Zero-Emission Vehicle Scenario Cost Analysis Using a Fuzzy Set-Based Framework

By

Timothy E. Lipman

UCD-ITS-RR-99-18

December 1999

Ph.D. Dissertation

Institute of Transportation Studies
One Shields Avenue
University of California, Davis
Davis, California 95616
Tel. 530/752-0247 Fax 530/752-6572
http://www.engr.ucdavis.edu/~its/
email: itspublications@ucdavis.edu

Zero-Emission Vehicle Scenario Cost Analysis Using A Fuzzy Set-Based Framework

BY

TIMOTHY EDWARD LIPMAN
B.A. (Stanford University) 1990
M.S. (University of California, Davis) 1998

DISSERTATION

Submitted in partial satisfaction of the requirements for the degree of

DOCTOR OF PHILOSOPHY

in

ECOLOGY

in the

OFFICE OF GRADUATE STUDIES

of the

UNIVERSITY OF CALIFORNIA

Davis

COMMITTEE IN CHARGE:

Prof. Daniel Sperling (Chair)
Prof. Paul P. Craig
Dr. Andrew F. Burke

1999

Acknowledgments

In addition to dissertation committee members Dan Sperling, Andy Burke, and Paul Craig, I would like to thank several individuals for their comments, assistance, and advice. First, I would like to thank Mark Delucchi, who graciously allowed me to use one of his models and whose work over the last ten years has been of great assistance to the effort described herein. The numerous references to his work are a testament to the research debt that I owe him. Second, I would like to thank Bob Moore and David Friedman of the ITS-Davis Fuel Cell Vehicle Modeling Center. Their advice and assistance was very helpful in completing the analysis of hydrogen and methanol fuel cell vehicles. Additionally, I would like to thank Dennis Corrigan of the Ovonic Battery Company and Jason Mark of the Union of Concerned Scientists for their advice and assistance. Finally, I would like to thank Susan Shaheen, for helping to make my years in Davis so enjoyable, and my parents, Peter and Beverly Lipman, for their love and encouragement.

This dissertation research was partially funded through an electric vehicle cost analysis research project sponsored by the California Air Resources Board and by two University of California Transportation Center dissertation grants. However, CARB and UCTC do not necessarily endorse the methods or findings herein.

Abstract

In this study, potential vehicle manufacturing costs, lifecycle costs, infrastructure support costs, and emission-related costs are compared for three potential zero-emission vehicle (ZEV) technology development and deployment scenarios. These scenarios include production of mid-sized battery electric vehicles, direct-hydrogen fuel cell vehicles, and direct methanol fuel cell vehicles from 2003 to 2026, and operation of the vehicles in California's South Coast Air Basin (SCAB) from 2003 to 2043. The study focuses on potential manufacturing cost reductions for electric motors, motor controllers, battery systems, hydrogen storage tanks, and fuel cell systems, due to the combined forces of production scale economies and technological progress.

Vehicle manufacturing and lifecycle costs are calculated by integrating vehicle component cost functions with a detailed vehicle performance and cost spreadsheet model. Fleet-level costs for vehicle operation, infrastructure development, and criteria pollutant and greenhouse gas emissions are calculated using a MATLAB/Simulink model developed by the author. In this regional-scale, fleet-level model, fuzzy set theory is used to characterize uncertainty in key input variables, and to propagate uncertainty through the calculation of vehicle, infrastructure, and emissions costs.

Findings are that estimated ZEV purchase prices drop steadily with production volume and technological progress, but that even in future, high-volume production the estimated purchase prices for all three ZEV types remain above those of comparable conventional vehicles. However, lifecycle costs for ZEVs in some cases become competitive with those of comparable conventional vehicles, especially for direct-hydrogen fuel cell vehicles. When infrastructure and emission-related costs are considered for vehicles used in the SCAB, total lifecycle costs for direct-hydrogen fuel cell vehicles are found to be below those of even low-emission gasoline vehicles by 2026, under central case assumptions. Meanwhile, total lifecycle costs for battery EVs and direct-methanol fuel cell vehicles are found to be between those of conventional and low-emission gasoline vehicles, again in the year 2026 central case. In general, the overall level of uncertainty in the calculation of total scenario net present values is considerable, and this level of uncertainty prevents the unequivocal determination of a least-cost ZEV technology pathway for the SCAB.

Table Of Contents

Table Of Contents (cont'd)

Table Of Contents (cont'd)

Table Of Contents (cont'd)

List of Tables

List of Tables (cont'd)

List of Tables (cont'd)

List of Figures

List of Figures (cont'd)

List of Figures (cont'd)

Abbreviations and Acronyms

Å = angstroms
AC = alternating current
Ah = ampere hour or ampere hours
AMI = American Methanol Institute
ANL = Argonne National Laboratory
AQMD = air quality management district
ASICs = application specific integrated circuits
atm = atmosphere or atmospheres of pressure
BAM = Ballard Advanced Materials
BCA = benefit-cost analysis
BPM = brushless permanent magnet
BEV = battery-powered electric vehicle
C = centigrade
CAFE = corporate average fuel economy
CARB = California Air Resources Board
CEC = California Energy Commission
CFC = chlorofluorocarbon
CH_4 = methane
cm^2 = square centimeter or square centimeters
cm^3 = cubic centimeter or cubic centimeters
CNG = compressed natural gas
CO = carbon monoxide
CO_2 = carbon dioxide
DC = direct current
DHFC = direct-hydrogen fuel cell
DHFCV = direct-hydrogen fuel cell electric vehicle
DMFC = direct-methanol fuel cell
DMFCV = direct-methanol fuel cell electric vehicle
DOE = U.S. Department of Energy
DTI = Directed Technologies Inc.
EDI = economic damage index
EEA = Energy and Environmental Analysis, Inc.
EIA = Energy Information Administration
EPA = U.S. Environmental Protection Agency
EV = electric vehicle
EVTECA = electric vehicle total energy cycle analysis
FCV = fuel cell electric vehicle
ft^3 = cubic foot or cubic feet
FUDS = federal urban driving schedule
g = gram or grams
g-CO_2-eq = grams of CO_2-equivalents
Gen1 = generation 1 (refers to NiMH battery technology)
Gen2 = generation 2 (refers to NiMH battery technology)
Gen3 = generation 3 (refers to NiMH battery technology)
Gen4 = generation 4 (refers to NiMH battery technology)

GHG = greenhouse gas
GJ = gigajoule or gigajoules
GM = General Motors Corporation
GWP = global warming potential
HFC = hydrofluorocarbon
HHV = higher heating value
HVAC = heating, ventilating, and air conditioning
H_2 = hydrogen
ICE = internal-combustion engine
ICEV = internal-combustion engine vehicle
IFC = International Fuel Cells Corporation
IGBT = insulated-gate bipolar transistor
IGT = Institute of Gas Technology
IPCC = Intergovernmental Panel on Climate Change
ITS-Davis = Institute of Transportation Studies - Davis
JPL = Jet Propulsion Laboratory
K = Kelvin or Kelvins
kg = kilogram or kilograms
kVA = kilovolt amperes
kW = kilowatt or kilowatts
kWh = kilowatt hour or kilowatt hours
L = liter or liters
LADWP = Los Angeles Department of Water and Power
LANL = Los Alamos National Laboratory
lb = pound
lbs = pounds
LEV = low-emission vehicle
LHV = lower heating value
Li-ion = lithium ion
mA = milliampere or milliamperes
mAh = milliampere hour or milliampere hours
MC = marginal cost
MEA = membrane-electrode assembly
MJ = megajoule or megajoules
mm = millimeter or millimeters
MMBTU = million British thermal units
MPa = megapascale or megapascales
MPF = manufacturing progress function
mW = milliwatt or milliwatts
MW = megawatt or megawatts
MWh = megawatt hour or megawatt hours
mV = millivolt or millivolts
m^2 = square meter or square meters
m^3 = cubic meter or cubic meters
M85 = a blend of 85% methanol with 15% gasoline

Abbreviations and Acronyms (cont'd)

M100 = neat methanol
NiMH = nickel-metal hydride
Nm = newton meter or newton meters
NMOG = non-methane organic gases
NO_x = nitrogen oxides
N_2O = nitrous oxide
OEM = original equipment manufacturer
OTA = Office of Technology Assessment
PEM = proton-exchange membrane
PM = particulate matter
PM_{10} = particulate matter less than 10 microns in diameter
PNGV = Partnership for a new Generation of Vehicles
psi = pounds per square inch
RTEC = Residential Transportation and Energy Consumption
SCE = Southern California Edison
SMR = steam methane reforming
SULEV = super ultra low-emission vehicle
SCAB = South Coast Air Basin
SCF = standard cubic foot or standard cubic feet
SO_x = oxides of sulfur
SO_2 = sulfur dioxide
TFN = triangular fuzzy number
U.S. = Unites States
V = volt or volts
VMT = vehicle miles traveled
W = watt or watts
Wh = watt hour or watt hours
ZEV = zero-emission vehicle

Chapter 1: Introduction

Introduction and Problem Context

Technological solutions to environmental problems continue to be of interest to regulators, industry, and the public. This is particularly true in the United States (U.S.) transportation sector, where efforts to alter travel behavior have often proven to be ineffective. Since travel behavior is difficult to change, many analysts believe that modifying vehicle technology is the best means to offset the environmental impacts of continued increases in vehicle miles traveled (VMT).[1] However, it is important to remember that even the best technological solutions are limited in scope, and no one type of solution can address all of the problems imposed by the vehicle-dominated transportation system in the U.S. Even very low emission vehicles, for example, do not solve the traffic congestion problems that plague many urban areas and lead to lost productivity, frustration, and a reduced quality of life for millions of U.S. citizens.

Studies of the social costs of motor vehicle use have shown that while the present system clearly provides large benefits to U.S. society, it also imposes substantial social costs. These costs occur in many forms, including direct costs paid by users, personal non-monetary costs, government service costs, and externality costs. By varying estimates, these motor vehicle related social costs (both private, paid costs and external, unpaid costs), totaled between $1.1 trillion and $2.8 trillion on an annualized basis for the U.S. in 1990. Of these total social costs, unpaid external costs accounted for $300 billion to $600 billion (Delucchi, 1996a; MacKenzie, et al., 1992; Miller and Moffett, 1993). Many of these costs are not unavoidable outcomes of the use of motor vehicle services. Rather, they represent the costs to society of motor vehicle use as mediated by specific technologies, and these technologies themselves are subject to change.

A variety of factors have contributed to the impetus to develop low-emission, "alternative-fuel" vehicles (AFVs) in the U.S. in recent years. These factors include lowered emissions standards for motor vehicles, including "zero-emission vehicle" mandates in California, New York, and Massachusetts; public concern about the various impacts of motor vehicle use on human health and the environment; and the desire of automobile manufacturers to be perceived as responsible corporations and technological leaders. In recent years, issues of public concern have included:

---

[1]Of course, reducing VMT and increasing vehicle occupancy rates are more direct solutions to the problems created by motor vehicle use than simply changing vehicle technology, because they get at the root causes of motor vehicle-related problems. Success at such efforts has historically been limited in most areas, but emerging information and communication technologies are making new types of solutions possible. Of course, VMT reduction and vehicle use efficiency improvement efforts can be pursued in parallel with efforts to improve the efficiency and environmental performance of vehicle technologies themselves.

- the persistent inability of some U.S. urban areas to achieve federal and state air quality standards, particularly in Southern California and in the Northeast;

- the potential climatic impacts of motor vehicle-related greenhouse gas (GHG) emissions;

- the overwhelming dependence of the transportation sector on petroleum; and

- the increasing share of oil imports relative to domestic production.

Over the past three decades in the U.S., since the original Clean Air Act of 1970 imposed the first restrictions on motor vehicle emissions and drew attention to the environmental impacts of transportation systems, the relative prominence of these issues has varied considerably. Petroleum dependence has occasionally been raised as an important issue in recent years, particularly during the Gulf War and when gasoline prices have temporarily risen. However, it is still much lower in prominence than during the 1970s and early 1980s when disruptions in oil markets caused high prices and shortages in supply, and raised the issue to the forefront. Nevertheless, the U.S. Department of Energy (DOE) is projecting that over 50% of the petroleum used in the U.S. will be imported in 2000, and that 65% will be imported by 2020 (EIA, 1998). These forecasts imply growing vulnerability to oil price shocks and supply disruptions, as well as balance of trade issues with $99.8 to $158.1 billion forecast for expenditures on imported oil in 2020 (EIA, 1998).

With regard to GHG emissions, the present level of concern is much greater in Europe than in the U.S., where support for the Kyoto Protocol to reduce GHG emissions has not been strong. The continuing trend of increasing global average temperatures might perhaps lead to a resurgence in concern about GHG emissions among the American public, but at present there appears to be insufficient political will to enact binding regulations to restrict GHG emissions. As the 2008-2012 timeframe for meeting the 7% reduction in GHGs (below 1990 levels) required by the Kyoto Protocol draws near, however, the issue is likely to become more politically prominent.

Urban air quality continues to be an important issue, with major restrictions on vehicle emissions being established in the sweeping Clean Air Act Amendments of 1990. In a relatively controversial move, the U.S. Environmental Protection Agency (EPA) has recently proposed new ozone and particulate matter (PM) standards that are even more stringent than the current standards that remain unattained in some U.S. urban areas. The EPA has justified these new regulations with analysis that shows that new standards are necessary to provide increased protection against a wide range of PM and ozone-related health effects. For example, the EPA estimates that even if Los Angeles County were to meet the existing PM standards, 400 to 1,000 deaths per year would still occur as a result of exposure to very fine PM (under 2.5 microns in diameter) that presently is not regulated (65650 Federal Register, 1996). Nationally, even though air quality has generally improved over the last 30

years, about 107 million people still live in counties with unhealthy air quality (U.S. EPA, 1998).

Concern for these issues among the public has led the automotive industry to begin to see the environmental attributes of the vehicles it sells as a potential point of competitive advantage. Companies in the industry are now vying to be perceived as environmentally responsible, and as leaders in improving vehicle environmental performance with new technologies. As Harry J. Pearce, vice chairman of General Motors, notes:

> [M]arket survey after market survey tells us environmental issues are increasingly important to our customers (Bradsher, 1999, p. D1).

Ironically, it may be that the greatest impetus for developing clean vehicles today is not great public concern about the impacts of motor vehicles on the environment *per se*, or even government regulations that require AFVs in fleets and in certain urban areas, but rather the desire of automobile manufacturers to cater to the environmental concerns that consumers report when surveyed. However, regardless of which social, regulatory, and economic factors are most responsible for leading manufacturers to develop new types of motor vehicles, it is becoming increasingly clear that an industrial revolution is underway. The ultimate outcome of this period of technological innovation in the automobile industry is impossible to predict, but it is likely that within a few decades a new "dominant design" for automobiles will emerge. This new dominant design will be based on lightweight materials, greater integration of electronics and information technologies into vehicle designs, and some form of hybrid power and/or propulsion system technology that likely will include a partial or full electric drive system.

Electric Vehicles and the Environment

In addition to natural gas, ethanol, and methanol combustion engine vehicles, of particular interest in recent years have been electric vehicles (EVs) that use some form of electric power and propulsion system. These include battery-powered EVs (BEVs), hybrid EVs that combine electric motors with small combustion engines, and fuel cell EVs (FCVs). All of these types of EVs promise improved efficiency relative to conventional vehicles. BEVs and FCVs offer the additional advantages of eliminated tailpipe emissions, flexibility of fuel supply, and quiet and smooth operation. They may also offer higher reliability and reduced maintenance requirements relative to conventional and hybrid vehicles that include a combustion engine.

EV technologies have developed rapidly in recent years, and a new wave of vehicle technology is emerging based on developments in power electronics, high-efficiency motors, battery and ultracapacitor energy storage systems, fuel cells, and lightweight materials. Every major automaker has now produced prototype or commercial EVs based on some type of battery or hybrid power system. General Motors and Honda have led the way in the U.S. market, with polished, production EVs currently available for lease in parts of California and Arizona.

Particularly given the explosion of automobile production and ownership that is occurring in the developing world, the timely development and transfer of environmentally friendly motor vehicle technologies has profound implications for not just national but also global health and environmental concerns. To emphasize this point, it is worth noting that China, currently with one of the lowest per-capita automobile ownership rates, is beginning to aggressively develop a motor vehicle industry. If the Chinese rate of motor vehicle ownership were to equal half of a vehicle per person in 50 years' time (less than the present U.S. average of about 70 vehicles per 100 people), and its current population growth rate of 0.83% per year continues, a staggering 950 million vehicles would be on the roads in China alone by 2050. Globally, 3 billion motor vehicles could be in use by 2050, if present trends continue (Sperling, 1995).

Despite the regional and international importance of the impacts of motor vehicle use, and the level of attention and research that has been focused on various aspects of EV technology development, few detailed, multi-dimensional studies have been conducted on the vehicle, infrastructure, and emission-related costs associated with introducing different types of EVs into one or more urban areas. Perhaps most attention has been focused on the potential air quality implications of EV use (Dowlatabadi, et al., 1990; Kazimi, 1997), and on the manufacturing costs of battery and fuel cell EVs (DeLuchi, 1992; Moomaw, et al., 1994; NYSERDA, 1995; OTA, 1995; U.S. DOE, 1995). Other studies have been conducted on the potential for EVs and FCVs to reduce greenhouse gas emissions and to alleviate petroleum dependency (Bentley, et al., 1992; Burke and Miller, 1997; Ogden, et al., 1994; U.S. DOE, 1998a).

In addition to these relatively narrowly-focused studies, a few efforts have been made to conduct multi-attribute analyses by examining more than one of these dimensions. Fulmer and Bernow (1995) conducted a partial social cost analysis of several types of AFVs, but did not include fuel cell vehicles and also did not estimate external costs other than those from air pollution. Hwang et al. (1994) studied the potential social benefits of EVs in California, but also did not examine fuel cell vehicles and did not include vehicle costs. Mark et al. (1994) examined emission and fuel saving potential of fuel cell vehicles (FCVs), but also did not include vehicle costs. Ogden et al. (1999) recently analyzed FCV costs and infrastructure costs, but did not analyze emissions. Berry (1996) assessed fuel and infrastructure costs and emissions associated with BEVs and various hybrid vehicles, including hydrogen internal-combustion engine (ICE) hybrids, but did not consider vehicle costs or fuel cell vehicles. Finally, Thomas et al. (1998a) studied vehicle costs, externality costs, and infrastructure costs for several different types of AFVs, including three types of hydrogen FCVs, but did not include an analysis of battery EVs.

An analysis of the relative costs associated with BEVs and FCVs is warranted because at present only BEVs and direct-hydrogen FCVs (DHFCVs) are capable of meeting the zero-emission vehicle (ZEV) mandate enacted by the California Air Resources Board (CARB). The original 1990 ZEV mandate required 10% of the vehicles offered for sale by major manufacturer sales in the state of California to be ZEVs by 2003, with 2% and 5% requirements for 1998 and 2001. New York and Massachusetts subsequently adopted the same vehicle sales requirements. The ZEV mandate was changed in 1996 to lift the

requirements for sales prior to 2003, and again in 1998 to allow some of the 10% ZEV requirement to be composed partial credits from other "near-ZEVs" that meet a complex set of emission-related and other technological criteria. However, even under the new, more flexible regulations, at least 40% of the ZEV credits required of major manufacturers (i.e., the "Big 7"), or 4% of overall sales, must come from "true ZEVs" that emit no criteria pollutants directly from their tailpipes (CARB, 1998b).

This dissertation research examines vehicle costs, infrastructure support costs, and monetized criteria pollutant and GHG values from fuel-cycle emissions associated with multi-year, transitional pathways toward BEV and FCV production and use. The focus of the analysis is California's South Coast region because approximately 40% of the state's ZEVs are expected to be sold in this region alone (Evashenk, 1999), and because the region's air quality problems make it the most important focus for ZEV technology. The analysis considers two different production volume scenarios for a major manufacturer, of a size comparable to General Motors (GM), Ford, or Toyota, in order to explore differences in vehicle and infrastructure costs associated with greater and lesser production volumes. In addition to BEVs and DHFCVs, the analysis also considers a third ZEV option that may ultimately prove important but for which less is presently known. This is the option of the direct-methanol FCV (DMFCV), whereby liquid methanol, rather than gaseous hydrogen, is reacted in the fuel cell. This option may offer many of the advantages provided by DHFCVs, without the associated hydrogen storage and hydrogen refueling infrastructure issues. The analysis also considers infrastructure support costs that are likely to be required to support the introduction of the vehicles, beyond the amortized costs that are included in the costs of fuel, and approximate monetized emission values for criteria pollutants and GHGs.

Dissertation Methods and Goals

The primary goal of this dissertation research is to compare the relative vehicle, infrastructure, and emission related costs of three different sets of ZEV technologies as they might be deployed in the South Coast Air Basin (SCAB), and to compare these costs to corresponding costs for conventional internal-combustion engine vehicles (ICEVs). Several hypotheses, discussed below, are tested with regard to these potential costs. An additional, methodological goal is to demonstrate how fuzzy set theory can be used in the context of the MATLAB/Simulink programming environment to characterize and propagate key uncertainties through a model. The following sections discuss important methodological issues underlying the analysis, and the hypothesis tests to be conducted.

Uncertainty in Energy and Transportation Policy Analysis

One crucial issue with regard to studying the various private and social costs associated with emerging technologies is that there is often considerable uncertainty associated with various elements of their cost and performance. Even technology component manufacturers themselves cannot be sure of future production costs, because materials costs change over time and unforeseen events can occur that affect production costs. The uncertainties for those outside of the industry are even greater because manufacturing cost data are proprietary

in nature and difficult to obtain. Other types of data also entail significant uncertainties, such as the emissions associated with fuel production technologies and feedstock extraction, and the damages to humans and the environment from changes in air quality.

A variety of different techniques are available to address and characterize such uncertainties, most of them with roots in mathematical probability theory. One of three basic strategies is typically employed to address uncertainty in policy analysis. The first option is to use mean or "best guess" values within a known range, and to ignore the underlying uncertainty. In policy analysis, this has historically been the most common procedure (Morgan and Henrion, 1990). Those who employ this method sometimes make the argument that variations above and below the mean will tend to cancel each other out, such that the final result would not be much different even if a more detailed approach were employed (Litman, 1996). The main problem with this method is that the same average value can be obtained from both very wide and very narrow ranges, so the level of uncertainty in a given variable is instantly lost when this method is used. There is thus no way, once the analysis is complete, to get a sense of the overall level of uncertainty in the analysis, or the relative importance of the uncertainty associated with each uncertain input variable.

A second approach is to choose a mean value in a range and proceed with the analysis, but to then conduct sensitivity analysis on each uncertain variable after the "base case" analysis has been completed. This can be done in a variety of ways. Methods include deterministic analysis, where one variable is changed at a time (to at least "high" and "low" cases, and possibly many more), deterministic joint analysis where more than one variable is changed at a time because the variables are not independent, or parametric analysis where one or more factor is varied along a continuous and well-established range. Use of this general approach is preferable to the first one, in that the range of uncertainty in each variable can be explored, and the relative importance of each variable to the final result can be assessed. The drawback, however, is that attention is often focused on the base case, and sometimes only this result gets reported and used by those who are interested in the study results. The results of sensitivity analyses are often buried in appendices in the back of the report, and they are frequently insufficiency addressed and discussed in report summaries. Furthermore, there is ample opportunity for those who wish to influence policy to choose whatever sensitivity runs best suit their cause, and to report only those results.

A third option is to attempt to propagate the uncertainty associated with the uncertain variables through every step of the analysis. This is more difficult, but it has several advantages. First, the final answer can readily be expressed in a manner that conveys the overall level of uncertainty in the analysis. Second, the need to do sensitivity analysis is greatly reduced. Third, sometimes enough research has been conducted on the range of variation in a particular variable to characterize it as a specific probability distribution, rather than a simple range. In this case, identifying a mean value is still possible, but all of the detail embodied in the underlying probability distribution is lost. This detail can be included if the full distribution is maintained, rather than collapsed into a point value. Finally, there is less opportunity for the results of the study to be mis-reported or misused, since the final answer is expressed as a range of values rather than a

series of single values from which a selection can be made. The disadvantages of methods that propagate uncertainty are that they are more computationally difficult, and that the final result may be far more ambiguous than if simplifying assumptions are used.

In the field of benefit-cost analysis (BCA), analyses of the first or second type have come to be known as deterministic BCA, while those of the third type are called probabilistic BCA (Morgan and Henrion, 1990). The most common manner though which the specifics of the uncertainty in one or more variables can be retained and carried through the analysis is to use a Monte Carlo technique. This technique has its roots in mathematical probability theory. It requires multiple trials to be conducted and that a random number generator be used to select a value from each probability distribution for each trial. This technique allows many different variables to be characterized with uncertainty, and the uncertainty in each variable to be propagated through the analysis.[2] Unlike in decision tree analysis, where the complexity of the analysis grows exponentially with the inclusion of each additional uncertain variable (with the exponent being the number of branches that are included), the total computational effort needed for a Monte Carlo analysis grows linearly with the number of uncertain variables (Morgan and Henrion, 1990). This difference clearly becomes very important for complicated analyses, when a large number of uncertain variables are included.

A further strength of the Monte Carlo method is that it can readily be used with simple and complex probability distributions. With some other methods, complicated probability distributions can be handled only with difficulty (e.g., those methods that involve discretizing continuous distributions so that they can be fit to a decision tree framework). Short et al. (1995) provide a useful discussion of Monte Carlo analysis, among several other techniques for the economic evaluation of energy technologies.

Uncertainty Characterization with Fuzzy Set Theory

Another technique that can be used to characterize and manipulate complex probability distributions for a large number of input variables is based in fuzzy set theory. Developed in 1965 by Lofti Zadeh at the University of California at Berkeley, fuzzy set theory is most well known for providing the mathematical basis for fuzzy logic. This technique of mapping input spaces into output spaces with fuzzy mathematics has been applied in many different settings where multivalent logic (as opposed to bivalent logic) is useful. Fuzzy logic has swept through the field of electronic controls over the past twenty or so years, first among engineers in Japan and Southeast Asia and more recently in the U.S. and Europe. Today many common household appliances incorporate some form of fuzzy logic into their operation.[3] Computer software packages, such as MATLAB by Mathworks, Inc., with its "Fuzzy Logic Toolbox," have recently been designed to provide fuzzy logic programming ability.

---

[2] I recently used this technique to conduct a probabilistic cost forecast of an EV drivetrain (Lipman and Sperling, 1997), and found it to be a useful and powerful technique.

[3] Such appliances are typically called “smart” or “intelligent” appliances, rather than “fuzzy logic” ones, because of the better connotations that those terms have.

The concept of "fuzziness" that underlies fuzzy set theory shares much in common with the concept of "randomness" that underlies probability theory, but the two are conceptually and theoretically distinct. Fuzzy set theory is really just an extension of classical set theory, which involves some of the most basic of all mathematical concepts such as set membership, set union, and set intersection. The source of fuzziness in fuzzy set theory is the lack of precisely defined class membership in a set. In classical set theory, a particular object or concept can either be in or out of a particular set, but not both. For example, the set of weekdays would include Monday, Tuesday, Wednesday, Thursday, and Friday. The set of weekend days would include Saturday and Sunday. These sets can be called "crisp" sets in that it is entirely clear and unambiguous that certain days are included or excluded. In fuzzy set theory, individual components of a set can have partial membership in that set. Again using the above example, fuzzy set theory would allow the day "Friday" to be partly in the set of weekdays and partly in the set of weekend days. The guiding principle to fuzzy set theory, the "fuzzy principle," is that "everything is a matter of degree" (Kosko, 1993).

Classical set theory has its roots in the philosophy of Aristotle and the other ancient Greeks, and within this paradigm there can only be crisp notions of set membership; an object or idea is either "A" or "not A." Fuzzy set theory is philosophically closer to the tenets of Buddhism, where instead of "A or not-A," the notion of "A and not-A" is allowed. A few hundred years before Aristotle lived, the Buddha was known to have often refused to be trapped by the bivalent logic that later would become the basis of much Western philosophy, mathematics, and science. He would engage in "noble silence" when asked questions that forced a bivalent answer, such as whether the universe was finite or infinite (Kosko, 1993).

Fuzzy set theory is much better suited than classical set theory to practical applications, where "shades of gray" predominate. Very little in real life is unambiguous, precisely defined, or "crisp." Albert Einstein put it well, in his 1952 book *Geometry and Experience*, when he wrote:

> [S]o far as the laws of mathematics refer to reality, they are not certain. And so far as they are certain, they do not refer to reality. (Quoted in Kosko, 1993, p. 3)

Fuzzy set theory assigns a degree of membership to every object in a set such that, for example, Friday could have a degree of membership of 0.6 in the set of weekdays and 0.4 in the set of weekend days. The following general "membership function" characterizes the concept of the degree of membership in a fuzzy set:

$$\mu_A: X \rightarrow [0, 1]$$

This means that the fuzzy set A is defined over a "universe of discourse" X to be between 0 and 1 (Bandemer and Gottwald, 1995). For practical applications, the range of variation of a given variable can be normalized to the range of from 0 to 1, so that this general expression can hold for all fuzzy set membership functions. As well as being discrete, with a specific membership degree, fuzzy sets can also be continuous such that the degree of membership varies along a

dimension of interest. Fuzzy set theory provides the conceptual underpinnings for fuzzy logic, but it also is a convenient and mathematically elegant framework for expressing the form of uncertain variables. The membership function for a fuzzy set can be very simple, or very (even arbitrarily) complex.

Despite being developed over thirty years ago, fuzzy set theory has only recently been applied in the field of environmental policy analysis. Dompere (1995) and Wang and Liang (1995) have applied fuzzy set theory to BCA, and Smith (1994) has developed a fuzzy set-based framework for the environmental appraisal of alternative road building projects in Queensland, Australia. Fuzzy set theory has also recently been used in environmental assessment of urban traffic patterns (Tao and Xinmiao, 1998), for production decision making in the German automobile industry (Altrock and Krause, 1994), for ecological impact classification (Silvert, 1997), and to capture uncertainty in estimating economic cash flows for engineering project evaluation (Chiu and Park, 1994).

The limited application of fuzzy set-based methods to environmental, energy, and transportation policy and planning issues to date is perhaps partially due to the fact that there are only a few approachable texts on the subject. Bandemer and Gottwald (1995) and Zimmerman (1991) are among the few thorough treatments available, although Kosko (1993) provides a highly approachable introduction to the topic. Much of the literature is notationally complex, intended for practitioners, and virtually unintelligible to others. It is clear, however, that fuzzy set theory can be a useful theoretical framework for dealing with complex, multi-criteria issues that commonly arise in policy and planning, and it is likely to become more widely used in such applications in the future.

While probability theory and fuzzy set theory both have the ability to allow the consideration and manipulation of uncertain variables, fuzzy set theory has two significant advantages. First, the fuzzy set extension principle, developed by Lofti Zadeh in 1975, allows the arithmetic operations of addition, subtraction, multiplication, and division to be used on triangular and trapezoidal fuzzy sets without the use Monte Carlo or Monte Carlo-type analysis (Zadeh, 1975). Some higher math functions have also been worked out with the extension principle, although they are less straightforward. The following notation is typically used for the addition, subtraction, and multiplication of fuzzy sets (Bandemer and Gottwald, 1995):[4]

Sum $S := A \oplus B$ determined as:

$$\mu_S(a) = \sup_{x \in \mathbf{R}} \min\{\mu_A(x), \mu_B(a - x)\} \text{ for all } a \in \mathbf{R}$$

Difference $S := A \ominus B$ determined as

$$\mu_S(a) = \sup_{x \in \mathbf{R}} \min\{\mu_A(x), \mu_B(x - a)\} \text{ for all } a \in \mathbf{R}$$

[4] See Appendix A for explanation of the notation in these expressions, as well as further discussion of fuzzy sets and the relationship between fuzzy set distributions and probability distributions.

Product $S := A \quad B$ determined as

$$\mu_S(a) = \sup_{\substack{x,y \in \mathbf{R} \\ a = xy}} \min\{\mu_A(x), \mu_B(y)\} \text{ for all } a \in \mathbf{R}$$

For simple triangular or trapezoidal "fuzzy numbers," the extension principle can be applied in a straightforward manner to allow basic arithmetic operations to proceed. The procedure is simply to apply the operation to each of the corresponding elements in each of the fuzzy set number sequences.[5] The resulting number is then also a fuzzy number, and its form is almost exactly the same answer as would be obtained by Monte Carlo analysis (see below for discussion). For fuzzy sets with more intricate membership functions, more complex algorithms, akin to Monte Carlo analysis but involving the use of "alpha-cuts" through the distributions, can be used to perform various mathematical operations.[6] Figure 1-1 depicts triangular fuzzy numbers, A_o and B_o, the sum of A_o and A_o, the sum of A_o and B_o, and the negative of A_o, as they would be calculated with the extension principle.

Figure 1-1: Sums and Negative of Triangular Fuzzy Numbers

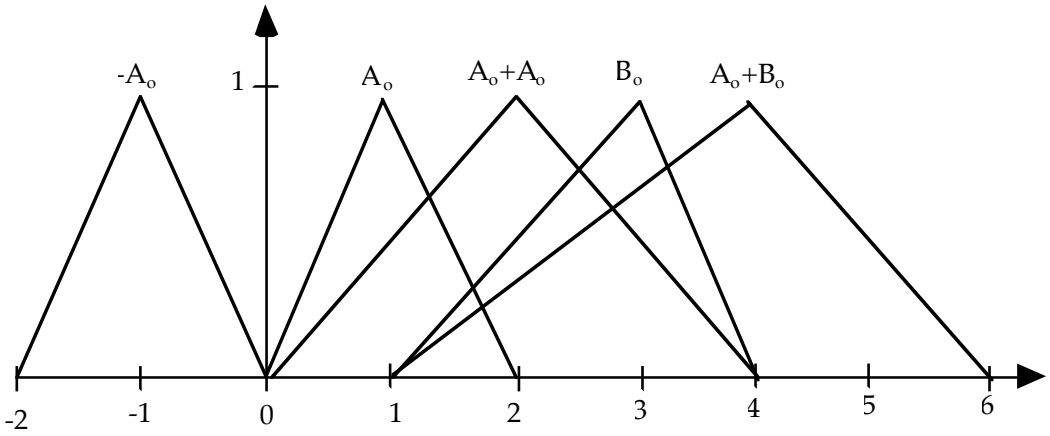

With multiplication and division of TFNs, the sides of the triangles (the left and right "descriptions" of the membership function, in the fuzzy set lexicon) are not exactly straight lines. They curve slightly, as shown in Figure 1-2. Note also in Figure 1-2 how when fuzzy multiplication is performed, the uncertainty is magnified even when just two uncertain variables are included.

---

[5] Unless fuzzy subtraction is being performed, in which case one of the variable vectors is reverse-ordered.

[6] The latest version of MATLAB (release 5.2) has the ability to perform mathematical operations on complex fuzzy sets, but the corresponding blocks for MATLAB's Simulink dynamic simulation package blocks have not yet been developed. One can call MATLAB's fuzzy math functions in from Simulink, but it is very cumbersome to do so because only one operation can be done at a time. As a result, I have for now confined myself to triangular distributions, but I would expect new Simulink blocks to be developed within a few years, and more complex distributions could then be included in fuzzy set-based Simulink models.

Figure 1-2: Fuzzy Set Multiplication in MATLAB

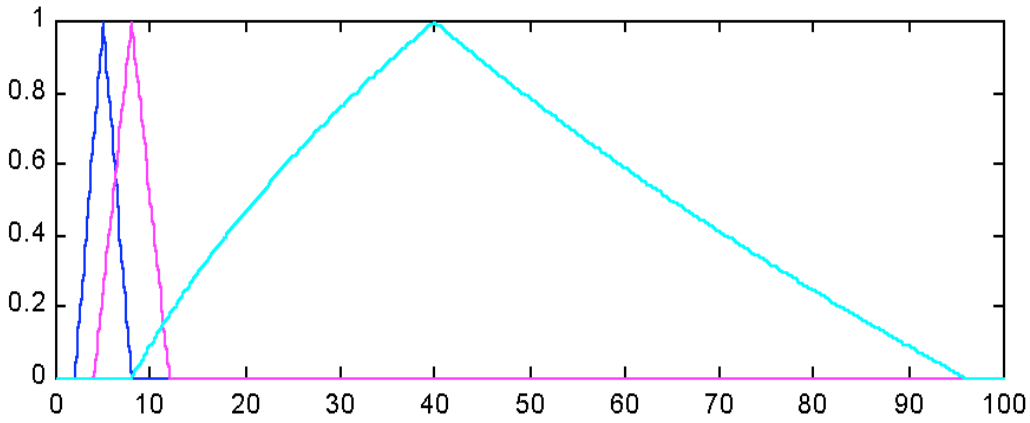

This distinction is not noted in all texts because in practice, it is only even theoretically significant where the shape of the triangle, as well as the spread of its points, is meaningful. If enough data are obtained to allow the analyst to characterize the shapes of the distributions, then the effect of the extension-principle fuzzy product/quotient discrepancy should be investigated. However, in some investigations where distributions with explicit shapes have been included, sensitivity of results to the extension principle result versus the "true" result have shown no effect on the final solution of using the results of the simpler method (Chiu and Park, 1994). If both types of solutions are to be compared, algorithms such as those in MATLAB's "fuzarith" function allow the more accurate result to be computed. One advantage of fuzzy set theory over probability theory is that the shapes of unusual distributions are easy to include; one can choose between standard or non-standard distributions easily (any convex distribution can be included).

The fuzzy set extension principle is useful in that it can reduce or even eliminate the number of Monte Carlo steps that may be required to propagate uncertainty through a given analysis. There may be occasions in which an analyst would like to include some uncertainty around a mean value, but has no reason to assume a specific functional form such as the normal distribution commonly assumed in probability-based Monte Carlo assessments. It may be felt that a value is likely to fall at a certain point or within a certain range, but that there is also some chance that it will be to either side. In this case, a triangular or trapezoidal fuzzy number could be specified, and through the use of the extension principle the fuzzy number could be manipulated without the use of the Monte Carlo technique.[7]

[7] This essentially amounts to simultaneously running central, high, and low cases in the same model, thereby eliminating the need to do separate runs or to maintain separate model structures. However, it has the additional advantage of allowing a range of interest to be collapsed (defuzzified) to the central value in order to compare it with other values, or to determine the effect of the level of uncertainty in one or more particular variable on the overall result and level of uncertainty.

In other cases, there may be a good reason to assume a more complex distributional form, and in this case the distribution could be specified as either a fuzzy set with a more complex membership function, or as a classical probability distribution. For example, the U.S. EPA has recently fit complex probability distributions to a number of pollutant-response and response-economic valuation effects reported in the literature, including for example a Weibull distribution with a mean of $4.8 million to estimates of the value of a statistical human life (U.S. EPA, 1997). In the case of a variable that includes the possibility of low-likelihood but potentially extreme outcomes, such as perhaps the risk associated with an accident for a train carrying nuclear waste through a populated area, it would be necessary to use a distribution with a "tail" rather than a triangular or trapezoidal distribution. In such cases, use of the extension principle to perform calculations would not be possible, and Monte Carlo-type techniques would be required. Figure 1-3 shows the result of adding a triangular fuzzy set distribution with a Gaussian distribution, using MATLAB's "fuzarith" function.

Figure 1-3: Fuzzy Set Addition in MATLAB

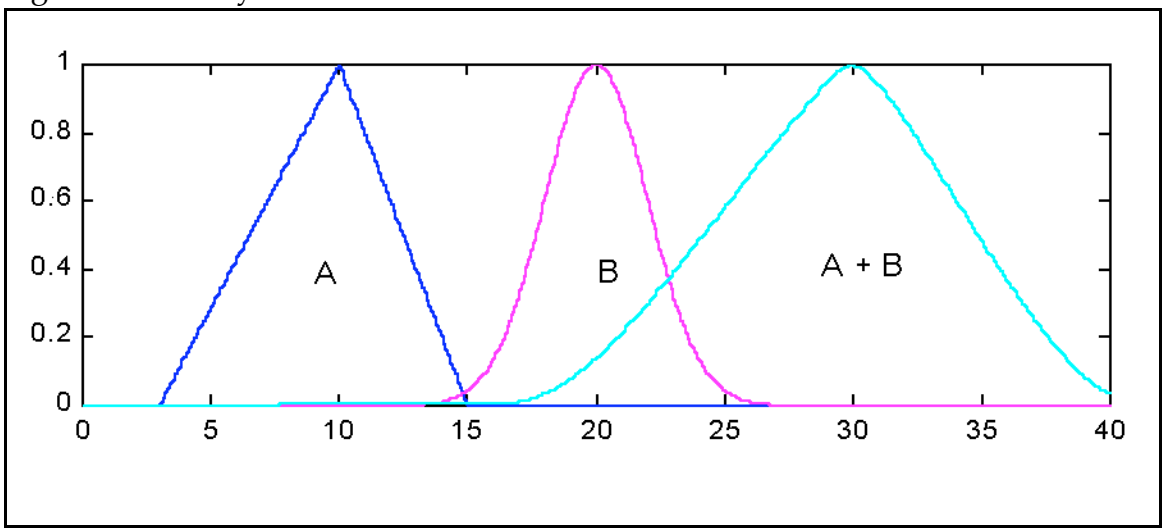

However, often the variables of interest in economic, technical, or policy analyses will have possible values that fall into relatively well-defined ranges, but simply are hard to "pin down" exactly. In such cases, the use of triangular or trapezoidal distributions can be appropriate. Since all of the distributions in this analysis can be satisfactorily characterized with TFNs, these TFNs are employed along with the extension principle to calculate fleetwide vehicle, infrastructure, and emission-related cost.

The fuzzy set-based fleet cost model developed here has been programmed in the Simulink environment of MATLAB, where a graphical user interface is employed and where system dynamics can be included. In the Simulink programming environment, unlike in the more fully-developed MATLAB workspace, the brand-new "fuzarith" function that is illustrated in Figures 1-2 and 1-3 has not yet been well-integrated. It can be called in from MATLAB only in a cumbersome and limited fashion. When this feature is better incorporated into Simulink in the form of a dedicated set of Simulink library

blocks, and with the help of further improvements in desktop computing power, it will be easier to avoid the extension principle altogether and perform large numbers of calculations using more detailed algorithms. Figure 1-4 depicts fuzzy multiplication in Simulink, using vectorized input variables and the fuzzy-set extension principle.

Figure 1-4: Fuzzy-Set Extension Principle Multiplication in Simulink

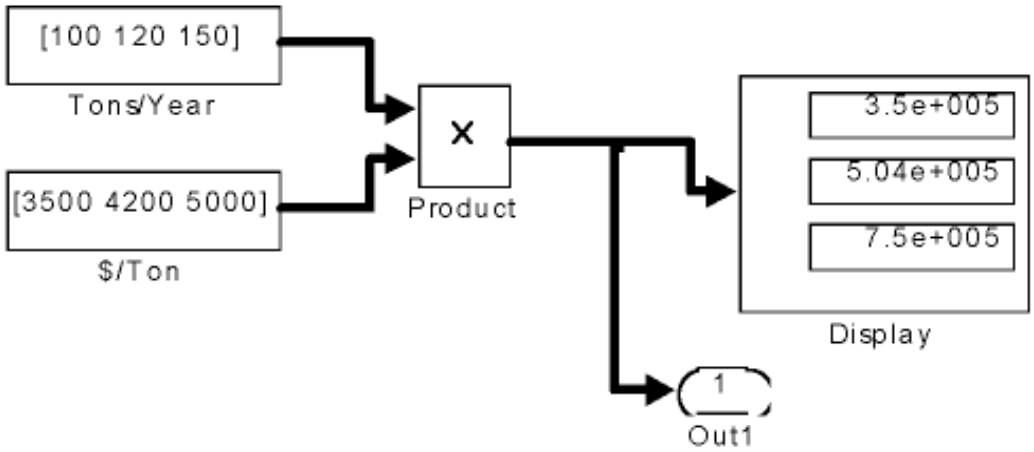

Using Fuzzy-Set Theory to Incorporate Qualitative Variables

A second potential advantage of fuzzy set theory is that it provides a coherent framework for including both quantitative and qualitative variables in an analysis. An important issue in the environmental policy analysis field is that it is often the case that it is only the variables that lend themselves to quantification that are included. Some factors, such as the economic damages to agricultural crops from pollution or tons of emissions from waste burned in an incinerator, can be reasonably well quantified, at the very least within a reasonable range. This cannot be as easily said for some other factors, such as aesthetic appreciation of the landscape, the cultural value of a natural asset, or the existence and bequest values of unspoiled wilderness to different individuals. Impact "quantifiability" and "severity" can easily be unrelated; in fact, Holdren (1982) has even argued that they may be inversely related. He argues that analysts that are "preoccupied with the quantifiable may confuse things that are countable with the things that count" (Holdren, 1982, p. 38).

Fuzzy set theory offers the ability to include qualitatively defined variables as well as quantitative ones in the same analytical framework by mapping such imprecise and subjective assessments as "very high," "high," "moderate," "low," and "very low" into fuzzy numbers. These can then be included in an analysis along with quantified variables (perhaps including some sort of preference weighting if appropriate). Figure 1-5 depicts graphically one suggestion for how this might be done (Smith, 1994). In this scheme, the five categories above could be expressed as the following triangular fuzzy numbers: very low [0.0, 0.0, 0.3], low [0.0, 0.0, 0.4], moderate [0.3, 0.5, 0.7], high [0.6, 1.0, 1.0], and very high [0.7, 1.0, 1.0].

Figure 1-5: Linguistic Ratings Expressed as Triangular Fuzzy Numbers

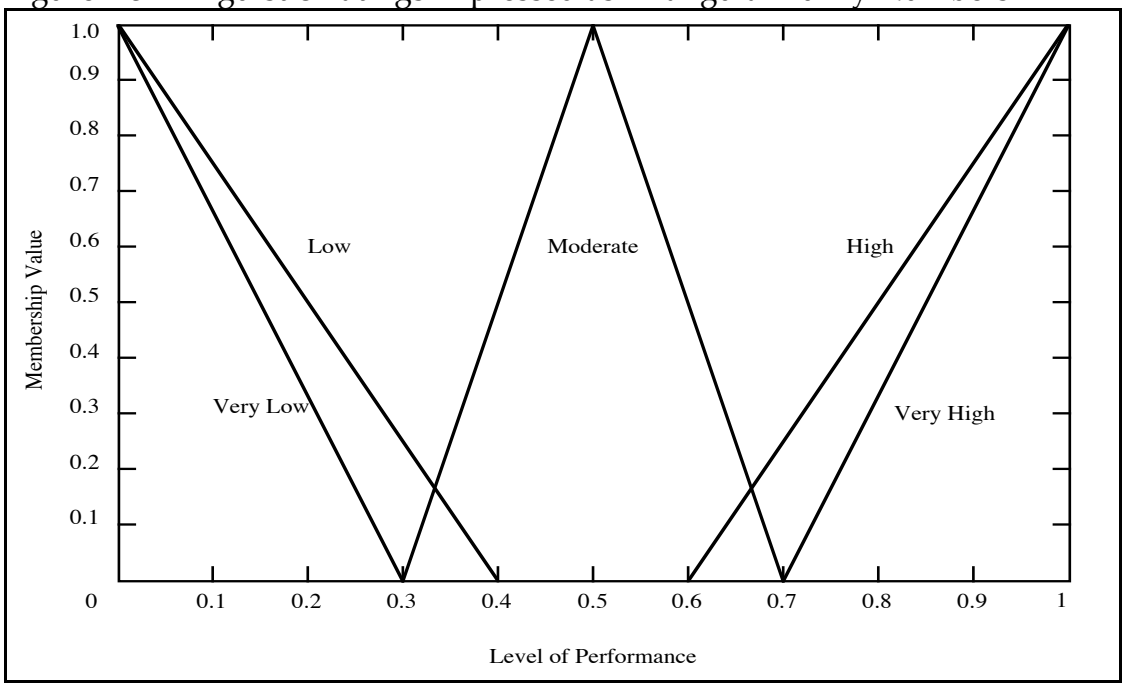

Due to these advantages, and its general flexible nature, fuzzy set theory is an attractive theoretical framework for probabilistic BCA or social cost analysis.[8] In order to perform a complex, multi-criteria analysis any number of cost categories can be specified and assessed using discrete or continuous fuzzy sets, a translation of qualitative assessments, and/or crisp values. If desired, any or all of these categories can be weighted to reflect the relative importance of each objective. Also, in order to account for differences in values and preferences, both fuzzy sets and weights can be defined from the perspective of individual stakeholders and interest groups, and the results can be analyzed and aggregated in various ways (Smith, 1994).

In the analysis conducted here, qualitative variables are not included because doing so would require consumers to be surveyed as to their subjective assessments of various vehicle attributes, and this is not presently possible since fuel cell vehicles are not yet available for drive clinics or home trials. In the future, however, such investigations will be possible for various ZEV types, as they have been recently for BEVs. It may in fact prove true that the values that consumers assign to qualitative differences between ZEVs and other vehicle types will be sources of significant overall differences between them, and that the positive values for perceived ZEV advantages will overwhelm negative values for perceived disadvantages. For now, however, we can only speculate about the values that consumers will place on ZEV attributes such as reduced vehicle noise, the absence of tailpipe emissions, the smooth and responsive acceleration of electric-drive, limited driving ranges for BEVs, the elimination of oil changes, and so on.

---

[8] Actually, "possibilistic BCA" may be the correct terms since fuzzy-set theorists now use the term "possibility theory" to distinguish it from probability theory.

Ranking of Fuzzy Sets or "Defuzzification"

In order to compare fuzzy sets in an absolute sense, it is necessary to determine the ranking order of the fuzzy set distributions. In the fuzzy set literature, this is known as determining the relative "dominance" of different fuzzy sets. There are a number of different ways in which this dominance-determination, or "defuzzification," procedure can be conducted, and in which fuzzy numbers can be compared. Most methods have focused on ranking triangular fuzzy numbers (TFNs), due to the popularity of their use in characterizing uncertain variables and computed values.

Chiu and Park (1994) review several different methods for comparing TFNs. First, Chang's method calculates the "mathematical expectation" of a TFN with form [a b c] as:

$$\text{mathematical expectation} = (c-a)(a+b+c)/6 \qquad (1\text{-}1)$$

Kaufman and Gupta have suggested three different methods. These include comparing the mode of each TFN (the 'b' parameter), comparing the range of each TFN (c-a), and comparing the following ranking parameter:

$$\text{ranking parameter} = (a+2b+c)/4 \qquad (1\text{-}2)$$

Clearly, comparing the mode of each TFN amounts to simply comparing the central case results of each set. Next, Jain's method involves calculating a "maximizing set" parameter. This is done by connecting the point with the largest possible value with a membership degree of 1, with the point with smallest possible value with a degree of membership 0, and then determining the intersection with the right representation of each TFN. Jain's method has been criticized for only considering the right representation of each TFN, and for therefore only reflecting the optimistic or pessimistic side of each variable (Abdel-Kader, et al., 1998). More complex variations of Jain's method have been devised, that consider both the right and left representations of each TFN, but these are difficult to employ in practice. Figure 1-6 depicts Jain's method in graphical form.

Figure 1-6:

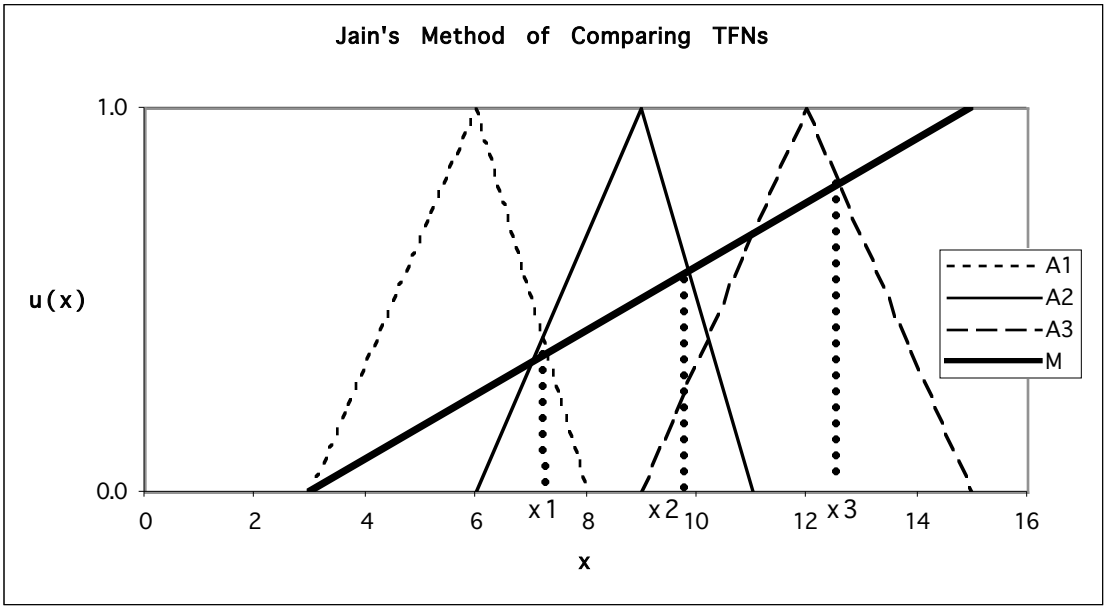

Finally, MATLAB's "defuzz" command allows the user to specify different procedures for collapsing fuzzy sets into "crisp" numbers so that they can be compared with other fuzzy sets that have been defuzzified in the same way. Built-in procedures include the "centroid" method and the "bisector" method. Additional methods can be defined by the user and called in with the "defuzz" command.

These different methods for ranking the relative dominance of TFNs often produce consistent results, although in some cases where TFNs are very close together some switching in rankings can occur with different methods (Chiu and Park, 1994). For this reason, it is preferable to use more than one method when comparing TFNs. The comparisons performed here (in Chapter 7) use Chang's method, comparison of the TFN modes, Kaufman and Gupta's ranking parameter, and MATLAB's "defuzz" command using the centroid and bisector methods.

Uncertainty Bands for Fuzzy Sets

In addition to the ranking of fuzzy sets using defuzzification techniques, it is also useful to have a measure to compare the range of variation of fuzzy sets. In this way, the relative level of uncertainty in each distribution can be assessed. Just as probability distributions can be evaluated with confidence intervals that define certain percentages of the distribution that fall within a given range, such as 95%, so too can uncertainty bands be defined for fuzzy sets. In principle, the uncertainty band for a fuzzy set can be defined at any given member ship function, or $\mu(x)$, value. For example, the uncertainty band could be defined as where $\mu(x)$ is equal to 0.5, 0.1, 0.05, or 0. For purposes of this analysis, and for the TFNs used here, the fuzzy set uncertainty band is defined as where $\mu(x)$ is equal to 0. The corresponding "x" values where $\mu(x)$ is equal to 0 are thus the "low" and "high" case values, below and above which values of "x" are considered to be unlikely, and the spread between the low and high values is

defined as the uncertainty band. Where $\mu(x)$ is equal to 1.0, the corresponding "x" value is most likely to be the actual value of "x"; this "x" value is thus the "central case" value.[9]

The calculation of uncertainty bands is useful in that it can show both in an absolute and relative sense the overall level of uncertainty that has been captured in an analysis. Depending on the degree of uncertainty in the results, and the degree to which the ranges of the different alternative overlap, it may or may not be possible to make unequivocal rankings of the results. In the case of the analysis conducted here, it is expected that the overall level of uncertainty will be considerable, due to the number of uncertain variables included and the relatively high level of uncertainty in several of them. It may thus not be possible to unequivocally rank the various ZEV scenarios in terms of the net present values of the total scenario costs over the period assessed here. However, depending on the degree to which the various defuzzification techniques produce consistent ranking results, less robust "likely" (but not unequivocal) conclusions may be possible. Furthermore, somewhat more specific conclusions with regard to the vehicle level cost results may prove to be more definitive if, for example, the relative level of uncertainty in the vehicle levels results is relatively low at certain points in time. In Chapter 7, the concept of the fuzzy set uncertainty band is discussed further, and both absolute and relative uncertainty bands are calculated for the high production volume, full scenario case results.

The Dynamics of Technology Manufacturing Costs

Every new technology progresses through a series of developmental stages, and for most successful mass-marketed technologies this progression culminates in automated, high-volume manufacture. Based largely on the work of William Abernathy and James Utterback, a picture of technological evolution has emerged within which new technologies move from a "fluid" phase to a "specific" phase (Utterback, 1994). The fluid phase is characterized by a focus on product innovation and the lack of a clear "dominant design" for the technology. Once a dominant design is established, the specific phase emerges and there is a "shakeout" of the market as competition shifts from a focus on product innovation to a focus on process innovation and lowering of production costs.

Neoclassical economics, while cognizant of the importance of technological progress in lowering production costs, bases production cost models on the concept of the short and long-run average cost curves (SRAC and LRAC). In their basic form, these curves assume a constant state of technology, and therefore that factor prices change only in response to changes in annual production volumes. The LRAC is typically depicted in a "U" shape, suggesting that costs rise with high levels of output, even in the long-term, although most would argue that firms would never choose to operate in this region. The generally "static" nature of the economic concept of the SRAC and LRAC is not particularly well suited to address the dynamics of emerging technologies. These technologies are often characterized by rapid progress in production process

[9] Trapezoidal fuzzy numbers, with a range of "x" values with membership function levels of $\mu(x) = 1.0$, can be used when a range of values (rather than a single value) is believed to have the highest likelihood.

automation, improved efficiency in any remaining manufacturing labor components, and traditional scale economies.

An alternative paradigm of understanding technology production costs traces its roots back to 1936, when T.P. Wright discovered a relationship between the labor hours needed to manufacture an airframe and the total number of airframes built. Wright found that each time the total quantity of airframes produced doubled, the labor hours required to assemble the airframe decreased by a stable percentage (Wright, 1936). Since this early work, thousands of studies have been conducted on the nature and variability of learning curves in industries as diverse as electric power, microchips, Japanese beer, airframes, and automobiles (Argote and Epple, 1990; Boston Consulting Group, 1972; Dino, 1985; Ghemawat, 1985; Yelle, 1983). These studies have allowed the concept of the learning curve, which initially considered only improvements in the labor component of production, to be extended to help explain the dynamics of overall production costs as technologies move from low-volume, prototype production, to "learned-out" mass production. These overall cost curves have come to be known as "manufacturing experience curves," or less commonly, "manufacturing progress functions."

Thus, in contrast with Wright's learning curves, experience curves capture more than just the labor component of the manufacturing cost reduction process. The experience curve describes the cost path of a manufactured product, beginning with the first and continuing to the 'nth' unit produced. While learning curves describe only improvements in the efficiency of the labor component of total manufacturing cost, the experience curve applies to reductions in cost of the entire value added by a company (i.e., all costs other than materials costs). Cost reductions are due to four primary factors: scale economies, technological improvements in production processes, improvements in product design (i.e. reduced parts counts and design for manufacturability), and improved production worker and organizational efficiency. In essence, the progress of a firm or industry along an experience curve for a new technology represents the steady decline in its inflation-corrected unit cost of manufacture.

While many different functional forms for the experience curve are possible and have been investigated, the most commonly used expression is the simple log-linear form shown in Equation 1-3.

$$C_N = C_1 * V_N^{(\log\partial / \log 2)} \qquad (1\text{-}3)$$

Where:
C_N = Cost of manufacturing nth unit
C_1 = Cost of manufacturing 1st unit
V_N = Cumulative production at nth unit
∂ = Experience curve slope

This relationship predicts that the constant dollar cost of adding value to a product falls by a fixed percentage with each doubling of accumulated manufacturing experience. For example, an 80% experience curve predicts that the constant dollar cost of a product will fall by 20% with each doubling of cumulative production volume. Hence, cost reductions are relatively dramatic

during the early stages of manufacture, as scale economies are captured and the production process is perfected, and then drop off as doublings in volume take longer to achieve.

Experience curve analyses are often applied retrospectively, or *ex post*. One classic example is in the early history of the automobile industry. Figure 1-7 depicts the decline in the price of the Model-T Ford from 1909 to 1923. During this period, the price fell from over $3,000 (in $1958) to under $1,000 (Abernathy and Wayne, 1974). Note that the same data plotted on a log-log scale in Figure 1-8 shows a good fit to the straight line of a log-linear experience curve with an 85% slope.

Figure 1-7: Price Path of Model-T Ford (1909-1923) with Standard Scale

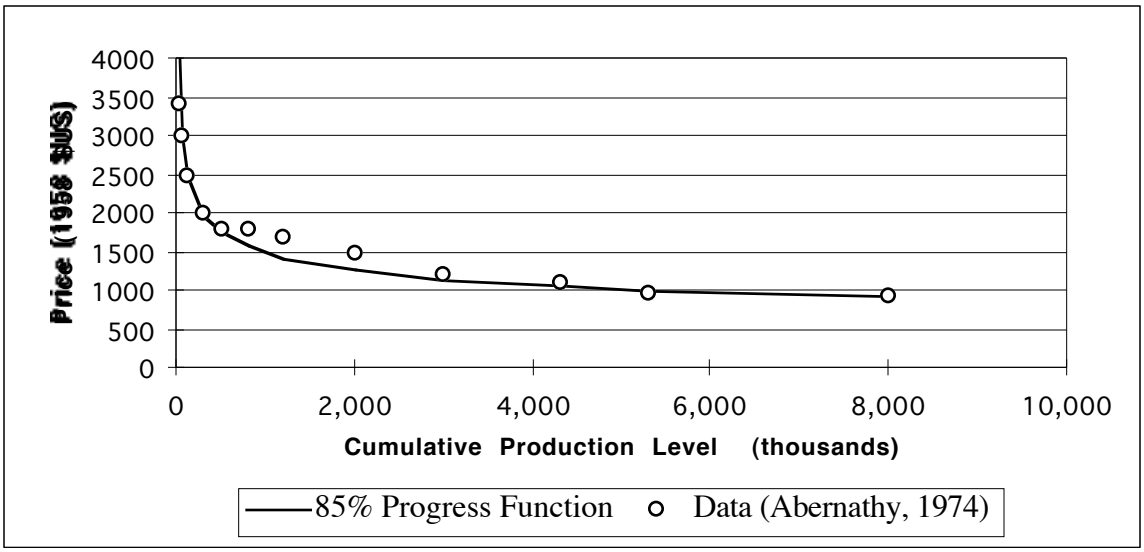

Source: (Abernathy and Wayne, 1974)

Figure 1-8: Price Path of Model-T Ford (1909-1923) with Log-Log Scale

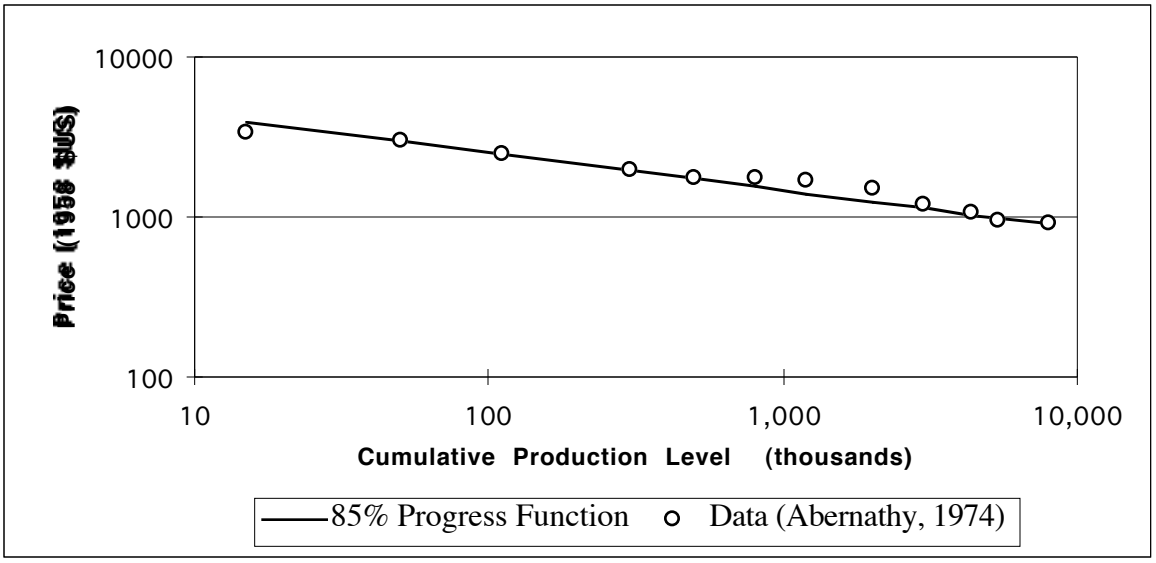

Source: (Abernathy and Wayne, 1974)

Since a landmark study by the Boston Consulting Group in 1972 that examined the evolution in unit costs of about 2,000 different products (Boston Consulting Group, 1972), many additional experience curve studies have been conducted. These studies have shown that the typical rate of unit cost reduction is very often in the range of 10% to 30% with each doubling of cumulative production experience, with rates of around 20% commonly observed (Dutton and Thomas, 1984; Ghemawat, 1985). This clustering of experience curve slopes has led to the common assumption of an 80% curve, for strategic technology forecasting purposes.

Thus, the manufacturing experience curve is an alternative method for analyzing and forecasting technology costs. It has proven to be a powerful technique, but a significant disadvantage is that when used for forecasting there is inevitably considerable uncertainty about the curve slope that should be assumed. The difference between a curve slope of 70% and one of 90% becomes great over a long forecast, and when a family of curves of different slopes are plotted in order to show different potential outcomes, the results can encompass a wide range of potential costs.

For this reason, the approach used in the EV technology component assessments conducted here is to first attempt to obtain manufacturer cost data that are expressed as a function of annual production, if possible. As mentioned above, this can be difficult because such data are proprietary, but most companies tend to analyze production costs in terms of annual production volume (i.e., with average cost curves), rather than in terms of accumulated production with experience curves. Thus, to the extent that data can be obtained from manufacturers, they tend to be in the prior form. If such data cannot be obtained, or cannot be accepted with confidence even if obtained, an alternative approach is to develop an original, annual production-based manufacturing cost analysis. This is very difficult to do because of the high quantity of data needed, and the noted difficulties in obtaining such data, but once accomplished it offers the advantages of documentability and the ability to explicitly forecast costs with improvements in any component of the cost forecast. With an original, detailed analysis, reductions in materials costs over time, improved materials utilization rates, changes in product design, and so on, can all be explicitly assessed. Finally, when neither of these approaches is practical, an experience curve analysis can be employed. As noted, this method entails considerable uncertainty, but because of the amount of historical data available to justify the basic pattern of cost reduction described by experience curves, it is a defensible and powerful method when more detailed analysis cannot be obtained or independently conducted.

For the primary technologies assessed in detail here, manufacturing cost data were obtained for electric vehicle motors and controllers, and a range of cost functions were developed as a function of production volumes and component sizes. Because of the importance of battery manufacturing costs to the BEV analysis (and to a lesser degree to the FCV analyses), an original, detailed analysis of nickel-metal hydride (NiMH) batteries was conducted. This was not done because no manufacturer cost data could be obtained; in fact, cost data were obtained from both Ovonic Battery Company and from Panasonic EV Energy. However, these data may not be reliable because of the established cost goals for EV battery technology, and the resulting propensity of manufacturers to forecast meeting those goals. A detailed analysis also allowed costs to be

forecast for future generations of the technology, based on improvements that currently are being demonstrated in laboratories. Finally, an experience curve analysis was used for proton-exchange membrane (PEM) fuel cell systems because of the extreme difficulty in obtaining either overall cost forecasts or the necessary data to conduct a detailed original analysis of this highly strategic, emerging set of technologies.[10]

Cost Categories Assessed

In principle, it would be useful to conduct a complete social cost analysis of producing and using these three types of EVs, and to compare the results to the social costs of producing and using conventional vehicles. In addition to the vehicle manufacturing and operating costs, infrastructure support costs, and emission-related costs from vehicle operation assessed in this analysis, one might also include: social costs associated with emissions from vehicle manufacture; social costs associated with changes in energy flows (i.e., the net value of petroleum import reductions); potential social costs associated with relative safety issues among the vehicle types; social costs associated with vehicle noise; and so on. The decision of which categories to include -- where to draw the boundaries around the system -- is difficult because of the many possible categories that could in theory be included. Even where data and tools are lacking to place dollar values on potential impacts, they can be assessed qualitatively and considered in the overall analysis though perhaps not aggregated into a single, final measure. The issue of what impacts to consider in a social cost analysis or BCA is an important one, and one that some analysts have suggested has been under-emphasized. For example, Socolow (1976) writes:

> [D]iscussions of the limitations of cost-benefit analysis nearly always emphasize uncertainties about the discount rate and contain caveats about the lack of sensitivity regarding who gets what. Only rarely do they call attention to the problem of drawing a boundary around the system being studied. As in idealized thermodynamics, the cost-benefit theory presupposes a system coupled with its surrounding in such a simple way that one can change the system without perceptibly affecting the surroundings. To do a sensible cost-benefit comparison of two alternative futures, one has to include in the "system" all the activities with which are associated large differences depending on which future is being considered.

A more complete social cost analysis would thus consider all of the categories of impacts that could possibly be sources of differences between the various EV types, and between EVs and conventional ICEVs. One complication, however, is that ICEV technology is also continuing to evolve. In order to properly conduct a complete social cost analysis that extends into the future, the analysis would have to assess likely changes in conventional vehicle technology

[10] As discussed in Chapter 3, one detailed analysis of PEM fuel cell manufacturing costs is available, but only for very high volume production.

in the baseline case, as well as forecasting all of the various cost components associated with the alternative cases. This type of effort, while certainly possible, would be beyond the scale of a dissertation project.

Thus, given the difficulties associated with forecasting the wide array of costs that would have to be assessed in a complete social cost analysis, this analysis focuses on the major cost categories that are likely to be sources of significant differences among the three ZEV types. The corresponding costs of current ICEV technology are examined as a reference for comparison, but the focus is on potential cost differences between the ZEV types. Hence, a complete social cost analysis of alternative future scenarios, including an ICEV baseline case, is not attempted here. It should be noted, however, that the structure of the MATLAB/Simulink model that has been developed to compute fleet-level costs is modular in nature. Thus, it will be possible to continue to develop it and to add modules to assess additional social cost categories. These may be added in future efforts when more is known about the relative performance of different ZEV types along various other dimensions. The considerable body of research on the potential social costs associated with additional categories of motor vehicle impacts will be useful in this regard. Such studies include those on costs associated with petroleum import reductions (Delucchi and Murphy, 1996; Leiby, 1997), fuel and vehicle safety (Swain, et al., 1998), vehicle noise and noise-related external costs (Delucchi and Hsu, 1996; MacDowall, 1990), and vehicle manufacturing emissions (U.S. DOE, 1998b).

Models, Scales, and Timeframe

This analysis combines the use of a vehicle-level manufacturing and lifecycle cost spreadsheet model with a fleet-level cost model. The vehicle-level model is a Lotus 1-2-3 spreadsheet model that computes vehicle manufacturing and operating costs and includes a detailed vehicle performance and energy use analysis (Delucchi, 1999). One advantage of using this model is that it includes many circular calculations that capture feedback effects with regard to component and vehicle weight and performance. For example, if battery technology improves such that a lighter battery pack can provide the same amount of energy, then the mass of the vehicle decreases. The calculated decrease in vehicle mass is slightly higher than the decrease in battery pack mass, because less vehicle body support structure is needed as well. The lighter vehicle then requires a slightly less powerful drivetrain to provide an equivalent level of performance, which also weighs less and further lightens the vehicle. The model calculates these component and vehicle mass changes iteratively, and converges on a solution after several iterations. It is thus capable of capturing vehicle mass compounding and decompounding effects, which may be important to lowering BEV and FCV costs as battery specific energy and fuel cell system specific power levels increase with technological improvements over time.

The fleet model is a MATLAB/Simulink model that computes overall fleet costs in each analysis year, along with additional infrastructure support costs, and criteria pollutant and GHG emissions and emission-related costs. The model has a vector dimension that allows a string of input variables to be entered and subsequent calculations to be performed simultaneously. Variables can be entered as three-element, triangular fuzzy-set distributions, or as four-element trapezoidal fuzzy-set distributions. The model then performs computations

based on the rules of the fuzzy set extension principle, thereby propagating uncertainty through the model.

The analysis thus encompasses three scales: a component scale in which cost functions for individual vehicle components are developed; a vehicle-level scale in which costs of purchasing and operating vehicles are computed; and a fleet scale in which overall costs of ownership and operation of multiple vehicles, infrastructure costs, and regional emission-related costs are computed. Figure 1-9 shows how cost functions and models are employed at each of these scales.

Figure 1-9: Analysis Scales and Models

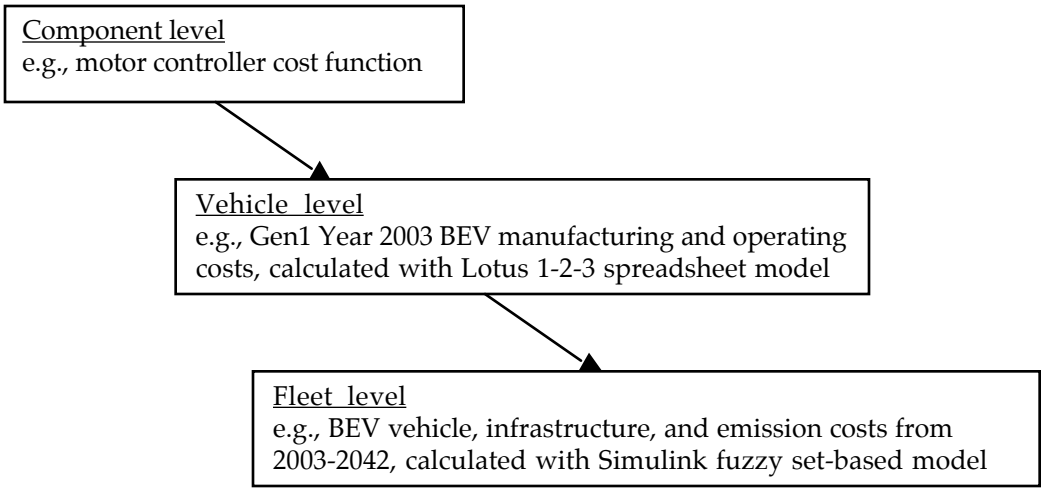

With regard to the timeframe chosen for the analysis, it is important to note that it is of course impossible to forecast technological evolution beyond a few years with any certainty. However, a fleet level analysis must consider a long enough timeframe to allow new vehicle types to penetrate the motor vehicle fleet in significant numbers. The motor vehicle stock turns over more rapidly than, for example, facilities for generating electricity or heating and cooling buildings. However, it still takes many years for new vehicle technologies to build market share, reach high volumes of production, and work their way into composing a substantial portion of the overall vehicle stock. It is thus important to consider a reasonably long timeframe when analyzing new motor vehicle technologies; otherwise, it is simply not possible for significant impacts to be realized. For this analysis, a relatively moderate timeframe of vehicle introduction is examined, from 2003-2026. Some analyses have gone further, examining AFV introduction through 2050 (e.g. Berry, 1996), but the limits of an analysis based on projections from present-day knowledge arguably are reached within the scope of such a long timeframe. For this reason, a more moderate timeframe is chosen for this analysis, although vehicle-operating costs are computed through year 2043.[11] Figure 1-10 presents additional analysis

[11] Vehicles that are introduced in 2026 are in use for up to 18 years under the vehicle lifetime estimates for BEVs and FCVs, although average annual mileage declines every year due to reduced vehicle use and attrition from accidents and vehicle retirement.

details, and shows the overall structure of the major components of the analysis effort. Note that only the MATLAB/Simulink model uses fuzzy sets as input variables and performs calculations using the fuzzy set extension principle. In order to determine the relative high, central, and low case vehicle level results with the Lotus 1-2-3 model, separate runs of the model are conducted with sets of low, central, and high case input variables in order to arrive at ranges of vehicle retail prices and levelized, lifecycle cost values. These ranges of levelized lifecycle cost values can then be input into the Simulink fleet-level model as three-element vectors that describe triangular fuzzy sets. This procedure is required because it is not possible to input variables as fuzzy sets into the Lotus 1-2-3 model, due to its structure, and as a result the low, central, and high cases have to be run independently in order to obtain ranges of vehicle-level results.

Figure 1-10: Analysis Flow Chart

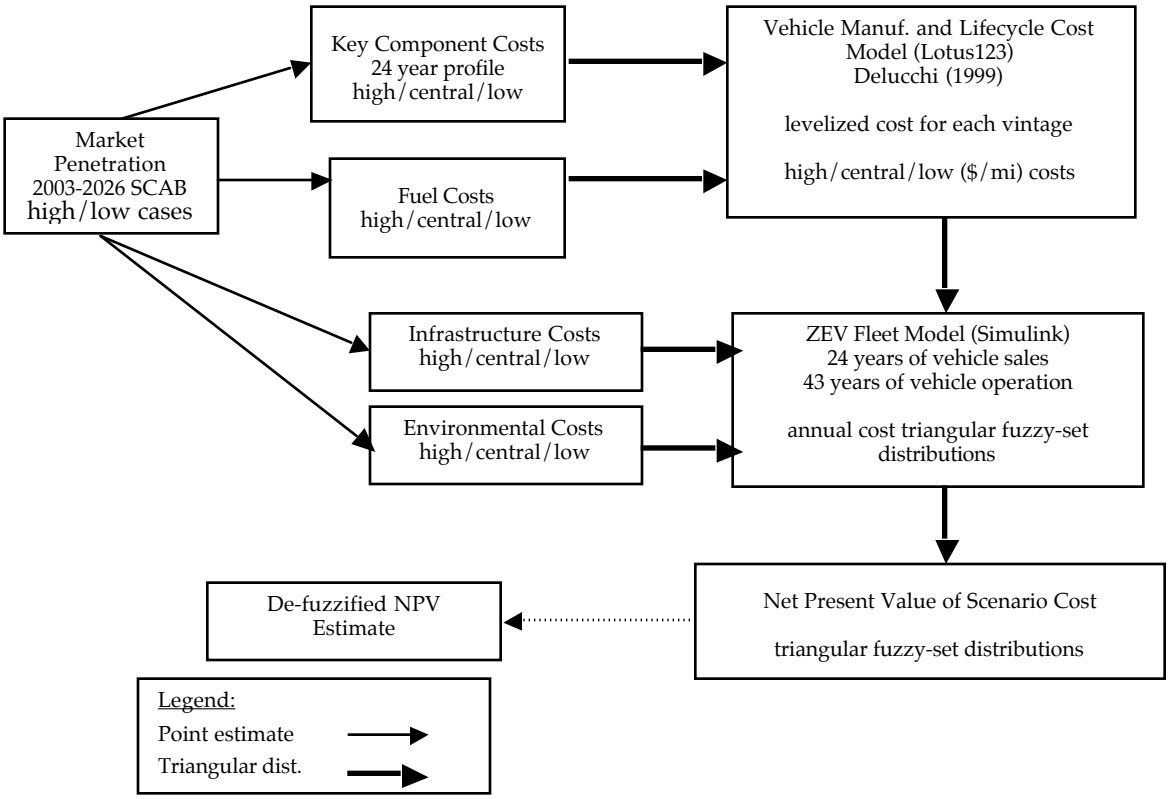

Hypothesis Tests

BEVs and FCVs are unlikely to appeal to consumers unless their purchase prices rival those of similar conventional vehicles. Government subsidies can help to offset near-term price differences, and automakers can absorb some losses initially, but these subsidies cannot be sustained indefinitely. However, it may be the case that the manufacturing costs of various types of EVs will exceed those of conventional vehicles even if high volumes of EV production are achieved. However, since EVs have relatively low fuel cycle emissions, total vehicle plus emission-related costs could in theory be lower for EVs than for conventional

vehicles, even if vehicle costs themselves are higher. Also, even if vehicle costs are higher, EV lifecycle costs could be comparable to lifecycle costs of conventional vehicles due to lower fuel and maintenance costs. Finally, DMFCVs might be more attractive from both a first cost and lifecycle cost perspective than either BEVs or DHFCVs because they require neither large battery packs nor compressed gas storage systems.

With regard to these notions, the following hypotheses are proposed:

Hypothesis 1:

H_1: Lifecycle costs for BEVs are always lower than lifecycle costs for DHFCVs and DMFCVs, under comparable production volume assumptions.

H_{1a}: Lifecycle costs for DHFCVs and/or DMFCVs in some cases drop below those of BEVs, under comparable production volume assumptions.

Hypothesis 2:

H_2: Under the high production volume scenarios, the purchase prices of BEVs, DHFCVs, and DMFCVs exceed those of comparable conventional vehicles in all cases.

H_{2a}: Under the high production volume scenarios, the purchase prices of BEVs, DHFCVs, and/or DMFCVs drop below those of comparable conventional vehicles in at least the low cost case.

Hypothesis 3:

H_3: In 2026, DMFCVs have higher initial prices and/or lifecycle costs than DHFCVs or BEVs.

H_{3a}: In 2026, DMFCVs have lower initial prices and lifecycle costs than DHFCVs and BEVs.

Hypothesis 4:

H_4: The net present value of vehicle, emissions, and infrastructure costs, over the time period 2003-2043, is lower for BEVs than for DHFCVs and DMFCVs.

H_{4a}: The net present value of vehicle, emissions, and infrastructure costs, over the time period 2003-2043, is lower for DHFCVs and/or DMFCVs than for BEVs.

The four hypotheses listed above can be either accepted or rejected based on the fleetwide purchase prices and lifecycle costs estimated in Chapters 2 through 4, along with the overall scenario vehicle, infrastructure, and emissions costs estimated in Chapters 2 through 6. The conclusions with regard to these hypotheses are presented in Chapter 7.

This page left intentionally blank

Chapter 2:
Manufacturing and Lifecycle Costs of Battery Electric Vehicles

Introduction

Due to the dual motivations of ZEV sales requirements in the U.S. and the desire to be perceived as "environmentally responsible" corporations, all of the world's major automakers are currently developing battery-powered EVs (BEVs), if not already producing them in pilot-scale. The most technologically advanced production BEV is General Motors' EV-1, which was entirely designed and optimized as a BEV. Made of lightweight materials, including an aluminum spaceframe covered with composite body panels, it is being produced in a state-of-the-art 100,000 square foot facility in Lansing, Michigan.

The EV-1 vehicle design and production facility are rife with innovations, with 23 patents awarded for vehicle designs alone (General Motors, 1996a). Novel developments include numerous electric drive system breakthroughs, an entirely redesigned heating, ventilating, and air conditioning (HVAC) system, a new electric power steering system, and a new braking system (General Motors, 1996a). The production of the vehicle involved the first-ever use of epoxy draw dies, instead of iron or steel, for a production vehicle (General Motors, 1996a). The use of such dies allowed die construction to be completed in 20 weeks versus the usual 38 to 45 weeks for metal dies (and at a fraction of the cost). This helped engineers meet a concept-to-production schedule of only nine months versus 2-3 years for a typical new vehicle launch (General Motors, 1996b).

Other BEVs currently in production by major manufacturers include the GM S-10 pickup, the Honda EV-Plus, the Nissan Altra, the Toyota RAV4, the Ford Ranger EV, and the Chrysler EPIC minivan (CARB, 1998a). In addition to these, other full-sized and small BEVs are also being developed or produced by major and minor automakers. These include vehicles produced by Renault and Peugeot, the Solectria Corporation conversion vehicles, and small "neighborhood" BEVs that include the Toyota Ecom, the Kewet El-Jet, and the Pivco Industries CityBee (Figenbaum, 1998). Interestingly, in early 1999 Ford purchased a majority stake in Pivco, which recently redesigned the CityBee into the two-seat, 2,050 pound "Th!nk" vehicle. Ford and Pivco plan to produce 5,000 Th!nk vehicles a year using a flexible manufacturing process facility, initially for sale in Scandinavia but scheduled for introduction in the U.S. in 2001 (Perry, 1999).

Most fundamentally, BEVs differ from conventional vehicles in that they use electrical energy stored in a battery pack to power an electric motor, rather than burning gasoline to power a combustion engine. They also may incorporate lightweight materials and be designed with low aerodynamic drag profiles in order to reduce the "road load," thereby reducing the size of the battery pack needed to provide a given driving range. BEVs are more efficient than conventional vehicles, when only the efficiency of the vehicle is considered, because electric motors are much more efficient than gasoline engines, many of the auxiliary systems needed for ICE vehicles can be eliminated or downsized, and electric drivelines eliminate much of the energy wasted by ICE vehicles

during idling and braking. ICE vehicle idling and braking losses amount to 10.8% of the energy used, by one estimate (OTA, 1995). Electric motor/controller systems tend to have efficiencies on the order of about 80% over city driving cycles, while gasoline engines have corresponding efficiencies of only 20-23% (OTA, 1995). However, when the complete fuel cycle is considered, including the efficiency of generating and distributing electricity and producing gasoline, BEVs and conventional vehicles have about the same primary energy efficiency (OTA, 1995).

Differences in the manufacturing costs of BEVs and conventional vehicles will to a large extent be driven by the costs of two key BEV subcomponents: the electrochemical battery pack, and the electric motor controller. EV motors themselves are lower in cost than battery packs or motor controllers, and thus tend to be less important cost drivers. However, different types of motors, such as alternating current (AC) induction, brushless permanent magnet (BPM), and switched reluctance, are characterized by different costs. At present, AC induction and BPM motors appear to be the leading candidates for use in EVs. BPM EV motors offer lighter weights and higher peak efficiencies than AC induction motors, but they are relatively new products that currently are produced in small, custom order lots by companies such as Unique Mobility, Inc., at relatively high cost. AC induction motors are produced in much higher volumes at present, by companies such as Baldor Electric, and the basic motor cores are modified with additional components (e.g., cooling jackets, encoders, wiring harnesses, etc.) for specific applications.

EV motor controllers for both motor types, on the other hand, consisting of a high power DC-AC inverter and a low power control section, are very costly at present. The inverter section designs used by most manufacturers incorporate insulated-gate bipolar transistor (IGBT) switching devices, and the cost of the IGBTs needed to control a typical size AC induction or BPM motor is on the order of $300-500. Concerted efforts are underway to decrease the present high costs of EV motor controllers, through controller design changes and cost reductions in key subcomponents.

Most important, BEV battery pack capital costs are crucial contributors to overall BEV manufacturing, lifecycle, and social costs. Advanced lead-acid batteries provide limited driving ranges of only about 60-70 miles, even in the highly efficient GM EV-1, and more exotic battery types are needed for longer driving ranges. These more advanced batteries, such as NiMH and lithium-ion (Li-ion), are currently produced in pilot scale quantities at costs in excess of $1,000 per kilowatt hour (kWh). Furthermore, such batteries may not last the lifetime of the vehicle, and battery capital costs may thus enter two or more times into calculations of the overall lifecycle costs of BEVs.

Finally, costs associated with support infrastructure and powerplant emissions of criteria pollutants and greenhouse gases contribute to the overall social costs of BEV production and use. These cost categories are discussed in a later chapter. Additional social costs associated with pollution from manufacturing batteries and other BEV components, with air toxic emissions from powerplants and fuel combustion, and with other social cost categories such as vehicle noise and oil import-related externalities, may be sources of significant social cost differences between BEVs and conventional vehicles. These

potential costs are not addressed in the scenario analyses conducted here, but they may be included in future revisions.

Market Penetration Assumptions

First, it is necessary to outline some basic elements of the scenarios considered, including assumptions regarding the future market penetration of BEVs and FCVs. Some attempts have been made to forecast BEV ownership and use (for example Golob, et al., 1996), but there is significant uncertainty regarding the level of consumer acceptance that new vehicle types will encounter. For BEVs, the unfamiliar vehicle attributes of limited driving range and long refueling time may severely restrict the market. The limited introduction of BEVs to date has not been especially successful, with only a few thousand total vehicles leased in California in 1997 and 1998. The GM EV-1 proved to be the most attractive to consumers and fleet operators, with 600 vehicles leased, while leases of Toyota RAV4s, Ford Rangers, GM S10 pickups, Honda EV Pluses, and Nissan Altras lagged behind with leases of 507, 500, 400, 300, and 30 vehicles, respectively (Kasler, 1999). However, some ultimately successful technologies initially met with limited consumer acceptance, and it is possible that BEVs will fall into this category. For example, in the first year of introduction, 1953, only 50 microwave ovens were sold (Purcell, 1998a).

Since the introduction of ZEVs in California, Massachusetts, and New York is governed by ZEV mandate requirements, the number of ZEVs that will be delivered for sale by major manufacturers starting in 2003 can be approximated. However, changes in the California ZEV mandate in November of 1998, provided automakers considerable flexibility in how they meet their ZEV mandate sales requirements. Now, a portion of the 10% EV sales mandate can be composed of "near ZEV" technology vehicles that meet certain criteria established by CARB. Vehicles that certify to super ultra low-emission vehicle (SULEV) standards, have "zero" evaporative emissions,[12] certify to meet on-board diagnostic requirements at 150,000 miles, and that have a performance and defects warranty period of 15 years or 150,000 miles, could qualify toward meeting a manufacturer's 10% ZEV sales requirement (CARB, 1998b). Such vehicles could earn varying fractions of a ZEV credit, known as a "partial ZEV credit" depending on the all-electric range that they offer, the "advanced ZEV componentry" that they incorporate, and their estimated fuel-cycle emissions of non-methane organic gases (NMOG).

Under these rules, it is possible that vehicles with no EV componentry could qualify for some partial ZEV credit, but only hybrid EVs would be able to generate more than 0.4 ZEV credits. Importantly, however, for major manufacturers (i.e., the "Big 7" that include General Motors, Ford, Daimler-Chrysler, Toyota, Honda, Nissan, and Mazda) only 60% of the 10% sales requirement, or 6% of a manufacturer's total sales, can be made up of partial ZEV credits. Only "pure ZEV" technology vehicles, with no tailpipe emissions, can be used to generate the remaining 4% of the credits. Assuming that the delivered vehicles are sold, the 4% estimate represents a lower bound on the number of ZEVs that will enter the vehicle fleets in the ZEV states. One final complication, however, is that the new ZEV mandate rules allow more than one

[12] CARB is currently determining the standards for "zero" evaporative emissions.

ZEV credit to be awarded to ZEVs sold prior to 2007 with driving ranges of over 100 miles. From 2003 to 2005, vehicles will receive 2-4 ZEV credits for driving ranges of 100-175 miles (with credits determined by linear interpolation within this range), and from 2006 to 2007 vehicles can receive 1-2 credits (CARB, 1998b).

Given these requirements, one scenario for production and use of ZEVs can be established under the assumption that manufacturers only produce ZEVs for the ZEV requirements in the U.S., and that they minimize the number of ZEVs that they need to produce under the current rules. CARB has estimated the number of vehicles that each major manufacturer would have to produce under these assumptions, and the additional assumption that the ZEVs have a driving range of 100 miles (Evashenk, 1999). These estimates, shown in Table 2-1, apply 1998 sales shares to an estimated total production of one million passenger cars and light trucks for these manufacturers in 2003-2006.

For purposes of this analysis, I assume production from a major manufacturer that holds 25% of the market in the ZEV states, although the size of the manufacturer can be easily varied. This 25% share compares with California market shares of 31% for GM, 20% for Ford, and 21% for Toyota, in 1998 (Evashenk, 1999). Since manufacturers would need to also produce vehicles for the Massachusetts and New York markets, the total number of ZEVs produced by each manufacturer would be approximately double what would be needed for the California market alone. Also, the total number of vehicles produced may increase slowly with increases in vehicle sales due to population growth.

Two basic ZEV production scenarios are considered in this analysis:

- a "low production scenario" that assumes only production for the U.S. market, conservative ZEV mandate compliance production levels, and no "take-off" in ZEV popularity; and

- a "high production scenario" that assumes production for a global market and steady, logistic (i.e., "S-shaped") growth in ZEV demand.

The parameters for the high production scenario are based on public market plans that have been announced by Toyota and DaimlerChrysler in the context of fuel cell vehicle introduction (Kalhammer, et al., 1998). This high production scenario is unlikely for the BEV case, given the market barriers currently confronting these vehicles, but is included for purposes of comparison with the fuel cell vehicle scenarios in the following chapters.[13]

The low production volume scenario assumes that two million vehicles are sold in California, New York, and Massachusetts in 2003, 2004, 2005, and 2006, and that ZEV production by a single major manufacturer is equal to 0.5% of this amount (10,000 vehicles) in 2003, 2004, and 2005, and 1% of this amount

---

[13] However, some analysts are relatively optimistic about future BEV sales. In its *Annual Energy Outlook 1999*, the EIA (1998) is forecasting U.S. sales of 299,000 BEVs by 2020. For a manufacturer with 25% of the market selling as many vehicles overseas as domestically, this would suggest an approximate production level of 150,000 vehicles per year, compared with the high production volume estimate of 186,000 BEVs per year here.

(20,000 vehicles) in 2006. The ZEV production estimates reflect the assumptions of 25% market share by a major manufacturer, that 2% of vehicles sold in 2003-2005 are ZEVs, since each ZEV gets 2 ZEV credits, and that 4% of the vehicles sold in 2006 are ZEVs. From 2007 to 2026, production is assumed to increase at a relatively slow rate of 5% per year above 2006 levels. Total ZEV production and the number of vehicles sold in the SCAB for this scenario, assuming that 40% of California sales are in the SCAB, are shown in Figure 2-1.

Figure 2-1:

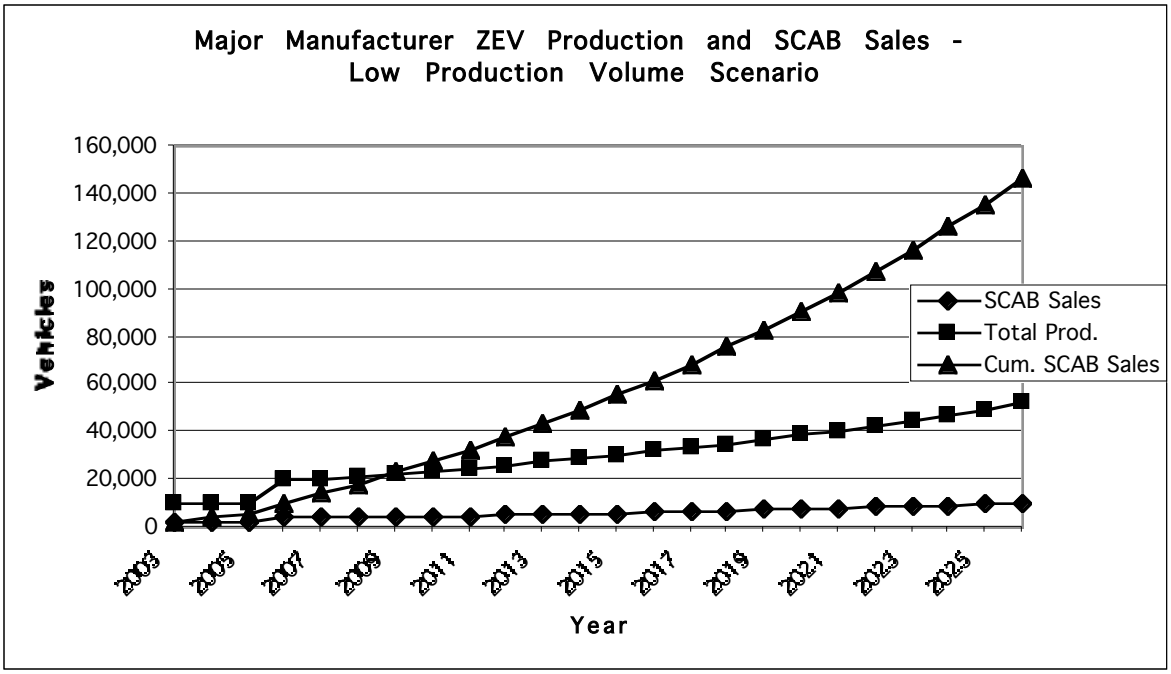

The high production volume scenario considers a global market for ZEVs, given the interest in ZEV technology in Europe and Japan. ZEV production and sales are assumed to follow a 50-year, S-shaped market penetration curve, with a slow start followed by a relatively rapid take-off and then a saturation phase. This pattern has been observed in many technological settings (Ray, 1989; Young, 1993). The production figures for this scenario were generated with a logistic growth function that was calibrated with ZEV production estimates that have been publicly stated by the Fuel Cell Alliance (consisting of DaimlerChrysler, Ford, and Ballard Power Systems), GM, and Toyota in the context of fuel cell vehicle introduction. The Fuel Cell Alliance has identified a potential projection schedule of 40,000 automotive fuel cell systems per year in 2004, and 100,000 systems per year by 2006[14] (Kalhammer, et al., 1998). GM and Toyota have announced that they will match these production goals, and Toyota has recently declared that it will be the first FCV manufacturer to market a mass-produced FCV, beginning in 2003 (Sacramento Bee, 1999).

[14] A final go/no-go decision on investment of >$1 billion to support these goals is expected late in 1999.

The logistic growth function is set to reach a global maximum of 600,000 ZEVs produced per year after 50 years, with an inflection point at 25 years. In order to match the initial production figures mentioned above, production for the global market is set at 20,000 vehicles in 2003 and 40,000 vehicles in 2004. Then, the logistic growth function is adopted for years 2005-2026 (yielding production of about 55,000 vehicles in 2005, 60,000 in 2006, and reaching about 270,000 vehicles in 2026).[15] The global market is assumed to be double the U.S. market, and the U.S. market, as above, is double the California market. Sales of ZEVs in California are thus about one-quarter of total global ZEV production (and sales in the SCAB are 40% of the California total and 10% of the global total). ZEV production and SCAB sales associated with this scenario are shown in Figure 2-2.

Figure 2-2:

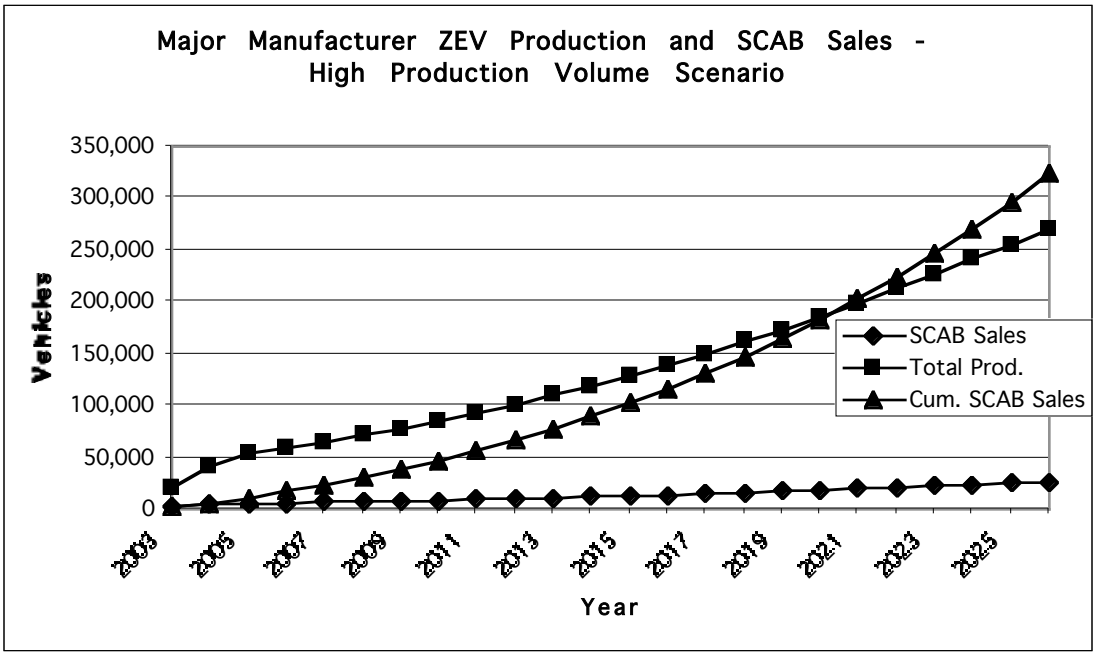

BEV Modeling Issues and Methods

Modeling the cost and performance of any vehicle type involves sizing drivetrain components to meet pre-established performance criteria. The selection of

---

[15] This production level is comparable to current production of the most popular models by single manufacturers. In 1998 North American production, Ford produced 406,937 Taurus vehicles, and Honda produced 432,096 Accord vehicles. In addition to the Taurus, Ford also produced 132,409 Contours, 148,984 Mustangs, and 194,095 Escorts (Automotive News, 1998). In principle, the Taurus, Contour, and Mustang could use essentially the same fuel cell driveline, and one supplier could also supply more than one automotive OEM. Thus, even the high production volume case levels assumed here are potentially somewhat conservative, but given the uncertain market response that FCVs will face, and the potential infrastructure issues, it would probably be tenuous to assume more dramatic FCV growth. In comparison, though, in a study for the American Methanol Institute (in what he calls a "modest" forecast), Nowell (1998) projects a global fleet of 40,000 methanol FCVs in 2004 and 35 million by 2020.

performance criteria can thus have a significant impact on the vehicle configuration that is analyzed, and on the resulting cost calculations. Some analysts argue that new vehicle types should meet the same or better performance criteria that conventional vehicles do, because consumers have come to expect this level of performance. Others argue that such performance criteria "set the bar" too high for alternative vehicle types, and that consumers might be forgiving of lower performance for vehicles that incorporate new technologies.

Vehicle performance is often assessed on established driving cycles, such as the Federal Urban Driving Schedule (FUDS) or the newer US-06 driving schedule. The FUDS is a much more gentle cycle than the US-06, with a top speed of about 56 miles per hour, versus about 80 miles per hour for the US-06, and the acceleration steps are softer. A vehicle whose performance is assessed and whose componentry is sized over the FUDS cycle will thus be unable to meet the performance requirements of the US-06. A better approach for determining the peak power required for a vehicle drivetrain is to use additional performance criteria, as supplements to a single driving cycle. This is commonly in the form of a 0 to 60 mile per hour acceleration time requirement, or a hill-climbing requirement. However, the amount of energy needed onboard the vehicle and the efficiency of the vehicle are traditionally based on repeated runs of the vehicle over a drive cycle.

For purposes of this analysis, the FUDS cycle is too gentle a drive cycle to make for a good comparison among ZEV types and between ZEVs and conventional ICEVs. FCVs in particular look very attractive when tested over the FUDS cycle because the low average power of the cycle corresponds well to the high efficiency that FCVs offer when the fuel cell system is operating at a relatively low percentage of its peak power. Conventional vehicles, in contrast, have relatively poor low-load efficiencies. They thus tend to fare better over higher power driving cycles, when compared with other vehicle types. One technique that Directed Technologies, Inc. (DTI) has developed, in working with the Ford Motor Company, is to multiply all the velocities of the FUDS cycle by 1.25 (Thomas et al., 1998a). The resulting drive cycle apparently closely mimics Fords' proprietary customer driving cycle, and its top speed of over 70 miles per hour and harder acceleration steps more closely match "real world" driving. This same procedure is adopted here for all of the analysis runs of BEVs and FCVs, using the Lotus 1-2-3 model. An additional drive cycle has thus been added to the model -- the "FUDS*1.25" cycle -- and the resulting vehicle efficiencies are somewhat lower than would be calculated if the regular FUDS cycle was used.

Another issue is the choice of vehicle driving range, because more energy needs to be stored onboard a higher range vehicle. Particularly for BEVs with expensive batteries, longer ranges imply higher vehicle purchase prices and, in general (although not without exception because of battery replacement cost issues), higher lifecycle costs. Using data from Lipman (1999a) that estimates the relationship between NiMH battery cost per kWh (and per kilogram (kg)) and cell capacity, the vehicle cost and performance model is capable of assessing the tradeoff in having a reduced range vehicle with higher power, smaller capacity cells. For example, in one set of runs, the purchase prices of NiMH Ford Taurus BEVs ranged from $24,590 for a 70-mile range vehicle, to $41,019 for a 220-mile

range vehicle (Delucchi, 1999). The trade-off to a lower range BEV, of course, is that from a consumer marketing standpoint lower range may adversely impact the market appeal of the vehicle. Market studies have attempted to assess consumers' "willingness-to-pay" for BEV driving range, with varying results, but since consumers are generally unfamiliar with the concept of limited vehicle ranges and long refueling times, it is unclear how valid these studies are.

Given these considerations, the assumption used here is that for BEVs the battery pack energy is held constant at about 29 kWh. For a 288-volt system, this implies that 100 ampere-hour (Ah) cells are used. The resulting driving ranges are between possible extremes, at about 110 to 130 miles. This assumption represents the "middle ground" between three possible choices as battery technology is improved: holding vehicle pack energy constant, holding vehicle range constant, and holding vehicle mass constant. If vehicle range is held constant with improved battery specific energy, the vehicle gets lighter and cheaper, but the capacity of the battery cells decreases (and the cost per kWh increases). If vehicle weight is held constant, on the other hand, the vehicle range increases and the vehicle cost increases slightly with the higher capacity battery pack. Holding battery pack energy constant as battery specific energy is increased allows for somewhat increased driving range, while at the same time decreasing the vehicle mass and peak power requirement. Table 2-2 presents key specifications and characteristics of the BEVs analyzed in this chapter.

As an aside, an interesting future analysis would be to focus on the choice of system voltage and the trade-off that exists between motor/controller costs and battery costs with changes in system voltage. Lower system voltages allow for fewer, higher capacity battery modules to be used and this reduces parts counts and costs in the battery pack. However, lower voltages increase the cost of the motor controller, where costs of the high power IGBT switching devices scale with current (i.e., at lower voltage, more current is needed to meet the vehicle's power requirement).

BEV Manufacturing Cost Studies

Several BEV cost studies were performed from 1994 to 1998 by various government agencies, coalitions, and research organizations. These studies report somewhat disparate results. All studies conclude that BEV costs will be higher than conventional vehicle costs in the near-term, but a few studies suggest that BEV costs could relatively quickly drop to levels comparable to those of conventional vehicles, particularly on a lifecycle basis (Moomaw, et al., 1994; U.S. DOE, 1995). Most studies suggest that BEV purchase prices are expected to remain a few to several thousand dollars higher than conventional vehicle prices, with lifecycle costs also remaining somewhat higher (Dixon and Garber, 1996; NYSERDA, 1995; OTA, 1995; U.S. GAO, 1994; Vyas, et al., 1998). Finally, one study concludes that BEV purchase prices are likely to remain much higher than conventional vehicle prices, through 2010 (Sierra Research, 1994). These BEV cost studies are reviewed in detail in Lipman (1999c), including discussion of the methods, assumptions, and results of each study. Table 2-3, below, summarizes the BEV purchase price results of the various studies. Note that in some cases the figures refer to full retail prices of BEVs, while in other cases the figures refer to incremental costs, relative to comparable conventional

vehicles. Table 2-4 summarizes BEV lifecycle cost results, for the studies that estimated BEV lifecycle costs.

Some of the variation in the reported results of BEV manufacturing costs can be explained by considering the vehicle classes, production volumes, and battery types considered in the various analyses. However, aside from these critical study parameters, considerable variation remains in the vehicle purchase price and lifecycle cost estimates reported in the tables. Parameters that help to account for the remaining differences in cost estimates include: the assumed performance of the vehicle (and in lieu of an explicit performance analysis the general sizing of components for a given vehicle type); the cost of the assumed battery type; and costs of accessories and additional equipment needed for the BEV such as battery chargers, HVAC systems, and electrical power steering units.

Also, most of these BEV cost studies are limited in that they are not coupled with vehicle performance models, and therefore have no way of relating the sizing of key vehicle components to the performance of the vehicle that is analyzed (the OTA study is the only exception). Lifecycle cost calculations tend to be based on assumed battery lifetimes, rather than on analysis of battery cycle life as a function of depth of discharge with a model that estimates average depth of discharge as a function of the size of the battery pack and average daily driving patterns. The studies also tend to assume that BEVs will be constructed in a similar manner as conventional vehicles (i.e., out of steel).

In order to form the basis of a more sophisticated analysis of BEV manufacturing and lifecycle costs, a motor vehicle cost and performance spreadsheet model has been developed by Mark Delucchi at the Institute of Transportation Studies - Davis (ITS-Davis). This model, documented in Delucchi (1999), calculates manufacturing and lifecycle costs of both mid-size (e.g. Ford Taurus) and subcompact (e.g. Ford Escort) class vehicles. The model is an integrated vehicle cost and performance model in that it designs a vehicle that satisfies range and performance requirements over a specific drive cycle, and then calculates the manufacturing and lifecycle costs of that vehicle. The model includes three major subparts: a vehicle cost and weight sub-model that is based on analysis of the costs and weights of about 40 vehicle subsystems; a vehicle energy use sub-model that calculates the forces that act on a vehicle as it goes through a second-by-second drive cycle; and a periodic ownership and operating cost sub-model that estimates fuel, maintenance, repair, and insurance costs.

As discussed above, key cost drivers for BEVs are the unique EV components that currently are not being produced in high "automotive" volumes. In order to couple the market penetration scenarios with calculations of BEV costs in a given year, it is necessary to develop cost estimates for these key components as a function of production volume. This is made difficult by the proprietary nature of manufacturing cost data for these emerging technologies, but such cost functions have been developed using data from various sources, including price quotes from suppliers of key component sub-materials. Furthermore, in order to allow for changes in vehicle power that arise from changes in vehicle weight and/or the demands of the assumed drive cycle, it is necessary to also estimate motor and controller costs as a function of the peak power that they can handle. Finally, due to the way in which the model sizes EV battery packs (and to generate cost estimates for small, peak power

battery packs for hybrid vehicles), it is necessary to also estimate battery costs as function of the ratio of specific power to specific energy that they can supply. Cost functions for EV motors, motor controllers, and battery packs are presented and discussed below, following a discussion of EV chassis costs.

Lightweight EV Chassis Costs

The vehicle mass compounding effect suggests that the cheapest vehicle will tend to be the lightest vehicle. This is especially true for BEVs since any reduction in vehicle mass translates directly into reduced drivetrain power needed to meet given performance criteria, and reduced battery pack capacity to achieve a given driving range. In other words, every kg of mass that is removed from the vehicle will reduce the vehicle's "road load" and will lead to smaller and cheaper motors, motor controller, and battery packs. Given this effect, some manufacturers have explored very lightweight vehicle chassis designs in order to arrive at light and efficient complete BEVs or hybrid EVs, with downsized and less expensive drivetrain and battery systems.

General Motors has been at the forefront of these efforts, with its Ultralight concept vehicle, developed in 1992, and the Impact/EV-1 production vehicle. These vehicles are among the most advanced ever engineered, and their chassis designs are highly innovative. The GM Ultralight has a body-in-white (BIW) mass of approximately 190 kg, including closures, or just 140 kg without closures (Mascarin, et al., 1995). The EV-1 aluminum spaceframe is made of just 165 parts, weighs a total of 132 kg, and is joined with 40% fewer spot welds (about 2,000) than a typical steel structure (General Motors, 1996c). The 12 composite body panels, some made of Reaction Injected Molded material and some of low-density Sheet Molding Compound, add 41 kg (an estimated 50% lighter than steel) for a total BIW mass of 173 kg (General Motors, 1996c; General Motors, 1996d). Coupled with a very low drag coefficient of 0.19 (General Motors, 1996a), the lightweight design leads to an impressive overall vehicle efficiency of only 0.185 kWh per mile, or 0.115 kWh per kilometer (OTA, 1995). Showing off the vehicle performance possible with these technological advances, General Motors set an EV record top speed of 183.8 miles per hour in 1994, using a modified EV-1 design with an even more remarkable drag coefficient of 0.137 (General Motors, 1996e).

Some analysts have gone even further with the lightweight chassis concept, suggesting "ultralight" EVs or hybrids, with complete BIW masses as low as 123 kg (Lovins, 1996; Mascarin, et al., 1995). At any rate, although some lightweight steel designs have been explored, lightweight vehicles in general would be based on the use of more specialized materials such as aluminum and composites. This raises the question of the relative costs of producing vehicles out of different materials, since materials such as composite fiber and aluminum have higher materials costs than steel, on a per weight basis (but, of course, the whole point is to use less weight of material). In order to investigate chassis manufacturing costs associated with lightweight chassis materials options, Energy and Environmental Analysis, Inc. (EEA) performed a vehicle chassis cost analysis under a subcontract to the ITS-Davis BEV cost study for CARB. EEA estimated costs of producing four different chassis designs, at production of 2,000, 20,000, and 200,000 units per year. In addition to traditional steel construction, EEA investigated composite carbon fiber, aluminum spaceframe,

and aluminum unibody construction, using a proprietary cost model developed by the IBIS Associates, Inc.

For a subcompact vehicle design, EEA found that aluminum unibody and aluminum spaceframe constructions would result in a 115-kg (41%) reduction in mass, relative to a 280-kg steel baseline structure, and that composite construction would result in a 69 kg (25%) reduction (EEA, 1998a). However, at high production volumes, the aluminum unibody and composite costs were estimated to be somewhat higher than the costs of the steel and aluminum spaceframe constructions. At production of 200,000 units per year, the costs of both the aluminum unibody and composite chassis were estimated to be about $4,300 per unit (including interior components), while the cost for the aluminum spaceframe chassis was about $3,900, and the cost of the steel chassis was about $3,800 (EEA, 1998a). At very low production of 2,000 units per year, the composite chassis was estimated to be much cheaper than the others, due to lower tooling costs, but this cost advantage disappears by the time production of 20,000 units per year is achieved. Thus, based on the EEA analysis, the aluminum unibody construction is the clear winner at high production volumes, in terms of the combination of cost and weight. Figure 2-3 (at end of chapter) shows the costs of the four different subcompact chassis constructions, at different production volumes, as estimated by EEA using the IBIS model.

Based on EEA's (1998a) analysis, that shows that some vehicle weight reduction measures can reduce weight and save cost at the same time (e.g., substituting a composite-plastic bumper for a steel one), and also on an estimate by Ledbetter and Ross (1990) that a 10% reduction in vehicle weight could be achieved with increased use of aluminum and plastic, Delucchi (1999) assumes that the weight of a conventional Taurus-class EV chassis could be reduced by about 370 pounds at a cost of $200 per vehicle. This assumption is adopted here as well (see below for further discussion), although more extreme weight reductions are arguably possible at reasonable cost (Lovins, 1996; Mascarin, et al., 1995). Further weight reductions would be beneficial in improving EV efficiency, and reducing drivetrain power requirements. However, even with the weight decompounding effect on lowering body and drivetrain costs, it is unclear if additional costs for weight reduction can be justified beyond the levels estimated with the IBIS model and reported in EEA (1998a).

The $200 per vehicle cost-of-weight-reduction estimate applies to high-volume chassis production of 200,000 units per year. In lower volume production, costs of building a specialized EV chassis would be considerably higher, as shown in the EEA analysis, particularly for production below 20,000 units per year. However, it probably makes sense for a manufacturer to produce a single reduced-weight chassis design for both the EV version of a vehicle model as well as the conventional version, given the relatively modest costs of doing so. Some support for assuming such a strategy comes from the increasing propensity of manufacturers to use cross-platform manufacturing strategies to provide consumers with body style choices, while at the same time reducing production costs. For example, the Volkswagen Golf GL, Volkswagen Jetta GLS, Volkswagen New Beetle, Skoda Octavia SLX, Audi TT Coupe, and Audi A3 are all produced from the same basic chassis platform, even though the retail prices of the final vehicles range from $17,000 to $40,000 (Krebs, 1999). Volkswagen has been the most successful at this strategy in recent years, now

producing half of its vehicles from just four basic platforms (with nearly 100% of production planned for those four platforms by 2001), but other manufacturers are following suit (Krebs, 1999). GM, Toyota, Honda, and Ford are now all pursuing "worldwide platform" strategies (Krebs, 1999).

Thus, if manufacturers will use the same platform for different body styles in order to achieve economies of scale, they very likely would attempt to use the same complete chassis for EV and conventional versions of the same body style if EV production were to reach substantial numbers. The reduced weight of the conventional vehicles would offer the manufacturer the benefit of greater fuel economy for those vehicles, which could aid in meeting fleet-averaged Corporate Average Fuel Economy (CAFE) standard requirements (and possibly other benefits of reduced drivetrain power requirements or greater vehicle performance as well). For the BEV cost model runs discussed below, the weight reductions and costs assumed by Delucchi (1999) are thus assumed for all EV production volumes, under the assumption that at least 200,000 mid-sized vehicle chassis are built for combined, "shared-platform" production of both the EV and conventional versions of the vehicle model. While any lightweight-bodied conventional vehicles would also carry a $200 cost penalty, this analysis assumes that these relatively modest costs are offset by ancillary benefits to automakers of approximately the same magnitude. These benefits could be in the form of weight decompounding effects, and/or through fleetwide efficiency improvements that allow the sale of more high-profit, light-duty trucks and sport-utility vehicles under CAFE regulations.

EV Drivetrain Costs

Propulsion systems designed specifically for BEVs are currently produced in small volumes and sold at high costs, although some hybrid EVs are beginning to see production in medium volumes of tens of thousands of units per year. As a result, component costs for hybrids are reaching more moderate levels, and they are forecast to decline further as production continues. For example, Toyota has disclosed that current costs of components for the Prius hybrid EV, in volumes of about 24,000 units per year, are about $700 for the motor, $1500 for the motor controller, and $1500 for the NiMH peak-power battery. These costs are expected to fall to $550, $800, and $800, respectively, for reductions of 21% in the motor cost and 47% in the controller and battery cost (EEA, 1998b). Also, fully electric power steering systems, a novel modification needed for EVs, cost Toyota only $100 for the Prius with a future expected cost of just $50 (EEA, 1998b).

At present, there are two primary choices of motor technology for use in EV drivetrains. Most vehicles in pilot-scale production today use AC induction systems, but some vehicles, such as the Toyota RAV4, use systems based on BPM motors. Both AC induction and BPM systems offer similar advantages over conventional direct-current (DC) brush motors. These include lighter motor weights, higher efficiencies, and lower service requirements (the brushes in DC brush motors wear out and require replacement). In general, AC induction motors provide high efficiencies over a wide range of operation, while BPM motors provide higher peak efficiencies. BPM motors also tend to be lighter, but they use rare earth magnets that are somewhat costly at present. Both of these

motor types require complicated control systems relative to DC brush motors, in order to operate from a DC source.

Both AC induction and BPM systems are good choices for use in EVs, and it is not clear which system will prove to be the most popular. The control systems needed for these types of motors are costly and complex, but the necessary electronics, particularly insulated-gate bipolar transistor (IGBT) power switching devices, have been improving rapidly. Continued progress in IGBT technology is expected, particularly with regard to the saturation characteristics of the devices and their switching energies. Inverters in general are expected to progress in terms of not only the cost and performance of the IGBT silicon chips, but also in packaging, controls, processors, and transducers (Hodkinson, 1997).

Recent statements by EV project managers at GM and Ford reflect the progress that has been made in reducing the cost and complexity of EV motor controllers over the past few years. Bob Purcell of GM reports that the second generation EV-1 motor controller has only three IGBTs, while the first generation had six. The new IGBTs have twice the power handling capability of the old ones, with equal precision levels. Overall, the new electric drive control system has half the mass, one-third fewer parts, and half the cost of the first generation system (Purcell, 1998b). John Wallace of Ford reports similar progress in the development of its system:

> [W]e have gone down in numbers and parts in the controller – it started out quite complicated. I can remember the original Ecostar controller, which was quite complex; then there was a two-board controller and now a one-board controller, and perhaps we will go down to a no-board controller basically by mounting control circuitry right on the motor. All that stuff is tearing out cost. (Wallace, 1998, p. 14)

These statements suggest that in addition to production scale economies, product innovation will lead to reduced EV drive system costs as the EV market matures.

Detailed cost estimates for EV motors and controllers have been developed based on a range of data sources, and are discussed below. Initial efforts to obtain data on motor and controller manufacturing costs from major manufacturers were generally unsuccessful due to the proprietary nature of the data. Ultimately, however, some manufacturers were willing to provide data on EV drivetrain costs at different production volumes in order to provide input for the UC Davis EV cost study for CARB (although in a few cases the data were only supplied under conditions of anonymity). These data, shown in Table 2-5, were supplemented with other motor and controller cost estimates, and analyses of materials and subcomponent costs, in order to develop high, central, and low case motor and controller cost functions that consider both production volume and the power rating of the system.

Cost Estimates for EV Motors

EV motor technology has improved dramatically since the basic DC motor technology used in the BEVs of the 1970s. Those motors had torque densities of about 3.1 newton meters (Nm) per kg, while permanent magnet motors with ferrite magnets introduced in about 1975 improved the density to over 4.0 Nm

per kg. Beginning in about 1980, permanaent magnet motors with rare earth samarium-cobalt magnets demonstrated torque densities of 6.0 to 8.0 Nm per kg, and improved samarium-cobalt magnet formulas (Sm_2CO_{17}) produced densities as high as 12.5 Nm per kg. Finally, the modern BPM motors of the 1990s, with neodymium-iron boron (Nd-Fe-B) rare earth magnets, have demonstrated torque densities of up to 25.0 Nm per kg (Ragone, et al., 1995).

As a starting point to estimating manufacturing costs of EV motors, it may be helpful to understand how costs may break down in terms of materials, labor, overhead, and other costs. In the conventional motor industry, aggregate data show that shop costs can be broken down as follows: materials (30-40%), direct labor (15-20%), energy costs (1-2%), and overhead, rents, depreciation, taxes, and interest (38-64%) (U.S. Commerce Dept., 1988). It is unclear, however, how well these data should apply to EV motors. Motors for EVs are designed for high efficiencies and low masses, and as a result they use more expensive materials for some subcomponents than do typical motors. The relative costs of materials, labor, and overhead are therefore likely to be somewhat different.

With regard to motors suitable for use in EVs, one motor manufacturer (who requested anonymity) supplied data that its 8 hp (nominal) DC electric vehicle drive motor has a retail price of about $2,200, and an original equipment manufacturer (OEM) cost of about $1,150 in quantities of 25 units. In smaller quantities, the OEM cost would range from about $1,600 to $1,200. The total manufacturing cost is about half the cost to the OEM, with a labor component of 22.3%, a materials component of 31.8%, and overhead costs of 45.9% (anonymous source). This motor is rated at only 8 hp, but it weighs 150 pounds and generates over 400 pounds per foot of torque when starting a vehicle from a standstill.

The same manufacturer also makes basic AC motors that they supply to both GM/Hughes and Solectria, as well as to many other companies. The motors supplied are just the basic core motor units that then require significant additional parts and assembly. Different motors are supplied to the two companies. The one for Hughes is liquid cooled with a special splined drive shaft, and it produces 50-80 kilowatts (kW), depending on controls, and 160 pounds per foot of torque at locked rotor. The motor for Solectria is the basic industrial design, rated at about 10 hp, with 100 volt, 3 phase windings. These motors are manufactured on the company's flexible flow AC motor production lines, and they therefore benefit from volume efficiencies even in relatively short production runs. The basic cost to OEM customers for these motors is about $390, not including extras such as cable assemblies, encoders, t-stats, and the liquid cooled package for the GM/Hughes motors. Of manufacturing cost, materials make up 53.5%, labor comprises 5.8%, and overhead adds 40.7%. The additional costs for assembling extra components include $10 for labor, and $70 for overhead, plus the costs of parts and overhead on parts (40% of parts cost).

BPM motors, with their rare earth samarium-cobalt or Nd-Fe-B magnets, are produced for traction applications by Unique Mobility in the United States, Siemens in Germany, and several companies in Japan. Relatively small motors for hybrid EVs and scooters are beginning to be mass-produced, but larger motors for BEVs are still manufactured on order and are not yet available “off-the-shelf.” Present, low-volume costs for BPM motors in the 50-75 kW range are thus still quite high, but costs are expected to decline in high volume production

to be only slightly higher than for AC induction motors. See Table 2-5 for manufacturer cost estimates for various sizes of complete BPM drive systems in different volumes of production (see Lipman (1999b) for separate cost estimates of motors and controllers).

In addition to manufacturer data, other motor cost data are available from government research programs. Argonne National Laboratory (ANL) has conducted research on EV motors, and detailed materials costs and high-volume manufacturing costs have been estimated for DC, AC induction, and BPM motors. The materials cost estimates for these motors are presented in Tables 2-6 through 2-8. For BPM motors, note that a substantial component of total materials cost (36.9%, as estimated by ANL) is the cost of the neodymium-iron boron magnet material.

With the materials cost breakdowns shown in Tables 2-6 through 2-8, Cuenca estimated total motor prices by adding costs for machining, winding, welding, and assembly. The assembly and testing process was estimated at 30% to 40% of the total manufacturing cost (Cuenca, 1995). To this total manufacturing cost, a gross profit margin of 20% was added to obtain a total cost to the OEM. Table 2-9 presents the results of Cuenca's analysis for three different motor types. Note that these prices were estimated for motors of different power ratings. As discussed above, consistent price comparisons of different types of motors are complicated by the lack of standards for rating motors, and the different performance characteristics of AC, DC, and BPM motors. See the following section for per-kW estimates of motor prices.

Finally, one other study of EV motor costs has been published in recent years. This assessment suggests that the mature production costs, per peak kW, of DC brush, BPM, AC induction, and switched-reluctance motors are $10 per kW, $10-15 per kW, $8-12 per kW, and $6-10 per kW, respectively (Rajashekara and Martin, 1995).

One advantage of detailed motor materials breakdowns is that it is possible to take account of per-pound price changes in specific motor components. For example, if the cost of the magnets used in the BPM motor were to drop from $50 per pound (lb) to $30 per lb, the new motor price could be calculated as follows (Cuenca, 1995):

- permanent magnets constitute 36.9% of motor materials costs (and by extension motor prices because assembly and profit are calculated in proportion to materials costs in ANL's analysis);

- the reduction from $50 per lb to $30 per lb is a 40% drop, yielding a 14.8% cost reduction (0.4 * 0.369 * 100%);

- a $520 motor would then sell for a price of $443 ($520 - (.148 * $520).

Core AC induction motors are currently produced in significant volumes and with relatively inexpensive materials. However, since the magnets alone constitute over a third of BPM motor materials costs, there is a significant potential for cost declines in Nd-Fe-B magnet material to drive overall cost reductions in BPM motors.

This Nd-Fe-B magnet material, the most powerful at ambient temperature currently known, was developed by the Sumitomo Corporation and first commercialized relatively recently in 1983. Estimating the cost of this material is somewhat complicated, but the Argonne estimate of $50 per pound is reasonable for high volume purchases, according to the Sumitomo Corp., which currently supplies magnet material to Unique Mobility, Inc. (Numajiri, 1997). The price charged to the OEM is dependent upon the volume of the order, the term of the contract, the commodity prices of the basic materials, the yen to $ exchange rate, and the form in which the material is shaped, among other factors. Sumitomo has licensed production of the material to other companies, some of which operate with lower labor costs in Korea than the Sumitomo operation does in Japan, but the quality of the Sumitomo product is better because they are the inventors of the product and most knowledgeable and adept at its manufacture (Numajiri, 1997). Sumitomo is currently expanding production, with capacity expected to double from 1997 to 2002-3, and this expansion is being driven to a significant extent by demand for motors in the automotive industry. This expansion in capacity and increased emphasis on producing motor magnet materials for automotive production could potentially result in a softening in prices. Sumitomo does not expect dramatic cost reductions because of relatively high costs for raw materials, but the company does consider costs of $40 per pound possible with a strong dollar, and a high-volume, long-term material supply order (Numajiri, 1997). This forecast suggests that BPM motors are likely to remain at least slightly higher in cost than AC induction motors, even when produced in similar volumes.

Cost Estimates for EV Motor Controllers

Just as EV motors have improved significantly in recent years, so too have EV motor controllers. The power controllers of the mid-1970s produced about 20 kilovolt-amperes (kVA) per cubic foot and about 0.5 kVA per pound. By the mid-1990s, these power densities had increased by more than five-fold, to over 110 kVA per cubic foot and to about 2.7 kVA per pound (Ragone, et al., 1995).

In addition to studying EV motors, ANL has also estimated near-term but high production volume costs for motor controller materials and assembly operations. For AC motor controllers with a 70-kW capacity, Roy Cuenca of ANL estimates that materials costs come to from $1,975 to $2,575, while for similar capacity BPM motor controllers materials costs range from $1,375 to $1,675 (Cuenca, 1996). Approximately two-thirds of total materials costs for AC controllers are for IGBTs (and uncertainty in this cost is cause for the range of values), while about one-half of the materials cost for BPM controllers is for IGBTs.

Once assembly costs and profit margins are added, Cuenca calculates costs of from $37.3 to $47.6 per kW for AC controllers, and from $26.7 to $32.1 per kW for BPM controllers. However, the study acknowledges that estimating costs on a per kW basis and using these estimates for controllers of other power ratings may not be a good approximation (Cuenca, 1996).

Given these high present costs, efforts are currently underway to reduce the costs of EV motor controllers. One such effort is SatCon Technology Corporation's Automotive Integrated Power Module program. SatCon has been awarded $10 million in funding from DOE to develop EV motor and

controller components, and it has recently received an order from GM's Opel division to produce power modules for the company's FCVs. The SatCon program seeks to reduce high volume (i.e., 10,000 to 200,000 units per year) controller manufacturing costs by selecting low cost materials, integrating subsystems to reduce parts counts, and utilizing low cost production techniques (Bonnice, 1999). Program goals are for post-2002 production of IGBT-based inverters and controller power modules, suitable for use with both AC induction and BPM motors, with selling prices of $14-19 per kW at 20,000 units per year, and $10-14 per kW at 200,000 units per year (Bonnice, 1999). These costs are applicable to devices with a 300V DC input level, and power levels in the 50-100 kW range. The ranges in costs reflect differences in costs for controllers across the 50-100 kW power range, uncertainties in future manufacturing costs, and potential differences is customer requirements.[16] The complete controller units are expected to have average efficiencies of 97% (Bonnice, 1999).

Cost Functions for EV Motors and Motor Controllers

Even though they are often characterized as such, motor and controller costs are not exact linear functions of rated power output. In the case of motors, costs may rise as a nearly linear function of nominal power rating, but this is not the case for motor controllers where some of the controller componentry does not change with higher power ratings. The issue of formulating cost functions for motors is further complicated by the fact that motors can be rated by continuous (nominal) output or peak output, and both of these ratings vary by system voltage. A motor can achieve a different peak power rating depending on the controller with which it is paired, and different types of motors appear to be capable of achieving different ratios of continuous to peak power. For example, one AC induction motor analyzed here has a continuous rating of 40 kW and a peak rating of 67 kW, yielding a peak to continuous ratio of 1.68. A typical DC brush motor has a continuous rating of 20 kW and a peak of 52 kW, yielding a ratio of 2.6. Finally, one BPM motor has a continuous rating of 32 kW, and this is also its peak rating for a ratio of 1.0, but a similar although slightly heavier 32 kW BPM motor has a peak rating of 53 kW, for a ratio of 1.65.

Given the above complications, various strategies can be used to approximate a per-kW price for motors. In his analysis, Cuenca divides the average OEM cost of a motor by its peak power rating to obtain what he terms a "specific cost." For the motors analyzed, he obtains the results shown in Table 2-10. It is unclear, however, how readily these results can be generalized to motors of different sizes than the ones analyzed. These estimates should be relatively accurate for motors close in size to those assessed (as should be the case for most motors used in passenger vehicle EV applications), but these relationships should probably not be presumed to extend to motors of much larger or smaller size.

In a study for the Office of Technology Assessment (OTA), a consultant (Energy and Environmental Analysis, Inc.) developed a cost function for AC induction motor/controller systems. This function includes a constant term, so

[16] e.g., switched reluctance motor drives would be at the high end of the range, while simple three-phase drives would be in the middle to the lower end of the range, depending on the power rating of the system.

the estimated cost is not purely a function of power rating, but the cost increment for increasing power is linear. This function is as follows (OTA, 1995):

Cost to the OEM = $300 + $30*kW (peak)

Of this total OEM cost, EEA/OTA estimates that roughly one-third of the cost is in the motor, and two-thirds are in the controller. This function is applicable to high-volume production of the propulsion system (i.e., a production level on the order of 100,000 units per year). EEA/OTA estimates that permanent magnet motors would cost 15-20% more, with similar production volumes.

Also, Vyas and Cuenca (1999) have estimated motor and controller costs for EVs, based on Cuenca's work and on data gathered under the auspices of the PNGV program. Under the assumption of high volume production (10,000 to 50,000 units per year initially, rising to 200,000 units per year), they estimated AC induction motor costs to the OEM of $7.50 per peak kW in 2000, falling to $6.00 per peak kW after 20 years. BPM motors were estimated to cost $9.00 per peak kW in 2000, and $7.00 after 20 years. Controllers for both systems are estimated to cost the OEM $20.00 per peak kW in 2000, falling to $5.00 per peak kW after 20 years (Vyas and Cuenca, 1999).

Table 2-11 compares cost estimates that would be predicted, using the OTA, Cuenca, and Vyas et al. methodologies, with high-volume forecasts provided by manufacturers. With regard to these estimates, it seems clear that there is reasonably good agreement between the EEA/OTA, Cuenca, and manufacturer estimates, while the Vyas et al. estimates are somewhat lower for 2000, and much lower for 2020 (only the Vyas et al. estimates project costs into the future). It is also clear that all of these drive system cost estimates are strong functions of peak power, with the Cuenca (1996) and Vyas et al. (1999) estimates being linear functions of peak power.

Based on consideration of all of the above information, I have developed central case, high, and low cost functions for EV motors and controllers. The data supplied by manufacturers and from other sources, while too sparse to allow detailed statistical analysis, are complete enough in terms of covering a range of system sizes and production volumes to allow relatively simple cost functions to be developed. The motor and controller cost functions, discussed below, were developed by examining all of the available data and then developing functions to match the data as well as possible. This was done by estimating parameters for materials costs, costs of adding value to materials, and manufacturer profit such that the final component costs estimated by the low, central, and high case cost functions matched the range of variation observed in the available data.

For motors, the high cost case reflects the use of a BPM motor, the central case reflects the use of an AC induction motor, and the low cost case also reflects the use of an AC induction motor, but reflects the relatively low motor costs estimated by Vyas and Cuenca (1999). For motor controllers, the high, medium, and low cost cases reflect different assumptions about the degree to which costs of key motor controller components will be reduced with production volume.

By considering three production volumes (2,000, 20,000 and 200,000 units per year), cost functions are developed that allow costs at other volumes to be

estimated by interpolating along curves that are fit to these three points. Costs estimates for the three different production volumes are based on the data discussed above and presented in the tables. Costs for the 20,000 units per year volume are also based on recent data on the costs of components for the Toyota Prius hybrid EV (EEA, 1998b). This is the first production vehicle with an electric driveline to be produced in volumes of over 20,000 units per year. Further supporting data and details on the development of the motor and motor controller cost functions can be found in Lipman (1999b).

The following cost functions differ somewhat from most of the cost functions discussed above (that assess motor and controller costs in terms of $/kW), in that I assume that for most cases motor costs are linear functions of the peak power rating of the motor, but that motor controller costs are weaker functions of their peak power rating. As discussed above, this is because only slightly higher rated (or more in parallel) IGBTs are required to supply higher power capabilities, along with perhaps slightly larger controller enclosures and cooling systems.

The BPM motor materials cost estimates are generally based on the Cuenca (1995) estimates shown above, with the exception that at the 200,000 per year production level, I assume that neodymium-iron boron magnet material can be purchased at $40 per pound (see above discussion). For AC induction motors, which are currently in mass production, a base price of $390 is assumed for a 50 kW motor, based on the quote mentioned above. Also based on data supplied by the manufacturer, additional costs of $150 per motor are assumed for the parts, labor, and overhead costs associated with adding cooling jackets, encoders, and cable housings (a liquid-cooled design is assumed). Since the tooling is already in place for these motors, and they are produced on flexible-flow production lines, I do not assume that the price is sensitive to production volume in the range of 2,000 to 200,000 units per year. The high, central, and low cost functions for BPM and AC induction EV motors are as follows:

<u>High Cost Case -- BPM Motor:</u>

2,000/yr: OEM price = 1.18 * (($10.16*kW-pk) + ($660+($15*kW-pk)))
or (simplified) = $779 + ($29.7 * kW-pk)

20,000/yr: OEM price = 1.18 * ((10.16*kW-pk) + (75+(1.8 * kW-pk)))
or (simplified) = $89 + ($14.1 * kW-pk)

200,000/yr: OEM price = 1.18 * ((9.4*kW-pk) + (1.2*kW-pk))
or (simplified) = $12.5 * kW-pk

Where:
1.18 = manufacturing cost + 18% supplier profit
10.16 (or 9.4) * kW-pk = materials cost
Additional term = cost of adding value to materials

Central Cost Case -- AC Induction Motor:
All volumes: OEM price = (kW-pk / 50) * ($470 + (1.4 * $50))
or (simplified) = $540 * (kW-pk / 50)

Where:
kW-pk / 50 = peak power scaling factor
$470 = selling price of 50 kW core motor, plus labor and overhead on extra parts
1.4 * $50 = extra parts plus 40% overhead on parts

Low Cost Case -- AC Induction Motor:
2,000/yr: OEM price = $9.00 * kW-pk

20,000/yr: OEM price = $7.50 * kW-pk

200,000/yr: OEM price = $6.00 * kW-pk

I also estimate three sets of controller cost functions (i.e., central case, high, and low), reflecting different assumptions about the degree to which motor controller costs will be reduced with increased production volume and accumulated manufacturing experience. For the high case cost functions, materials cost estimates underlying the 20,000 per year and 200,000 per year cases are based primarily on ANL's estimates for items such as the microprocessor ($200); driver stage board ($175); DC-DC converter ($70); current sensor ($120); ripple capacitors ($60); and hardware, chassis, and cooling ($150). For the 2,000 per year case, the cost function is based on data supplied by manufacturers for controller costs at this relatively low volume. Costs are considerably higher at this volume relative to production at 20,000 units per year, presumably reflecting higher materials costs, processing costs, and amortized fixed costs. Controller costs may also be higher at low volumes because it is generally not cost-effective to design application specific integrated circuits (ASICs) for low volume production. In higher volumes, ASICs chips can be used in place of assemblages of individual transistors and resistors, reducing cost and also reducing system volume, mass, and cooling load (Brandmeyer, 1997). The up-front costs associated with designing an ASICs-based system preclude doing so at low volumes, but at higher volumes significant cost savings can result as these fixed costs are spread over more and more units.

IGBT costs for the high case cost functions are based on a recent paper by Hodkinson (1997), and consultation with an electronics industry expert for an estimate of recent and likely near-term declines in IGBT costs. Hodkinson (1997) examines wire bond, lead frame, and intelligent power module type IGBTs for 70 kW (peak) AC induction and BPM drive systems, and concludes that wire bond packaging provides the lowest silicon cost for EV motor controllers. He estimates that the current silicon cost for a 70 kW AC induction inverter is $300, based on the use of three 1200 volt, 100 amp six-pack IGBT modules, and that the silicon cost for a 70 kW BPM inverter is $200, based on the use of two such modules. For these higher cost case functions, the higher IGBT cost estimates (i.e., $300) are assumed for a 70 kW system, and then they are scaled linearly for different inverter power ratings, since silicon costs scale to current capacity (for

constant system voltages). The 2,000 per year and 20,000 per year estimates assume current IGBT module costs, while the 200,000 per year estimate includes a slightly lower cost estimate that reflects a projected 20% decrease in IGBT costs over the next 2-3 years, relative to current costs (Harvey, 1998).

The central case and low case controller cost functions are primarily based on cost target data from SatCon Technology Corporation's Automotive Integrated Power Module program (see above). These data are used to estimate cost functions for production volumes of 20,000 units per year and 200,000 units per year. Cost functions for the 2,000 unit per year cases are matched to average (central case) and lower (low case) data supplied by Unique Mobility and Solectria (SatCon is focused on higher volumes of production, and did not supply cost estimates for 2,000 units per year). Based on information supplied by SatCon, the central case functions are most suitable for estimating costs of AC induction motor controllers, assuming most likely progress in reducing costs. The slightly lower low cost functions are more suitable for BPM motor controllers, or for AC induction systems with optimistic progress in reducing costs.

The same functional form was used as shown above for the high cost case functions, but the parameters were adjusted so that the overall cost estimates reflect the cost targets. These cost functions, documented in detail in Lipman (1999b), simplify to the following functions when the materials cost, labor cost, overhead cost, and manufacturer profit components are consolidated into a fixed component and a component that varies with system peak power:

<u>High Cost Case – Motor Controller:</u>
2,000/yr: OEM price = $3,298 + ($9.13 * kW-pk)

20,000/yr: OEM price = $1,363 + ($7.10 * kW-pk)

200,000/yr: OEM price = $907 + ($4.81 * kW-pk)

<u>Central Cost Case -- Motor Controller:</u>
2,000/yr: OEM price = $3,283 + ($6.07 * kW-pk)

20,000/yr: OEM price = $418 + ($10.76 * kW-pk)

200,000/yr: OEM price = $312 + ($7.60 * kW-pk)

<u>Low Cost Case -- Motor Controller:</u>
2,000/yr: OEM price = $3,234 + ($5.43 * kW-pk)

20,000/yr: OEM price = $392 + ($9.44 * kW-pk)

200,000/yr: OEM price = $262 + ($6.94 * kW-pk)

The specific motor and controller cost estimates used for each BEV, and based on the above cost functions, are shown in Appendix B.

Key Uncertainties

It is important to note that there are inherent uncertainties in making cost estimates of this sort. Perhaps most fundamentally, raw material and subcomponent costs, such as for Nd-Fe-B magnets or IGBT power switches, are subject to change over time and not always in predictable ways. Even factors such as the relative strength of the yen or deutschemark to the dollar can have an impact. Also, suppliers will face different factory costs depending on the region in which they locate, for such costs as labor, environmental compliance, and so on. Suppliers can also trade off labor for capital, at the expense of capital investments that must be amortized over several years, and this will affect the cost of adding value to materials. Factors such as these emphasize the need to consider a range of cost estimates for each key component, as it is impossible (even for the manufacturers themselves) to forecast future costs with certainty.

BEV Battery Costs

Many different types of batteries have been researched and tested for use in BEVs and hybrid EVs in recent years. Batteries suitable for use in BEVs are in various stages of development, depending on the battery type. The three most likely choices of battery chemistry for use in near to mid-term production BEVs appear at present to be advanced lead-acid, NiMH, and Li-ion. Other battery types that have been considered, but that no longer appear to be leading candidates, include sodium-sulfur batteries, sodium-nickel chloride batteries, zinc-bromine batteries, and nickel-cadmium batteries. Lithium polymer batteries are another possible option, although one that apparently is only under investigation by a few companies, such as 3M Corp.

With regard to these three battery types, sealed lead-acid batteries are a relatively mature product, produced by such companies as Johnson Controls, Inc., Horizon Battery Company, and Japan Battery Storage Company. Nickel metal hydride batteries are currently in pilot-scale to low volume production by such companies as GM Ovonic (a joint venture between Ovonic Battery Company and General Motors), Panasonic EV Energy, Varta, Yuasa, and SAFT. Company product literature reports that GM Ovonics is achieving a specific energy of 70 watt hours (Wh) per kg with modules of 85 Ah and 13.2 (GM Ovonic, n.d.). Panasonic's batteries achieve a reported 63 Wh per kg, with a 95-Ah, 12-volt (V) design (Panasonic EV Energy Co., n.d.). Meanwhile, lithium-ion batteries are currently in pilot-scale production by Sony and SAFT. SAFT has demonstrated small batteries with a specific energy of 105 Wh per kg, while Sony has reported 100 Wh per kg at the cell level (Kalhammer, et al., 1995). Factories to produce larger production volumes of NiMH and Li-ion batteries are currently under construction, with production expected in the next one to two years.

In addition to being at different stages of development, these battery types also share different characteristics. Advanced lead-acid batteries have the advantage of using relatively inexpensive materials, and thus have relatively low manufacturing costs and selling prices. I have recently analyzed in detail the potential manufacturing costs and selling prices of lead-acid batteries, and found that selling prices of about $110 per kWh should be possible for a company that produced batteries by licensing an existing battery design (Lipman, 1999a). Table 2-12 shows these selling price estimates, along with retail and wholesale selling

price quotes for Johnson Controls lead acid batteries. However, advanced lead-acid batteries have specific energy values on the order of only 35-40 Wh per kg. This means that BEVs using lead-acid batteries will have relatively low driving ranges, and this is likely to be a market barrier for these vehicles. For example, even the highly efficient GM EV-1 achieves only 60-70 miles per charge of practical driving, when equipped with a lead-acid battery pack.

Given the low specific energy of lead-acid batteries, all automobile manufacturers have shifted their attention to nickel and/or lithium based batteries. GM is now starting to equip the EV-1 with NiMH batteries produced by GM Ovonics, and the Toyota RAV4-EV and Honda EV Plus also use NiMH batteries. At present, the Nissan Altra EV is the only vehicle that is equipped with Li-ion batteries. The driving ranges reported for these vehicles are 60-80 miles for the lead-acid version of the EV-1, with up to 120 miles expected for the NiMH version, 80-100 miles for the Toyota RAV4-EV and Honda EV Plus, and 120 miles for the Nissan Altra EV (CARB, 1998c). Under "real world" conditions, Honda reports that users are getting about 75 miles of range with the EV Plus (Osawa and Kosaka, 1998), and by some accounts the Nissan Altra EV is at present only getting about half of the 120 mile range that it is supposed to have.

Determining costs of these recently developed, advanced EV batteries is complicated by two factors. First, as with manufacturing cost data for EV motors and controllers, cost data for batteries are highly proprietary and difficult to obtain. Second, since the data necessarily come from the manufacturers themselves, who have a vested interest in demonstrating the promise of the particular technology that they manufacture, one cannot be sure how much to trust any cost data that can be obtained. For example, with regard to NiMH EV batteries, I have obtained manufacturing cost estimates at different production volumes from both GM Ovonics and Panasonic. GM Ovonics' estimates are shown in Figure 2-4, while Panasonic has requested that their estimates remain confidential.

Figure 2-4:

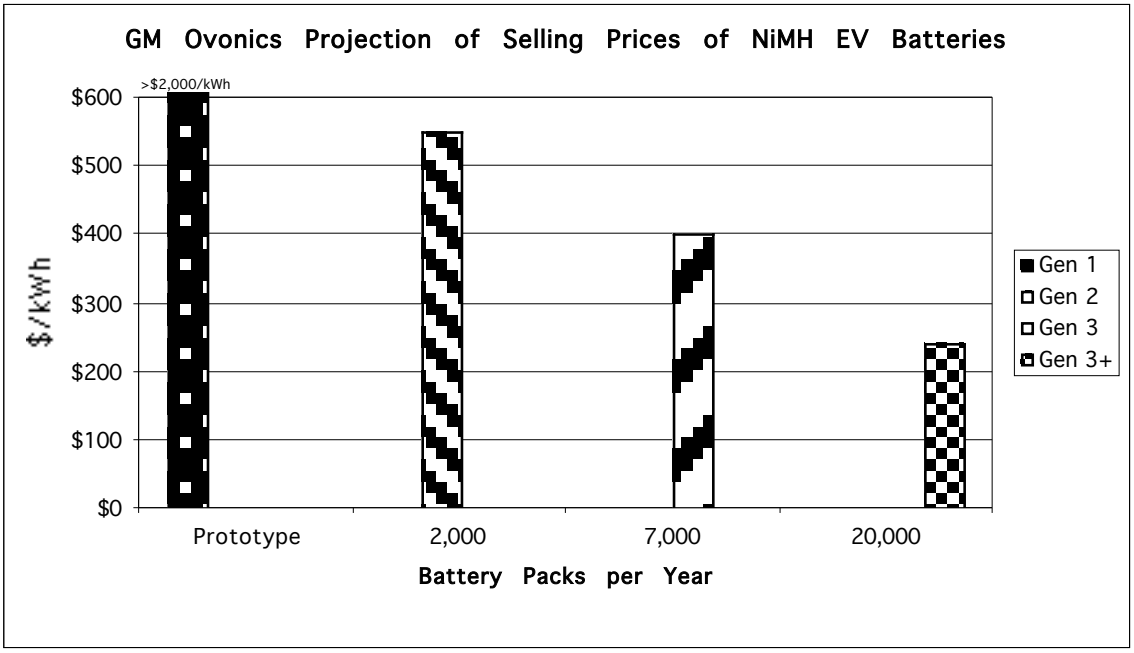

Source: (Adams, 1995)

Since none of the supporting details associated with these estimates are provided, however, it is impossible to analyze them in detail. In order to arrive at more justifiable estimates of battery production costs, I have therefore chosen to perform a detailed cost analysis of NiMH batteries.[17] A parallel investigation of the manufacturing costs of Li-ion EV batteries is underway at ANL, but the results of the study are not yet available. As discussed below, the investigation of NiMH battery manufacturing costs includes an analysis of the potential costs of a future generation NiMH battery design with a specific energy of 120 Wh per kg. This is similar to the specific energy that relatively near-term Li-ion batteries are likely to achieve, so pending the release of the ANL study, this case can serve as a reasonable surrogate for the performance (if not the cost) of Li-ion EV batteries.

The general methodology employed in the NiMH battery cost analysis is to make use of a battery performance model developed at ITS-Davis by Dr. Andy Burke (1999) to determine battery design specifications for potential NiMH battery designs. Using these specifications, quantities of the various materials needed to manufacture a given battery are estimated. These materials are then costed by obtaining quotes from battery component suppliers. Finally, additional battery manufacturing and selling costs are estimated based on a variety of sources. The study considers a range of production volumes, in order estimate the reductions in manufacturing costs that occur through economies of scale in materials purchase, and in other factory costs.

A detailed analysis of the manufacturing costs of NiMH batteries is especially warranted because some of the materials used in the NiMH battery

[17] This investigation was conducted to support a recent analysis of the costs of manufacturing BEVs for the California Air Resources Board.

have relatively high costs at present. Some of these materials are not "raw materials" but instead are "value-added materials" that require prior processing steps. As a result, the costs of these materials should themselves drop somewhat over time, as production volumes increase and production processes improve in design and efficiency. In fact, due to the relatively high costs of novel NiMH battery materials, successful commercialization of NiMH EV batteries is likely to depend on cost reductions in key materials. A major focus of the analysis discussed below is therefore to assess the potential for cost reductions in key battery materials, including active materials for electrodes, grid substrate materials, and separator materials.

NiMH Batteries for EVs

Typical NiMH EV battery cells have a capacity of 90-100 Ah. These 1.2-V battery cells are typically designed in a prismatic configuration, with negative and positive electrode plates sandwiched with layers of separator material. The negative electrode plates are composed of nickel or other metal grids that are pasted with a nickel hydride alloy, while the positive electrode plates are composed of a nickel foam substrate that is coated with spherical nickel hydroxide. Further details of specific battery materials are discussed below.

Figure 2-5:

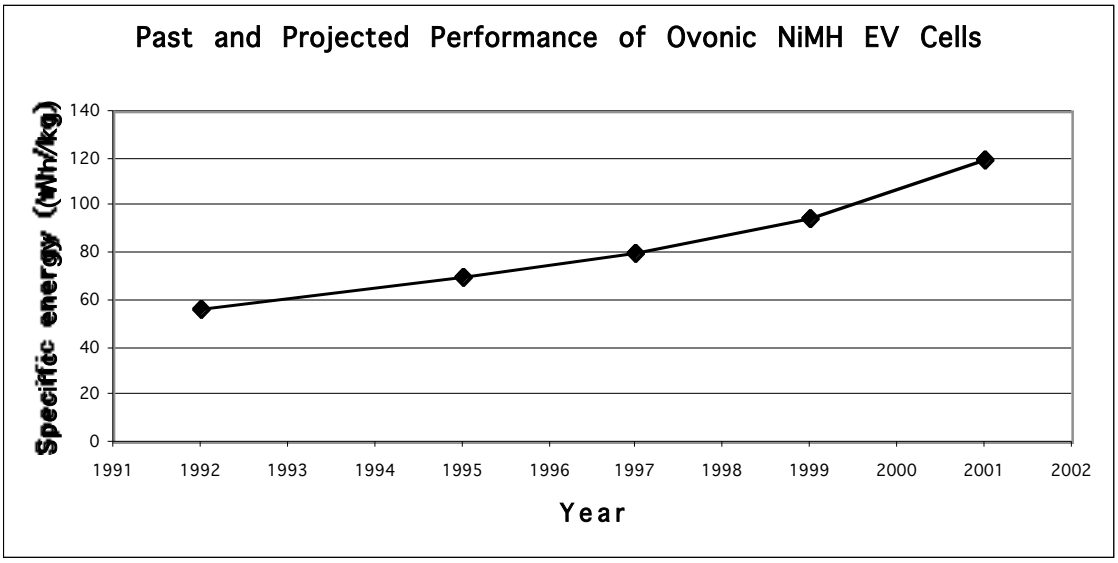

Source: (Corrigan, et al., 1997)

Also, four production levels are analyzed in order to assess potential volume discounts in materials purchasing arrangements, and to explore the potential for economies of scale through reductions in per-unit fixed costs and labor requirements. The first production level is pilot-scale production of 350 vehicle battery packs per year (about 10,800 kWh/yr). This production level implies the manufacture of about 9,100 modules, or about 100,000 cells. The next production level is 7,700 vehicle packs per year (about 240 megawatt hours (MWh)/yr), or about two hundred thousand modules. These modules would be composed of about 2 million cells, depending on the configuration of the module. The third production level is high volume, mature production of 20,000

vehicle battery packs per year (about 624 MWh/yr). This production level implies the manufacture of about five hundred thousand modules, for a total production of over five million cells per year. Finally, a very high volume case is included, wherein 100,000 vehicle packs per year are manufactured (about 3,124 MWh/yr). These packs are composed of 2.6 million modules, and 26 million cells. All of these cases assume that 26 modules are used for each battery pack, with a resulting nominal pack voltage of 312 or 343 volts. Table 2-13 summarizes the cases examined in this analysis, and a few of the key estimates underlying each case. These and other estimates and assumptions are explained in more detail in the tables at the end of the chapter.

NiMH Battery Materials

Nickel is the most abundant material used in NiMH battery construction, as the anode grids and grid tabs are almost entirely composed of nickel, and the cathode foam substrate, anode active material, and cathode active material are substantially composed of nickel. The price of nickel is rather volatile, and analysis of the 27 month history of nickel trading on the London Metal Exchange (prior to April, 1998) reveals a high price of approximately $9,000 per tonne (or $9.00 per kg) in September, 1995, and a low price of $5,600 per tonne (or $5.60 per kg) early in 1998. The recent low price of nickel has reportedly caused one large supplier, Inco, Inc., to curtail production in order to prevent further nickel price declines.

New York nickel dealer prices closely track the London Metal Exchange prices, although they tend to be approximately 4-5% higher. These nickel exchange prices provide an indicator of the overall world nickel market, but these prices for raw nickel do not necessarily translate directly into per weight costs of the nickel used in various components of NiMH batteries. First, battery-grade nickel suitable for use in the negative and positive active materials costs somewhat more than that of generic raw nickel, on the order of $7-8 per kg versus $5-6 per kg. Second, processing and delivery costs must be included for products that require processing (rather than using raw nickel directly as an input), and the resulting prices for specific nickel-based products can therefore be much higher than the general market price for unprocessed nickel.

For example, Vista Metals, Inc. of Seekonk, Massachusetts, produces nickel tabs for use in the battery industry. These 0.005 gauge tabs are manufactured in widths of from one-eighth of an inch to three-eighths of an inch, and they are composed of a 201 alloy that is approximately 99.5% nickel. Prices in small orders of 25 to 100 pounds are on the order of $20 per pound ($44/kg), while larger orders of 1,000 pounds would cost just over $10 per pound ($22/kg) (Almeida, 1998). These prices are based on the current low price of nickel of approximately $2.50 per pound ($5.60/kg), and they would be adjusted with changes in the raw nickel price. Thus, for this nickel-based battery subcomponent, the final cost is almost four times the cost of raw nickel, even with high volume purchasing.

Because of the processing costs associated with manufacturing nickel-based battery components, their costs have been estimated explicitly, by gathering data from specific subcomponent material suppliers. For the computations of possible costs of different hydride alloys (Table 2-14), and of estimating the value-added share associated with production of spherical nickel

hydroxide and nickel foam (Figures 2-6 and 2-7 below), a battery-grade nickel cost of $7.50 per kg has been chosen, based on data in Sandrock (1997) and from battery manufacturers. This compares to an early-1999 prevailing cost of generic nickel of about $5.60 per kg.

Nickel Hydride Alloy Anode Material

Battery manufacturers use proprietary formulations for the nickel hydride materials used in the anode plates, and the exact specifications of these hydride materials are company secrets. Some manufacturers are using transition metal-based hydrides (AB_2), while most are using misch-metal based hydrides (AB_5). This analysis is for a transition metal-based hydride battery, and these hydrides are primarily composed of nickel, titanium, zirconium, vanadium, and chromium. For this analysis, the focus is on AB_2 hydride-based batteries because AB_2 hydrides have several advantages over AB_5 hydrides that may ultimately make them better choices for EV batteries. These advantages include higher hydrogen storage capacities, better oxidation and corrosion resistance, and higher volumetric electrode capacities (Liu, et al., 1996). AB_2 hydride alloys also are reported to have higher tolerance to impurities than AB_5 hydride alloys, and to potentially have lower processing costs associated with removing impurities (Magnuson and Gibbard, 1994).

The general composition of AB_2 hydride alloys is $(Ti_{2-x}Zr_xV_{4-y}Ni_y)_{1-z}Cr_z$. These alloys are designated as AB_2 because the Ti-Zr and Ni-V atomic fractions are in the ratio of 1:2. Transition metal hydrides with varying compositions have commonly been reported in the literature, and analysis of the relative advantages of different hydride compositions is an active area of research (Knosp, et al., 1998).

Deriving a cost for transition-metal hydride alloy material is complicated by variations in the chemical form of the various hydride alloys that can be used, and by the range of different costs for each metal that are observed in metals markets. Materials costs for titanium, vanadium, and zirconium are quite variable depending on the grade and form of the material required. For example, vanadium chips can be purchased in large quantities from Oremet Wah-Chang (an Allegheny-Teledyne subsidiary, formerly Teledyne Wah-Chang) for approximately $55.00 per pound (Jansen, 1998). Meanwhile, vanadium in a vanadium-nickel alloy sells for approximately $23.10 per kg, and in the "ferro" form, the cost can be as low as $11.39 per kg (Sandrock, 1997). Titanium chips in grade 2 or 3 sell for about $3.50 per pound, titanium sponge dust sells for about $4.50 per pound, and zirconium sponge sells for about $7.50 per pound, in a minus-20 mesh (Jansen, 1998).

Other metals that are sometimes used as additives in the production of the hydride alloy include chromium, manganese, cobalt, aluminum, and iron. Chromium sells for approximately $4.00 per pound at the present time, although this cost has fluctuated somewhat in recent years (Slagle, 1998). Of these other metal additives, only cobalt is expensive, with a price of nearly $60.00 per kg. Manganese, aluminum, and iron all have prices in the range of $0.44 to $2.30 per kg, in forms suitable for the formation of alloys (Sandrock, 1997).

Transition metal prices have been relatively stable for the past few years, and they are not expected to change appreciably in the near future (Slagle, 1998). A few years ago, chromium prices were somewhat lower than they are today, at

nearly $3.00 per pound, but this was substantially lower than the price was a few years prior to that. Thus, the cost of chromium has rebounded somewhat from a low of a few years ago, but still is relatively low compared to what it has been in the past several years.

I examined the materials costs for various hydride formulations available in the academic literature, and also discussed the present costs of suitable hydride alloys with industry experts. Table 2-14 presents cost estimates for different transition metal hydrides, based on formulas that are available in the literature. For comparison, I also include an analysis of a mischmetal (AB_5) alloy. Metals cost estimates are taken from the sources discussed above, and from Sandrock (1997).

These calculations show that production of a transition metal hydride with a cost of <$10.00 per kg is possible, particularly given that the formulas used have not necessarily been optimized for low manufacturing cost. A high volume cost estimate of $9.00 per kg for a metal hydride powder seems reasonable, given that the relatively expensive metals vanadium and zirconium can, to some degree, be substituted with titanium and nickel (respectively) in order to reduce costs, and that some of these metals are available at lower costs than assumed in the above analysis. The hydride production process requires that the hydride materials are melted together before being powdered, and there are opportunities to use metal alloys with combinations of various metals, rather than the pure form assumed for most of the metals in the tables. Also, some metals are available on the scrap market, or as byproducts from other industrial processes. For example, in addition to the titanomagnetite source that is mined in South Africa, Russia, and China to produce pure vanadium and vanadium-nickel alloys, vanadium is also available from fly ash residues from petroleum production. Approximately 16% of the world's vanadium production comes from this source (Andersson and Rade, 1998). Furthermore, the costs associated with melting and powdering the alloy are relatively small at high volumes.

Thus, based on the above analysis, and consultations with industry experts, hydride powder costs of $12.00 per kg are assumed for pilot-scale production, and costs as low as $9.00 per kg are estimated for high volume production. In the higher-cost case I also consider the possibility that hydride costs do not drop below $12.00 kg, in case inadequate scrap or byproduct materials are available to meet demand, or in case the high production levels assumed here (up to 100,000 packs per year) result in upward pressure on nickel, titanium, vanadium, zirconium, and/or chromium prices. It is important to note that the use of magnesium based hydrides could lead to lower hydride costs than $9.00 per kg (and potentially better performance -- see below), but since the use of magnesium hydrides is still under development, their use has not been assumed in NiMH battery Gen1 through Gen3. See Table 2-15, below, for further details of materials cost estimates for the different cases examined.

Spherical Nickel Hydroxide Cathode Material

Another key material to the construction of NiMH battery cells is spherical nickel hydroxide ($Ni(OH)_2$). This material forms the basis of the active material used in the positive electrode battery plates. Several manufacturers in the U.S., Canada, Europe, and Japan currently produce spherical nickel hydroxide. The Tanaka Corporation in Japan is the premier vendor, but Stark Chemical and the OMG

Company in Ohio also produce this material. OMG quotes a price of $14.00-15.00 per kg in large orders, depending on the specific grade required (Montgomery, 1997). Inco also produces this product, reportedly at a somewhat lower cost than OMG. Some industry experts believe that this material could potentially be produced for about $8.00 per kg, with improvements in processing techniques and equipment. Such improvements are actively being pursued in the both the U.S. and Japan, and in Japan, Ishikawajima-Harina Heavy Industries and Fujisaki Electric reportedly make high-quality spherical nickel hydroxide using a new type of nozzle developed by Fujisaki. The system reportedly produces particles one-sixth to one-fourth the size of the currently available product, and the companies say the new product can improve battery quality, and cut the cost of battery manufacturing (CALSTART, 1998).

Figure 2-6 shows the percentage of the total cost of the hydroxide that is the cost of the nickel needed for its production, and the percentage of the cost that is the cost of adding value. This analysis generally supports industry projections of about $8.00 per kg, because even at this cost, the value added still exceeds the cost of the nickel input. Thus, based on price quotes and an analysis of materials costs, I assume that nickel hydroxide costs $15.00 per kg in pilot-scale production, and that the cost drops steadily to as low as $8.00 per kg in the most optimistic, high-volume scenarios.

Figure 2-6:

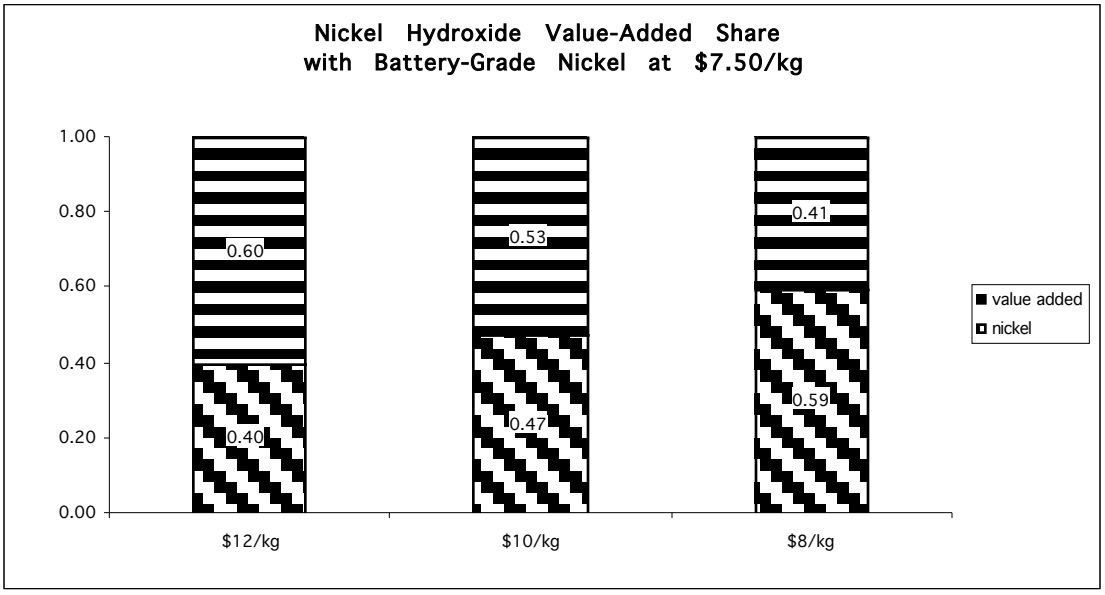

Cobalt Oxide Cathode Material

Cobalt oxide is used in the production of the positive plates, as an additive in small quantities. This material can be purchased for about $65.00-75.00 per kg, depending on order size (Montgomery, 1997). The quantities of cobalt oxide needed for the various battery designs are shown in the detailed cost tables at the end of the chapter.

Nickel Foam Cathode Substrate

The positive electrodes in NiMH EV batteries typically consist of a foam or felt nickel substrate material that is pasted with nickel hydroxide active electrode material and then dried and compressed. Nickel foam is used because it allows the production of a battery with a high level of active mass utilization, resulting in a greater amp-hour capacity than is possible with the current limits of sintered electrode technology. The standard nickel foam material, produced by companies such as the Eltech Systems Corp., is a 1.6 millimeter (mm) foam that weighs roughly 500 g per square meter (m^2). The Eltech product is produced with an electrolytic process, although the use of a carbonyl process is also possible. A 40 kWh battery would use roughly 75-100 m^2 of this material.

In order sizes of 1-2 million m^2 per year, the price of the Eltech material is presently in the range of $15.00-16.00 per m^2 (Cahill, 1997). At higher production volumes of several million m^2, prices of $12.00-14.00 per m^2 are considered possible, but this production volume is much higher than Eltech's current capacity of about 800,000 m^2 per year, and these prices are thus somewhat speculative (Cahill, 1997). The cost of nickel becomes an increasingly important variable at these production volumes, and low prices are thus more likely if the cost of nickel stays low. Nickel foam prices as low as $10.00 per m^2 are expected in the future by some analysts (Reisner, et al., 1996), but process breakthroughs may be required to realize these lower prices.

Figure 2-7 shows the percentages of the total price of the nickel foam that is the cost of the nickel needed for its production, the cost of the urethane foam that is used as a substrate during production (before being eventually vaporized), and the percentage of the price that is the cost of adding value, along with supplier profit. The urethane foam cost is estimated to be $1.63 per m^2, based on a cost estimate for SIF foam in a 110 PPI grade of $2.25 per board foot, cut to the proper width (Glennon, 1998). The foam would then shaved to a thickness of 1.6 mm before being coated with nickel. At $16.00 per m^2, the cost of adding value substantially exceeds the cost of the raw material input. Even at $10.00 per m^2, the raw material input accounts for less than 50% of the total cost. This suggests that $10.00 per m^2 is a reasonable estimate for high volume production in a competitive, mature battery industry. Based on this analysis and the supplier price quoted above, I use estimates of $20.00 per m^2 for production volumes of 350 packs per year, $15.00-16.00 per m^2 for production volumes of 7,700 packs per year, $14.00-15.00 per m^2 for production volumes of 20,000 packs per year, and $10.00-14.00 per m^2 for production volumes of 100,000 packs per year.

Figure 2-7:

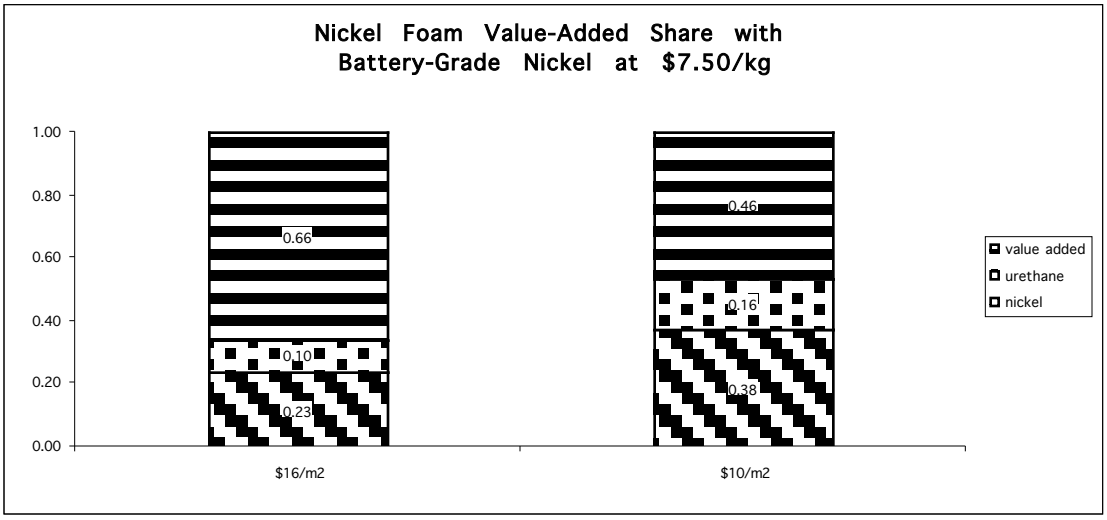

Metal Mesh or Grid Anode Substrate

The construction of the anode requires the use of a grid substrate, that acts both to support the metal hydride active material and as a current collector. The specific design of the substrate is not important, and any type of wire mesh, perforated metal, or expanded metal can be used (Fetcenko, et al., 1992). At present, nickel or nickel alloy is used for this purpose, although in principle it may be possible to use other less expensive metals. Initially, I assume the use of expandable nickel grid that is purchased in roll form and cut to the proper size. The cost of this material is presently about $0.30 per linear foot (Gifford, 1998). This cost is assumed for the Gen1 cases, but for the Gen2 and Gen3 technologies I assume that a less-expensive substrate can be used, with a cost of $0.10-0.15 per linear foot ($0.10-0.12 for 100,000 packs per year). This assumption is based on the fact that manufacturers are exploring the use of less expensive grid materials, and a variety of common metals could be manufactured in the proper form at a cost of about $0.10 per foot. This cost is equivalent to a cost of nearly $20 per kg,[18] and this would be sufficient to cover the metal input cost, and the costs of processing, plating, packaging and delivery, for such materials as nickel-plated stainless steel, copper, or iron. SAFT has recently stated that they have begun using nickel-plated steel for their negative electrode grids (Madery and Liska, 1999).

Separator Material

The separator material used in the NiMH EV battery is a 0.005-inch thick polypropylene material. This material is presently produced by only a few U.S., European, and Japanese companies, including the Freudenberg Company in Germany and the Hollingsworth-Vose Company in the U.S. The raw fiber used in producing the separator material is manufactured in Japan, and since the separator material demands the finest grade of fiber produced today, the cost of the basic fiber material used in the separator is greater than the cost of coarser

[18]Assuming a grid that is 0.025 cm thick, 8 cm wide, 90% open, and with a density of 8.8 mg/cm^3.

fibers produced for other purposes. Once obtained, the fibers are then blended and then processed to produce a "wettable" surface. Finally, a washing process is used to clean and finish the material. The cost of this material is currently in the range of $2.50-3.00 per m^2, depending on order size (Bennett, 1997). These costs are expected to perhaps $2.00-2.25 per m^2 decline as the market for NiMH batteries develops and the market for the separator material becomes more competitive.

Electrolyte Material

NiMH batteries use a liquid potassium hydroxide (KOH) electrolyte. Electrolyte requirements of approximately 2.0 grams per Ah are reported for nickel cadmium batteries (Scott and Rusta, 1978), and manufacturers of NiMH cells confirm that this is also the electrolyte fill level used for practical NiMH batteries (although levels as high as 4.5 grams (g) per Ah have been reported in the literature). KOH is produced and sold at a variety of locations around the country, and its final delivered cost is partly a function of how far it is transported. In small, drum quantities, KOH can be purchased for approximately $0.50 per pound. In tanker truck quantities of 45,000 pounds, the purchase price drops to $0.20 to $0.25 per pound, depending on transport distance (Banisch, 1998).

The standard product is a 45% KOH solution, whereas NiMH battery production calls for a 30% solution. The lower volume production scenario analyzed here would require approximately 60,000 pounds of 45% KOH per year, which would then be diluted to 90,000 pounds of 30% solution. The higher volume scenario would require approximately 1.2 million pounds of 45% solution. The electrolyte needs for the lower volume scenario could be met with electrolyte delivered in 55-gallon drums, since approximately 15 drums per month would be sufficient. The cost of KOH supplied in this form is assumed to be $0.50 per pound for the 45% solution, or $0.33 for the final 30% solution. For the higher volume scenarios, it is more reasonable to assume that the solution would be delivered by tanker truck, in 45,000-pound lots. For the 7,700 pack per year scenario, between 26 and 27 truck deliveries would be required per year, so deliveries would be taken about twice a month and the solution would be stored onsite in a storage tank between deliveries. The larger volume scenarios would require either more frequent deliveries, or multiple truck deliveries with larger storage tanks. At these volumes, the cost is assumed to be $0.20 per pound for the 45% solution, resulting in a final cost of $0.13 per pound for the 30% solution.

Casing Material

Various metal product companies and tool and die shops produce steel casings suitable for battery applications. Hudson Tool and Die, in New York, is a large metalworking operation that produces orders of metal casings in a huge range of pre-determined shapes, sizes, and tolerances. However, the casings that they produce have curved edges, while prismatic battery designs require casings with square edges. Even though they do not manufacture exactly the right type of case, they are familiar with that type of product and they were able to offer an approximate price quote on square edge designs in low and high volumes. For stainless steel cases that are approximately four inches wide, two inches deep, and six inches high, they estimate that in lower volumes of ten to fifty thousand

units per year, the cost for the cases and covers could be as high as $7.00-8.00 for each case/cover assembly. At higher volumes of over 100,000 units per year, the cost of the case would drop to approximately $3.00 per unit (Hynes, 1998).

Bison ProFab in New York confirms the price of at least $8.00 per case for the container and lid in quantities of a few thousand units per year, and suggests that costs could be as high as $13 per case in smaller volumes. In quantities of hundreds of thousands of units per year, it would be cost-effective to set up an automated extruding process for production of the cases. Bison estimates that this would reduce costs by approximately two-thirds, with resulting unit costs on the order of $3.00 per case (Pladson, 1998). Containers can also be produced from rolled tubes that are shaped through extrusion or die-like expansion processes and then fitted with a bottom piece, or they can be deep-drawn.

For this analysis, I use cost estimates for a rolled tube that is extruded into the proper shape.[19] A bottom piece is welded to the shaped container, and the resulting assembly is then leak-tested before delivery. These cost estimates are similar to those discussed above for the other processes. See the tables at the end of the chapter for details.

Lid, Terminals, and Miscellaneous Hardware

The costs of the terminals and pressure vents that are incorporated into the lid of each battery cell container are quite variable depending on production volume and the manufacturing processes used. In low volumes, these pieces would be custom machined at high per-unit costs, while in larger volumes it becomes economical to mass produce them with tool and die production lines, and to use metal stamping processes for some components.

The parts that compose each battery lid are the lid itself, two terminals, a vent, and other miscellaneous parts including a vent spring and O-rings. In low volume production, these parts would cost approximately $16 per lid assembly, while in higher volume production of over 2,000 packs per year, the costs would fall to about $2.80 per assembly, with the terminals and terminal assembly accounting for approximately $1.90 of this total. These cost estimates are based on quotes to battery manufacturers, from various suppliers of these parts.

Finally, there are some minor hardware costs associated with assembling separate cells into a module. I estimate that these battery terminal interconnects and module compression straps would add approximately $1.50 to the cost of each module.

Estimates of Key Materials Costs

Table 2-15 presents the principal materials cost estimates used in the analysis, for each case examined. In each case, except for the pilot-scale case, two different sets of materials cost estimates were used based on my assessment of a reasonable range of costs for each key material. In one case, relatively high materials cost estimates were used, and in the other case relatively low materials cost estimates were used. In this way, a range of manufacturing costs and selling prices was estimated for each case.

---

[19] These estimates were developed for a battery manufacturer by a supplier, and provided to me by the manufacturer.

Other Factory Costs

Labor and overhead rates, and costs associated with administration, marketing and distributing the battery have been derived from a variety of sources, including conversations with various battery manufacturers, and published cost estimates for other battery types (Hasuike, 1991; Quinn, et al., 1989). Distribution and service costs are assumed to be proportional to the weight of the battery, and thus are a lower percentage of costs for NiMH batteries than for lead-acid batteries (see tables for details). Costs associated with "marketing and other corporate costs" can be highly variable depending on the structure of the company, the number of product lines that it has, it's marketing strategy and requirements for marketing expenditures, the amount spent on product R&D, licensing arrangements, and other factors.

Given these uncertainties, I consider a range of costs for this category, from 2% of selling price in the lower cost cases (assuming direct sales to OEMs with no associated marketing costs, and no licensing costs), to 7% of selling price in the higher cost cases. Since the estimates for labor, overhead, marketing/corporate costs, warranty, and profit are expressed as a function of manufacturing cost or selling price, they vary for each case when the high and low materials cost estimates are used. Thus, to some degree, uncertainty in these parameters is incorporated into the analysis even when the percentages themselves do not vary.

With regard to manufacturer profit, it is reasonable to assume that the level of profit per module is more or less constant even as production volume increases. This is because automobile manufacturers tend to set the level of profit that they allow their suppliers to make. If profit margin is assumed to be constant, then the dollar profit per module is much higher in low volume production, when manufacturing costs are high. It is unlikely that automotive customers would allow profits to vary in this manner. For this analysis, the targeted level of profit is assumed to be approximately $40 per module.

Results of NiMH Battery Manufacturing Cost and Selling Price Analysis

Some representative results of the manufacturing cost analysis for 90-100 Ah NiMH cells are presented in Tables 2-16 through 2-20. These tables show detailed results of the cost analysis for one representative case for each technology generation (see Lipman (1999a) for a complete set of tables). Table 2-21 presents final selling prices and effective battery prices (including salvage value -- see discussion below) for each case examined. Figure 2-8 presents the results of the analysis in graphical form. The data presented in the figure are mean values for the range of selling prices that are shown in the tables. Figure 2-9 shows the difference between the high and low estimates for one technology at each production volume. The figure shows estimated prices for Gen1 technology at 350 packs per year, Gen2 technology at 7,700 packs per year, and Gen3 technology for 20,000 and 100,000 packs per year. Figure 2-4 presents selling price projections that were developed independently by GM Ovonics (Adams, 1995). The two projections compare favorably, particularly at the 20,000 pack per year level for Gen3 technology, where GM Ovonics projects a price of $240 per kWh, and this analysis results in a projected range of prices of $239-279 per kWh.

Figure 2-8:

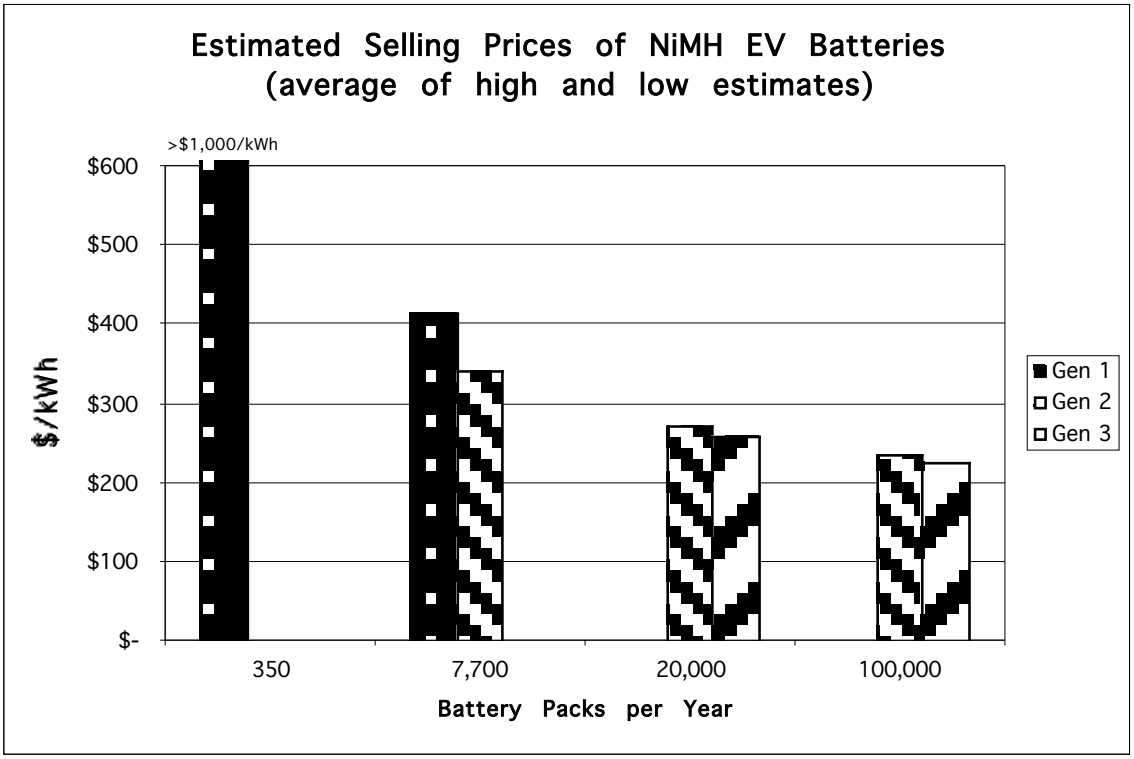

Figure 2-9:

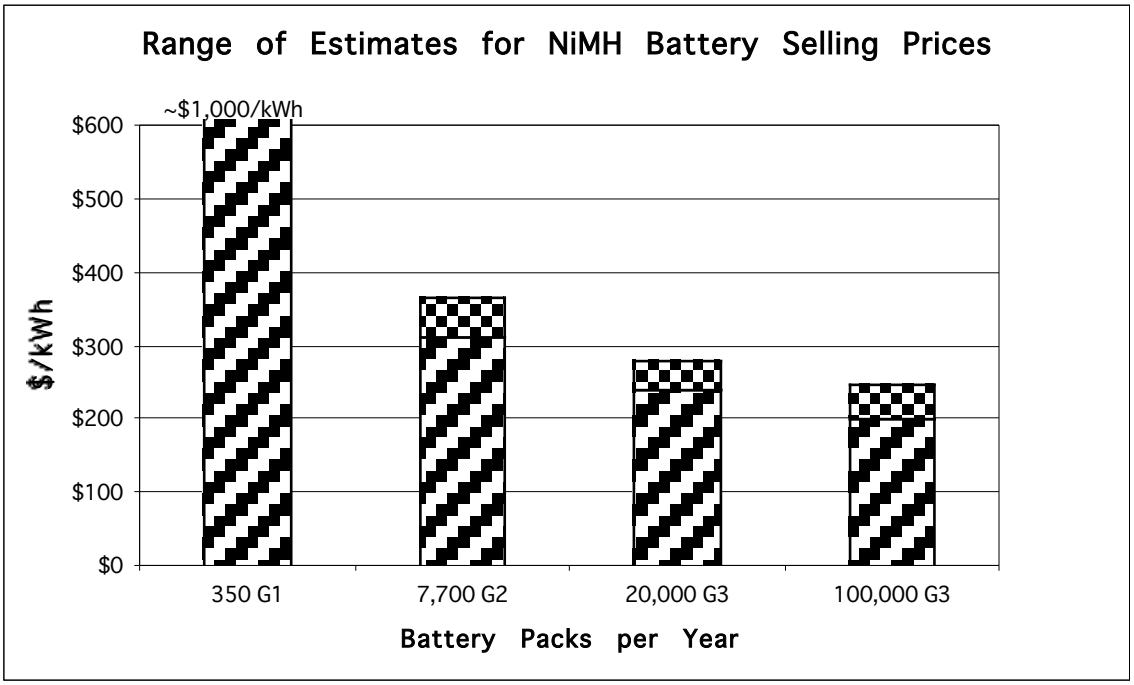

Potential Further Cost Reductions

It is important to note that the "effective" prices of NiMH batteries could be lower than the sale prices shown in Figures 2-8 and 2-9 for two reasons. First, the fact that NiMH batteries contain substantial quantities of nickel means that it likely would be economically attractive to recover this material at the end of the batteries' useful life. In contrast to the case of lead-acid batteries, where lead sells for only about $1.00 per kg and battery recycling efforts are driven largely by the desire to prevent lead from entering landfills, a NiMH battery recycling industry could presumably be driven by the opportunity to recover nickel and resell it at the prevailing price of $5.00-6.00 per kg. Recent research in Japan has shown that 96% of the nickel and cobalt in NiMH battery electrodes can be recovered, using sulfuric acid and oxalic acid recovery techniques (Zhang, et al., 1999).

Tables 2-16 through 2-20 show the potential salvage value of NiMH batteries, assuming that 40% of the battery weight is recovered as nickel, that the recovered nickel is sold at $5.60 per kg, and that processing costs consume 25% of the salvage value (in reality, of course, processing costs would be dependent on the scale of the recycling operation and the nature of the processes used). These figures show that battery salvage could result in a return of about 6-9% of battery selling price at the end of battery life, thereby lowering the "effective price" of the battery.

Second, it is possible that a secondary market for EV batteries may develop. Once the performance of a battery pack drops to a level below which it is not suitable for use in an EV, it could be reconfigured for other, less-demanding uses, such as load-leveling utility power systems or providing electrical energy storage for remote photovoltaic, fuel-fired generator, or other "off the grid" systems. This market has not yet been established, so I do not quantify the potential impact on battery "effective prices," but Ovonic Battery Company believes that the value of used NiMH EV batteries could potentially be comparable to the present cost of lead-acid batteries since they may be able to provide similar performance and cycle life once their useful life as an EV battery expires (Corrigan, 1998).

Furthermore, it is important to note that the above discussion of the costs of key NiMH battery value-added materials, such as nickel foam and nickel hydroxide, stopped short of pointing out that the costs of these materials could potentially drop to levels below those assumed here. In high volume production, many common products have total manufacturing costs that are only 25-30% higher than the cost of raw materials, whereas even the lowest costs assumed here for nickel foam and nickel hydroxide include costs of adding value that are on the order of the value of the underlying materials cost. Thus, further cost reductions of 20-25% in these materials may be possible with process innovation and increases in production volume. For nickel foam, cost reductions could become even more substantial if a suitable material could be produced without the use of the urethane substrate that is currently used in the nickel foam production process.

Finally, new active materials for NiMH EV batteries are currently under development, and the future use of these materials could result in performance improvements and cost reductions that would lead to prices significantly below those shown here. For example, Ovonic Battery Company is currently being

funded by NIST to develop magnesium-based metal hydride alloys that could potentially lower the weight of hydride needed by a factor of two, at a lower hydride cost than assumed here for the Ni-Ti based hydrides (Corrigan, 1998). The combination of these factors could reduce the cost of metal hydride material needed for a given level of anode performance by more than 50%. Work is also underway to increase the utilization of nickel hydroxide electrodes by up to about 50%, making use of quadrivalent nickel in the nickel electrode (Corrigan, 1998). Together, these two approaches could result in significant cost reductions in future generation NiMH batteries.

In order to account for this future potential of NiMH batteries that use next-generation active materials, costs of additional "Gen4" cases are also estimated. The detailed results for one of these cases are shown in Table 2-20. These cases assume that a magnesium-based hydride material with a storage capacity of approximately 600 milliampere hours (mAh) per gram can be produced in powdered form at a cost of $5-7 per kg (based on analysis of the potential costs of one recently-published magnesium hydride formula (Cui and Luo, 1999), using a calculation similar to those shown in Table 2-14). These cases also assume somewhat higher theoretical hydroxide utilization levels (363 mAh/g versus 291 mAh/g for Gen3). More fundamentally, these cases assume that the significant hydride stability and cycle life degradation problems that magnesium-based hydrides currently face are solved.

The 100,000 pack per year, higher cost cases also assume slightly lower costs for other battery materials than used in the Gen3 100,000 pack per year, higher cost cases (reflecting the likelihood that by the time Gen4 hydride materials become available, other materials costs may be nearer the lower end of the assumed ranges). As such, these examples represent somewhat optimistic future cases. However, the results ($155 to $211 per kWh, depending on the case) do not appear to be overly optimistic given the expectations of some manufacturers. Costs as low as $100 to $150 per kWh are expected by Ovonic Battery Company for batteries that use the next-generation, magnesium-based hydride materials (Corrigan, 1998). Based on the estimates made here, selling prices per kWh of these Gen4 modules would be about 25% lower than Gen3 cells produced in volumes of 20,000 packs per year and 100,000 packs per year (see Table 2-21).

The specific NiMH battery cost estimates used for each BEV case are shown in Appendix B. These cost estimates are reported in units of $ per pound, which is the form in which they are entered into the Lotus 1-2-3 spreadsheet model.

BEV Fuel and Maintenance Costs

Residential electricity prices in the Los Angeles area are currently about $0.10 per kWh, but the California Energy Commission (CEC) expects them to drop to about $0.08 per kWh by 2007 (Goeke, et al., 1998). Table 2-22 shows the CEC projections for residential electricity rates for various California utilities from 1998 to 2007.

Both Southern California Edison (SCE) and Los Angeles Department of Water and Power (LADWP) provide special rates to BEV owners. These rates are designed to reward off-peak electricity use, which helps the utilities to load-level demand and make electricity generation more efficient. These rates are

somewhat complicated because in order to determine peak versus off-peak demand, the utilities must install an additional electricity meter. The rates for BEV owners include a fixed daily or monthly cost, that helps to cover the cost of installing the time-of-use (TOU) meter, and a variable, per kWh cost. SCE has two different BEV TOU rate structures. The first one consists of a $0.12 meter charge per day, plus peak and off-peak rates of $0.29583 per kWh and $0.04085 per kWh during the summer, and $0.08969 per kWh and $0.04425 per kWh during the winter (Southern California Edison, 1998a). The second rate structure consists of both a $0.26 per day customer charge and a $0.12 per day meter charge, along with peak and off-peak rates of $0.24181 per kWh and $0.04085 per kWh during the summer, and $0.07342 per kWh and $0.04425 per kWh during the winter (Southern California Edison, 1998b). The second rate structure could potentially save money for customers that must use electricity during the peak period, which is defined as noon to 9 PM, every day. Clearly, these rate structures are designed to incentivize BEV recharging during off-peak periods.

The LADWP BEV TOU rate structure differs from the SCE structures in that there are two different peak periods, "high peak" and "low peak," and there is no distinction made between summer and winter electricity use. Also, the peak periods are defined as occurring during the week, from Monday to Friday, with weekends considered off-peak. The high peak period is from 1 PM to 5 PM, and the low peak period is from 10 AM to 1 PM and from 5 PM to 8 PM. The remaining period is a "base period" from 8 PM to 10 AM Monday through Friday, and all day Saturday and Sunday. The rate structure consists of a $6.00 monthly meter charge, plus a high peak rate of $0.17047 per kWh, a low peak rate of $0.11463 per kWh, a base rate of $0.06454 per kWh, and a discount for energy used to charge BEVs during the base period of $0.025 per kWh (LADWP, 1999).

Using LADWP's estimate of approximately 300 kWh per month for BEV recharging for an average user, and assuming that all BEV recharging occurs off-peak, these rates would yield average charges to an BEV owner of about $0.055 per kWh and $0.081 per kWh for the two SCE plans. The charge under the LADWP plan would be about $0.059 per kWh. There is thus some uncertainty in what charging would cost a BEV owner in the Los Angeles area, depending on whether or not they happen to be an SCE or an LADWP customer, whether or not they choose a TOU rate plan, which plan they choose (if an SCE customer), and when they actually choose to recharge their vehicle. Therefore, I use three different average electricity rates in the vehicle lifecycle cost calculations, for the central, high, and low cost cases. For the central case, I assume an electricity rate of $0.065 per kWh. This rate allows for the fact that some BEV charging might occur on-peak, even if the customer is operating under a TOU rate plan. For the high case, I use the non-TOU plan CEC rate projection of $0.08 per kWh, which also corresponds to the rate that an SCE "Plan 2" customer might pay if they used 300 kWh per month of electricity and charged off-peak, instead of on-peak.[20] For the low case, I use a rate of $0.055 per kWh, which is the least that a customer could expect to pay under the present SCE "Plan 1" rate structure.

---

[20] They would not choose this plan unless they expected to charge on-peak a significant percentage of the time, but at times they might be able to shift to off-peak charging, thus realizing a rate of about $0.08 per kWh.

BEV Maintenance and Repair Costs

Some analysts have suggested that maintenance and repair costs for BEVs may be much lower than for ICEVs due to the fewer moving parts and greater simplicity of electric drive systems, lower operating temperatures, lack of emission control systems, and reduced lubrication requirements. For example, Delucchi (1999) cites several studies that assume 50% lower maintenance costs for BEVs. Also cited are several studies of maintenance costs for BEVs actually in use, including England's electric milk delivery fleet. These studies report reductions in maintenance and repair costs of 35% to 60%, relative to costs for ICEVs.

Some analysts have been less optimistic about reduced maintenance and repair costs for BEVs, such as Dixon and Garber (1996) who assume that costs for BEVs will range from being the same as for ICEVs to being 33% lower. Also, in a recent Delphi survey, Vyas et al. (1997) found that the EV experts surveyed believe that early BEVs, introduced in 2000, will have about 20% higher fuel and maintenance costs than ICEVs, but that by 2020 BEVs will have about 15% lower fuel and maintenance costs.

For the lifecycle cost model used here, Delucchi (1999) concludes that BEVs will have about 25% lower maintenance and repair costs than ICEVs, once costs for BEV battery maintenance (but not replacement) are included. However, they assume that BEVs produced in low volume production will have no such advantage because of unfamiliarity with BEV technology in early years, and the potential for problems with technology that is new. The relative maintenance and repair costs for BEVs and ICEVs were estimated in detail by dividing components into different categories, based on whether the components were the same for both types of vehicles, whether the components provide a similar function but are different in detail (e.g., motor/controller systems versus ICE engines), and whether the components are entirely unique to one vehicle type or the other. Maintenance and repair costs were then estimated for "same" and "unique ICEV" components based on data for ICEV maintenance and repair, and for "similar" and "unique BEV" components based on the relative complexity of the systems.

The lifecycle cost results presented below reflect these estimated maintenance and repair costs. Maintenance and repair costs for Generation 1 vehicles thus have no cost advantage for BEVs, other than for differences due to the unique ICEV and BEV components. Maintenance and repair costs for the Generation 1 BEVs analyzed here are calculated to be $424 per year, on a levelized basis, compared with costs of $492 per year for ICEVs. Maintenance and repair costs for the Generation 2 and 3 BEVs reflect a 10% advantage over ICEVs, for "same" and "similar" components, along with differences due to the unique components. The calculated maintenance and repair costs for the Generation 2 and 3 BEVs amount to about $401 per year. Maintenance and repair costs for Generation 4 vehicles reflect a 30% advantage for BEVs, along with differences due to unique components. The calculated maintenance and repair costs for the Generation 4 BEVs amount to about $355 per year. These estimates are somewhat higher than other estimates of BEV maintenance and repair costs, which typically assume about 50% lower costs for BEVs. They may therefore be somewhat conservative, but they are probably more carefully

calculated than in most other BEV cost studies and they may prove to be more accurate.

BEV Consumer Cost and Lifecycle Cost Results

In order to produce consumer purchase cost and lifecycle costs for BEVs in each analysis year, the vehicle cost and performance model was run under assumptions for manufacturer production in each year, for each case (i.e. high cost, central cost, and low cost), and for each of the two production volume scenarios. For each model run, the motor cost, controller cost, battery cost, and electricity cost were varied. Also, some additional vehicle component costs and weights vary in the model depending on whether the vehicle technology production/development level is classified as "low," "medium," or "high." These components include items such as the onboard vehicle charger, for which three different sets of cost estimates are included in the model, and motors and motor controllers, for which different weights are specified depending on the level of development category. For purposes of this analysis, Generation 1 vehicles were considered to have a low development level, Generation 2 vehicles and Generation 3 vehicles were considered to have a medium development level, and Generation 4 vehicles were considered to have a high development level.

The following procedure was used to perform the model runs. First, for each vehicle generation included in the analysis, important vehicle characteristics such as vehicle weight and motor peak power requirement were calculated in the model depending on the characteristics of the battery pack assumed for that vehicle generation. For example, in vehicle Generation 1, the Gen2 NiMH battery technology was assumed, with a specific energy of 80 Wh per kg. The vehicle range was then defined so that the model would calculate the needed battery pack energy to be approximately 29 kWh. Given the 288-volt system assumed in the model, this size battery pack implies 100 Ah cells, which are the ones analyzed above.[21] Once the battery pack was sized in this manner, the total vehicle weight and peak power were calculated in the model. Next, component costs for the battery, motor, and controller, and electricity costs were determined for the particular production volume in that model year. This was done by calculating costs of the motors and controllers at 2,000 units per year, 20,000 units per year, and 200,000 units per year for the motor and controller of the proper power rating (i.e., 82 kW for Generation 1, 76 kW for Generation 2, etc.) using the low, central case, and high cost functions presented above. Then, a production volume function was fitted to the cost estimates using regression analysis. For batteries, costs were estimated at 7,700 units per year, 20,000 units per year, and 100,000 units per year based on the above analysis (only the latter two estimates were required for Gen4 batteries), and a continuous function was estimated with the regression procedure. The functional form that typically produced the highest r-squared value was a power function, with the following form:

---

[21] As noted above, there is a choice to be made between holding battery pack energy constant, holding vehicle range constant, or holding vehicle weight constant. Of these three choices, holding battery pack energy constant is the "middle ground" and it is the choice made here.

$$\text{Component cost (to the OEM)} = A * (PV)^B$$

Where:
PV = annual production volume in units per year
A and B are constants estimated through regression analysis

The calculated r-squared values were always over 0.87, and typically in the range of 0.91 to 0.99.[22] The various component cost functions, and the corresponding correlation and r-squared values, are shown in Table 2-23. The motor cost, controller cost, and battery cost functions estimated with the regression analyses were then entered into a spreadsheet, where component costs were calculated at each particular production volume for each model year and for the low, central case, and high cost cases. These component costs are shown in Tables B-1 and B-2 in Appendix B.

The calculated component costs were then entered and the vehicle cost model was run for each case (high, central, and low), for each year of the analysis, for that vehicle generation. Then, the procedure was repeated for the next generation of vehicles, with new vehicle specifications calculated if there was an assumed change in battery technology. For example, the Generation 2 vehicles were assumed to be equipped with Generation 3 NiMH batteries, which have a battery specific energy of 90 Wh per kg. The use of these batteries results in an increased range of 115 miles, even though the energy in the battery pack is held constant, because the vehicle is now lighter. The lower battery pack mass results in a mass decompounding effect from reduced support structure mass and a smaller drivetrain (e.g., the peak power required from the motor drops to 76 kW, from 82 kW in Generation 1, since the vehicle mass is reduced).

After the results were obtained for each case in the lower production volume scenario, component costs were estimated to reflect the production volumes in the higher volume scenario, and the model was run again for each case. The higher production volume estimates reach a peak of about 270,000 vehicles per year in the final year of the analysis, and this production volume is higher than the highest production volumes considered in the above drivetrain and battery cost analyses. Since further economies of scale are likely to be minimal at production volumes from 100,000 units per year to 300,000 units per year,[23] no economies of scale beyond production of 100,000 batteries per year and 200,000 drivetrain components per year were assumed for the central and high cost cases. For the low cost case, however, economies of scale for battery production above 100,000 units per year and drivetrain production above 200,000 units per year were extrapolated for the actual production volume, using the functions shown in Table 2-23. As expected, this produced only minor further decreases in final vehicle costs.

The vehicle purchase cost and lifecycle cost estimates for each scenario, along with key vehicle characteristics for each vehicle generation, are presented

---

[22] Values of 1.00 were obtained where the function was estimated with two higher production volume points, to obtain a better fit for the later generation, higher production volume cases. See Table 2-23.

[23] For example, see the chassis production cost estimates in Figure 2-3, where cost reductions beyond production of just 20,000 units per year are rather slow.

in Tables 2-24 and 2-25. Vehicle purchase costs for the two scenarios are shown in Figure 2-10 (at end of chapter), as a function of production volume. These results show that under the assumptions of this analysis, where battery pack energy is kept constant and battery performance improvements lead to a combination of increased range and decreased vehicle weight, vehicle consumer costs drop from a high of over $40,000 in the lower production highest cost case, to just over $24,000 in the higher production, lowest cost case. Even at production of about 270,000 units per year, however, initial purchase costs for the least expensive BEVs remain substantially higher than the $20,155 price of the gasoline ICE Taurus. In the central case, the lowest cost BEV has a purchase price that is about $5,800 higher than the $20,155 price of the ICE Taurus, and the low and high case vehicles have prices that are about $4,200 and $6,900 higher. From a lifecycle cost perspective, however, the least expensive BEV approaches parity with the conventional vehicle. Its $0.4136 cost per mile is within 1.7¢ per mile of the $0.3968 per mile lifecycle cost of the gasoline ICE. With a cost of $0.4415 per mile, the central case, high production volume, year 2026 BEV lifecycle cost remains about 4.5¢ per mile higher than that of the gasoline Taurus.

BEV Fleet Cost Results

With the calculated costs of owning and operating BEVs in each analysis year, total fleetwide costs of BEVs operated in the SCAB can be calculated. The levelized per-mile lifecycle cost estimates calculated in the vehicle-level model, corresponding to the average costs of owning and operating each vehicle in each year, can be used to calculate total fleet costs in each year. Then, discounted net present values for the entire fleet can be calculated.

These calculations have been performed in the Simulink model, using the same VMT schedule used in the Lotus 1-2-3 model to determine the levelized costs shown in Tables 2-24 and 2-25. The model first uses a VMT formula to closely reproduce a driving schedule that has been observed through the Energy Information Administration's Residential Transportation and Energy Consumption (RTEC) surveys, and then calculates an average annual VMT by assuming a 165,000 mile vehicle life. The RTEC data and the driving schedule calculated with the formula are shown in Table 2-26. With the exception of the first two years, in which the formula slightly underestimates VMT, the calculated results match the RTEC data quite closely, to within a few percent in most years. The model then calculates the levelized vehicle owning and operating costs using the average annual VMT estimate, 9,523 miles per year, and a 3.1% discount rate, over a calculated vehicle life of 17.3 years.

In order to more accurately calculate the fuel-cycle emissions associated with BEV and FCV use (in Chapter 6), the Simulink model uses the variable driving schedule estimated with the VMT formula, rather than the average annual VMT estimate. This makes the structure of the Simulink model more complicated, because the proper VMT estimate must be matched with each vintage of vehicle in each analysis year, but it more accurately represents the driving schedule profile, and thus annual emissions, of a typical vehicle. In order to reproduce the same net present value of vehicle owning and operating costs estimated in the Delucchi model with the average VMT estimate and a 3.1% discount rate, with the variable VMT estimates, a slightly different discount rate of 3.65% is needed. This discount rate is therefore selected as a central case value

for the net present value calculations (the sensitivity of results to the choice of a discount rate is discussed in Chapter 7). The net present values of fleetwide vehicle owning and operating costs, for each case, are shown in Tables 2-27 and 2-28. These estimates assume the same 165,000-mile and 17.3-year average vehicle lives assumed in Delucchi (1999).

It is worth noting that the RTEC driving schedule was of course developed through survey data collected from owners of gasoline ICEV vehicles. A reasonable question is to what extent BEVs will be driven along this same VMT driving schedule. Since there are only a few hundred conversion BEVs and no production BEVs that have been in use for more than a few years, this is an open question. On one hand, one might speculate the BEVs will be driven less because of their limited driving ranges and resulting unsuitability for long trips. On the other hand, though, BEVs may be used preferentially within a household for short trips, since they are easy to operate, would save "wear and tear" on any ICEVs in the household, and do not suffer the "cold start" emissions problem.

Interestingly, Honda has recently published data on the first year of use of the Honda EV-Plus vehicles. The results show that for the eight users for which annual projected driving data were published, a range of 4,769 miles per year to 17,263 miles per year was observed, with an average of 9,189 miles (Osawa and Kosaka, 1998). Honda further reports that overall driving data for 24 EV-Plus customers reveals an average annual mileage of 14,783 miles, of which 78.4% or 11,590 miles, was driven in the EV-Plus (Osawa and Kosaka, 1998). This is very close to the RTEC estimate for new conventional vehicles. Thus, some available evidence suggests that BEVs may be driven at similar annual VMT levels as conventional vehicles. Clearly, however, data collected over many years will be needed in order to compare the relative VMT driving schedules over the full lives of BEVs and conventional vehicles. For the FCVs analyzed in the following chapters, the vehicle cost and performance model is set to analyze FCVs with driving ranges similar to those of conventional vehicles. There is therefore no basis to assume that the annual driving schedule will be different (but of course it could ultimately prove to be due to fuel cost differences, variations in vehicle lifetimes, or other factors).

Tables and Large Figures for Chapter 2

Table 2-1: CARB ZEV Production Projections for California Market

	1998 Production		Production Projections			
	market share	production	2003	2004	2005	2006
GM	0.305	276,926	305,098 tot. 6,102 ZEV	305,098 tot. 6,102 ZEV	305,098 tot. 6,102 ZEV	305,098 tot. 12,204 ZEV
Ford	0.198	179,538	197,802 tot. 3,956 ZEV	197,802 tot. 3,956 ZEV	197,802 tot. 3,956 ZEV	197,802 tot. 7,912 ZEV
Toyota	0.209	189,290	208,547 tot. 4,171 ZEV	208,547 tot. 4,171 ZEV	208,547 tot. 4,171 ZEV	208,547 tot. 8,342 ZEV
Honda	0.161	145,855	160,693 tot. 3,214 ZEV	160,693 tot. 3,214 ZEV	160,693 tot. 3,214 ZEV	160,693 tot. 6,428 ZEV
Nissan	0.067	60,683	66,856 tot. 1,337 ZEV	66,856 tot. 1,337 ZEV	66,856 tot. 1,337 ZEV	66,856 tot. 2,674 ZEV
Chrysler	0.043	38,855	42,808 tot. 856 ZEV	42,808 tot. 856 ZEV	42,808 tot. 856 ZEV	42,808 tot. 1,712 ZEV
Mazda	0.018	16,516	18,196 tot. 364 ZEV	18,196 tot. 364 ZEV	18,196 tot. 364 ZEV	18,196 tot. 728 ZEV
Total	1.001	907,663	1,000,000 20,000 ZEV	1,000,000 20,000 ZEV	1,000,000 20,000 ZEV	1,000,000 40,000 ZEV

Source: (Evashenk, 1999)

Table 2-2: BEV Specifications and Characteristics

Component and Specification	Gen 1 Vehicles	Gen 2/3 Vehicles	Gen 4 Vehicles
NiMH Battery Pack:			
Technology	Generation 2	Generation 3	Generation 4
Pack energy	29.0 kWh	29.0 kWh	29.2 kWh
Pack maximum power	88.3 kW	82.3 kW	73.8 kW
Pack mass	804 kg	714 kg	538 kg
Maximum power density	242 W/kg	254 W/kg	302 W/kg
Pack specific energy (c/3)	80 Wh/kg	90 Wh/kg	120 Wh/kg
Cell capacity	100 Ah	100 Ah	100 Ah
Motor/controller:			
Type[a]	AC induction	AC induction	AC induction
Peak power rating	82 kW	76 kW	69 kW
System voltage	288 V	288 V	288 V
Vehicle driving range	109 miles	115 miles	126 miles
Vehicle drag coefficient	0.24	0.24	0.24
Vehicle efficiency: (wall outlet-to-wheels)			
On "FUDS*1.25" cycle[b]	75.2 mpg-eq (HHV) 2.05 mi/kWh	79.7 mpg-eq (HHV) 2.18 mi/kWh	87.1 mpg-eq (HHV) 2.38 mi/kWh
On FUDS cycle[b]	88.3 mpg-eq (HHV) 2.41 mi/kWh	92.7 mpg-eq (HHV) 2.53 mi/kWh	96.6 mpg-eq (HHV) 2.64 mi/kWh
Vehicle curb mass	1,560 kg	1,460 kg	1,306 kg
0-60 acceleration time	9.3 sec	9.4 sec	9.4 sec

Notes: FUDS = federal urban driving schedule; HHV = higher heating value; NiMH = nickel-metal hydride.

[a] High cost estimates reflect the use of a brushless permanent magnet motor/controller system.

[b] Vehicle efficiency values are approximate because vehicle efficiency is difficult to calculate accurately, and different models will produce different vehicle efficiency estimates. Values for efficiency on FUDS cycle are slightly inaccurate because when modeled over the FUDS cycle vehicle components are resized slightly, and drivetrain power and vehicle mass decrease relative to the values shown in the table. For comparison, the ICE Taurus has a calculated 20.1 mpg fuel economy over the FUDS cycle.

Table 2-3: Summary of BEV Purchase Price Estimates from Various Studies

Cost Study	Purchase Price[a]			
Argonne Nat'l Lab Vyas, 1999 #68:	2000 (<10K/yr)	2005 (10-40K/yr)	2010 (>40K)	2020 (>40K/yr)
Subcompact BEV	$18,500 - 41,400	$18,300 - 35,900	$17,800 - 32,900	$17,700 - 30,300
Minivan BEV	$27,300 - 63,500	$27,100 - 53,900	$26,300 - 49,400	$26,000-44,100
-Booz-Allen & Hamilton (1995):	1998	2000	2002	2004
Compact BEV	40,000/yr $28,173	41,000/yr $25,606	107,00/yr $20,060	243,000/yr $18,290
Office of Technology Assessment (1995):	Subcompact 2005	Mid-size 2005	Subcompact 2015	Mid-size 2015
Incremental Price (Retail Price Effect)	(24,000/yr) $8,090 - $56,600	(24,000/yr) $10,920 - $74,100	(24,000/yr) $2,260 - $25,560	(24,000/yr) $3,175 - $33,090
Sierra Research (1994):	1998	2002	2006	2010
Small Passenger BEV Incremental Price	$10,000 - 27,143	$7,000 - 17,254	$4,250 - 20,280	$10,000 - 22,726
U.S. GAO (1994):	Handbuilt	1000/yr	10,000/yr	100,000/yr
Compact BEV	$42,700	$28,700	$27,000	$18,300
NAVC Moomaw, 1994 #71	1995 (prototype)		1998 (20,000/yr)	
Purpose-Built BEV	$60,515		$22,945	
U.S. DOE (1995):	1998		2005	
Minivan BEV	$25,409-30,739		$20,318-22,254	
Rand Institute (1996):	1998-2002			
Compact BEV Incremental Price	$3,320-$15,000			

Note:

[a]Or incremental price where noted.

Table 2-4: Summary of BEV Lifecycle Cost Estimates from Various Studies

Cost Study	Lifecycle Cost[a]			
Argonne Nat'l Lab Vyas, 1999 #68:	2000 (<10K/yr)	2005 (10-40K/yr)	2010 (>40K/yr)	2020 (>40K/yr)
Subcompact BEV	$0.30-0.72/mi	$0.27-0.60/mi	$0.25-0.48/mi	$0.24-0.42/mi
Minivan BEV	$0.44-1.08/mi	$0.39-0.89/mi	$0.37-0.72/mi	$0.33-0.60/mi
NYSERDA	1998	2000	2002	2004
Booz-Allen & Hamilton (1995):	40,000/yr	41,000/yr	107,00/yr	243,000/yr
Compact BEV	$0.36/mi	$0.33/mi	$0.27/mi	$0.24/mi
NAVC Moomaw, 1994 #71			1998 (20,000/yr)	
Purpose-Built BEV			$0.24/mi	
Rand Institute (1996):	1998-2002		post 2002	
Passenger BEV Lifetime Incr. Cost	$1,316-$11,251		$1,234-$6,459	
Minivan BEV Lifetime Incr. Cost	$608-$15,799		$1,023-$7,920	
U.S. DOE (1995):	1998		2005	
Minivan BEV	$0.24-0.39/mi		$0.22-0.37/mi	
U.S. GAO (1994):	Near Term		Long Term	
Compact BEV	$0.53/mi		$0.31/mi	

Note:

[a]Or lifetime incremental cost where noted.

Table 2-5: EV Drivetrain Prices in Medium and High Volume Purchases

Motor/Controller System	Nom. Power Rating (Peak)	Price ($)	Type	Source
Advanced DC Brush	16.3 kW (62 kW)	900 (mot.) 700 (ctr.) 1,600 tot.	Medium vol. (>1,000 units)	Kochek, 1995 (motor); Booz-Allen, 1995 (controller)
Solectria AC Induction	unavail. (56 kW)	2,475 2,295 2,130	OEM cost@: 5,000/yr 10,000/yr 20,000/yr	TDM, 1997
Unique Mobility BPM	32 kW (53 kW)	6,100 4,009 2,405	OEM cost@: 2,000/yr 10,000/yr 100,000/yr	Barnes, 1998
Unique Mobility BPM	75 kW (100 kW)	8,028 3,537	OEM cost@: 2,000/yr 20,000/yr	Rankin, 1998
AC Induction	unavail. (50 kW)	2,000-3,000	High vol. target	Withheld by request
AC Induction	unavail. (50 kW)	10,000 3,400 1,300	OEM cost@: 3,000/yr 10,000/yr 20,000/yr	Withheld by request

Notes: AC = alternating current; BPM = brushless permanent magnet; DC = direct current.

Table 2-6: ANL Estimates of Materials Costs for 40 kW (continuous), 67 kW (peak) AC Induction Motors

Components	Mass (lb)	% of mass	Cost ($)	$/lb	% of cost
Core laminations, stator	51	44.6	110	2.16	43.0
Core laminations, rotor	28	24.5	60	2.14	23.5
Field winding (copper)	12.3	10.8	25	2.03	9.8
Housing (magnesium)	7.3	6.4	25	3.42	9.8
Shaft	7.0	6.1	3.5	0.50	3.0
Rotor conductor (alum.)	3.7	3.2	7.5	2.03	1.0
Miscellaneous	5.0	4.4	25	5.00	9.8
Total	114.3	100	256	2.24	100

Source: (Cuenca, 1995)

Table 2-7: ANL Estimates of Materials Costs for 20 kW (continuous), 52 kW (peak) DC Motors

Components	Mass (lb)	% of mass	Cost ($)	$/lb	% of cost
Core laminations, rotor	33.3	23.4	85	2.6	29.8
Core laminations, poles	29.5	20.8	65	2.2	22.8
Frame	29.0	20.4	20	0.7	7.0
Armature windings	10.3	7.2	21	2.0	7.4
Pole windings	9.5	6.6	19	2.0	6.7
Commutator	10.5	7.4	30	2.9	10.5
Shaft	9.3	6.5	5	0.5	1.8
Housing flanges	5.0	3.5	10	2.0	3.5
Miscellaneous	6.0	4.2	30	5.0	10.5
Total	142.3	100	285	2.0	100

Source: (Cuenca, 1995)

Table 2-8: ANL Estimates of Materials Costs for 32 kW (continuous), 32 kW (peak) BPM Motors

Components	Mass (lb)	% of mass	Cost ($)	$/lb	% of cost
Stator core	24.0	27.8	68	2.8	20.9
Stator winding	11.0	12.7	22	2.0	6.8
Housing	21.0	24.3	50	2.4	15.4
Rotor	16.0	18.5	26	1.6	8.0
Magnets	2.4	2.8	120	50.0	36.9
Attachment band	0.5	0.6	6	12.0	1.8
Shaft	5.5	6.4	3	0.6	0.9
Miscellaneous	6.0	6.9	30	5.0	9.2
Total	86.4	100	325	3.76	100

Source: (Cuenca, 1995)

Table 2-9: ANL Estimates of Prices for AC, DC, and BPM Motors

Element	AC 40 kW ($)	DC 20 kW ($)	BPM 32 kW ($)
Material cost	256	285	325
Assembly/testing (at 30%)	115	120	80
Assembly/testing (at 40%)	175	190	140
Total manufacturing cost	370-430	400-475	405-465
Gross margin (20%)	75-85	80-95	80-93
OEM price per unit	445-515	480-570	485-558

Source: (Cuenca, 1995)

Table 2-10: ANL Estimates of Specific Costs of Various Motors

Parameter	AC	DC	BPM
Average cost to OEM ($)	480	525	520
Maximum power (kW)	67	52	32
Specific cost ($/kW)	7.2	10.1	16.3

Source: (Cuenca, 1995)

Table 2-11: Comparison of Drivetrain "Cost to OEM" Estimates

System Type and Peak Rating	EEA/OTA Function[a]	Cuenca Estimate	Vyas et al. Estimate 2000/2020	Manuf. Forecast[b]
AC Induction				
50 kW peak	$1,800	$2,225-2,740	$1,375/$550	$2,130
70 kW peak	$2,400	$3,115-3,836	$1,925/$770	
90 kW peak	$3,000	$4,005-$4,932	$2,475/$990	
BPM				
50 kW peak	$1,890	$2,150-2,420	$1,450/$600	$2,405
70 kW peak	$2,520	$3,010-3,388	$2,030/$840	
90 kW peak	$3,150	$3,870-4,356	$2,610/$1,080	

Notes:

[a]For BPM, assumes that one-third of system cost is that of the motor, and that BPM motor costs are 15% higher than AC induction motor costs (reflecting statements in the OTA report).

[b]AC induction forecast is for Solectria 56 kW (peak) system at 20,000 units/yr, and BPM forecast is for 53 kW (peak) system at 100,000 units/yr (see above tables).

Table 2-12: Estimated and Observed Sealed Lead Acid Battery Prices (1998$)

Battery	**Voltage**	**Cap.**	**Manufacturer List**	**Retail Price**	**Wholesale (>100 mod./mo.)**
JC U1-31B	12 V	31 Ah	$100/mod. $269/kWh	$75/mod. $202/kWh	$39-55/mod. $105-149/kWh
			$150/mod.[a] $403/kWh[a]	$115/mod.[a] $309/kWh[a]	$70-80/mod.[a] $188-215/kWh[a]
JC GC1245V	12 V	45 Ah	$134/mod. $298/kWh	$98/mod. $218/kWh	$68-75/mod. $151-167/kWh
JC GC1265V	12 V	65 Ah	$160/mod. $246/kWh	$135/mod. $208/kWh	$90-110/mod. $138-169/kWh
Lipman(1999a) Estimate	12 V	75 Ah	N/A	N/A	$97-102/mod. $107-113/kWh

Notes:

[a]Battery module list, retail, and wholesale cost circa 1993, and in 1993$. Manufacturer list price is the price listed by Johnson Controls, retail price is the actual small order price by Cell-Con, Inc., and wholesale price is the large order (>100 modules/month) order price from Cell-Con, Inc.

Source: Johnson Controls battery costs from Mumma (1998).

Table 2-13: Cases Examined for NiMH Battery Production for BEVs

Production Level/ Technology	**350 packs/yr**	**7,700 packs/yr**	**20,000 packs/yr**	**100,000 packs/yr**
Generation 1 (~70 Wh/kg)	90 Ah cells 11 cells/module 30% overhead 25% labor	90 Ah cells 11 cells/module 20% overhead 16% labor	Not examined	Not examined
Generation 2 (~80 Wh/kg)	Not examined	100 Ah cells 10 cells/module 20% overhead 16% labor shorter plates	100 Ah cells 10 cells/module 12% overhead 10% labor shorter plates	100 Ah cells 10 cells/module 8% overhead 5% labor shorter plates
Generation 3 (~90 Wh/kg)	Not examined	Not examined	100 Ah cells 10 cells/module 12% overhead 10% labor shorter plates better hydride	100 Ah cells 10 cells/module 8% overhead 5% labor shorter plates better hydride
Generation 4 (~120 Wh/kg) Future Technology	*Not examined*	*Not examined*	*100 Ah cells* *10 cells/module* *12% overhead* *10% labor* *Mg-based hydride* *better hydroxide*	*100 Ah cells* *10 cells/module* *8% overhead* *5% labor* *Mg-based hydride* *better hydroxide*

Table 2-14: Costs of Nickel-Hydride Alloys (with pure alloying metals)

Alloy and Materials	Weight (kg)	Cost per kg	Cost per Wgt
$V_{22}Ti_{17}Zr_{16}Ni_{39}Cr_7$[a]			
Vanadium	1.12068	$23.10	$25.89
Titanium	0.8143	$9.92	$8.08
Zirconium	1.45952	$16.53	$24.13
Nickel	2.28969	$7.50	$17.17
Chromium	0.364	$8.82	$3.21
Total:	6.04819	**$12.97**	$78.47
$Ti_{0.5}Zr_{0.5}Mn_{0.9}Cr_{0.9}Ni_{0.4}$[b]			
Titanium	0.02395	$9.92	$0.24
Zirconium	0.04561	$16.53	$0.75
Manganese	0.049446	$2.29	$0.11
Chromium	0.0468	$8.82	$0.41
Nickel	0.023484	$7.50	$0.18
Total:	0.18929	**$8.95**	$1.69
$V_{15}Ti_{15}Zr_{16}Ni_{31}Cr_6Co_6Fe_6$[c]			
Vanadium	0.7641	$23.10	$17.65
Titanium	0.7185	$9.92	$7.13
Zirconium	1.45952	$16.53	$24.13
Nickel	1.82001	$7.50	$13.65
Chromium	0.312	$8.82	$2.75
Cobalt	0.35358	$57.87	$20.46
Iron	0.3351	$0.44	$0.15
Total:	5.76281	**$14.91**	$85.92
$V_{0.2}Ti_{0.2}Zr_{0.8}Ni_{0.8}Mn_{0.8}Co_{0.15}Al_{0.05}$[d]			
Vanadium	0.010188	$23.10	$0.24
Titanium	0.00958	$9.92	$0.10
Zirconium	0.072976	$16.53	$1.21
Nickel	0.046968	$7.50	$0.35
Manganese	0.043952	$2.29	$0.10
Cobalt	0.0088395	$57.87	$0.51
Aluminum	0.001349	$1.60	$0.00
Total:	0.1938525	**$12.91**	$2.50
$Ni_{3.5}Co_{0.8}Al_{0.3}Mn_{0.4}Mm$[e]			
Nickel	0.205485	$7.50	$1.54
Cobalt	0.047144	$57.87	$2.73
Aluminum	0.008094	$1.60	$0.01
Manganese	0.021976	$2.29	$0.05
Mischmetal	0.0575	$7.00	$0.40
Total:	0.340199	**$13.92**	$4.74

Notes: Where necessary, costs were converted from per pound costs to per kg costs using 2.204 lbs/kg. Quantities of materials were calculated by multiplying the molecular weight of each metal by the coefficient given in the chemical formula. The overall $/kg estimate was computed by dividing the total cost of metals by the total weight.

[a] Hydride formula is from (Fetcenko, et al., 1992).

[b] Hydride formula is from (Liu, et al., 1996).

[c] Hydride formula is from (Knosp, et al., 1998).

[d] Hydride formula is from (Venkatesan, et al., 1994).

[e] Hydride formula is from (Sakai, et al., 1992).

Table 2-15: Estimated Cost Ranges for Key NiMH Battery Materials

Production Level/ Technology	**350 packs/yr**	**7,700 packs/yr**	**20,000 packs/yr**	**100,000 packs/yr**
Generation 1 (~70 Wh/kg)	AG @$0.30/ft. CF @$20/m^2 MH @$12/kg NH @$15/kg SP @$3.00/$m^2$	AG @$0.30/ft. CF @$15-16/m^2 MH @$10-12/kg NH @$10-12/kg SP @$2.50-2.75/$m^2$	Not examined	Not examined
Generation 2 (~80 Wh/kg)	Not examined	AG @$0.10-0.15/ft. CF @$15-16/m^2 MH @$10-12/kg NH @$10-12/kg SP @$2.50-2.75/$m^2$	AG @$0.10-0.15/ft. CF @$14-15/m^2 MH @$9-12/kg NH @$9-10/kg SP @$2.25-2.50/$m^2$	AG @$0.10-0.12/ft. CF @$10-14/m^2 MH @$9-12/kg NH @$8-10/kg SP @$2.00-2.50/$m^2$
Generation 3 (~90 Wh/kg)	Not examined	Not examined	AG @$0.10-0.15/ft. CF @$14-15/m^2 MH @$9-12/kg NH @$9-10/kg SP @$2.25-2.50/$m^2$	AG @$0.10-0.12/ft. CF @$10-14/m^2 MH @$9-12/kg NH @$8-10/kg SP @$2.00-2.50/$m^2$
Generation 4 (~120 Wh/kg) Future Technology	*Not examined*	*Not examined*	*AG @$0.10-15/ft.* *CF @$14-15/m^2* *MH @$6-7/kg* *NH @$9-10/kg* *SP @$2.25-2.50/$m^2$*	*AG @$0.10-12/ft.* *CF @$10-12/m^2* *MH @$5-6/kg* *NH @$8-9/kg* *SP @$2.00-2.25/$m^2$*

Notes: AG = anode grid; CF = cathode foam; MH = metal hydride; NH = spherical nickel hydroxide; SP = separator. Gen4 case assumes that stability and performance improvements allow magnesium-based hydrides to become practical anode materials.

Table 2-16: NiMH Battery Manufacturing Costs in Pilot-Scale Production
(350 battery packs/year, 90 Ah cells (Gen1), 1.19 kWh/module, 31 kWh/pack)

Component	Materials (cost/qty.)	Materials (qty./mod)	Total ($/mod)	Total ($/kWh)
Plate Production:				
anode grids[a]	$0.30/ft	97.441 ft	$29.23	$24.61
cathode foam substrate[b]	$20.00/$m^2$	2.665 m^2	$53.30	$44.86
hydride alloy for anode[c]	$12.00/kg	3.13 kg	$37.23	$31.34
$Ni(OH)_2$ for cathode[d]	$15.00/kg	4.404 kg	$66.06	$55.61
cobalt oxide for cathode[e]	$70.00/kg	0.132 kg	$9.25	$7.79
grid tabs for electrodes[f]	$23.00/kg	0.259 kg	$5.96	$5.02
Mat'ls for Plate Production			**$201.04**	**$169.22**
Battery Assembly:				
KOH electrolyte[g]	$0.72/kg	1.98 kg	$1.43	$1.20
separator material[h]	$3.00/$m^2$	10.38 m^2	$31.14	$26.21
lid/terminals/pressure vent	$16.00/set	11 sets	$176.00	$148.15
containment	$7.50/cont.	11 containers	$82.50	$69.44
misc. hardware	$1.50/set	1 set	$1.50	$1.26
Mat'ls for Battery Assembly			**$292.56**	**$246.26**
Total Materials Cost:			**$493.60**	**$415.49**
Overhead (30% of manuf. cost)			$329.07	$276.99
Labor (25% of manuf. cost)			$274.22	$230.83
Total Manufacturing Cost:			**$1,096.88**	**$923.30**
Distribution and Service[i]			$5.66	$4.76
Marketing and Corporate Costs (10% of selling price)			$128.20	$107.91
Warranty (4% of selling price)			$51.28	$43.17
Profit (n/a for pilot)			$0.00	$0.00
Total Selling Price:			**$1,282.03 per module**	**$1,079.15 per kWh**
Less (Salvage Value)[j]			($30.68)	($25.82)
Total Effective Price[k]			**$1,251.35 per module**	**$1,053.33 per kWh**

Notes:
See text for sources of material cost estimates.

[a] Grids are assumed to be composed of nickel or nickel plated metal, and the quantity of material required was calculated by multiplying the height of each plate by the number of plates used.

[b] The nickel foam substrate material is assumed to be 1.6 mm thick prior to pasting and compression, and the quantity of material required was calculated by multiplying the area of each plate by the number of plates used.

[c] Quantity estimated by calculating the volume of the plates, subtracting the volume of the grids, and multiplying by the density of the hydride. The hydride density is estimated to be 5.69 g/cm^3.

[d] Quantity estimated by calculating the volume of the plates, subtracting the volume of the foam substrate, and multiplying by the density of the hydroxide. The hydroxide density is estimated to be 4.15 g/cm^3.

[e] Assuming that cobalt oxide content is 3% of the spherical nickel hydroxide content.

[f] Grid tabs are estimated to be 1.9 cm wide and 3.1 cm long. They are .005 inches or .0127 cm in thickness, and they are assumed to be composed of nickel with a density of 8.8 gm/cm^2.

[g] Assumes 2.0 g KOH electrolyte per Amp-hour (see text for source).

[h] Assuming that each electrode plate is inserted into a separator "envelope" and that the surface area of separator is thus twice the total plate surface area.

[i] Assuming same distribution and service cost per kg as in lead acid case, and in (Quinn, et al., 1989), of $0.31 per kg.

[j] Salvage value is based on an estimate that 40% of the battery weight can be reclaimed as nickel, that reclaimed nickel has a value of $5.60 per kg, that the weights of Gen1, Gen2, and Gen3 cells are 1.66 kg, 1.55 kg, and 1.38 kg, respectively, and that 25% of the salvage value is lost to processing costs.

[k] Effective price is selling price minus undiscounted salvage value.

Table 2-17: NiMH Battery Manufacturing Costs in Medium Volume Production
(7,700 battery packs per year, 100 Ah cells (Gen2), 1.2 kWh/module, 31 kWh/pack)

Component	Materials (cost/qty.)	Materials (qty./mod)	Lower Materials and Corporate Costs: Total ($/mod)	Lower Materials and Corporate Costs: Total ($/kWh)	Higher Materials and Corporate Costs: Total ($/mod)	Higher Materials and Corporate Costs: Total ($/kWh)
Plate Production:						
anode grids[a]	$0.10-0.15/ft	70.89 ft	$7.09	$5.91	$10.63	$8.86
cathode foam substrate[b]	$15-16/$m^2$	1.951 m^2	$29.26	$24.38	$31.21	$26.01
hydride alloy for anode[c]	$10-12/kg	3.092 kg	$30.92	$25.77	$37.11	$30.92
$Ni(OH)_2$ for cathode[d]	$10-12/kg	4.299 kg	$42.99	$35.82	$51.59	$42.99
cobalt oxide for cathode[e]	$65.00/kg	0.129 kg	$8.38	$6.99	$8.38	$6.99
grid tabs for electrodes[f]	$15.00/kg	0.210 kg	$3.15	$2.63	$3.15	$2.63
Mat'ls for Plate Production			**$121.80**	**$101.50**	**$142.07**	**$118.39**
Battery Assembly:						
KOH electrolyte[g]	$0.29/kg	2.00 kg	$0.58	$0.48	$0.58	$0.48
separator material[h]	$2.50-2.75/$m^2$	7.57 m^2	$18.93	$15.78	$20.83	$17.36
lid/terminals/pressure vent	$2.80/set	10 sets	$28.00	$23.33	$28.00	$23.33
containment	$2.90/cont.	10 cont.	$29.00	$24.17	$29.00	$24.17
misc. hardware	$1.50/set	1 set	$1.50	$1.25	$1.50	$1.25
Mat'ls for Battery Assembly			**$78.01**	**$65.01**	**$79.91**	**$66.59**
Total Materials Cost:			**$199.81**	**$166.51**	**$221.98**	**$184.98**
Overhead (20% of manuf. cost)			$62.44	$52.03	$69.37	$57.81
Labor (16% of manuf. cost)			$49.95	$41.63	$55.49	$46.25
Total Manufacturing Cost:			**$312.20**	**$260.17**	**$346.84**	**$289.04**
Distribution and Service[i]			$4.81	$4.00	$4.81	$4.00
Marketing and Corporate Costs (2% or 7% of selling price)			$7.54	$6.28	$30.93	$25.78
Warranty (4% of selling price)			$15.08	$12.57	$17.68	$14.73
Profit (12% of manuf. cost)			$37.46	$31.22	$41.62	$34.68
Total Selling Price:			**$377.10 /mod.**	**$314.25 /kWh**	**$441.88 /mod.**	**$368.23 /kWh**
Less (Salvage Value)[j]			($26.04)	($21.70)	($26.04)	($21.70)
Total Effective Price[k]			**$351.06 /mod.**	**$292.55 /kWh**	**$415.84 /mod.**	**$346.53 /kWh**

Notes: Same as previous table.

Table 2-18: NiMH Battery Manufacturing Costs in High Volume Production
(20,000 battery packs per year, 100 Ah cells (Gen3), 1.2 kWh/module, 31 kWh/pack)

Component	Materials (cost/qty.)	Materials (qty./mod)	Lower Materials and Corporate Costs: Total ($/mod)	Lower Materials and Corporate Costs: Total ($/kWh)	Higher Materials and Corporate Costs: Total ($/mod)	Higher Materials and Corporate Costs: Total ($/kWh)
Plate Production:						
anode grids[a]	$0.10-0.15/ft	71.69 ft	$7.17	$5.97	$10.75	$8.96
cathode foam substrate[b]	$14-15/$m^2$	1.840 m^2	$25.76	$21.47	$27.60	$23.00
hydride alloy for anode[c]	$9-12/kg	2.433 kg	$21.90	$18.25	$29.20	$24.33
$Ni(OH)_2$ for cathode[d]	$9-10/kg	4.055 kg	$36.49	$30.41	$40.55	$33.79
cobalt oxide for cathode[e]	$65.00/kg	0.122 kg	$7.91	$6.59	$7.91	$6.59
grid tabs for electrodes[f]	$15.00/kg	0.248 kg	$3.73	$3.11	$3.73	$3.11
Mat'ls for Plate Production			**$102.96**	**$85.80**	**$119.73**	**$99.78**
Battery Assembly:						
KOH electrolyte[g]	$0.29/kg	2.00 kg	$0.58	$0.48	$0.58	$0.48
separator material[h]	$2.25-2.50/$m^2$	7.18 m^2	$16.15	$13.46	$17.94	$14.95
lid/terminals/pressure vent	$2.80/set	10 sets	$28.00	$23.33	$28.00	$23.33
containment	$2.61/cont.	10 cont.	$26.10	$21.75	$26.10	$21.75
misc. hardware	$1.50/set	1 set	$1.50	$1.25	$1.50	$1.25
Mat'ls for Battery Assembly			**$72.33**	**$60.27**	**$74.12**	**$61.77**
Total Materials Cost:			**$175.28**	**$146.07**	**$193.85**	**$161.55**
Overhead (12% of manuf. cost)			$26.97	$22.47	$29.82	$24.85
Labor (10% of manuf. cost)			$22.47	$18.73	$24.85	$20.71
Total Manufacturing Cost:			**$224.72**	**$187.27**	**$248.53**	**$207.11**
Distribution and Service[i]			$4.56	$3.80	$4.56	$3.80
Marketing and Corporate Costs (2% or 7% of selling price)			$5.74	$4.78	$23.42	$19.52
Warranty (4% of selling price)			$11.48	$9.56	$13.39	$11.15
Profit (18% of manuf. cost)			$40.45	$33.71	$44.74	$37.28
Total Selling Price:			**$286.94 /mod.**	**$239.12 /kWh**	**$334.63 /mod.**	**$278.86 /kWh**
Less (Salvage Value)[j]			($24.70)	($20.58)	($24.70)	($20.58)
Total Effective Price[k]			**$262.25 /mod.**	**$218.54 /kWh**	**$309.94 /mod.**	**$258.28 /kWh**

Notes: Same as previous table.

Table 2-19: NiMH Battery Manufacturing Costs in High Volume Production
(100,000 battery packs per year, 100 Ah cells (Gen4), 1.2 kWh/module, 31 kWh/pack)

Component	Materials (cost/qty.)	Materials (qty./mod)	Lower Materials and Corporate Costs: Total ($/mod)	Lower Materials and Corporate Costs: Total ($/kWh)	Higher Materials and Corporate Costs: Total ($/mod)	Higher Materials and Corporate Costs: Total ($/kWh)
Plate Production:						
anode grids[a]	$0.10-0.12/ft	49.21 ft	$4.92	$4.10	$5.91	$4.92
cathode foam substrate[b]	$10-12/$m^2$	1.360 m^2	$13.60	$11.33	$16.32	$13.60
hydride alloy for anode[c]	$5-6/kg	1.607 kg	$8.03	$6.69	$9.64	$8.03
$Ni(OH)_2$ for cathode[d]	$8-9/kg	3.497 kg	$27.97	$23.31	$31.47	$26.22
cobalt oxide for cathode[e]	$65.00/kg	0.105 kg	$6.82	$5.68	$6.82	$5.68
grid tabs for electrodes[f]	$15.00/kg	0.197 kg	$2.96	$2.47	$2.96	$2.47
Mat'ls for Plate Production			**$64.31**	**$53.59**	**$73.11**	**$60.93**
Battery Assembly:						
KOH electrolyte[g]	$0.29/kg	2.00 kg	$0.58	$0.48	$0.58	$0.48
separator material[h]	$2.00-2.25/$m^2$	5.27 m^2	$10.54	$8.78	$11.86	$9.88
lid/terminals/pressure vent	$2.80/set	10 sets	$28.00	$23.33	$28.00	$23.33
containment	$1.90/cont.	10 cont.	$19.00	$15.83	$19.00	$15.83
misc. hardware	$1.50/set	1 set	$1.50	$1.25	$1.50	$1.25
Mat'ls for Battery Assembly			**$59.62**	**$49.68**	**$60.94**	**$50.78**
Total Materials Cost:			**$123.93**	**$103.27**	**$134.05**	**$111.71**
Overhead (8% of manuf. cost)			$11.40	$9.50	$12.33	$10.27
Labor (5% of manuf. cost)			$7.12	$5.94	$7.70	$6.42
Total Manufacturing Cost:			**$142.44**	**$118.70**	**$154.08**	**$128.40**
Distribution and Service[i]			$3.48	$2.90	$3.48	$2.90
Marketing and Corporate Costs (2% or 7% of selling price)			$3.71	$3.09	$14.82	$12.35
Warranty (4% of selling price)			$7.42	$6.18	$8.47	$7.06
Profit (20% of manuf. cost)			$28.49	$23.74	$30.82	$25.68
Total Selling Price:			**$185.55 /mod.**	**$154.62 / kWh**	**$211.66 /mod.**	**$176.39 /kWh**
Less (Salvage Value)[j]			($18.87)	($15.72)	($18.87)	($15.72)
Total Effective Price[k]			**$166.68 /mod.**	**$138.90 /kWh**	**$192.80 /mod.**	**$160.66 /kWh**

Notes: Same as previous table.

Table 2-20: NiMH Battery Manufacturing Costs in High Volume Production
(100,000 battery packs per year, 100 Ah cells (Gen4), 1.2 kWh/module, 31 kWh/pack)

Component	Materials (cost/qty.)	Materials (qty./mod)	Lower Materials and Corporate Costs: Total ($/mod)	Lower Materials and Corporate Costs: Total ($/kWh)	Higher Materials and Corporate Costs: Total ($/mod)	Higher Materials and Corporate Costs: Total ($/kWh)
Plate Production:						
anode grids[a]	$0.10-0.12/ft	49.21 ft	$4.92	$4.10	$5.91	$4.92
cathode foam substrate[b]	$10-12/m^2	1.360 m^2	$13.60	$11.33	$16.32	$13.60
hydride alloy for anode[c]	$5-6/kg	1.607 kg	$8.03	$6.69	$9.64	$8.03
$Ni(OH)_2$ for cathode[d]	$8-9/kg	3.497 kg	$27.97	$23.31	$31.47	$26.22
cobalt oxide for cathode[e]	$65.00/kg	0.105 kg	$6.82	$5.68	$6.82	$5.68
grid tabs for electrodes[f]	$15.00/kg	0.197 kg	$2.96	$2.47	$2.96	$2.47
Mat'ls for Plate Production			**$64.31**	**$53.59**	**$73.11**	**$60.93**
Battery Assembly:						
KOH electrolyte[g]	$0.29/kg	2.00 kg	$0.58	$0.48	$0.58	$0.48
separator material[h]	$2.00-2.25/m^2	5.27 m^2	$10.54	$8.78	$11.86	$9.88
lid/terminals/pressure vent	$2.80/set	10 sets	$28.00	$23.33	$28.00	$23.33
containment	$1.90/cont.	10 cont.	$19.00	$15.83	$19.00	$15.83
misc. hardware	$1.50/set	1 set	$1.50	$1.25	$1.50	$1.25
Mat'ls for Battery Assembly			**$59.62**	**$49.68**	**$60.94**	**$50.78**
Total Materials Cost:			**$123.93**	**$103.27**	**$134.05**	**$111.71**
Overhead (8% of manuf. cost)			$11.40	$9.50	$12.33	$10.27
Labor (5% of manuf. cost)			$7.12	$5.94	$7.70	$6.42
Total Manufacturing Cost:			**$142.44**	**$118.70**	**$154.08**	**$128.40**
Distribution and Service[i]			$3.48	$2.90	$3.48	$2.90
Marketing and Corporate Costs (2% or 7% of selling price)			$3.71	$3.09	$14.82	$12.35
Warranty (4% of selling price)			$7.42	$6.18	$8.47	$7.06
Profit (20% of manuf. cost)			$28.49	$23.74	$30.82	$25.68
Total Selling Price:			**$185.55 /mod.**	**$154.62 /kWh**	**$211.66 /mod.**	**$176.39 /kWh**
Less (Salvage Value)[j]			($18.87)	($15.72)	($18.87)	($15.72)
Total Effective Price[k]			**$166.68 /mod.**	**$138.90 /kWh**	**$192.80 /mod.**	**$160.66 /kWh**

Notes: Same as previous table.

Table 2-21: Selling and (Effective) Prices for 90-100 Ah NiMH BEV Batteries

Production Level/ Technology	**350 packs/yr**	**7,700 packs/yr**	**20,000 packs/yr**	**100,000 packs/yr**
Generation 1 90 Ah/cell (~70 Wh/kg)	$1,079/kWh ($1,053/kWh)	$386-441/kWh ($360-415/kWh)	Not examined	Not examined
Generation 2 100 Ah/cell (~80 Wh/kg)	Not examined	$314-368/kWh ($293-347/kWh)	$249-292/kWh ($227-271/kWh)	$209-260/kWh ($188-239/kWh)
Generation 3 100 Ah/cell (~90 Wh/kg)	Not examined	Not examined	$239-279/kWh ($219-258/kWh)	$201-248/kWh ($180-227/kWh)
Generation 4 100 Ah/cell (~120 Wh/kg)			*$186-211/kWh ($170-195/kWh)*	*$155-176/kWh ($139-161/kWh)*

Notes: Generation 4 is a somewhat speculative case, based on specifications of active materials that are in the laboratory research and development phase. Effective prices, shown in parentheses, are selling prices less salvage value.

Table 2-22: Projected Residential Sector Electricity Prices in California (1995$)

Year	**PG&E (cents/kWh)**	**SMUD (cents/kWh)**	**SCE (cents/kWh)**	**LADWP (cents/kWh)**
1998	10.09	7.81	10.51	9.25
1999	9.84	7.62	10.26	9.03
2000	9.58	7.42	9.99	8.79
2001	9.32	7.21	9.71	8.55
2002	7.90	6.14	8.38	6.78
2003	7.50	6.44	7.95	7.07
2004	7.61	6.77	8.01	7.40
2005	7.77	7.14	8.06	7.76
2006	7.96	7.54	8.23	8.16
2007	7.86	7.55	8.07	8.17

Source: (Goeke, et al., 1998).

Table 2-23: Component Cost Functions

Component	Cost Functions	Applicable Prod. Volume Range	Correlation (r^2 value)
82 kW motor (Gen1):			
High case - BPM ($)	Cost =18692(PV)$^{-0.24816}$	2,000-200,000 units/yr	-0.9345 (0.87)
Central case – AC ($)	Cost = 886	2,000-200,000 units/yr	N.A.
Low case – AC ($)	Cost =1450.9(PV)$^{-0.08805}$	2,000-200,000 units/yr	-0.9983 (0.99)
82 kW contr. (Gen1):			
High case ($)	Cost =24927(PV)$^{-.0.24643}$	2,000-200,000 units/yr	-0.9862 (0.97)
Central case ($)	Cost =33551(PV)$^{-.0.30340}$	2,000-200,000 units/yr	-0.9565 (0.91)
Low case ($)	Cost =37456(PV)$^{-0.32306}$	2,000-200,000 units/yr	-0.9539 (0.91)
Gen2 NiMH (Gen1):			
High case ($/kg)	Cost =86.38(PV)$^{-.0.1285}$	7,700-100,000 units/yr	-0.9440 (0.89)
Central case ($/kg)	Cost =88.69(PV)$^{-.0.1396}$	7,700-100,000 units/yr	-0.9598 (0.92)
Low case ($/kg)	Cost =92.60(PV)$^{-.0.1531}$	7,700-100,000 units/yr	-0.9736 (0.95)
76 kW motor (Gen2-3):			
High case - BPM ($)	Cost =17536(PV)$^{-0.24905}$	2,000-200,000 units/yr	-0.9362 (0.87)
Central case – AC ($)	Cost = 821	2,000-200,000 units/yr	N.A.
Low case – AC ($)	Cost =1344.8(PV)$^{-0.08805}$	2,000-200,000 units/yr	-0.9983 (0.99)
76 kW contr. (Gen2-3):			
High case ($)	Cost =24883(PV)$^{-.0.24818}$	2,000-200,000 units/yr	-0.9857 (0.97)
Central case ($)	Cost =38453(PV)$^{-.0.31966}$	2,000-200,000 units/yr	-0.9525 (0.91)
Low case ($)	Cost =39607(PV)$^{-0.33243}$	2,000-200,000 units/yr	-0.9523 (0.91)
Gen3 NiMH (Gen2-3):			
High case ($/kg)	Cost =46.71(PV)$^{-.0.07260}$	20,000-100,000 units/yr	-1.000 (1.00)
Central case ($/kg)	Cost =50.85(PV)$^{-.0.08862}$	20,000-100,000 units/yr	-1.000 (1.00)
Low case ($/kg)	Cost =57.00(PV)$^{-.0.10821}$	20,000-100,000 units/yr	-1.000 (1.00)
69 kW motor (Gen4):			
High case - BPM ($)	Cost =2592.4(PV)$^{-0.09011}$	20,000-200,000 units/yr	-1.000 (1.00)
Central case – AC ($)	Cost = 745	2,000-200,000 units/yr	N.A.
Low case – AC ($)	Cost =1358.1(PV)$^{-0.09733}$	20,000-200,000 units/yr	-1.000 (1.00)
69 kW contr. (Gen4):			
High case ($)	Cost =10464(PV)$^{-.0.17480}$	20,000-200,000 units/yr	-1.000 (1.00)
Central case ($)	Cost =4745.6(PV)$^{-.0.14225}$	20,000-200,000 units/yr	-1.000 (1.00)
Low case ($)	Cost =4537.8(PV)$^{-0.14847}$	20,000-200,000 units/yr	-1.000 (1.00)
Gen4 NiMH (Gen4):			
High case ($/kg)	Cost =68.15(PV)$^{-.0.11163}$	20,000-100,000 units/yr	-1.000 (1.00)
Central case ($/kg)	Cost =65.23(PV)$^{-.0.11334}$	20,000-100,000 units/yr	-1.000 (1.00)
Low case ($/kg)	Cost =62.34(PV)$^{-.0.11535}$	20,000-100,000 units/yr	-1.000 (1.00)

Notes: AC = AC induction motor; BPM = brushless permanent magnet motor; Cost = Cost to OEM; PV = production volume. Correlations are -1.000 for cases in which functions were estimated with only two points.

Table 2-24: Mid-Sized BEV Consumer Costs and Lifecycle Costs (Low Production Volume Scenario)

	Vehicle Characteristics	Production Volume	Low Case (1997$)	Central Case (1997$)	High Case (1997$)
Generation 1					
2003	109 mile range	10,000 vehicles/yr	$35,578 (56.61 ¢/mi)	$37,080 (59.12 ¢/mi)	$40,198 (63.68 ¢/mi)
2004	82 kW drivetrain	10,000 vehicles/yr	$35,578 (56.61 ¢/mi)	$37,080 (59.12 ¢/mi)	$40,198 (63.68 ¢/mi)
2005	Gen2 NiMH battery	10,000 vehicles/yr	$35,578 (56.61 ¢/mi)	$37,080 (59.12 ¢/mi)	$40,198 (63.68 ¢/mi)
2006	(29.0 kWh pack)	20,000 vehicles/yr	$33,842 (54.25 ¢/mi)	$35,389 (56.80 ¢/mi)	$38,068 (60.86 ¢/mi)
	1,560 kg curb weight				
Generation 2					
2007	115 mile range	20,600 vehicles/yr	$30,259 (52.20 ¢/mi)	$31,557 (54.55 ¢/mi)	$33,932 (58.28 ¢/mi)
2008	76 kW drivetrain	21,630 vehicles/yr	$30,161 (52.06 ¢/mi)	$31,468 (54.43 ¢/mi)	$33,816 (58.12 ¢/mi)
2009	Gen3 NiMH battery	22,712 vehicles/yr	$30,087 (51.95 ¢/mi)	$31,409 (54.34 ¢/mi)	$33,741 (58.02 ¢/mi)
2010	(29.0 kWh pack)	23,847 vehicles/yr	$30,001 (51.83 ¢/mi)	$31,322 (54.21 ¢/mi)	$33,627 (57.87 ¢/mi)
	1,460 kg curb weight				
Generation 3					
2011	115 mile range	25,039 vehicles/yr	$29,929 (51.72 ¢/mi)	$31,262 (54.12 ¢/mi)	$33,553 (57.77 ¢/mi)
2012	76 kW drivetrain	26,291 vehicles/yr	$29,842 (51.59 ¢/mi)	$31,177 (54.00 ¢/mi)	$33,440 (57.62 ¢/mi)
2013	Gen3 NiMH battery	27,606 vehicles/yr	$29,772 (51.48 ¢/mi)	$31,118 (53.91 ¢/mi)	$33,357 (57.50 ¢/mi)
2014	(29.0 kWh pack)	28,986 vehicles/yr	$29,685 (51.36 ¢/mi)	$31,033 (53.79 ¢/mi)	$33,257 (57.38 ¢/mi)
	1,460 kg curb weight				
Generation 4					
2015	126 mile range	30,436 vehicles/yr	$26,218 (44.23 ¢/mi)	$27,232 (46.04 ¢/mi)	$28,943 (48.75 ¢/mi)
2016	69 kW drivetrain	31,957 vehicles/yr	$26,203 (44.22 ¢/mi)	$27,175 (45.95 ¢/mi)	$28,870 (48.64 ¢/mi)
2017	Gen4 NiMH battery	33,555 vehicles/yr	$26,183 (44.20 ¢/mi)	$27,136 (45.89 ¢/mi)	$28,798 (48.54 ¢/mi)
2018	(29.3 kWh pack)	35,233 vehicles/yr	$26,139 (44.13 ¢/mi)	$27,078 (45.80 ¢/mi)	$28,741 (48.46 ¢/mi)
2019	1,306 kg curb weight	36,995 vehicles/yr	$26,081 (44.04 ¢/mi)	$27,039 (45.74 ¢/mi)	$28,670 (48.36 ¢/mi)
2020		38,844 vehicles/yr	$26,046 (43.99 ¢/mi)	$26,984 (45.65 ¢/mi)	$28,614 (48.28 ¢/mi)
2021		40,787 vehicles/yr	$25,987 (43.90 ¢/mi)	$26,943 (45.59 ¢/mi)	$28,535 (48.16 ¢/mi)
2022		42,826 vehicles/yr	$25,944 (43.83 ¢/mi)	$26,888 (45.50 ¢/mi)	$28,481 (48.08 ¢/mi)
2023		44,967 vehicles/yr	$25,895 (43.76 ¢/mi)	$26,856 (45.45 ¢/mi)	$28,408 (47.98 ¢/mi)
2024		47,216 vehicles/yr	$25,851 (43.69 ¢/mi)	$26,800 (45.37 ¢/mi)	$28,356 (47.90 ¢/mi)
2025		49,576 vehicles/yr	$25,801 (43.62 ¢/mi)	$26,761 (45.30 ¢/mi)	$28,284 (47.80 ¢/mi)
2026		52,055 vehicles/yr	$25,760 (43.55 ¢/mi)	$26,704 (45.22 ¢/mi)	$28,230 (47.72 ¢/mi)

Table 2-25: Mid-Sized BEV Consumer Costs and Lifecycle Costs (High Production Volume Scenario)

	Vehicle Characteristics	Production Volume	Low Case (1997$)	Central Case (1997$)	High Case (1997$)
Generation 1					
2003	109 mile range	20,000 vehicles/yr	$33,842 (54.25 ¢/mi)	$35,389 (56.80 ¢/mi)	$38,068 (60.86 ¢/mi)
2004	82 kW drivetrain	40,000 vehicles/yr	$32,399 (52.25 ¢/mi)	$33,990 (54.84 ¢/mi)	$36,288 (58.46 ¢/mi)
2005	Gen2 NiMH battery	54,570 vehicles/yr	$31,719 (51.35 ¢/mi)	$33,308 (53.93 ¢/mi)	$35,428 (57.36 ¢/mi)
2006	(29.0 kWh pack)	59,850 vehicles/yr	$31,613 (51.17 ¢/mi)	$33,212 (53.76 ¢/mi)	$35,294 (57.15 ¢/mi)
	1,560 kg curb weight				
Generation 2					
2007	115 mile range	65,460 vehicles/yr	$28,499 (49.58 ¢/mi)	$29,925 (52.14 ¢/mi)	$31,843 (55.46 ¢/mi)
2008	76 kW drivetrain	71,520 vehicles/yr	$28,373 (49.35 ¢/mi)	$29,835 (52.00 ¢/mi)	$31,689 (55.25 ¢/mi)
2009	Gen3 NiMH battery	78,070 vehicles/yr	$28,247 (49.21 ¢/mi)	$29,711 (51.82 ¢/mi)	$31,562 (55.08 ¢/mi)
2010	(29.0 kWh pack)	85,110 vehicles/yr	$28,147 (49.05 ¢/mi)	$29,602 (51.65 ¢/mi)	$31,412 (54.87 ¢/mi)
	1,460 kg curb weight				
Generation 3					
2011	115 mile range	92,680 vehicles/yr	$28,025 (48.87 ¢/mi)	$29,515 (51.52 ¢/mi)	$31,301 (54.72 ¢/mi)
2012	76 kW drivetrain	100,790 vehicles/yr	$27,928 (48.72 ¢/mi)	$29,407 (51.36 ¢/mi)	$31,157 (54.53 ¢/mi)
2013	Gen3 NiMH battery	109,460 vehicles/yr	$27,819 (48.56 ¢/mi)	$29,384 (51.33 ¢/mi)	$31,101 (54.47 ¢/mi)
2014	(29.0 kWh pack)	118,690 vehicles/yr	$27,724 (48.41 ¢/mi)	$29,339 (51.29 ¢/mi)	$31,020 (54.38 ¢/mi)
	1,460 kg curb weight				
Generation 4					
2015	126 mile range	128,500 vehicles/yr	$24,936 (42.29 ¢/mi)	$26,068 (44.25 ¢/mi)	$27,307 (46.43 ¢/mi)
2016	69 kW drivetrain	138,890 vehicles/yr	$24,873 (42.19 ¢/mi)	$26,063 (44.24 ¢/mi)	$27,282 (46.41 ¢/mi)
2017	Gen4 NiMH battery	149,840 vehicles/yr	$24,805 (42.09 ¢/mi)	$26,041 (44.21 ¢/mi)	$27,240 (46.36 ¢/mi)
2018	(29.3 kWh pack)	161,360 vehicles/yr	$24,751 (42.01 ¢/mi)	$26,036 (44.21 ¢/mi)	$27,216 (46.34 ¢/mi)
2019	1,306 kg curb weight	173,430 vehicles/yr	$24,684 (41.90 ¢/mi)	$26,016 (44.19 ¢/mi)	$27,177 (46.29 ¢/mi)
2020		186,020 vehicles/yr	$24,630 (41.82 ¢/mi)	$26,010 (44.18 ¢/mi)	$27,158 (46.28 ¢/mi)
2021		199,090 vehicles/yr	$24,570 (41.73 ¢/mi)	$25,994 (44.16 ¢/mi)	$27,120 (46.23 ¢/mi)
2022		212,610 vehicles/yr	$24,525 (41.66 ¢/mi)	$25,990 (44.15 ¢/mi)	$27,102 (46.22 ¢/mi)
2023		226,520 vehicles/yr	$24,469 (41.57 ¢/mi)	$25,990 (44.15 ¢/mi)	$27,102 (46.22 ¢/mi)
2024		240,790 vehicles/yr	$24,426 (41.51 ¢/mi)	$25,990 (44.15 ¢/mi)	$27,102 (46.22 ¢/mi)
2025		255,330 vehicles/yr	$24,370 (41.42 ¢/mi)	$25,990 (44.15 ¢/mi)	$27,102 (46.22 ¢/mi)
2026		270,100 vehicles/yr	$24,335 (41.36 ¢/mi)	$25,990 (44.15 ¢/mi)	$27,102 (46.22 ¢/mi)

Table 2-26: Estimates of Vehicle Miles Traveled by Vehicle Age

Vehicle Age (Years)	RTEC Data[a]	VMT Formula[b]	Average Value[c]
1	12,780	11,561	9,523
2	13,635	13,973	9,523
3	12,277	13,208	9,523
4	12,197	12,485	9,523
5	11,210	11,801	9,523
6	10,612	11,155	9,523
7	11,058	10,545	9,523
8	10,162	9,968	9,523
9	9,614	9,421	9,523
10	9,167	8,906	9,523
11	8,720	8,419	9,523
12	8,391	7,957	9,523
13	8,061	7,522	9,523
14	7,261	7,110	9,523
15	6,460	6,721	9,523
16	5,737	6,353	9,523
17	5,416	6,005	9,523
18	5,114	5,677	2,857
19	4,829	5,365	0
20	4,559	5,072	0

Notes:

[a] Data from Residential Transportation Energy Consumption survey (EIA, 1993b).

[b] These are the estimates used in the Simulink model. The estimates are derived from the following formula, in Delucchi (1999):

$$Cumulative\ VMT(miles) = \left[266,799 + (-270,021 \times Veh.\ Age)^{-0.0563}\right]$$

[c] These values were calculated by Delucchi (1999) assuming a total vehicle life of 165,000 miles. Using the driving schedule calculated with the above formula, this results in a vehicle life of 17.3 years.

Table 2-27: Fleetwide Vehicle Ownership and Operating Costs for BEVs by Year (2000$) - Low Production Volume Scenario

Year	Low Case	Central Case	High Case
2003	$71,513,741	$74,684,550	$80,445,064
2004	$157,947,571	$164,950,723	$177,673,579
2005	$239,649,283	$250,274,963	$269,578,985
2006	$382,429,785	$399,751,567	$429,773,749
2007	$533,432,460	$557,618,177	$598,404,933
2008	$682,255,991	$713,204,125	$764,397,058
2009	$831,425,192	$869,242,001	$930,846,514
2010	$981,305,163	$1,026,027,540	$1,098,066,266
2011	$1,132,295,538	$1,184,049,075	$1,266,592,787
2012	$1,284,740,463	$1,343,664,475	$1,436,753,174
2013	$1,439,071,798	$1,505,352,757	$1,609,032,033
2014	$1,595,631,460	$1,669,413,378	$1,783,859,063
2015	$1,727,870,423	$1,806,915,947	$1,928,978,234
2016	$1,856,587,031	$1,940,122,258	$2,069,106,259
2017	$1,989,321,895	$2,077,286,994	$2,213,302,804
2018	$2,126,180,061	$2,218,649,266	$2,362,016,793
2019	$2,267,332,101	$2,364,641,617	$2,515,523,121
2020	$2,388,698,795	$2,489,829,642	$2,646,601,911
2021	$2,506,439,442	$2,611,355,645	$2,773,404,320
2022	$2,631,383,320	$2,740,352,652	$2,908,193,374
2023	$2,741,297,644	$2,853,625,466	$3,025,998,345
2024	$2,851,517,740	$2,967,246,287	$3,144,293,910
2025	$2,969,421,385	$3,088,897,667	$3,271,067,162
2026	$3,094,158,268	$3,217,588,343	$3,405,315,839
2027	$2,925,776,081	$3,041,922,261	$3,218,442,769
2028	$2,687,635,950	$2,793,816,251	$2,955,169,825
2029	$2,458,832,139	$2,555,391,539	$2,702,172,001
2030	$2,238,659,923	$2,325,906,005	$2,458,673,826
2031	$2,026,481,236	$2,104,713,360	$2,223,952,202
2032	$1,830,917,175	$1,901,236,052	$2,008,536,193
2033	$1,645,642,530	$1,708,742,170	$1,804,984,564
2034	$1,466,286,375	$1,522,496,469	$1,608,096,424
2035	$1,292,437,916	$1,342,019,365	$1,417,301,012
2036	$1,123,595,461	$1,166,696,998	$1,232,000,503
2037	$959,221,432	$996,056,949	$1,051,644,114
2038	$798,924,149	$829,616,628	$875,813,314
2039	$642,192,124	$666,886,600	$703,913,075
2040	$488,586,292	$507,371,501	$535,488,168
2041	$337,658,865	$350,634,845	$370,024,474
2042	$188,996,331	$196,250,471	$207,096,151
2043	$42,188,269	$43,806,051	$46,227,880
NPV in 2000 (3.65% d.r.)	$26,655,722,955	$27,779,411,066	$29,525,907,762

Table 2-28: Fleetwide Vehicle Ownership and Operating Costs for BEVs by Year (2000$) - High Production Volume Scenario

Year	Low Case	Central Case	High Case
2003	$137,064,846	$143,507,525	$153,765,282
2004	$429,684,552	$450,558,865	$481,248,879
2005	$829,688,548	$870,652,679	$928,125,545
2006	$1,264,379,617	$1,327,367,640	$1,413,552,459
2007	$1,707,045,975	$1,792,912,522	$1,908,583,565
2008	$2,167,439,613	$2,278,122,978	$2,424,055,190
2009	$2,651,536,598	$2,788,206,943	$2,966,034,720
2010	$3,161,576,903	$3,325,499,339	$3,536,680,657
2011	$3,699,559,607	$3,892,896,678	$4,139,100,326
2012	$4,268,044,875	$4,492,582,725	$4,775,537,150
2013	$4,869,245,985	$5,128,647,420	$5,450,161,153
2014	$5,505,373,806	$5,803,844,278	$6,165,522,717
2015	$6,081,644,452	$6,406,964,803	$6,796,433,309
2016	$6,669,751,377	$7,021,609,769	$7,437,150,620
2017	$7,296,290,615	$7,678,488,686	$8,122,005,318
2018	$7,963,025,278	$8,379,713,777	$8,853,086,705
2019	$8,670,610,046	$9,126,469,643	$9,631,372,062
2020	$9,373,346,661	$9,870,708,752	$10,405,911,287
2021	$10,058,728,147	$10,599,188,398	$11,162,434,283
2022	$10,744,969,619	$11,330,879,949	$11,921,924,982
2023	$11,461,303,486	$12,094,798,930	$12,715,263,624
2024	$12,220,271,523	$12,903,591,235	$13,555,650,428
2025	$13,018,435,967	$13,753,433,365	$14,439,231,634
2026	$13,852,243,169	$14,640,937,003	$15,362,268,343
2027	$13,219,449,163	$13,974,150,326	$14,658,218,836
2028	$12,225,662,139	$12,924,491,133	$13,553,412,854
2029	$11,263,494,693	$11,908,193,125	$12,483,595,504
2030	$10,329,707,505	$10,921,266,288	$11,444,624,833
2031	$9,421,298,482	$9,960,301,236	$10,433,042,168
2032	$8,568,569,917	$9,061,120,055	$9,489,369,569
2033	$7,749,444,506	$8,198,235,653	$8,585,025,813
2034	$6,948,230,978	$7,353,648,353	$7,699,971,394
2035	$6,162,690,642	$6,524,918,420	$6,831,697,409
2036	$5,390,573,165	$5,709,482,999	$5,977,608,937
2037	$4,629,811,563	$4,905,211,765	$5,135,288,506
2038	$3,878,866,126	$4,110,466,457	$4,303,186,477
2039	$3,135,807,386	$3,323,233,223	$3,479,045,064
2040	$2,398,631,610	$2,541,996,773	$2,661,179,861
2041	$1,665,778,313	$1,765,341,155	$1,848,110,264
2042	$936,295,445	$992,257,415	$1,038,780,016
2043	$209,403,985	$221,919,970	$232,324,824
NPV in 2000 (3.65% d.r.)	$106,756,263,470	$112,625,945,746	$118,673,507,799

Figure 2-3:

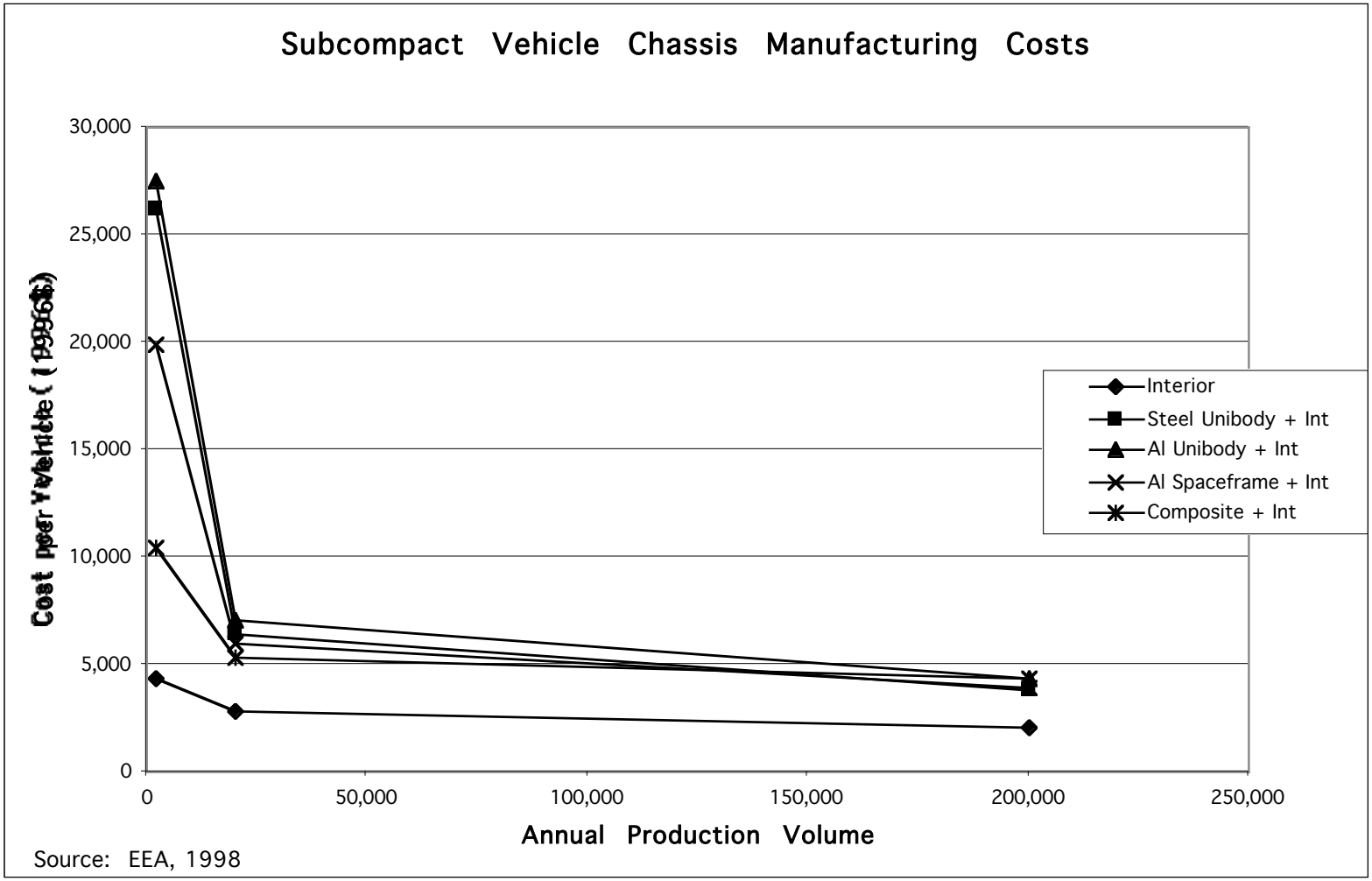
Subcompact Vehicle Chassis Manufacturing Costs
30,000
25,000
20,000
15,000
10,000
5,000
0
0
50,000
100,000
150,000
200,000
250,000
Annual Production Volume
Interior
Steel Unibody + Int
Al Unibody + Int
Al Spaceframe + Int
Composite + Int
Source: EEA, 1998

Figure 2-10:

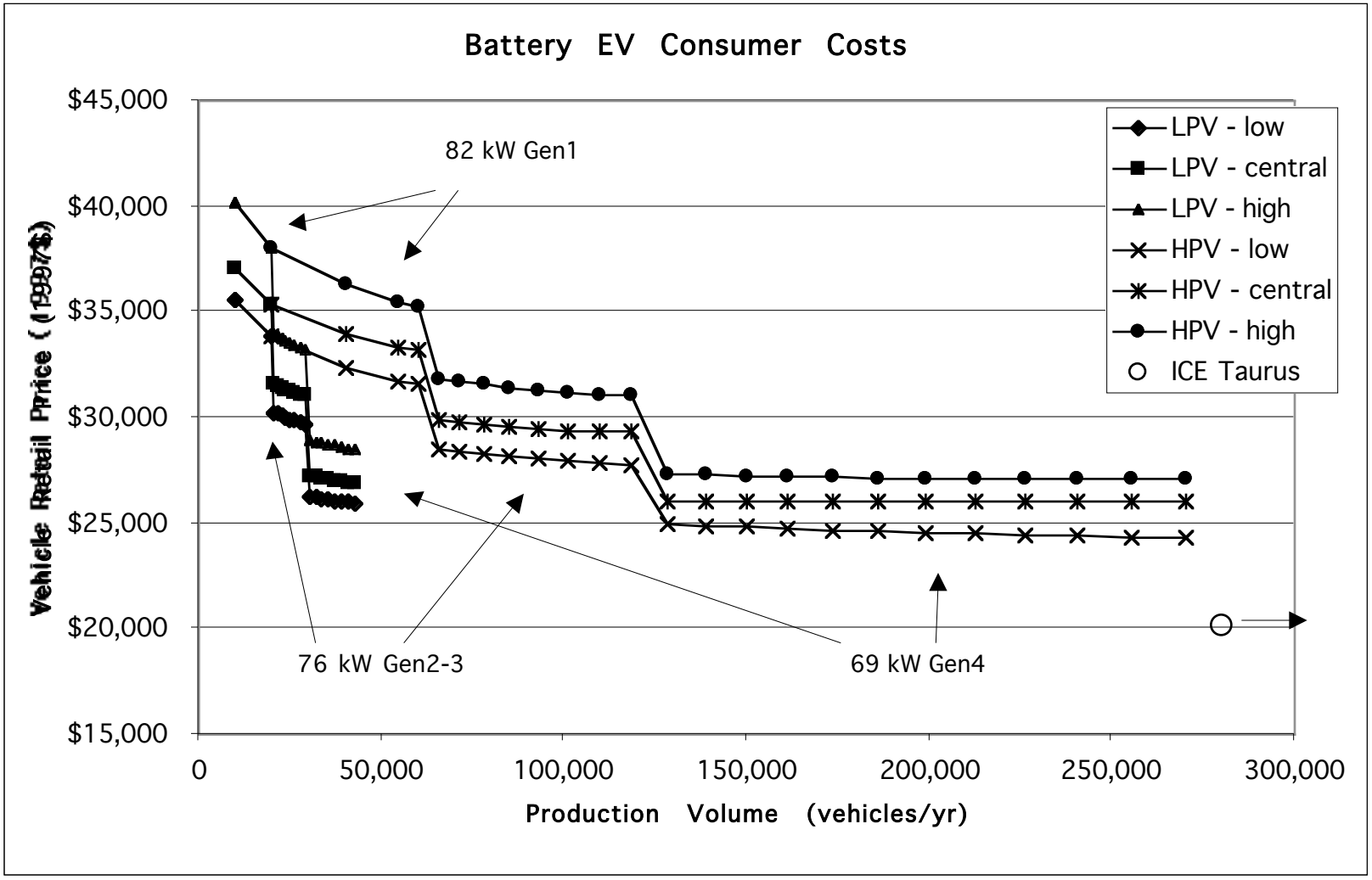
Battery EV Consumer Costs
$45,000
$40,000
$35,000
$30,000
$25,000
$20,000
$15,000
Vehicle Retail Price (1997$)
0
50,000
100,000
150,000
200,000
250,000
300,000
Production Volume (vehicles/yr)
82 kW Gen1
76 kW Gen2-3
69 kW Gen4
LPV - low
LPV - central
LPV - high
HPV - low
HPV - central
HPV - high
ICE Taurus

Chapter 3:
Manufacturing and Lifecycle Costs of Direct-Hydrogen Fuel Cell Vehicles

Introduction

A rapidly emerging alternative to purely battery-powered EVs is to combine the same electric drivetrain with a fuel cell or hybrid fuel cell/battery power system. The resulting vehicle could have many of the same advantages of the BEV, in particular the potential for zero tailpipe emissions of criteria pollutants and GHGs as well as the advantages of electric drive (e.g., maximum torque from zero speed and shift-free acceleration to maximum speed), without the disadvantages of limited driving range and long refueling time. As with gasoline hybrid vehicles, there are many different configurations possible for fuel cell vehicles (FCVs). First, there are several different types of fuel cell systems, including PEM fuel cells, alkaline fuel cells, solid-oxide fuel cells, and phosphoric-acid fuel cells, among others. For transportation applications, PEM fuel cells are considered the best choice, primarily because they operate near ambient temperatures. Second, FCVs could be powered with hydrogen stored on-board the vehicle, with hydrogen produced on-board the vehicle from a liquid fuel such as methanol or gasoline, or with methanol directly. Third, the fuel cell power system could be coupled with a peak-power battery power system, in order to reduce the size of the fuel cell system and to capture regenerative braking energy, or a simpler system could be used with a somewhat larger fuel cell system and no peak-power battery. FCVs that use hydrogen that is stored onboard the vehicle, instead of being produced on the vehicle through a reforming process, are known as direct-hydrogen FCVs (DHFCVs).

While just a few years ago, FCVs were considered impractical as a near-term option for ZEV technology, rapid developments in fuel cell component, stack, and system performance and design have made near-term introduction of FCVs possible. World leaders in FCV development include the DaimlerChrysler Corporation, which has produced four generations of prototype FCVs known as NECAR I-IV (Daimler-Benz, 1996; Veit, 1998), the Ford Motor Company, Toyota Motor Company, and General Motors. The recently unveiled DaimlerChrysler NECAR IV is a Mercedes-Benz A-class DHFCV that uses a liquid hydrogen storage tank, a compact fuel cell system with no battery hybridization, and a 55-kW electric drivetrain. Figure 3-1 shows a cutaway drawing of the NECAR IV.

Figure 3-1: The DaimlerChrysler NECAR IV DHFCV

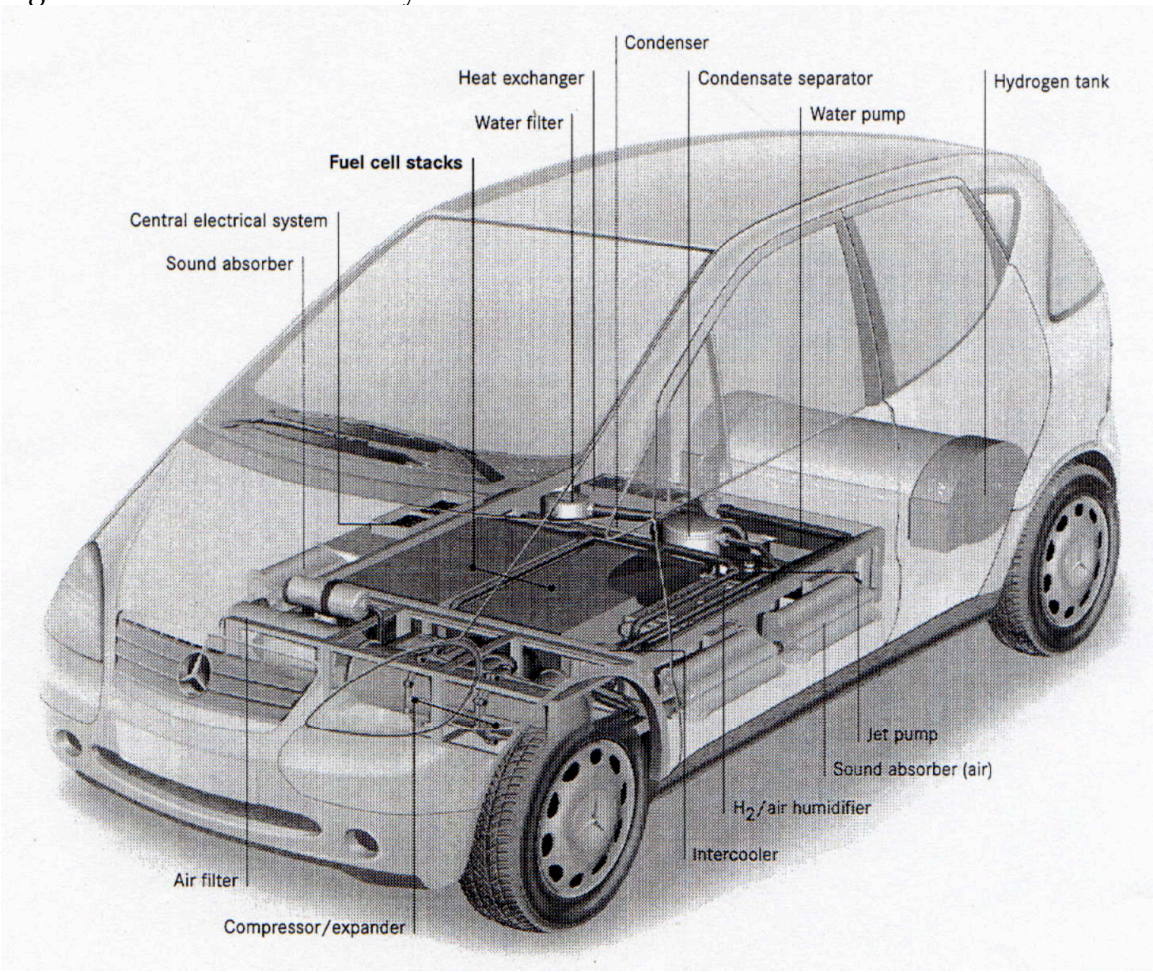

Source: (DaimlerChrysler, 1999a)

Recently, a partnership was forged between DaimlerChrysler, Ford, and Ballard Power Systems of Canada (the world leader in developing PEM fuel cell system technology) to form the "Fuel Cell Alliance." This joint venture has led to the formation of three new companies, including Dbb Fuel Cell Engines, Electric Drive Company (ECo), and Ballard Automotive. The focus of the alliance is to commercialize fuel cell systems for transportation applications by accumulating "sufficient production volume to achieve commercial costs" (Dircks, 1998). The alliance has targeted 2004 as the date by which it aims to introduce FCVs. Within the alliance, Ballard Power Systems is held 20% by DaimlerChrysler, 15.1% by Ford, with the remainder traded on the NASDAQ and Toronto exchanges. Dbb, which receives fuel cell stacks from Ballard Power Systems and produces complete fuel cell "engines," is held 51% by DaimlerChrysler, 27% by Ballard, and 22% by Ford. ECo, which produces electric motors and controllers, is held 62% by Ford, 17% by DaimlerChrysler, and 21% by Ballard. Finally, Ballard Automotive is the marketing company for the alliance (Dircks, 1998).

Meanwhile, Toyota and GM are apparently developing fuel cell technology "in-house," although various GM subsidiaries have purchased Ballard fuel cell stacks in the past. Toyota has demonstrated two FCVs, one

running on direct hydrogen stored in hydride storage, and another running on liquid methanol that is reformed into hydrogen. Toyota has announced that it plans to reach market with a "mass-produced" FCV in 2003, one year before DaimlerChrysler and Ford (Sacramento Bee, 1999). Smaller automakers have also announced their intent to produce fuel cell vehicles. Honda is planning to produce 300 fuel cell vehicles in 2003, using the EV Plus as a base vehicle and probably running on reformed methanol (Fuel Cells 2000, 1999). Also, Nissan and Volkswagen have recently unveiled prototype vehicles that use Ballard stacks, and Mazda and Renault (partnered with Volvo) have produced concept vehicles (Dircks, 1998).

These various efforts are indicative of the level of research and development attention that the world's automakers are applying to FCV introduction. Many technical achievements have been made in recent years through these efforts, and the remaining technical hurdles to FCV introduction primarily involve those associated with the various potential fuel reformation or storage systems, as well as system optimization and integration issues. Increasingly, it seems that manufacturing cost and fuel infrastructure issues, rather than technical feasibility, are the major barriers to FCV introduction.

Direct-Hydrogen FCVs

DHFCVs would in principle be simpler than non-direct FCVs, because they would not require the use of a fuel reformer. However, practical on-board hydrogen storage systems remain an obstacle. Using a reformed liquid fuel eliminates the need for hydrogen storage, but invokes the complexities of developing a compact, low-cost, and responsive fuel processer system (which is in essence a miniature chemical plant), associated efficiency losses of the fuel processors (30-40%), and the need for a gas cleanup system to remove carbon monoxide from the hydrogen stream. In addition, the need for a rapid transient response can lead to substantial fuel utilization losses for reformed fuel systems.

DHFCVs could employ a hybrid power system, with batteries or ultracapacitors used to help meet peak power demands, or they could have an exclusively fuel cell power system. The use of batteries or capacitors would enable the recapture of braking energy through regenerative braking, but it would also involve additional system complexity. Of the present concept vehicles, Daimler-Chrysler's NECAR line and the Ford P2000 are not hybridized, while Toyota's two vehicles, the Renault/Volvo vehicle, the fuel cell version of the GM EV1, Nissan's prototype, and VW's prototype all use batteries, and Mazda's vehicle uses ultracapacitors (Dircks, 1998). However, of these, only the Ford P2000, the Mazda vehicle, one of the Toyota vehicles, and the Daimler-Chrysler NECAR IV are DHFCVs. For reformed fuel systems, hybridization of the fuel cell power system with batteries is one approach to achieving transient response at high fuel utilization.

DHFCVs could be refueled with hydrogen produced in a variety of different ways. Hydrogen can be produced from fossil fuels via steam reformation of natural gas, partial oxidation of heavy oil, or coal gasification. Hydrogen can also be produced without fossil fuel feedstocks via electrolysis of water, either with solar energy or with conventional electricity supplied through the grid. The lowest cost current method of hydrogen production is through steam reformation of natural gas, and this is the most likely pathway for

producing hydrogen for DHFCVs in the near-term. Two basic strategies have been investigated (Berry, 1996; Moore and Raman, 1998): 1) hydrogen production at a large, centralized natural gas steam reformation facility, followed by delivery to local service stations by trucks or pipelines, and 2) hydrogen production at small natural gas steam reformation facilities located at service stations. The latter strategy is attractive because it eliminates the need for shipping or piping the hydrogen in from a remote location, but it also has a few potential drawbacks. First, any pollutant emissions associated with the reformer operations would be located in-basin, whereas the centralized facility could be located out of the immediate urban area and airshed. Second, for safety reasons it is unclear if local regulations would allow small-scale reformers to be located at service stations. Natural gas steam reforming takes place at approximately 850° centigrade (C) (Moore and Raman, 1998), and the presence of these high temperatures in the proximity of hydrogen storage containers may present a safety hazard.

However, it is worth noting that stationary phosphoric acid fuel cell systems, currently used for backup power at hospitals and factories, are routinely sited along with complementary reformer systems. As discussed below, recent analyses have shown that the decentralized production scenario can be economically attractive, assuming natural gas and electricity prices in the Los Angeles area. This scenario eliminates the immediate need for the construction of hydrogen pipelines, and it avoids the large electricity use and attendant greenhouse gas emission issues (and boil-off problems) associated with liquefying hydrogen and delivering it by truck. For these reasons, fuel costs, infrastructure costs, and emissions associated with the scenario of decentralized hydrogen production at service stations are included in this analysis of DHFCV deployment. Costs associated with other scenarios are also discussed where relevant.[24]

DHFCV Modeling Issues and Methods

One interesting issue with regard to DHFCVs is whether or not hybridization of the fuel cell power system with a battery system provides a net efficiency advantage. Recent modeling results from the Fuel Cell Vehicle Modeling Center at ITS-Davis have suggested that the benefits of hybridization for DHFCVs depend on the vehicle duty cycle. When modeled over the relatively gentle FUDS cycle, the fuel efficiency of the hybridized, mid-sized DHFCV exceeded that of the non-hybridized version by about 10%. Relative efficiencies of the two vehicles were about 0.50 kWh per mile and 0.55 kWh per mile, with the non-hybridized version equipped with a 75-kW (net) fuel cell system and the hybridized version equipped with a 40-kW (net) fuel cell system and a NiMH battery pack (Friedman, 1999). However, when tested over the more aggressive US-06 driving cycle, the efficiency of the non-hybridized version exceeded that of the hybridized version, with relative efficiencies of about 0.69 kWh per mile and 0.75 kWh per mile (Friedman, 1999). The hybridization control strategy was not

[24] Future efforts may compare the costs associated with different scenarios of hydrogen production.

necessarily fully optimized in this analysis, and further optimization could well improve the modeled efficiency of the hybridized system.

Similar modeling efforts by Ford Motor Company and DTI for DOE produced very similar results for mid-sized direct-hydrogen fuel cell (DHFC) aluminum-intensive Ford Sable. When tested over the FUDS cycle, the hybridized version, equipped with a 40-kW fuel cell system and a lead-acid battery pack, was estimated to have an efficiency of 0.51 kWh per mile (Oei, et al., 1997b). In comparison, the non-hybridized version (80-kW fuel cell system) had an estimated efficiency of 0.55 kWh per mile (Oei, et al., 1997a).

Thus, on relatively gentle driving cycles the hybridized DHFCV designs appear to be superior. The reduced efficiency of the smaller fuel cell system is more than compensated by the ability of the battery pack to capture braking energy that is lost in the non-hybridized version. Over more aggressive driving schedules, however, the lower efficiency of the fuel cell in the hybridized version may overwhelm the regenerative braking advantage. This finding is tentative at present, though, and further optimization of the hybrid vehicle control strategy could change the results for tests on aggressive driving cycles. For purposes of this analysis, the hybrid configuration is assumed, but it is important to note that the ultimate conclusion of which system type is "best" will depend on consideration and optimization of a complex set of performance, efficiency, cost, and system packaging factors.

Another issue is that hybrid vehicles can be either charge depleting or charge sustaining. With charge depleting hybrids, the battery pack is slowly discharged over the driving range of the vehicle and must then be recharged from an outlet with a battery charger. Charge sustaining hybrids use electricity generated from the fuel cell system (or generator in an ICE hybrid) to recharge the battery periodically, when the fuel cell system is operating at less than peak power. From a consumer standpoint, it is probably preferable for hybrid vehicles to be charge sustaining because this obviates the need for battery recharging as well as refueling. For the analysis model runs conducted here, the vehicles are assumed to be charge sustaining and the battery pack is recharged with electricity generated with the fuel cell system. This assumption results in slightly higher fuel and lifecycle costs than if the electricity were supplied from an outlet, because the cost of electricity generated with hydrogen in the fuel cell is generally somewhat higher than the cost of grid-supplied electricity (depending of course on the exact hydrogen and electricity costs assumed).

Another important modeling issue is the assumed performance of the fuel cell stack itself. The fundamental description of fuel cell stack performance is the polarity plot, which describes the relationship between cell voltage and current density and thus provides the power density at any operational point. Fuel cell stack performance is considerably better when pure oxygen is used as the oxidant than when air is used, and since much experimental data reflects the use of pure oxygen, care must be taken to ensure that operation with air is being characterized. Stack performance also increases with oxidant pressure, but higher pressures involve greater compressor power and this introduces a parasitic loss that affects the net power of the stack. Including parasitic losses due to compression/expansion and other system auxiliaries is thus critical, particularly if operation significantly above ambient pressure is assumed.

With regard to these issues, DTI assumes relatively optimistic stack performance, using polarity plots with a DOE-goal maximum power density of 646 milliwatts (mW) per square centimeter (cm^2) (1.076 A/cm^2 at 0.6 V), and relatively low parasitic losses (Thomas, et al., 1998a). Ogden et al. (1998) use a simple formula to characterize stack voltage/current behavior, rather than a family of polarity plots, with a constant assumed voltage drop due to compression of 80 millivolts (mV). The peak power density calculated with the equation is over 800 mW per cm^2, which is optimistic performance for a hydrogen/air stack. Delucchi (1992) used a family of polarity plots in the Lotus 1-2-3 model used here, but once again with optimistic assumed performance that yielded a peak power density of 781 mW per cm^2. The polarity plots also included one with an unrealistically high maximum pressure of nearly 4.5 atmospheres.[25]

In order to reasonably characterize stack operation with air as the oxidant, a new family of polarity plots has been entered into the model based on runs of the hydrogen fuel cell stack model developed at ITS-Davis (Friedman and Moore, 1998). These plots provide somewhat lesser performance than assumed by the other efforts described above, but they are almost certainly more realistic for actual stack performance using air as the oxidant gas for the foreseeable future. The peak power density for this family of plots is 545 mW per cm^2 (990 milliamperes (mA)/cm^2 at 0.55 V), obtained at 3.0 atmospheres of air pressure. The polarity plots originally used in Delucchi (1992) and the newer ones used here are shown in Figure 3-2.

[25] i.e., the relatively simple compressor characterization used in the model assumed a relatively high efficiency of 82% and did not sufficiently penalize high-pressure operation. The model would thus choose to operate along the 4.5 atm plot, when in reality the parasitic loss penalty would be prohibitive at such high air pressure levels.

Figure 3-2:

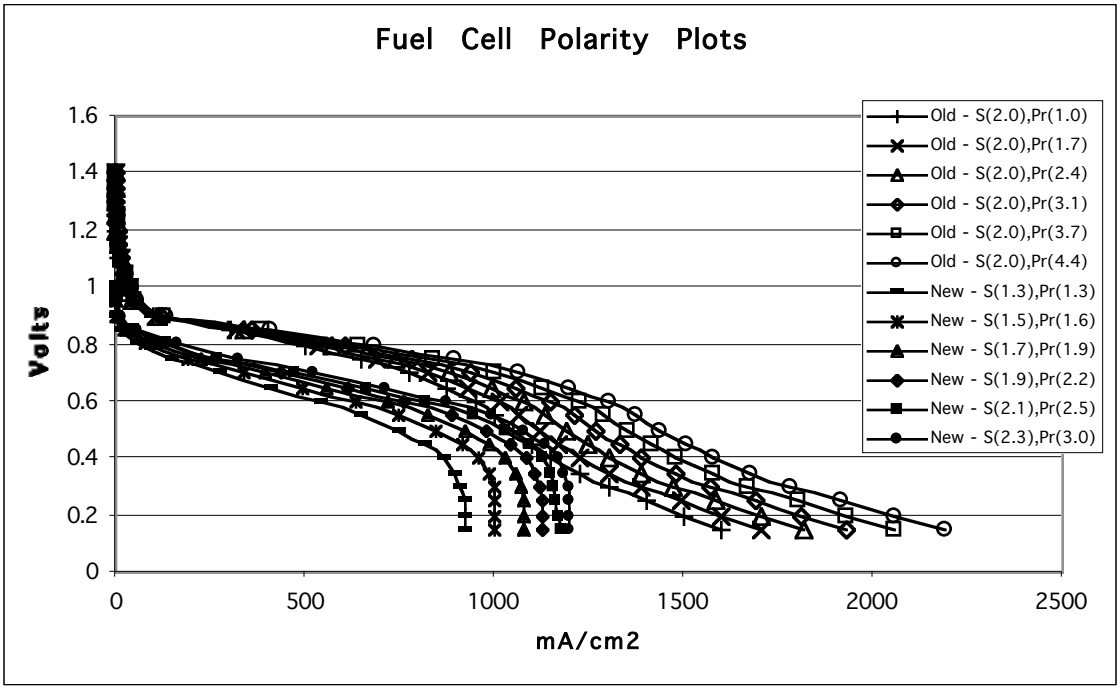

Notes: S = stoichiometric ratio; Pr = air pressure in atmospheres.

As discussed below, substantial improvements are expected in packaging of fuel cell stacks and auxiliary systems, resulting in higher overall system power densities. Improving fundamental cell performance would require breakthroughs in fuel cell catalysis itself, and it is unclear to what extent this will be possible. The types of improvements that would shift the actual polarity plots outward are therefore much less likely to occur than engineering and design improvements that would allow cells of typical performance to be packaged into more compact and lightweight overall system configurations. In fact, efforts at present tend to be focused on substituting cheaper and lighter-weight materials for flowfield plates and reducing catalyst loadings, while maintaining existing performance levels, rather than on improving performance with more exotic and costly materials (U.S. DOE, 1998c; U.S. DOE, 1998d).

Hydrogen FCV Manufacturing Costs

The few previous studies that have addressed the potential manufacturing costs of complete DHFCVs include DeLuchi (1992) and Thomas et al. (1998a). Thomas et al. (1998a) estimate that a mid-sized DHFCV with a 38.1 kW fuel cell system, a 40.3 kW lead-acid battery, and an 82-kW motor/controller system would have an initial production cost of $110,398 and a mass-production cost of $20,179. DeLuchi (1992) estimates that a mid-sized DHFCV with a 400-kilometer (248-mile) range would have a full retail price (i.e., cost of vehicle production, plus manufacturer and dealer markups) of $25,446. A 250-kilometer (155-mile) range DHFCV would have a retail price of $23,183 (DeLuchi, 1992). Also, Ogden et al. (1999) estimate that the fuel cell system, peak power battery, motor and controller, and compressed hydrogen storage system for a 77.5 kW DHFCV

would cost $3,600 to $7,000 in mass production, but they do not estimate complete vehicle costs.

The following analysis estimates manufacturing costs for DHFCVs under a range of different production volumes, using the same production assumptions as for the BEVs analyzed in Chapter 2. In addition to the novel battery, motor, and motor controller components used in BEVs, whose costs are variable with production volume, DHFCVs also include fuel cell system components, and a hydrogen storage system.

Common EV Component Costs

Some novel FCV component costs would be nearly identical to those for BEVs. These include the electric motor, the motor controller, the gearbox, the electric power steering unit, and the high-efficiency HVAC system. Costs for the electric motor and controller depend on their peak power rating, and thus may be a source of difference between vehicle types of different masses, but otherwise would be identical as used in BEVs and FCVs. The Generation 2-4 DHFCVs analyzed here tend to have slightly lower masses than the BEVs of the corresponding technology generation, and they therefore have somewhat less powerful and cheaper drive systems.[26] Thus, the same cost functions for these components are used as for the BEVs in the previous chapter, although the actual component costs vary because of different power ratings. The same costs are assumed for the other auxiliary components (e.g., gearbox, HVAC, power steering) as were used for the BEVs.

PEM Fuel Cell System Costs

PEM fuel cell technology has improved dramatically in recent years, and system power density and overall performance are now adequate for vehicle applications. For example, in 1989, Ballard was achieving fuel cell stack power densities of approximately 100 W per liter (L). By 1996, over 1100 W per L were achieved (Ballard Power Systems Inc., 1998). Thus, in just seven years more than an order of magnitude improvement in stack power density was realized. Given the success of these performance improvements, Ballard is now shifting attention to cost reduction as a major research and development focus:

> [D]uring 1998 the Company's development activities for transportation applications focused on achieving continued reduction in fuel cell costs. The required cost reductions are being achieved by concentrating efforts in four main areas. First is the selection of low cost materials without compromising existing fuel cell performance. Second is ensuring that selected materials are consistent with the use of low cost, high volume manufacturing processes. Third is developing product designs that have inherent high yield and low scrap rates combined with eliminating

---

[26] The Generation 1 BEVs and DHFCVs have almost the same total mass, and therefore both have 82 kW drive systems. The Generation 2 BEVs have a 76 kW drive system, compared with 70 kW for the Generation 2 DHFCVs. The Generation 3 BEVs have a 69 kW drive system, compared with 65 kW for the Generation 3 DHFCVs.

> components and parts. Finally, Ballard is forming supplier relationships that will allow the manufacture of fuel cells in volumes that will result in sufficient economies of scale to drive the final costs down. (Ballard Power Systems Inc., 1998, p. 18)

Since PEM fuel cells systems for motor vehicles are still in prototype production, manufacturing costs and selling prices are quite high. For example, Ballard is currently leasing fuel cell systems for approximately $10,000 per net-kW to automotive customers (Otto, 1999). These lease costs cover amortized R&D expenditures as well manufacturing costs, but even manufacturing costs themselves are presently in the range of $1,500 to $5,000 per kW, by varying estimates (Ekdunge and Raberg, 1998; Thomas, et al., 1998a).

Arriving at estimates for the manufacturing costs of automotive PEM fuel cell systems in higher production volumes is difficult for several reasons. First, few detailed cost analyses have been conducted for which results are available in the public domain. Second, the detailed studies that have been published have focused on manufacturing costs under very high volume production conditions, thus shedding little light on potential near- and medium-term production costs. Third, as with NiMH batteries, cost reductions in overall PEM systems will depend on cost reductions in key subcomponents, such as membrane-electrode assemblies (MEAs) and compressor systems. Finally, PEM fuel cell technology is continuing to evolve, and further improvements in the technology may result in reduced system costs as performance is increased and system optimization occurs. For example, until recently it was necessary to include a humidifier system in order to maintain optimal stack operation, but recent improvements in MEA design have allowed proper humidification to be achieved without an auxiliary system, thus simplifying the system and reducing parts counts and costs (Bahar, 1996). DOE estimates that present fuel cell system technology would cost $500 per kW to manufacture (including a fuel processor), even if production volume was 500,000 units per year (Patil and Ohi, 1998). This suggests that continued design and materials improvements will be required to achieve DOE's cost goal of $35 per kW (excluding fuel processor) for automotive PEM fuel cell systems.

Given the issues associated with estimating fuel cell system costs, including the lack of publicly available cost estimates for a range of PEM fuel cell system production volumes, a different method is used here to estimate future PEM fuel cell system costs than was used to estimate NiMH battery and EV drivetrain manufacturing costs. Instead of attempting to estimate manufacturing costs over a range of production volumes, this method combines a manufacturing progress function analysis with the detailed, high volume production cost estimates that have been made. In this way, manufacturing costs can be forecast from the high levels that currently are observed under prototype production, to the much lower costs that will be possible under high volume, "learned out" production. In the sections that follow, key fuel cell materials cost issues are discussed, followed by a review of manufacturing cost estimates for complete fuel cell systems. Additional background on the use of manufacturing experience curve/progress function analysis is then provided. Finally, results of the PEM fuel cell manufacturing progress function (MPF) analysis are presented.

Key PEM Fuel Cell Materials Costs

The key components of the fuel cell system are the MEA and the bipolar flowfield plates. Additional components include cooling plates, an air compressor, heat exchangers, an air filtration system, a system controller, and miscellaneous gas tubes and assembly hardware. The fuel cell membrane itself is an ionomer membrane, composed of perfluorinated sulfonic acid polymers. These perfluorinated membranes were originally developed by DuPont, which produces the Nafion™ family of membranes, in 1966. These membranes have a higher tensile strength than the sulfonic acid polymers used previously, and they have demonstrated lifetimes of over 60,000 hours at 80 °C., compared with only about 3,000 hours for the membranes used in the 1955-1966 era (Steck, 1995). Other membrane manufacturers today include Dow Chemical, W.L. Gore Associates Inc, Asahi Chemical, and Ballard Advanced Materials (BAM). BAM has been experimenting with lower cost, aromatic-based hydrocarbon membranes, and the exhibited performance has exceeded those of the DuPont and Dow membranes. The drawback thus far has been membrane lifetime, with early generation BAM2G membrane being restricted to only 500-600 hours of operation, and newer BAM3G membrane exhibiting about 2,500 hours of operation in a commercial Ballard stack (Steck, 1995).

Sulfonic acid membranes are currently produced in low volumes, with list prices of $750-$800 per m^2 for the DuPont Nafion-115 and Nafion-117 membranes, and over $1,600 per m^2 for the Dow membrane (Lomax, et al., 1997; Steck, 1995). Costs of $100 per square meter have been projected for volume production of the Gore membrane (Bahar, 1996). Lomax et al. (1997) calculate that in very high volume production needed to produce 500,000 FCVs per year, ionomer membranes could be produced at much lower costs. The required materials costs are shown to vary with membrane thickness, to as low as $0.60 per m^2 for a 5 micron membrane (Lomax, et al., 1997).

On either side of the membrane, the MEA also consists of a platinum catalyst layer and a gas diffusion electrode, which is composed of relatively low cost, porous carbon material. At present, only platinum catalysts (or binary metal catalysts with platinum as a major constituent) are suitable for use in PEM fuel cells. Platinum currently has a market price of about $360 per troy ounce (Kitco Inc., 1999), which equals $11.58 per gram. Recent efforts to reduce platinum catalyst loading levels have shown that MEAs with cathode loadings of <0.60 mg per cm^2 and anode loadings of <0.25 mg per cm^2 can produce equivalent performance to the platinum black MEAs used in Ballard Mark V stacks, which had total catalyst loading levels of 8.0 mg per cm^2 (Ralph, et al., 1997).[27] In small cells, high performance levels have been maintained with cathode loadings as low as 0.10-0.11 mg per cm^2, and total (anode plus cathode) loadings as low as 0.10 mg per cm^2 have been reported (Ralph, et al., 1997). In general, total catalyst loadings of 0.20-0.30 mg per cm^2 are considered feasible with future progress, without compromising performance (Bahar, 1996; Donitz, 1998). These levels would translate into an additional cost of $23-29 per square meter of MEA.

---

[27] Loadings of 8 mg/cm^2 would result in costs of over $10,000 for a passenger vehicle sized stack, for platinum alone!

The platinum catalyst is applied to the membrane as an "ink," in combination with carbon support material, ionomer, and organic solvent. The costs of these additional materials are insignificant compared to the cost of the catalyst (less than 0.2%), and could easily be subsumed by minor fluctuations in the cost of platinum. The costs of the carbon paper used in the gas diffusion electrodes, produced in high volumes, have been quoted at about \$5.00 per m^2 (Lomax, et al., 1997). However, the materials costs are less than \$1.00 per m^2, and this suggests the potential for lower costs in very high volume production (Lomax, et al., 1997). Assuming membrane materials costs of \$76.30 per kg, platinum costs of \$11.14 per gram (and a total loading of 0.25 mg/cm^2), and carbon paper costs of \$5.00 per m^2, Lomax et al. (1997) calculate total MEA materials costs of \$38.45 per square meter. Under high volume production conditions, they calculate processing costs of \$0.684 per square meter, and a total MEA cost after mark-up of \$47.04 per m^2.

Manufacturing costs of bipolar flow field plates are variable, depending on the material used as well as production volume. In previous space applications, expensive plate materials such as titanium or nickel were used to assure long stack service lives and reliability. The prototype PEM stacks currently being produced use solid graphite flow field plates, but these too are quite expensive and also are difficult to machine. In a study for Ford and DOE, DTI examined potential manufacturing costs of different alternative plate materials and designs, including carbon-polymer composite, amorphous carbon, three-piece metallic, and unitized metallic constructions. They conclude that the unitized metallic and carbon-polymer composite constructions offer the lowest potential costs. The plate costs are shown to vary with cell active area, but for plates of 250-450 cm^2, the unitized metallic and carbon polymer plate constructions are shown to yield costs of from about \$0.60 to \$0.90 per cell (Lomax, et al., 1997).

These bipolar plate cost projections, while much lower than earlier estimates by Arthur D. Little of bipolar plate costs of \$149 per kW (cited in Bahar, 1996), are actually only slightly lower than other recent estimates for flow field plate costs based on composite graphite technology. For example, the Institute of Gas Technology (IGT) has been under contract with DOE to develop low-cost bipolar plates. With subcontractors the Stimsonite Corporation and the Superior Graphite Corporation, IGT evaluated several possible plate material compositions and selected a hydrophilic composite graphite formulation (the details are proprietary). This material was then molded into different sizes of bipolar plates, sample cells were built, and the designs were tested against conventional machined graphite plates. Performance was only slightly reduced when the molded plates were used. The performance difference between the cells using the two plate types amounted to a loss of about 15 mV at 400 mA per cm^2 with the molded plates, or about 3% (U.S. DOE, 1998c). IGT estimates that in commercial quantities, materials costs for the blended plate material will be approximately \$1.46 per pound, or \$4.10 per kW (U.S. DOE, 1998c). They further estimate that manufacturing costs will be under \$6 per kW, making for a total bipolar plate cost of about \$10 per kW (U.S. DOE, 1998c). Also, Energy Partners, L.C. has recently announced that manufacturing composite graphite plates in a new high-speed process will reduce plate costs from \$100 per piece to \$1.50 per piece (Hydrogen and Fuel Cell Letter, 1999a).

Since these flowfield plates are bipolar, the per-piece costs estimated by Energy Partners correspond to the per-cell costs estimated by DTI. The IGT estimate of $10 per kW translates into about $1.65 per cell (or plate), assuming that cells based on their 300 cm^2 plates achieve 0.55 W per cm^2. Thus, the DTI estimates of bipolar plate costs of under $1.00 per cell are somewhat lower than the recent estimates by Energy Partners and IGT of $1.50-$1.65 per cell. However, the DTI estimates assume that less expensive carbon polymer or steel plate materials can be used, while Energy Partners and IGT are focusing on the use of composite graphite materials.

Based on the MEA and bipolar plate cost estimates discussed above, overall fuel cell stack costs were calculated by DTI, with different ratios of active cells to cooling cells, and also for different cell active areas. Manufacturing costs of under $20 per kW were calculated for cell active areas of 200 cm^2 and higher, assuming active to cooling cell ratios of 3:1 or 4:1, and the unitized metallic or composite-polymer plate constructions (Lomax, et al., 1997). It is important to note, however, that the costs estimated by DTI only apply to very high volume stack production of 500,000 units per year. Manufacturing costs in lower volume production would presumably be considerably higher, but intermediate production volumes were not considered in the DTI study.

Costs of PEM Fuel Cell Power Systems for EVs

A few cost analyses for complete PEM fuel cell systems have been published. These tend to fall into two categories: experience curve analyses, and production volume-based analyses. An experience curve analysis of PEM fuel cells was recently published by Rogner (1998). He estimated three different experience curves, with slopes of 0.76, 0.81, and 0.93, and initial costs for complete fuel cell systems of $2,500, $4,500, and $10,000 per kW, at 2 megwatts (MW) of cumulative production. After 100,000 MW of production, these three curves project widely differing costs of about $2,500 per kW (for initial cost of $10,000 per kW and slope of 0.93), $200 per kW (for initial cost of $4,500 per kW and slope of 0.81), and $25 per kW (for initial cost of $2,500 per kW and slope of 0.76). Also, Willand (1996) has presented a Daimler-Benz fuel cell system cost forecast that appears to be based on a MPF analysis, but is not explicitly identified as such. This forecast shows costs declining from 100,000 deutsche marks (DM) per kW initially (with 1 unit of cumulative production) to about 1,000 DM per kW at a cumulative production level of about 5,000 units, and then further to 300-500 DM per kW or 600-800 DM per kW after production of about 250,000 units (the curve forks into two branches beyond 5,000 units of cumulative production).

Ekdunge and Raberg (1998), of AB Volvo, present an analysis of present and projected materials costs for PEM fuel cells stacks for motor vehicles. They show materials costs of $1,220 per kW at present, with costs of $825 per kW for bipolar plates, $120 per kW for membrane material, and $243 per kW for catalyst. Based on these materials costs, they suggest overall costs of $5000 per kW. In mass production, with platinum catalyst loadings of 0.155 g per kW, they suggest that materials costs could be reduced to $49 per kW (Ekdunge and Raberg, 1998).

As discussed above, a detailed analysis of the manufacturing costs of PEM fuel cell stacks in high-volume production has recently been conducted by DTI, for the Ford Motor Company and DOE's Office of Transportation Technologies.

This study examined four different approaches to manufacturing fuel cell stack mechanical parts, and considered a high volume production level of 500,000 units per year. This study concluded that a complete fuel cell stack manufacturing cost as low as about $20 per kW is possible for complete 70 kW (gross) fuel cell stacks, using either carbon-polymer composite or unitized metallic flowfield plate compositions (Lomax, et al., 1997). A subsequent study by DTI included cost estimates for additional fuel cell system components such as compressors, heat exchangers, a humidification system, safety devices, and a control system. Also produced in automotive volumes of 300,000-500,000 units per year, these additional system components were estimated to add about $14.35 per kW to the cost of the 70 kW system (Thomas, et al., 1998a).

Thus, at the present time, a detailed, high-volume PEM fuel cell system cost analysis has been conducted, but no detailed lower-volume manufacturing cost estimates are publicly available. In order to bridge the gap between today's pilot-scale PEM fuel cell manufacturing cost, and the manufacturing costs that are possible in high-volume production, a MPF analysis can be used. This analysis can then be fitted to assumptions of market penetration and component production in order to arrive at PEM fuel cell system manufacturing costs in a given year. By combining the MPF analysis with a high-volume cost analysis or cost target, some protection can be afforded against the problem of potentially forecasting unrealistically low $ per kW costs at high levels of accumulated production.

Learning Curves, Experience Curves, and Manufacturing Progress Functions

The first example that appears in the literature of an analysis of systematic cost reduction in manufacturing occurred in 1936, when T.P. Wright published a paper about his discovery of a relationship between the labor hours needed to manufacture an airframe and the total number of airframes built. Wright found that each time the total quantity of airframes produced doubled, the labor hours required to assemble the airframe decreased by a stable percentage (Wright, 1936). Wright coined the term "learning curve" to describe this logarithmic pattern of reduced labor effort and manufacturing cost. Since this early work, thousands of studies have been conducted on the nature and variability of manufacturing cost reduction as a function of accumulated output, in industries as diverse as electric power, microchips, Japanese beer, consumer electronics, and automobiles (Argote and Epple, 1990; Boston Consulting Group, 1972; Dino, 1985; Dutton and Thomas, 1984; Ghemawat, 1985; Yelle, 1983). The term "learning curve" is often used generically to describe various types of cost decline and/or efficiency improvement, but many analysts prefer to reserve the term for labor efficiency improvement only, as in Wright's study of airframe production.

The Manufacturing Experience Curve

Thus, defined as applying to the labor component of manufacturing only, learning curves capture only a portion of manufacturing cost reductions. They describe improvements in the efficiency of the labor component of total manufacturing cost, while the term that has come to be used to describe the curve that describes progress in the entire per unit manufacturing cost is the "manufacturing experience curve." Learning curves can account for important

sources of cost reduction for products in low-volume production, where assembly operations are often done by hand, and for products whose production is not amenable to automation. For most products, the production process becomes highly automated relatively rapidly, and learning curves become correspondingly less relevant.

In essence, the experience curve describes the cost path of a manufactured product, beginning with the first and continuing to the 'nth' unit produced. Cost reductions are typically due to four primary factors: scale economies, technological improvements in production processes, improvements in product design (i.e., reduced parts counts and design for manufacturability), and improved production worker and organizational efficiency. The progress of an industry along an experience curve for a new technology represents the steady decline in its inflation-corrected unit cost of manufacture.

In the seminal work on experience curves, the Boston Consulting Group suggested that experience curves could alternatively be construed to reflect the progress in the cost of adding value to a product (i.e., all manufacturing costs other than materials costs), rather than the entire manufacturing cost (Conley, 1970). They suggested that this distinction could be important for products where materials costs represented a large share of total manufacturing cost, and where cost declines in materials were likely to follow a different pattern than the overall unit cost decline. In practice, however, experience curves have almost always been analyzed in terms of total manufacturing costs or product prices, without regard for the materials cost/value added cost distinction.

Experience curves are now commonly presented and discussed in the management literature, and they are used in industry, government agencies, and academia to assess historic cost reductions and to project potential future progress. Some uses of experience curves in the context of analyzing energy technologies are discussed below. In general, economists tend to be skeptical of experience curve-type analyses, preferring instead more traditional cost models that assess costs in terms of annual production, rather than accumulated production. In one critique of experience curve theory, British economists Hall and Howell (1985) sought to critique the common assumption of 80% experience curve slopes, and found some variations in curve slopes to support their critique (see the below discussion on the variability in experience curve slopes for more detail). However, when assessing Boston Consulting Group data on the historical reductions in costs of microchips and Japanese beer with both experience curve models and traditional "current rate of output" economic models, they found that both model forms provided good fits to the data. For microchips, the experience curve and current output rate models produced R^2 values of 0.93 and 0.92, respectively, while for Japanese beer the R^2 values were 0.97 and 0.98, respectively (Hall and Howell, 1985). Despite their caveats about using experience curve models, the authors were forced to conclude that both model types can be suitable, and that they can produce similar results (depending of course on the model parameters used).

The Manufacturing Progress Function

MPFs are similar to experience curves, except that MPFs describe the pattern of manufacturing costs for a particular firm in an industry, while experience curves describe industry-wide cost reductions. In principle, if market shares in an

industry were stable over time, one could estimate an industry-wide experience curve by aggregating the MPFs of the firms in an industry and calculating a market share-weighted average of the progress function slopes. However, this would require analysis of the MPFs of all of the firms in an industry – a daunting task. In practice, experience curve analysis is used when the available data or the forecast of interest is for industry-wide production, and MPF analysis is used if an individual firm is the unit of analysis of interest.

Several different functional forms for MPFs and experience curves have been investigated, but the most commonly used expression is the simple log-linear form shown in Equation 3-1:[28]

$$C_N = C_1 * V_N^{(\log\partial / \log 2)} \qquad (3\text{-}1)$$

Where:
C_N = Cost of manufacturing nth unit
C_1 = Cost of manufacturing 1st unit
V_N = Cumulative production at nth unit
∂ = Experience curve slope

This relationship predicts that the constant dollar cost of manufacturing a product falls by a fixed percentage with each doubling of accumulated manufacturing experience. For example, an 80% curve predicts that the constant dollar cost of a product will fall by 20% with each doubling of cumulative production volume. Hence, cost reductions are relatively dramatic during the early stages of manufacture, as scale economies are captured and the production process is perfected, and then drop off as doublings in volume take longer to achieve.

Ex Post and Ex Ante Analyses

Experience curve and MPF analyses are often applied retrospectively, or *ex post*. One classic example is the reduction in manufacturing cost of the Model-T Ford from 1909 to 1923, shown in Chapter 1. Another, much more recent example can be found in the fuel cell field. Figure 3-3 shows the reduction in manufacturing costs to date for the 200-kW stationary phosphoric acid fuel cell systems manufactured by ONSI, a division of United Technologies, of which 144 units had been sold as of September 1997. This figure shows that ONSI has been on a relatively aggressive 75% experience curve, and that it expects to stay on it with its current and future cost reduction programs.

---

[28] There are some variations in how this equation is expressed mathematically. Such forms as $C_N = C_1 * V_n^{-b}$ and $Log C_N = \frac{Log A \square Log N}{Log 2} + Log C_1$ are mathematically equivalent to Equation 1, although the value of "b" in the first formula is not directly equivalent to the value of the experience curve slope value in Equation 1.

Figure 3-3: IFC/ONSI 200-kW Phosphoric Acid Fuel Cell System Cost Reduction

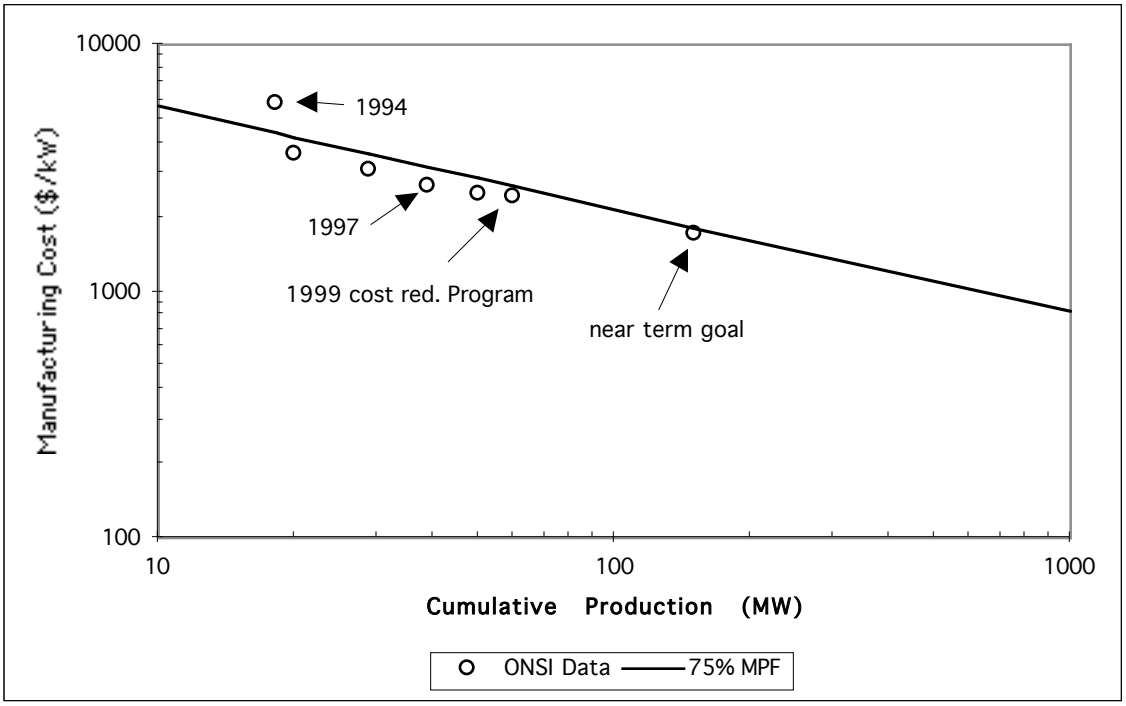

Source: (Whitaker, 1998)
Note: Data read from chart – may be slightly inaccurate.

Experience curves are also commonly used *ex ante*, as a forecasting tool. For example, the Energy Information Administration (EIA) uses an experience curve formula in the National Energy Modeling System in order to forecast the potential future capital costs of different types of energy production technologies. These forecasts form an important part of the EIA's Annual Energy Outlook, and recently the model has been expanded to account for international learning effects (Petersik, 1997).

Experience curve models are also being used to assess the capital costs of new energy technologies in a recent modeling effort in Sweden. This model uses endogenous experience curves to capture the dynamics of cost reductions for electricity generating systems based on photovoltaics and fuel cells (Mattson and Wene, 1997). Also, the Shell International Petroleum planning group has used experience curve models to describe cost reductions in energy commodities, such as gasoline and electricity, and found similar cost reduction rates as have been found for manufactured products. They have also used experience curves to forecast the potential costs of future energy production technologies, and this analysis has led to the following observations:

> [N]ew technologies steadily progress along their learning curves, first capturing niche markets and, by 2020 become fully competitive with conventional energy sources. Progression reflects an 80% experience curve for PM solar and 85% for wind and biomass. This is not unlike the progression of oil 100 years ago (80%) and slower than that of electricity in the USA over 1926-1970, which achieved 75%. (Shell International Petroleum, 1994, p. 96)

Furthermore, in the current European automobile industry, experience curves are used to negotiate component prices between suppliers and assembly firms. A component price is negotiated that is between the present manufacturing cost for the component and the experience curve-based prediction for the cost of the component at the end of the production run for that vehicle (typically four years). This price allows component manufacturers to realize an overall profit, but they actually lose money in the early years of production when manufacturing costs exceed the negotiated price, and then they more than make up the deficit in later years (Hinterhuber, 1997).

The difficulty with conducting *ex ante* experience curve analyses is that it is impossible to know with certainty what experience curve or MPF slope is appropriate for the product in question. Even if some production cost data are available to estimate the initial part of the curve, experience curve and MPF slopes are not always stable for a given product, and simply extrapolating the entire curve from the initial portion may not be accurate. In order to contend with this issue, some form of probabilistic analysis is warranted. This could take the form of simply forecasting two or more different cases, with different corresponding curve slopes, or a more elaborate type of analysis such as Monte Carlo simulation (as in Lipman and Sperling, 1997).

An additional difficulty with *ex ante* MPF cost forecasts, and one that is rarely noted in the literature, is that if a forecast is extended far enough, it may be the case that at some point an unrealistically low cost will be forecast. The nature of the logarithmic function shown above is such that percentage reductions in manufacturing cost take longer and longer to achieve with higher levels of accumulated production, but the formula will continue to calculate reductions in manufacturing costs indefinitely if allowed to do so. *Ex post* analyses of some products provide evidence that technologies with very long product life cycles may eventually reach a plateau in manufacturing cost, even if they very closely followed a certain curve slope up until that point.

For example, consider the case of laser diodes produced by Sony starting in 1982. These devices have been produced in great numbers because they are components of a highly successful consumer product, the compact disc player. Figure 3-4 shows manufacturing cost data for this product from 1982 until 1994, and a set of three manufacturing progress functions with different slopes. Three interesting features are apparent in this figure. First, the overall pattern of cost reduction is reasonably well approximated by an 80% curve slope. Second, the data do not perfectly track any given curve slope, but rather "wander" considerably. The early production history of the product closely tracks a 75% curve slope, but extending this would have yielded an unrealistically optimistic cost forecast. Third, there is clear evidence of a manufacturing cost plateau at cumulative production levels of over about 10 million units. The cost at this point of 140 Yen is equal to about one dollar, and this either represents a lower bound on the manufacturing cost of the product or is simply the point at which Sony stopped attempting to further reduce the cost. Thus, there is a potential danger to extending experience curve and MPF analysis too far, without regard for a possible lower limit on the manufacturing cost of the product. This point will be discussed further below.

Figure 3-4: Sony Laser Diode Manufacturing Costs (1982-1994)

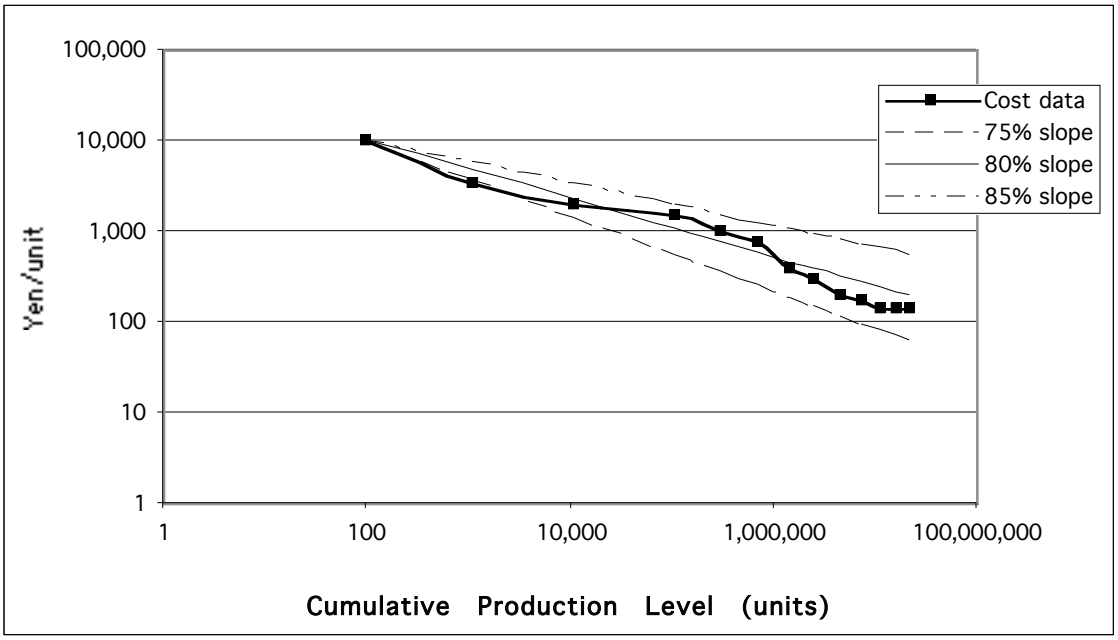

Source: (Wood, 1998; Wood and Brown, 1998)

Experience Curve and MPF Slope Variation

Returning to the first caveat discussed above with regard to performing *ex ante* cost forecasts, care must be taken in applying MPFs and experience curves due to variations in curve slopes within and between industries. According to one study of about 100 experience curves, slopes do vary significantly across industries, as Figure 3-5 illustrates, but they are typically between 70% and 85% (implying cost reductions of 30% to 15% with each doubling of accumulated output). While in some cases a curve of a certain slope seems to describe the cost path for most firms in an industry -- a 70% curve for dynamic RAM chips is one example -- experience curve slopes often vary within an industry (Ghemawat, 1985). MPF slopes also vary, and the nature of the variation (shown in Figure 3-6) is quite similar to that observed for experience curve slopes.

Figure 3-5: Experience Curve Slope Variation

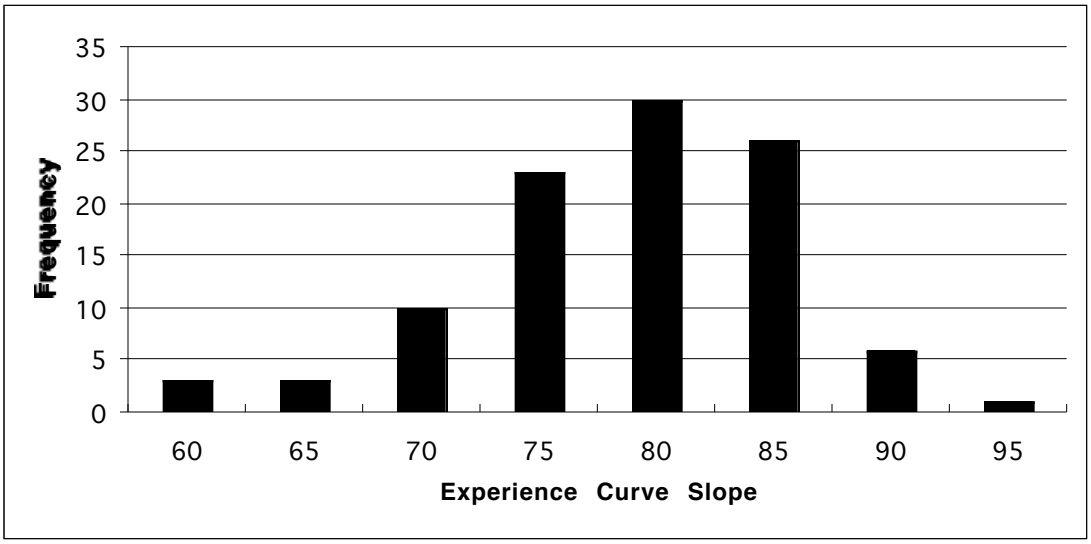

Source: (Ghemawat, 1985)

Figure 3-6: MPF Slope Variation

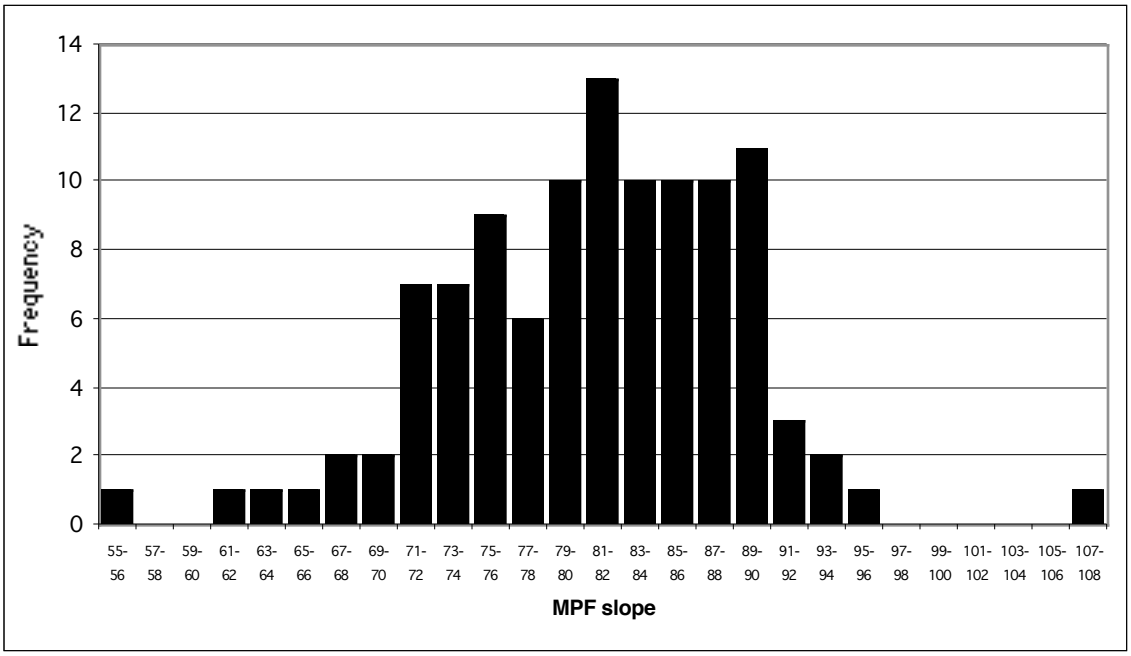

Source: (Dutton and Thomas, 1984)

Many explanations are possible for these variations in experience curve and MPF slopes. Variation between industries might be explained by such factors as the degree of product complexity, market structure, and industry maturity. Variation among individual firms in the same industry can occur for many reasons, including relative levels of vertical integration, corporate work ethics, research and development expenditures, and access to technical information.

While some findings suggest that curve slopes are relatively stable throughout a product's life-cycle, it is worth noting that some research suggests that this may only be true through the duration of a development stage (e.g. introduction, take-off and growth, maturity, etc.) (Dino, 1985). However, even if stable, it is difficult to determine actual experience curves and MPFs precisely and accurately, and controlling for possible sources of variation between studies has been a persistent problem in interpreting the literature. For instance, the proprietary nature of cost data sometimes necessitates the use of product price data as a proxy for actual manufacturing costs. This can be problematic because the relationship between manufacturing cost and retail price is difficult to discern, and may not be stable. In research in which price data were analyzed, perhaps variations in the price-cost relationship that were observed, at least in part, rather than actual variations in the rate of decline of manufacturing cost. An additional complication with many studies is the difficulty in controlling for variations in product performance, durability, and quality over time. Experience curve analyses are most convincing, and probably have the most predictive power, where product design is relatively stable and where at least some manufacturing cost data are available. At any rate, while considerable efforts have been directed toward understanding these issues for a few industries, there remains insufficient evidence to warrant broad conclusions as to the causal factors for experience curve slope consistency or variation in different settings.

Manufacturing Progress Function Assumptions

In order to apply the MPF cost analysis framework, it is necessary to assess the present cumulative production level and manufacturing cost of PEM fuel cell systems, for a specific manufacturer. At the present time, the world leader in producing PEM fuel cell systems for vehicle applications is Ballard Power Systems, of Vancouver, Canada. As of 1998, Ballard had produced a total of about 5 MW of PEM fuel cell stacks (Savoie, 1998). Estimating the manufacturing cost at the present time is more difficult, since data on the manufacturing costs of Ballard stacks are not publicly available. Ballard stacks currently lease for as much as $10,000 per net-kW, but these lease prices include a contribution to engineering and development costs (Otto, 1999), and because of Ballard's unique position in the market may not be directly related to present manufacturing costs. Among other manufacturers, Energy Partners estimates current manufacturing costs of about $2,500 per kW for its hydrogen/air fuel cell system (U.S. DOE, 1998c).

DTI estimates a present manufacturing cost of about $1,500-2,000 per net-kW for complete fuel cell systems, depending somewhat on the system's power output. Using a formula that they provide, a 70-kW system would have a present cost of about $97,920, or $1,400 per kW, while a smaller, 30-kW system would have a present cost of about $64,960, or $2,165 per kW (Thomas, et al., 1998a). These estimates may be somewhat low, given that the present cost of the stationary phosphoric acid fuel cell systems produced by ONSI is approximately $2,500-3,000 per kW (Whitaker, 1998). As DTI notes, however, the manufacturing costs of PEM fuel cell systems for vehicle applications may be lower than for stationary phosphoric acid systems, even at the present time. Fuel cells for vehicles need only be built for operating lives of several thousand hours, as opposed to tens or even hundreds of thousands of hours for stationary

systems. Vehicle systems would also operate near peak power much less of the time (Thomas, et al., 1998a).

Rogner (1998) contended with the uncertainty in the present cost of PEM fuel cell systems by considering a very wide range of values for this parameter, from $10,000 per kW to $2,500 per kW. This range is probably unnecessarily wide, but given the present uncertainty in this parameter, a range of values should be included. Based on the estimates discussed above, I choose a central case estimate of $2,200 per kW, with a low value of $1,500 per kW and a high value of $3,000 per kW.

Next, MPF slope values must be selected. As discussed above and shown in Figure 4, the historical range of variation in this parameter is typically between 70% and 90%, with a few exceptional high and low cases. In one analysis, Thomas et al. (1998b) used a MPF to connect their high-volume PEM fuel cell system cost estimate with their present cost estimate of $1,500 per kW, and calculated the resulting slope at 81.9%. This is one possible approach, but the calculated slope would be different with a different estimate for the present PEM system cost, which as discussed above is uncertain. It is therefore preferable to consider a range of slope values, and to use the data on historical MPF slopes to guide the choice of estimates. I use the commonly assumed value of 80% for the central case estimate, with 75% and 85% for the low and high cases.

As discussed above, one potential concern with experience curve and MPF analyses is that if carried out far enough, they may at some point forecast costs that are unreasonably low. One way to prevent this is to impose some lower limit on the cost forecast, but arriving at a reasonable lower limit is not generally straightforward. Furthermore, doing so may introduce undue conservatism to the analysis and rob it of one of its strengths, namely the ability to capture the long-term and often dramatic cost reductions that are sometimes observed for products that are highly successful and do survive to reach high levels of accumulated production. Despite this concern, however, the possibility of forecasting unrealistically low manufacturing costs with experience curve and MPF analyses should be considered. Particularly for technologies that may have very long product life cycles, and/or for cases in which steep curves are assumed, bounding an MPF analysis with a cost target or very high volume manufacturing cost estimate could prevent an overly optimistic forecast.

Another way to bound a cost forecast would be to use estimates for materials costs in high volume production, if they can be obtained, plus an increment for processing costs that is based on an analysis of the processing costs for a similar mature product. This approach is reasonable because when products reach high-volume, automated production, materials costs often dominate the total manufacturing cost. However, estimating "ultimate" materials costs can be difficult, particularly if the product uses any relatively novel components or materials that themselves have the potential for cost reduction, or if there are opportunities to eventually substitute for less expensive materials in some subcomponents.

Another approach would be to use an established cost goal as a lower bound, under the assumption that companies will be satisfied if costs reach this level and will not strive to reduce them further. For example, in the case of PEM fuel cell systems, the Partnership for a New Generation of Vehicles (PNGV) has established year 2004 cost targets of $40 per kW for fuel cell systems (stack and

auxiliaries) and $10 per kW for fuel processors (Teagan, et al., 1998). Also, Kalhammer et al. (1998) have identified cost targets for automotive fuel cell system components of $20 per kW for PEM fuel cell stacks, $20 per kW for fuel processors, and $20 per kW for "balance of plant" auxiliary components. These cost targets could be used to bound MPF forecasts.

Alternately, the detailed, very high-volume cost estimates developed by DTI provide a possible lower bound. Of course, costs could ultimately be lower than even these optimistic estimates due to unforeseen changes in product design or the development of enabling technologies. However, the estimation methodology used by DTI was specifically designed to identify the lowest cost PEM stack design configuration, and the choice of a production volume of 300,000 units per year suggests that it would be difficult to construe a lower cost case. I choose to bound the forecast with DTI's high-volume PEM fuel cell system cost estimate, believing that the risk of estimating an unrealistically low cost with an unbounded forecast is greater than the risk of conservatism that this choice will introduce. This lower bound is given by Equation 3-2, and it varies somewhat with the size of the stack (Thomas, et al., 1998a).

$$C_{HV} = 1{,}073 + P_N \left[3.27 + \frac{5.34 + 27 \cdot L_P}{P_D} \right] \qquad (3\text{-}2)$$

Where:
C_{HV} = high volume cost of PEM fuel cell system (in $)
P_N = net fuel cell peak power output, in kW
L_P = total cell platinum catalyst loading in mg/cm^2
P_D = cell peak power density, in W/cm^2

Using values of 0.25 mg per cm^2 for the total platinum catalyst loading (anode plus cathode) and 0.545 W per cm^2 for the cell peak power density (DTI assumes 0.646 W/cm^2) gives the simpler Equation 3-3:

$$C_{HV} = 1{,}073 + 25.45 \cdot P_N \qquad (3\text{-}3)$$

Where:
C_{HV} = high volume cost of PEM fuel cell system (in $)
P_N = net fuel cell peak power output, in kW

For fuel cell stack sizes in the 60 to 80-kW range, that would be used for non-hybridized DHFCVs, the DTI estimate produces values of about $39-43 per kW. For smaller fuel cell systems used in hybrid vehicles, in the range of 20 to 40 kW, costs would be $79 per kW and $52 per kW, respectively. DOE (1998c) and Kalhammer et al. (1998) have identified cost targets of $35-40 per kW for 50-kW automotive systems, compared to the 50-kW system estimate of $47 per kW ($43 per kW if a power density of 0.646 W/cm^2 is assumed) using the DTI formula. Thus, using either established cost goals or the DTI high-volume estimate as a lower bound would produce similar results for 50-kW systems.

Results of PEM Fuel Cell MPF Analysis

The results of the MPF analysis for the future costs of automotive PEM fuel cell systems, using the assumptions described above, are shown in Figure 3-7. The five sets of assumptions used to generate the curves shown produce significantly different results. The central case, using a present value of $2,200 per kW and an 80% MPF slope, predicts that the high volume DTI estimates of $47 per kW to $52 per kW for 40 to 50-kW systems will not be achieved until a cumulative production volume of several hundred thousand MW is achieved. The more conservative case suggests that such cost level will not be achieved even after 10 million MW of accumulated production. The case using the 75% curve predicts that the high volume cost estimates will be reached with a cumulative production level of about 20 thousand MW.

Figure 3-7: PEM Fuel Cell MPF Cost Forecast

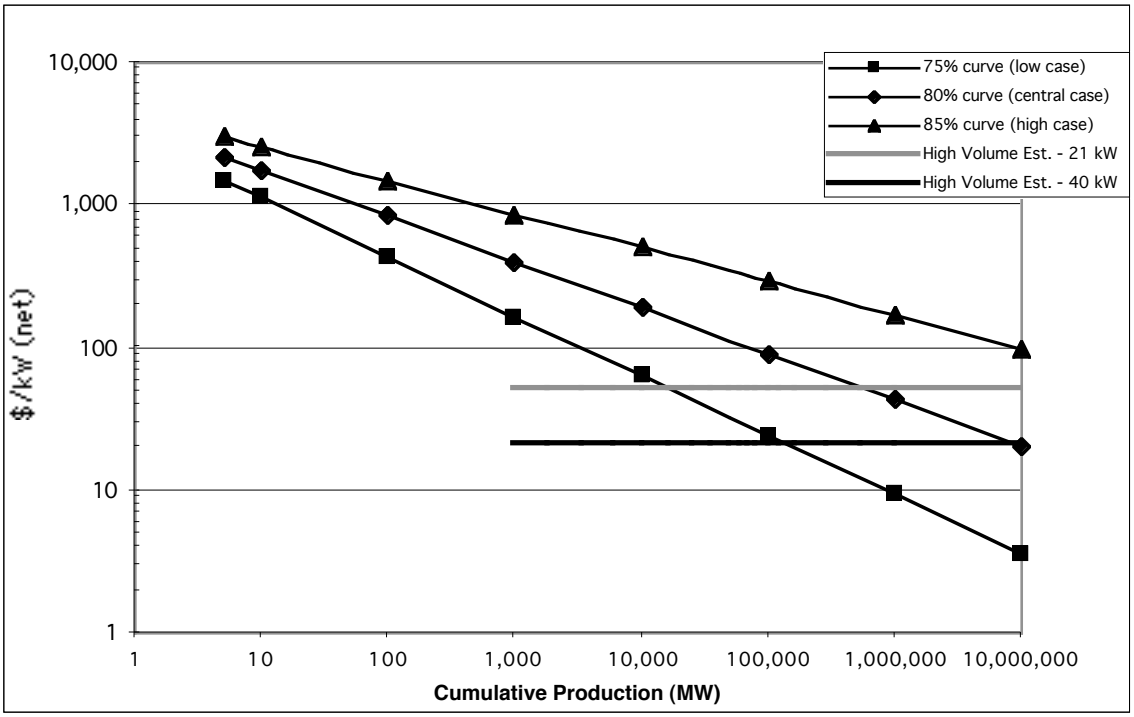

Figure 3-7 also shows that an "unbounded" 75% curve forecasts costs below the DOE goal of $35 per kW at cumulative production volumes of greater than 50,000 MW. This example shows the potential for forecasting costs that may be unrealistically low using MPF or experience curve techniques, particularly for optimistic cases in which relatively steep curve slopes are assumed. It is interesting to note that while 70-75% curve slopes are at the low end of the observed ranges shown in Figure 3-7, the Daimler-Benz fuel cell cost forecast (Willand, 1996) closely matches a 70% MPF when plotted in terms of cumulative production volume on a log-log scale (Lipman and Sperling, 1997). Such steep curves may be observed relatively rarely, but they are possible, particularly for products whose manufacture is amenable to automated production, and where substantial investments are made into product and process engineering innovations. However, as the Sony laser diode example

shows, it is unclear if such steep curve slopes can be maintained for long periods of time. It is also worth noting that the cumulative production level of 50,000 MW, beyond which the 75% curve drops below the DOE goal (and DTI high-volume forecasts), would be achieved in just eight years by a manufacturer that produced 20,000 70-kW systems in the first year and ramped up production at an incremental rate of 20,000 systems per year.

Based on the histogram of MPF slopes observed historically, a good choice for a central case estimate is the Case 3 MPF forecast that employs an 80% curve slope. Cases 2 and 4 represent likely upper and lower bounds, while low likelihood, extreme cases could be plotted with 70% and 90% slopes. Table 3-1 presents numerical results for these cases, using the DTI projection of $76.55 per kW for 21-kW (net) systems as a lower bound.[29]

Since Ballard is continually producing fuel cell stacks, at a rate of approximately 1 MW per year at present, the MPF forecast assumes a cumulative production level of 10 MW in 2003 (up from 5 MW in 1998). This analysis also considers the fact that Ballard/Dbb is currently supplying fuel cell systems to more than one automaker, and is likely to continue to do so for some time due to its monopolistic position in the market. Through the Fuel Cell Alliance, Ballard is closely allied with DaimlerChrysler and Ford, but has also supplied fuel cell systems to Honda, Nissan, and General Motors in recent years. I therefore assume that fuel cell system supplier production is double the FCV production of the single automaker analyzed. This supplier production forecast is probably conservative, given the additional contributions to production of fuel cell systems for buses, and possible learning and scale economy "spillovers" from production of stationary fuel cell systems.

In the cost analysis model runs conducted here, the MPF cost forecasts are used unless the forecast cost is lower than would be predicted by Equation 3-3 for the particular system size used in that vehicle generation. If the cost obtained with the MPF forecast is ever lower than the high-volume cost estimate, then the high-volume estimate is used instead, as a lower bound. This procedure turns out to be important, because the system cost that is forecast with the MPF function in the high production volume, low case (with a 75% curve), reaches a low value of $21.75 per kW in 2026. This is substantially lower than the $76.55 per kW estimated with Equation 3-3 for the 21-kW system used in Generation 4 vehicles. Figure 3-8 shows the fuel cell system cost estimates used in the DHFCV cost model runs.

---

[29] The lower bound for the 21-kW system is relevant for this analysis, since this is the size fuel cell system used in the Generation 4 vehicles when cumulative production volumes may be high enough to reach the lower bound estimate. Fuel cell systems are modular in nature, which means that experience gained building various sizes of stacks contribute to cost reductions for all sizes of systems. Thus, it is unnecessary to conduct separate experience curve analyses for the 21-40 kW (net) systems analyzed here.

Figure 3-8:

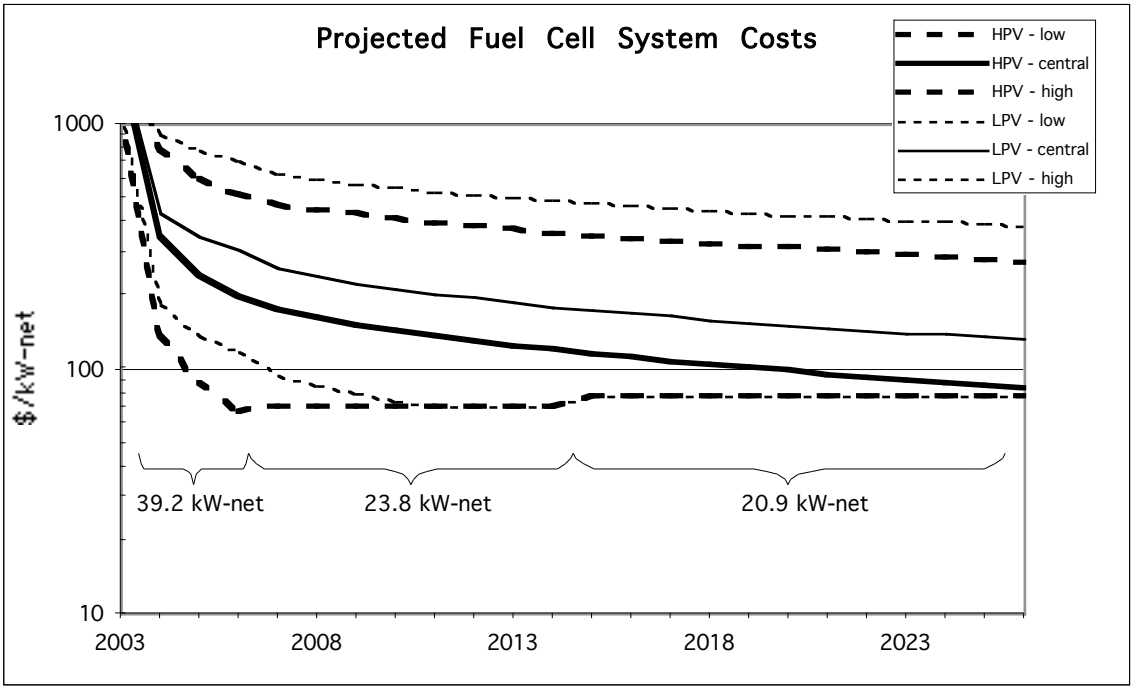

PEM Fuel Cell Stack and System Power Density and Specific Power

As discussed above, PEM fuel cell stack power densities have increased by approximately an order of magnitude in the past several years, to about 1 kW per L and 1 kW per kg at present. Ballard has packaged a 30-kW fuel cell stack into a cubic foot of volume (1.06 kW/L) and they are currently developing a design that will produce 50 kW in the same volume, for a power density of 1.77 kW per L (Brown, 1998). Lynntech, Inc. is also exploring compact, low-cost fuel cell stack designs. They have been exploring designs using metal rather than graphite flowfield plates, to reduce cell thickness, and they have constructed stacks with 0.967 kW per kg and 0.846 kW per L (Murphy, et al., 1998). They believe that stacks with 1.5 kW per kg and 1.2 kW per L will be possible with further optimization, including the weight and volume of endplates and hardware (Murphy, et al., 1998).

The state-of-the-art for overall system specific power is represented by the DaimlerChrysler NECAR IV, which achieves a total system specific power of 5 kg per kW (DaimlerChrysler, 1999b). This represents a dramatic improvement relative to earlier NECAR versions. For example, the NECAR I, developed in 1994, was powered by a 50-kW fuel cell system that required 12 separate stacks and had a specific power level of 21 kg per kW (0.048 kW/kg). The NECAR II was also powered by a 50-kW system, but it was configured into just two stacks and had a greatly reduced mass of 6 kg per kW (0.167 kW/kg). The 1997 NEBUS was fitted with a 10-stack, 250-kW fuel cell system that achieved 5.6 kg per kW (0.179 kW/kg). Finally, the 1999 NECAR IV achieved 5 kg per kW for a 70-kW system (0.2 kW/kg). Daimler-Benz engineers believe that they can further improve specific power by 20% to 40% in the near future, resulting in system masses of 3-4 kg per kW (DaimlerChrysler, 1999b). The DOE goals for a 50-kW

fuel cell system power density (including thermal, air, and water management and control systems but excluding fuel processing) are for 0.35 kW per L and 0.35 kW per kg by 2000, and 0.50 kW per L and 0.50 kW per kg by 2004 (U.S. DOE, 1998c).

The fuel cell stack and system mass and volume estimates assumed in this analysis are based on the above data for present power density performance, and projected future improvements. The estimates for fuel cell stacks, auxiliary systems, and complete systems are shown in Table 3-2. These estimates reflect overall system values of 0.25 kW per kg and 0.35 kW per L for Generation 1, 0.33 kW per kg and 0.40 kW per L for Generations 2 and 3, and 0.50 kW per kg and 0.45 kW per L for Generation 4. These estimates result in achievement of the DOE goal for specific power, and nearly achieving the goal for power density, but by 2015 rather than 2004.

Hydrogen Storage Tank Costs

Hydrogen can be stored onboard FCVs using a range of different storage technologies. The simplest method is to store hydrogen as a gas in pressurized cylinders, but it can also be stored in metal hydrides, adsorbent carbons, carbon nanotubes, glass microspheres, or as a cryogenic liquid (Banerjee and T-Raissi, 1994; Dillon, et al., 1997; Duret and Saudin, 1994; Ewald, 1998; James, et al., 1997). Cryogenic liquid hydrogen storage can also be combined with either high pressure storage or metal hydride storage, achieving some of the advantages of both types of systems (Berry and Aceves, 1998). Another recently developed option is to store hydrogen in solid alkaline hydride form, where the hydride can then be combined with water in order to evolve hydrogen gas (Powerball Technologies, 1999). Each of these methods has advantages and disadvantages with regard to technical feasibility, energy density, cost, safety, and refueling time (Table 3-3). Thus, a complex set of trade-offs is involved in the choice of a hydrogen storage technology, and at the moment there is no clear winner for all applications.

Potential Hydrogen Storage Technologies

Compressed-gas storage, at pressures of 3000 to 8000 pounds per square inch (psi) (20.7 to 55.2 megapascales (MPa)), is the simplest and most economical, but provides a relatively low volumetric energy density. The energy density can be increased by greater pressurization, but at pressures of 8000 psi (55.2 MPa) and above it becomes difficult to maintain a high test-safety factor. Perceived safety issues and high refueling station costs for ultra high-pressure delivery suggest that a storage pressure of around 5000 psi would be a good compromise. Recently developed fiber-reinforced composite storage tanks, made of aluminum wrapped with fiberglass, kevlar, or carbon, are lighter and stronger and more resistant to impacts than are all-metal tanks. The Al-carbon composite is the lightest and strongest but also the most expensive. Banerjee and T-Raissi (1994) report that Al-fiberglass, Al-Kevlar and Al-carbon tanks with a design pressure of 5000 psi (34.5 MPa) and a fuel volume of 5 cubic feet (ft^3) (0.14 cubic meters (m^3)) cost $1,060, $1,259, and $3,086 respectively (in 1990$) and weigh 131 kg, 94 kg, and 45 kg respectively. Even lighter fiber-wrapped tanks have recently been developed, based on the use of very thin (5 mil) laminated, metallized polymeric bladders, resulting in tank weights that are 30-40% lower

than when aluminum or plastic bladders are used (James, et al., 1997). Such tanks storing 6.8 kg of hydrogen (or 11.4 ft^3 at 5000 psi) would weigh just 50.3 kg (see Table 3-3). Current research efforts include those by the Thiokol Corporation, which is currently under contract with DOE to develop lightweight composite, 5000 psi storage tanks that are "conformable" in shape to ease packaging in motor vehicles (U.S. DOE, 1998c).

Liquid-hydrogen cryogenic systems are relatively compact and light, but quite complex, consisting of vacuum-insulated, heat-shielded, double-walled containers with pumps and heat exchangers. The most serious drawback is that on account of the extremely low storage temperature (20K -- near absolute zero), a substantial amount of fuel will boil off. Estimates of boil-off of 1.8% per day from a 130 L tank have been reported (Banerjee and T-Raissi, 1994), although more recent estimates are as low as about 1% per day (Ewald, 1998). Another major drawback is that 25% to 45% of the energy content in liquefied hydrogen is required for liquefaction, compared to about 9% needed to compress hydrogen to 20 MPa. Also, the safety hazards posed by the boiled-off hydrogen gas make indoor or confined-space parking impractical, unless systems are developed to adsorb, burn, or safety-vent the released hydrogen (Hansel, et al., 1993).

Vehicle refueling times for liquid hydrogen systems are somewhat variable depending on the need to cool tanks, refueling lines, and couplings. Complete refueling times, including cooling from ambient temperatures, of under 20 minutes have recently been reported, and reductions to 10 minutes are considered achievable with continued advances in refueling system development (Tachtler and Szyszka, 1994). Peschka and Escher (1993) report a state-of-the-art refueling time of between 4 and 4.5 minutes with a cold tank, but warm refueling lines. Starting with the tank at ambient temperature as well, they have achieved a 15-minute total refueling time.

Another interesting option is a hybrid gas per liquid cryogenic storage system that could be refueled with either pressurized hydrogen gas or liquid hydrogen. This cryogenic pressurized system avoids the boil-off problem of liquid hydrogen storage because the boiled-off gas is retained in the tank (as long as the vehicle were driven about 10 km per day to use some of the boiled-off fuel). Even with no driving, the system could retain one-third of its full capacity of liquid hydrogen indefinitely. Insulated cryogenic pressure vessel engineering and thermodynamic analyses have been conducted by James et al. (1997) and Aceves et al. (1998). James et al. (1997) estimate energy densities of 17.7 megajoules (MJ) per kg and 4.1 MJ per L for a 5000 psi capable system that stores 6.8 kg of hydrogen, based on the use of lightweight materials. Aceves et al. (1998) estimate densities of 20.0 MJ per L and 4.2 MJ per kg for two different 3600 psi systems that store 5 kg of hydrogen, based on multi-layer vacuum super-insulation and microsphere insulation. James et al. (1997) estimate a volume production cost of $611 for the 6.8-kg capacity system. While the system could be refueled with either liquid hydrogen or high-pressure gas, the energy stored could only be maximized with liquid hydrogen refueling (refueling with gaseous hydrogen at 3600 psi would provide about 1/3 the range of liquid fuel). The flexibility in refueling with either gas or liquid means that in principle drivers could pay the additional costs associated with liquid refueling only when they

needed the additional range, and could refuel with cheaper pressurized gas when more moderate driving ranges were needed.

Another type of hydrogen storage technology is metal hydride based, where hydrogen is stored in the interatomic spaces of a metal. Hydrogen is absorbed as the metal (typically powdered) is cooled and then evolved as the metal is heated. Hydrides are safe and reliable, and some types operate at moderate temperatures and pressures, but they are heavy and expensive (Table 3-3). Research efforts have primarily focused on Fe-Ti hydrides, La-Ni hydrides, Mg-hydrides, and Ti-Zr-V hydrides (Banerjee and T-Raissi, 1994). An ideal hydride would have a low temperature of hydrogenation and dehydrogenation, high hydrogen storage capacity, fast refueling capability, and low cost. As might be expected, none of the hydride materials available today provide all of these characteristics. Mg-hydrides can store up to 7.6% hydrogen by weight, but have a high dissociation temperature of approximately 290°C, while hydrides that operate at lower temperatures (from 20-80°C) can store only 1.3 to 5.5% hydrogen by weight (Banerjee and T-Raissi, 1994).

H-Power, a New Jersey company, has obtained a patent on a reduced-iron/oxidized-iron (oxidation/reduction) hydrogen-generation system (Werth, 1992). The process begins with iron oxide (Fe_3O_4) and a reducing gas (hydrogen or carbon monoxide), off-board the vehicle. The reducing gas and the iron oxide are reacted at high temperature (about 800-1,100° C if hydrogen is used) to produce reduced iron and steam. If pure hydrogen is used as the reducing gas, the reaction requires an external source of heat; if enough carbon monoxide (CO) is added, no external heat source is needed, because the reaction becomes exothermic. The reduced iron is transferred to the vehicle and stored as a powder in metal tubes. To produce hydrogen fuel on-board the vehicle, the iron-reduction reaction is reversed. Steam or hot water (over 50° C) is reacted with the reduced iron to produce hydrogen and iron-oxide. This hydrogen-generation (iron-oxidation) reaction takes place between 25° C and 900° C, but below about 500° C, a catalyst, probably a noble metal, is required. The catalyst may be alloyed with the metal, mixed with the water, or introduced in other ways. Overall cost, complexity, and performance will determine the balance between the use of a catalyst and the use of external heat. The fuel cycle is completed when the oxidized iron is removed from the vehicle to undergo the initial reduction (regeneration) reaction.

Hydrogen also can be stored at low temperatures and moderate pressures on high-surface-area adsorbing materials. Several different activated carbon adsorbents have been investigated. At 150-160K, hydrogen can be stored both as adsorbed molecules at the surface of activated carbon and as compressed gas in interstitial spaces (Hansel, et al., 1993). The level of adsorbency increases with better surface treatment of the carbon medium and decreased temperature. Research at Syracuse University has demonstrated that 12-13% by carbon weight of hydrogen can be stored at 77 Kelvins (K) and 55 atmospheres (atm) (Young, 1992). Costs increase with such low temperatures, but a temperature of 150 K with a pressure of 55 atm has been demonstrated to provide an adequate level of adsorption for vehicular applications (Young, 1992). In general, adsorbed carbon systems offer the advantages of a moderately high gravimetric energy density, a high degree of dormancy, and better safety than compressed gas systems. They suffer from a low volumetric energy density, a high degree of system

complexity, and the problem of gaseous impurities being readily adsorbed and reducing storage efficiency (Banerjee and T-Raissi, 1994).

Another carbon-based storage option is to store hydrogen in carbon nanotubes, which have been shown to have a high hydrogen uptake (Chambers, et al., 1998; Chen, et al., 1999; Dillon, et al., 1997). Graphite nanofibers have reportedly stored over 20 L of hydrogen per gram of material, with about 16 L of hydrogen being stored reversibly (Chambers, et al., 1998). In these investigations, it took several hours of hydrogen uptake at high initial pressure (112 atm) and ambient temperature (25 °C) to achieve these adsorption levels, but desorption was much faster, on the order of 5-10 minutes (Chambers, et al., 1998). The observed gravimetric storage densities were an astounding 43%-58%, counting only the weight of the adsorbent and the hydrogen (i.e., no containment or auxiliaries). These storage densities are far higher than for any other known system, including liquid hydrogen storage.

Also, hydrogen storage in single-walled carbon nanotubes, with diameters of 16.3 angstroms (Å) and 20 Å, has been demonstrated to provide volumetric storage densities of 45 to 50 kg of hydrogen per m^3 (Dillon, et al., 1997). These storage densities are again higher than for any other, non-carbon based system. The corresponding gravimetric storage densities are 3-4%, which are comparable to the best hydrides and are exceeded only by liquid hydrogen and compressed gas in carbon-polymer cylinders (Dillon, et al., 1997).

Finally, exciting results have been recently reported for studies of alkali-doped, multi-walled carbon nanotubes. Hydrogen storage levels of up to 14% by weight have been demonstrated with potassium-doped nanotubes (for the carbon material itself, not for a complete system with containment and auxiliaries), and storage levels of up to 20% by weight have been demonstrated with lithium-doped nanotubes (Chen, et al., 1999). The nanotubes must be heated to temperatures of 200 to 400 °C prior to absorption and for desorption, but in laboratory experiments absorption capacity remained at 90% of the original level after 20 absorption/desorption cycles (Chen, et al., 1999). More research and development will clearly be required before such carbon nanotube systems are available for automotive or other practical hydrogen storage applications. However, if cost, cyclability, and safety criteria can be met, these early results suggest that such systems may be developed in the near future for use where weight and volume are important constraints.

Another recently developed hydrogen storage option is to mix solid alkaline hydrides (also known as hydrolysis hydrides) with water in order to evolve gaseous hydrogen. Potential hydrides include those based on sodium, calcium, magnesium, potassium and lithium. In an investigation of the potential for generating hydrogen with several potential hydride formulations, Kong et al. (1999) found that CaH_2 and LiH produced the highest hydrogen yields, of about 96% and 90% respectively. $LiAlH_4$ was also found to produce a high yield of hydrogen per unit mass. Kong et al. (1999) also found that the rates of the reactions were easier to control when water vapor, rather than liquid water, was used as a reactant, and that the rates of heat production were also reduced. Interestingly, a recent joint venture between the Natex Corporation and Powerball Industries has formed Powerball Technologies, a company that is commercializing "powerball" technology. This technology involves forming solid sodium hydride (NaH) into small (ping-pong ball sized) balls that are

coated with plastic, stored in a tank with water, and then mechanically opened to release hydrogen via the exothermic reaction of NaH with water. In theory, one gallon of NaH balls in water, with 65% of the volume made up of the hydride, could evolve 287 grams of hydrogen. The practical yield is lower, however, because some hydrogen is left behind in NaOH solution. The systems developed to date seem to allow about 125 grams of hydrogen to be evolved for every gallon of solution (Powerball Technologies, 1999). Powerball Technologies is currently selling the hydride balls for $1-30 per gallon, depending on order size, and a storage and dispensing system with an 8-gallon capacity currently sells for $1,450 (Powerball Technologies, 1999). This system reportedly produces 11,795 L of hydrogen (about 1 kg) from each 8-gallon tank of hydroxide balls (Powerball Technologies, 1999). Based on these values, the system does not look like it will be very attractive unless its weight and cost can be reduced (see Table 3-3 for comparisons with other systems).

Other potential hydrogen storage systems include glass microspheres, liquid organic hydrides, and combined liquid hydrogen and metal hydride systems. These technologies are at the basic research or primary research and development stage. Table 3-3 provides details on the costs, performances, and refueling times of the hydrogen storage systems discussed above.

Hydrogen Storage for PEM FCVs

For light-duty motor vehicle applications, hydrogen storage system weight, volume, and safety requirements are especially critical. Metal hydrides, despite offering superior safety, will not be practical until weight and cost can be substantially reduced. Liquid hydrogen is generally more impractical than other systems because of its high boil-off rate and the complexity and duration of refueling compared to conventional gasoline tanks (Banerjee and T-Raissi, 1994). Carbon adsorption may become practical, particularly if refueling time can be decreased, and carbon nanotube systems are an exciting but still unproven option. Compressed gas storage probably is the most practical means of storage for the near-term. The containers are relatively simple, commercially available, and capable of being refueled quickly. Moreover, experience with compressed natural gas (CNG) refueling stations provides insight into the optimal design and management of compressed hydrogen stations (Ogden, et al., 1994).

Thus, for this analysis, hydrogen storage in compressed gas cylinders is assumed. Compressed gas storage systems are relatively bulky relative to liquid hydrogen systems, but the Ford P2000 vehicle and proof-of-concept designs have demonstrated that it is possible to package compressed hydrogen tanks (holding about 6.0 kg of hydrogen at 5000 psi) into a mid-sized vehicle, albeit with some loss of trunk space (Oei, et al., 1997b; Oei, et al., 1997a). The lightest and most attractive storage tanks are the recent designs based on the use of a thin, metallized polymeric bladder that is then wrapped in carbon fiber, as discussed above, although these tanks are not yet in commercial production. James et al. (1997) and Berry and Aceves (1998) estimate that these lightweight storage tanks can achieve a storage density of 13.5% by weight, at a pressure of 5000 psi. This translates into a total tank weight of 50.3 kg for 6.8 kg of hydrogen stored, or a 37.0 kg tank for 5.0 kg of hydrogen stored. Delucchi (1992) has estimated that valves, regulators, and hoses would add about 30 pounds (13.6 kg) to compressed hydrogen systems, thus lowering the storage

density to about 9.7% by weight (for a system that stores about 7 kg of hydrogen). For the analysis here, the 5000 psi hydrogen storage tanks used in Generation 1 DHFCVs are assumed to attain somewhat more typical hydrogen storage densities of 10% by weight for the tank alone and 7.9% for the complete system. Generation 2-4 storage systems are assumed to be fully optimized and to achieve the full potential of 9.7% hydrogen storage by weight.

DTI has estimated near-term and high production volume costs for both more conventional aluminum-lined and novel polymer-lined cylinders, based on analysis of the costs of similar cylinders for storing CNG. In general, the cost of a hydrogen cylinder rated for gas storage at 5000 psi will be somewhat higher than for a 3600 psi CNG cylinder due to the extra carbon fiber wrapping needed to support the higher pressure, at an equivalent test safety factor. DTI estimates that 39% more fiber would be needed for the 5000 psi hydrogen tanks (Thomas, et al., 1998a). The current selling prices of 3600 psi CNG cylinders produced in relatively low volumes is about $420 per kg of stored CNG. Once the materials costs are adjusted to account for the extra fiber (and the additional weight of gas that can be stored at 5000 psi is taken into account), the corresponding price of a hydrogen storage tank would be about $510 per kg of stored hydrogen. In very high volume production, DTI estimates that tanks storing 6.8 kg of hydrogen would cost from $570 to $1,111, depending on the cost of carbon fiber and the figure of merit of the tank (Thomas, et al., 1998a).[30] These estimates correspond to $84 per kg and $163 per kg of stored hydrogen. The range of estimates is based on low and high T-1000 carbon fiber costs of $8.80 per kg and $22.00 per kg, and tank figures of merit of 2.2×10^6 inches and 1.3×10^6 inches. The lower cost and higher figure of merit estimates reflect the use of the lightweight polymer bladder (and cheaper carbon fiber), and the higher cost and lower figure of merit reflect the use of an aluminum liner (and more expensive fiber).

Based on these cost calculations, ranges of hydrogen storage cylinder costs for DHFCVs can be estimated. Assuming that the high volume production cost estimates apply to manufacture of 200,000 units per year or more, and that the $510 per kg estimate applies to manufacture of several hundred to a few thousand units per year, approximate cost to production volume relationships can be established by assuming the logarithmic form shown in Figure 3-9. These relationships are based on a range of costs of from $500 to $600 per kg of stored hydrogen (with $550/kg as a central estimate) for orders of 2,000 units per year (corresponding to $4,202-5,042/gigajoule (GJ) on a lower heating value (LHV) basis), and a range of costs of from $84 to $163 per kg of stored hydrogen (with $124/kg as a central estimate) for orders of 200,000 units per year ($706-$1,370/GJ on a LHV basis).

[30] The tank figure of merit is the operating pressure (5000 psi here), times the safety factor (typically 2.25), times the internal volume of the tank, divided by the tank weight.

Figure 3-9:

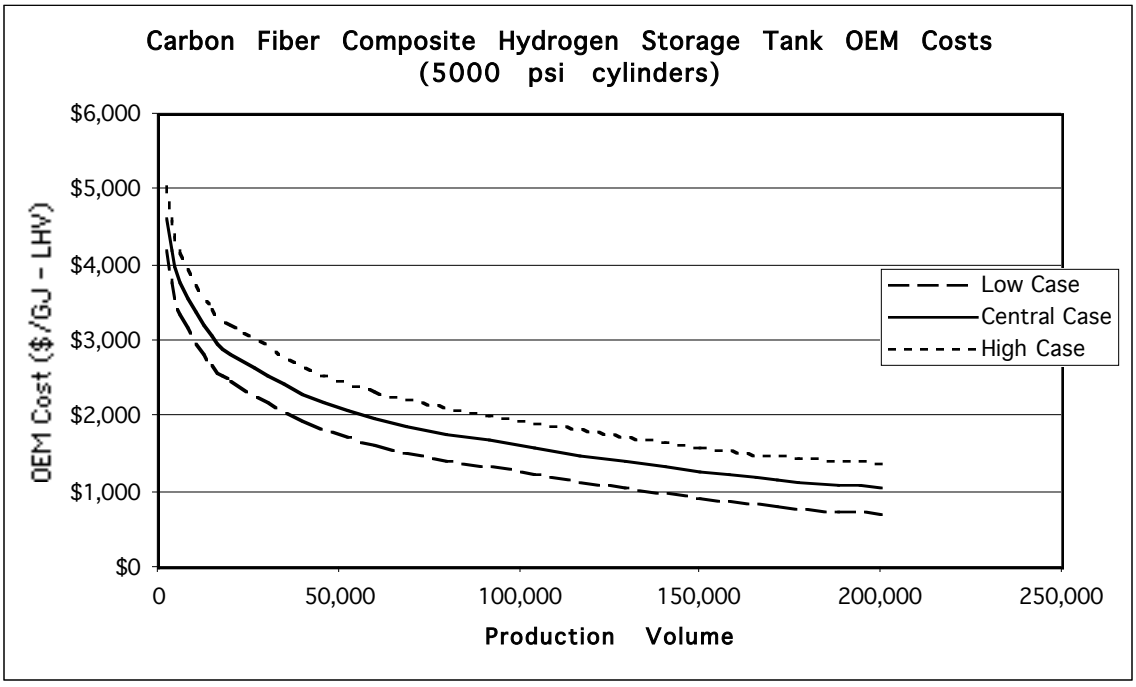

Peak Power Battery Costs

As discussed above, DHFCVs can operate with or without the assistance of a peak-power battery pack. Manufacturers have designed DHFCVs that are not hybridized, but some of the current designs that have been shown in public do include the use of batteries. These battery packs are optimized for high power, rather than high energy as for BEVs, and they use much smaller capacity cells so that an adequate voltage can be supplied from a relatively small battery pack.

As well as providing relatively high specific energy for BEVs, NiMH battery chemistry is also a good choice for high power battery designs for hybrid vehicles. In fact, given the high costs of NiMH battery materials, this battery type may ultimately find its best markets in the hybrid vehicle market, where the battery pack is much smaller and therefore less of a contribution to the overall cost of the vehicle. It is possible to design NiMH cells in such a way as to increase cell specific power, although this tends to decrease cell specific energy. For hybrid vehicles, this is a good trade-off since battery pack energy storage needs are relatively modest (e.g., in a charge-sustaining hybrid all of the energy needed to provide driving range is stored in the fuel tank, and even in a charge-depleting hybrid most of the energy is stored in the fuel tank).

One issue with modeling costs of different battery cell sizes is that many different designs are possible, and these designs give varying results for the effect of cell plate size on the specific power of the cell. The specific power of the cell can generally be improved by increasing the plate count and decreasing plate thickness. However, manufacturer data show that considerable specific power can also be gained simply by making the plates shorter, holding plate count constant. This is because current can be collected more efficiently through a

smaller plate. Thus, there are two effects to consider. First, cell power can be increased through specific changes in the battery design, and second there is an "automatic" increase in cell power as plate size is decreased.

For this analysis, Dr. Burke's model was modified[31] to account for the latter effect, by including values for the resistivity of various materials, and the model was then used to analyze battery designs for different cell sizes. Table 3-4, below, shows the characteristics of these different cell size designs, based on the "Gen3" technology discussed above, as calculated with the battery performance model. This table shows that cell specific power generally increases as plate area and cell capacity are decreased, with the exception of the 80 Ah case (which apparently is not well optimized for peak power).

The manufacturing costs and selling prices of these 10 Ah to 150 Ah cells have been estimated by making a few adjustments to the assumptions used for the 100 Ah reference cell. First, a different packaging scheme was assumed for the smallest cell sizes, with the 10 Ah cells packaged in 10-cell "multibloc" modules. These modules have internal cell connectors, so that only one set of terminal hardware is used for each 10-cell, 12V module. This packaging scheme reduces containment and hardware costs, and probably more accurately reflect the strategy that manufacturers would actually employ for smaller cells, relative to the simpler "1 cell, 1 container" assumption.[32] Second, costs of the battery containers were assumed to scale in proportion to their surface area. As in the analysis of the 100 Ah cells, both low and high price estimates were made in order to capture some of the uncertainty in key battery materials cost and corporate level cost parameters.

The following figures present selling price estimates for different battery cell sizes, at different production volumes. Figures 3-10 and 3-11 show prices as a function of $ per kWh and $ per kg. Figure 3-12 shows the results when the values at a production level of 20,000 packs per year are normalized to the value for the reference 100 Ah cell, in order to show the relative range of variation. As can be seen, prices of the smaller cells are considerably less variable as a function of cell weight than they are as function of cell energy, but they are not a constant function of either parameter.

---

[31] By him, with some assistance from me in obtaining the necessary input values.

[32] The trade-off to this strategy is that it is much harder to replace a single failed cell in a module that is composed of several cells.

Figure 3-10

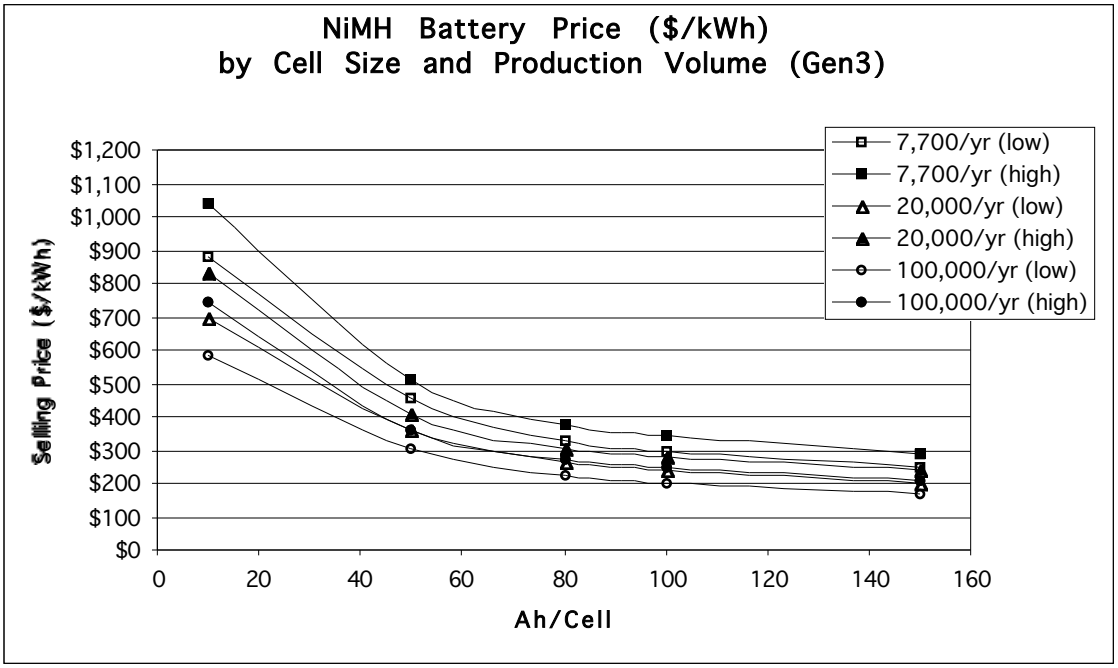

Figure 3-11

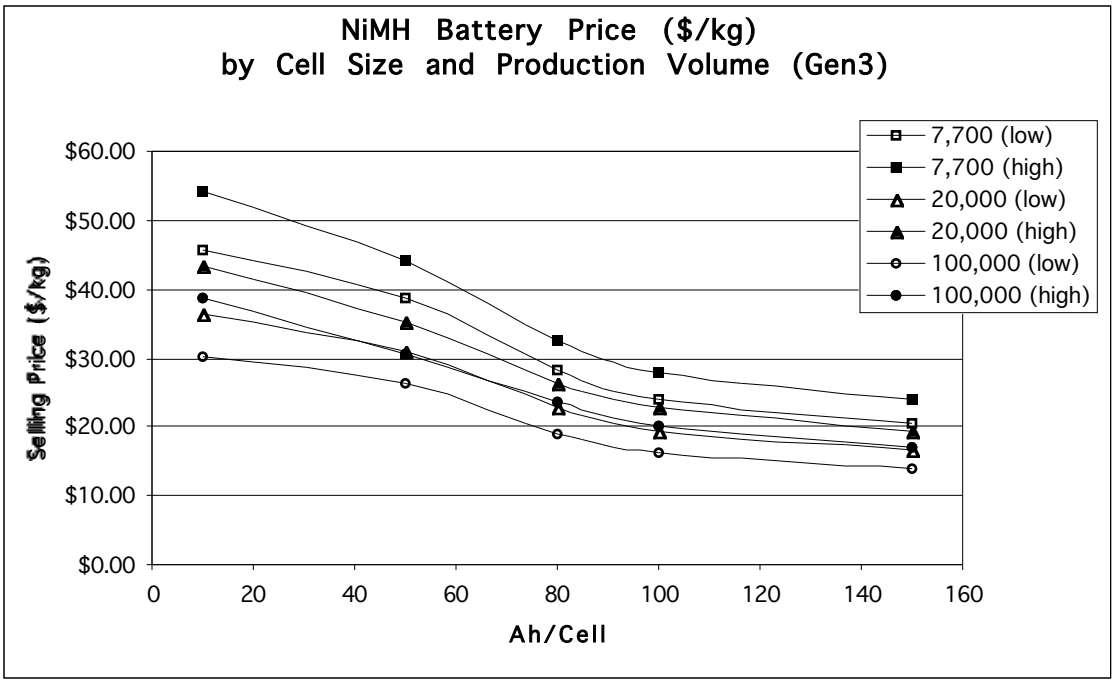

Figure 3-12

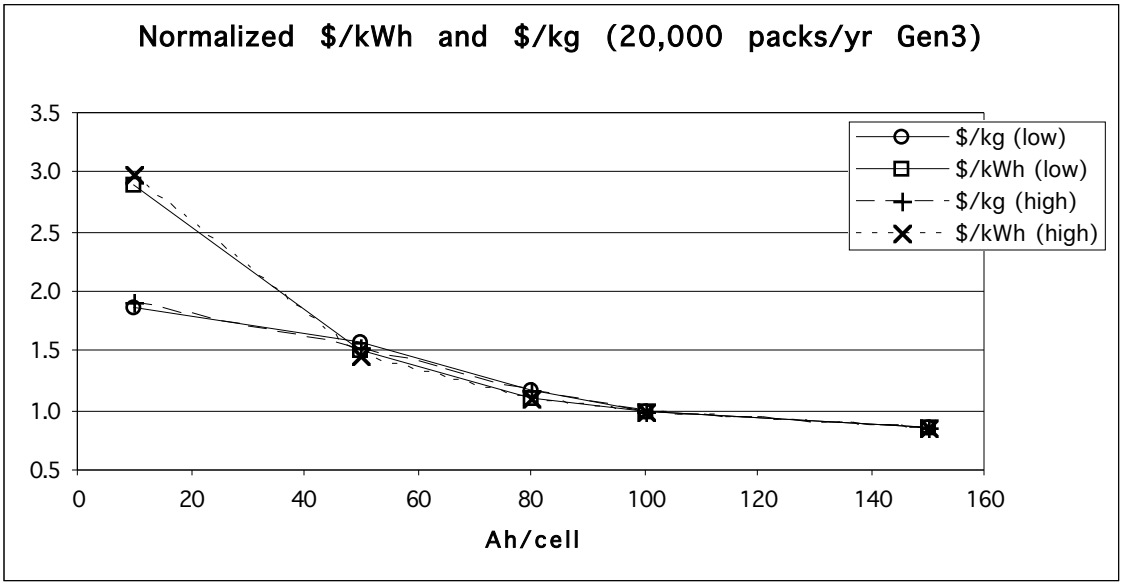

Figure 3-13 shows that, when normalized to the 100 Ah case, the dollar per kg and dollar per kWh prices of the Gen4 modules are somewhat less variable over the range of sizes of from 60 Ah to 20 Ah than are the prices of the Gen3 modules.[33] As in the Gen3 cases, the flattening of the price per kg curves shown in Figure 3-13 between 60 Ah and 20 Ah is due to the assumption that the 20 Ah modules are packaged in "multibloc" containers, each holding five cells, resulting in a reduction in hardware costs. The reduced variation in costs of the Gen3 modules with cell sizes from 60 Ah to 20 Ah is presumably due in part to the earlier introduction of the "multibloc" strategy (at 20 Ah vs. 10 Ah for Gen3). In general, the Gen4 modules have considerably lower prices than Gen3 modules when prices are expressed as a function of price per kWh, but prices are very similar when expressed as a function of price per kg. This is due to the lighter weights of the Gen4 modules, compared to Gen3 modules of the same capacity. OEM price results for all of the Gen4 module cases are shown in Table 3-5, both as a function of price per kWh and price per kg.

[33]60 Ah and 20 Ah Gen3 modules were not analyzed, but the corresponding prices can be approximated by examining trends in the prices of the 80 Ah, 50 Ah, and 10 Ah Gen3 modules.

Figure 3-13:

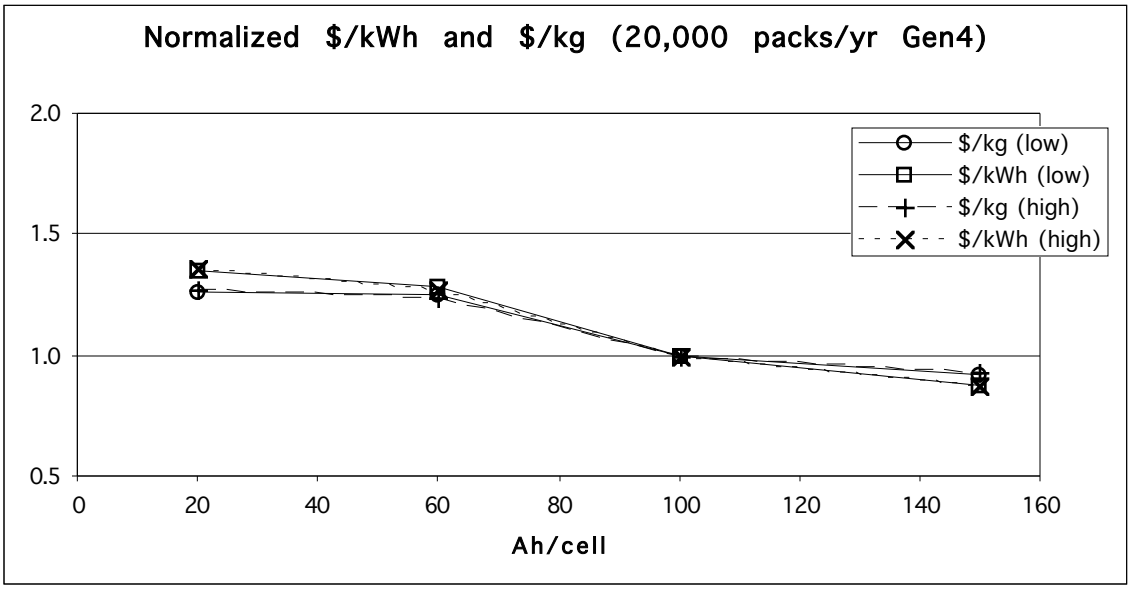

Costs of Peak Power Batteries for Modeled DHFCVs

Hybrid DHFCVs include a battery or ultracapacitor pack that complements the primary fuel cell power system used in the vehicle. In principle, any point along the continuum of battery to fuel cell power could be used as a design configuration. On one extreme, one could have a small "range extender" fuel cell stack, combined with a relatively large and powerful battery pack. Or, one could have a fuel cell stack that would almost be large enough to provide a given level of performance with no battery, coupled with a very small battery or ultracapacitor pack. Optimizing the configuration of the hybridized components is complicated by the need to consider both performance and cost criteria.

From a more practical perspective, a limitation arises from the specific power available for a certain battery type. One could use ultracapacitors instead of batteries to achieve higher specific power levels, but in any case the specific power required of the peak power device cannot be exceeded, given a certain power fuel cell system. For NiMH batteries in the 20 Ah to 60 Ah size range, specific power levels of 570 to 630 W per kg have recently been demonstrated by the Ovonic Battery Company (Ovshinsky, et al., 1998). These high specific power levels, compared to 300 to 350 W per kg for 100 Ah NiMH modules, represent a significant improvement over those demonstrated just a few years ago. This level of performance suggests that modern NiMH batteries are well suited for hybrid vehicle applications when they are optimized for specific power.

The determination of required battery energy capacity for a hybrid vehicle is necessarily somewhat subjective, since the choice depends on the level of performance that the vehicle is designed to have. At one extreme, the battery pack could have just enough capacity to recapture regenerative braking energy over a modest driving cycle on flat terrain. At the other extreme, the battery could be sized to have enough capacity to allow the vehicle to operate at peak

power over its entire driving range, so that it could carry a very heavy load or pull a trailer.

For the DHFCVs analyzed here, the configuration of the fuel cell system and battery pack was determined by setting the vehicle driving range at 300 miles[34] and then sizing the fuel cell system and battery pack. The components were sized such that sufficient battery capacity exists to recapture regenerative braking energy and to meet vehicle performance tests, while ensuring that the specific power required of the battery system does not exceed the limitations of the technology. The battery capacity needed to recapture the braking energy over the "FUDS*1.25" cycle is relatively modest, but more battery energy is required if the vehicle is required to operate at near peak power for a significant amount of time (e.g., to climb a long hill, to carry a heavy load, or to accelerate many times in succession).

For Generation 1 vehicles, the limit on battery specific power was assumed to be 600 W per kg, based on Ovonic Battery Company data (Ovshinsky, et al., 1998), for a 5.76 kWh battery pack (using 240 1.2 volt, 20Ah cells). The use of this battery pack resulted in the requirement for a 39.2 kW net-power fuel cell system. For Generation 2 and 3 vehicles, the peak power limit of the battery was assumed to be 625 W per kg. Coupled with improvements in fuel cell system component specific power levels, discussed elsewhere, and the resulting "decompounded" reduction in overall vehicle mass, this resulted in the reduced fuel cell system net power requirement of 23.8 kW. For Generation 4 vehicles, the battery pack size was scaled back slightly to 5.18 kWh (implying 18 Ah cells), the specific power limit was raised to 650 W per kg (based on the use of "Generation 4" NiMH battery technology), and the fuel cell system net power requirement was then 20.9 kW.

As noted above, these relatively large (for a hybrid vehicle) battery packs are capable of supplying considerably more energy than needed for operation under the regime of the "FUDS*1.25" driving cycle, or any of the other established driving cycles. Ultracapacitors or very high power, thin-foil, lead acid batteries would provide a better match to the idealized hybridization needs of most fuel cell vehicles, since under almost any reasonable driving conditions high power operation is needed only for brief periods. However, the use of NiMH batteries, with moderately high power combined with high energy density, has the advantage of allowing for a robust vehicle design that can operate at high power for extended periods of time if needed. An additional advantage is that a 5-6 kWh, 600 W per kg battery pack is capable of providing about 45 kW of power, so in theory the vehicle could be designed with a bypass system to allow operation on batteries only for several miles, under a reduced power mode. This could be useful in the event of a fuel cell system problem or if the vehicle were to

---

[34] Unlike BEVs, DHFCV costs do not vary greatly with driving range since only the fuel tank directly increases in size and cost with greater range (compared to the battery pack for BEVs). Increases in fuel tank size translate relatively weakly into greater body structure mass and drivetrain size. However, with bulky compressed hydrogen storage, fuel storage volume becomes an important constraint. Packaging storage cylinders large enough to provide driving ranges much in excess of 300 miles in a mid-sized vehicle becomes impractical for storage pressures of 5000 psi. Sensitivity of cost results to assumed driving range for all vehicle types is discussed in Chapter 7.

run out of hydrogen. Further details of the vehicle configurations and component characteristics assumed in this analysis are provided in Table 3-2.

Hydrogen FCV Fuel and Maintenance Costs

As discussed above, the most plausible initial scenarios for producing hydrogen for DHFCVs are via small-scale steam reformation of natural gas at service stations, or in larger scales at a centralized facility. The centrally produced hydrogen fuel could then be compressed into a liquid and delivered to filling stations by tanker trucks. At present, approximately 20,000 liquid hydrogen tanker trailer truck deliveries are made each year in the U.S., so there is already a well-defined infrastructure for this delivery method (Moore and Raman, 1998). In the longer term, a network of hydrogen pipelines could be constructed to eliminate the need to liquefy and deliver hydrogen with trucks. The capital costs of pipeline construction are quite high, however, on the order of $1 million per mile in urban areas by one estimate (Ogden, et al., 1999). As a result, this is not a feasible near-term option when the number of DHFCVs to be supported is relatively low, but eventually it could become an attractive option.

Moore and Raman (1998), of Air Products and Chemicals, Inc., have examined decentralized production of hydrogen via steam methane reforming (SMR), as well as centralized SMR at two different production scales. In the decentralized case, hydrogen is estimated to be produced at a cost of $3.57 per kg ($30 per GJ LHV and $25 per GJ higher heating value (HHV)) at a $9.6 million station that produces 2.7 tonnes per day of hydrogen (enough to refuel approximately 500 vehicles). Hydrogen production at centralized facilities was examined at a level of 27 tonnes per day in the smaller scale case, while the larger scale case was for production of 270 tonnes per day. Moore and Raman (1998) assumed that the hydrogen would be shipped by tanker truck an average of 500 miles (800 km) to either 10 fueling stations (small case) or 100 fueling stations (large case). Each fueling station would thus receive 2.7 tonnes of hydrogen per day, which would be enough to refuel about 500 vehicles each day. Each filling station would have enough storage capacity to last about 1.5 days, in case truck deliveries were delayed on any given day (i.e. about 4.5 tons of storage capacity). These assumptions yielded delivered hydrogen costs of about $3.35 per kg ($28 per GJ LHV and $24 per GJ HHV) with the smaller reformer, and about $2.35 per kg ($20 per GJ LHV and $17 per GJ HHV) with the larger reformer. The smaller scale production case implies a capital investment of about $63 million, while the larger case implies a capital cost of about $259 million (Moore and Raman, 1998). Thus, according to this analysis, the costs of producing hydrogen via SMR at decentralized, local facilities is comparable to the costs of production and delivery with relatively small-scale, centralized SMR, and about 50% higher than the cost of production with large-scale, centralized SMR.

Ogden et al. (1999) have examined production of hydrogen via steam reforming of natural gas at both service stations and centralized facilities, across a range of production scales. Of the options discussed above, they found that centralized production and truck delivery of liquid hydrogen was the most expensive option at most production scales, followed by centralized production with pipeline distribution, and then onsite production with conventional and advanced reformer technology. While onsite production with conventional reformer technology was found to have the highest costs at the low production

level of 100,000 standard cubic feet (SCF) per day, of about $40 per GJ (HHV), costs were estimated to drop rapidly with production scale. With production of 366,000 SCF per day, costs of onsite, conventional SMR were comparable to the liquid delivery and gaseous pipeline options, at about $20 per GJ (HHV). At production of 1 million SCF per day and 2 million SCF per day, costs of onsite, conventional SMR production were estimated to be somewhat lower than the other options, reaching a low value of about $12 per GJ (HHV). Onsite SMR production with advanced reformer technology, of the type used in fuel cell co-generation plants such as ONSI Corporation's PC-25 200-kW, phosphoric acid fuel cell unit, was found to be the least expensive option at all production levels. This was largely due to reduced reformer costs relative to the conventional SMR option, and the elimination of costs associated with liquefying hydrogen for truck delivery and of developing pipelines for distributing gaseous hydrogen. The overall ranges of costs estimated were from about $20-30 per GJ (HHV) for liquid hydrogen delivered by truck (over a range of production of from 0.1 to 2.0 million SCF per day), about $18-27 per GJ (HHV) for hydrogen delivered by pipeline, $12-40 per GJ (HHV) for onsite production with conventional reformers, and about $11-25 per GJ (HHV) for onsite production with advanced reformers (Ogden, et al., 1999). The local production scenario assumed energy prices in the Los Angeles area of $2.80 per GJ for natural gas and $0.03 per kWh for electricity (off-peak).

In a similar analysis of onsite hydrogen production with advanced fuel cell system reformers, Thomas et al. (1998c) have shown that delivered costs of hydrogen are sensitive to both the production volume of the reformer "appliances" as well as the number of supported vehicles. For example, for a station using a SMR unit produced in "one of a kind" production, supporting 100 vehicles (and producing 56 kg of hydrogen per day), delivered hydrogen costs were estimated at about $4.30 per kg (or $36 per GJ LHV and $30 per GJ HHV). When the same sized station used an SMR unit produced in 10,000 unit quantities, delivered hydrogen costs dropped to about $1.50 per kg ($13 per GJ LHV and $11 per GJ HHV). These costs are estimated to decline further when the scale of the plant is increased to support 1,000 and 10,000 vehicle fleets. At the 10,000 vehicle fleet support level, the delivered costs of hydrogen are estimated to range from about $2.00 per kg ($17 per GJ LHV and $14 per GJ HHV) in the single-unit plant, to about $1.20 per kg ($10 per GJ LHV and $8 per GJ HHV) with plants produced in 10,000 unit quantities (Thomas, et al., 1998c).

For comparison with these estimates, it is worth noting that a hydrogen dispensing station opened in May of 1999, at the Munich airport in Germany. The station provides both liquid hydrogen fuel, which is trucked in from a nearby liquid hydrogen production plant, and gaseous fuel that is produced from an advanced pressure electrolyzer at the airport. The gaseous hydrogen is sold at a price of DM 0.65 ($0.34) per standard cubic meter, or about $27 per GJ (HHV) (or $34 per GJ on a LHV basis), and the liquid hydrogen is sold at a price of DM 1.10 ($0.59) per L, or about $59 per GJ (HHV) (Hydrogen and Fuel Cell Letter, 1999b). Thus, the early German experience suggests costs considerably higher than the Ogden et al. (1999) estimates for distribution of liquid hydrogen (the Munich prices are reported to barely cover costs of fuel production and delivery), but it does not offer insights into potential costs of hydrogen production via decentralized SMR. Also, the costs of electricity and other inputs

used in producing the liquid and gaseous fuel in Germany were not disclosed, and they may be higher than the costs assumed by Ogden et al. (1999) for hydrogen production in the U.S. However, the Ogden et al. (1999) estimates for onsite hydrogen production via electrolysis range from about $25-35 per GJ, and thus agree well with the $27 per GJ price of gaseous hydrogen produced through electrolysis at the Munich airport.

Thus, hydrogen production at service stations via SMR of natural gas with conventional reforming technology is expected to cost from $12-40 per GJ (HHV), depending on the hydrogen production scale, the cost of the reformer system, and other assumptions. Similarly, production with advanced reformer technology is expected to yield delivered hydrogen costs of $8-30 per GJ (HHV). Given the various factors and uncertainties behind these figures, it is important to consider a range of potential hydrogen fuel costs. However, the rather wide range of costs estimated for hydrogen production in the studies discussed above can be narrowed somewhat by considering the numbers of DHFCVs that would be in the fleet in any given year, and the number of refueling stations that might be needed to support that fleet.

In the context of analyzing the costs associated with providing an initial level of baseline hydrogen refueling stations, in Chapter 5, the issue is discussed of the minimum level of refueling infrastructure that would be required in order to make FCV purchases feasible for consumers. For a region the size of the South Coast, approximately 100 refueling stations would be needed to assure consumers that there would be a station within several miles of their homes and workplaces (see Chapter 5 for details). These stations could be constructed over a five-year period such that in the first year, a skeletal infrastructure of only 20 refueling stations is available, but that 20 additional stations are added every year for five years. Since the reformer systems currently built by the ONSI division of International Fuel Cells (IFC) and marketed by Praxair, Inc., are modular systems that can be increased in size as the fleet grows, the refueling stations built initially can be rather small, when the size of the fleet is small. The refueling stations can then be increased in size with the growth of the fleet, and hydrogen can be sold at a lower cost.

Thus, assuming that 100 refueling stations are built over five years, the ratio of the vehicles in the fleet to the number of stations is as shown in Table 3-6, for the low and high production volume scenarios. Based on these estimates and on the relationships shown in Thomas et al. (1998c) for delivered hydrogen costs as a function of the number of vehicles supported, narrower ranges than shown above can be estimated for hydrogen costs for each generation of vehicles. These estimates, also shown in Table 3-6, assume that reformers are built in relatively small production runs of 20-100 units. Hydrogen costs are estimated to be in the range of $14-21 per GJ (HHV) for Generation 1, $11-15 per GJ for Generation 2, $10-13 per GJ for Generation 3, and $8-11 per GJ for Generation 4, with slight differences in the ranges for the low and high production volume scenarios.

DHFCV Maintenance and Repair Costs

Potential maintenance and repair costs for DHFCVs are difficult to estimate because there has not yet been any direct experience with FCVs under real-world operating conditions. A fleet of FCV taxis has just begun to operate in

London, but they have not been in use long enough yet for maintenance and repair data to be gathered. The first FCV demonstration project in the U.S. is scheduled to start in California in 2000, with five to ten vehicles in the first year. This demonstration may yield some insight into potential FCV maintenance and repair costs, but obviously not for several years and in any event the data gathered on the fleet are likely to be held as proprietary by Ford and DaimlerChrysler. Furthermore, while there are only a few detailed cost studies that include maintenance and repair costs for BEVs, such as Vyas et al. (1998), there are even fewer for FCVs.

As with BEVs, maintenance are repair costs for DHFCVs are estimated in the Lotus 1-2-3 model by separating out maintenance and repair costs for components that are the same as in ICEVs, components that are similar, components that are unique to ICEVs, and components that are unique to FCVs. The same maintenance and repair costs for FCVs are assumed as for ICEVs for the common components, and of course unique ICEV components have no maintenance and repair costs for FCVs. As with BEVs, the same and similar components for DHFCVs are assumed to have a 0%, 10%, or 30% advantage relative to ICEVs depending on the development level of the vehicles. For the unique fuel cell and hydrogen storage system components in FCVs, maintenance and repair costs are assumed to be modest due to the relative simplicity of these systems. Fuel cell system maintenance and repair costs are estimated to be about $40 per year, and hydrogen storage systems are assumed to only need periodic leak detection, with an average cost of about $10 per year (Delucchi, 1999). These assumptions result in maintenance and repair cost estimates of $475 per year for Generation 1 DHFCVs, $449 per year for Generation 2 and 3 DHFCVs, and $397 per year for Generation 4 DHFCVs, relative to $492 per year for the ICE Taurus (all on a levelized basis).

DHFCV Consumer Cost and Lifecycle Costs Results

As in the BEV cost analysis, the vehicle cost and performance model was run under assumptions for manufacturer production in each year, for each case (i.e. high cost, central cost, and low cost), and for each of the two production volume scenarios. In addition to variations in motor costs, controller costs, and battery costs, as in the BEV analysis, fuel cell system costs, hydrogen storage tank costs, and hydrogen fuel costs were also varied using the cost estimates discussed above. Also as in the BEV analysis, some minor component costs and some component weights vary in the model depending on whether the vehicle technology production/development level is classified as "low," "medium," or "high." As with BEVs, Generation 1 DHFCVs were assigned a low development level, Generation 2 and Generation 3 DHFCVs were assigned a medium development level, and Generation 4 DHFCVs were assigned a high development level.

A similar procedure was used to perform the model runs as was described in Chapter 2 for the BEV analysis. First, for each vehicle generation, important vehicle characteristics such as vehicle weight, battery and fuel cell power requirements, and drivetrain peak power were calculated in the model depending on the characteristics of the fuel cell system and battery pack assumed for that vehicle generation (see above discussion of fuel cell and battery sizing for more details). Next, component costs for the battery, motor, controller, fuel

cell system, and hydrogen storage tank, as well as hydrogen fuel costs, were determined for the particular production volume in that model year. This was done by developing similar cost functions for each component and power rating as shown in Table 2-23 for BEV components, with the exception that the "bounded MPF" technique was used to estimate fuel cell system costs, rather than the production volume based approach used for the other components. These component cost estimates are shown in Tables B-3 and B-4 in Appendix B.

The calculated component costs were then entered and the vehicle cost model was run for each case (high, central, and low), for each year of the analysis, for that vehicle generation. Then, the procedure was repeated for the next generation of vehicles, with new vehicle specifications calculated for Generation 2 and Generation 4 vehicles, and for each production volume scenario.

As in the BEV analysis, no economies of scale beyond production of 100,000 batteries per year and 200,000 drivetrain and hydrogen storage tank components per year were assumed for the central and high cost cases. For the low cost case, however, economies of scale for battery production above 100,000 units per year and drivetrain and hydrogen storage tank production above 200,000 units per year were extrapolated for the actual production volume. Once again, this produced only minor further decreases in final vehicle costs.

The vehicle purchase cost and lifecycle cost estimates for each scenario, along with key vehicle characteristics for each vehicle generation, are presented in Tables 3-7 and 3-8. Vehicle purchase costs for the two scenarios are shown in Figure 3-14 (at end of chapter), as a function of production volume. These results show that under the assumptions of this analysis, where a 300-mile vehicle range is assumed, vehicle consumer costs drop from a high of over $175,000 in the lower production highest cost case, to just over $24,000 in the higher production, lowest cost case. At the highest volume production of about 270,000 units per year, initial purchase costs for the least expensive DHFCVs remain about $5,700 higher than the $20,155 price of the gasoline ICE Taurus (about $4,000 and $12,600 higher in the low and high cost cases).

Vehicle costs drop rapidly after the first year of introduction largely due to reductions in the cost of the fuel cell system. Since the level of cumulative DHFC production at the time the first DHFCVs are introduced in 2003 is only 10 MW, system costs are still on the order of $1,125 per kW, $1,750 per kW, and $2,550 per kW (for the low, central, and high cost cases) at that point. However, just one year of production at the levels assumed for 2003 (10,000 and 20,000 vehicles in the low and high production volume cases) is enough to increase the cumulative production levels for the next year to 794 MW and 1,578 MW (assuming supplier production of twice as many 26.7 kW-net systems needed by the single large automaker whose production is modeled in this analysis). This much higher base of cumulative production in Year 2004 leads to substantially lower DHFC system costs, as computed by the MPF-based cost function, and to lower overall vehicle costs. DHFC system cost reductions continue to drive vehicle cost reductions in subsequent years, along with cost reductions in other components and optimized vehicle designs, but more and more gradually.

From a lifecycle cost perspective, the least expensive DHFCV (the low cost case vehicle in year 2026) nearly achieves cost parity with the conventional vehicle. Its $0.4006 cost per mile is within a half of a cent per mile of the $0.3968

per mile lifecycle cost of the gasoline ICE. Even the central case, year 2026 vehicle in high volume production has a comparable lifecycle cost, at $0.4019 per mile, as the ICE Taurus. As is discussed further in Chapter 7, one assumption behind these lifecycle cost estimates is that fuel taxes contribute about 1.75¢ per mile to the lifecycle costs of both the gasoline Taurus and the DHFCVs. If a government policy were enacted to eliminate taxes on hydrogen, in order to encourage its use, then the lifecycle cost of the year 2026 low cost case DHFCV would be about 1.37¢ per mile lower than that of the ICE Taurus, and the lifecycle cost of the year 2026 central case DHFCV would be about 1.24¢ per mile lower.

DHFCV Fleet Cost Results

With the calculated costs of owning and operating DHFCVs in each analysis year, total fleetwide costs of DHFCVs operated in the SCAB have been calculated. As with BEVs, these calculations have been performed in the Simulink model, using the same underlying VMT schedule used in the Lotus 1-2-3 model to determine the levelized costs shown in Tables 3-7 and 3-8. The net present values of fleetwide vehicle owning and operating costs, for each case, are shown in Tables 3-9 and 3-10. These estimates assume the same 165,000-mile and 17.3-year average vehicle lives assumed in Delucchi (1999), and the same variable VMT schedule and 3.65% discount rate discussed in Chapter 2.

Tables and Large Figures for Chapter 3

Table 3-1: Results for PEM Fuel Cell Cost Forecast for Various Cases (for 21-kW net power system)

Cumulative Production Level (MW)	Low Case: 75% MPF slope ($/net kW)	Central Case: 80% MPF slope ($/net kW)	High Case: 85% MPF slope ($/net kW)
5	$1,500.00	$2,200.00	$3,000.00
10	$1,125.21	$1,760.16	$2,550.29
100	$432.71	$838.73	$1,486.36
1,000	$166.40	$399.66	$866.28
10,000	$76.55	$190.44	$504.89
100,000	$76.55	$90.75	$294.26
1,000,000	$76.55	$76.55	$171.50
10,000,000	$76.55	$76.55	$99.95

Table 3-2: DHFCV Specifications and Characteristics (300-mile driving range)

Specification	Gen 1 Vehicles	Gen 2/3 Vehicles	Gen 4 Vehicles
Fuel Cell System:			
Gross power	50.0 kW	30.0 kW	26.0 kW
Net power	39.2 kW	23.8 kW	20.9 kW
Compressor efficiency	70%	75%	80%
Net system efficiency[a]	40.1%	39.2%	39.0%
Power density – stack	0.0353 ft^3/kW (1.000 kW/L)	0.0294 ft^3/kW (1.202 kW/L)	0.0200 ft^3/kW (1.767 kW/L)
Power density – aux.	0.0660 ft^3/kW (0.535 kW/L)	0.0589 ft^3/kW (0.600 kW/L)	0.0585 ft^3/kW (0.604 kW/L)
System power density	350 W/L	400 W/L	450 W/L
Specific power - stack	1 kg/kW	0.85 kg/kW	0.67 kg/kW
Specific power – aux.	3 kg/kW	2.15 kg/kW	1.33 kg/kW
System specific power	4 kg/kW (250 W/kg)	3 kg/kW (333 W/kg)	2 kg/kW (500 W/kg)
NiMH Battery Pack:			
Pack energy	5.76 kWh	5.76 kWh	5.18 kWh
Pack maximum power	48.5 kW	51.3 kW	48.7 kW
Pack mass	81.2 kg	82.1 kg	74.8 kg
Maximum power density	599 W/kg	625 W/kg	651 W/kg
Pack specific energy (c/3)	69 Wh/kg	69 Wh/kg	68 Wh/kg
Cell capacity	20 Ah	20 Ah	18 Ah
Motor/controller:			
Peak power rating	82 kW	70 kW	65 kW
System voltage	288 V	288 V	288 V
Hydrogen storage system:			
Tank pressure	5000 psi	5000 psi	5000 psi
Weight of hydrogen[b]	8.00 kg	7.39 kg	6.94 kg
Total system weight[c]	101 kg	75.7 kg	71.7 kg
Inner/outer tank volume	12.86/15.78 ft^3	11.87/14.56 ft^3	11.15/13.68 ft^3
Storage density[d]	7.9%	9.7%	9.7%
Vehicle drag coefficient	0.24	0.24	0.24
Vehicle efficiency:[e]			
On "FUDS*1.25" cycle	38.2 mpg-eq (HHV) 298.8 mi/MMBTU	41.7 mpg-eq (HHV) 326.6 mi/MMBTU	44.2 mpg-eq (HHV) 346.4 mi/MMBTU
On FUDS cycle[f]	44.5 mpg-eq (HHV) 355.8 mi/MMBTU	47.8 mpg-eq (HHV) 382.6 mi/MMBTU	50.1 mpg-eq (HHV) 401.1 mi/MMBTU
Vehicle curb mass	1,563 kg	1,330 kg	1,227 kg
0-60 mph accel. time	9.3 sec	9.4 sec	9.4 sec

Notes: FUDS = Federal Urban Driving Schedule; HHV = higher heating value; NiMH = nickel-metal hydride.

[a] For vehicles tested over the "FUDS*1.25" cycle.

[b] For a range of 300 miles.

[c]Includes weight of tank plus 13.6 kg for valves, regulators, and hoses.

[d]Weight of hydrogen divided by weight of total system times 100%.

[e]Vehicle efficiency values are approximate because vehicle efficiency is difficult to calculate accurately, and different models will produce different vehicle efficiency estimates. Efficiencies in mpg-equivalents would be about 1.09 times *higher* on a LHV basis due to the relative HHV/LHV values for gasoline and hydrogen.

[f]Values are slightly inaccurate because when modeled over the FUDS cycle vehicle components are resized slightly, and drivetrain power and vehicle mass decrease relative to the values shown in the table. For comparison, the ICE Taurus has a calculated 20.1 mpg fuel economy over the FUDS cycle.

Table 3-3: Characteristics of Hydrogen Storage Systems

Storage system	Installed fuel system energy density[a] (MJ/L)	(MJ/kg)	Container cost[b] ($-OEM/GJ)	Refuel time[c] (minutes)	Station cost[d] ($/GJ)
Gasoline tank[e]	32.4	34.0	$20	2-3	$0.6
Carbon/alum. cylinder @5000 psi (34.4 MPa)[f]	2.5	11.5	$4,250 .	2-3	$4-6
Cryogenic liquid[g]	4.4-5.4	19.2-28.6	$600-1,000	4-15	$3.5-5 ($11)
Iron oxidation/red.[h]	5.8?	5.0?	$500?	?	$3?
Cryoadsportion[i]	2.1	6.3	$2,000-4,000	5	$4-5
Cryogenic pressurized[j]	4.1-5.8	9.5-20.0	$750?	2-15	$4-11
FeTi metal hydride[k]	2-4	1-2	$3,300-6,000	20-30	$3-4
Organic liquid hydride[l]	0.5	1.0	?	6-10	?
Carbon nanotubes[m]	6.0?	4.8?	$900-920?	10-15?	?
Sodium hydride balls[n]	2.5?	1.2	$12,100	2	?

Notes: HHV = higher heating value; GJ = gigajoule; LHV = lower heating value; MJ = megajoule; OEM = original equipment manufacturer.

[a] Weight and volume of container, fuel, and auxiliaries.

[b] Cost to the OEM, per GJ (LHV) of storage capacity.

[c] Time to deliver fuel; does not include time to pull in, pull out, or pay.

[d] The full owning and operating cost of the station. The cost of H_2 is not included here.

[e] Energy density was calculated assuming that an empty gasoline tank weighs 12 kg, and that the ratio of the outside displacement of a tank to its inner capacity is 1.075:1. The estimate of the cost of the tank is based on data in the American Council for an Energy-Efficient Economy (ACEEE, 1990).

[f] Carbon-wrapped aluminum-lined high-pressure vessel. The cost estimates are from (Thomas, et al., 1998a), who examined costs of 3600 psi natural gas cylinders and scaled the estimates to account for the extra carbon fiber wrapping needed for 5000 psi H_2 storage (39% more fiber). The figures in parentheses are Thomas et al.'s extrapolations to volume production of the cylinders, assuming high and low carbon fiber costs of $22 per kg and $8.80 per kg, respective tank figures of merit of 1.3×10^6 inches and 2.2×10^6 inches, and a tank storage capacity of 6.8 kg. The storage densities assume the use of recently developed, lightweight tanks using very thin (5 mil), metallized polymeric bladders, and an additional weight of 13.6 kg for valves, regulators and hoses. The estimate of station cost is from Lipman and Delucchi (1996).

[g] The energy densities are from Aceves et al. (1998) and James et al. (1997). The tank cost estimate is from (James, et al., 1997). The station costs are based on data in DeLuchi (1989). The estimate of the station mark-up in parentheses includes the cost of liquefying H_2 (about $6/GJ); the other estimate does not. According to Peschka and Escher (1993), the DLR BMW LH_2 tanks can be refilled in 4-4.5 minutes when they are cold. Tachtler and Szyszka (1994) and Peschka and Escher (1993) report complete refueling times of just under 20 minutes and 15 minutes respectively, including cooling of the tank, fueling line, and couplings.

[h] Joe Maceda (1991) of H-Power gives the following performance specifications for this system: 22.66 Wh-electricity per cubic inch of storage, and 366 Wh-electricity per pound of storage, assuming 50% H_2-to-power efficiency on a LHV basis (42% HHV basis). This translates into 11.7 MJ/L and 6.8 MJ/kg, but these values refer to the actual iron storage media only, and do

not include metal tubes, steam and water lines, fuel lines, pumps (if any), separators, pre-heaters (if any), insulation, or the overall enclosure. Since the station would not have compressors or coolers, the station mark-up should be less than the mark-up for compressed, liquid, or cyroadsorbed H_2. The developers of this system believe that refueling can be performed quickly (Werth, 1992).

[i] Young (1992) estimates 6.83 MJ/kg and 1.92 MJ/L (including fuel) for a carbon adsoprtion system storing hydrogen at 55 atm and 150 K. In another paper from the same research group, Amankwah et al. (1990) estimate 7.2 MJ/kg and 2.4 MJ/L (they assume kevlar-wrapped tanks). For the calculations shown in the table, including auxiliaries is assumed to reduce these energy-density values by 15%. The refueling station would require a compressor, refrigerator, and vacuum pump. Amankwah et al.'s (1990) estimate of the station cost was used, except that a cost of $0.07/kWh was assumed for electricity. The cost of the container is based on statements in Amankwah et al. (1990) indicating that the vessel would cost more than an LH_2 vessel, but less than half as much as a hydride system.

[j] This system stores liquid and/or pressurized H_2 gas, thereby alleviating the boil-off problem with LH_2 storage. The system could retain one-third of its full capacity of liquid hydrogen indefinitely. Insulated pressure vessel engineering and thermodynamic studies have been made by James et al. (1997), Berry and Aceves (1998), and Aceves et al. (1998). James et al. (1997) estimate 17.7 MJ/kg and 4.1 MJ/L for a 5000 psi capable system, based on the use of lightweight materials. Aceves et al. (1998) estimate 20.0 MJ/L and 4.2 MJ/kg for two different 3600 psi systems, using multi-layer vacuum super-insulation and microsphere insulation. Berry and Aceves (1998) report estimates of 13.2 MJ/kg and 5.8 MJ/L for a 20.6 MPa (3000 psi) capable system that stores 11.4 kg of liquid H_2, and 9.5 MJ/kg and 5.2 MJ/L for a 34.4 MPa (5000 psi) capable system that stores 10.3 kg of liquid H_2. The system cost estimate shown is from (James, et al., 1997), of $611 for a system capable of storing 6.8 kg of H_2. The system could be refueled with either LH_2 or high-pressure gas, but the energy stored could only be maximized with LH_2 refueling (refueling with gas only would provide about 1/3 the range of liquid fuel). Refueling station costs reflect the less expensive, near-term option of refueling with gaseous H_2, and accepting the lower storage density, and the higher cost option of dispensing liquid H_2 (including the cost of liquefaction).

[k] The hydride cost estimates are based on data in DeLuchi (1989) and James et al. (1997). Magnesium hydrides would offer nearly a three-fold higher gravimetric energy density, and would be 3-4 times less expensive than FeTi hydrides, but they are not yet suitable for vehicular applications because of their high dissociation temperature of about 300 °C.

[l] In this system methylcyclohexane (MCH), a liquid, would be carried on-board the vehicle and dehydrogenated by an on-board reformer to produce hydrogen and toluene. The system would be very bulky and heavy for several reasons: 1) the effective volumetric and mass density of hydrogen in MCH is low; 2) two large tanks would be needed -- one for the MCH, and one for the toluene; and 3) the reformer itself would be large and heavy, even assuming major improvements over current models.

[m] Calculations assume that 50 kg H_2/m^3 can be stored in a 20 Å nanotube system, based on data in Dillon et al. (1997). Their calculations assume an outer container weight that is equal to the nanotube weight divided by 3.5, and an exterior volume that is 1.075 times the inner volume. The system cost estimates assume high volume carbon nanofiber cost of $4.40 per kg, based on cost estimates for production of 4.5 million kg per year (Hydrogen and Fuel Cell Letter, 1997), and an additional $180-200 per GJ cost for the low-pressure outer tank and valves. Chambers et al. (1998) report much higher storage densities for graphite nanotubes, of up to 58% by weight for active material alone, but adsorbing the H_2 apparently takes many hours.

[n] This system would use a tank of plastic covered NaH balls mixed with water to evolve hydrogen when the balls are mechanically opened. The resulting NaOH solution would then need to be drained prior to refueling. Figures are based on data supplied by Powerball

Technologies of $1,450 for an 8 gallon, 136 pound, 48.0 L (exterior volume) storage tank and delivery system, capable of producing 11,795 L (or about 1 kg) of H_2. One gallon of hydride balls, with 65% of the volume composed of NaH, would weigh 4.78 kg. They currently sell for $1-30 per gallon, depending on order size (Powerball Technologies, 1999).

Table 3-4: NiMH Cell Characteristics Based on Gen3 Technology Assumptions

Cell Capacity	**Cell/Module Specific Energy (C/3 rate)**	**Cell/Module Specific Power (peak to .8 V)**	**Plate Area (per plate)**	**Cell/Module Weight**
10 Ah	72.1/60.8 Wh/kg	648/547 W/kg	60 cm^2	0.18/0.21 kg
50 Ah	120.7/91.3 Wh/kg	343/260 W/kg	72 cm^2	0.54/0.71 kg
80 Ah	120.7/93.7 Wh/kg	235/183 W/kg[a]	98 cm^2	0.86/1.11 kg
100 Ah	113.6/88.1 Wh/kg	304/235 W/kg	92 cm^2	1.14/1.47 kg
150 Ah	117.0/88.9 Wh/kg	254/193 W/kg	180 cm^2	1.67/2.19 kg

Note: [a]Not a misprint -- specific power decreases from 100 Ah to 80 Ah for the particular 80 Ah battery design analyzed.

Table 3-5: Selling Price Estimates for Gen3 and Gen4 NiMH EV Batteries

Generation and Cell Size	Low Cost Case	High Cost Case	Average
Generation 3 @ 20,000/yr:			
10 Ah	$694.53/kWh ($36.24/kg)	$829.61/kWh ($43.28/kg)	$762.07/kWh ($39.76/kg)
50 Ah	$359.95/kWh ($30.85/kg)	$409.24/kWh ($35.08/kg)	$384.60/kWh ($32.97/kg)
80 Ah	$263.08/kWh ($22.75/kg)	$305.45/kWh ($26.42/kg)	$284.27/kWh ($24.59/kg)
100 Ah	$239.12/kWh ($19.52/kg)	$278.86/kWh ($22.76/kg)	$258.99/kWh ($21.14/kg)
150 Ah	$203.70/kWh ($16.74/kg)	$237.59/kWh ($19.53/kg)	$220.65/kWh ($18.14/kg)
Generation 3 @ 100,000/yr:			
10 Ah	$580.89/kWh ($30.31/kg)	$740.22/kWh ($38.62/kg)	$660.56/kWh ($34.47/kg)
50 Ah	$306.84/kWh ($26.30/kg)	$358.18/kWh ($30.70/kg)	$332.51/kWh ($28.50/kg)
80 Ah	$220.51/kWh ($19.07/kg)	$271.45/kWh ($23.48/kg)	$245.98/kWh ($21.28/kg)
100 Ah	$200.88/kWh ($16.40/kg)	$248.05/kWh ($20.25/kg)	$224.47/kWh ($18.33/kg)
150 Ah	$171.36/kWh ($14.08/kg)	$206.83/kWh ($17.00/kg)	$189.10/kWh ($15.54/kg)
Generation 4 @ 20,000/yr:			
20 Ah	$251.76/kWh ($25.18/kg)	$287.93/kWh ($28.79/kg)	$269.85/kWh ($26.99/kg)
60 Ah	$238.69/kWh ($24.91/kg)	$269.02/kWh ($28.07/kg)	$253.86/kWh ($26.49/kg)
100 Ah	$186.14/kWh ($19.89/kg)	$211.10/kWh ($22.56/kg)	$198.62/kWh ($21.23/kg)
150 Ah	$162.36/kWh ($18.38/kg)	$185.00/kWh ($20.94/kg)	$173.68/kWh ($19.66/kg)
Generation 4 @ 100,000/yr:			
20 Ah	$211.29/kWh ($21.13/kg)	$240.23/kWh ($24.02/kg)	$225.76/kWh ($22.58/kg)
60 Ah	$199.23/kWh ($20.79/kg)	$225.66/kWh ($23.55/kg)	$212.45/kWh ($22.17/kg)
100 Ah	$154.62/kWh ($16.52/kg)	$176.39/kWh ($18.85/kg)	$165.51/kWh ($17.69/kg)
150 Ah	$133.94/kWh ($15.16/kg)	$153.63/kWh ($17.39/kg)	$143.79/kWh ($16.28/kg)

Table 3-6: Delivered Hydrogen Cost Ranges for Production Via Onsite SMR

DHFCV Fleet in SCAB	**Number of Refueling Stations**	**Ratio of Vehicles:Stations**	**Delivered H2 Cost [$/GJ HHV] *[$/MMBTU HHV]***
Generation 1:			
2,000-10,000 (LPV)	20-80	100-125	[16.00 18.00 21.00] *[16.84 18.94 22.11]*
2,000-17,400 (HPV)	20-80	100-218	[14.00 18.00 21.00] *[14.73 18.94 22.11]*
Generation 2:			
14,100-27,800 (LPV)	100	141-278	[12.00 14.00 15.00] *[12.63 14.74 15.79]*
24,000-47,500 (HPV)	100	240-475	[11.00 13.00 14.00] *[11.58 13.68 14.74]*
Generation 3:			
32,800-49,300 (LPV)	100	328-493	[11.00 12.00 13.00] *[11.58 12.63 13.68]*
56,700-89,600 (HPV)	100	567-896	[10.00 11.00 12.00] *[10.53 11.58 12.63]*
Generation 4:			
55,400-128,00 (LPV)	100	554-1,280	[9.00 10.00 11.00] *[9.47 10.53 11.58]*
102,400-292,700 (HPV)	100	1,024-2,927	[8.00 9.00 10.00] *[8.42 9.47 10.53]*

Notes: LPV = low production volume; HPV = high production volume.

Table 3-7: Mid-Sized DHFCV Consumer Costs and Lifecycle Costs (Low Production Volume Scenario)

	Vehicle Characteristics	Production Volume	Low Case (1997$)	Central Case (1997$)	High Case (1997$)
Generation 1					
2003	82 kW drivetrain	10,000 vehicles/yr	$93,589 (125.29 ¢/mi)	$129,894 (171.92¢/mi)	$176,265 (233.77¢/mi)
2004	29.2 kW-net fuel cell	10,000 vehicles/yr	$42,067 (62.70 ¢/mi)	$57,175 (81.55 ¢/mi)	$86,802 (118.46 ¢/mi)
2005	5.76 kWh battery	10,000 vehicles/yr	$39,583 (59.75 ¢/mi)	$52,505 (75.99 ¢/mi)	$79,363 (109.31 ¢/mi)
2006	(NiMH 600 W/kg)	20,000 vehicles/yr	$36,661 (56.46 ¢/mi)	$48,467 (71.17 ¢/mi)	$73,321 (102.09 ¢/mi)
	1,563 kg curb weight				
Generation 2					
2007	70 kW drivetrain	20,600 vehicles/yr	$30,676 (47.26 ¢/mi)	$37,574 (55.81 ¢/mi)	$52,498 (73.98 ¢/mi)
2008	23.8 kW-net fuel cell	21,630 vehicles/yr	$30,291 (46.83 ¢/mi)	$36,878 (55.00 ¢/mi)	$51,299 (72.51 ¢/mi)
2009	5.76 kWh battery	22,712 vehicles/yr	$29,971 (46.48 ¢/mi)	$36,299 (54.33 ¢/mi)	$50,301 (71.29 ¢/mi)
2010	(NiMH 625 W/kg)	23,847 vehicles/yr	$29,693 (46.17 ¢/mi)	$35,804 (53.76 ¢/mi)	$49,442 (70.25 ¢/mi)
	1,330 kg curb weight				
Generation 3					
2011	70 kW drivetrain	25,039 vehicles/yr	$29,473 (45.59 ¢/mi)	$35,368 (52.55 ¢/mi)	$48,680 (68.64 ¢/mi)
2012	23.8 kW-net fuel cell	26,291 vehicles/yr	$29,375 (45.47 ¢/mi)	$34,978 (52.82 ¢/mi)	$47,995 (67.81 ¢/mi)
2013	5.76 kWh battery	27,606 vehicles/yr	$29,276 (45.39 ¢/mi)	$34,622 (52.12 ¢/mi)	$47,375 (67.07 ¢/mi)
2014	(NiMH 625 W/kg)	28,986 vehicles/yr	$29,178 (45.26 ¢/mi)	$34,294 (51.34 ¢/mi)	$46,804 (66.38 ¢/mi)
	1,330 kg curb weight				
Generation 4					
2015	65 kW drivetrain	30,436 vehicles/yr	$26,571 (40.86 ¢/mi)	$30,246 (45.25 ¢/mi)	$40,884 (57.83 ¢/mi)
2016	20.9 kW-net fuel cell	31,957 vehicles/yr	$26,496 (40.78 ¢/mi)	$30,037 (45.02 ¢/mi)	$40,511 (57.39 ¢/mi)
2017	5.18 kWh battery	33,555 vehicles/yr	$26,423 (40.71 ¢/mi)	$29,843 (44.80 ¢/mi)	$40,160 (56.99 ¢/mi)
2018	(NiMH 650 W/kg)	35,233 vehicles/yr	$26,349 (40.63 ¢/mi)	$29,658 (44.60 ¢/mi)	$39,824 (56.59 ¢/mi)
2019	1,227 kg curb weight	36,995 vehicles/yr	$26,276 (40.55 ¢/mi)	$29,479 (44.40 ¢/mi)	$39,500 (56.22 ¢/mi)
2020		38,844 vehicles/yr	$26,207 (40.48 ¢/mi)	$29,309 (44.22 ¢/mi)	$39,168 (55.83 ¢/mi)
2021		40,787 vehicles/yr	$26,136 (40.41 ¢/mi)	$29,146 (44.04 ¢/mi)	$38,870 (55.49 ¢/mi)
2022		42,826 vehicles/yr	$26,067 (40.34 ¢/mi)	$28,989 (43.86 ¢/mi)	$38,569 (55.14 ¢/mi)
2023		44,967 vehicles/yr	$26,001 (40.27 ¢/mi)	$28,837 (43.70 ¢/mi)	$38,331 (54.87 ¢/mi)
2024		47,216 vehicles/yr	$25,933 (40.20 ¢/mi)	$28,690 (43.54 ¢/mi)	$38,062 (54.56 ¢/mi)
2025		49,576 vehicles/yr	$25,869 (40.13 ¢/mi)	$28,547 (43.38 ¢/mi)	$37,803 (54.26 ¢/mi)
2026		52,055 vehicles/yr	$25,803 (40.06 ¢/mi)	$28,409 (43.23 ¢/mi)	$37,552 (53.97 ¢/mi)

Table 3-8: Mid-Sized DHFCV Consumer Costs and Lifecycle Costs (High Production Volume Scenario)

	Vehicle Characteristics	Production Volume	Low Case (1997$)	Central Case (1997$)	High Case (1997$)
Generation 1					
2003	82 kW drivetrain	20,000 vehicles/yr	$91,763 (122.28 ¢/mi)	$128,078 (169.56¢/mi)	$173,975 (230.70¢/mi)
2004	29.2 kW-net fuel cell	40,000 vehicles/yr	$36,331 (55.33 ¢/mi)	$49,256 (72.11 ¢/mi)	$75,208 (104.35 ¢/mi)
2005	5.76 kWh battery	54,570 vehicles/yr	$33,029 (51.54 ¢/mi)	$43,088 (64.69 ¢/mi)	$64,839 (91.85 ¢/mi)
2006	(NiMH 600 W/kg)	59,850 vehicles/yr	$31,750 (50.09 ¢/mi)	$40,440 (61.55 ¢/mi)	$59,999 (86.07 ¢/mi)
	1,563 kg curb weight				
Generation 2					
2007	70 kW drivetrain	65,460 vehicles/yr	$27,753 (43.77 ¢/mi)	$32,578 (49.83 ¢/mi)	$44,403 (63.96 ¢/mi)
2008	23.8 kW-net fuel cell	71,520 vehicles/yr	$27,616 (43.63 ¢/mi)	$32,072 (49.26 ¢/mi)	$43,486 (62.88 ¢/mi)
2009	5.76 kWh battery	78,070 vehicles/yr	$27,486 (43.49 ¢/mi)	$31,628 (48.76 ¢/mi)	$42,678 (61.92 ¢/mi)
2010	(NiMH 625 W/kg)	85,110 vehicles/yr	$27,359 (43.36 ¢/mi)	$31,230 (48.32 ¢/mi)	$41,968 (61.09 ¢/mi)
	1,330 kg curb weight				
Generation 3					
2011	70 kW drivetrain	92,680 vehicles/yr	$27,234 (42.89 ¢/mi)	$30,909 (47.28 ¢/mi)	$41,349 (59.68 ¢/mi)
2012	23.8 kW-net fuel cell	100,790 vehicles/yr	$27,118 (42.77 ¢/mi)	$30,622 (46.95 ¢/mi)	$40,787 (59.02 ¢/mi)
2013	5.76 kWh battery	109,460 vehicles/yr	$27,004 (42.65 ¢/mi)	$30,358 (46.66 ¢/mi)	$40,267 (58.41 ¢/mi)
2014	(NiMH 625 W/kg)	118,690 vehicles/yr	$26,897 (42.54 ¢/mi)	$30,115 (46.39 ¢/mi)	$39,785 (57.85 ¢/mi)
	1,330 kg curb weight				
Generation 4					
2015	65 kW drivetrain	128,500 vehicles/yr	$24,763 (38.67 ¢/mi)	$27,111 (41.51 ¢/mi)	$35,354 (51.19 ¢/mi)
2016	20.9 kW-net fuel cell	138,890 vehicles/yr	$24,686 (38.59 ¢/mi)	$26,952 (41.34 ¢/mi)	$35,032 (50.82 ¢/mi)
2017	5.18 kWh battery	149,840 vehicles/yr	$24,805 (38.51 ¢/mi)	$26,801 (41.18 ¢/mi)	$34,725 (50.47 ¢/mi)
2018	(NiMH 650 W/kg)	161,360 vehicles/yr	$24,541 (38.44 ¢/mi)	$26,658 (41.02 ¢/mi)	$34,433 (50.14 ¢/mi)
2019	1,227 kg curb weight	173,430 vehicles/yr	$24,475 (38.37 ¢/mi)	$26,524 (40.87 ¢/mi)	$34,154 (49.82 ¢/mi)
2020		186,020 vehicles/yr	$24,411 (38.31 ¢/mi)	$26,394 (40.73 ¢/mi)	$33,888 (49.52 ¢/mi)
2021		199,090 vehicles/yr	$24,350 (38.24 ¢/mi)	$26,273 (40.60 ¢/mi)	$33,634 (49.23 ¢/mi)
2022		212,610 vehicles/yr	$24,293 (38.18 ¢/mi)	$26,191 (40.51 ¢/mi)	$33,443 (49.01 ¢/mi)
2023		226,520 vehicles/yr	$24,240 (38.13 ¢/mi)	$26,115 (40.42 ¢/mi)	$33,264 (48.80 ¢/mi)
2024		240,790 vehicles/yr	$24,187 (38.07 ¢/mi)	$26,043 (40.34 ¢/mi)	$33,093 (48.61 ¢/mi)
2025		255,330 vehicles/yr	$24,138 (38.02 ¢/mi)	$25,974 (40.27 ¢/mi)	$32,929 (48.42 ¢/mi)
2026		270,100 vehicles/yr	$24,093 (37.98 ¢/mi)	$25,910 (40.19 ¢/mi)	$32,772 (48.24 ¢/mi)

Table 3-9: Fleetwide Vehicle Ownership and Operating Costs for DHFCVs by Year (2000$) - Low Production Volume Scenario

Year	Low Case	Central Case	High Case
2003	$158,275,157	$217,181,459	$295,314,738
2004	$270,503,553	$365,512,271	$506,574,001
2005	$352,035,942	$468,630,390	$656,342,127
2006	$495,292,731	$648,073,225	$914,715,751
2007	$628,728,002	$805,180,515	$1,125,082,057
2008	$754,657,988	$949,634,060	$1,312,319,720
2009	$880,410,541	$1,093,117,871	$1,497,213,505
2010	$1,006,426,791	$1,236,287,829	$1,680,755,330
2011	$1,132,152,465	$1,377,461,468	$1,861,567,743
2012	$1,259,178,002	$1,521,270,163	$2,042,067,866
2013	$1,388,321,375	$1,665,968,248	$2,223,508,660
2014	$1,519,720,472	$1,810,605,965	$2,406,418,438
2015	$1,637,280,268	$1,934,986,714	$2,561,058,473
2016	$1,753,655,076	$2,056,626,104	$2,711,101,626
2017	$1,873,574,284	$2,181,803,817	$2,865,272,602
2018	$1,997,295,193	$2,310,887,649	$3,023,916,642
2019	$2,125,087,822	$2,444,158,482	$3,187,446,620
2020	$2,202,904,776	$2,507,354,807	$3,254,619,873
2021	$2,293,572,783	$2,588,505,930	$3,341,957,408
2022	$2,404,118,752	$2,696,508,264	$3,464,315,350
2023	$2,499,204,991	$2,784,457,983	$3,557,046,814
2024	$2,600,281,144	$2,882,149,367	$3,667,755,722
2025	$2,711,301,199	$2,992,568,558	$3,797,589,317
2026	$2,828,845,554	$3,110,072,399	$3,936,208,170
2027	$2,676,989,081	$2,937,315,779	$3,712,976,660
2028	$2,461,507,090	$2,696,831,948	$3,405,620,155
2029	$2,254,768,590	$2,465,755,202	$3,111,543,165
2030	$2,055,897,649	$2,243,868,144	$2,829,450,870
2031	$1,864,357,343	$2,031,118,580	$2,558,459,054
2032	$1,685,231,467	$1,833,962,907	$2,308,144,362
2033	$1,514,510,101	$1,646,865,517	$2,071,188,030
2034	$1,349,352,149	$1,466,118,719	$1,842,495,386
2035	$1,189,317,726	$1,291,206,188	$1,621,446,318
2036	$1,033,895,455	$1,121,561,641	$1,407,306,330
2037	$882,623,958	$956,676,918	$1,199,502,813
2038	$735,097,534	$796,113,766	$997,440,276
2039	$590,853,013	$639,379,387	$800,495,112
2040	$449,500,222	$486,022,052	$608,013,243
2041	$310,627,742	$335,589,983	$419,476,036
2042	$173,855,761	$187,681,892	$234,404,097
2043	$38,807,395	$41,878,274	$52,282,454
NPV in 2000 (3.65% d.r.)	$25,505,920,633	$29,353,806,344	$38,279,383,314

Table 3-10: Fleetwide Vehicle Ownership and Operating Costs for DHFCVs by Year (2000$) - High Production Volume Scenario

Year	Low Case	Central Case	High Case
2003	$308,945,426	$428,400,282	$582,872,995
2004	$652,988,494	$882,156,226	$1,231,768,322
2005	$1,046,175,871	$1,375,781,002	$1,936,392,118
2006	$1,461,195,790	$1,883,278,021	$2,647,899,175
2007	$1,842,884,328	$2,314,787,361	$3,203,215,894
2008	$2,231,507,867	$2,741,638,529	$3,735,254,009
2009	$2,642,083,783	$3,189,662,751	$4,291,083,518
2010	$3,076,612,064	$3,661,235,759	$4,873,847,984
2011	$3,533,102,804	$4,151,157,076	$5,478,718,905
2012	$4,016,513,280	$4,667,494,763	$6,114,299,972
2013	$4,529,817,714	$5,214,632,180	$6,785,187,879
2014	$5,074,973,926	$5,794,619,340	$7,493,805,324
2015	$5,592,873,102	$6,334,431,968	$8,142,993,100
2016	$6,129,094,601	$6,890,447,069	$8,807,712,494
2017	$6,700,832,961	$7,483,752,826	$9,515,711,850
2018	$7,309,548,301	$8,115,510,652	$10,268,450,729
2019	$7,956,398,984	$8,786,861,070	$11,066,983,462
2020	$8,536,312,454	$9,351,551,672	$11,711,963,401
2021	$9,128,735,914	$9,927,901,448	$12,353,041,217
2022	$9,746,689,642	$10,537,354,324	$13,028,155,551
2023	$10,394,666,924	$11,181,657,963	$13,746,241,934
2024	$11,093,871,645	$11,894,799,082	$14,567,727,313
2025	$11,831,985,079	$12,655,364,638	$15,452,532,082
2026	$12,600,840,283	$13,448,719,863	$16,374,924,492
2027	$12,032,365,291	$12,828,122,350	$15,601,212,782
2028	$11,136,147,043	$11,863,249,559	$14,415,511,551
2029	$10,269,411,975	$10,931,260,464	$13,270,764,622
2030	$9,428,682,792	$10,027,829,641	$12,162,015,144
2031	$8,611,223,607	$9,150,012,571	$11,085,693,614
2032	$7,835,289,929	$8,320,702,878	$10,072,492,950
2033	$7,086,202,142	$7,522,036,817	$9,098,871,973
2034	$6,353,389,710	$6,741,272,245	$8,148,171,582
2035	$5,634,852,429	$5,976,392,849	$7,217,910,412
2036	$4,928,344,848	$5,225,039,978	$6,305,312,525
2037	$4,232,011,769	$4,485,288,744	$5,408,112,023
2038	$3,544,490,596	$3,755,587,146	$4,524,543,938
2039	$2,864,083,857	$3,033,850,558	$3,652,023,477
2040	$2,189,513,865	$2,318,751,866	$2,788,881,205
2041	$1,519,706,679	$1,609,012,718	$1,933,553,809
2042	$853,778,664	$903,637,786	$1,085,034,177
2043	$190,906,465	$202,015,030	$242,478,354
NPV in 2000 (3.65% d.r.)	$99,189,538,605	$109,603,716,180	$137,656,167,098

Figure 3-14:

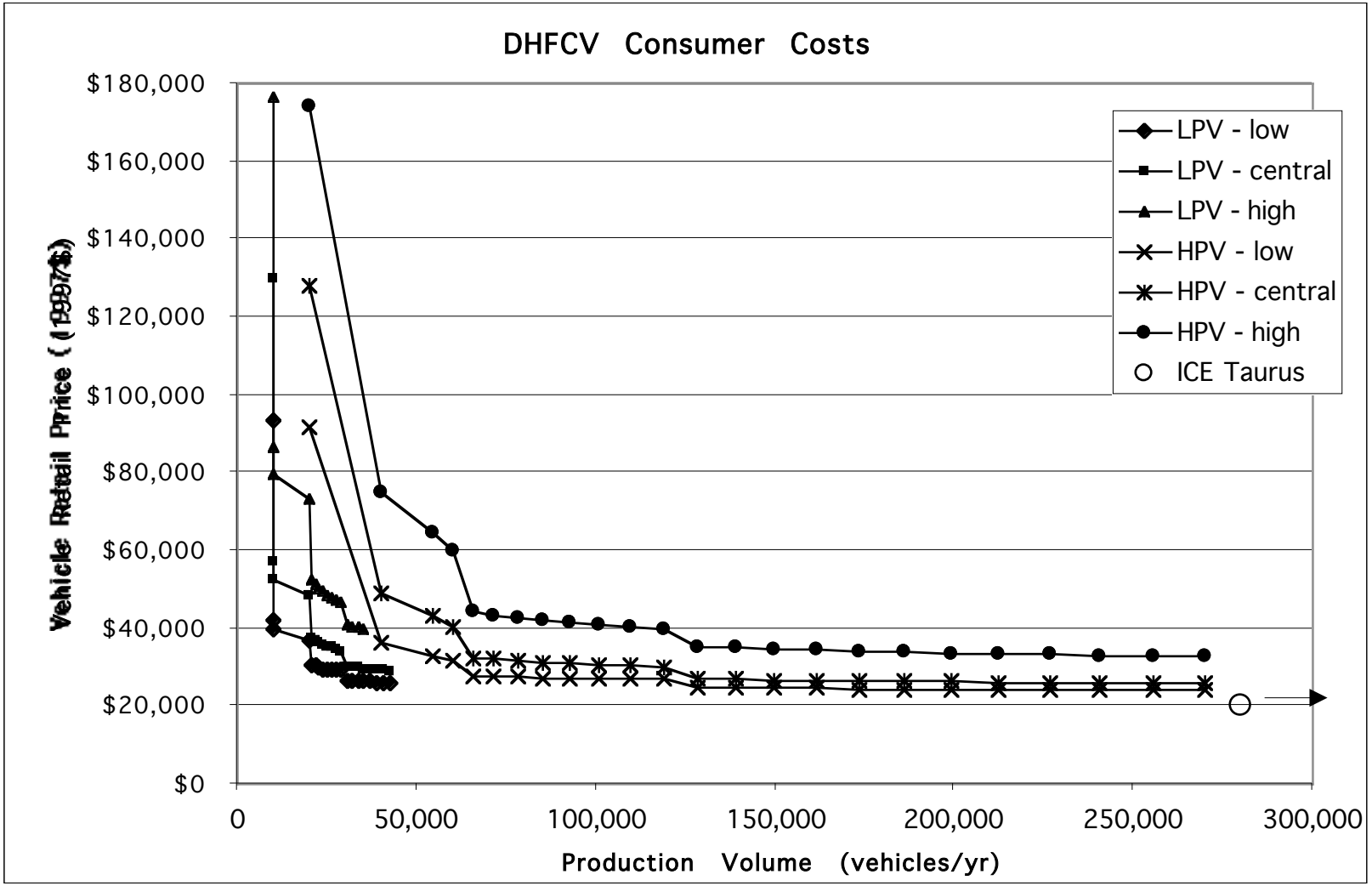
DHFCV Consumer Costs
$180,000
$160,000
$140,000
$120,000
$100,000
$80,000
$60,000
$40,000
$20,000
$0
0
50,000
100,000
150,000
200,000
250,000
300,000
Production Volume (vehicles/yr)
LPV - low
LPV - central
LPV - high
HPV - low
HPV - central
HPV - high
ICE Taurus

Chapter 4:
Manufacturing and Lifecycle Costs of Direct-Methanol Fuel Cell Vehicles

Introduction

Methanol is a leading contender as a FCV fuel because it can be stored as a non-cryogenic liquid and because it can be reformed more easily (i.e., at lower temperature) than gasoline. Several automotive companies are developing FCVs that would run on methanol; Daimler-Benz, and Toyota displayed methanol FCVs at the 1997 Frankfurt Auto Show, and General Motors, through its German subsidiary, Opel, displayed a methanol fuel cell van at the 1998 Detroit Auto Show (Nowell, 1998). These methanol vehicles would run on methanol that would then be reformed into hydrogen onboard the vehicle before being used in the fuel cell.

In addition to this option, however, methanol could also potentially be used directly to run the fuel cell, without the need to first produce gaseous hydrogen. This possibility is particularly intriguing, in that it means that a direct-methanol fuel cell (DMFC) vehicle could combine some of the best features of DHFCVs and ICEVs. Like DHFVCs, DMFC vehicles (DMFCVs) would produce no tailpipe emissions of criteria pollutants (although they would produce carbon dioxide (CO_2) in addition to water vapor) but, unlike DHFCVs, DMFCVs would require only slightly modified fuel storage and delivery systems relative to gasoline ICEVs. Since methanol could be stored as a liquid at ambient temperatures, the bulky and/or costly fuel storage systems needed for DHFCVs would be eliminated. Furthermore, the costly, inefficient, and complicated fuel processor systems needed for methanol or gasoline reformate FCVs would be unnecessary with DMFCVs.

While not as versatile as hydrogen, methanol can be derived from a variety of different renewable and non-renewable feedstocks including natural gas, wood, coal, municipal solid wastes, agricultural products and by-products, and sewage, as well as from the large oceanic reserves of methane hydrates (Nowell, 1998). Methanol is harder to ignite than gasoline, burns about 60% slower, and burns cooler, such that the energy release in a methanol fire is about one-fifth that of a similar quantity of burning gasoline (Nowell, 1998). Methanol fires are also easier to extinguish, since water is effective. As a result of these differences, the U.S. EPA has estimated that the use of methanol in place of gasoline as the primary automotive fuel in the U.S. could reduce the number of automotive fires from about 180,000 to about 20,000 annually, and reduce the number of resulting deaths from 750 down to about 50 (U.S. EPA projection, cited in Nowell, 1998).

From an environmental perspective, methanol mixes well in water and thus disperses and biodegrades much more readily than gasoline (Malcolm Pirnie, 1999). However, because it mixes and disperses well it is less detectable as a groundwater contaminant when it escapes from storage tanks. Methanol is somewhat more toxic than gasoline if ingested, with 80-150 ml constituting a typical lethal dose (U.S. EPA, 1994), versus 115-470 ml for gasoline. Unlike

gasoline, however, methanol is apparently not carcinogenic (Malcolm Pirnie, 1999; U.S. EPA, 1994).

Direct-Methanol Fuel Cells for Vehicles

Direct-methanol PEM fuel cells are an emerging technology. They are presently at an earlier research and development stage than are hydrogen PEM fuel cells, with a development "gap" of approximately ten years. Organizations that are investigating the potential use of DMFCs for vehicle applications include Ballard Power Systems, DaimlerChrysler, Los Alamos National Laboratory (LANL), and NASA's Jet Propulsion Laboratory (JPL), among others. Unfortunately, due to the proprietary nature of these investigations, and since DMFC research efforts are confined to relatively few organizations, much less information is publicly available on the state-of-the art of development of DMFCs than is available for DHFCs. In 1997, JPL DMFC technology was licensed by a Los Angeles company, DTI Energy, Inc. (NASA, 1997). In August 1999, Ballard licensed the technology from DTI Energy, and has an agreement that will allow it to sublicense the technology to its alliance members DaimlerChryslyer and Ford under certain conditions (Ballard, 1999). As a result of these licensing agreements, technical details of the JPL technology are no longer being made available to outside researchers. Of the various government and industrial DMFC investigations in the U.S. and Canada, only the LANL findings are currently being reported (U.S. DOE, 1998d).

Hydrogen PEM fuel cells currently have better performance than methanol PEM fuel cells because hydrogen oxidation at the anode in the hydrogen fuel cell is more rapid than the oxidation of methanol at the anode of the methanol fuel cell (Scott, et al., 1998). The oxidation kinetics are inherently slower for methanol fuel cells because the oxidation of methanol requires six electrons to be transferred, rather than two for hydrogen oxidation. Also, intermediates are formed during methanol oxidation that then require the adsorption of an oxygen containing species in order for CO_2 to be produced (Scott, et al., 1998).

Also, unlike in hydrogen fuel cells, platinum is not sufficiently active as a methanol oxidation electrocatalyst. Other catalyst formulations are needed, and the platinum-ruthenium (Pt-Ru) binary catalyst presently appears to offer the best performance. The ruthenium in this formulation allows a surface oxide to form in the potential range needed for methanol oxidation (Scott, et al., 1998). Present overall catalyst loadings for DMFCs are still quite high, on the order of 2.5 mg per cm^2 (U.S. DOE, 1998d). These levels are analogous to the catalyst loading levels used in DHFCs ten years ago, when membranes were filled with "platinum black" bulk catalyst material at levels as high as 4 mg per cm^2 per electrode (in order to assure adequate performance with this bulk catalysis technology). Subsequent optimization has reduced catalyst loadings for DHFCs to less than an order of magnitude below the levels of 10 years ago by utilizing the platinum as a "thin film" catalyst layer supported on a conductive carbon substrate. Present total (anode plus cathode) catalyst loadings for DHFCs are typically about 0.25 mg per cm^2, with levels as low as 0.04 mg per cm^2 being investigated (U.S. DOE, 1998d). DMFC researchers are confident that when DMFC stacks begin to be optimized for cost and manufacturability with supported catalysts, rather than being overloaded with "bulk" catalyst to assure

performance in the laboratory, significant reductions in anode catalyst loadings will be possible (Moore, 1999; U.S. DOE, 1998d).

Another interesting feature of DMFCs is that they can be fueled with either methanol in vapor form, or with liquid methanol. The liquid fuel option is currently under more intense research and development because of the energy penalty associated with vaporizing liquid methanol. Also, when vaporized methanol is used, carbon dioxide mixes with unused fuel vapor in the exhaust stream, thereby complicating the process of reusing the unreacted fuel (Scott, et al., 1998).

In addition to relatively low catalyst utilization (because of the use of bulk catalysts), the other crucial issue for DMFCs is that during operation some methanol fuel "crosses over" the polymer membrane, resulting in a loss of cell voltage and a decrease in efficiency. For a given set of operating conditions, the crossover current density tends to be relatively constant over the range of cell voltages typical for DMFCs (about 0.25 to 0.6 V), while the cell current density follows the typical pattern of increasing with lower voltages. This pattern has led to the conclusion that DMFCs should always be operated at relatively high cell current densities, where the ratio of cell current density to crossover current density is highest. For automotive applications, this suggests that a DMFC would have to be used in a hybrid power system, where the fuel cell always operates near its peak power level and a battery pack is used to "load follow" the power demands of the vehicle.

However, in a recent analysis of methods to optimize DMFC operation using an experimental state-of-the-art DMFC at LANL, Moore et al. (1999a) found that methanol crossover currents could be reduced by varying the methanol concentration and solution feed rate at the anode. By optimizing the fuel concentration and feed rate as a function of the different operating points, they were able to reduce the methanol crossover flux, particularly at low power levels. With the optimized methanol concentration/feed rate fuel control strategy, the methanol crossover current was reduced by about 50% at low power levels, and the voltage efficiency was also increased slightly. The optimized strategy produced a higher fuel utilization rate at low power, and allowed the overall conversion efficiency curve to be much flatter than for a single set of anode fuel feed conditions. The optimized strategy yielded a conversion efficiency of over 30% over a wide range of cell power density, from 70 to 230 mW per cm^2 (Moore, et al., 1999a).

Based on this optimized fuel control strategy, Moore et al. (1999b) then compared complete DMFC systems to DHFC systems for motor vehicle applications with regard to the relative volumes needed for just the fuel cell stack and fuel storage systems for the two system types. First, since methanol has about five times the energy density of hydrogen at 5000 psi, the authors calculated that the storage volume of a methanol tank that would provide a driving range of 350 miles for a DMFCV would be about 72 L. This is 40% of the 180 L needed for a 5000 psi hydrogen storage tank that would provide a DHFCV with a similar range (i.e., since a state-of-the-art DMFC has only about 50% of the fuel conversion efficiency of the DHFC, the storage volume needs to be 40% that of the DHFCV, not 20%). Next, the state-of-the-art LANL DMFC demonstrates a maximum power density that is about 45% that of a modern DHFC (at the cell level). Since DHFC systems have achieved a power density of 1 kW per L, a 60-

kW system would require about 60 L, or 240 L total including the hydrogen storage tank. If the DMFC system were to achieve this same volume, the stack and auxiliaries would need to fit into a volume of about 170 L (allowing 70 L for the methanol tank), necessitating a power density of 0.35 kW per L, or 35% of the DHFC system power density. The authors conclude that this condition would be met if current state-of-the-art DMFC results were extrapolated from the cell to stack level. Expected future reductions in methanol crossover currents would lead to the 0.35 kW per L power density condition being exceeded substantially. Thus, Moore et al. (1999b) conclude that given a similar fuel cell stack and fuel storage volume of about 240 L, a DMFCV stack (based on current cell performance) could be expected to achieve the same 350 mile driving range as a DHFCV.[35]

Finally, looking into the future, Moore et al. (1999b) examine the impact on DMFC performance of projected improvements in reducing methanol crossover currents. If crossover currents can be reduced by 90%, presumably with the use of a new membrane type that blocks methanol while maintaining high protonic conductivity, and if cell voltage losses can be decreased by 0.1 V, then overall DMFC performance would improve substantially. These advances would allow the maximum power density for the DMFC to exceed 0.3 W per cm^2, up from about 0.25 W per cm^2 in present state-of-the-art DMFCs. This is about 55% of the typical 0.545 W per cm^2 maximum DHFC power density discussed in Chapter 3. These advances would also allow the overall fuel conversion efficiency for the DMFC to reach about 75% of the conversion efficiency of the DHFC (Moore, et al., 1999b).

Direct-Methanol Fuel Cell System Modeling Issues

The critical differences between direct-methanol PEM fuel cell systems and direct-hydrogen PEM systems are: lower electrochemical fuel conversion efficiencies for DMFCs, lower maximum power densities for DMFCs, differences in optimal anode catalyst types and potentially in anode catalyst loading levels, potential differences in optimal bipolar plate thicknesses (due to thermal management issues), potential auxiliary system differences, and fuel storage and delivery system differences. Since DMFCs are at a relatively early stage of development, arriving at potential specifications for future systems is clearly somewhat speculative. However, the current state-of-the-art, represented by small DMFC stacks constructed at LANL, and projected future improvements such as those discussed above, provide sufficient information to characterize potential DMFC system parameters and to analyze complete DMFCVs using the Lotus 1-2-3 vehicle cost and performance spreadsheet model.

First, DMFC maximum power density and the stack power produced at different operating points are determined by fuel cell polarization behavior. As discussed in Chapter 3 for DHFCs, a family of polarity plots that relate cell current density to cell voltage for different operating parameters typically

---

[35] Moore et al. (1999b) only considered the system volume issue, and did not consider the potential relative masses of the two system types. System mass differences, if any, would translate into different total vehicle masses and drivetrain power requirements, and this could lead to a slightly different conclusion. Potential DMFC system masses are explicitly considered in this analysis.

characterizes this behavior. For DMFCs, the primary focus at present is to minimize methanol crossover currents by optimizing fuel feed conditions at the anode (as in the efforts discussed above). This is a relative non-issue for DHFCs, where pure hydrogen is always supplied, and as a result attention is focused on improving performance by optimizing the air pressure and flow rate conditions at the cathode. For DMFCs, the cathode conditions are also important, but reducing methanol crossover is the immediate research priority and relatively little attention is being paid to examining operation under different air pressure regimes. Polarity plots for different air pressure levels, relatively common in the DHFC literature, are thus absent in the DMFC literature.

For purposes of this analysis, a baseline set of DMFC performance data has been obtained from experimental results for operation of the LANL DMFC stack. These data represent state-of-the-art DMFC stack performance as of February, 1998. The polarity plots in the data set characterize the stack under different fuel concentration and feed rate conditions, and for different operating temperatures, but not for different air pressure levels. In order to approximate the family of polarity plots that might be observed with different air pressure levels, I have used the following procedure. First, based on Moore et al.'s (1999a) analysis for optimizing DMFC stack performance by varying fuel feed conditions, I generated a composite fuel cell polarity plot by combining sections of plots for three different sets of conditions, that yield the best overall performance. This optimization suggests using low methanol concentrations at low cell current densities, and higher methanol concentrations at higher current densities, in order to maximize performance at each operating point. Figure 4-1 shows the three individual polarity plots and the composite polarity plot.

Figure 4-1:

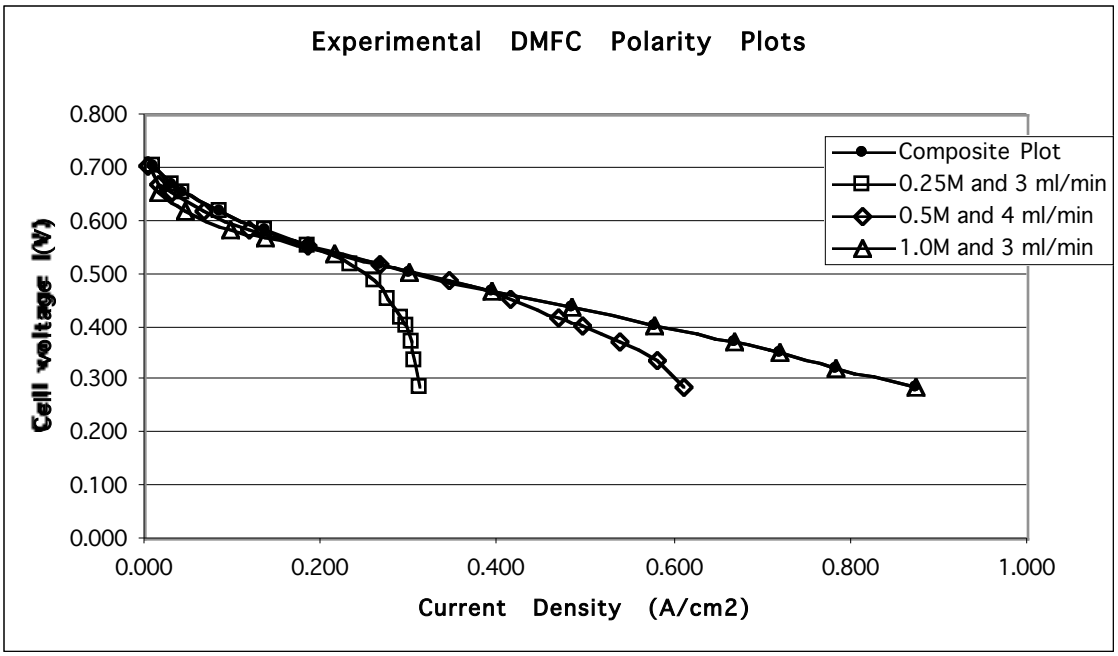

Note: Data are for DMFC operation at 100° C.

Next, based on this composite polarity plot, which represents performance for an air pressure level of 30 psi (2.05 atm), additional polarity plots have been created by assuming the same absolute change in cell voltage with air pressure as observed in the DHFC model data shown in Figure 3-2. This procedure, suggested by Bob Moore at the Fuel Cell Vehicle Modeling Center at UC Davis (Moore, 1999) as a reasonable approximation, will of course probably not be exactly accurate because of known differences in the response to air pressure between the two stack types (e.g., the impact on methanol crossover in DMFC stacks). However, it should provide a reasonably good first-order characterization of DMFC stack performance under different cathode-side pressure conditions -- until a full set of actual experimental or modeled data becomes available. These polarity plots are used in the Lotus 1-2-3 model to estimate PEM stack performance when liquid methanol is used directly as the fuel. Figure 4-2 shows the family of polarity plots that result from this procedure.

Figure 4-2:

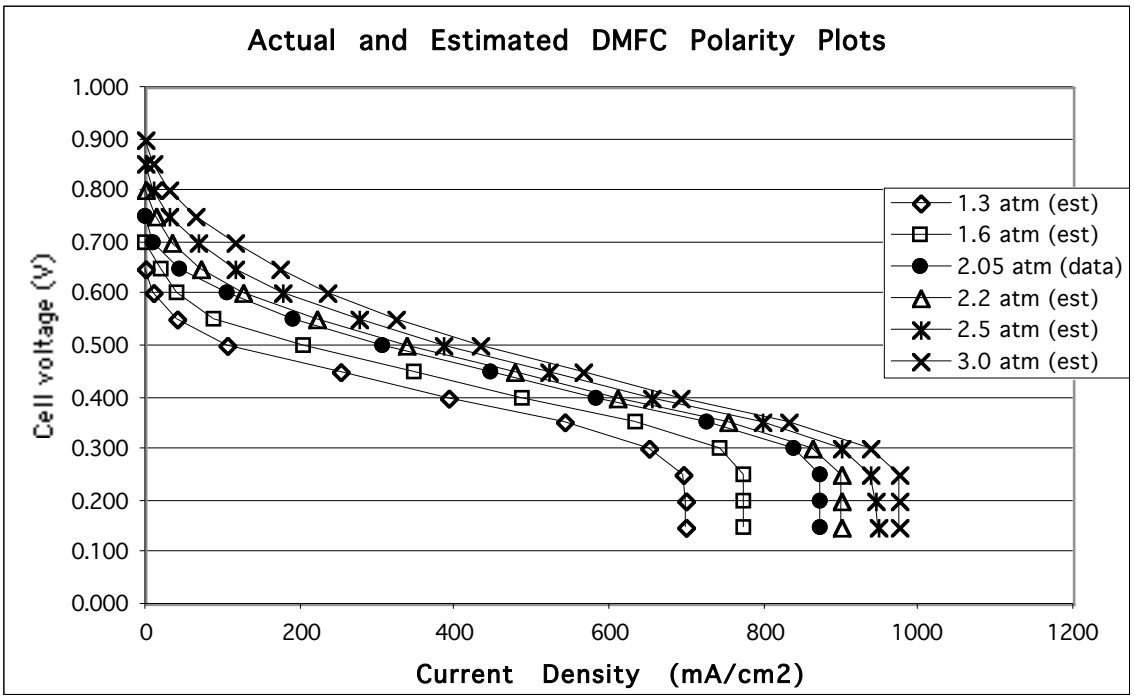

Note: The experimental data plot at 2.05 atm and the 2.2 atm plot are close together because they are separated by an air pressure difference of only 0.15 atm.

As noted above, it is also important to characterize the power density of the DMFC stack in order to account for the fact that a DMFC stack producing a given level of nominal or net power output may be larger and heavier than a DHFC stack of similar output power. The overall volumetric and gravimetric power densities of a fuel cell stack (in W per L and W per kg) are related to the maximum power density of the individual cells (in W per cm^2), as well as the thicknesses of the cells and the densities of the stack materials used. The polarity plots shown above yield a maximum power density of 0.291 W per cm^2 (831 mA per cm^2 at 0.35 volts on the 3.0 atm pressure curve). This is higher than the

maximum of 0.25 W per cm^2 observed in the LANL experimental data at a pressure of 2.05 atm, but lower than the projected levels of over 0.30 W per cm^2 with expected future reductions in methanol crossover losses (Moore, et al., 1999b). The figure of 0.291 W per cm^2 is about 53% of the maximum power density of 0.545 W per cm^2 that is typical of DHFCs operated on pure hydrogen and air.

There are some early indications that DMFC cell thicknesses might ultimately be thinner than DHFC cell thicknesses. Use of a liquid fuel provides a thermal management advantage for the stack, and this might allow DMFC cells to be thinner than DHFC cells. A DMFC "short stack" built at LANL has achieved a cell packing density of 5 cells per cm, for a stack cell pitch of 2mm, compared to the current state-of-the-art for DHFC cells of about 3mm (Moore, et al., 1999b; U.S. DOE, 1998c). However, this stack has yet to be fully tested to assure that single-cell performance levels can be duplicated, and it is also not a full-sized stack. It is therefore important to be cautious about naively accepting this stack cell pitch as practical for DMFCs in automotive (or other) applications.

Given the uncertainty about the bipolar plate materials that will ultimately be used in both DHFCs and DMFCs, and other details of the stack geometries (cell pitch, number of cooling cells, etc.) there is at this time no compelling argument that the relative power densities of DMFC and DHFC stacks will be significantly different than the relative power densities at the cell level. It is possible that thinner cell pitch and a reduced number of cooling cells will alter the extrapolation in favor of DMFCs, but it is also possible that DMFCs will require different (and maybe denser) bipolar plate materials to be used, given the corrosivity of liquid methanol. If DMFCs and DHFCs both have a stack cell pitch of 3mm for full-sized cells, and the hydrogen fuel cell area needed to produce a given amount of maximum power is 53% that of the methanol fuel cell area (0.291 W per cm^2 for DMFCs vs. 0.545 W per cm^2 for DHFCs), then the methanol fuel cell area needed to produce 341 W would be 1180 cm^2, while for the hydrogen fuel cell the area would be 625 cm^2. The corresponding cell volumes would be 188 cubic centimeters (cm^3) for the direct-hydrogen cell, and 354 cm^3 for the direct-methanol cell, also in the ratio of 0.53:1. Thus, as Moore et al. (1999b) conclude, absent differences in cell pitch, plate materials, or cooling cell configurations, the most reasonable assumption for now is that the overall stack power densities for DMFCs and DHFCs will be in rough proportion to their relative cell power densities.

The auxiliary systems required by the two PEM fuel cell types are another source of potential difference, but there is at present no solid basis for assuming any significant differences in auxiliary system weights, volumes, or efficiencies. DMFCs would require a small amount of water to be cycled through the fuel system to dilute the methanol as it is fed to the anode. However, since the water will be recycled, this will result in a very minor addition to the system mass, and one that could easily be offset by other differences, such as smaller heat exchangers or fewer cooling cells in the stack itself. Both systems would require a compressor/expander system to pressurize the stack on the cathode side of the cells (assuming that they operate significantly above ambient pressure), and they would require similar control electronics.

Another critical difference between DHFCs and DMFCs that must be addressed is the lower fuel conversion efficiency for DMFC stacks. DMFC

conversion efficiencies are expected to improve with methanol crossover reductions, but even with forecast improvements they will be lower than for DHFCs. Under dynamic operation conditions, current DMFC fuel utilization levels are on the order of 75-80% (Moore, et al., 1999a). Under optimized conditions, however, experiments at LANL have shown that fuel utilization levels of 90% can be realized (U.S. DOE, 1998d). Further reductions in methanol crossover losses, with improved membrane and cell designs, will improve both dynamic and steady-state fuel utilization levels. The reduction in fuel use efficiency for DMFCs due to methanol crossover has been included in the Lotus 1-2-3 model by adding a parameter that accounts for the efficiency loss. Table 4-1 presents the DMFC system conversion efficiency estimates included in the model for Generation 1 and Generation 2 DMFCVs (90% and 95% respectively), as well as gravimetric and volumetric DMFC stack and system power densities. Based on present and projected DMFC cell power densities, the DMFC stack power density estimates assume that Generation 1 DMFC stacks achieve about 50% the power density of *current* DHFC technology (i.e., 2.0 kg per kW and 2.0 L per kW versus 1.0 kg per kW and 1.0 L per kW for DHFC stacks). I assume that Generation 2 DMFC stacks achieve a 20% improvement over these levels (i.e., 1.6 kg per kW and 1.6 L per kW. These projected stack power density levels are almost certainly conservative, but it is at this point not possible to know if DMFC developers will have the same relative success at improving power densities as have for DHFC developers, due to the differences between the two stack types. The fuel cell auxiliary system power densities for DMFCVs are assumed to be the same as for the DHFCVs in the same time period. The other potential system differences between DMFCs and DHFCs mentioned above, including catalyst type and loading differences and fuel storage and delivery system differences, will be addressed below in the sections on DMFC system costs.

Direct-Methanol FCV Scenarios

Since DMFCs are at a somewhat earlier developmental stage than DHFCs, DMFCVs will not be production ready in the 2003-2004 time frame assumed here for the introduction of BEVs and DHFCVs. However, there are many similarities between DMFCVs and DHFCVs, and DMFCs are actively being researched in industrial, governmental, and university laboratories. Given these considerations, it is probably reasonable to assume that DMFCVs could potentially be introduced in the third generation of vehicles considered here, beginning in 2011. This is a somewhat optimistic introduction date, given the technical issues still facing direct-methanol fuel cell operation, but it is useful to recall that only a few years ago the introduction of DHFCVs seemed many years away, and now it appears that such vehicles could be introduced by 2003-2004.

Large manufacturers choosing to commercialize DMFCVs would need to introduce other ZEVs in the years from 2003-2010, in order to meet their ZEV mandate commitments. For purposes of this analysis, I assume that these Generation 1 and 2 vehicles are the same Generation 1 and 2 BEVs analyzed in Chapter 2, and that the DMFCV and BEV scenarios are differentiated starting with the Generation 3 vehicles. An alternative would be for an automaker to introduce DHFCVs for the 2003-2010 timeframe and then to switch to DMFCVs, but this would involve conducting two parallel FCV research and development

efforts.[36] This would probably involve greater corporate expense than initially introducing BEVs, whose development is already relatively advanced for most automakers. A future addition to this analysis may be to include the DHFCV to DMFCV transition pathway, with a consideration of possible "spillovers" from DHFCV development to DMFCV development. The production volume and SCAB sales assumptions for each vintage and generation of BEVs and DMFCVs, in the high and low production volume cases, are the same as described in Chapter 2.

Direct-Methanol FCV Manufacturing Costs

Only a few studies have examined the manufacturing costs of methanol FCVs. These studies have considered the case of methanol FCVs with onboard reformers that convert liquid methanol fuel into gaseous hydrogen. The gas stream from the reformer is then fed into the fuel cell stack much like in a DHFCV (the principal difference being that the reformate hydrogen stream is diluted with other gases, unlike the nearly pure hydrogen gas used in DHFCVs). There do not appear to be any published studies of the potential manufacturing costs of DMFCVs. Cost studies for indirect-methanol FCVs include those by Engineering Systems Management, Inc. (1992), DeLuchi (1992), and DTI (Thomas et al., 1998a). These studies are briefly discussed below, followed by a discussion of the DMFCV component cost estimates used for the analysis conducted here.

The Engineering Systems Management (ESM) study was conducted for the U.S. Department of Energy. It compared the capital and lifecycle costs of cars, vans, and buses of the following types: conventional gasoline ICE, ethanol ICE, CNG ICE, battery electric, and fuel cell (with methanol as the fuel). For cars and vans, the fuel cell was assumed to be of the PEM type, while for buses both PEM and phosphoric acid fuel cells were considered. The FCVs were assumed to have a fuel cell/battery hybrid power system. Data for several different battery types were available in the ESM model for use in evaluating BEV costs, but for the FCV cases batteries were assumed to be one of three generic types, corresponding to low, medium, and high performance.

The ESM study assumed fuel cell costs provided in a 1985 Jet Propulsion Lab study (Hardy, 1985). Costs were shown for phosphoric acid fuel cells and for PEM fuel cells, and these costs are $250 per kW and $165 per kW, respectively. Other specific cost assumptions for the three FCV configurations analyzed are provided in Table 4-2. Curiously, cost estimates for methanol reformers are not discussed in the ESM study, and in fact the very inclusion of a methanol reformer is not discussed. The ESM study concludes that methanol FCV manufacturing costs will be $15,997 with a low performance battery, $16,426 with a medium performance battery, and $15,466 with a high performance battery (in $1992). These estimated FCV "capital costs" are simply the sums of the costs of the "basic vehicle" and the additional FCV components, with no mark-ups for additional factory-level, division-level, corporate-level, and dealer-level costs.

---

[36] At present it seems that only DaimlerChrysler is doing R&D on both hydrogen FCVs and DMFCVs, although some other companies, such as Toyota, are developing both direct-hydrogen and reformer based FCV systems.

DeLuchi (1992) estimated manufacturing costs and retail prices for a mid-sized, indirect-methanol FCV that uses a hybrid power system. The assumed power system consists of a 25-kW fuel cell system coupled with a bipolar lithium-sulfide battery pack. For a methanol FCV with a 560-kilometer (348-mile) range, DeLuchi estimated a vehicle retail price of $24,810. This retail price figure is based on an estimated $180 per kW OEM cost for the complete fuel cell system, including the fuel cell stack, system auxiliaries, and the reformer system (DeLuchi, 1992).

The DTI study estimates that mid-sized, indirect-methanol FCVs would have mass production costs of $20,356 to $21,076 (Thomas et al., 1998a). These cost estimates appear to be manufacturing costs, without retail-level markups. The cost estimates are for hybrid power system vehicles, with a 45-kW fuel cell system (with a total cost of $2,143-2,370) and a 43-kW battery pack (with a cost of $774-785). Methanol processor costs are assumed to be $10 to $20 per kW, for a total of $444 to $917 in the analyzed system configuration. DTI has been focusing on gasoline partial-oxidation reformer technology, and they have not yet analyzed methanol reformer costs in detail.

Common EV Component Costs

As with DHFCVs, DMFCVs would use similar motors, controllers, gearboxes, electric power steering systems, and high-efficiency HVAC systems used in BEVs. As with the other vehicle types, motor and controller costs for DMFCVs are estimated with the same types of production volume-based cost functions discussed in Chapter 2. As with BEVs and DHFCVs, absolute costs for motors and controllers at a particular production volume are determined by the motor/controller system power rating, and this is a function of the mass of the particular vehicle (and the performance required of it). The drive system power levels needed for the Generation 1 and Generation 2 DMFCVs are shown in Table 4-1. Cost estimates for the other novel EV components are the same as described in Chapter 2 for BEVs.

Direct-Methanol Fuel Cell System Costs

As discussed above, DMFC stacks differ from DHFC stacks primarily in the lower power densities and lower fuel conversion efficiencies of DMFC stacks, differences in anode catalyst types and potentially in optimal loading levels, and possible differences in membrane materials. Until some of the technical issues facing DMFCs are solved, it will of course be difficult to arrive at detailed stack cost estimates, but approximate estimates can be made based on what is known today about the differences between DMFC and DHFC stacks.

In the context of the MPF-based approach used to estimate near-term DHFC system costs, it seems likely that costs for DMFC systems will be similar to those of DHFC stacks at corresponding early levels of cumulative production. At the present cumulative DHFC production level of about 5 MW for Ballard, much of the estimated $1,500-2,500 per kW manufacturing cost is attributable to labor, because the stacks are being carefully built by hand, and to auxiliary system costs, because the some of the auxiliary components are specialty items that are not yet being mass-produced. The stack cost is also no doubt considerable, because the graphite bipolar plates have a high materials cost and are being machined rather than molded, and because MEA costs are still high.

When DMFC production by a single manufacturer reaches 5 MW, per-kW manufacturing costs could be higher than for DHFCs today because the lower stack power density means that larger cells and stacks will be required to produce an equivalent amount of net power, and also because anode catalyst loadings might be higher. Membrane costs might also be higher, depending on what types of membranes or membrane treatments are developed to limit methanol crossover.

On the other hand, DMFC manufacturing costs at that time could be expected to benefit from experience in producing DHFC stack components, which may then be supplied by mature industries. Bipolar plates may at that point be mass-produced, and suitable auxiliary system components such as compressors and heat exchangers may be available "off-the-shelf." The potentially greater availability and lower cost of these components in several years could allow DMFC costs to be lower in prototype production than DHFC costs are now.

Thus, in early stages of DMFC production, there are arguments for both higher and lower manufacturing costs than for DHFCs today. Labor costs will still be a heavy burden, because cumulative production levels of only 5-10 MW mean that mass-production will not yet have started, and stacks will be hand-built. The resulting labor costs could easily mask relatively small differences in component costs. There is therefore at this time no clearly compelling reason to assume that the $1,500-2,500 per kW range of costs estimated for DHFCs at 5 MW of cumulative production is not also reasonable for a manufacturer producing DMFCs at roughly the same stage. As Figure 3-8 makes clear, the range of MPF slope values assumed for DHFCs captures a relatively wide range of potential future manufacturing costs, and as with DHFCs this also allows for uncertainty in the relative ease with which costs will be reduced for DMFCs as production proceeds (once again there are arguments both for and against why DMFC system costs might drop more or less quickly than DHFC system costs).

With regard to a lower bound on DMFC system costs, however, it does seem that in high volume production, once labor costs are a relatively low percentage of total manufacturing cost and materials costs dominate, differences between the stack types might be significant. The power density (and potential catalyst cost) differences between DHFC and DMFC stacks might prevent DMFC systems from attaining the same level of cost as estimated by DTI for DHFC stacks in very high volume production. These potential cost differences can be estimated by using DTI's system cost equation (Thomas, et al., 1998a), shown below as Equation 4-1, and adjusting it to account for likely differences between DHFC and DMFC stacks.

$$C_{HV} = 1{,}073 + P_N \left[3.27 + \frac{5.34 + 27 \cdot L_P}{P_D} \right] \qquad (4\text{-}1)$$

Where:
C_{HV} = high volume cost of PEM fuel cell system (in $)
P_N = net fuel cell peak power output, in kW
L_P = total cell platinum catalyst loading in mg/cm^2
P_D = cell peak power density, in W/cm^2

First, relative to DHFC peak power densities of about 0.545 W per cm^2, DMFCs would have peak power densities perhaps 50-60% as high at the cell level. The peak power density of a DMFC stack with the cell polarity plots developed above would be 0.291 W per cm^2, or 53% of the DHFC value. Second, DMFCs at present have high catalyst loading levels of about 2 mg per cm^2 on each electrode. However, unlike for DHFCs, efforts have not yet commenced to reduce catalyst loadings for low-cost manufacture by maximizing the amount of available catalyst surface area per unit mass of catalyst. On the cathode side, there is no reason to assume any difference in catalyst type or loading level, because the cathode catalyst function is the same in both stack types (i.e. to facilitate the separation of oxygen molecules into oxygen atoms). On the anode side, however, pure platinum catalysts have not proven to be effective for operation on liquid methanol, and binary Pt-Ru catalysts have shown much more favorable characteristics. Catalyst formulations of 1:1 Pt to Ru, on an atomic ratio basis, have been used in the recent LANL work (Moore, et al., 1999b). On a mass basis, this translates into a Pt:Ru ratio of 1.93:1 (Pt has a mass number of 195.09 g per mole and Ru has a mass number of 101.07 g per mole). Although it is not yet clear what Pt:Ru ratio is optimal, this estimate corresponds well with other Pt:Ru mass ratios of 2:1 to 2.33:1 that have been reported in the literature for recent DMFC stack investigations (Scott, et al., 1998).

With regard to Pt and Ru prices, Pt has a price of about $400 per troy ounce (the average was $394 per troy ounce in 1997), while Ru has a much lower price, ranging from $39-45 per troy ounce in 1997 (AMM Online, 1999). From a cost perspective, an equivalent anode catalyst loading for DMFCs and DHFCs would thus favor the DMFC stack. Since low catalyst loadings have not yet been used in DMFC stacks, however, it is unclear if the ~0.05 mg per cm^2 anode loadings currently used in DHFC stacks will produce acceptable results for DMFCs. Given the uncertainty about the level of anode Pt-Ru catalyst loading that will ultimately prove satisfactory for DMFCs, three different levels of catalyst loadings are assumed here, for the low, central, and high cost cases. The low cost case assumes that, as with DHFCs, a loading of 0.05 mg per cm^2 of catalyst (Pt-Ru) will prove satisfactory for the anode side of the MEA. The central case assumes that a loading 0.10 mg per cm^2 will be necessary, and the high case assumes that a loading of 0.20 mg per cm^2 will be needed. When the relative prices of Pt-Ru catalysts and Pt catalysts are considered (with Pt at $395 per troy ounce and Ru at $45 per troy ounce), and the peak power density of 0.291 W per cm^2 is included, the following high-volume, "learned-out" DMFC system cost functions can be calculated:

<u>Low Case:</u>

$$C_{HV} = 1{,}073 + 43.41 \cdot P_N \qquad (4.2)$$

Where:
C_{HV} = high volume cost of PEM fuel cell system (in $)
P_N = net fuel cell peak power output, in kW

Central Case:

$$C_{HV} = 1{,}073 + 46.64 \times P_N \qquad (4\text{-}3)$$

Where:
C_{HV} = high volume cost of PEM fuel cell system (in $)
P_N = net fuel cell peak power output, in kW

High Case:

$$C_{HV} = 1{,}073 + 53.10 \times P_N \qquad (4\text{-}4)$$

Where:
C_{HV} = high volume cost of PEM fuel cell system (in $)
P_N = net fuel cell peak power output, in kW

In comparison with the estimates discussed in Chapter 3 for high volume production of DHFC systems (with a peak power density of 0.545 W per cm2), the central case formula (Equation 4-3) projects somewhat higher costs for DMFC systems. Costs estimated for 20-kW systems are about 27% higher ($79 per kW for the DHFC system versus $100 per kW for the DMFC system), while for costs for 50-kW stacks are about 44% higher ($47 per kW for the DHFC system versus $68 per kW for the DMFC system). Figure 4-3 shows the per-kW system costs estimated by Equations 4-2 through 4-4, relative to the DHFC system costs estimated with Equation 3-3, by system net power rating.

Figure 4-3:

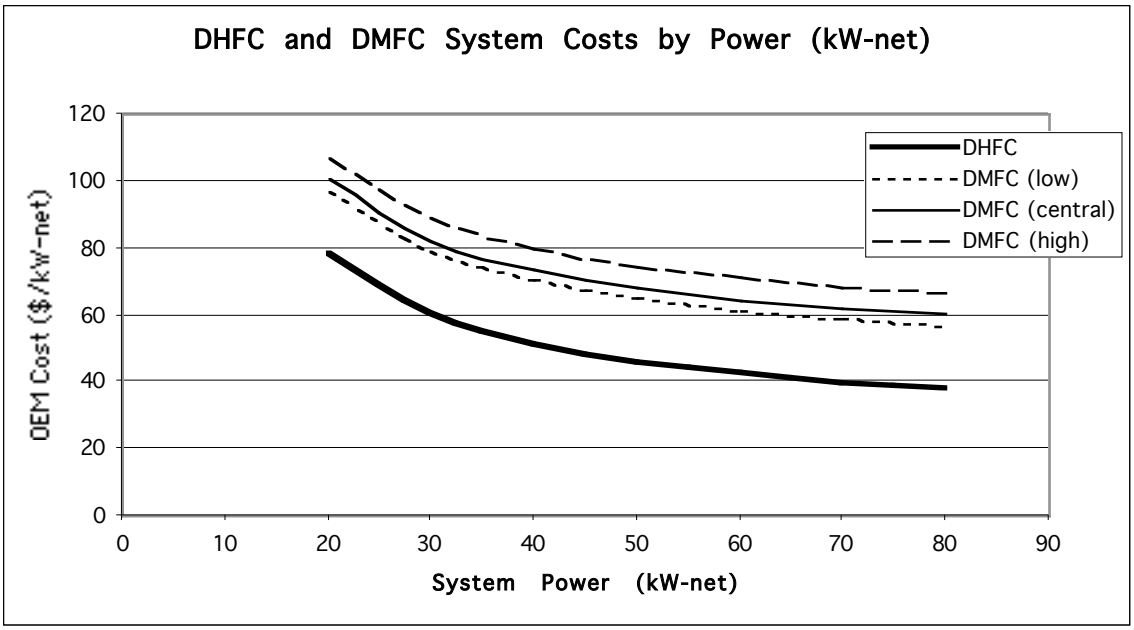

With regard to the MPF analysis of DMFC systems, I have made similar assumptions as in the analysis of DHFC systems. The cumulative production

level for the supplier of DMFC systems, when Generation 1 DMFCVs are introduced in 2011, is also assumed to be 10 MW.[37] DMFC system costs thus follow the same MPF curves calculated for DHFC systems, but they are bounded with the above cost functions, rather than with the somewhat lower cost function (Equation 3-3) estimated for DHFC systems. For the 26.7 kW (net) DMFC system used in Generation 1 DMFCVs, the lower-bound system costs are $83.60 per kW-net (low case), $86.83 per kW-net (central case), and $93.28 per kW-net (high case). For the 21.9 kW (net) DMFC system used in Generation 2 DMFCVs, the lower-bound system costs are $92.41 per kW-net (low case), $95.64 per kW-net (central case), and $102.10 per kW-net (high case).

Methanol Storage System Costs

One slight drawback for DMFCVs (and methanol reformate FCVs and other methanol-fueled vehicles) relative to gasoline-powered vehicles is that in order to be "methanol compatible," any rubber and aluminum parts used in conventional fuel storage and delivery systems would need to be replaced with synthetic rubber and nickel-plated aluminum parts. This is necessary in order to prevent leaching of aluminum and certain types of plasticizers and fillers (EA Engineering, 1999). However, the automobile industry has built approximately 15,000 methanol "flexible-fuel" vehicles (Nowell, 1998), so these modifications are not novel and should not entail significant additional cost.

In the Lotus 1-2-3 model, costs for methanol storage tanks are calculated as a function of the weight of fuel stored, relative to the weight of fuel stored in the ICE Taurus. For a 300-mile range, the DMFCVs require 74.0 kg of fuel for Gen 1 vehicles and 64.8 kg of fuel for Gen 2 vehicles, compared with 44.4 kg of fuel for the ICE Taurus. The DMFCVs are more efficient than the ICE Taurus, but methanol contains only about 21,610 BTUs per kg, compared with about 44,760 BTUs per kg for reformulated gasoline (on a higher heating value basis). The resulting costs for methanol storage tanks are about $45 (Gen 1) and $39 (Gen 2) at the manufacturing cost level, compared with $27 for the ICE Taurus. Once fuel lines, valves, the first tank of fuel, and the various division, corporate, and dealer markups are included, the retail-level cost of the methanol storage system reaches $120 (Gen 1) and $104 (Gen 2) per vehicle.

Peak Power Battery Costs

Moore et al. (1999a) have shown that an optimized fuel feed strategy can reduce methanol crossover at low power levels, and allow power densities for DMFC stacks to be relatively constant over a wider range of power levels than with operation under a single anode feed condition. Thus, contrary to conventional wisdom, DMFCs could potentially be used in "pure" rather than hybrid form and could be the sole power source for a vehicle.

However, just as with DHFCs, there are three other potential justifications for using DMFCs in a hybrid configuration with peak power batteries. First, although the optimized fuel feed strategy improves the shape of the fuel

---

[37] The MPF cost estimates are not very sensitive to this parameter because cumulative production levels quickly dwarf the initial cumulative production level, even in the low production volume scenario.

conversion efficiency curve, there still is a drop-off in efficiency at high power levels. Second, the inclusion of batteries in the vehicle power system allows some braking energy to be recaptured. Because of these two factors, there may be an efficiency benefit to hybridization under at least some driving conditions. Third, from a cost perspective, there is a clear potential advantage to hybridization early in the commercialization phase for DMFCVs, when DMFC system costs are high. Battery costs are also higher in lower volume production, but they do not approach the $1,000-2,000 per kW costs likely for fuel cell systems when they are first introduced. For these reasons, and for an "apples-to-apples" comparison with the DHFCVs analyzed in Chapter 3, DMFCVs for this analysis are assumed to be hybridized with the same NiMH peak power batteries as are the DHFCVs. The potential costs of non-hybridized DHFCVs and DMFCVs are discussed briefly in Chapter 7.

Methanol FCV Fuel and Maintenance Costs

Estimating fuel and maintenance costs for methanol FCVs is difficult because maintenance requirements for these vehicles are speculative at this time, and because of uncertainty about methanol costs in the future. The ESM (1992) study estimated costs for fuel and maintenance for methanol FCVs, and the overall results are shown in Table 4-3. In this study, methanol costs were assumed to be $0.89 ($1992) per gallon in 1992 (or $15.62 per million British thermal units (MMBTU)), and they were then inflated through 2001 using a rate of 4.5% per year.

The American Methanol Institute (AMI) reports spot methanol prices and contract methanol prices for the U.S. Gulf Coast from 1989 to 1998 (AMI, 1999c). According to these data, prices were relatively stable from 1989 to 1993, at about $0.40 to $0.50 per gallon ($7.02 to $8.77 per MMBTU, LHV). In 1994, there was a price surge with spot prices reaching levels as high as $1.00 per gallon ($17.54 per MMBTU). From 1995 to 1997 prices receded to the $0.40 to $0.60 range ($7.02 to $10.53 per MMBTU), and in 1998 spot prices reached a low of just over $0.30 per gallon ($5.26 per MMBTU).

In its *Annual Energy Outlook 1999*, the EIA has forecast consumer-level M85 (a blend of 85% methanol with 15% gasoline) prices from 1997 until 2020 (EIA, 1998). These estimates, originally in 1997$, were inflated to 2000$ using a rate of 3% per year, and are shown in Figure 4-4 along with the EIA's forecast for gasoline prices over the same period. Corresponding prices for neat methanol (M100) were calculated from these estimates, accounting for the 85%/15% relative contributions of M100 and gasoline to M85. For this analysis, high case, central case, and low case methanol prices were estimated based on the high, average, and low values projected by EIA over the period from 1997 to 2020. These estimates, of $10.97, $14.01, and $15.16 per MMBTU, are also shown in Figure 4-4.

Figure 4-4:

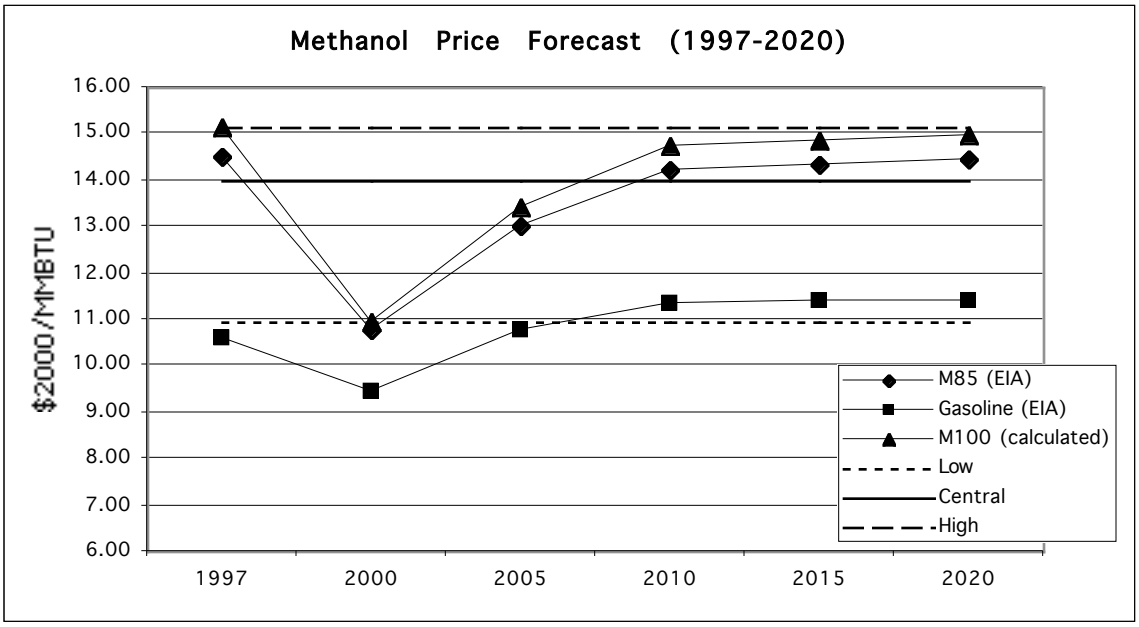

Note: M100 prices were calculated from M85 and gasoline price estimates in EIA (1998).

DMFCV Maintenance and Repair Costs

As with DHFCVs, potential maintenance and repair costs for DMFCVs are somewhat speculative because of the lack of real-world experience with this vehicle type. Calculations of maintenance and repair costs for DMFCVs for this analysis follow the same general procedure discussed for BEVs and DHFCVs, where components are separated into common, similar, and unique categories and maintenance and repair costs are estimated for each category. The result of this procedure is that Generation 1 DMFCVs have levelized maintenance and repair costs of about $465 per year, compared to about $492 per year for the ICE Taurus, and Generation 2 DMFCVs have levelized maintenance and repair costs of about $411 per year.

DMFCV Consumer Cost and Lifecycle Costs Results

As in the analysis of BEVs and DHFCVs, the Lotus 1-2-3 vehicle cost and performance model was run under assumptions for manufacturer production in each year, for each case (i.e. high cost, central cost, and low cost), and for each of the two production volume scenarios. The number of variables altered for each run was similar to the analysis of DHFCVs, except that fuel storage system costs were constant (see above) and not a function of production volume as in the case of the high pressure hydrogen storage system. Thus, for DMFCVs, motor costs, controller costs, battery costs, fuel cell system costs, and methanol fuel costs were varied. Also as in the previous analyses, some minor component costs and weights vary in the model depending on whether the vehicle technology development level is classified as "low," "medium," or "high." To be consistent with the analyses of the other vehicles, Generation 1 DMFCVs (introduced in 2011 when Generation 3 BEVs and DHFCVs are introduced) were assigned a

medium development level, and Generation 2 DMFCVs were assigned a high development level.

A similar procedure was used to perform the model runs as has been described in the previous chapters. First, for each vehicle generation, important vehicle characteristics such as vehicle weight, battery and fuel cell power requirements, and drivetrain peak power were calculated in the model depending on the characteristics of the fuel cell system and battery pack assumed for that vehicle generation. Next, component costs for the battery, motor, controller, and fuel cell system were determined for the particular production volume in that model year. This was done by developing similar cost functions for each component and power rating as shown in Table 2-23 for BEV components, except that as with DHFCVs the "bounded MPF" technique was used to estimate fuel cell system costs, rather than the production volume based approach used for the other components. A slight difference between the projected DMFC system cost estimates and the DHFC system cost estimates is that for DMFC systems, the assumed lower bound on costs was slightly different for the "low," "central," and "high" cost cases (see above discussion of DMFC system costs). These component cost estimates are presented in Table B-5 and B-6 in Appendix B.

The calculated component costs and forecast methanol fuel costs were then entered and the vehicle cost model was run for each case (high, central, and low), for each year of the analysis, for that vehicle generation. Then, the procedure was repeated for the next generation of vehicles, with new vehicle specifications calculated for Generation 2 vehicles, and for each production volume scenario.

As in the other analyses, no economies of scale beyond production of 100,000 batteries per year and 200,000 drivetrain and hydrogen storage tank components per year were assumed for the central and high cost cases. For the low cost case, however, economies of scale for battery production above 100,000 units per year and motor/controller production above 200,000 units per year were extrapolated for the actual production volume. Once again, this produced only minor further decreases in final vehicle costs.

The vehicle purchase cost and lifecycle cost estimates for each scenario, along with key vehicle characteristics for each vehicle generation, are presented in Tables 4-3 and 4-4. Vehicle purchase costs for the two scenarios are shown in Figure 4-5 (at end of chapter), as a function of production volume. These results show that under the assumptions of this analysis, where a 300-mile vehicle range is assumed, vehicle purchase costs drop from a high of over $122,000 in the lower production highest cost case, to about $24,000 in the higher production, lowest cost case. At the highest volume production of about 270,000 units per year, and with central case component and fuel costs, initial purchase costs for the year 2026 DMFCVs remain at $25,302, or about $5,150 higher than the $20,155 price of the gasoline ICE Taurus (about $3,850 and $11,800 higher in the low and high cost cases).

As with DHFCVs, vehicle costs drop sharply after the first year of introduction largely due to reductions in the cost of the fuel cell system. Since the level of cumulative DMFC production at the time the first DMFCVs are introduced in 2011 is only 10 MW, system costs are still on the order of $1,125 per kW, $1,750 per kW, and $2,550 per kW (for the low, central, and high cost cases)

at that point. However, just one year of production at the levels assumed for 2011 (25,039 and 92,680 vehicles in the low and high production volume cases) is enough to increase the cumulative production levels for the next year to 1,347 MW and 4,959 MW (assuming supplier production of twice as many 26.7 kW-net systems needed by the single large automaker whose production is modeled in this analysis). This much higher base of cumulative production in Year 2012 results in substantially lower DMFC system costs, and to lower overall vehicle costs.

From a lifecycle cost perspective, as in the DHFCV case, the least expensive DMFCV (the low cost case vehicle in year 2026) nearly achieves cost parity with the conventional vehicle. Its $0.4073 cost per mile is just over a cent per mile more than the $0.3968 per mile lifecycle cost of the gasoline ICE Taurus. However, the year 2026 central case estimate of $0.4352 per mile is nearly four cents per mile more than the lifecycle cost of the ICE Taurus.

DMFCV Fleet Cost Results

With the calculated costs of owning and operating DMFCVs in each analysis year, total fleetwide costs of DMFCVs operated in the SCAB have been calculated. As with the other vehicle types, these calculations have been performed in the Simulink model, using the same underlying VMT schedule used in the Lotus 1-2-3 model to determine the levelized costs shown in Tables 4-3 and 4-4. The net present values of fleetwide vehicle owning and operating costs, for each case, are shown in Tables 4-5 and 4-6. These estimates assume the same 165,000-mile and 17.3-year average vehicle lives assumed in Delucchi (1999), and the same variable VMT schedule and 3.65% discount rate discussed in Chapter 2.

Tables and Large Figures for Chapter 4

Table 4-1: DMFCV Specifications and Characteristics (300-mile driving range)

Specification	State-of-the-Art circa Feb. 1998	Gen 1 Vehicles (2011-1014)	Gen 2 Vehicles (2015-2023)
Fuel Cell System:			
Gross power		34.0 kW	27.5 kW
Net power		26.7 kW	21.9 kW
Compressor efficiency		75%	80%
Net system efficiency[a]		24.7%	26.1%
Power density – stack	0.100 ft^3/kW (0.350 kW/L)	0.0707 ft^3/kW (0.500 kW/L)	0.0566 ft^3/kW (0.624 kW/L)
Power density – aux.		0.0589 ft^3/kW (0.600 kW/L)	0.0585 ft^3/kW (0.604 kW/L)
System power density		273 W/L	307 W/L
Specific power - stack	~3 kg/kW	2.00 kg/kW	1.60 kg/kW
Specific power – aux.		2.15 kg/kW	1.33 kg/kW
System specific power		4.15 kg/kW (241 W/kg)	2.93 kg/kW (341 W/kg)
Avg. Fuel Utilization (including crossover loss)	~80% dynamic ~90% steady-state	90%	95%
NiMH Battery Pack:			
Pack energy		5.76 kWh	5.18 kWh
Pack maximum power		51.2 kW	48.5 kW
Pack mass		82.1 kg	74.8 kg
Maximum power density		624 W/kg	649 W/kg
Pack specific energy (c/3)		69 Wh/kg	68 Wh/kg
Cell capacity		20 Ah	18 Ah
Motor/controller:			
Peak power rating		72 kW	65 kW
System voltage		288 V	288 V
Methanol storage tank:			
Weight of methanol		74.03 kg	64.8 kg
Tank volume (inner)		3.30 ft^3	2.89 ft^3
Vehicle drag coefficient		0.24	0.24
Vehicle efficiency:[b]			
On "FUDS*1.25" cycle		25.4 mpg-eq (HHV) 203.3 mi/MMBTU	28.9 mpg-eq (HHV) 231.5 mi/MMBTU
On FUDS cycle[c]		31.6 mpg-eq (HHV) 252.9 mi/MMBTU	35.1 mpg-eq (HHV) 280.5 mi/MMBTU
Vehicle curb mass		1,381 kg	1,241 kg
0-60 mph accel. time		9.4 sec	9.4 sec

Notes: FUDS = Federal Urban Driving Schedule; HHV = higher heating value; NiMH = nickel-metal hydride.

[a]For vehicles tested over the "FUDS*1.25" cycle.

[b]Vehicle efficiency values are approximate because vehicle efficiency is difficult to calculate accurately, and different models will produce different vehicle efficiency estimates. Efficiencies in mpg-equivalents would be about 1.05 times *higher* on a LHV basis due to the relative HHV/LHV values for gasoline and methanol.

[c]Values are slightly inaccurate because when modeled over the FUDS cycle vehicle components are resized slightly, and drivetrain power and vehicle mass decrease relative to the values shown in the table. For comparison, the ICE Taurus has a calculated 20.1 mpg fuel economy over the FUDS cycle.

Table 4-2: Results of ESM (1992) FCV Capital and Operating Cost Analysis

	Methanol FCV with Low Performance Battery	Methanol FCV with Medium Performance Battery	Methanol FCV with High Performance Battery
Vehicle Cost:			
Basic vehicle	$5,369.49	$5,369.61	$5,369.76
Battery	$629.06	$1,624.20	$1,077.93
Motor	$1,012.88	$957.74	$918.93
Controller	$2,398.94	$2,268.33	$2,176.42
Transmission	$247.89	$234.39	$224.90
Fuel Cell (PEM)	$4,881.96	$4,515.52	$4,241.51
Fuel Tank	$356.38	$356.38	$356.38
Accessories	$1,100.00	$1,100.00	$1,100.00
Total Capital Cost	$15,996.60	$16,426.18	$15,465.82
Lifecycle Cost:			
Fuel	$4,274.00	$4,274.00	$4,274.00
Tires	$586.04	$568.91	$556.85
Battery Replacement	$0.00	$0.00	$0.00
Insurance	$4,471.47	$4,471.47	$4,471.47
Parking and Tolls	$619.96	$619.96	$619.96
Title, Reg. and License	$595.89	$607.64	$581.38
Salvage Value	($902.19)	($901.26)	($895.94)
Total Operating and Capital Cost	$32,230.29	$32,655.41	$31,662.06

Table 4-3: Mid-Sized DMFCV Consumer Costs and Lifecycle Costs (Low Production Volume Scenario)

	Vehicle Characteristics	Production Volume	Low Case (1997$)	Central Case (1997$)	High Case (1997$)
Generation 1					
2003	Gen 1 BEVs	10,000 vehicles/yr	See Table 2-24		
2004		10,000 vehicles/yr			
2005		10,000 vehicles/yr			
2006		20,000 vehicles/yr			
Generation 2					
2007	Gen 2 BEVs	20,600 vehicles/yr	See Table 2-24		
2008		21,630 vehicles/yr			
2009		22,712 vehicles/yr			
2010		23,847 vehicles/yr			
Generation 3					
2011	72 kW drivetrain	25,039 vehicles/yr	$66,977 (92.75 ¢/mi)	$91,581 (124.43 ¢/mi)	$122,783 (164.35¢/mi)
2012	26.7 kW-net fuel cell	26,291 vehicles/yr	$30,463 (49.31 ¢/mi)	$39,451 (61.29 ¢/mi)	$57,755 (83.85 ¢/mi)
2013	5.76 kWh battery	27,606 vehicles/yr	$29,012 (47.66 ¢/mi)	$36,629 (57.98 ¢/mi)	$53,054 (78.28 ¢/mi)
2014	(NiMH 624 W/kg)	28,986 vehicles/yr	$28,304 (46.86 ¢/mi)	$35,200 (56.32 ¢/mi)	$50,559 (75.22 ¢/mi)
	1,381 kg curb weight				
Generation 4					
2015	65 kW drivetrain	30,436 vehicles/yr	$25,545 (42.39 ¢/mi)	$29,997 (48.76 ¢/mi)	$42,032 (63.29 ¢/mi)
2016	21.9 kW-net fuel cell	31,957 vehicles/yr	$25,501 (42.34 ¢/mi)	$29,520 (48.25 ¢/mi)	$41,154 (62.25 ¢/mi)
2017	5.18 kWh battery	33,555 vehicles/yr	$25,459 (42.29 ¢/mi)	$29,132 (47.81 ¢/mi)	$40,424 (61.38 ¢/mi)
2018	(NiMH 649 W/kg)	35,233 vehicles/yr	$25,414 (42.24 ¢/mi)	$28,802 (47.44 ¢/mi)	$39,796 (60.64 ¢/mi)
2019	1,241 kg curb weight	36,995 vehicles/yr	$25,371 (42.20 ¢/mi)	$28,514 (47.11 ¢/mi)	$39,242 (59.99 ¢/mi)
2020		38,844 vehicles/yr	$25,332 (42.15 ¢/mi)	$28,260 (46.83 ¢/mi)	$38,751 (59.42 ¢/mi)
2021		40,787 vehicles/yr	$25,288 (42.11 ¢/mi)	$28,032 (46.57 ¢/mi)	$38,303 (58.89 ¢/mi)
2022		42,826 vehicles/yr	$25,247 (42.06 ¢/mi)	$27,824 (46.34 ¢/mi)	$37,895 (58.42 ¢/mi)
2023		44,967 vehicles/yr	$25,207 (42.02 ¢/mi)	$27,634 (46.12 ¢/mi)	$37,515 (57.97 ¢/mi)
2024		47,216 vehicles/yr	$25,167 (41.97 ¢/mi)	$27,457 (45.92 ¢/mi)	$37,161 (57.56 ¢/mi)
2025		49,576 vehicles/yr	$25,129 (41.93 ¢/mi)	$27,293 (45.74 ¢/mi)	$36,833 (57.18 ¢/mi)
2026		52,055 vehicles/yr	$25,089 (41.89 ¢/mi)	$27,139 (45.57 ¢/mi)	$36,524 (56.82 ¢/mi)

Table 4-4: Mid-Sized DMFCV Consumer Costs and Lifecycle Costs (High Production Volume Scenario)

	Vehicle Characteristics	Production Volume	Low Case (1997$)	Central Case (1997$)	High Case (1997$)
Generation 1					
2003	Gen 1 BEVs	20,000 vehicles/yr	See Table 2-25		
2004		40,000 vehicles/yr			
2005		54,570 vehicles/yr			
2006		59,850 vehicles/yr			
Generation 2					
2007	Gen 2 BEVs	65,460 vehicles/yr	See Table 2-25		
2008		71,520 vehicles/yr			
2009		78,070 vehicles/yr			
2010		85,110 vehicles/yr			
Generation 3					
2011	72 kW drivetrain	92,680 vehicles/yr	$65,891 (91.49 ¢/mi)	$90,596 (121.63 ¢/mi)	$121,406 (162.63¢/mi)
2012	26.7 kW-net fuel cell	100,790 vehicles/yr	$27,070 (45.52 ¢/mi)	$33,858 (54.81 ¢/mi)	$48,468 (72.70 ¢/mi)
2013	5.76 kWh battery	109,460 vehicles/yr	$26,933 (45.37 ¢/mi)	$31,968 (52.64 ¢/mi)	$44,918 (68.41 ¢/mi)
2014	(NiMH 624 W/kg)	118,690 vehicles/yr	$26,873 (45.30 ¢/mi)	$31,009 (51.54 ¢/mi)	$43,020 (66.14 ¢/mi)
	1,381 kg curb weight				
Generation 4					
2015	65 kW drivetrain	128,500 vehicles/yr	$24,449 (41.19 ¢/mi)	$26,930 (45.35 ¢/mi)	$36,186 (56.44 ¢/mi)
2016	21.9 kW-net fuel cell	138,890 vehicles/yr	$24,400 (41.14 ¢/mi)	$26,608 (44.98 ¢/mi)	$35,503 (55.65 ¢/mi)
2017	5.18 kWh battery	149,840 vehicles/yr	$24,352 (41.09 ¢/mi)	$26,341 (44.68 ¢/mi)	$34,930 (54.99 ¢/mi)
2018	(NiMH 649 W/kg)	161,360 vehicles/yr	$24,308 (41.04 ¢/mi)	$26,114 (44.43 ¢/mi)	$34,434 (54.41 ¢/mi)
2019	1,241 kg curb weight	173,430 vehicles/yr	$24,266 (41.00 ¢/mi)	$25,917 (44.21 ¢/mi)	$33,997 (53.91 ¢/mi)
2020		186,020 vehicles/yr	$24,224 (40.95 ¢/mi)	$25,742 (44.01 ¢/mi)	$33,606 (53.46 ¢/mi)
2021		199,090 vehicles/yr	$24,184 (40.91 ¢/mi)	$25,588 (43.84 ¢/mi)	$33,252 (53.05 ¢/mi)
2022		212,610 vehicles/yr	$24,148 (40.87 ¢/mi)	$25,457 (43.69 ¢/mi)	$32,954 (52.71 ¢/mi)
2023		226,520 vehicles/yr	$24,114 (40.83 ¢/mi)	$25,339 (43.56 ¢/mi)	$32,683 (52.40 ¢/mi)
2024		240,790 vehicles/yr	$24,079 (40.80 ¢/mi)	$25,302 (43.52 ¢/mi)	$32,433 (52.11 ¢/mi)
2025		255,330 vehicles/yr	$24,047 (40.76 ¢/mi)	$25,302 (43.52 ¢/mi)	$32,202 (51.85 ¢/mi)
2026		270,100 vehicles/yr	$24,017 (40.73 ¢/mi)	$25,302 (43.52 ¢/mi)	$31,987 (51.60 ¢/mi)

Table 4-5: Fleetwide Vehicle Ownership and Operating Costs for DMFCVs (with BEVs in early years) by Year (2000$) - Low Production Volume Scenario

Year	Low Case	Central Case	High Case
2003	$71,513,741	$74,684,550	$80,445,064
2004	$157,947,571	$164,950,723	$177,673,579
2005	$239,649,283	$250,274,963	$269,578,985
2006	$382,429,785	$399,751,567	$429,773,749
2007	$533,432,460	$557,618,177	$598,404,933
2008	$682,255,991	$713,204,125	$764,397,058
2009	$831,425,192	$869,242,001	$930,846,514
2010	$981,305,163	$1,026,027,540	$1,098,066,266
2011	$1,262,077,652	$1,406,446,842	$1,603,716,297
2012	$1,434,026,856	$1,636,673,655	$1,931,328,360
2013	$1,564,868,738	$1,802,890,778	$2,171,942,740
2014	$1,694,556,100	$1,963,666,394	$2,400,366,368
2015	$1,809,959,274	$2,097,948,455	$2,584,830,091
2016	$1,924,729,848	$2,227,261,661	$2,758,719,249
2017	$2,043,647,112	$2,359,303,728	$2,934,078,650
2018	$2,166,990,120	$2,494,676,590	$3,111,891,479
2019	$2,295,077,903	$2,633,858,979	$3,292,942,884
2020	$2,403,640,146	$2,751,797,631	$3,450,457,244
2021	$2,508,968,593	$2,865,567,960	$3,602,952,984
2022	$2,621,756,995	$2,986,502,882	$3,762,801,823
2023	$2,719,798,364	$3,091,313,012	$3,905,316,658
2024	$2,818,330,747	$3,196,201,006	$4,048,033,521
2025	$2,924,768,436	$3,308,942,461	$4,199,257,456
2026	$3,038,245,052	$3,428,613,223	$4,358,005,030
2027	$2,870,046,537	$3,241,996,937	$4,134,731,878
2028	$2,590,355,258	$2,906,506,240	$3,705,436,398
2029	$2,351,407,670	$2,622,622,452	$3,334,480,544
2030	$2,142,749,491	$2,381,206,825	$3,019,329,425
2031	$1,943,339,039	$2,151,826,429	$2,721,374,974
2032	$1,757,052,141	$1,940,885,717	$2,450,419,735
2033	$1,579,415,067	$1,741,573,724	$2,196,007,750
2034	$1,407,524,492	$1,549,440,506	$1,951,353,349
2035	$1,240,910,779	$1,363,846,497	$1,715,559,547
2036	$1,079,015,970	$1,184,112,284	$1,487,701,860
2037	$921,383,533	$1,009,637,149	$1,266,988,291
2038	$767,584,244	$839,911,780	$1,052,758,249
2039	$617,143,345	$674,353,148	$844,246,466
2040	$469,639,129	$512,488,460	$640,846,503
2041	$324,651,343	$353,814,210	$441,909,675
2042	$181,767,121	$197,851,900	$246,832,755
2043	$40,580,174	$44,145,107	$55,043,339
NPV in 2000 (3.65% d.r.)	$26,789,316,942	$30,126,171,724	$37,077,138,512

Table 4-6: Fleetwide Vehicle Ownership and Operating Costs for DMFCVs (with BEVs in early years) by Year (2000$) - High Production Volume Scenario

Year	Low Case	Central Case	High Case
2003	$137,064,846	$143,507,525	$153,765,282
2004	$429,684,552	$450,558,865	$481,248,879
2005	$829,688,548	$870,652,679	$928,125,545
2006	$1,264,379,617	$1,327,367,640	$1,413,552,459
2007	$1,707,045,975	$1,792,912,522	$1,908,583,565
2008	$2,167,439,613	$2,278,122,978	$2,424,055,190
2009	$2,651,536,598	$2,788,206,943	$2,966,034,720
2010	$3,161,576,903	$3,325,499,339	$3,536,680,657
2011	$4,198,554,171	$4,713,743,907	$5,402,509,604
2012	$4,830,401,899	$5,528,612,476	$6,533,884,209
2013	$5,345,973,093	$6,137,640,087	$7,365,933,466
2014	$5,897,757,453	$6,766,123,922	$8,203,517,926
2015	$6,422,387,257	$7,335,372,113	$8,931,736,556
2016	$6,968,718,108	$7,916,879,505	$9,660,469,869
2017	$7,555,140,341	$8,537,110,696	$10,429,731,125
2018	$8,182,958,025	$9,198,181,044	$11,242,038,498
2019	$8,853,517,677	$9,901,658,210	$12,099,680,765
2020	$9,520,637,235	$10,599,628,833	$12,951,852,770
2021	$10,171,972,278	$11,279,144,778	$13,785,024,897
2022	$10,825,316,421	$11,959,063,268	$14,620,319,728
2023	$11,507,938,433	$12,668,493,955	$15,488,742,698
2024	$12,231,929,138	$13,422,255,491	$16,403,015,116
2025	$12,993,548,232	$14,218,353,204	$17,359,523,569
2026	$13,789,335,607	$15,053,552,454	$18,354,083,829
2027	$13,151,619,189	$14,358,501,514	$17,534,573,359
2028	$11,990,057,062	$13,005,700,567	$15,838,102,901
2029	$10,985,306,477	$11,855,557,653	$14,387,770,695
2030	$10,087,582,648	$10,859,170,303	$13,146,091,771
2031	$9,214,595,713	$9,897,793,132	$11,953,927,664
2032	$8,385,812,097	$8,995,374,384	$10,846,601,365
2033	$7,585,510,581	$8,129,140,993	$9,789,606,323
2034	$6,802,344,216	$7,283,471,946	$8,759,880,214
2035	$6,034,219,706	$6,455,802,423	$7,754,310,251
2036	$5,278,665,485	$5,643,375,759	$6,769,430,194
2037	$4,533,804,072	$4,844,036,658	$5,802,517,206
2038	$3,798,047,876	$4,055,961,716	$4,851,450,664
2039	$3,069,577,868	$3,277,079,393	$3,913,500,709
2040	$2,347,144,866	$2,505,892,279	$2,986,802,241
2041	$1,629,408,481	$1,740,150,556	$2,069,703,787
2042	$915,536,536	$978,098,362	$1,160,881,739
2043	$204,729,340	$218,753,275	$259,367,394
NPV in 2000 (3.65% d.r.)	$108,144,079,821	$118,913,993,264	$142,838,640,483

Figure 4-5:

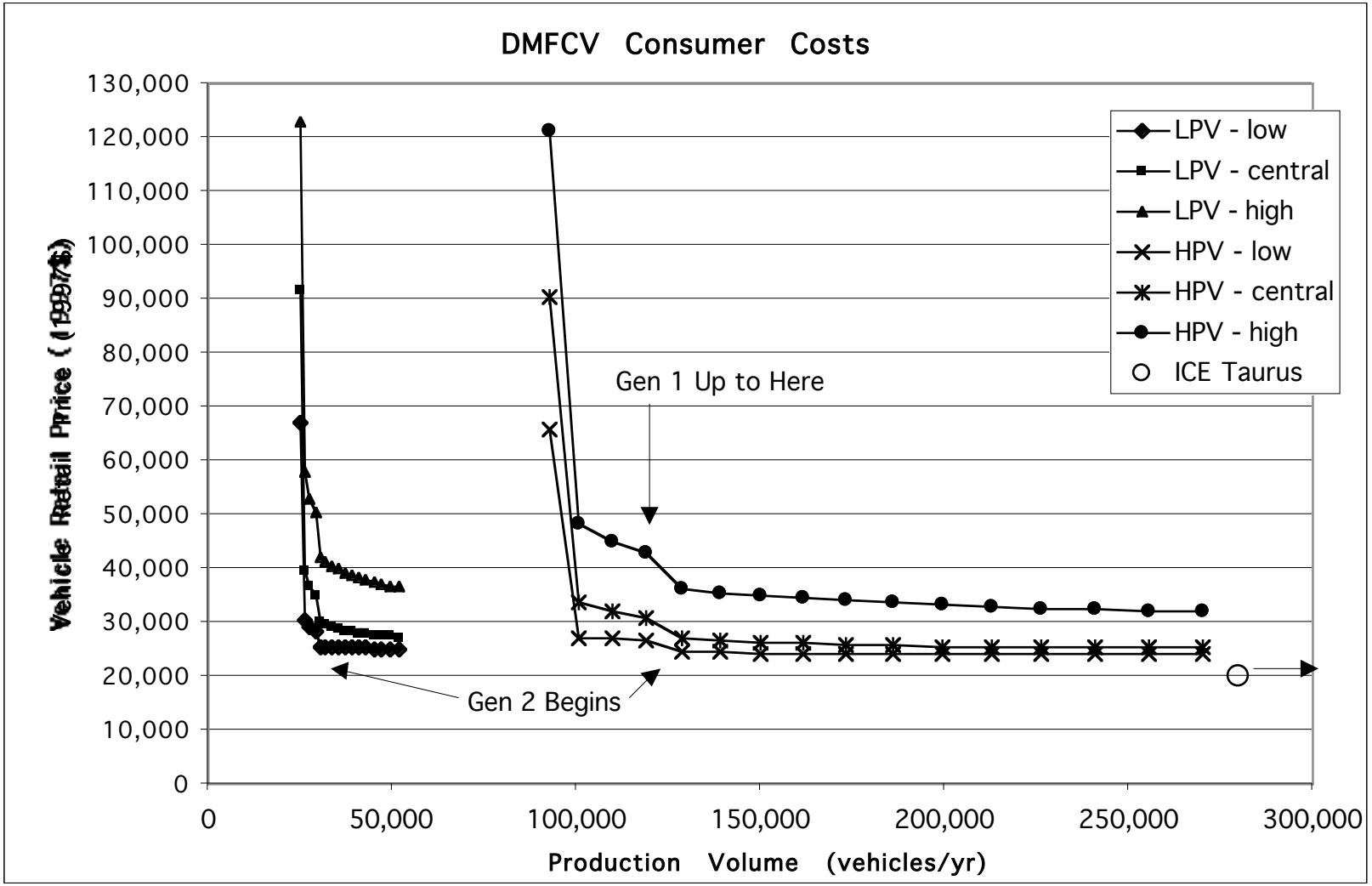
DMFCV Consumer Costs
130,000
120,000
110,000
100,000
90,000
80,000
70,000
60,000
50,000
40,000
30,000
20,000
10,000
0
0
50,000
100,000
150,000
200,000
250,000
300,000
Production Volume (vehicles/yr)
LPV - low
LPV - central
LPV - high
HPV - low
HPV - central
HPV - high
ICE Taurus
Gen 1 Up to Here
Gen 2 Begins

This page left intentionally blank

Chapter 5:
Infrastructure Support Costs for BEV and FCV Fleets in the South Coast Air Basin

Introduction

To a significant extent, costs associated with the infrastructure needed to refuel battery and fuel cell EVs are included in the fuel cost estimates used in the previous chapters. Delivered costs for electricity, methanol, and hydrogen include a contribution to the amortized capital cost of fuel production plants and associated equipment. However, some additional infrastructure-related costs will arguably be needed to support the introduction of the vehicles. The expenditures associated with this additional infrastructure vary for the three types of ZEVs analyzed here. The purpose of this chapter is to estimate these costs, so that the effect of their inclusion on the total costs associated with each scenario can be estimated.

For BEVs, basic on-board recharging units are included with the vehicle costs estimates. These recharging units would allow for 110-volt recharging from a standard outlet, such as in the vehicle owner's garage. In addition to the small recharging units included with the vehicles, however, additional potential BEV recharging infrastructure includes public charging stations. These higher power, 220-volt charging stations would increase the attractiveness of BEV purchase and use because they would allow for rapid "opportunity" charging at worksites, shopping centers, airports, and other locations. Several such charging stations are already in place in the Los Angeles area, but additional stations would improve the attractiveness of using BEVs, as the number of BEVs in the region grows.

For DHFCVs, the delivered fuel cost estimates used in this analysis include the costs of modifications to fueling stations so that they can dispense gaseous hydrogen. However, the assumptions used in developing the hydrogen fuel cost estimates are somewhat optimistic in that the costs of just the number of refueling stations needed to support a given number of vehicles are included. For example, Ogden et al. (1998) estimate that a fleet of 18,400 DHFCVs could be refueled from two service stations that each dispense 1 million SCF of hydrogen to 650 cars per day. While this is no doubt technically true, it is highly questionable whether anyone would purchase a vehicle that could only be refueled at two stations in the entire Los Angeles area. In order for any DHFCVs to be sold, it seems that a minimum skeleton of refueling infrastructure would need to be provided such that the capacity to dispense hydrogen is initially much greater than required by the vehicles sold in the first few years. This gap could then be allowed to close slowly, and eventually new refueling stations could be added to meet additional demand. The net effect of this strategy would be to make investments in refueling stations earlier than if they were only added as a simple function of the number of vehicles, thus raising the net present value of costs associated with the provision of that infrastructure.

For DMFCVs, a similar baseline methanol distribution infrastructure would be needed. Also, the methanol cost estimates used do not include the

costs of refueling station modifications needed to dispense methanol. New methanol storage and refueling infrastructure will be needed for DMFCVs because, though a liquid fuel, methanol is not compatible with conventional gasoline storage tanks and refueling lines and pumps.

Thus, the following chapter estimates the investments that would need to be made in refueling infrastructure in order to support the levels of vehicle purchase and use assumed in the scenarios.

Battery EV Infrastructure Costs

In addition to the in-vehicle or garage chargers sold along with BEVs, the development of a network of public recharging stations would make BEV purchases more attractive to consumers. BEVs based on near-term NiMH battery technology will have rather limited ranges of approximately 100-120 miles, and even the more advanced NiMH batteries assumed here for later generation BEVs would not provide driving ranges of over 150 miles per charge. The ability to "opportunity" charge at shopping centers, transit stations, airports, worksites, and other locations, via a network of public charging stations, would help to ease consumer concerns about limited BEV driving ranges. Incentives associated with public charging stations, in the form of free electricity and/or preferential parking space siting, could provide additional inducements to consumers contemplating the purchase of a BEV over a conventional vehicle.

There currently is a considerable infrastructure of public charging stations in the SCAB, primarily located at shopping centers, transit stations, and worksites (particularly parking lots at public utility offices). As of April 5, 1999, there were 292 charging stations in Los Angeles, Orange, Riverside, and San Bernardino counties (Edison EV, 1999a). More of these stations use inductive charger technology than use conductive charger technology, with 181 of the chargers (or 62%) being of the inductive variety. Los Angeles County has the most chargers, 179, with the remainder roughly evenly spread over the other three counties (Edison EV, 1999a).

The costs of installing public BEV charging stations depend on the charging technology used, the number of chargers being installed, and site-specific installation costs. The cost of installing a single 220-volt charger averages about $6,000, while the installation of two chargers with wiring for two additional ones can cost up to $20,000 (Edison EV, 1999b). The chargers themselves cost about $2,000 for a GMATV Magne Charge (inductive) unit, and about $1,800 for an EV International Series 200 (conductive) unit (Edison EV, 1999b).

There is no established formula for the number of public charging stations that would ideally support a given sized fleet of BEVs, but a reasonable order-of-magnitude estimate is that each 100 BEVs sold would be supported by the installation of one inductive and one conductive charging station. If this level of charging station installation were to be supported for the first 20 years of vehicle introduction, then a substantial charging station network would be available for vehicle charging in subsequent years.

As discussed above, the most expensive additional charging station would cost about $10,000, in the case where two chargers were installed with wiring for two others, and the least expensive station additional station would cost about

$2,550.[38] Thus, assuming that two charging stations are installed for each 100 vehicles sold over a 20-year period, and using a central case cost assumption in the middle of the assumed range, the cost of additional public BEV charging stations can be estimated with a triangular fuzzy-set distribution as follows:

> EV infrastructure cost/100 vehicles sold = [$5,100 $12,550 $20,000] (for 20 years)

Hydrogen FCV Infrastructure Costs

Several recent analyses have been conducted on the costs of hydrogen refueling stations that employ small-scale steam methane reformers to produce hydrogen from natural gas delivered by pipeline. These analyses include those by Moore and Raman (1998), Berry (1996), Ogden et al. (Ogden, et al., 1999), and Thomas et al. (1998a).

Moore and Raman (1998) of Air Products and Chemicals, Inc. have examined the costs of small natural gas reformer systems constructed on-site. They estimate a facility cost of $9.6 million for a station that can support refueling of 500 vehicles per day (for a per vehicle cost of $2,400 assuming one refill every eight days). These stations produce 2,700 kg of hydrogen per day, at a net cost of $3.57 per kg (or $30 per GJ LHV and $25 per GJ HHV) (Moore and Raman, 1998).

In a comparison of various hydrogen production pathways, Berry (Berry, 1996) estimated production costs for an on-site steam methane reformer capable of producing about one ton (455 kg) of hydrogen per day. He estimates that the facility would have a capital cost of $2.2 million, and that hydrogen could be delivered at a cost of about $4.30 per kg (or $36 per GJ LHV and $30 per GJ HHV) (Berry, 1996).

Ogden et al. (1999) analyzed the costs of relatively large steam methane reformer production and refueling stations, on the same order of size as assessed by Air Products. Their analysis assumes the use of advanced reformer technologies in stations designed to dispense 1 million SCF (2,370 kg) of hydrogen per day, or enough to support the refueling of an estimated 654 cars per day. Each such station is estimated to cost $3.4 million, or about $370 per supported vehicle (apparently assuming an infrequent refill rate of once per 14 days). They calculate the same per vehicle cost for fleets of both 18,400 FCVs and 1.41 million FCVs, assuming that the number of service stations scales evenly with the number of supported vehicles (i.e., two service stations support the 18,400 vehicle fleet and 153 service stations support the 1.41 million vehicle fleet).

DTI has estimated both near-term and high volume costs for different sizes of factory-built (as opposed to custom on-site construction) SMR systems, and has calculated per vehicle costs depending on system production volume and the size of the vehicle fleet supported. The premise behind such analyses is that economies of scale in manufacturing many small systems may rival the production economies that occur with large-scale, centralized steam reforming

[38] In the case where the wiring is already in place, a conductive charger is installed, and Edison EV's lower end installation cost of $750 is assumed.

plants in producing economical hydrogen. In one analysis, DTI estimated single unit production costs of $221,900, $256,000, and $447,000 per station for systems capable of producing 36.3 kg, 72.5 kg, and 272 kg per day of hydrogen, respectively, and corresponding 10,000 unit production costs of $33,400, $39,950, and $76,000 per unit (Thomas, et al., 1998b). In another analysis, delivered costs of hydrogen were shown to be sensitive to both the production volume of the SMR "appliances" as well as the number of supported vehicles. For example, for stations supporting 100 vehicles (and producing 56 kg of hydrogen per day), delivered hydrogen costs were estimated at about $4.30 per kg for appliances produced in single units, declining to about $1.50 per kg for appliances produced in 10,000 unit quantities (Thomas, et al., 1998c). The corresponding capital costs per supported vehicle were approximately $2,800 per vehicle and $300 per vehicle. These costs decline when the scale of the plant is increased to support 1,000 and 10,000 vehicle fleets. At the 10,000 vehicle fleet support level, the delivered costs of hydrogen range from about $2.00 per in the single-unit plant to about $1.20 per kg with plants produced in 10,000 unit quantities. Under these conditions, the corresponding capital costs per vehicle decline sharply to approximately $700 per vehicle and $130 per vehicle (Thomas, et al., 1998c).

More recently, DTI has conducted a detailed analysis of the costs of manufacturing reformers, compressors, and storage and dispensing systems needed for very small hydrogen refueling stations capable of refueling 6-7 cars per day (i.e., a fleet of 50 vehicles that refuel about every 8 days). They estimate a cost of $11,830 for the natural gas reformer (with six reformer sub-assemblies), $11,200 for a primary compressor system (with two compressors for added reliability), $9,670 for pressurized gaseous hydrogen storage tanks and valve systems (six small tanks, each holding 6.6 kg of hydrogen), and $1,600 for a backup pumping and compression system. These estimates, which yield a total system cost of $34,300 (or $686 for each supported vehicle), were made in order to estimate the infrastructure costs associated with supporting a fleet of 500,000 FCVs that is deployed over a six year period. Thomas et al. assume that the 10,000 service stations needed to support a fleet of this size are also deployed over six years. As such, these estimates assume moderate production volumes for the fueling station components, such that components for 1,667 service stations are produced each year. Hence, these estimates are most appropriate for a maturing hydrogen refueling station industry (and one based on low capacity refueling stations), rather than a nascent one where component production volumes would be substantially lower.

These analyses show that for decentralized SMR plants, both delivered hydrogen costs and capital costs per vehicle are variable depending on the estimated capital costs of the facility and the size of the facility examined. The hydrogen fuel cost ranges assumed in the above DHFCV lifecycle cost analysis capture some of this uncertainty as it affects fuel costs. However, in order to estimate the additional costs associated with initiating a hydrogen refueling infrastructure, it is also necessary to consider the fact that at first it will be necessary to have more refueling stations than are strictly needed to support the numbers of vehicle that are sold. This is because a minimal infrastructure is necessary to provide reasonable geographic coverage, even to support a few hundred or thousand vehicles, assuming that they are not all sold to fleets where central refueling is an option. For this very reason, it is likely that early FCVs

will be placed in fleets, where they can be conveniently refueled at a dedicated facility. However, if FCVs are to be a reality as consumer products, then a more general refueling infrastructure will need to be provided.

One way to estimate these additional infrastructure costs is to assume that in addition to hydrogen fuel costs, which have been calculated to sufficiently cover the capital costs of refueling infrastructure that is used "ideally," there will also be a cost penalty associated with providing excess refueling capacity. Initially, this excess capacity will necessarily be quite large, just as today many public battery EV recharging stations are unused much of the time. As the number of FCVs grows, however, the level of excess capacity will decrease and a more ideal ratio of refueling capacity to vehicle fleet size can be approached. This raises the question of what level of "skeleton" infrastructure would be necessary to induce consumers to buy FCVs, without their needing to deviate wildly from their typical driving patterns in order to refuel. In theory, experience with the provision of methanol for methanol fueled vehicles could yield some insights into this question. However, because most of the methanol vehicles sold to date have not been dedicated methanol vehicles but rather methanol "flexible fuel" vehicles that can also use gasoline, the fact that some service stations were never converted to provide methanol never imposed a serious barrier to users of these vehicles.

The DTI analysis discussed above shows that the costs of delivering hydrogen by relatively small reforming and refueling stations, that support 100 to 1,000 vehicles each, decline sharply from factory production of a single unit to a production run of just 100 units. If these 100 refueling stations were deployed in the SCAB (which has an area of about 12,000 square miles) in approximately a grid pattern, then each station would be on average about 11 miles apart. The furthest one could get from a station, if one were in the middle of one square in the grid, would be about 7.8 miles away. These stations could ultimately support a total fleet of only 10,000-100,000 vehicles, so additional larger stations would need to be added before long, but initially they could form the basis of the skeletal infrastructure needed to assure consumers that adequate fuel would be available. Assuming this initial production run of 100 stations was built and deployed over five years, the cost in each year would be in the range of $1.4 to $9 million.[39] These investment levels are assumed here, for the first five years of each DHFCV scenario:

> DHFCV infrastructure cost/year = [$1,400,000 $5,200,000 $9,000,000]
> (for first five years only)

This initial infrastructure would be under-utilized at first, but after a period of time it would represent a relatively small margin of excess production capacity for the overall refueling system. Eventually, these small stations could fulfill the role of providing a modest level of reserve production capacity, in the event that one of the larger stations, built later, were to be down for maintenance or repair. In theory, they could even be uprooted, replaced by larger stations, and then

[39] i.e., 20 plants per year times DTI's estimates of $70,000 for a 100 vehicle station and $450,000 for a 1,000 vehicle station.

relocated to other regions that were following California's lead in introducing DHFCVs.

Methanol FCV Infrastructure Costs

Methanol FCVs would be refueled with liquid methanol that would be delivered by trucks to filling stations, just as gasoline is delivered today. In fact, some methanol infrastructure already exists in California and in other U.S. states, distributing a blend of 85% methanol with gasoline (M85). Although currently dispensing M85, these storage and distribution systems are also M100 compatible (CEC, 1999a).

The American Methanol Institute (AMI) reports that from 1997 to 1999, global methanol demand grew relatively slowly, from about 25.4 million metric tons in 1997 to about 26.8 million metric tons in 1999 (AMI, 1999b). Production capacity grew somewhat faster during the same period, such that 80% of production capacity was in use in 1997 and 76% was expected to be in use in 1999 (AMI, 1999b). About 5.4 million metric tons of new production capacity are planned for completion in 1999 and 2000, in various areas of the world that include Delaware, Chile, Trinidad, Guinea, and the Middle East (AMI, 1999a). However, continued growth in demand is also expected, and the AMI forecasts relatively stable production capacity utilization percentages of about 80% through 2005 (AMI, 1999b).

The 20% average unused production capacity, representing some 7-9 million metric tons or about 2.5-3.3 billion gallons, could in theory support several million methanol FCVs. As a result, no additional methanol production facility expansion would be necessary to support the use of methanol FCVs for many years. Furthermore, with the impending reduction in demand for methanol to make methyl tertiary butyl ether (MTBE), due to controversy surrounding its use as a reformulated gasoline additive, methanol production capacity is likely to further outstrip demand. In 1999, forecast methanol demand for MTBE was only slightly behind demand for formaldehyde production as the number one use of methanol, with 7.2 million metric tons of the total global demand of 26.8 million metric tons being used in MTBE production (AMI, 1999b).

Unfortunate for the prospects of introducing methanol FCVs in California is the fact that the number of methanol stations in the state has begun to slowly dwindle in recent years. Storage tanks and pumps for M85, which could be easily used to dispense neat methanol, were added to filling stations in California under 10-year agreements between municipalities and fuel providers starting in about 1988. These agreements have begun to expire, and while there were once about 100 methanol filling stations in the state (EA Engineering, 1999), the number is currently approximately 40. As of April 1999, the CEC reports that there are 21 public M85 dispensing sites in Southern California, and an additional 17 sites in Northern California (CEC, 1999b). These stations and those in other states have supported about 15,000 methanol vehicles that have been operating in the U.S. over the past decade (EA Engineering, 1999). However, most of these methanol vehicles are "flexible-fuel" vehicles that can be fueled with M85 or with pure gasoline.

The storage and pumping systems needed for methanol are quite similar to those for gasoline, with the exception being that methanol can leach plasticizers and fillers from some types of dispenser hoses (EA Engineering,

1999). Since these impurities could clog vehicle fuel filters, certain types of hoses are required for methanol delivery systems in order to prevent leached impurities from mixing with the fuel.

The costs associated with adding methanol storage and delivery systems to existing filling stations have recently been estimated by EA Engineering, Science, and Technology, Inc., in a study for the American Methanol Foundation (EA Engineering, 1999). This study examined the costs associated with adding a methanol refueling station alongside gasoline facilities, and the costs to refurbish a gasoline facility to allow methanol to be dispensed instead.

The components of a methanol storage and delivery system include a double-walled storage tank, a fuel dispenser, a vapor recovery system, and various hoses, pipes, and fittings. In principle, the storage tank could be located above ground, but safety codes and space restrictions will necessitate below ground storage in most areas. Methanol storage tanks can be made of carbon steel, fiberglass, or stainless steel, but due to the high costs of stainless steel, fiberglass and carbon steel/fiberglass composite tanks are more common (carbon steel tanks must be coated with fiberglass to prevent corrosion) (EA Engineering, 1999). In the case where an existing gasoline dispensing pump is converted to use with methanol, the existing gasoline storage tank could be used if it is "methanol compatible," meaning that it meets all of the current regulations and also does not contain any components known to be reactive with methanol. CEC guidelines do not specifically recommend the storage of neat methanol in tanks that previously held gasoline or diesel, but a recent CEC report discusses this as a low-cost option (CEC, 1999a).

Vapor recovery systems include both stage-I vapor recovery, which recovers vapors emitted during storage tank refilling, and stage-II vapor recovery, which recovers vapors emitted during vehicle refueling. These systems would be similar to the corresponding systems for gasoline storage and dispensing facilities, but they would require the use of methanol compatible components. Methanol compatible fuel and vapor hoses are made with special polymer liners and synthetic rubber, and metal components for dispensers and nozzles would need to be made from iron or nickel-plated aluminum, rather than the aluminum used for gasoline dispensing systems (CEC, 1999a; EA Engineering, 1999).

The costs calculated by EA Engineering (1999) associated with installing new, 10,000 gallon, underground and aboveground methanol storage tanks and delivery systems are shown in Table 5-1. Costs for converting an existing gasoline storage tank and delivery system, either through tank cleaning or by installing a fiberglass "tank-within-a-tank," are shown in Table 5-2. The results indicate that the tank cleaning scenario is the most economical solution, with a cost of about $19,000, while installing a new fiberglass tank liner and auxiliary systems would cost about $31,000. Installing a new, aboveground tank and delivery system would cost about $56,000, while the new underground tank and delivery system would cost about $62,000. A final option, to remove an existing tank in a multi-tank field and replace it with a new double-walled tank and delivery system, was estimated to be the most expensive option with a cost of about $70,000 (EA Engineering, 1999).

The CEC reports a similar set of cost estimates, based on the experience gained with providing M85 at various fueling stations in California. The CEC

estimates the costs of installing a new, below-ground 12,000 gallon methanol storage tank and distribution system at $80,000 to $100,000, compared with $50,000 for an above-ground system. Meanwhile, costs of inspecting, cleaning, and retrofitting a below-ground gasoline storage tank and distribution system are an estimated $9,000 to $28,500 (CEC, 1999a).

While as discussed above there currently are a few dozen remaining methanol fueling stations in California, the number of these stations is expected to decline over the next few years because the agreements under which the stations are maintained will have expired. Thus, the refueling infrastructure situation that DMFCVs would face upon their introduction in 2007 would probably be similar to that faced by DHFCVs in 2003; there would be a general dearth of refueling stations to support the first vehicles sold.

However, unlike the fuel cost estimates used for hydrogen for DHFCVs, the methanol fuel cost estimates used here do not include a contribution to the costs of modifications to refueling stations needed to dispense the fuel. Thus, in addition to the need to provide a skeletal infrastructure of methanol refueling stations to support early generation vehicles, additional infrastructure expenditures will be necessary to provide refueling stations for more vehicles in later years.

The methanol refueling station cost estimates discussed above include the addition of a 10,000 gallon methanol storage tank to an existing service station, and they also include the installation of a two-hose dispensing station. The dispensing station could refuel up to 20 vehicles per hour, assuming a six-minute refueling time for a 13-14 gallon fuel tank, if the dispenser were used to its maximum capacity (EA Engineering, 1999). Of course, in reality refueling stations are never used to their maximum capacity, as there are idle periods in between vehicle refuelings. The lengths of these idle times will of course vary depending on the time of day and the location of the refueling station. As an approximation, if a 50% capacity utilization factor is assumed for the methanol dispenser over a sixteen hour per day period (assuming 0% utilization for the other eight hours), then each such station could support 160 DMFCV refuelings per day. If one refueling is assumed per vehicle every 8 days, then each such station could support 1,280 total DMFCVs.

The calculation of the infrastructure support costs for DMFCVs thus includes two components. First, costs are included for the provision of an initial, baseline infrastructure to support vehicle introduction. As with DHFCVs, an initial roll-out of 100 refueling stations is assumed, evenly spread over a five year period. Second, additional costs are included for the modifications to subsequent stations needed to support a growing fleet of DMFCVs. Following the above calculation, one station is added for each 1,280 vehicles sold. These refueling station investments are assumed to be made for as long as additional DMFCVs are being introduced, or for an additional eleven years after the initial five-year methanol fueling station roll-out. After this period, even with longer scenarios of DMFCV introduction than examined here, investments in infrastructure may no longer be needed because early generation DMFCVs will begin to be retired and the growth in the fleet will slow down. In the case of the low market penetration scenario, these assumptions would lead to the addition of methanol pumps at 355 refueling stations in the SCAB from 2016 to 2026, in addition to the 100 stations modified from 2011-2015. In the high production volume scenario, a

total of about 1,700 stations would be modified from 2016 to 2026. These stations would have the theoretical capacity to support more than double the number of vehicles in the DMFCV fleets assessed here.

The methanol refueling station modification costs are derived from the above EA Engineering estimates, reflecting different strategies for the provision of methanol fuel at existing service stations. The low end estimate of $16,000 is for cleaning and re-using an existing tank that is converted from gasoline to methanol, the central case estimate of $62,000 is for provision of a new 10,000 gallon underground storage tank, and the high cost estimate of $70,000 is for removing an existing tank and reinstalling a new tank.[40] Thus, the following DMFCV infrastructure cost estimates are included in the model:

DMFCV infr. cost / year = [$320,000 $1,240,000 $1,400,000]
(from 2011-2015)

And,

DMFCV infr. cost / 1,280 new vehicles = [$16,000 $62,000 $70,000]
(from 2016-2026)

Infrastructure Support Cost Results

Tables 5-3 to 5-7 show the calculated infrastructure costs by year for BEVs, DHFCVs, and DMFCVs, as well as the net present values of the cost streams. Figures 5-1 and 5-2 compare the net present values of the additional infrastructure support cost estimates for the various scenarios.[41] For both the low and high volume production cases, the BEV scenario has the highest additional infrastructure support costs, followed by the DMFCV/BEV scenario, and the DHFCV scenario. However, it must be noted that these cost estimates do not include the full costs of infrastructure for all of the scenarios, and they therefore are not directly comparable. For the DHFCV scenario, the bulk of the infrastructure costs associated with constructing, operating, and maintaining the hydrogen refueling stations are included in the estimated costs of hydrogen that are used in the vehicle lifecycle cost calculations. Also, the DMFCV scenario cost estimates include costs for BEV recharging stations in early years, before the DMFCVs are introduced.

---

[40] This would presumably be required in some areas due to space constraints.

[41] Figures 5-1 and 5-2 can be interpreted by realizing that the larger the value of the membership function $\mu(x)$, the more likely is the corresponding NPV estimate. Hence, the most likely value occurs at $\mu(x) = 1$. As the value of $\mu(x)$ declines to either side, the likelihood of the NPVs decline until $\mu(x) = 0$. See Appendix A for definitions of fuzzy sets, the relationship between fuzzy sets and probability distributions, and a discussion of fuzzy set mathematics.

Figure 5-1:

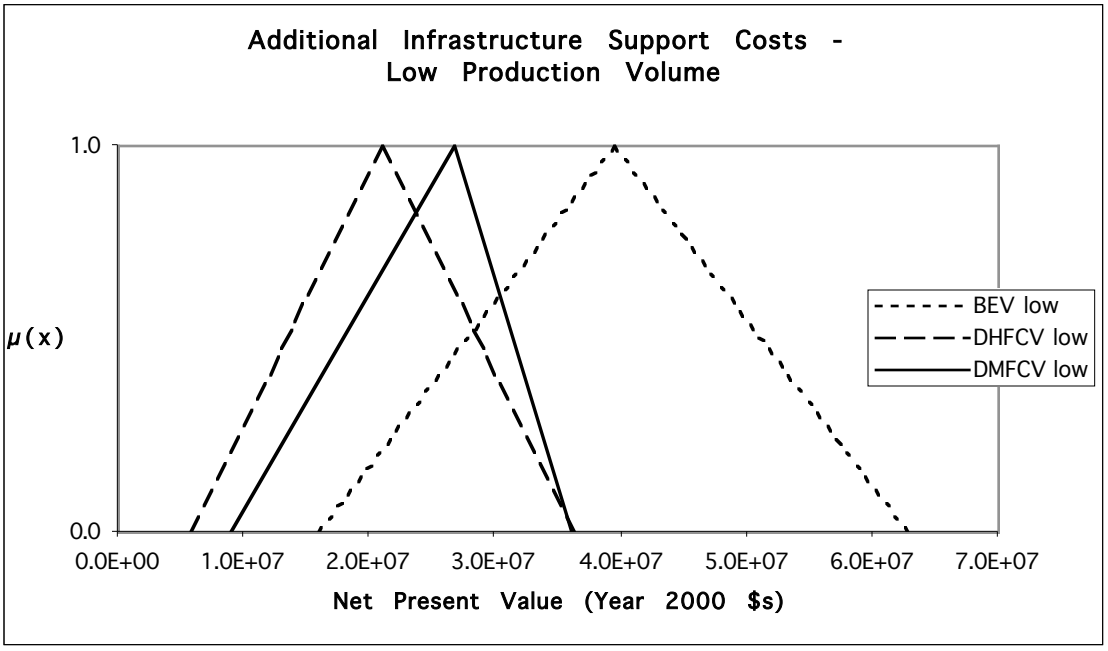

Figure 5-2:

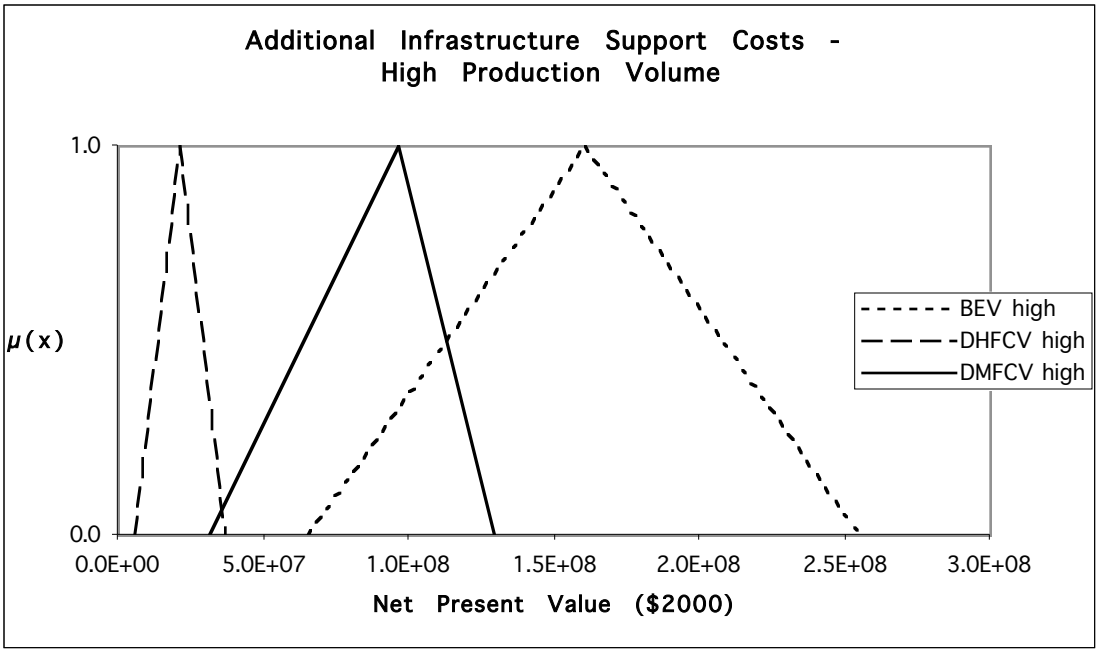

In Chapter 7, these costs are analyzed for each scenario, relative to costs for vehicles and emissions. Also, infrastructure support costs are estimated on a per-vehicle basis in order to clarify the implications of including additional infrastructure support costs in estimates of the total costs associated with producing and using the different ZEV types.

Tables for Chapter 5

Table 5-1: Costs of Adding New Methanol Storage and Dispensing System to Existing Facility

	Urban Underground Tank	Rural Aboveground Tank
Materials:		
10,000 gallon double-walled storage tank	$17,553	$25,850
Interstitial leak detector probe	$1,200	$1,200
Fill adapters, overfill, and ball float valves	$640	$640
1/3 hp submersible turbine pump w/leak detect	$1,426	$1,426
Dispenser, nozzles, hoses, and fittings	$8,645	$8,645
Vent valve and flame arrestors	$1,580	$1,580
Download piping	$300	$1,000
Product and vent piping	$390	$650
Subtotal	$31,734	$40,991
Contingency	$3,173	$3,963
Materials total	$34,907	$44,954
Labor:		
Install tank, piping, vent system, etc.	$25,000	$10,000
Labor contingency	$2,500	$1,000
Labor total	$27,500	$11,000
Total materials and labor	$62,407	$55,954

Source: (EA Engineering, 1999)

Table 5-2: Costs of Converting a Gasoline Storage and Dispensing System to Methanol at an Existing Facility

	Clean Tank	Tank Liner
Materials:		
Interstitial leak detector probe	$1,200	$1,200
Fill adapters, overfill, and ball float valves	$640	$640
1/3 hp submersible turbine pump w/leak detect	$1,426	$1,458
Dispenser, nozzles, hoses, and fittings	$8,645	$8,645
Vent valve and flame arrestors	$1,580	$1,580
Product piping	$300	$300
Vent piping	$390	$390
Subtotal	$14,181	$14,213
Contingency	$1,418	$1,421
Materials total	$15,599	$15,634
Labor:		
Refurbish 10,000 gallon underground tank	$3,250	$9,677
Excavate to expose top of tank		$4,000
Labor contingency	$325	$1,400
Labor total	$3,575	$15,077
Total materials and labor	$19,174	$30,711

Source: (EA Engineering, 1999)

Table 5-3: Additional Infrastructure Support Costs for BEVs by Year (2000$) – Low Production Volume Scenario

Year	Low Case	Central Case	High Case
2003	$510,000	$1,255,000	$2,000,000
2004	$510,000	$1,255,000	$2,000,000
2005	$510,000	$1,255,000	$2,000,000
2006	$1,020,000	$2,510,000	$4,000,000
2007	$1,050,600	$2,585,300	$4,120,000
2008	$1,103,130	$2,714,565	$4,326,000
2009	$1,158,312	$2,850,356	$4,542,400
2010	$1,216,197	$2,992,799	$4,769,400
2011	$1,276,989	$3,142,395	$5,007,800
2012	$1,340,841	$3,299,521	$5,258,200
2013	$1,407,906	$3,464,553	$5,521,200
2014	$1,478,286	$3,637,743	$5,797,200
2015	$1,552,236	$3,819,718	$6,087,200
2016	$1,629,807	$4,010,604	$6,391,400
2017	$1,711,305	$4,211,153	$6,711,000
2018	$1,796,883	$4,421,742	$7,046,600
2019	$1,886,745	$4,642,873	$7,399,000
2020	$1,981,044	$4,874,922	$7,768,800
2021	$2,080,137	$5,118,769	$8,157,400
2022	$2,184,126	$5,374,663	$8,565,200
2023	$0	$0	$0
2024	$0	$0	$0
2025	$0	$0	$0
2026	$0	$0	$0
2027	$0	$0	$0
2028	$0	$0	$0
2029	$0	$0	$0
2030	$0	$0	$0
2031	$0	$0	$0
2032	$0	$0	$0
2033	$0	$0	$0
2034	$0	$0	$0
2035	$0	$0	$0
2036	$0	$0	$0
2037	$0	$0	$0
2038	$0	$0	$0
2039	$0	$0	$0
2040	$0	$0	$0
2041	$0	$0	$0
2042	$0	$0	$0
2043	$0	$0	$0
NPV in 2000 (3.65% d.r.)	$16,002,257	$39,378,104	$62,753,951

Table 5-4: Additional Infrastructure Support Costs for BEVs by Year (2000$) – High Production Volume Scenario

Year	Low Case	Central Case	High Case
2003	$1,020,000	$2,510,000	$4,000,000
2004	$2,040,000	$5,020,000	$8,000,000
2005	$2,783,070	$6,848,535	$10,914,000
2006	$3,052,350	$7,511,175	$11,970,000
2007	$3,338,460	$8,215,230	$13,092,000
2008	$3,647,520	$8,975,760	$14,304,000
2009	$3,981,570	$9,797,785	$15,614,000
2010	$4,340,610	$10,681,305	$17,022,000
2011	$4,726,680	$11,631,340	$18,536,000
2012	$5,140,290	$12,649,145	$20,158,000
2013	$5,582,460	$13,737,230	$21,892,000
2014	$6,053,190	$14,895,595	$23,738,000
2015	$6,553,500	$16,126,750	$25,700,000
2016	$7,083,390	$17,430,695	$27,778,000
2017	$7,641,840	$18,804,920	$29,968,000
2018	$8,229,360	$20,250,680	$32,272,000
2019	$8,844,930	$21,765,465	$34,686,000
2020	$9,487,020	$23,345,510	$37,204,000
2021	$10,153,590	$24,985,795	$39,818,000
2022	$10,843,110	$26,682,555	$42,522,000
2023	$0	$0	$0
2024	$0	$0	$0
2025	$0	$0	$0
2026	$0	$0	$0
2027	$0	$0	$0
2028	$0	$0	$0
2029	$0	$0	$0
2030	$0	$0	$0
2031	$0	$0	$0
2032	$0	$0	$0
2033	$0	$0	$0
2034	$0	$0	$0
2035	$0	$0	$0
2036	$0	$0	$0
2037	$0	$0	$0
2038	$0	$0	$0
2039	$0	$0	$0
2040	$0	$0	$0
2041	$0	$0	$0
2042	$0	$0	$0
2043	$0	$0	$0
NPV in 2000 (3.65% d.r.)	$65,150,132	$160,320,423	$255,490,714

Table 5-5: Additional Infrastructure Support Costs for DHFCVs by Year (2000$) – Low and High Production Volume Scenarios

Year	Low Case	Central Case	High Case
2003	$1,400,000	$5,200,000	$9,000,000
2004	$1,400,000	$5,200,000	$9,000,000
2005	$1,400,000	$5,200,000	$9,000,000
2006	$1,400,000	$5,200,000	$9,000,000
2007	$1,400,000	$5,200,000	$9,000,000
2008	$0	$0	$0
2009	$0	$0	$0
2010	$0	$0	$0
2011	$0	$0	$0
2012	$0	$0	$0
2013	$0	$0	$0
2014	$0	$0	$0
2015	$0	$0	$0
2016	$0	$0	$0
2017	$0	$0	$0
2018	$0	$0	$0
2019	$0	$0	$0
2020	$0	$0	$0
2021	$0	$0	$0
2022	$0	$0	$0
2023	$0	$0	$0
2024	$0	$0	$0
2025	$0	$0	$0
2026	$0	$0	$0
2027	$0	$0	$0
2028	$0	$0	$0
2029	$0	$0	$0
2030	$0	$0	$0
2031	$0	$0	$0
2032	$0	$0	$0
2033	$0	$0	$0
2034	$0	$0	$0
2035	$0	$0	$0
2036	$0	$0	$0
2037	$0	$0	$0
2038	$0	$0	$0
2039	$0	$0	$0
2040	$0	$0	$0
2041	$0	$0	$0
2042	$0	$0	$0
2043	$0	$0	$0
NPV in 2000 (3.65% d.r.)	$5,652,495	$20,994,982	$36,337,469

Table 5-6: Additional Infrastructure Support Costs for DMFCVs (with BEVs in early years) by Year (2000$) – Low Production Volume Scenario

Year	Low Case	Central Case	High Case
2003	$510,000	$1,255,000	$2,000,000
2004	$510,000	$1,255,000	$2,000,000
2005	$510,000	$1,255,000	$2,000,000
2006	$1,020,000	$2,510,000	$4,000,000
2007	$1,050,600	$2,585,300	$4,120,000
2008	$1,103,130	$2,714,565	$4,326,000
2009	$1,158,312	$2,850,356	$4,542,400
2010	$1,216,197	$2,992,799	$4,769,400
2011	$320,000	$1,240,000	$1,400,000
2012	$320,000	$1,240,000	$1,400,000
2013	$320,000	$1,240,000	$1,400,000
2014	$320,000	$1,240,000	$1,400,000
2015	$320,000	$1,240,000	$1,400,000
2016	$399,463	$1,547,917	$1,747,648
2017	$419,438	$1,625,320	$1,835,039
2018	$440,413	$1,706,598	$1,926,805
2019	$462,438	$1,791,945	$2,023,164
2020	$485,550	$1,881,506	$2,124,281
2021	$509,838	$1,975,620	$2,230,539
2022	$535,325	$2,074,384	$2,342,047
2023	$562,088	$2,178,089	$2,459,133
2024	$590,200	$2,287,025	$2,582,125
2025	$619,700	$2,401,338	$2,711,188
2026	$650,688	$2,521,414	$2,846,758
2027	$0	$0	$0
2028	$0	$0	$0
2029	$0	$0	$0
2030	$0	$0	$0
2031	$0	$0	$0
2032	$0	$0	$0
2033	$0	$0	$0
2034	$0	$0	$0
2035	$0	$0	$0
2036	$0	$0	$0
2037	$0	$0	$0
2038	$0	$0	$0
2039	$0	$0	$0
2040	$0	$0	$0
2041	$0	$0	$0
2042	$0	$0	$0
2043	$0	$0	$0
NPV in 2000 (3.65% d.r.)	$8,810,422	$26,659,367	$36,147,002

Table 5-7: Additional Infrastructure Support Costs for DMFCVs (with BEVs in early years) by Year (2000$) – High Production Volume Scenario

Year	Low Case	Central Case	High Case
2003	$510,000	$1,255,000	$2,000,000
2004	$510,000	$1,255,000	$2,000,000
2005	$510,000	$1,255,000	$2,000,000
2006	$1,020,000	$2,510,000	$4,000,000
2007	$1,050,600	$2,585,300	$4,120,000
2008	$1,103,130	$2,714,565	$4,326,000
2009	$1,158,312	$2,850,356	$4,542,400
2010	$1,216,197	$2,992,799	$4,769,400
2011	$320,000	$1,240,000	$1,400,000
2012	$320,000	$1,240,000	$1,400,000
2013	$320,000	$1,240,000	$1,400,000
2014	$320,000	$1,240,000	$1,400,000
2015	$320,000	$1,240,000	$1,400,000
2016	$399,463	$1,547,917	$1,747,648
2017	$419,438	$1,625,320	$1,835,039
2018	$440,413	$1,706,598	$1,926,805
2019	$462,438	$1,791,945	$2,023,164
2020	$485,550	$1,881,506	$2,124,281
2021	$509,838	$1,975,620	$2,230,539
2022	$535,325	$2,074,384	$2,342,047
2023	$562,088	$2,178,089	$2,459,133
2024	$590,200	$2,287,025	$2,582,125
2025	$619,700	$2,401,338	$2,711,188
2026	$650,688	$2,521,414	$2,846,758
2027	$0	$0	$0
2028	$0	$0	$0
2029	$0	$0	$0
2030	$0	$0	$0
2031	$0	$0	$0
2032	$0	$0	$0
2033	$0	$0	$0
2034	$0	$0	$0
2035	$0	$0	$0
2036	$0	$0	$0
2037	$0	$0	$0
2038	$0	$0	$0
2039	$0	$0	$0
2040	$0	$0	$0
2041	$0	$0	$0
2042	$0	$0	$0
2043	$0	$0	$0
NPV in 2000 (3.65% d.r.)	$31,395,921	$96,112,579	$129,166,298

This page left intentionally blank

Chapter 6:
Air Pollutant and Greenhouse Gas Emissions from BEVs and FCVs Used in the South Coast Air Basin

Introduction

BEVs and certain types of FCVs are considered "zero-emission vehicles" because they produce no emissions of criteria pollutants directly from the power systems used in the vehicles. However, the term ZEV is something of a misnomer because all vehicles have emissions associated with their operation. Even BEVs and DHFCVs would produce particulate emissions from tire and brake wear and road dust, for example, and BEVs might emit trace quantities of gases such as hydrogen during battery recharging. Furthermore, all FCVs might emit trace quantities of pollutants simply because there are trace quantities of pollutants in urban air. This air is used as an oxidant gas in FCVs, and passing it through the fuel cell will remove oxygen but not necessarily some of the pollutants that the air contains.[42] Hence, a realistic definition of a "ZEV" would be a vehicle that emits no exhaust pollutants directly from its power system that can be measured above background levels as "net" emissions.

Another issue is that DMFCVs, and indirect-methanol and gasoline FCVs, would have NMOG emissions associated with refueling and with fuel evaporation (also known as "diurnal" emissions) when fuel in the tank and fuel lines heats up. In California, total NMOG emissions from conventional vehicle refueling and fuel evaporation are expected to actually exceed NMOG tailpipe emissions by about 2010, as fleet-average NMOG emissions are slowly being ratcheted-down (CARB, 1997). As a result, CARB is examining new standards for reducing these emissions. For ZEVs, refueling and evaporative emissions would have to be "zero" in order for vehicles to receive ZEV credits under CARB rules. However, CARB is still determining the standards for these emissions and what "zero" really means. Negative-pressure refueling systems are being developed, as well as technologies for trapping evaporative emissions, but minor emissions from these sources would seem to be inevitable over the lifetimes of the vehicles as these control systems degrade or malfunction.

This chapter reviews the literature and fills remaining gaps associated with estimating the full fuel-cycle emissions associated with the operation of BEVs, DHFCVs, and DMFCVs. The goal is to arrive at reasonable ranges of "in-basin" and "out-of-basin" emissions associated with fuel feedstock extraction and production, fuel production and delivery, fuel use, and hydrogen compression (for DHFCVs), for vehicles used in the SCAB. Considered are emissions of NMOG, oxides of nitrogen (NOx), CO, fine particulates (PM_{10}), oxides of sulfur (SO_x), and an assortment of direct and indirect GHGs. Not considered are all other pollutants, such as air toxics, emissions from vehicle manufacture and scrappage, and emissions of PM_{10} from tire and brake wear and road dust. The

[42] Although any CO is likely to remain in the fuel cell system, either in a filtration trap or as a slow build-up on the platinum catalyst, which has a high affinity for CO.

emphasis here is on assessing emissions that are likely to be sources of significant difference among the vehicle types assessed, rather than on comprehensively assessing all emissions from every stage of vehicle and fuel production, use, and retirement. For a broader assessment of BEV emissions, including emissions from vehicle manufacture, see the Electric Vehicle Total Energy Cycle Analysis (EVTECA) recently conducted collaboratively by several national laboratories (U.S. DOE, 1998b).

Finally, included here are approximate damage or control costs for each pollutant, for both in-basin and out-of-basin emissions, in order to translate pollutant magnitudes into cost estimates. These damage or control values are limited in important ways, discussed below, but they are reasonably well-established values for monetizing emissions from vehicles, fuel production facilities, and powerplants. They clearly could (and should) be refined further. However, conducting a full social cost analysis of any one pollutant for a particular region, let alone all of the pollutants addressed here, could easily constitute a PhD dissertation if done thoroughly, given the complexities of pollutant dispersion, atmospheric chemistry, human and other receptor exposure, and dose-response. Hence, for purposes of this analysis, damage and control cost estimates from the literature are reviewed, and ranges of values are chosen for each pollutant, but original pollutant damage or control cost analysis is not performed. The distinction is made between in-basin and out-of-basin emissions because damage and control cost values for the SCAB are considerably higher than those for other regions, and at a minimum two sets of damage and/or control cost value ranges should be used. Also, because of the region's air quality problems, it is of regulatory and policy interest to separately analyze in-basin emissions.

BEV Fuel Cycle Emissions

Emissions from utility power plants that are associated with BEV recharging will cause social costs through damages to humans and the environment, and/or through emission control costs (to the extent that emissions are controlled or offset by controls on other sources). Estimates of BEV-related emissions of criteria pollutants and GHGs are discussed below, followed by the choice of emissions and damage/control cost estimates to include in the Simulink model. Emissions associated with gasoline ICEV use, for comparison purposes, are discussed in Chapter 7.

Emissions from Electricity Production for the South Coast

BEVs produce no tailpipe emissions, but would likely be recharged with electricity produced by utility power plants. Solar recharging is another option, and one with no associated operational emissions, but solar recharging could only take place during the day and only very effectively during times of moderate to high insolation. A few solar EV charging stations have already been designed and built in California, but since most EV recharging is expected to be done at night at individual households, it is most reasonable to assume that in the near-term EVs will be recharged from utility power plants.

The most detailed analyses of utility emissions associated with EV recharging in the SCAB involve the use of utility dispatch models to analyze scenarios of utility emissions both with and without demand from EV

recharging. These studies include those by (Dowlatabadi, et al., 1990), Yau et al. (1993), Hwang et al. (1994), CARB (1996), Acurex Environmental Corporation (1996a), and Rau et al. (1996). Additional studies include those by Wang et al. (1990) and Austin and Caretto (1995).

Hwang and Taylor (1997) have recently reviewed several of these studies, and they show that the different studies used different estimating methodologies, and as a result arrived at significantly different conclusions regarding EV emissions impacts in the SCAB. Most fundamentally, Hwang and Taylor point out that Wang et al. (1990) and Austin and Caretto use an "average" emission estimating methodology, while Hwang et al. (1994) and CARB (1996) use a "marginal" method. The marginal method assumes that the electricity required for EV recharging is the last increment to a utility's load profile, while the average method assumes that the emission factors associated with EV recharging are those for the system in general, including base load plants. Marginal emissions estimates are in principle more accurate, but they require using an electric utility dispatch model, both with and without the assumed EV related electricity demand, in order to estimate the magnitude of emissions.

Table 6-1 presents the results of the studies that report actual emission factors associated with EV recharging. Some of the studies do not report g per kWh emissions factors, and therefore are not included in the table. Also, CARB only reported emission factors for HCs and NO_x, so no CO, SO_x, or PM emission factors are reported for this study.

Of these studies, the most detailed, up-to-date, and thoughtful analyses appear to be Rau et al (1996), Acurex (1996), and Hwang et al. (1994). The Rau et al. (1996) study was conducted under the auspices of the EVTECA project to study the full fuel-cycle emissions impacts of BEVs (U.S. DOE, 1998b). The EVTECA was conducted by several U.S. national laboratories and was originally intended to include analyses of the emissions impacts of EV use in four U.S. cities, including Los Angeles, Houston, Chicago, and Washington, D.C. Unfortunately, funding for the study was insufficient to allow analysis of all four cities, and only the Houston and Washington, D.C. scenarios were examined in detail. The Hwang et al. (1994) study relied on an extended set of ELFIN model utility emission scenario runs originally conducted for an earlier EDF study (Chapman, et al., 1994). The original analysis only considered year 2010 emissions, while the Hwang et al. (1996) study included emissions estimates for every year from 1998 to 2010. Finally, the Acurex (1996) analysis was also based on ELFIN model runs that were conducted in 1995 by the CEC. These runs included EV recharging scenarios for 2000, 2005, and 2010, assuming two different ratios of on-peak to off-peak recharging, and two different EV efficiency estimates.

Details of Marginal EV Recharging Emissions Analyses

Even though the full EVTECA Los Angeles scenario analysis was never completed, the underlying Rau et al. (1996) utility dispatch analysis included an assessment of utility emissions for the Los Angeles region, for the year 2010. One interesting feature of this analysis is that in addition to considering average and marginal emissions associated with EV use, the study also assessed "incremental" emissions. Incremental and marginal emissions differ in the Rau et al. (1996) analysis in that incremental emissions are the emissions that result from EV use considering the fact that the introduction of EVs causes a change in

utility planning and capacity expansion. The additional demand generated from EVs causes the utilities to develop new capacity relatively quickly, because even though most EV recharging occurs at night, some recharging is expected for the late afternoon and adds to peak demand. In the absence of EV introduction, new capacity is developed more slowly as just the base load grows. In the incremental analysis, the new capacity that is developed to meet the demand for EVs is also available meet the demands of the native load, and redispatching of electricity occurs relative to the base case. In contrast, the Rau et al. (1996) marginal emissions analysis assumes that the extra generating capacity needed for EV recharging is built in any event. The marginal emissions are simply the difference between simulation runs both with and without EVs. Thus, use of the incremental emission results is most appropriate when comparing scenarios or policies that include EV use with policies or scenarios that do not. Meanwhile, use of the marginal emissions analysis is most appropriate for exploring perturbations in the level of EV use, in scenarios in which significant EV use is anticipated and planned.

The Rau et al. (1996) utility emissions analysis simulates EV recharging loads by estimating the number of vehicles that are being charged at any time of the day, in five minute intervals, and the amount of power needed for each vehicle at that time as a function of the battery depth of discharge (i.e., power demanded drops off near the end of the charge cycle). The Rau et al. (1996) analysis includes several vehicle types, with battery pack sizes ranging from 16.9 kWh to 54.8 kWh, and four battery types including lead-acid, sodium-sulfur, nickel-cadmium, and NiMH. The analysis considers an "unconstrained" recharging scenario, in which both fleet and household vehicles are connected to the system when they reach their final daily destination, and three "constrained" charging scenarios whereby charging is delayed until the peak load has occurred. The least drastic restricted charging scenario, where charging is delayed until 5pm and unconstrained thereafter, produces very little change in emissions relative to the fully unconstrained case. The more drastic other cases, however, where most charging is delayed until after 10pm, produce significant though not generally dramatic changes in emission factors (with most factors decreasing somewhat under the constrained cases). The analysis also considers two different levels of EV market penetration, and two different choices of generating technology for additional capacity expansions (combined cycle and combustion turbine). Under the "low" penetration case, demand would be 1,609 GWh annually and under the "high" case demand would be 3,758 GWh annually, in the Los Angeles area. The emission factors for the two different penetration scenarios are generally very similar, with slight increases or decreases in NO_x emissions from low to high case being the only notable exceptions. Also, Rau et al. (1996) consider cases in which dispatch is determined by least-cost criteria, and in which dispatch is constrained by the need to meet the 1990 CAAA sulfur dioxide (SO_2) emission cap. They conclude that emission constrained dispatch is only relevant to the Commonwealth Edison utility in Chicago, because the other utilities analyzed will emit SO_2 at levels below the EPA allowance through 2010.

The Rau et al. (1996) analysis differs from the other utility analyses mentioned above in that it considers the computation of a reliability index in the context of utility decisions to add new capacity. Most other studies use the

assumption that if only off-peak demand is added, the utilities will not need to add new capacity. However, this conclusion does not accurately reflect the actual utility planning process, which relies on a reliability index to determine the adequacy of the system to meet demand. The Rau et al. (1996) analysis considers the fact that any additional off-peak load also contributes to the computation of the reliability index, and that a non-zero increase in system capacity is implied even under constrained recharging. The reliability index is non-linear, so the needed increase in system capacity with off-peak additional load only is smaller than the increase when some additional load is added to the peak demand period. The important result, however, is that some additional capacity is needed even if the peak demand level is not increased, in order to maintain the same reliability index as before the additional load has been included.

The Hwang et al. (1994) study uses marginal emissions estimates generated by Chapman, using the Elfin model, for every year from 1998 to 2010. One key assumption underlying these runs is that the load profile is "semi-controlled," with 66% of recharging occurring between midnight and 6 AM. This assumption results in some increment to demand during the peak period, but less than in the "uncontrolled" scenario considered in the original Chapman et al. (1994) analysis. Another important assumption is that 73% of the electricity demanded is in the South Coast Edison (SCE) service area, and that 27% is in the Los Angeles Department of Water and Power (LADWP) service area.

The Acurex (1996) EV recharging emission estimates are based on a series of ELFIN runs conducted by the CEC for EV recharging in the SCAB. The ELFIN runs assessed marginal emissions associated with EV recharging in 2000, 2005, and 2010, while the Acurex (1996) study focused on three scenarios: EV recharging in 1992 using average emission factors, EV recharging in 2010 using incremental emission factors and 80% off-peak recharging, and EV recharging in 2010 using incremental emission factors and 95% off-peak recharging. The ELFIN runs included distinctions between emissions in the basin, emissions in California but out of the basin, emissions in other areas of the U.S., and emissions outside the U.S. (this last category represented emissions associated with less than 1% of total generation). The ELFIN runs assumed an escalating EV power demand from 2000 to 2010, such that total power demand in 2010 would be 1,192 GWh per year (3,138 million vehicle miles and an average EV efficiency of 0.38 kWh per mile including transmission losses). The overall Acurex analysis also considered emissions associated with feedstock production and transportation for fuels used in electricity production, but these emissions were later "zeroed-out" because they were assumed to occur outside of the SCAB (the focus of the Acurex study was in-basin emissions).

Shown in Table 6-1 are the results of the Rau et al. (1996) analysis for the two Los Angeles area utilities, the results of the ELFIN runs for 2010 used in the Acurex (1996) study, and the results of the Hwang et al. (1994) analysis for 2001 and 2010. The Rau et al. (1996) results are for marginal utility emissions, assuming that recharging is unconstrained, for the low and high EV market penetration levels, and for two different choices of additional power generation technology (combined cycle and combustion turbine). The Acurex study did not consider particulate matter and sulfur dioxide emissions.

BEV Recharging Emissions Estimates for the Model

The above discussion illustrates the many complexities involved in estimating emissions associated with BEV recharging. Important factors include: the specific region and utility network being analyzed, the number and type of BEVs being recharged, any constraints that may be imposed on the time of day of recharge (or voluntarily adopted due to pricing mechanisms), the nature of the new generating capacity added to meet the additional BEV demand, the effects of any constraints imposed by emission-control regulations, and assumptions about the nature of the BEV load (i.e., average, marginal, or incremental). With regard to considering these factors, the Rau et al. (1996) study is the most comprehensive analysis conducted to date. No other study combines a detailed, dispatch-model generated analysis with an assessment of the impacts of BEV use in different region, and with an assessment of average, incremental, and marginal emissions.

As studies that analyze BEV recharging emissions in the SCAB, the Rau et al. (1996), Hwang et al. (1994), and Acurex (1996) studies are all reasonably thorough. Furthermore, they all provide useful data in that they present actual marginal emission factors, in g per kWh or lb per GWh, rather than overall percentage emission reductions relative to another case (e.g., Yau et al. (1993) and Wang et al. (1990) only present percentage emission reductions relative to emissions from conventional vehicles). One advantage of the Rau et al. (1996) study is that the various cases analyzed provide considerable flexibility in applying the results. One limitation, though, is that it includes a consideration of in-basin and out-of-basin emissions for SCE and LADWP BEV recharging loads, but only for total and incremental emissions, and not for marginal emissions. Emission reductions in the SCAB are much more highly valued than emission reductions elsewhere, and an important strength of the emissions analysis that underlies the Hwang et al. (1994) study is that it separates marginal emissions by the regions in which they are expected to occur. Rau et al. (1996) chose not to analyze the "in-basin vs. out-of-basin" impacts of marginal emissions associated with BEV recharging because of uncertainty with regard to where the facilities added to meet the additional BEV demand would be located.

Given these issues, high, central, and low case estimates for both in-basin and out-of-basin emissions were calculated as follows. First, the Rau et al. (1996) values were adjusted so that composite SCE and LADWP emission factors, and in-basin and out-of-basin fractions could be determined. For each marginal emission scenario of additional generating capacity (combustion turbine and combined cycle), marginal emission factors were estimated using the assumption, from Chapman et al. (1994), that 72% of future BEV electricity demand will be from the SCE system, and 28% will be from the LADWP system. Then, in-basin and out-of-basin emission factors were calculated assuming that the same in-basin to out-of-basin energy fractions and emission factor ratios apply to the revised Rau et al. (1996) values as are observed in the average Hwang et al. (1994) values.[43] Once these adjustments were made, central case

[43] An analysis of the in-basin and out-of-basin breakdowns of incremental system emissions, along with the new capacity needed to meet EV demand, showed that the 55%/45% average in/out share in Hwang et al. (1994) could very likely apply to the Rau et al. (1996) marginal emission data if most new capacity is added outside the basin, but some is added in the basin.

estimates were calculated by averaging the Hwang et al. (1994) 2000-2010 mean values, the adjusted Rau et al. (1996) values that assume addition of combined cycle facilities, and the adjusted Rau et al. (1996) values that assume addition of combustion turbine facilities. For in-basin emissions, the values were weighted by an in-basin energy fraction of 0.55 to arrive at weighted emission factors. For out-of-basin emissions, an energy fraction of 0.45 was applied, and the upstream emission factors were then added. The low case and high case values were developed in a similar fashion, except instead of averaging the three sets of values, all of the minimum values were used for the low case and all of the maximum values were used for the high case. These emission factors are shown in Table 6-2.

Since these emission factors are now weighted with the fraction of energy generated in and out of the basin, each kWh of electricity delivered must be multiplied by both the in-basin emission factors and the out-of-basin emission factors to estimate total emissions. Or, if the in-basin versus out-of-basin distinction is not needed, the total emission factors, also shown in Table 6-2, can be used.

A few important caveats are in order with regard to the choices of emission factors in the above analysis. First, the time period of analysis is from 2000 to 2010 for the Hwang et al. (1994) study, and 2010 for the Rau et al. (1996) study. In the present analysis, BEVs are introduced through 2026 in the BEV scenarios. This means that BEVs are recharged from 2003 through about 2042, since the vehicle lifecycle cost calculations are carried out over about a 16-year vehicle life. Clearly, any changes in the electricity generation fuel mix over this period, beyond what are forecast for 2010, could influence marginal system emissions associated with BEV recharging. To some extent, the potential for these changes is addressed by including the Rau et al. (1996) emission estimates for different new-facility technologies, but in addition to these new facilities and the regular facility turnover included in the models for the period up to 2010, some additional base-load facilities will be replaced from 2010 to 2042. The addition of these new facilities could change the facility dispatch order relative to the model runs used in the two studies, and this could then in turn alter the marginal emissions associated with BEV recharging. The use of marginal emission estimates may mitigate this concern relative to the use of average emission estimates, which surely will change over time as new facilities are added, but only to the extent that the marginal generating facilities are more stable than the system average. Also, it should be noted that somewhat lower marginal emissions may be possible in the later years of the analysis because of the replacement of older facilities, and the fact that cleaner, new base-load facilities may contribute to marginal BEV recharging emissions in times of low electricity demand.

Second, the electricity production "landscape" is changing in California due to the deregulation of the utility industry. Independent energy providers have been allowed entry into the market, and consumers now have a choice of electricity providers. One aspect of this transition is that consumers have the option to pay a premium price for electricity derived partly or wholly from renewable sources. These sources include hydropower and windmills, and in addition to being based on renewable resources they also tend to be characterized by low operational emissions of criteria pollutants and GHGs. One

could speculate that BEV owners will be more likely to choose energy providers that use production systems based on renewable sources, because they are likely to have higher than average levels of environmental concern, and to be affluent enough to afford the premium prices associated with renewable electricity production. On the other hand, they may be somewhat more sensitive to higher electricity prices because their electricity expenditures will be higher than those of most households. To the extent that BEV owners do choose electricity provision plans with substantial renewable production components, one could argue that the correct marginal emission estimates to assign to the recharging of those BEVs are those emission factors associated with the provision plans that they select. These marginal emission factors will tend to be lower than those that were estimated by the dispatch models for the system as a whole, given the projected future mix of electricity generating technologies that was assumed prior to deregulation.

Furthermore, under deregulation, electric generating facilities in California have been divested to private owners. These owners have incentive to sell as much electricity as they can, and in order to do so they may need to add emission control equipment to limit total emissions under the provisions of the RECLAIM program. Per-kWh emissions associated with BEV recharging may thus be reduced, relative to levels estimated prior to deregulation. The CEC is currently performing some new Multisim model runs to estimate BEV recharging emissions in the SCAB and elsewhere in California (Tanghetti, 1999). In doing so, they are attempting to consider the potential impact of deregulation on utility decisions regarding future levels of emission control. These model runs will support a revision of the full fuel-cycle analysis of emissions from the production and distribution of transportation fuels, originally conducted by Acurex (1996a). The results of the CEC analysis are anticipated in August, 1999. However, despite the use of the new Multisim model in place of Elfin, and the inclusion of some different assumptions than were used previously, CEC analysts do not expect that the results will be much different than those from the Elfin runs that underlie several of the studies discussed above (Tanghetti, 1999).

Thus, due to changes in the electricity generating industry from deregulation, it is possible that the marginal emissions associated with BEV use during the period assessed here will be somewhat lower than those calculated using the emission factor estimates discussed above, particularly for the post-2010 period. The emissions factors at the low end of the proposed ranges are thus probably more likely to be appropriate than those at the high end, and even the low-end numbers may be conservative. More careful and thorough analyses of the marginal emissions associated with BEV recharging in the future will consider the potential impact of future environmental regulations on utility operations and technology choices, and the impact of utility industry deregulation on potential scenarios of BEV recharging and the associated marginal emissions.

Additional Upstream Emissions from Fuel Production and Distribution

In addition to emissions from the powerplants themselves, there are additional sources of fuel-cycle emissions associated with extraction, production, and distribution of coal and natural gas. These emissions are not generally considered when BEV recharging emissions are compared with gasoline ICEV

tailpipe emissions, but they are sometimes (and should be) considered in full fuel-cycle analyses and comparisons. Delucchi (1997) and Delucchi and Lipman (1997) have recently updated Delucchi's earlier fuel-cycle analysis, and have produced updated emissions estimates for the coal and natural gas fuel cycles for years 2000 and 2015. The year 2015 estimates are assumed for this analysis, since 2015 is near the midpoint of the scenario analyses considered here. It should be noted that there also are potential upstream emissions associated with hydropower, geothermal, and renewable electricity production, but these emissions tend to be small in magnitude. They are not considered here because most of the marginal powerplant electricity for BEV recharging is from coal and natural gas facilities.

Applying these upstream emission estimates for coal and natural gas production requires an estimate for the amount of BEV recharging electricity in the SCAB that comes from powerplants using these fuels. Of the marginal emission analyses discussed above, only Hwang et al. (1994) clearly show the fuel mixes that underlie the utility dispatch model runs for marginal BEV recharging in the SCAB. They show powerplant fuel mixes for each year from 1998 to 2010. According to these figures, the coal share fluctuates between 17% and 32% of total production, and the natural gas share fluctuates between 44% and 83% (Hwang, et al., 1994). There is no clear pattern associated with these fluctuations; in some years either the coal or natural gas share is relatively high and the other is relatively low, and in other years the situation is reversed. There also is no clear trend over the 1998-2010 period assessed in the study. In comparison, Delucchi (1997) includes estimates for marginal BEV recharging fuel mix breakdowns in six different regions of the U.S. For the "West" region, he shows a mix of 56% coal, 11% fuel oil, and 33% natural gas; but this large region includes all of the Rocky Mountain States as well as the states further west. It thus includes a much larger number of powerplants than those used to supply electricity to the SCAB, and a higher proportion of coal and oil fired plants. For comparison, the CEC breakdowns on supply technologies, as an average for the state and including imports, are 19.5% coal (10.1% in-state and 9.4% out-of-state), 21.4% large hydroelectric (13.9% in-state and 7.5% out-of-state), 34.8% natural gas (32.2% in-state and 2.6% out-of-state), 13.9% nuclear, <0.1% oil and diesel, 10.2% "eligible" renewables, 2.3% other biomass and waste, 4.5% other geothermal, 2.1% other small hydroelectric, 0.3% other solar, and 1.0% other wind (CEC, 1999c).

In order to account for the potential annual variations in marginal powerplant fuel mix associated with BEV recharging in the SCAB, the low and high-end coal and natural gas fuel mix numbers can be used to define the ends of a range of upstream emission factors. Since the emission factors are expressed in terms of grams of pollutant per MMBTU of fuel input, they must be converted into grams per kWh of electricity produced using an a powerplant efficiency estimate. Delucchi's (1997) estimates for powerplant efficiencies in 2015 were assumed for this analysis (he also shows estimates for 2000, but like the emission figures they are only slightly different). The assumed coal plant efficiency is 34.9% and the assumed natural gas turbine plant efficiency is 42.2%. Table 6-2 shows the high, central, and low upstream emission estimates that result from these calculations. The central case estimates are simple averages of the high and low estimates.

Greenhouse Gas Emissions from BEV Recharging

In addition to criteria pollutant emissions, BEV recharging also produces emissions of GHGs. As with criteria pollutant emissions, the full fuel-cycle associated with BEV recharging includes combustion emissions of GHGs as well as upstream emissions from fuel extraction, production, and transport. In addition, there are emissions of nitrous oxide from corona discharges along power lines, as the electricity is transmitted to the end user.

These electricity generation GHG emissions are estimated and documented in detail in Delucchi (1997) and Delucchi and Lipman (1997), along with estimates for various other transportation fuel-cycles. Other electricity-generation GHG estimates, specific to the marginal emissions associated with BEV recharging, have been developed by Wang (1996) and Bentley et al. (1992). However, the latter analysis only considered CO_2 emissions and excluded emissions of other radiatively active gases.

As in the above upstream criteria pollutant emission calculation, the calculations used here for GHG emissions from BEV recharging rely on the emission estimates documented in Delucchi (1997) and Delucchi and Lipman (1997) for CO_2 and other GHG emissions from various stages in the natural gas-to-electricity and coal-to-electricity fuel-cycles. The calculations of GHG emissions, in grams of CO_2-equivalents (g-CO_2-eq) per kWh of electricity generated, are based on the estimated emissions of 1,096 g-CO_2-eq per kWh for coal plants in 2015, and 570 g-CO_2-eq per kWh for natural gas plants in 2015 (Delucchi, 1997).[44] However, unlike the relatively broad "West Region" BEV recharging fuel mix estimates documented in Delucchi (1997), emission estimates here have been calculated using the natural gas and coal fuel mix estimates for marginal BEV recharging in the SCAB discussed above. In order to assess the impact of these fuel mix changes, emissions of GHGs were calculated assuming each of the 13 fuel mixes given in Hwang et al. (1994) for the years 1998-2010. The lowest and highest of these values were then taken to be the low case and high case emission estimates, and a central case estimate was calculated as the average of the low and high values. Table 6-3 shows all of these emission estimates, as well as Delucchi's (1997) "West Region" estimate (for comparison).

Hydrogen FCV Fuel Cycle Emissions

Emissions of criteria pollutants and GHGs associated with the use of hydrogen FCVs are confined to emissions from hydrogen production and distribution, since the only net emissions from the vehicles themselves would be of water vapor. As discussed above, hydrogen can be produced in various ways, including steam reformation of natural gas (on a variety of different scales), coal gasification, and electrolysis of water. The most likely near-term scenarios to support the use of FCVs in the SCAB would probably be to either produce hydrogen through SMR at a centralized facility located outside of the immediate urban area and to deliver it as a liquid in tanker trucks, or to produce it with decentralized reformers located at service stations. Production by SMR at a

[44] Natural gas boiler and natural gas turbine powerplants produce virtually identical emissions of GHGs (569 g-CO2-eq/kWh for boiler plants versus 570 g-CO2-eq/kWh for turbine plants), so distinguishing between the contributions of these two types of plants is unnecessary.

central facility and distribution by pipeline is another option, but one that is only likely in the longer term due to the high capital costs of pipeline construction. Natural gas used to produce hydrogen for FCVs will likely be transported from West Texas or Western Canada, in order to meet the incremental demand (Acurex, 1996a).

The emission estimates discussed below will focus on full fuel-cycle emissions associated with the decentralized production option. This option was assumed for the hydrogen infrastructure cost and fuel cost estimates used in the previous chapters. Emissions associated with the hydrogen production process are thus assumed to occur entirely with the SCAB. An interesting subsequent investigation would be to assess the relative emissions and associated costs from the other production options, where hydrogen production emissions might occur outside of the air basin, but where there would be some distribution, fugitive, and electricity-related emission sources located with the air basin.

Fortunately, there is an existing small-scale reformer technology that provides some insight into potential emissions associated with decentralized SMR hydrogen production. The ONSI division of the International Fuel Cells Corporation (IFC) produces a small reformer for use with their PC-25 stationary phosphoric acid fuel cell system, and the emissions from these reformers have been measured by IFC. These emission estimates can be combined with estimates of emissions from natural gas production, hydrogen distribution, and hydrogen compression to produce reasonable ranges of estimates of total fuel-cycle emissions from refueling DHFCVs with hydrogen produced in a decentralized fashion.

Upstream Emissions from Natural Gas Extraction and Production

Hydrogen production from natural gas first generates "upstream" pollutant and GHG emissions from the natural gas fields themselves, from gas leaks and flares, and from processing of the natural gas. Processing is necessary for natural gas because its composition as extracted varies widely, water vapor and excess inert gases must be removed, and also because some constituents are removed for higher value uses.

Emissions from natural gas production have been estimated by Delucchi (1997), Darrow (1994), and Acurex (1996a; 1996b). The Darrow (1994) emission estimates have been analyzed and put into the context of emissions associated with producing fuel for hydrogen FCVs, and converted into units of grams of pollutant per MMBTU of hydrogen produced, by Thomas et al. (1998a). I have performed similar analyses with the Acurex (1996a-b) and Delucchi (1997) data. Table 6-4 reports the emission estimates, as converted into these units.

There is considerable variability in these emission estimates due to differences in the data sources and assumptions used by the authors. Also, only Delucchi (1997) estimated SO_x and PM emissions, and Acurex (1996a-b) examined only CO_2 and methane (CH_4) emissions and not emissions of other GHGs. As discussed in the following sections, the emission estimates shown in the table for natural gas extraction and production are used to generate high, central, and low estimates for overall fuel-cycle emissions associated with hydrogen production from decentralized SMR.

Emissions from Small-Scale Steam Methane Reforming

The reformer used with the IFC/ONSI 200-kW PC-25 phosphoric acid fuel cell system is a good surrogate for the type of reformer that might be used to produce hydrogen at service stations. Now marketed by Praxair Corporation, the reformer is modular in nature and can be configured to produce from 3,000 cubic feet to 30,000 cubic feet of hydrogen per hour (Praxair Corp., 1999). If run continuously, and coupled with sufficient storage systems, a fleet of about 40 to 400 FCVs could be supported with reformers in this size range. This relatively small-scale system is different with respect to efficiency and emissions than the larger scale reformers currently used to produce hydrogen commercially, and thus it is more appropriate to analyze for the scenario examined here. For example, the IFC reformer burns 9.4% of the natural gas that it uses to produce steam, compared to about 17% for larger SMR systems (the rest of the natural gas is reacted chemically to produce hydrogen). Overall, it uses 0.18 MMBTU of natural gas to produce a kg of hydrogen, while the larger systems use 0.19 MMBTU of natural gas (Thomas, et al., 1998a). The difference in the fuel fraction is significant because burned natural gas produces some NO_x and CO, while the natural gas used as the chemical feedstock produces only hydrogen and CO_2.

Criteria pollutant emissions measured from the ONSI/IFC reformer system are shown in Table 6-4. Several of these reformers are in use in the SCAB, and the emission levels that they produce are sufficiently low that the South Coast Air Quality Management District has exempted PC-25 reformer siting from air quality permit regulations (SCAQMD, 1997). GHG emissions from the reformer process, also shown in the table, were calculated with the estimate that the natural gas that is chemically reacted in the reformer produces the same amount of CO_2 as natural gas burned in a boiler, or 53,590 grams of CO_2 per MMBTU of natural gas (DeLuchi, 1991). The natural gas burned to raise steam produces about 59,070 grams of CO_2-equivalent GHG emissions, due to additional emissions of CO, NO_x, nitrous oxide (N_2O), and unburned methane gas (DeLuchi, 1991; Thomas, et al., 1998a). Using the 9.4% fuel fraction and 0.18 MMBTU of natural gas per kg of hydrogen estimates for the IFC/ONSI system, total GHG emissions per MMBTU of hydrogen produced were calculated as a weighted average of these two emission factors.

Emissions from Hydrogen Compression

Hydrogen compression at the service station is necessary so that onboard, high-pressure hydrogen storage tanks can be refilled. This compression requires considerable electrical energy, with which there are associated fuel-cycle emissions. In order to estimate these emissions, compression electricity requirements have been estimated, and the same emission factors developed above for marginal BEV recharging have been assumed.

The ratio of compression energy to hydrogen energy can be calculated with formulas for the amount of energy needed to compress the gas, and the energy content of hydrogen. Assuming adiabatic compression, Thomas et al. (1998a) derive the following formula for calculating this ratio:

$$\frac{E_c}{E_h} = 0.0352 \left(\frac{n}{\eta_c} \left(\frac{P_o}{P_i} \right)^{\frac{0.296}{n}} - 1 \right) \qquad (6-1)$$

Where:
E_c = energy needed for compression (MMBTU)
E_h = energy of hydrogen (MMBTU)
n = number of compressor stages
η_c = compressor/motor efficiency
P_o = outlet pressure (psi)
P_i = inlet pressure (psi)

With a four-stage compressor, a 15 psi inlet pressure, a 6,000 psi outlet pressure (needed to fill 5,000 psi storage tanks), and a compressor motor efficiency of 65%,[45] the calculated compression energy per MMBTU of hydrogen is 0.12086 MMBTU. In other words, about 12% of the energy of the hydrogen is needed for compression. This is equal to 35.42 kWh per MMBTU of hydrogen, or 4.016 kWh per kg of hydrogen. In principle, the compression energy requirements could be reduced if the reformer is operated at elevated pressure and the compressor inlet pressure is raised, or if the number of compression stages can be reduced. Compression ratios of over 5:1 require lubricating oil for the compressor, however, and this can be problematic with hydrogen (Thomas et al., 1998a). The conservative assumption is therefore to assume a four-stage compressor in order to achieve the 400:1 compression ratio needed if the reformer is operated at ambient (15 psi) pressure.

With this compression energy requirement, the emissions associated with hydrogen compression at the refueling station can be calculated. These values are shown in Table 6-4, separated into in-basin and out-of-basin portions, including upstream fuel production and distribution contributions. As an aside, the cost of electricity needed for hydrogen compression was included in the estimates for the cost of delivered hydrogen, discussed in Chapter 3. Since the station and fuel cost estimates were developed by Thomas et al. (1998a), who developed the above compression energy formula, the calculated compression energy requirements used in the station cost calculations should be very similar to the 12% value discussed above.

Total Emissions from Hydrogen Production and Compression

Total emission estimates for hydrogen production and compression have been calculated with the above estimates. These emissions have been separated into in-basin and out-of-basin portions assuming that all upstream feedstock extraction and fuel production activities occur outside of the SCAB, that some fuel distribution and marketing emissions occur inside the SCAB, that the fuel reformers themselves are inside the SCAB, and that some of the electricity is

[45] Thomas et al. (1998a) assume a 93% electric motor driving a 70% efficient compressor, for a net efficiency of 65%.

produced in-basin and some is produced out-of-basin (using the same assumptions as above for marginal emissions associated with BEV recharging).

High case, central case, and low case values were calculated assuming the corresponding values for electricity production, and the range of values shown in Table 6-4 for upstream emissions of NMOG, NO_x, and CO from natural gas production from the Acurex (1996a-b), Delucchi (1997), and Thomas et al. (1998a) studies. Since only Delucchi (1997) estimated PM and SO_x emissions from upstream production of natural gas, these values are used for all three out-of-basin case. Also, since Acurex did not examine non-CO_2 and CH_4 GHG emissions from upstream natural gas production, and since Thomas et al.'s values are based on Delucchi's model, the Delucchi (1997) GHG values are used for all three cases as well. The total in-basin and out-of-basin emission estimates for hydrogen compression are shown in Table 6-4.

Methanol FCV Fuel Cycle Emissions

Most of the methanol used in the world, and all the methanol currently used as a vehicle fuel in California, is produced by steam reformation of natural gas. Most of the methanol used in California is produced in Canada and delivered by barge, but a small amount comes from Texas and is delivered by rail (Acurex, 1996a). In the future, methanol may be produced from a combination of partial oxidation and steam reformation of natural gas, rather than from steam reformation alone, and it may be produced from entirely different feedstocks and in other regions. For example, methanol can readily be produced from coal or biomass, and recent evidence suggests that production of methanol through a combined natural gas and biomass process can offer lower costs and greater benefits than when either process is used alone (Borgwardt, 1998).

The methanol fuel-cycle emission estimates discussed below and shown in Table 6-5 are based primarily on data in Acurex (1996a; 1996b) and Delucchi (1997). The methanol production criteria pollutant emission figures discussed below are based on the Acurex analysis that considered methanol production from natural gas, coal, and biomass in 1992 and 2010. This study was used because it focused on methanol production specifically for use in Southern California. The study assumed natural gas production in Canada with steam reforming in 1992, and 50% in Canada and 50% in Indonesia in 2010, through a combination of advanced steam reformation and partial oxidation.

Other upstream emission factors are shown for both the Acurex and Delucchi analyses. In the Acurex study, the methanol produced from natural gas reforming was assumed to be delivered to California by tanker ship, stored in bulk and mixed to M85 at a storage depot within the SCAB, delivered to local stations by tanker truck, and then stored underground at local stations. In the case where methanol was produced from, production was assumed to occur in Utah from coal produced in U.S. mines. The methanol would be then be transported to Southern California by rail, and stored and distributed as above. Finally, the biomass production scenarios assumed methanol production through gasification techniques from California biomass, storage in Sacramento, transport to Los Angeles via pipeline, and bulk storage and distribution in the SCAB as above (Acurex, 1996a).

Upstream Emissions from Methanol Production

Methanol production via steam reformation of natural gas is the most likely pathway by which methanol will be produced in the near-term. By the later years of this analysis other potential pathways are possible, based on coal or biomass feedstocks, or a combination of feedstocks. However, in order to keep the present analysis manageable, emissions associated with the most likely pathways are considered. These pathways are methanol production through steam reforming and production through a combined steam reforming and partial oxidation process.

Steam reformation of natural gas to methanol begins with the dissociation of natural gas into CO, H_2, CO_2, CH_4, and light hydrocarbons. To produce methanol, this gas mixture, known as synthesis gas or syngas, is then pressurized in a reactor. Crude methanol is produced when CO and CO_2 are catalyzed with H_2, and the crude methanol is then refined into chemical grade methanol (Acurex, 1996a). When methanol is produced from biomass or coal, the synthesis gas is produced through a biomass or coal gasification process. Conventional steam reforming of natural gas can produce 0.782 moles of methanol per mole of natural gas, with 63.6% thermal efficiency, while the Battelle-Columbus Laboratory biomass to methanol production system can produce 1.477 moles of methanol from 100 kg of biomass, with 51% net thermal efficiency (Borgwardt, 1998). Interestingly, the methanol yield from the same feedstocks may be increased by 10-13% through a combined natural gas/biomass process because when combined the fuels have a more optimal ratio of hydrogen to carbon for the production of methanol (Borgwardt, 1998). Table 6-5 shows estimates of the emissions of criteria pollutants and GHGs from the various stages of the methanol production fuel-cycle. The data are for the case of production by advanced steam reformation of natural gas, as well as the year 2010 Acurex scenario where some production occurs through the combined steam reforming and partial oxidation process.

Methanol FCV Evaporative Emissions and Vehicle GHG Emissions

In theory, methanol FCVs could produce emissions of hydrocarbons during refueling and through diurnal evaporative losses. Methanol is considerably less photoreactive than the evaporative hydrocarbons emitted by ICE vehicles, with approximately 0.37 times the reactivity (Thomas, et al., 1998a), but it still has some ozone-forming potential. Assuming a higher fuel efficiency for a methanol FCV, (and thus less fuel storage) than a methanol ICE vehicle, Thomas et al. (1998a) calculate that a methanol FCV would emit about 0.02 g per mile, or 0.6 g per gallon equivalent, of NMOG. This value is converted into g per MMBTU of methanol and shown in Table 6-5.

However, in order for DMFCVs to quality as ZEVs under the latest rules proposed by CARB, these evaporative emissions would have to be eliminated through some sort of evaporative emissions control system. In fact, even partial ZEV credit vehicles would have to certify to zero evaporative hydrocarbon emissions under the baseline criteria requirement, although CARB has not yet determined exactly how "zero" evaporative emissions are to be defined and certified (CARB, 1998b). Hence, the assumption made here is that DMFCVs will necessarily be equipped with an evaporative emission control system, and that the resulting evaporative emissions will be negligible.

Also, unlike DHFCVs, DMFCVs would emit CO_2 directly because methanol is a hydrocarbon fuel. An estimate for these direct GHG emissions has been calculated assuming that all of the carbon content of the methanol is converted to CO_2 (i.e., that any unreacted methanol is recycled back through the system). This assumption is consistent with the zero evaporative emission condition above. The direct GHG emission estimate is shown in Table 6-5.

Valuation of Air Pollutants and GHGs

The monetary valuation of air pollutant and GHG emissions is controversial. In order to estimate damage or control cost values, a series of calculations and modeling steps are required, and significant uncertainties are involved in each step. Estimating damage or control costs for emissions that will occur in the future entails even greater uncertainties due to potential changes in background pollution levels, population patterns and densities, climatological and meteorological variables, and potential control technologies. The development of damage values for emissions involves estimating emissions of a pollutant or GHG in a given year or other time period, determining the impact of those emissions on ambient air quality (or atmospheric concentrations of GHGs), estimating the impacts that result from the change in air quality (or GHG concentrations), and finally valuing the various impacts. Determining control cost values involves assessing the marginal costs of controlling emissions using a certain control technology.

Given the complexities associated with valuing pollutant emissions, and because of the lengthy timeframe of this analysis and the uncertainty underlying the geographic location of some future emission sources, the intent of the following analysis is merely to estimate the approximate monetary values associated with emissions in each of the scenarios, based on values found in the air pollution and GHG literatures. A comprehensive analysis, while clearly desirable, would be an enormous undertaking that would require multiple, expensive runs of urban airshed models and heroic assumptions regarding the locations of new electricity and hydrogen generating facilities, future emissions inventories and air quality levels, population growth patterns, and so on.

Perhaps the greatest limitation to performing such an analysis is that there is at present no fully credible model for estimating fine particulate matter (PM) formation and dispersion, but PM tends to be associated with high social costs because ambient PM concentrations are correlated with human mortality. Until better PM emission, formation, dispersion, and impact models are developed, considerable uncertainty will remain regarding the magnitude of the contribution to ambient PM concentrations from transportation fuel cycles, and the overall human and ecological welfare impacts of transportation fuel cycle emissions.

Moreover, the valuation of GHG emissions is perhaps even more controversial than that of air pollutants. On one hand, and unlike air pollutants, most GHGs are believed to have generally similar impacts on climate regardless of they are emitted.[46] Thus, the geographic location of gas release is less of an issue. However, the ultimate impact of GHGs on climate is enormously complex

[46] However, indirect GHGs can have different impacts depending on the altitude at which they are emitted.

and controversial, and the economic impacts of the resulting climatological changes, even if those climatological changes could be agreed upon, are far from straightforward.

Thus, both the emissions associated with BEV and FCV fuel cycles and the damages or other costs that result from them entail significant uncertainties. While few would dispute that air pollutant and GHG releases are likely to result in some level of social cost, the exact level of cost for a given pollutant in a given region is difficult to estimate precisely. This problem is a good example of where employing an analysis method that allows for uncertainty is useful, because at least to some extent the significant uncertainties associated with emission levels and values can be included. The following sections review the recent literature on air pollutant and GHG damage and control cost values (for areas relevant to the fuel-cycles considered here), and estimate reasonable ranges of values to include for each pollutant species. Finally, the results of computations of the range of values of air pollutant and GHG emission-related costs are presented for each scenario.

Emission Values for Criteria Pollutants

As discussed above, criteria pollutant emissions can be valued with damage cost and control cost methods, as well as several others such as the contingency valuation method. The damage cost method is based on estimating actual damage costs from pollutants, and the control cost method is based on assessing the costs of controlling emissions of the pollutant. Conceptually, damage cost values should be used if the emissions are likely to occur, since actual damages will result from the emissions, and control costs should be used if the emissions are likely to be controlled. Some argue that control cost values can be used as a proxy for damage costs, but in principle this will only be accurate if environmental regulations have been set at economically efficient levels, such that the marginal cost of control is equal to the marginal damage cost. There is at present no clear consensus among state and federal agencies for which set of values should be used, or if values from another method are preferable. Many agencies and utilities seem to be using control cost based values, but other agencies, such as the Federal Energy Regulatory Commission, prefers to use damage function based values. It argues that the "limitations of the damage function approach can be overcome with current and future research, while alternative approaches are subject to inherent flaws that cannot be improved through further research" (EIA, 1995a, p. 25).

Damage and control cost values for air pollutant emissions have recently been an issue for several states in the context of efforts to plan utility operations and expansions. A recent report by DOE's Energy Information Administration (EIA) (1995a) reviews the efforts that states have made to consider, and in some cases place monetary values on, externalities from electricity generation. The report notes that about half of the states in the U.S. consider externalities in the utility integrated resource planning process, but only seven states use explicit monetary values in these planning efforts. These states are California, Massachusetts, Minnesota, New York, Nevada, Oregon, and Wisconsin (EIA, 1995a). After examining case studies of utility planning in California, Massachusetts, and Wisconsin, the EIA report concludes that the inclusion of externality values in the utility planning process has had a negligible impact on

the planned resource mix for utilities in these states, primarily because thus far there has been little need for new capacity. Additional reasons include the fact that low natural gas prices have made natural gas power plants the technology of choice to meet future demands, and because utilities have had relatively little experience with renewable technologies other than hydroelectric power (EIA, 1995a). The criteria pollutant values used by the utilities in these states are generally based on the control cost method, and they are shown in Table 6-6.

In California, the CEC directed in 1990 that the costs associated with environmental compliance be included in assessments of the cost-effectiveness of power generation (EIA, 1995a). In order to aid in utility planning efforts, in a 1992 report the CEC developed both damage and control cost based emission values for various regions within the state. These values are also shown in Table 6-6.

In a study for DOE's Office of Transportation Technologies, Wang and Santini (1994) developed both damage and control cost criteria pollutant emission values for various U.S. regions. These values are not based on detailed, original analyses, but rather on regression analysis of the relationship between emission values and air pollutant concentrations and population exposures in the various regions. As such, these values are intended to be used as interim values for environmental technology cost/benefit analyses until more detailed estimates become available. A few representative sets of these values are shown in Table 6-6.

McCubbin and Delucchi (1996) and Small and Kazimi (1995) have analyzed damage values of air pollutants emitted from motor vehicles. McCubbin and Delucchi estimated values for the entire U.S., for all urban areas in the U.S. (aggregated), and for Los Angeles. They conducted their analysis by examining the change in ambient air quality that would result from reductions in motor vehicle use of 10% and 100%, and estimating the resulting reductions in damages to human health. Their analysis considered several permutations, under which upstream and road dust emissions were included and excluded. Small and Kazimi (1995) performed a similar analysis for the South Coast region by examining the links between emissions of NMOG, NO_x, and SO_x on morbidity from ozone, morbidity from particulates, and mortality from particulates. Representative results from McCubbin and Delucchi (1996), along with Small and Kazimi's (1995) results, are shown in Table 6-6.

Examining the damage and control cost values in Table 6-6 reveals that control costs tend to be higher than damage costs, with the exception of values for PM and some of the values for SO_x. This implies that most pollutants are "over-controlled" and that PM, and perhaps SO_x as well, are "under-controlled." However, the complications discussed above for deriving these values suggest that these conclusions are not very robust. The values also show some disparities in values for similar regions, for the same estimation method. For example, CEC's control cost values for the desert Southwest are somewhat different than the values that the state of Nevada has adopted, and there are significant differences between the CEC (1992), McCubbin and Delucchi (1996) and Small and Kazimi (1995) damage values for emissions in the SCAB.

Given the controversial nature of emission values, and the complexities associated with deriving them, the approach adopted here is simply to define two ranges of approximate values for each pollutant. The first range is for

emissions that occur within the SCAB, and the second is for emissions that occur in other regions. With regard to the second set of emission values, it is important to note that most of the out-of-basin emissions that are relevant to the fuel cycles considered here are associated with electricity generation and production of natural gas, coal, and methanol feedstocks. Most of these activities that contribute to electricity, hydrogen, and methanol use in the SCAB will take place in other regions in California, in other areas of the western U.S., and perhaps in western Canada. Thus, the out-of-basin emission factors should focus on values that have been developed for these regions. Also, the assumption here is that the marginal emissions associated with the introduction of BEVs and FCVs will occur, and that damage values should therefore be used, with the exception of NO_x emissions in the SCAB. These emissions are regulated under the Regional Clean Air Incentives Market (RECLAIM) program, which requires that any potential increases in NO_x emissions by large emitters (such as electric utilities and refineries) be either controlled or offset (SCAQMD, 1997). The Clean Air Act Amendments of 1990 (CAAA) restrict SO_x emissions in a similar manner on a nationwide level in order to control acid rain, but none of the 261 plants that are required to comply with Phase I of Title IV of the CAAA are in California or any other western state (EIA, 1997). As a result emission offsets for new sources of SO_x are not currently required in the South Coast (CEC, 1997). CAAA Title IV Phase II requirements, taking effect in 2000, are more stringent but still will almost exclusively affect eastern and mid-western powerplants (EIA, 1997). Thus, for purposes of this analysis, control cost values are more appropriate for in-basin emissions of NO_x, but damage costs are more appropriate for the other pollutants and for out-of-basin emissions.

In order to develop emission value ranges, the following procedure was used. First, the relevant values (discussed below) from Table 6-6 were inflated to Year 2000 values using the GDP implicit price deflator index (National Science Foundation, 1999).[47] Then, for in-basin emission values, the lower of the CEC values for the South Coast and the McCubbin and Delucchi (1996) Los Angeles values were adopted as the central case values, and the higher values were taken as high case values. The low case values were the CEC values for Ventura Country, which are presumably representative of emission values at the edge of the air basin, where lower damage or control costs may be possible. The NO_x values were taken as the CEC NO_x control cost values for central and high cases, and the CEC Ventura County control cost values for the low values.

For out-of-basin emissions, CEC damage values for the San Joaquin Valley, Sacramento Valley, South Central Coast, and desert Southwest, Wang and Santini's Houston area damage values, and ECO Northwest's western Oregon damage values were considered. Of the regional estimates available, these areas were considered to be possible areas in which out-of-basin emissions relevant to the electricity, hydrogen, and methanol fuel cycles might occur. High case values were taken to be the highest of these values, low case values were the lowest values, and central case values were the average of the six regional sets of values (or the average of as many values as were made for each pollutant

[47] The latest NSF index has values up to 1997. For 1998-2000, an average increase of 3% per year was assumed (percentage increase values for 1995, 1996, and 1997 were 2.85%, 2.93%, 3.00%, respectively).

among the six sets). These final estimates, along with the inflated (2000$) values used to calculate them, are shown in Table 6-7.

Damage Costs for GHGs

Marginal damage cost estimates for GHGs have been published by several authors in recent years including Fankhauser (1994), Cline, (1992), Hammitt et al. (1996), Nordhaus (1994) and Tol (Tol, 1995; Tol, 1999). These estimates, among others, are reviewed and compared in the recent Intergovernmental Panel on Climate Change (IPCC) *Climate Change 1995* report (Pearce, et al., 1996), and in Tol (1999). In addition to reviewing other results, Tol's recent (1999) paper presents new marginal damage cost estimates based on a more complex and detailed analysis using the latest version of the FUND model.

These damage cost estimates can be useful for planning purposes, even as the development of actual carbon taxes, to internalize potential GHG-related externalities, remains controversial. Goodland and Serafy (1998) have recently advocated a two-stage GHG internalization process, whereby potential emissions are first valued with damage cost estimates for planning purposes in order to "level the field of comparison among alternative energy sources for new investments" (p. 90). Later, actual carbon taxes are imposed once a taxation scheme can be agreed upon. They note that rather high taxes of $100-200 per tonne of carbon would be required to induce significant shifts in technologies and fuels, but that much more modest taxes could generate substantial revenues. These revenues could be targeted to investments in conservation, renewable energy R&D, pilot projects, education, and so on. A tax of $25 per tonne would generate approximately $50 billion per year for OECD countries, but $5 billion per year, from a tax of only $2.50 per tonne, could be used to triple the current level of investment in renewable energy (Goodland and Serafy, 1998). An important point remains, however, that even in the absence of carbon taxes, GHG damage estimates can be used to help provide decision-makers and the public with information about the full costs and benefits of different technology development and investment strategies.

The differences among the GHG marginal damage estimates made to date arise due to differences in the models used to assess climate changes and damages, and due to other important assumptions. For example, Cline's (1992) results show a wide range with the upper bound results arising from high benchmark estimates of climate change, a long time horizon and relatively low discount rate, and assumed continuous vulnerability to climate change. Differences in each of these assumptions can all have significant effects on the calculation of marginal damages, along with assumptions about: the values of health risks for individuals of different income categories; the relative linearity of damages with increases in regional temperatures; and the extent to which some effects are functions of the pace of climate change, rather than its extent (Pearce, et al., 1996; Tol, 1999).

One additional issue with regard to estimating marginal damage costs for GHGs is that the global warming potential (GWP) index that is useful for comparing the radiative forcing effects of different gases from a scientific perspective is not ideal for comparing gases from an economic perspective. Radiatively active gases other than CO_2, such as chlorofluorocarbons (CFCs), N_2O and CH_4, may have different economic effects, relative to the effects of CO_2,

than their GWP value would indicate. For example, CO_2 has a crop fertilization effect that can be a benefit from an economic perspective, and in addition to being GHGs, CFCs are potent ozone depletors that can ultimately produce negative economic effects unrelated to their radiative forcing. The GWP index has also been criticized because the overall relationship between radiative forcing and impact may be non-linear, and also because the GWP index does not including discounting over time (Reilly, 1992; Schmalensee, 1993).

In light of these shortcomings, Reilly (1992) and Hammitt et al. (1996) have proposed the use of an alternate index to weigh the impacts of different gases. In addition to accounting for the relative lifetimes and radiative forcing potencies of different greenhouse gases, this economic damage index (EDI) goes a step further than the GWP index to compare greenhouse gases by analyzing them with respect to the potential economic impacts that they may exert. The EDI's focus is on the effects rather than the magnitude of climate change, and as a result it is able to account for potentially important effects that are unrelated to forcing, such as those mentioned above.

The EDI, as defined by Hammitt et al. (1996), is the reduction in emissions of a standard gas (CO_2) that would be required to offset the incremental damage that would otherwise result from increased emissions of a particular greenhouse gas. It can also be defined as the partial derivative of the present value of economic welfare loss with respect to the emissions of a particular greenhouse gas, relative to the partial derivative of welfare loss with respect to CO_2 emissions. Hammitt et al. (1996) define the EDI equation as follows:

$$EDI_i = \frac{\frac{\partial}{\partial e_i} W[C(t)]}{\frac{\partial}{\partial e_o} W[C(t)]} = \frac{\int_0^\infty \Delta C_i(t)\,\gamma_i(t)\,dt}{\int_0^\infty \Delta C_o(t)\,\gamma_o(t)\,dt} \qquad (6\text{-}2)$$

Where:

EDI_i = the economic damage index for gas i

e_i = emissions of gas i

e_o = emissions of reference gas, CO_2

W[C(t)] = the economic welfare loss due to the time path of GHG concentrations, C(t)

$\Delta C_i(t)$ = the change in the concentration of gas i

$\Delta C_o(t)$ = the change in the concentration of the reference gas, CO_2

$\gamma_i(t)$ = the marginal social cost of an additional unit concentration of gas i

$\gamma_o(t)$ = the marginal social cost of an additional unit concentration of the reference gas, CO_2

Hammitt et al. (1996) base the calculation of EDI values on a simple damage function that relates economic damages to the magnitude of temperature change over time. The damage function is as follows:

$$W[\Delta T(t)] = \int_0^{\infty} (1/1+r)^t \; \alpha \; GDP(t) \; D[\Delta T(t)]dt \qquad (6\text{-}3)$$

Where:
W[ΔT(t)] = economic damages from a change in average global temperature
r = the discount rate
α = a scaling constant
GDP(t) = gross world product
D[ΔT(t)] = economic damage function, related to magnitude of temperature change
ΔT(t) = the increase in global annual-mean surface temperature from its 1990 value

In addition to simple damage functions, where damages are a linear, quadratic, or cubic function of delta-T, Hammitt et al. (1996) also investigate a more complex, "hockey-stick" damage function. This function can be varied from a quadratic function to a highly convex function by varying the parameter γ from 0 to 1 (in a slightly more complex version of the function shown above). The authors chose a γ value of 0.1, resulting in a highly convex function that might represent the possibility of catastrophic damages with high levels of delta-T.

In addition to the work by Reilly (1992) and Hammitt et al. (1996), Tol (1999) also develops damage index values for CH_4 and N_2O, relative to CO_2, using the FUND model. These values are shown in Table 6-8 along with various GWP values, the Reilly (1992) values, and the Hammitt et al. (1996) values for various cases.

Also shown in Table 6-8 are the values assumed by Delucchi (1997) and Delucchi and Lipman (1997) in computing overall CO_2-equivalent emission values for various fuel-cycles. These values were chosen based on the various Reilly (1992) and Hammitt et al. (1996) EDI values (see Delucchi and Lipman (1997) for more details). Since these weighting factors were used to compute the CO_2-equivalent emission values used for most of the fuel-cycle emissions analyzed here, no further corrections are needed. Where additional calculations have been done here that involve emissions of non-CO_2 GHGs, the values shown at the bottom of the table were used to produce overall CO_2-equivalent emission values.

Once various emissions of GHGs have been translated into the common metric of CO_2-equivalent emissions using the EDI-based values, it is finally necessary to choose damage values for emissions of CO_2-equivalents. However, as discussed above, there is considerable uncertainty in these damage values. The greatest damages as estimated by most models are from sea level rise, with somewhat lesser damages due to extreme weather and small contributions from species loss, malaria, and agriculture-related damages, but different models show different relative levels of impacts among these categories, and different regional distributions of damages (Pearce, et al., 1996; Tol, 1999). Due to the underlying uncertainties, the IPCC is at present suggesting the use of a rather wide range of values, of from $5 to $125 (in 1990$) per tonne of carbon (Pearce, et al., 1996).

Many agencies are still using default values of zero at present for planning purposes, but the Global Environmental Facility, supported by the World Bank and the United Nations Development Program, has been using "unit abatement cost" estimates of $20-25 per tonne of carbon for the past several years (Goodland and Serafy, 1998).

Tol's recent (1999) study includes both an analysis of damages with and without equity weights, and a detailed sensitivity analysis. These values calculated with "equity-weighting" assume that the impacts of climate change exert greater proportional damage on individuals who have less income, thus assuming a non-linear effect of utility on monetary income. Most other studies make the simplifying assumption that OECD damage values apply to the entire world. The inclusion of this equity-weighting effect raises the damage values calculated with the FUND model from $9 and $23 per tonne of carbon (with 3% and 5% discount rates) to $26 and $60 per tonne, respectively (Tol, 1999). Thus, equity-weighting is an important issue that can potentially raise damage values by nearly 300%. Tol's (1999) sensitivity analysis is based on 2,500 Monte Carlo runs and uncertainties in the following parameters: climate sensitivity; sensitivity in response of sea levels, hurricanes, floods, and storms; the atmospheric lives of CO_2, CH_4 and N_2O; GDP and population growth rates; dollar impacts; the value of a statistical life; and several other parameters. The results show a log-normal distribution of carbon emission values for each discount rate assessed (0%, 1%, 3%, 5%, and 10%), with a skew toward the lower end values and a wide overall spread. For example, for the 3% discount rate, equity-weighted values ranged from about $25 per tonne of carbon up to over $500 per tonne, with a mean value of $92 per tonne (Tol, 1999).

The various GHG damage cost estimates made by the authors mentioned above are shown in Table 6-9, along with my choices for high, central, and low damage values to use for the period of analysis in this study. For the calculations performed here, a range of values was estimated using Tol's (1999) 2011-2020 emission year value at a 5% discount rate as a central case value, and the $5 and $125 per tonne values suggested by IPCC as ends of the likely range of damages as low case and high case values. These values were inflated to Year 2000 $s using GDP implicit price deflator data (see footnote 47 for details), and converted from damages per tonne of carbon to damages per tonne of CO_2.

Results

Figures 6-1 through 6-6 present total fuelcycle emissions (in tons) of each pollutant for the period from 2003 to 2043, for each ZEV type and for each case. The figures present the results for the high production volume scenario; the results for the low production volume scenario show the same pattern as shown in the figures, only with lower overall magnitudes of emissions. Table 6-10 shows the results for both the high and low production volume scenarios. Note that the DMFCV results include emissions associated with the BEVs that are introduced in 2003-2010, prior to the introduction of DMFCVs in 2011.

Figure 6-1:

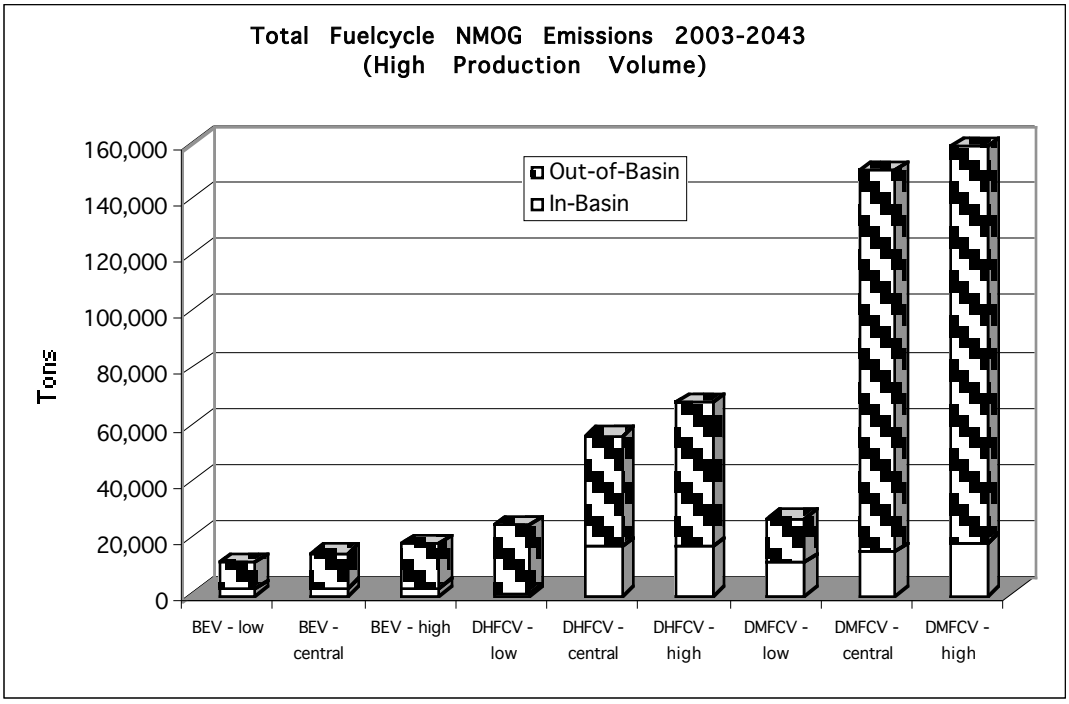

Figure 6-1 shows that fuelcycle NMOG emissions are likely to be lowest for BEVs, followed by DHFCVs and then DMFCVs. There is considerable uncertainty about in-basin emissions of NMOG for DHFCVs, as Acurex estimates in-basin emissions of over 9 grams per MMBTU of hydrogen from the natural gas distribution stage in the fuelcycle, while Delucchi estimates no NMOG emissions from natural gas distribution. There is also considerable uncertainty regarding out-of-basin NMOG emissions for DMFCVs. This is because Acurex estimates emissions of nearly 40 grams of NMOG per MMBTU of methanol for methanol production, while Delucchi estimates no emissions of NMOG from methanol production. In both of the these cases, the Acurex values are used for the central case, because the Acurex analysis focused on criteria pollutants and also is specific to fuel use in the SCAB.

Figure 6-2:

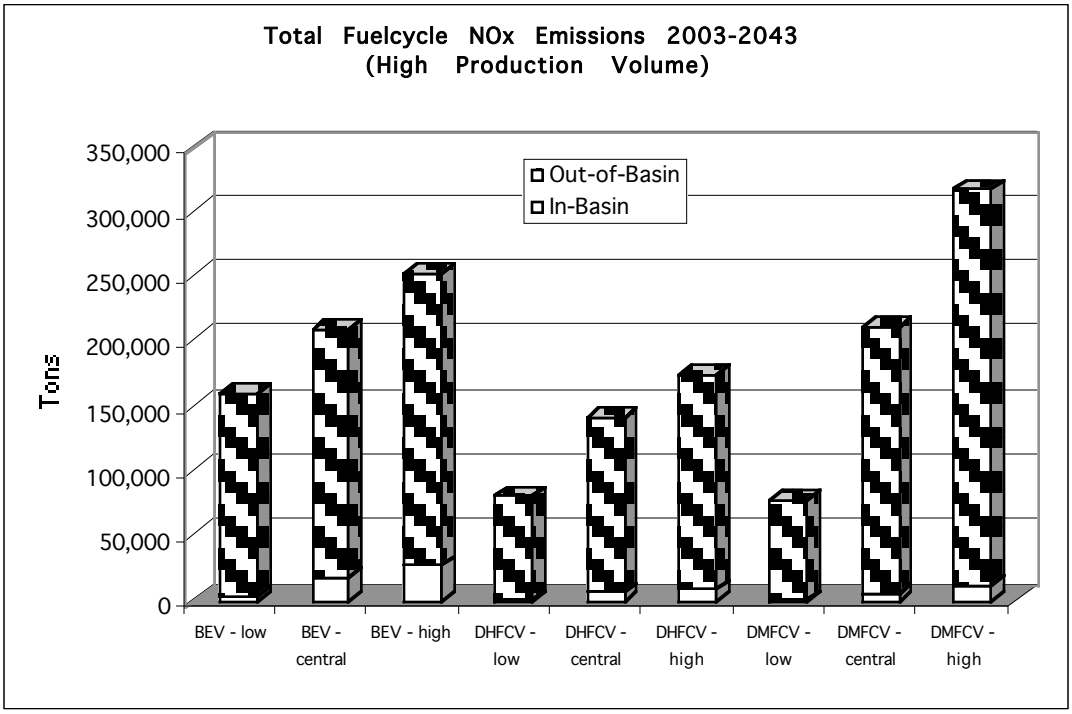

Figure 6-2 shows that fuelcycle NO_x emissions are likely to be lowest for DHFCVs. BEVs and DMFCVs have similar emission levels for the central cases, but there is considerable uncertainty with regard to DMFCV NO_x emissions. The majority of fuelcycle NO_x emissions are out-of-basin for all ZEV types.

Figure 6-3:

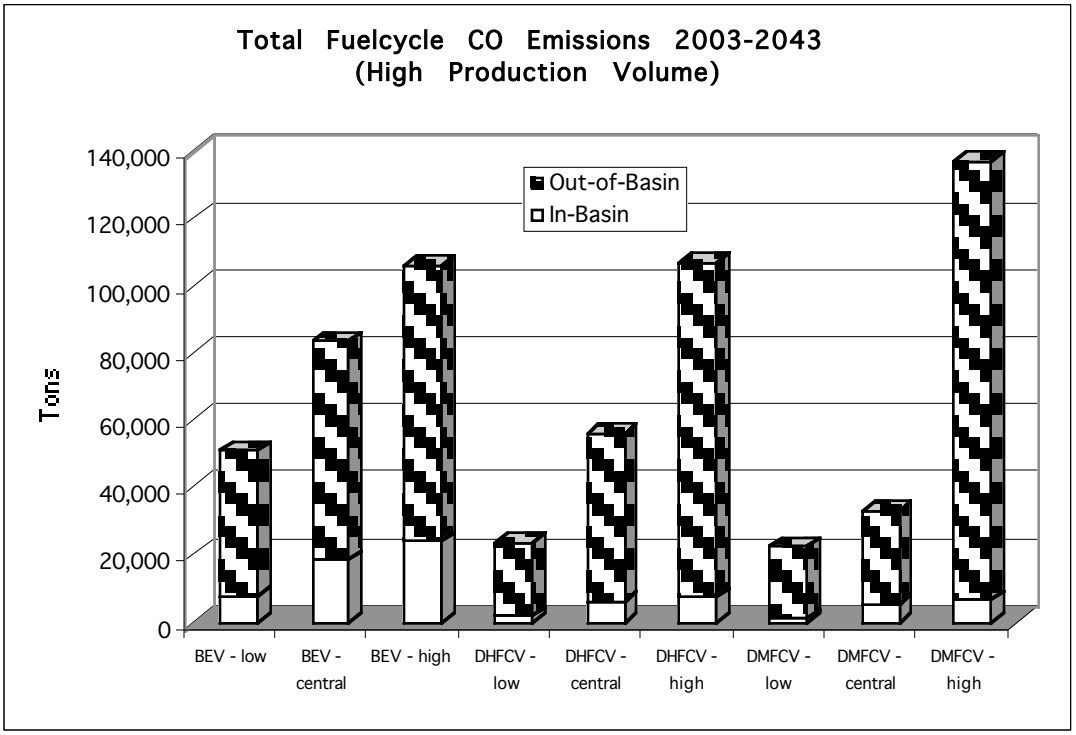

Figure 6-3 shows that CO emissions are likely to be lowest for DMFCVs, followed by DHFCVs and BEVs. However, Delucchi (1997) estimates relatively high CO emissions of 33 grams per MMBTU of methanol, from the methanol feedstock extraction and production stage of the fuelcycle, compared with only 0.5 grams per MMBTU in the Acurex (1996b) analysis. With the higher CO emissions estimate, reflected in the "DMFCV-high" case, fuelcycle CO emissions from the DMFCV scenario would be higher than for the other two scenarios.

Figure 6-4:

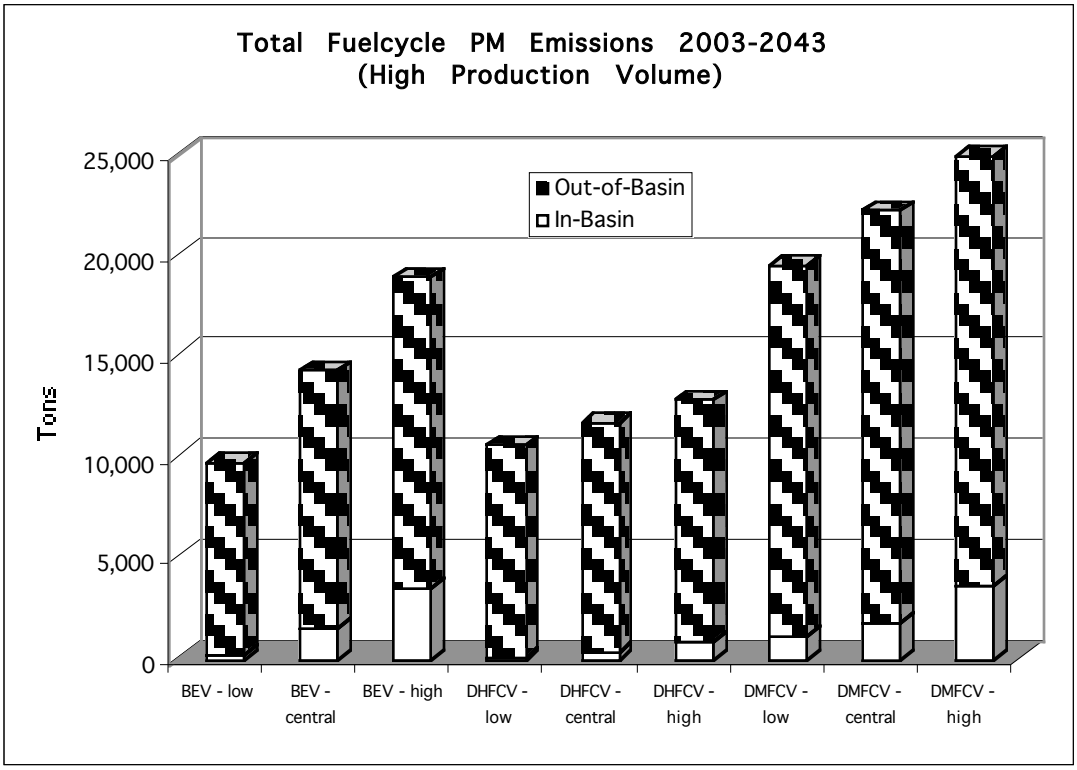

Figure 6-4 shows that fuelcycle PM emissions are likely to be lowest for the DHFCV scenario, followed by the BEV scenario and then the DMFCV scenario. Acurex (1996b) did not estimate PM emissions, so these results are based on Delucchi's estimates for the methanol and hydrogen fuelcycles, and studies of the marginal emissions associated with electricity production for BEV recharging and hydrogen compression.

Figure 6-5:

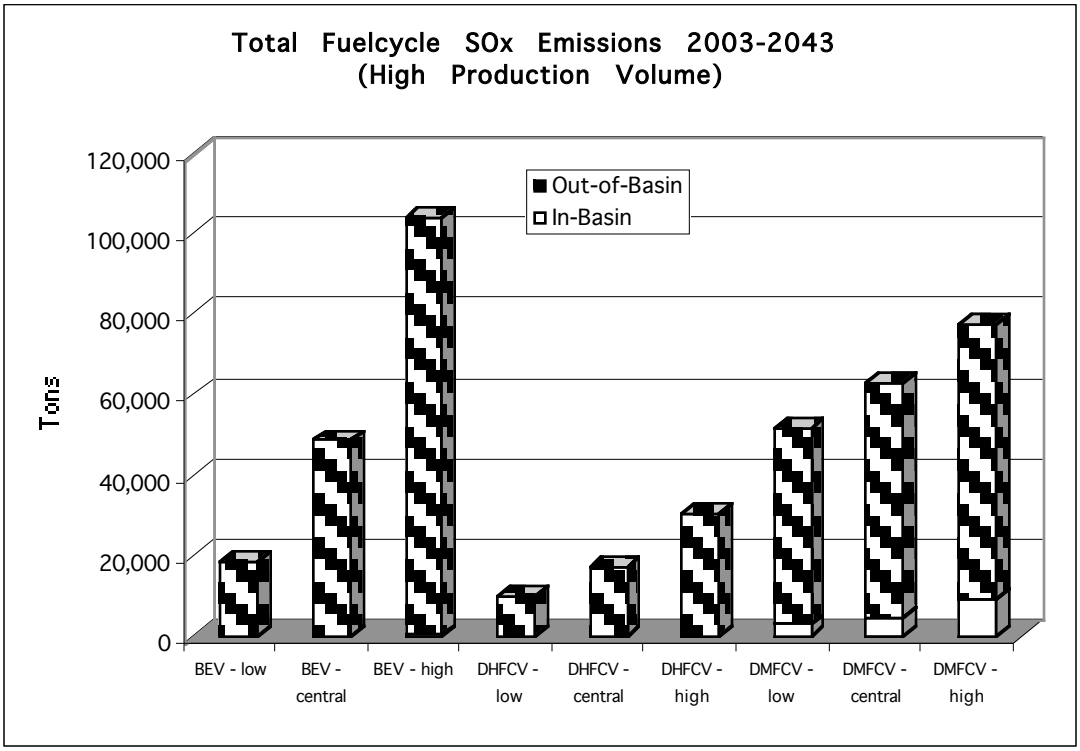

Figure 6-5 shows that SO_x emissions are also likely to be lowest for the DHFCV scenario, followed by the BEV scenario and then the DMFCV scenario. SO_x emissions may be highest for BEVs due to the fact that some coal-fired powerplants have relatively high SO_x emissions. If these powerplants provide a significant amount of the electricity used to recharge BEVs, then SO_x emissions are higher than if natural gas and other types of power plants are primarily used. In-basin emissions of SO_x are only significant for the DMFCV scenario, since there are some SO_x emissions associated with delivery of liquid methanol to refueling stations in the basin. Once again, Acurex (1996b) did not estimate SO_x emissions, so these results are based on Delucchi (1997) and studies of emissions from electricity production.

Figure 6-6:

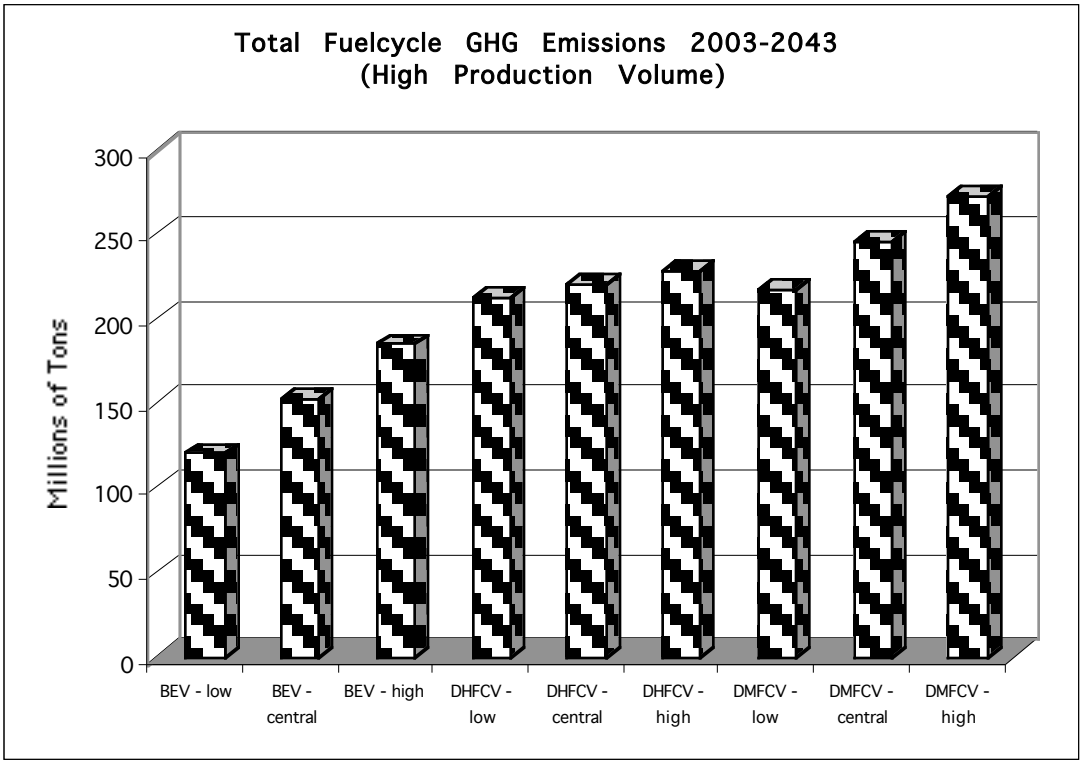

Figure 6-6 shows that fuelcycle GHG emissions are likely to be lowest for BEVs, followed by DHFCVs and DMFCVs. These differences are in part due to different fuelcycle GHG emissions for production of electricity, hydrogen, and methanol, and in part due to differences in the efficiencies of BEVs, DHFCVs, and DMFCVs. These emission estimates include GHG emissions from feedstock extraction and production; electricity, methanol, and hydrogen production and distribution for vehicle refueling; electricity production for hydrogen compression; and tailpipe CO_2 emissions from DMFCV operation. They do not include potential other sources of GHG emissions from vehicle operation, such as hydrofluorocarbon (HFC) emissions from leaking or damaged vehicle air conditioning systems.

Figures 6-7 through 6-10 show cost estimates for monetized emissions of criteria pollutants and GHGs.[48] These estimates were calculated in the Simulink model using triangular fuzzy-set distributions for in-basin and out-of-basin emission factors and in-basin and out-of-basin damage (or control cost) values. The criteria pollutant cost estimates are aggregates of costs for all five of the criteria pollutants assessed. Also, the net present values of the cost streams were calculated using a discount rate of 3.65%. The sensitivity of results to the choice of a discount rate is discussed in Chapter 7.

---

[48] Figures 6-7 to 6-10 can be interpreted by realizing that the larger the value of the membership function $\mu(x)$, the more likely is the corresponding NPV estimate. Hence, the most likely value occurs at $\mu(x) = 1$. As the value of $\mu(x)$ declines to either side, the likelihood of the NPVs decline until $\mu(x) = 0$. See Appendix A for definitions of fuzzy sets, the relationship between fuzzy sets and probability distributions, and a discussion of fuzzy set mathematics.

Figure 6-7:

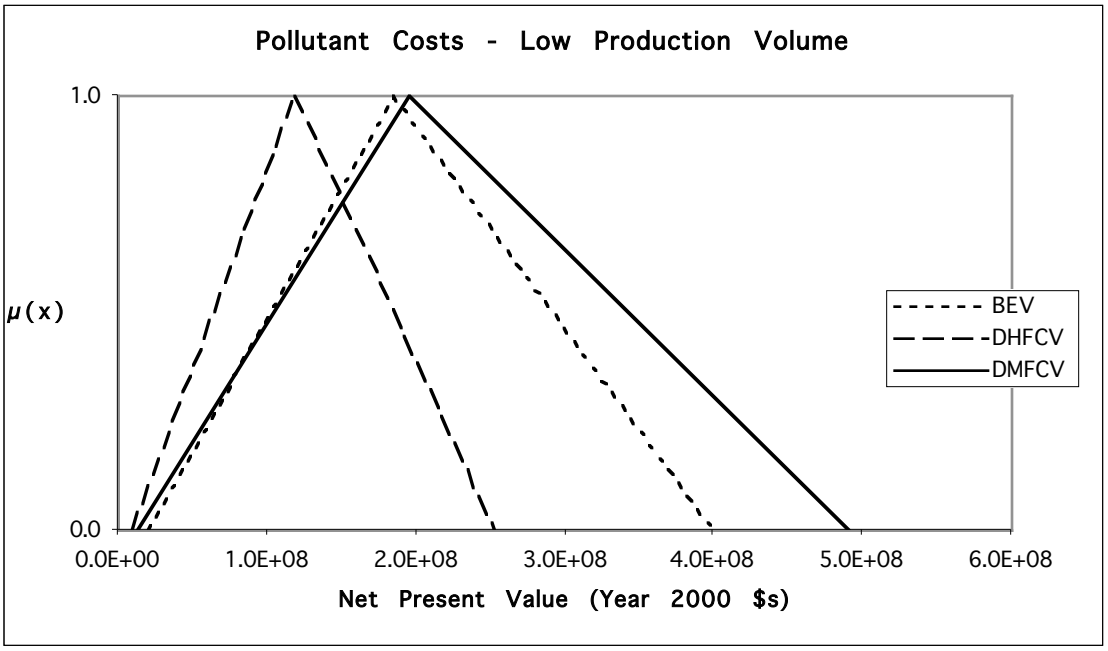

Figure 6-8:

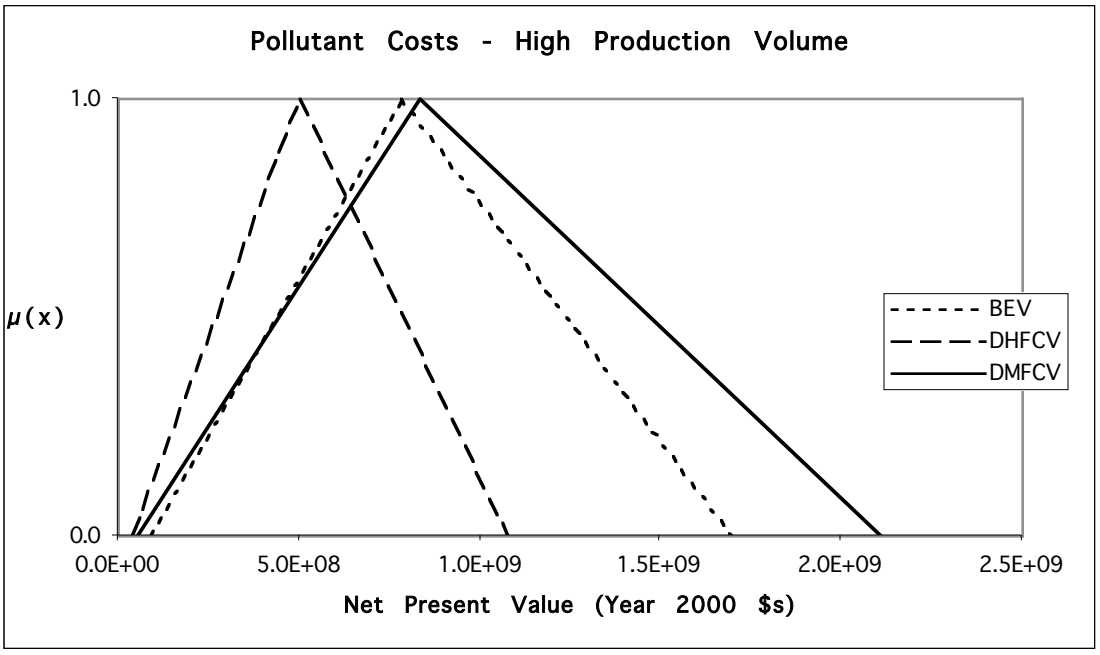

Figures 6-7 and 6-8 show that the aggregate net present value of criteria pollutant costs is lowest for DHFCVs, with somewhat higher costs for BEVs and DMFCVs. The net present value of costs for BEVs is slightly lower than for DMFCVs in the central cost case, and considerably lower in the high cost case. There is more than an order of magnitude of difference between the low cost and high cost cases for all three ZEV types. This shows that, given the

parameters used in this analysis, there is significant uncertainty with regard to the costs associated with fuelcycle emissions for these vehicle types.

Figure 6-9:

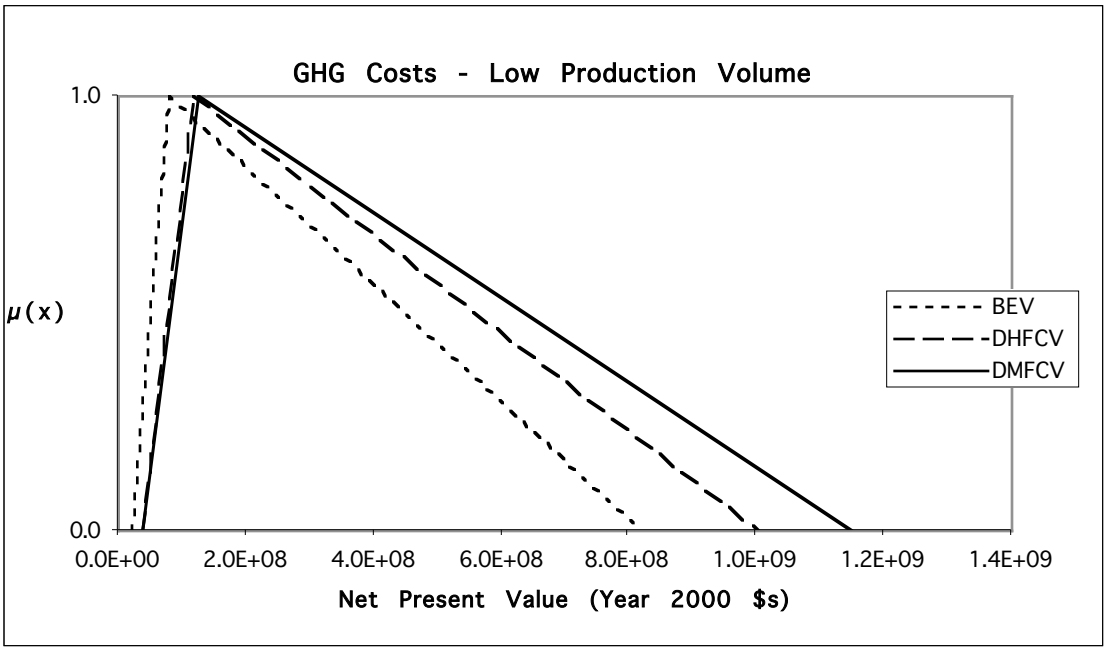

Figure 6-10:

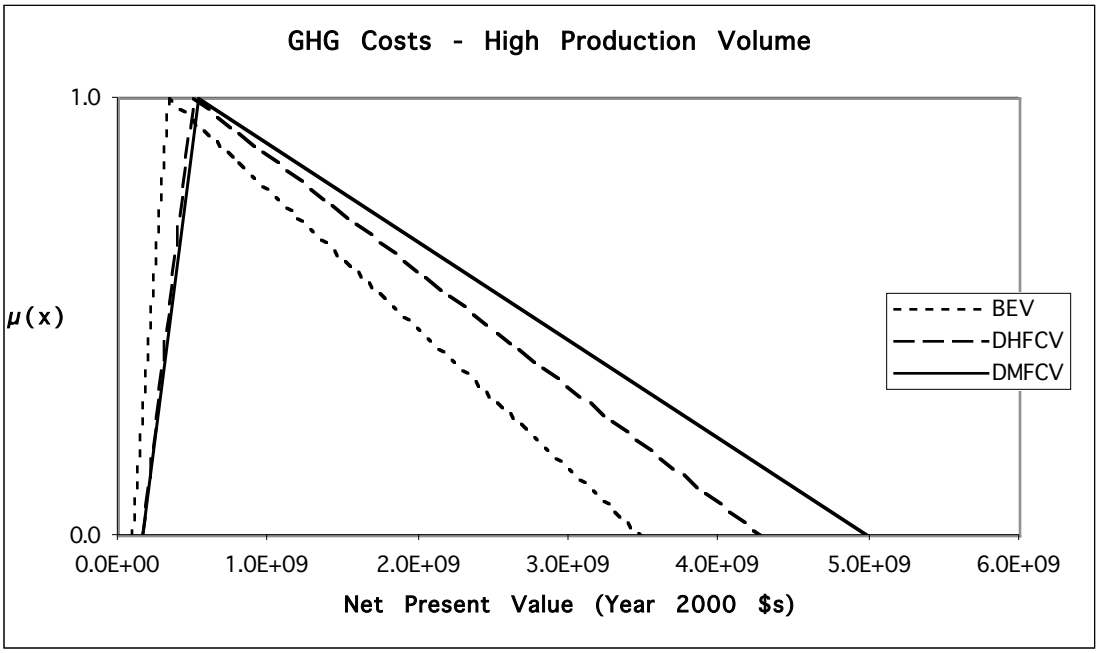

Figures 6-9 and 6-10 show that the net present value of monetized GHG emissions is comparable for all three ZEV types. BEVs have the lowest net present value of costs, followed by DHFCVs and then closely by DMFCVs. Once again, there is more than an order of magnitude of difference between the low

cost and high cost cases for each ZEV type. Table 6-11 presents these same results in tabular form.

Tables and Large Figures for Chapter 6

Table 6-1: Marginal Powerplant Emission Factors Associated with EV Charging in the SCAB (g/kWh)

Study	NMOG	CO	NOx	PM_{10}	SOx
Austin and Caretto (1995):					
2001 total	0.053	0.29	0.68	0.16	0.61
CARB (1996):					
2010 in-basin	0.008	N.E.	0.05[a]	N.E.	N.E.
2010 total	0.026	N.E.	0.46	N.E.	N.E.
Hwang et al. (1994):					
2001 in-basin	0.011	0.027	-0.054[b]	0.022	0.004
2001 total	0.012	0.054	0.58	0.028	0.31
2010 in-basin	0.016	0.06	0.04	0.027	0.003
2010 total	0.013	0.06	0.42	0.028	0.28
Rau et al. (1996) SCE[c]:					
2010 low EV, CC	0.018	0.14	0.39	0.032	0.005
2010 high EV, CC	0.018	0.13	0.37	0.032	0.005
2010 low EV, CT	0.018	0.14	0.40	0.032	0.005
2010 high EV, CT	0.018	0.15	0.41	0.032	0.005
Rau et al. (1996) LADWP[c]:					
2010 low EV, CC	0.014	0.32	0.69	0.023	0.005
2010 high EV, CC	0.014	0.29	0.61	0.027	0.005
2010 low EV, CT	0.005	0.33	0.97	0.014	0.005
2010 high EV, CT	0.009	0.31	0.91	0.018	0.005
Acurex (1996) 80% off-peak:					
2010 in-basin (49.0% energy)	0.008	0.043	0.048	N.E.	N.E.
2010 in CA (21.7% energy)	0.012	0.045	0.053	N.E.	N.E.
2010 in U.S. (29.3% energy)	0.003	0.006	0.309	N.E.	N.E.
2010 other (0.02% energy)	0.000	0.000	0.001	N.E.	N.E.
2010 total (100% energy)	0.023	0.094	0.411	N.E.	N.E.
Acurex (1996) 95% off-peak:					
2010 in-basin (57.7% energy)	0.012	0.041	0.041	N.E.	N.E.
2010 in CA (17.9% energy)	0.011	0.042	0.063	N.E.	N.E.
2010 in U.S. (24.4% energy)	0.003	0.007	0.298	N.E.	N.E.
2010 other (0.03% energy)	0.000	0.000	0.001	N.E.	N.E.
2010 total (100% energy)	0.026	0.090	0.403	N.E.	N.E.

Notes: CO = carbon monoxide; N.E. = not est.; NMOG = non-methane organic gases; NOx = oxides of nitrogen; PM_{10} = particulate matter less than 10 microns in diameter; SOx = oxides of sulfur.

[a] These emissions are assumed to be zero under the cap and trade RECLAIM program.

[b] Emissions are negative because the incremental EV demand causes retrofits to be made that lower emissions, relative to the base case.

[c] These are marginal emissions under unconstrained recharging. CC refers to the case in which generating capacity is added with a combined cycle utility plant, and CT refers to the case in which generating capacity is added with a combustion turbine utility plant. Emission factors were converted from lb/MWh to g/kWh.

Table 6-2: Combustion, Upstream, and Total Emission Factors for EV Recharging in the SCAB (g/kWh)

	Energy Fraction	NMOG	CO	NOx	PM_{10}	SOx
Combustion Emissions:						
Hwang et al. (1994) in-basin 2000-2010 avg.	0.55	0.016	0.056	0.029	0.026	0.004
Hwang et al. (1994) out-of-basin:						
CA 2000-2010 avg.	0.147	0.004	0.054	0.239	0.012	0.004
Northwest 2000-2010 avg.	0.106	0.007	0.052	0.815	0.031	0.842
Southwest 2000-2010 avg.	0.202	0.019	0.128	2.229	0.054	1.288
Out-of-basin weighted avg.	0.45	0.010	0.070	1.110	0.029	0.661
Adjusted Rau et al. (1996) in-basin 2010:						
Combined cycle added	0.55	0.020	0.171	0.169	0.002	0.00008
Combustion turbine added	0.55	0.017	0.174	0.200	0.002	0.00008
Adjusted Rau et al. (1996) out-of-basin 2010:						
Combined cycle added	0.45	0.013	0.214	0.846	0.063	0.011
Combustion turbine added	0.45	0.011	0.217	1.000	0.057	0.011
Upstream Emissions:						
Calculated from Delucchi (1997)						
Low case	N.A.	0.032	0.138	0.233	0.024	0.069
Central case	N.A.	0.043	0.181	0.308	0.028	0.089
High case	N.A.	0.055	0.223	0.384	0.032	0.109
Total Emissions:						
Modeled in-basin:[a]						
Low case	0.55	0.009	0.031	0.016	0.001[b]	0.000
Central case	0.55	0.010	0.073	0.073	0.006[b]	0.001
High case	0.55	0.011	0.096	0.110	0.014[b]	0.002
Modeled out-of-basin:[a]						
Low case	0.45	0.036	0.170	0.614	0.037	0.074
Central case	0.45	0.048	0.256	0.752	0.050	0.191
High case	0.45	0.061	0.321	0.884	0.060	0.407
Total in-basin + out-of-basin						
Low case	N.A.	0.045	0.093	0.630	0.038[b]	0.074
Central case	N.A.	0.058	0.222	0.825	0.056[b]	0.192
High case	N.A.	0.072	0.289	0.994	0.074[b]	0.409

Notes: CO = carbon monoxide; N.E. = not estimated; NMOG = non-methane organic gases; NOx = oxides of nitrogen; PM_{10} = particulate matter <10 microns in diameter; SOx = oxides of sulfur.

[a] These emission factors are weighted by the in-basin/out-of-basin energy fraction. The upstream emissions were added to the out-of-basin factors, assuming that all upstream emissions occur out of the SCAB. Each kWh of delivered electricity should thus have applied both an in-basin and out-of-basin factor to calculate total emissions, or the total in-basin + out-of-basin factors can be used.

[b] Estimates do not include emissions from road dust and tire and brake wear.

Table 6-3: GHG Emissions from BEV Recharging in the SCAB

Fuel Mix Year/Case	Marginal Fuel Mix[a]	Emission Factor Year	GHGs[b] (grams CO_2-eq per kWh)
1998	27%C/63%NG/10%O	2015	659
1999	30%C/59%NG/11%O	2015	669
2000	24%C/66%NG/10%O	2015	643
2001	19%C/79%NG/2%O	2015	659
2002	17%C/81%NG/2%O	2015	649
2003	32%C/66%NG/2%O	2015	728
2004	22%C/68%NG/10%O	2015	633
2005	24%C/64%NG/12%O	2015	633
2006	19%C/44%NG/37%O	2015	473
2007	19%C/49%NG/32%O	2015	500
2008	20%C/72%NG/8%O	2015	633
2009	19%C/73%NG/8%O	2015	627
2010	20%C/69%NG/11%O	2015	617
Low Case	19%C/44%NG/37%O	2015	473
Central Case	Avg. case	2015	601
High Case	32%C/66%NG/2%O	2015	728
Delucchi (1997) "West Region"	56%C/11%F/33%NG	2015	917[d]

Notes: C = coal-fired powerplant; CO_2-eq = carbon dioxide equivalents; F = fuel oil-fired powerplant; GHGs = greenhouse gases; NG = natural gas-fired powerplant; O = other fuel powerplant.

[a] Fuel mixes are from Hwang et al. (1994). Other fuel powerplant sources are wind, solar, hydro, and/or geothermal plants. These are assumed to contribute to total GHG emissions only through emissions of N_2O from corona discharges during distribution through power lines, and not through any upstream contributions.

[b] These estimates include distribution losses (8% loss) and contributions from nitrous oxide emissions from powerline corona discharges. Thus, they are grams CO_2-eq per kWh from the power plug.

[c] Emission factors are from Delucchi (1997). They are 1,096 g-CO_2-eq/kWh for coal-fired powerplants and 570 g-CO_2-eq/kWh for natural gas-fired powerplants.

[d] Emissions were back-calculated from g/mile to g/kWh using the estimate in Delucchi (1997) of 0.293 kWh/mile for BEV efficiency.

Table 6-4: Fuelcycle Emissions for Hydrogen Produced by Small-Scale Steam Reformation of Natural Gas (g/MMBTU of H2 (LHV) delivered)

	GHGs (gCO_2-eq)	NMOG	CO	NOx	PM_{10}	SOx
Natural Gas Production:						
Acurex (1996b) - 1992	1,299[a]	(0.3) 4.8	(0.0) 0.0	(0.0) 0.0	N.E.	N.E.
Acurex (1996b) – 2010	1,296[a]	(0.0) 5.1	(0.0) 0.0	(0.0) 0.0	N.E.	N.E.
Delucchi (1997)[b]	15,831	12.7	28.6	34.9	1.6	1.6
Thomas et al. (1998a)	19,451[c]	27.1	19.7	63.6	N.E.	N.E.
Natural Gas Distribution:						
Acurex (1996b) - 1992	[16,543][a]	(9.8) 15.6	(1.0) 5.6	(1.8) 24.4	N.E.	N.E.
Acurex (1996b) – 2010	[20,014][a]	(9.5) 15.8	(1.1) 6.7	(1.7) 20.4	N.E.	N.E.
Delucchi (1997)[b]	[4,221]	[0.0]	[17.5]	[28.6]	[3.2]	[1.6]
Hydrogen Production:						
Thomas et al. (1998a)[d]		(0.0295)	(0.0215)	(0.0074)	N.E.	N.E.
Author estimate	(85,919)[e]					
Hydrogen Compression:[f]						
In-basin:						
Low case	(16,771)[g]	(0.31)	(1.09)	(0.56)	(0.04)	(0.00)
Central case	(21,273)[g]	(0.35)	(2.60)	(2.59)	(0.20)	(0.03)
High case	(25,775)[g]	(0.40)	(3.38)	(3.89)	(0.51)	(0.08)
Out-of-basin:						
Low case		1.27	6.02	21.74	1.30	2.62
Central case		1.72	9.07	26.63	1.77	6.78
High case		2.16	11.36	31.30	2.12	14.40
Total Emissions:						
Modeled in-basin:						
Low case	(122,742)[g]	(0.34)	(1.11)	(0.57)	(0.04)[h]	(0.00)
Central case	(127,244)[g]	(9.88)	(3.72)	(4.29)	(0.20)[h]	(0.03)
High case	(131,746)[g]	(9.93)	(4.50)	(5.60)	(0.51)[h]	(0.08)
Modeled out-of-basin:						
Low case		14.0	12.7	42.1	6.06	5.80
Central case		22.6	28.8	82.0	6.54	9.96
High case		29.3	57.4	95.0	6.89	17.58

Notes: CO = carbon monoxide; GHGs = greenhouse gases; N.E. = not estimated; NMOG = non-methane organic gases; NOx = oxides of nitrogen; PM_{10} = particulate matter less than 10 microns in diameter; SOx = oxides of sulfur. Values in parentheses are in-basin emissions. Values in brackets are mostly out-of-basin but may contain an in-basin component. All others are out-of-basin.

[a] Emission values include CO_2 and CH_4 only. Grams of CH_4 converted to grams of CO_2-equivalents using a weighting value of 22.

[b]Converted from g/MMBTU of CH_4 to g/MMBTU of H_2 using conversion efficiency estimate of 1.588 MMBTU of CH_4 to produce 1 MMBTU of H_2, calculated from small-scale SMR efficiency of 0.18 MMBTU CH_4 to produce 1 kg of H_2 (Thomas et al., 1998a).

[c]Based on earlier (1991) Delucchi value.

[d]Data originally from International Fuel Cells Corporation.

[e]Assumes 9.4% of fuel is burned and 90.6% is chemically reacted in small-scale SMRs, based on data in Thomas et al. (1998a).

[f]Values were calculated using a hydrogen compression requirement of 35.42 kWh of electricity for each MMBTU of hydrogen – see text for details.

[g]Some GHG emissions occur out-of-basin, but since GHG damages do not depend on the location of emission, out-of-basin emissions are included in the in-basin estimates.

[h]Estimates do not include emissions from road dust and tire and brake wear.

Table 6-5: Fuelcycle Emissions for Methanol Produced by Steam Reformation of Natural Gas (g/MMBTU of methanol (LHV) delivered)

	GHGs (gCO_2-eq)	NMOG	CO	NOx	PM_{10}	SOx
Feedstock Extraction, Production, and Distribution:						
Acurex (1996b) - 1992	4,677[a]	17.9	0.5	1.1	N.E.	N.E.
Acurex (1996b) – 2010[b]	4,454[a]	17.1	0.5	1.1	N.E.	N.E.
Delucchi (1997)	10,708	6	33	44	2	2
Methanol Production:						
Acurex (1996b) -1992	32,059[a]	39.2	7.9	24.1	N.E.	N.E.
Acurex (1996b) – 2010[b]	19,956[a]	39.2	6.3	15.1	N.E.	N.E.
Delucchi (1997)	11,999	0	6	43	0	2
Methanol Distribution, Storage, and Delivery						
Acurex (1996b) - 1992	[394][a]	(8.3) 0.5	(0.05) 0.1	(0.35) 7.4	N.E.	N.E.
Acurex (1996b) - 2010[b]	[3,232][a]	(6.7) 3.7	(1.3) 0.9	(1.4) 63.1	N.E.	N.E.
Delucchi (1997)	[5,196]	[5]	[14]	[35]	[7]	[21]
Vehicle Emissions:						
Author Estimate[c]	(72,530)					
Thomas (1998a)		(10.53)[d]				
Total Emissions:						
Modeled in-basin:						
Low case	(90,000)[e]	(5.0)	(0.05)	(0.35)	(0.5)[f]	(1.4)
Central case	(100,433)[e]	(6.7)	(1.3)	(1.4)	(0.7)[f]	(2.1)
High case	(110,000)[e]	(8.3)	(1.4)	(3.5)	(1.4)[f]	(4.2)
Modeled out-of-basin:						
Low case		6.5	6.6	23.6	7.6	20.8
Central case		60.0	7.7	79.3	8.3	22.9
High case		62.1	53.0	122.0	8.5	23.6

Notes: CO = carbon monoxide; GHGs = greenhouse gases; N.E. = not estimated; NMOG = non-methane organic gases; NOx = oxides of nitrogen; PM_{10} = particulate matter less than 10 microns in diameter; SOx = oxides of sulfur. Values in parentheses are in-basin emissions. Values in brackets are mostly out-of-basin but may contain an in-basin component. All others are out-of-basin.

[a] Emission values include CO_2 and CH_4 only. Grams of CH_4 converted to grams of CO_2-equivalents using a weighting value of 22.

[b]These values assume that methanol is produced via a combined steam reforming and partial oxidation process (i.e., 50% SMR and 50% partial oxidation) and also that 50% of the production is in Indonesia and 50% is in Canada, versus 100% Canada for the 1992 values.

[c]Calculated assuming all of the carbon in the methanol is emitted as CO_2.

[d]Converted from an evaporative emissions estimate of 0.6 g/gallon, using 57,000 BTU/gallon (LHV). This estimate accounts for the relatively low photoreactivity of methanol, so it is a reactivity-weighted emission factor. These emissions would need to be controlled in order for DMFCVs to earn ZEV credits, so they are assumed to be zero for this analysis.

[e]Some GHG emissions occur out-of-basin, but since GHG damages do not depend on the location of emission, out-of-basin emissions are included in the in-basin estimates.

[f]Estimates do not include emissions of road dust and from tire and brake wear.

Table 6-6: Damage and Control Cost Values for Criteria Pollutants ($/ton per year)

Source/Location	Type	NMOG	CO	NOx	PM_{10}	SOx
CEC (1992) South Coast ($1989)	Damage Control	6,911 18,900	3 9,300	14,483 26,400	47,620 5,500	7,425 19,800
CEC (1992) Ventura County ($1989)	Damage Control	286 21,100	0 I.A.	1,647 16,500	4,108 1,800	286 21,100
CEC (1992) Bay Area ($1989)	Damage Control	90 10,200	1 2,200	7,345 10,400	24,398 2,600	90 10,200
CEC (1992) San Diego ($1989)	Damage Control	98 17,500	1 1,100	5,559 18,300	14,228 1,000	98 17,500
CEC (1992) San Joaquin Valley ($1989)	Damage Control	3,711 9,100	0 3,200	6,473 9,100	3,762 5,200	3,711 9,100
CEC (1992) Sacramento Valley ($1989)	Damage Control	4,129 9,100	0 5,000	6,089 9,100	2,178 2,800	4,129 9,100
CEC (1992) North Coast ($1989)	Damage Control	467 3,500	0 I.A.	791 6,000	551 900	467 3,500
CEC (1992) N. Central Coast ($1989)	Damage Control	803 9,100	0 I.A.	1,959 9,100	2,867 900	803 9,100
CEC (1992) S. Central Coast ($1989)	Damage Control	286 9,100	0 I.A.	1,647 9,100	4,108 900	286 9,100
CEC (1992) Southwest Desert ($1989)	Damage Control	157 3,500	0 2,900	439 6,000	680 5,700	157 3,500
ECO Northwest (1987) – W. Oregon[a] ($1989)	Damage	N.E.	N.E.	839	1950	N.E.
EIA (1995a) – Nevada[b] ($1992)	Control	1,012	1,012	7,480	4,598	1,716
EIA (1995a) - Oregon[b] ($1992)	Control	N.E.	N.E.	3,500	3,000	0
EIA (1997) – CAAA, Title IV[c]	Control	N.E.	N.E.	N.E.	N.E.	113-322
McCubbin and Delucchi (1996) – Los Angeles[d] ($1991)	Damage	472 – 3,892	27 - 163	5,933 - 70,515	11,204 - 141,140	30,418 - 190,400
McCubbin and Delucchi (1996) – United States[d] ($1991)	Damage	91 – 898	9 - 82	998 - 14,705	544 - 13,726	2,540 - 20,502
PG&E – CA facilities[e] ($1996)	Control	4,236	N.E.	9,120	2,624	4,486
PG&E – Pacific NW[e] ($1996)	Control	0	N.E.	292	556	298
SCE – CA facilities[e] ($1992)	Control	22,462	N.E.	31,448	6,804	23,490
Small and Kazimi (1995) – South Coast ($1992)	Damage	2,920	N.E.	10,670	N.E.	109,900
Wang and Santini (1994) - Chicago[f] ($1994)	Damage Control	2,700 8,150	N.E. 2,440	5,380 7,990	10,840 4,660	3,600 9,120
Wang and Santini (1994) – Houston[f] ($1994)	Damage Control	3,540 15,160	N.E. 2,680	6,890 17,150	5,190 2,780	2,910 3,590

Notes: CAAA = Clean Air Act Amendments of 1990: CO = carbon monoxide; I.A. = district is in attainment; N.E. = not estimated; NMOG = non-methane organic gases; NOx = oxides of nitrogen; PG&E = Pacific Gas and Electric; PM_{10} = particulate matter less than 10 microns in diameter; SCE = Southern California Edison; SOx = oxides of sulfur. CEC (1992) values are from EIA (1995a).

[a] These values are reported in Wang and Santini (1994).

[b]These values were adopted by the states for use in state utility planning decisions.

[c]These values are based on experience by eastern and midwestern state utilities in meeting CAAA Title IV SOx regulations. The $322 per ton control cost is for using scrubbers, and the $113 per ton control cost is for modifying a plant to burn lower sulfur coal.

[d]These values were estimated by assuming a 10% decrease in motor vehicle emissions, and then estimating the resulting change in ambient air quality and reduction in damages. The values shown are the results when upstream emissions and road dust are included. The authors also calculate results excluding these emission sources, and the resulting damage values are higher than the ones shown. Values were converted from $/kg to $/ton using 907.2 kg/ton.

[e]These values, documented in EIA (1995a) are used by the utility in planning decisions for the region shown.

[f]These values were estimated through regression analysis of pollutant concentration and population levels in the region.

Table 6-7: Inflated and Modeled Values for Criteria Pollutants (2000$/ton per year)

Source/Location	NMOG	CO	NOx	PM_{10}	SOx
In-Basin:					
CEC (1992) South Coast	9,570	4	36,559[a]	65,944	10,282
McCubbin and Delucchi (1996) L.A.	1,147	105	N.E.	17,537	26,194
CEC (1992) Ventura	396	0	22,849[a]	5,689	396
In-Basin Modeled Values:					
Low Case	396	0	22,849[a]	5,689	396
Central Case	1,147	4	36,559[a]	17,537	10,282
High Case	9,570	105	36,559[a]	65,944	26,194
Out-of-Basin:					
CEC (1992) Sacramento Valley	5,718	0	8,432	3,016	5,718
CEC (1992) San Joaquin Valley	5,139	0	8,964	5,210	5,139
CEC (1992) S. Central Coast	396	0	2,281	5,689	396
CEC (1992) Southwest Desert	217	0	608	942	217
Wang and Santini (1994) Houston	4,218	0	8,210	6,184	3,467
ECO Northwest (1987) W. Oregon	N.E.	N.E.	1,162	2,700	N.E.
Out-of-Basin Modeled Values:					
Low Case	217	0	608	942	217
Central Case	3,138	0	4,943	3,957	2,988
High Case	5,718	0	8,964	6,184	5,718

Notes: I.A. = district is in attainment; N.E. = not estimated; PG&E = Pacific Gas and Electric; SCE = Southern California Edison. Values were inflated based on GDP implicit price deflator data from 1990-97, and assumed continued growth of 3% per year from 1998-2000. See text for details.

[a] These are control cost values because NOx emissions are strictly controlled in the SCAB under the RECLAIM program. All other values are damage cost based.

Table 6-8: Global Warming Potential (GWP) and Economic Damage Index (EDI) Values for GHGs (on a mass basis)

GWPs	**CH_4**	**N_2O**	**CFC-12**	**HFC-134a**	**CO**	**NMOG**	**NOx**
IPCC:[a]							
20-year horizon	56	280	6,400-6,800 (net) 6,000-6,800 (net) 7,800 (direct only)	3,400	7	31	30[b]
100-year horizon	21	310	6,600-6,800 (net) 6,200-7,100 (net) 8,100 (direct only)	1,300	3	11	7[b]
500-year horizon	6.5	170		420	2	6	2[b]
Martin/Michaelis (1992):[c]							
50-year horizon	26.5	270			3	8.8	3
Bruhl (1993):[d]							
50-year horizon	10-13						
100-year horizon	6-8						
EDIs							
Reilly (1992):[e]							
Linear damages	21	201	2,140		0.9		
Quadratic damages	74	208	7,309		2.9		
Quadratic damages + CO_2 fertilization	92	260	9,119		3.7		
Hammitt et al. (1996):[f]							
Middle case	11.0	354.8	9,067				
Damage exponent = 1	27.21	354.7	9,279				
Damage exponent = 3	5.10	340.1	8,527				
'Hockey stick' damages	6.07	319.4	7,910				
Low climate sensitivity	10.03	353.4	9,028				
High sensitivity	12.33	356.6	9,142				
Discount rate = 1%/yr.	3.73	322.2	7,950				
Discount rate = 5%/yr.	23.70	366.2	9,596				
IS92c emission/GDP	22.16	345.2	8,934				
IS92e emission/GDP	8.01	399.2	10,272				
Emission year 2005	6.78	364.0	9,423				
Emission year 2015	3.96	373.5	9,779				
Minimum	49.69	296.7	7,286				
Maximum	2.92	403.6	10,507				
Tol (1999):[g]							
1995-2004 emissions	14	348					
Used in Delucchi (1997) and Delucchi and Lipman (1997)	22	355	7,435	2,000	2	3.7/1.5	-3

Notes: CFC = chlorofluorocarbon; CH_4 = methane; CO = carbon monoxide; CO_2 = carbon dioxide; HFC = hydrofluorocarbon; NMOG = non-methane organic gases; NOx = oxides of nitrogen; N_2O = nitrous oxide.

[a] The results for CH_4, N_2O, CFC-12, and HFC-134a are from IPCC (1996a).

CH_4: The estimate includes the indirect effects of tropospheric O_3 production and stratospheric water vapor production.

CFC-12: The first range shows the net GWPs that result from varying, from the minimum to the maximum value, the relative efficiency of bromine and chlorine in removing ozone, other parameters held constant. The second range shows the net GWPs that result from varying the magnitude of cooling in the lower stratosphere. The third line shows the GWP due to the direct radiative forcing effect only. In calculating these values, Daniel et al. (1995) (reported in IPCC, 1996a) assumed that O_3-depleting gases can be compared in a globally averaged sense, that future CO_2 levels are constant, and that indirect effects for each gas depend linearly on its contribution to chlorine or bromine release in the stratosphere.

CO, NMHCs, NO_X: These estimates, from the 1990 IPCC report (Shine, et al., 1990) are preliminary estimates of total direct-plus-indirect GWPs. The IPCC has essentially disavowed these earlier estimates of total GWPs, on the grounds that it is not yet possible to estimate indirect effects accurately for these relatively short-lived and poorly mixed gases.

[b]The GWPs originally published in Shine et al. (1990) were: 150, 40, and 14, for the 20-, 100-, and 500-year time horizons. However, those values were in incorrect due to an error in the calculation of O_3 inventory changes (Johnson, et al., 1992). The corrected values are shown here (for emissions of NO_X at earth's surface) (Johnson, et al., 1992).

[c]The results for the 50-year time horizon are from modeling done by Harwell Laboratories of the Energy Technology Support Unit (ETSU) in Great Britain (Martin and Michaelis, 1992). The ETSU work appears to improve upon the early IPCC work in some respects: it re-estimates the global-warming effect of ground level O_3; it accounts for the effects of CO, NMHCs, and NO_X emissions on CH_4 concentrations; and it distinguishes between emissions of NO_X at ground level and emissions at higher levels.

[d]Bruhl (1993) modeled GWPs under two scenarios, one in which emissions increase over time, and another in which the concentration and lifetime of CH_4 is fixed. The former yields higher GWPs, because increasing concentrations of CH_4 (in the face of a relatively constant amount of the scavenger, OH) result in a longer average lifetime for CH_4. Bruhl explains that his estimate of the indirect GWP of CH_4 is lower than the IPCC's estimate of the indirect effect because the IPCC probably overestimated the production of O_3 due to CH_4.

[e]Reilly (1992) bases his estimates on a highly simplified model of greenhouse gas atmospheric behavior. He assumes that a doubling of trace gas concentrations would cause a welfare loss of $38 billion in the agricultural sector, and that damages to all economic sectors would be six times the agricultural-sector losses. Reilly further assumes that the agricultural damages would be double the amount shown if it were not for the beneficial effect of carbon fertilization. Estimates are shown for three cases: i) economic damages rise linearly with trace gas concentrations; ii) economic damages rise as a quadratic function with trace gas concentrations, and iii) economic damages rise as a quadratic function with trace gas concentrations but CO_2 fertilization causes linear benefits with CO_2 concentration.

[f]Hammitt et al. (1996) base their EDI calculations on a simple climate model, the Integrated Science Assessment Model, and calculate several different indices by varying their climate change and economic damage assumptions. Shown first is the index for the 'middle case', which assumes a 3%/yr. discount rate, a damage function exponent of 2, a 2.5 °C temperature rise with a doubling in trace gas concentrations, the IS92a emission scenario, and an emission year of 1995. Other cases vary one of these assumptions while keeping the others constant. The 'hockey stick' damage function is a function that can be varied from a quadratic damage function to a very convex 'catastrophic' type function -- the one assessed here is quite convex (see Hammitt et al. [1996] for details). The 'minimum' and 'maximum' indices are the high and low values for 81 different combinations of input assumptions. The EDIs do not include the indirect effect of CH_4 or halocarbons on H_2O or O_3, or the effects of CO_2 fertilization.

gTol's estimates are based on runs of the FUND model, version 1.6. He assumes an IS92a emission scenario, emissions between 1995 and 2004, a time horizon until 2100, and a 3% discount rate (Tol, 1999).

Table 6-9: GHG Marginal Damage Cost Estimates – Net Present Values Discounted to Period of Emission (1990$/tC except where noted)

Source	Type[a]	1991-2000	2001-2010	2011-2020	2021-2030
Marginal Damage Estimates:[b]					
Nordhaus - 1991	MC		7.3 (0.3-65.9)[c]		
Ayers and Walter - 1991	MC		30-35		
Nordhaus –1994	BCA	5.3 (12.0)[d]	6.8 (18.0)[d]	8.6 (26.5)[d]	10.0 (N.E.)[d]
Cline - 1992	BCA	5.8-124	7.6-154	9.8-186	11.8-221
Peck and Teisberg - 1994	BCA	10-12	12-14	14-18	18-22
Fankhauser - 1995	MC	20.3 (6.2-45.2)[c]	22.8 (7.4-52.9)[c]	25.3 (8.3-58.4)[c]	27.8 (9.2-64.2)[c]
Maddison - 1995		5.9	8.1	11.1	14.7
	MC	6.1	8.4	11.5	15.2
Tol (1999) – 5% discount rate	MC	11 [317, 171, 60, 26, 6][e]	13 [311, 157, 48, 18, 3][e]	15	18
Values Used for State Utility Planning:[f] ($1992/ton-$CO_2$)					
EIA (1995a) – California		9			
EIA (1995a) – Massachusetts		24			
EIA (1995a) – Minnesota		9.8			
EIA (1995a) – Nevada		24			
EIA (1995a) – New York		1			
EIA (1995a) – Oregon		25			
EIA (1995a) – Wisconsin		15			
Modeled Values:					
Low Case		1.81 (2000$/t$CO_2$) [5.00 (1990$/tC), 6.63 (2000$/tC)]			
Central Case		5.43 (2000$/t$CO_2$) [15.00 (1990$/tC), 19.89 (2000$/tC)]			
High Case		45.21 (2000$/t$CO_2$) [125.00 (1990$/tC), 165.77 (2000$/tC)]			

Notes: BCA = benefit cost analysis; CO_2 = carbon dioxide; GHG = greenhouse gas; MC = marginal cost analysis; N.E. = not estimated.

[a] Estimates derived through marginal cost analyses are based on slight perturbations to a baseline; estimates derived through BCA are shadow values.

[b] Estimates are as reported in an IPCC review by Pearce et al. (1996) and in Tol (1999).

[c] Estimates in parentheses are 90% confidence interval.

[d] Estimates in parentheses are expected values with assumed variable probability distributions, estimates outside parentheses are "best-guess" estimates that assume that all underlying variables assume their central positions.

[e] Values in brackets are with equity-weighting (see text) and for discount rates of 0%, 1%, 3%, 5%, and 10%. The values reported for emissions from 1991-2000 are actually for 1995-2004, and those for 2001-2010 are for 2005-2014.

[f] Note that estimates are $/ton-$CO_2$, not ton-C, and in $1992.

Table 6-10: Total Fuelcycle Emissions of Criteria Pollutants -- 2003-2043 (Tons)

	NMOG	NOx	CO	PM_{10}	SOx
BEVs:					
Low Production Volume					
Low Case	(522)	(927)	(1,797)	(58)	(0)
	2,086	35,585	9,853	2,144	4,289
Central Case	(580)	(4,231)	(4,231)	(348)	(58)
	2,782	43,583	14,837	2,898	11,070
High Case	(638)	(6,375)	(5,564)	(811)	(116)
	3,535	51,233	18,604	3,477	23,588
High Production Volume					
Low Case	(2,296)	(4,082)	(7,910)	(255)	(0)
	9,186	156,665	43,376	9,441	18,881
Central Case	(2,552)	(18,626)	(18,626)	(1,531)	(255)
	12,247	191,876	65,320	12,758	48,735
High Case	(2,807)	(28,067)	(24,495)	(3,572)	(510)
	15,564	225,557	81,905	15,309	103,848
DHFCVs:					
Low Production Volume					
Low Case	(134)	(225)	(437)	(16)	(0)
	5,515	22,334	5,003	2,387	2,285
Central Case	(3,892)	(1,690)	(1,465)	(79)	(12)
	8,902	27,022	11,344	2,576	3,923
High Case	(3,911)	(2,206)	(1,773)	(201)	(32)
	11,541	37,421	22,610	2,714	6,925
High Production Volume					
Low Case	(590)	(990)	(1927)	(69)	(0)
	24,305	98,437	22,049	10,521	10,069
Central Case	(17,153)	(7,448)	(6,458)	(347)	(52)
	39,236	119,097	50,000	11,354	17,292
High Case	(17,240)	(9,722)	(7,812)	(885)	(139)
	50,868	164,930	99,652	11,962	30,521
DMFCVs:[a]					
Low Production Volume					
Low Case	(2,490)	(356)	(391)	(250)	(667)
	3,524	18,512	5,157	4,060	10,789
Central Case	(3,312)	(1,531)	(1,483)	(405)	(1,013)
	(29,165)	46,693	6,699	4,548	13,174
High Case	(4,086)	(2,970)	(1,803)	(833)	(2,025)
	30,320	68,606	29,059	4,761	16,063
High Production Volume					
Low Case	(11,440)	(1,423)	(1,365)	(1,148)	(3,101)
	15,855	7,7125	21,500	18,332	49,069
Central Case	(15,246)	(6,056)	(5,834)	(1,793)	(4,692)
	134,848	20,6091	27,417	20,409	58,456
High Case	(18,830)	(12,205)	(6,986)	(3,668)	(9,384)
	140,026	30,6017	13,0391	21,257	68,748

Notes: In-basin emissions are in parentheses, out-of-basin emissions are not in parentheses.

[a] Emissions estimates include emissions from BEVs introduced from 2003-2010, prior to DMFCV introduction in 2011.

Table 6-11: Total Net Present Values of Pollutant Costs for Fleetwide Emissions from 2003 to 2043 (2000$)

	Criteria Pollutants	GHGs
BEVs:		
Low Production Volume		
Low Case	$20,039,012	$21,262,329
Central Case	$184,586,390	$81,048,583
High Case	$399,444,696	$817,404,479
High Production Volume		
Low Case	$85,149,838	$90,347,961
Central Case	$784,345,103	$344,391,911
High Case	$1,697,321,735	$3,473,317,842
DHFCVs:		
Low Production Volume		
Low Case	$8,257,177	$37,447,045
Central Case	$118,684,530	$116,461,645
High Case	$253,068,791	$1,003,963,033
High Production Volume		
Low Case	$35,126,838	$159,303,384
Central Case	$504,739,512	$495,439,208
High Case	$1,074,299,105	$4,270,956,766
DMFCVs:[a]		
Low Production Volume		
Low Case	$13,193,792	$36,071,699
Central Case	$195,052,547	$123,547,905
High Case	$490,480,531	$1,148,773,411
High Production Volume		
Low Case	$53,758,923	$157,899,724
Central Case	$831,137,656	$538,137,206
High Case	$2,111,071,971	$4,982,920,837

Notes: Net present values were calculated with a 3.65% discount rate.

[a] Cost estimates include costs associated with emissions from BEVs introduced from 2003-2010, prior to DMFCV introduction in 2011.

Chapter 7:
Analysis and Conclusions

> "They will have to realize that the era of their terrific progress and even more terrific income and wealth based on cheap oil is finished. They will have to find new sources of energy. Eventually they will have to tighten their belts; eventually all those children of well-to-do families who have plenty to eat at every meal, who have their cars, and who act almost as terrorists and throw bombs here and there, they will have to rethink all these aspects of the advanced industrial world. And they will have to work harder…"
>
> -- The Shah of Iran (1973) Quoted in Yergin (1991, p. 626)

Introduction

These portentous remarks, made by the Shah of Iran more than twenty-five years ago, have yet to prove true. The price of oil is much lower than predicted by experts in the mid-1980s (see Figure 7-1, below), and the price of gasoline in the U.S. is currently near a twenty-year low, in real terms (Davis, 1997). Meanwhile, the U.S. stock market is booming, with major indices near their all-time highs. Many young internet company workers, who five years ago took relatively low-paying jobs at startup firms, have suddenly found themselves to be millionaires as their stock options have been caught in an internet stock "feeding frenzy." The most popular vehicles in automobile showrooms are sport-utility vehicles, with low fuel economies and high profits for automakers. Light-duty truck sales have exceeded 40% of total light-duty vehicle sales since 1994, up from about 20% in the mid-1970s (Davis, 1998). In fact, as of 1998, light-duty trucks composed 44.5% of the light-duty fleet in the U.S. (NHTSA, 1998). As a result of this trend toward larger and heavier automobiles, the light-duty vehicles sold in the U.S. in 1996 and 1997 are on average less efficient than the vehicles sold in any year since 1980 (NHTSA, 1998). Therefore, for the first time in many years, the average new vehicle sold today is likely to be less efficient than the scrapped vehicle that it is replacing.

Figure 7-1:

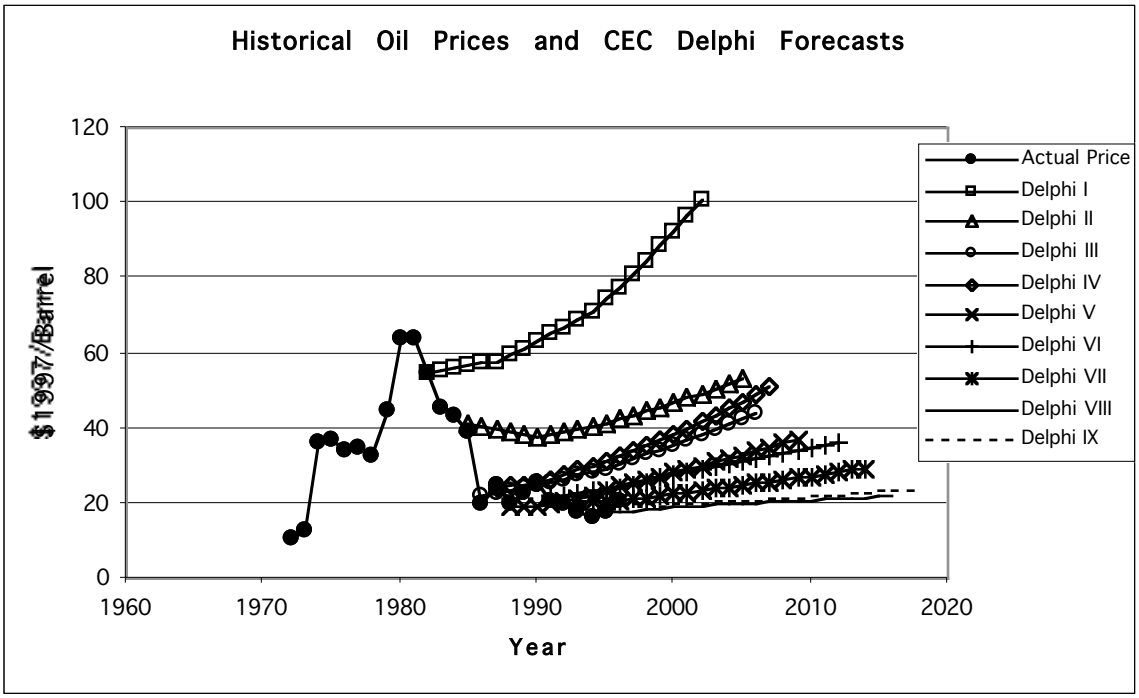

Source: (CEC, 1998)

Despite the recent prosperity felt by the "haves" in the U.S., however, there are indications that the Shah's warning may still be valid, and ultimately may prove true. There is still disagreement among experts as to the date when crude oil will become scarce. However, the 1.6 trillion remaining barrels of oil (discovered and undiscovered reserves), estimated in the last U.S. Geological Survey study in 1993 (U.S.G.S., 1998), would be used in about 60 years even at present worldwide consumption levels of about 70 million barrels per day (Davis, 1998). With forecast increases in demand, all of the crude oil that is economically and politically feasible to recover will likely be gone by about the middle of the next century. There are opportunities to fabricate gasoline-like fuels with "gas-to-liquids" processes, possibly for many more years, but the costs at which such fuels could be offered in the market are not yet well-established. Furthermore, urban air quality concerns remain an important transportation policy driver in the U.S., where millions of people live in counties with unhealthy air. And, while concern over climate change and the resulting potential impacts are lower in the U.S. than in Europe, as the largest emitter of GHGs the U.S. is likely to face increasing pressure from other countries to curb emissions.

Emerging EV technologies offer the potential to alleviate some of these concerns. Some of the top scholars and analysts in the transportation and energy fields feel that a transportation energy system based mainly on renewable fuel sources, and hydrogen and electricity as energy carriers, is ultimately the only way in which the nation's mobility needs can be met in a manner that is sustainable, environmentally benign, and climate stabilizing (Lovins and Williams, 1999; Ogden and Williams, 1989; Sperling and DeLuchi,

1989). There are several pathways by which EVs could help bridge the looming gap between today's fossil-fuel dominated transportation system and this utopian vision of the future. The key enabling technology may prove to be the fuel cell; an inherently clean and elegant type of device that is free from the Carnot efficiency limit that applies to all heat engines.

This transition, if it is to occur, will have substantial costs. But, as the following analysis suggests, once the initial costs of the transition have been absorbed, the lifecycle costs of owning and operating the EVs of the future may well be comparable to those of conventional vehicles. If externality values are considered as well, the total social costs associated with the use of some types of EVs, used in the SCAB and possibly other areas, may actually be lower than those for even low-emission conventional vehicles. The following sections compile and analyze the vehicle, infrastructure, and emission cost results estimated in the previous chapters, conduct further sensitivity analysis on key variables not included in the fuzzy-set based model, and discuss key policy and regulatory issues.

Fleetwide Results

With the fleet-level vehicle, infrastructure, and emissions costs calculated in Chapters 2 through 6, the relative costs of the BEV, DHFCV, and DMFCV scenarios can be compared. First, however, Figure 7-2 shows that for the BEV low production volume case, vehicle costs dominate infrastructure and emissions costs. Figure 7-3 shows the same data plotted on a logarithmic scale. This scale allows the cost estimates for infrastructure, criteria pollutants, and GHGs to be seen more clearly, although the uncertainty in the vehicle cost estimates tends to be concealed. Interestingly, infrastructure, criteria pollutant, and GHG related costs are all within about an order of magnitude for each ZEV type. Figures 7-3 through 7-8 show the fleet-level results for BEVs in the high production volume scenario, as well as the results for the DHFCV and DMFCV scenarios, also plotted on logarithmic scales.[49]

[49] Figures 7-2 to 7-14 can be interpreted by realizing that the larger the value of the membership function $\mu(x)$, the more likely is the corresponding NPV estimate. Hence, the most likely value occurs at $\mu(x) = 1$. As the value of $\mu(x)$ declines to either side, the likelihood of the NPVs decline until $\mu(x) = 0$. See Appendix A for definitions of fuzzy sets, the relationship between fuzzy sets and probability distributions, and a discussion of fuzzy set mathematics.

Figure 7-2:

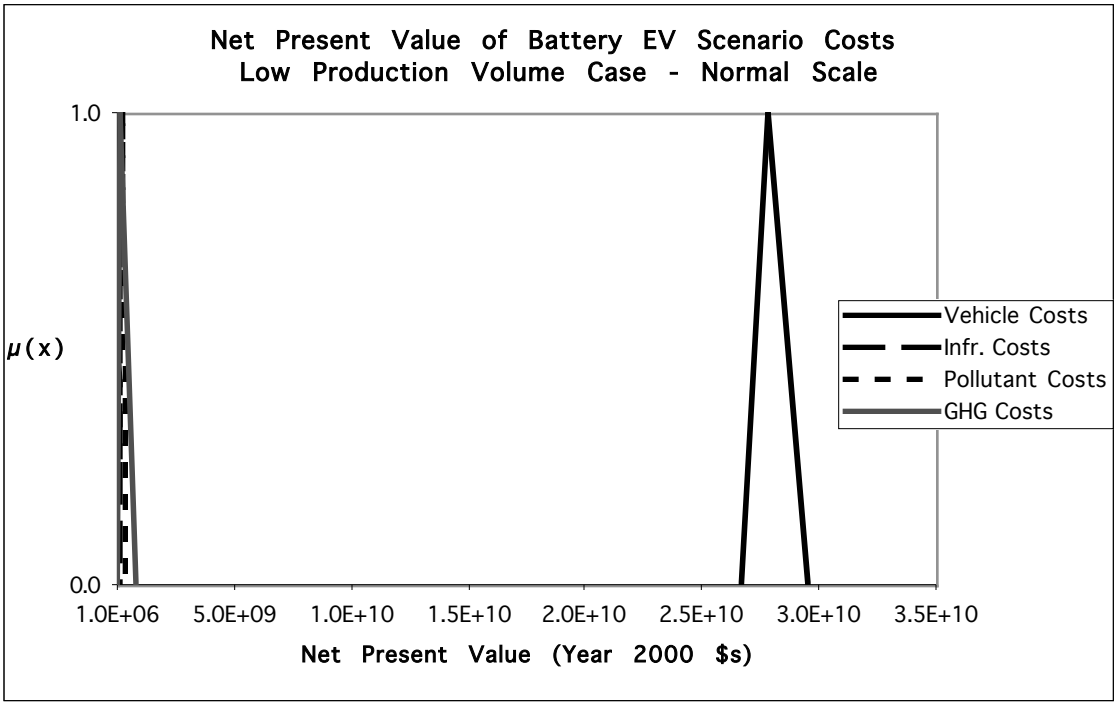

Figure 7-3:

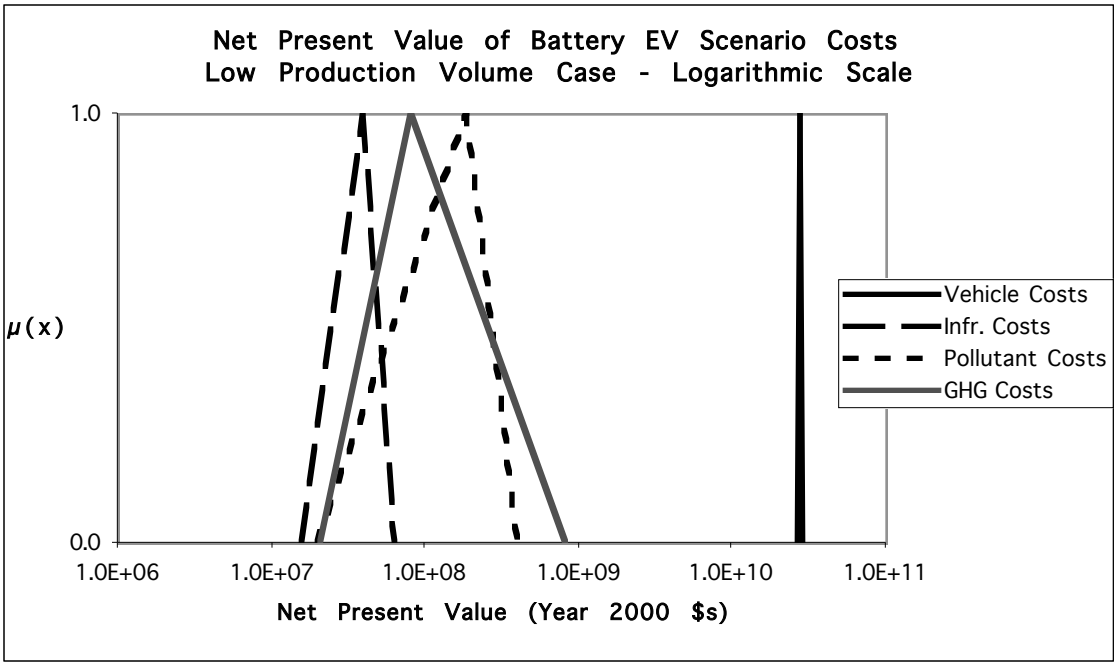

Figure 7-4:

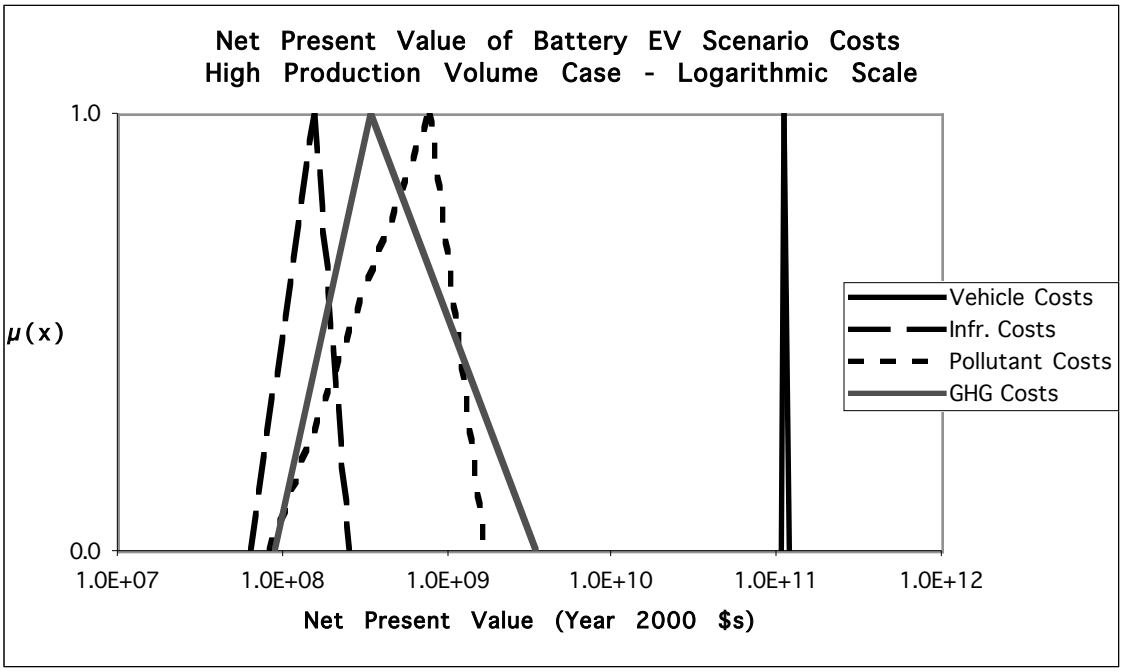

Figure 7-5:

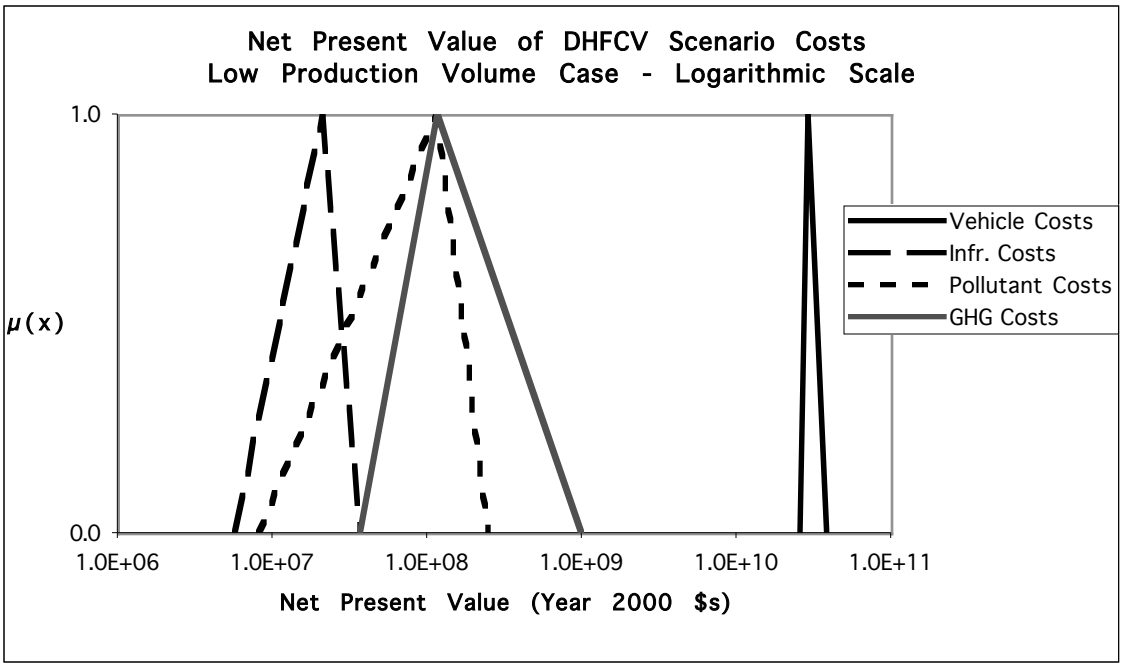

Figure 7-6:

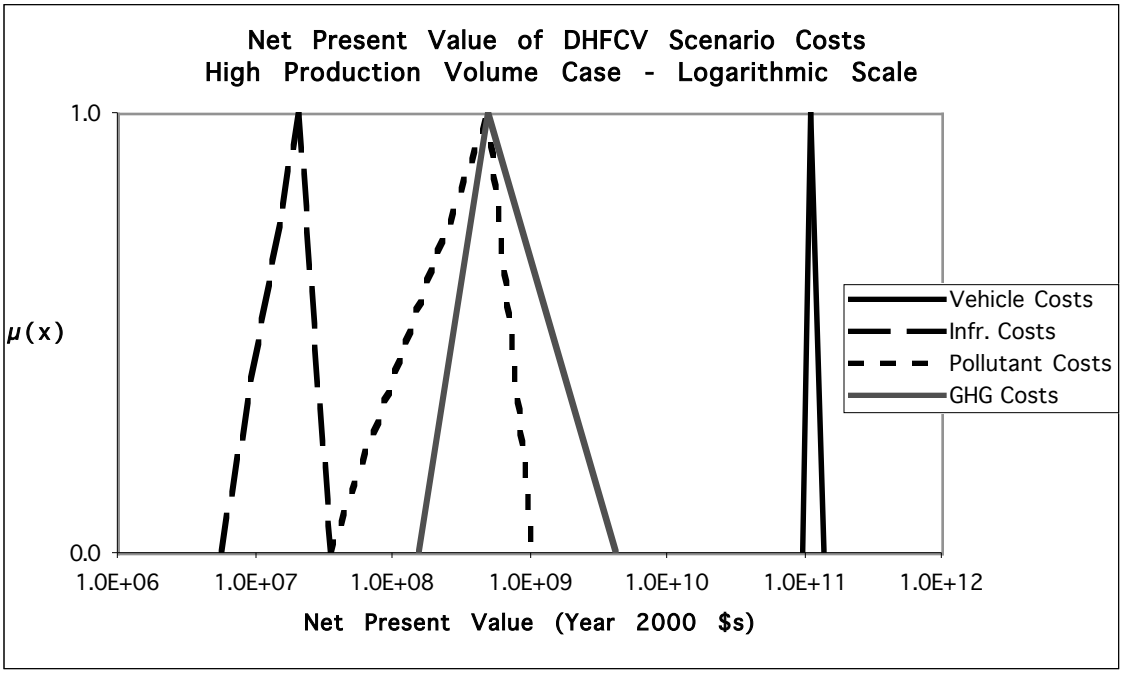

Figure 7-7:

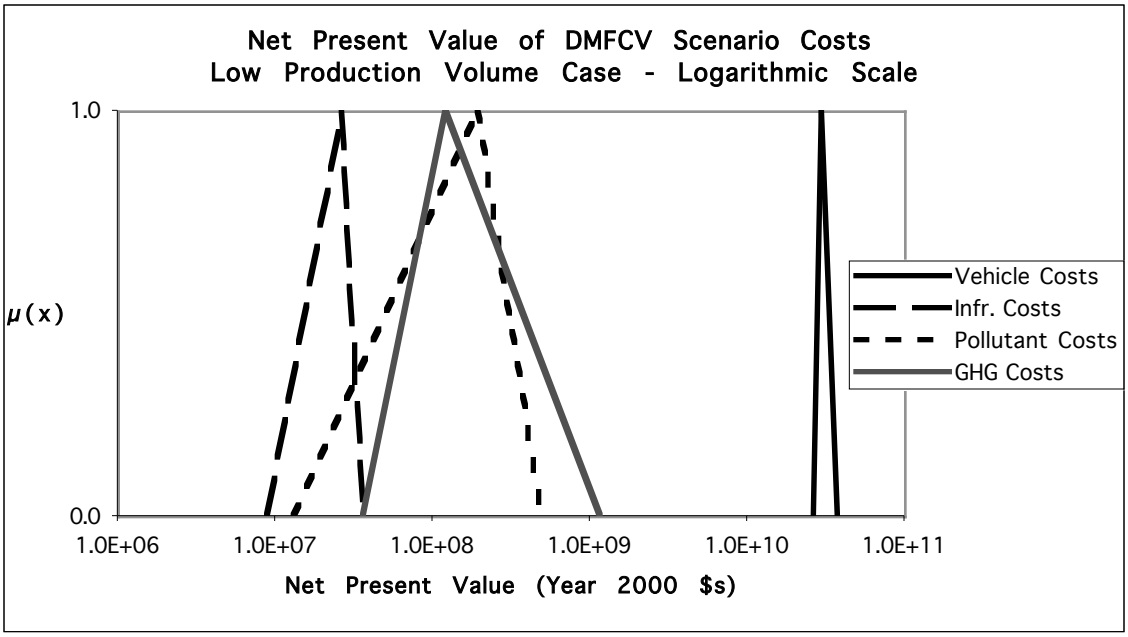

Figure 7-8:

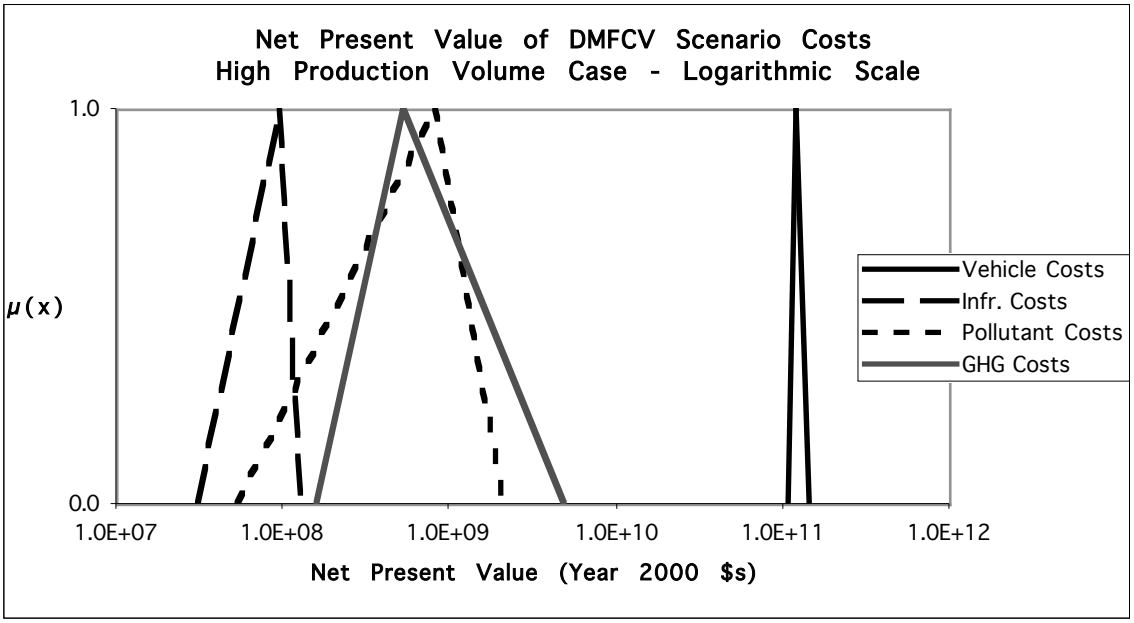

In order to put these scenario-level cost estimates in perspective, it is helpful to compare them with the costs of operating a conventional vehicle fleet. Assuming that a comparable conventional fleet of mid-sized gasoline ICEVs can be operated at a levelized cost of 39.68 cents per mile (i.e., the cost calculated with the Lotus 1-2-3 model for a $20,155 Taurus and with gasoline at $1.20 per gallon), the net present value of owning and operating costs for a fleet of ICEVs the same size as the low production volume fleet of ZEVs would be $22.2 billion (from 2003 to 2043, using a 3.65% discount rate). With an ICEV fleet size the same as that prescribed by the high production volume ZEV scenario, the net present value of vehicle owning and operating costs would be $94.8 billion (again using the same 3.65% discount rate as used to calculate the NPV estimates in Figures 7-3 through 7-8).

Thus, in the low production volume case, the NPV of BEV owning and operating costs is 20% higher than the cost of a comparable conventional vehicle case with low BEV costs, 25% higher with central BEV costs, and 33% higher with high BEV costs. In the high production volume scenario, the NPV of BEV owning and operating costs is 13% higher than for comparable ICEVs with low BEV costs, 19% higher with central BEV costs, and 25% higher with high BEV costs. For DHFCVs, the NPV of vehicle owning and operating costs with a low production volume fleet is 15% higher than for ICEVs with low DHFCV costs, 32% higher with central DHFCV costs, and 73% higher with high DHFCV costs. With a high production volume fleet, the relative costs of the DHFCV and ICEV fleets are 5% higher, 16% higher, and 45% higher, with low DHFCV costs, central DHFCV costs, and high DHFCV costs, respectively. Meanwhile, for DMFCVs (with BEVs as the "Gen1" 2003-2007 vehicles), the NPV of vehicle owning and operating costs with a low production volume fleet is 21% higher than for ICEVs with low DMFCV/BEV costs, 36% higher with central DMFCV/BEV costs, and 67% higher with high DMFCV/BEV costs. Finally, for DMFCVs in the high production volume scenario, the NPV of vehicle owning and operating costs is

14% higher than for ICEVs with low DMFCV/BEV costs, 25% higher with central DMFCV/BEV costs, and 51% higher with high DMFCV/BEV costs. Figures 7-9 and 7-10 present the scenario cost NPVs for the different vehicle types, with fleet sizes from the low and high production volume scenarios.

Figure 7-9: Relative Fleet NPVs for ICEVs and ZEVs – Low Prod. Volume

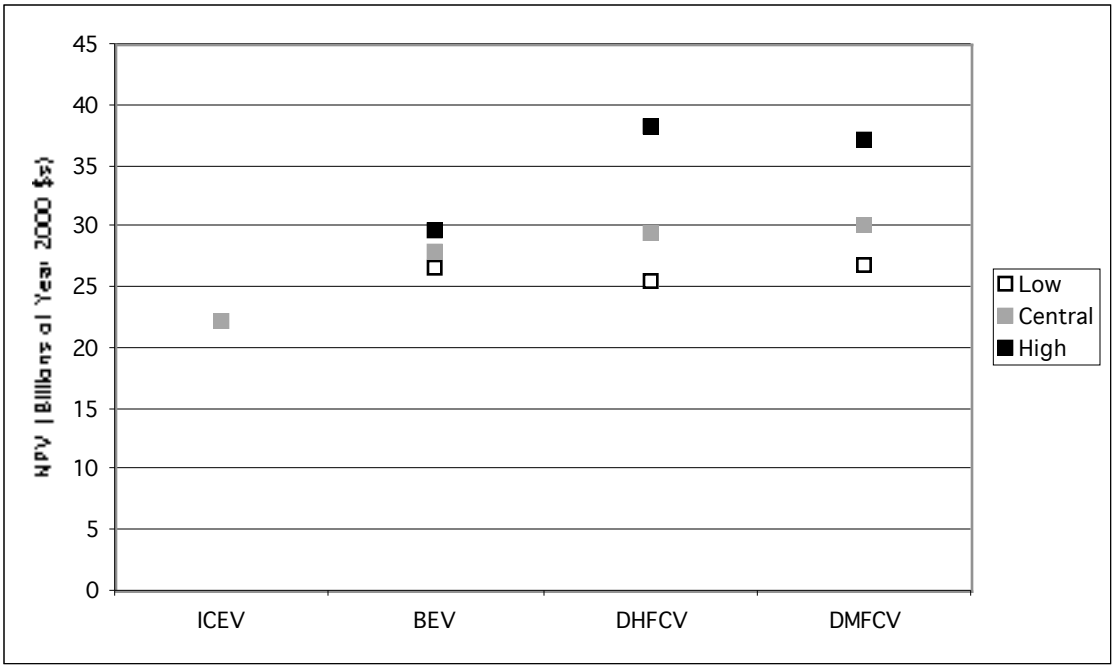

Figure 7-10: Relative Fleet NPVs for ICEVs and ZEVs – High Prod. Volume

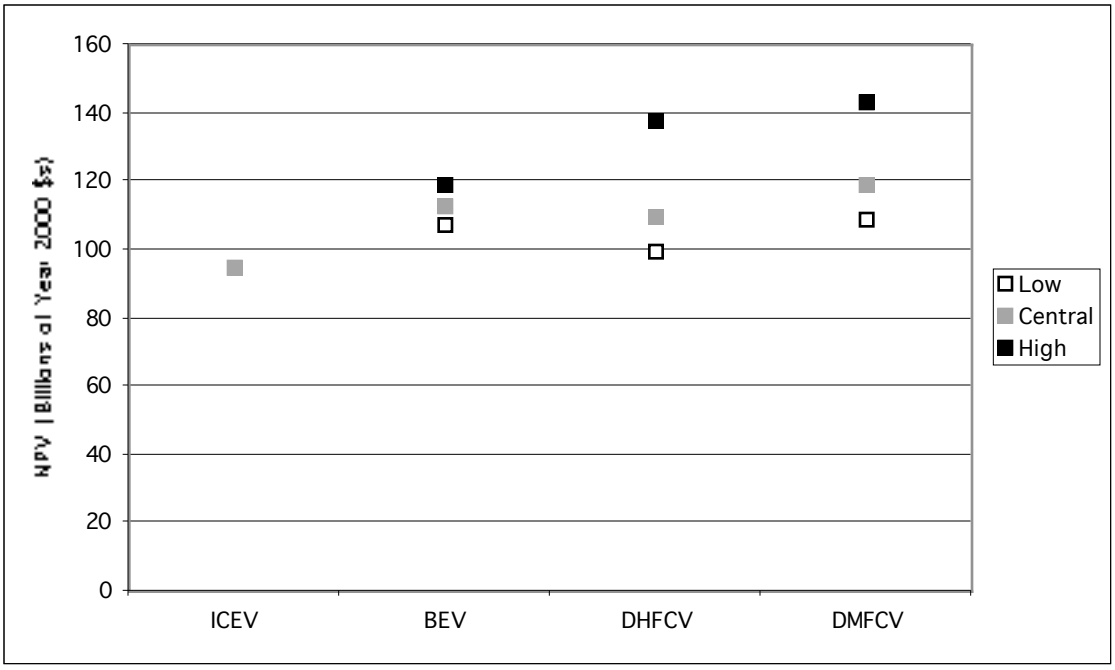

Fleetwide Comparisons of ZEV Types

In order to compare the relative costs associated with different ZEV types, as characterized by triangular fuzzy sets, it is necessary to determine the ranking order of the relevant triangular fuzzy set distributions. As discussed in Chapter 1, there are several different methods that have been developed for ranking TFNs. The various methods often produce consistent results, but sometimes where TFNs are very close together different methods will produce different ranking orders. For this reason, it is preferable to use more than one method when comparing TFNs. The following comparisons use Chang's method, comparison of the TFN modes, Kaufman and Gupta's ranking parameter, and MATLAB's "defuzz" command using the centroid and bisector methods.

Comparison of Vehicle Costs

Figures 7-11 and 7-12 compare the fleet-level vehicle lifecycle cost net present values for the three ZEV types in the low and high production volume scenarios. These figures show that scenario-wide BEV costs are generally lowest, except when only the central case is considered in the high production volume scenarios. DHFCV scenario costs are generally ranked second, followed by DMFCV costs.

Figure 7-11:

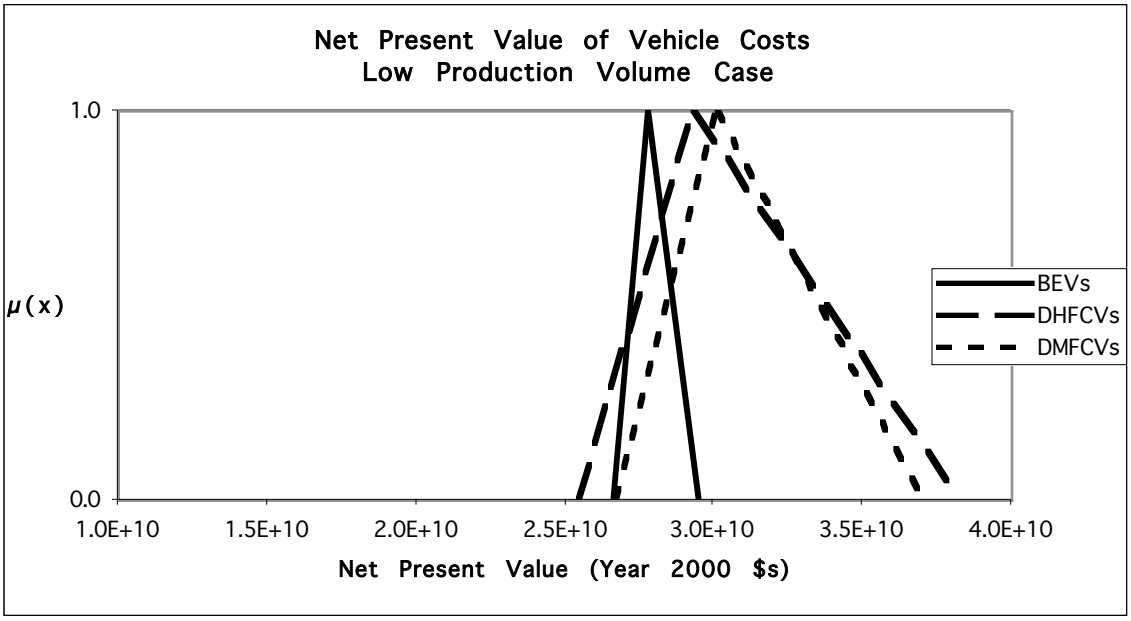

Chang's Method	BEV<DMFCV<DHFCV
TFN Modes	BEV<DHFCV<DMFCV
Kaufman and Gupta's Method	BEV<DHFCV<DMFCV
MATLAB Defuzz/Centroid Method	BEV<DHFCV<DMFCV
MATLAB Defuzz/Bisector Method	BEV<DHFCV<DMFCV

Figure 7-12:

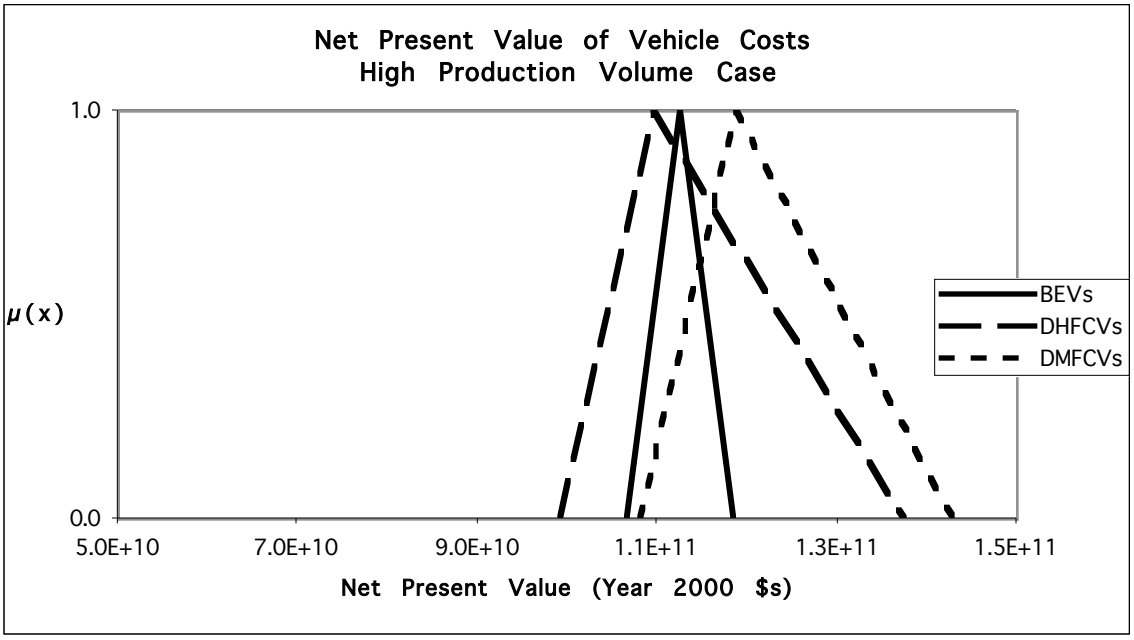

Chang's Method	BEV<DMFCV<DHFCV
TFN Modes	DHFCV<BEV<DMFCV
Kaufman and Gupta's Method	BEV<DHFCV<DMFCV
MATLAB Defuzz/Centroid Method	BEV<DHFCV<DMFCV
MATLAB Defuzz/Bisector Method	BEV<DHFCV<DMFCV

Comparison of Vehicle and Infrastructure Costs

Figures 7-13 and 7-14 compare the fleet-level net present values for the three ZEV types, when additional infrastructure support costs are included along with vehicle costs, in the low and high production volume scenarios. The inclusion of infrastructure costs does not have an effect on the ranking order for the different ZEV types, using the various defuzzification measures.

Figure 7-13:

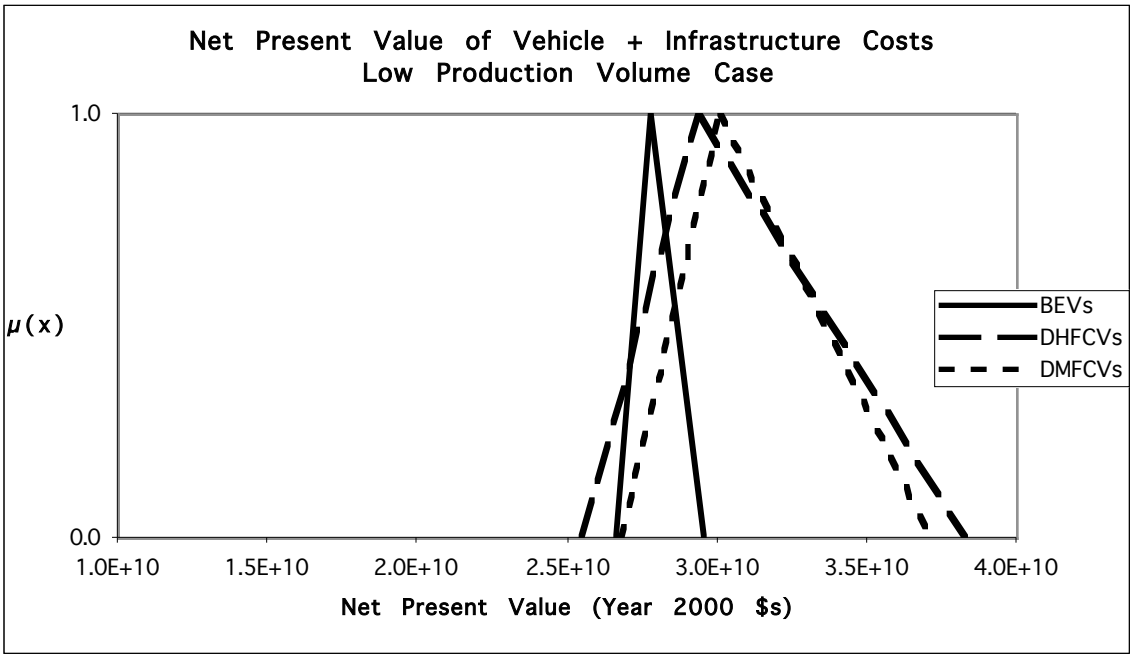

Chang's Method	BEV<DMFCV<DHFCV
TFN Modes	BEV<DHFCV<DMFCV
Kaufman and Gupta's Method	BEV<DHFCV<DMFCV
MATLAB Defuzz/Centroid Method	BEV<DHFCV<DMFCV
MATLAB Defuzz/Bisector Method	BEV<DHFCV<DMFCV

Figure 7-14

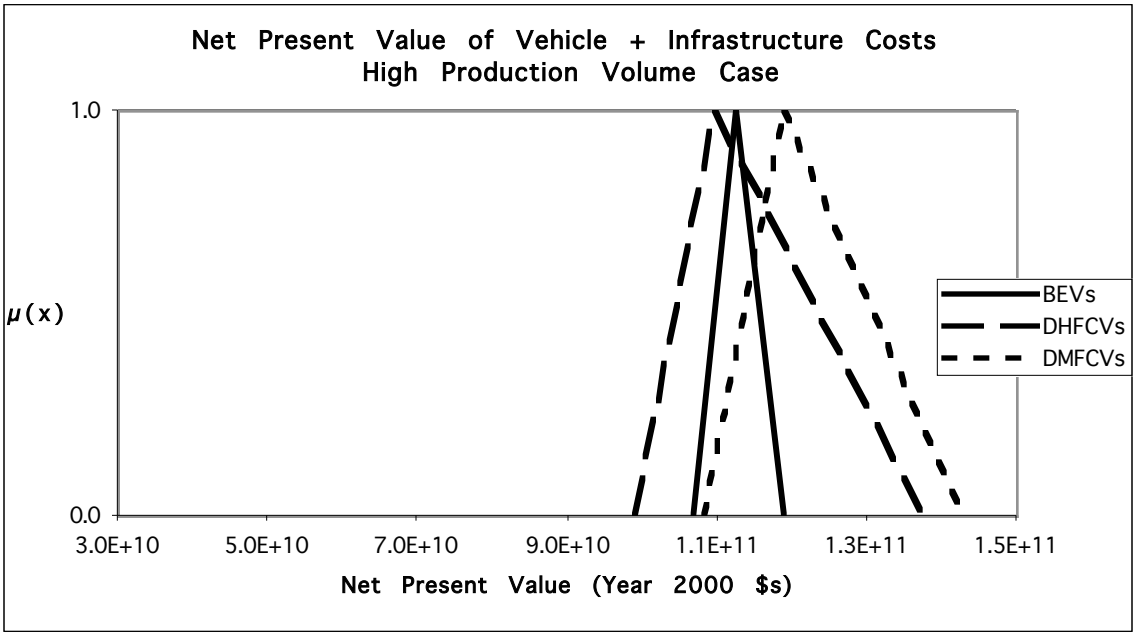

Chang's Method	BEV<DMFCV<DHFCV
TFN Modes	DHFCV<BEV<DMFCV
Kaufman and Gupta's Method	BEV<DHFCV<DMFCV
MATLAB Defuzz/Centroid Method	BEV<DHFCV<DMFCV
MATLAB Defuzz/Bisector Method	BEV<DHFCV<DMFCV

Comparison of Vehicle, Infrastructure, and Emission Costs

Figures 7-15 and 7-16 compare the fleet-level net present values for the three ZEV types, when additional infrastructure support costs and emission costs are included along with vehicle costs, in the low and high production volume scenarios. The rankings again remain relatively unchanged, although in the high production volume scenarios Chang's method now ranks the DHFCV scenario ahead of the DMFCV scenario, as do all of the other methods.

Figure 7-15:

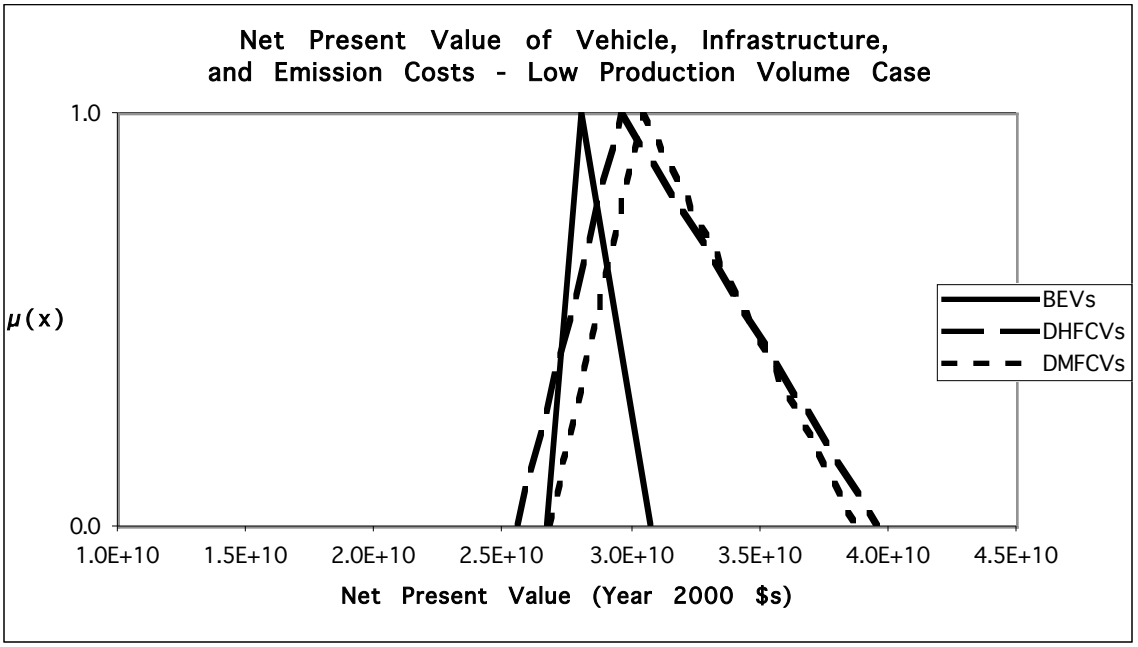

Chang's Method	BEV<DMFCV<DHFCV
TFN Modes	BEV<DHFCV<DMFCV
Kaufman and Gupta's Method	BEV<DHFCV<DMFCV
MATLAB Defuzz/Centroid Method	BEV<DHFCV<DMFCV
MATLAB Defuzz/Bisector Method	BEV<DHFCV<DMFCV

Figure 7-16:

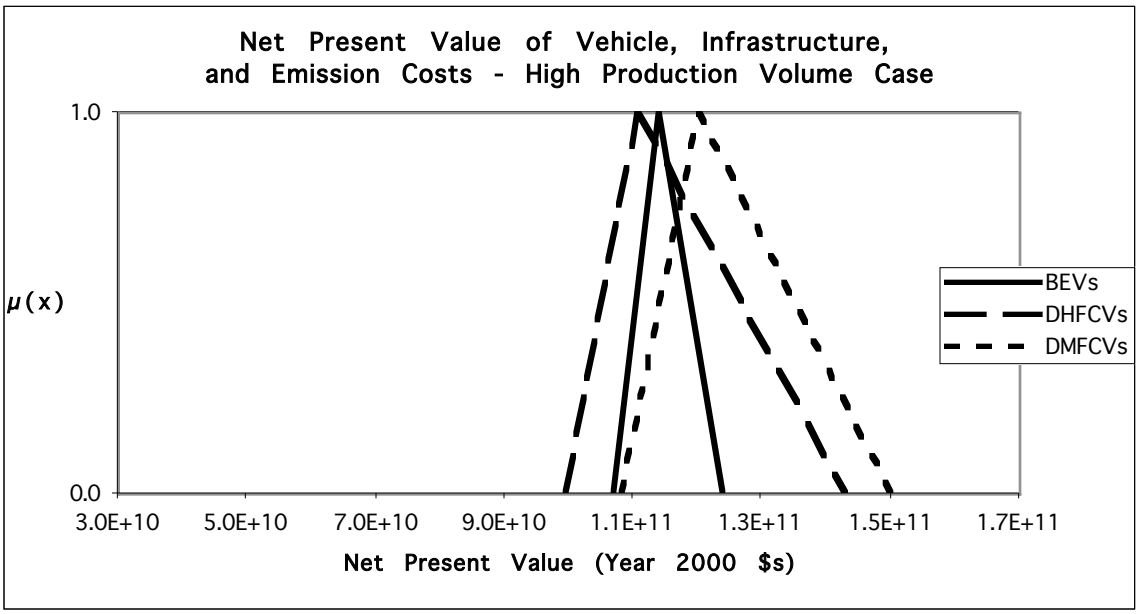

Chang's Method	BEV<DHFCV<DMFCV
TFN Modes	DHFCV<BEV<DMFCV
Kaufman and Gupta's Method	BEV<DHFCV<DMFCV
MATLAB Defuzz/Centroid Method	BEV<DHFCV<DMFCV
MATLAB Defuzz/Bisector Method	BEV<DHFCV<DMFCV

Once again, in order to put these total scenario NPV estimates in perspective, it is useful to compare them with the total vehicle plus emissions-related NPV estimates associated with the operation of comparable conventional ICEV fleets over the same time period. When emission-related costs are included for conventional vehicles (using the fuelcycle emissions estimates shown in Table 7-2 and the same ranges of in-basin and out-of-basin damage values as used for the ZEVs), and the total scenario NPV estimates are compared with vehicle plus emissions plus infrastructure costs for ZEVs, the differences between the discounted costs of operating ICEVs and ZEVs diminish relative to the discounted vehicle ownership and operation estimates presented above. For BEVs, total scenario NPVs in the low production volume scenario are 10% to 11% higher than for ICEVs in the low, central, and high cost cases. In the high production volume scenario, the NPVs for BEVs exceed those of ICEVs by only 4% to 5%. For DHFCVs, total scenario NPVs in the low production volume scenario are 6% higher, 16% higher, and 43% higher than the ICEV NPVs, in the low, central, and high cost cases. In the high production volume scenario, the low case NPV for the DHFCV scenario is actually 4% lower than for the ICEVs, 1% higher in the central case, and 21% higher in the high case. For the DMFCV low production volume scenario, the low, central, and high case NPVs are 11%, 19%, and 40% higher than the ICEV NPVs. Finally, in the DMFCV high production volume scenario, the scenario NPVs exceed those for ICEVs by 5%, 10%, and 27%, in the three cases. Figures 7-17 and 7-18 present these relative NPV estimates graphically.

Figure 7-17: Total Scenario NPVs for ICEVs and ZEVs – Low Prod. Volume

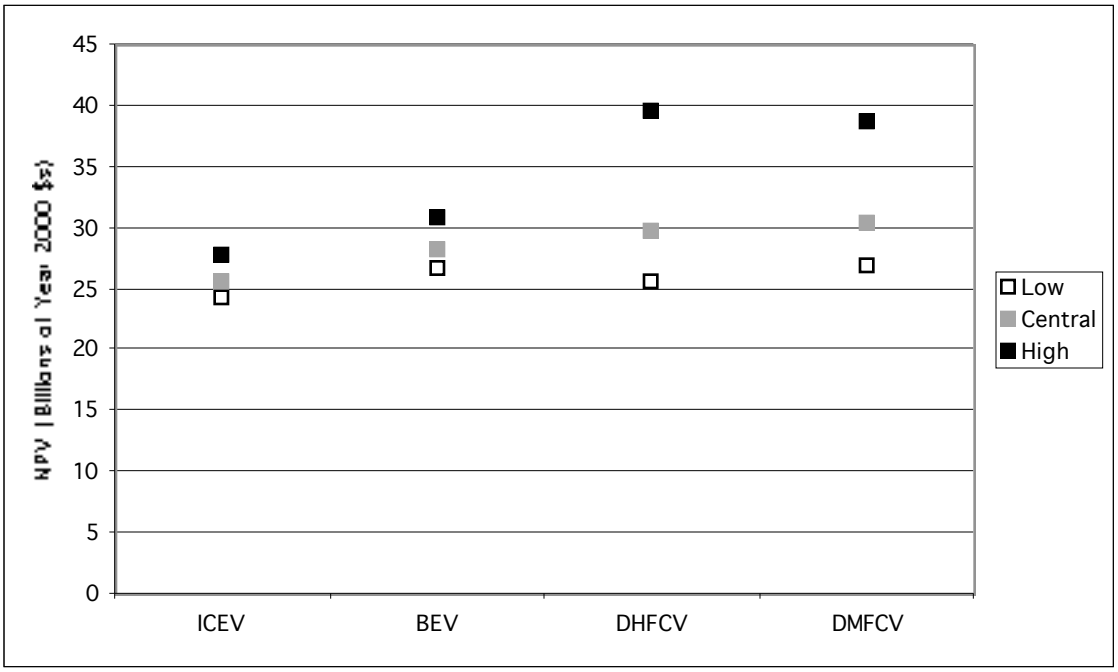

Figure 7-18: Total Scenario NPVs for ICEVs and ZEVs – High Prod. Volume

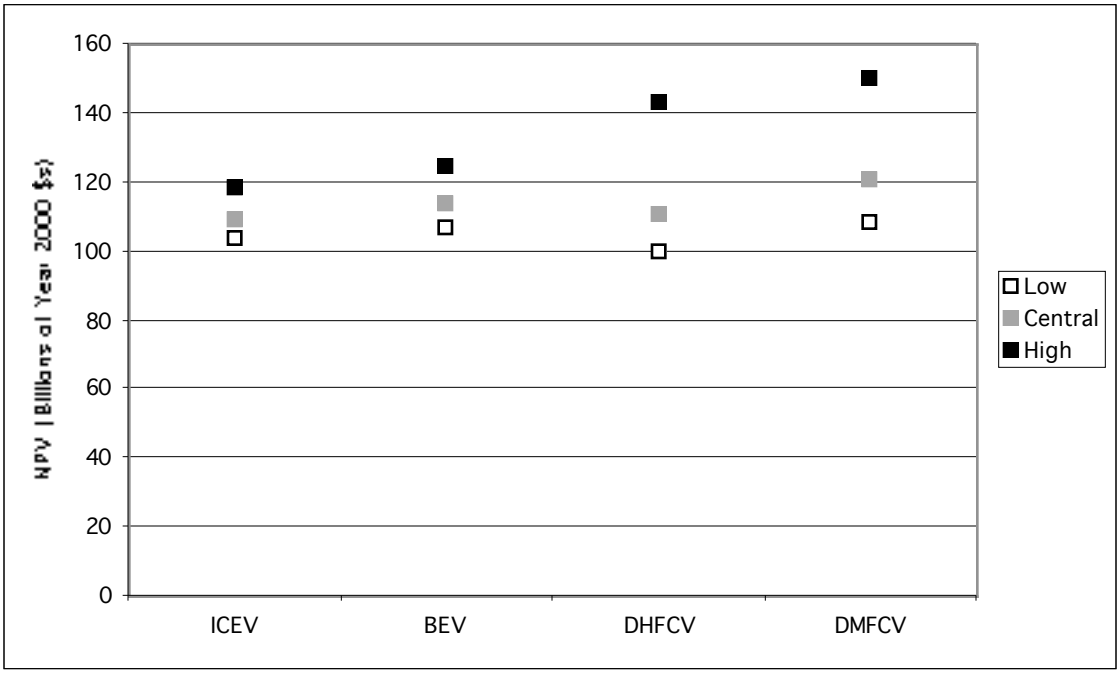

It is important to note that in all of these cases, the FCV scenarios are characterized by a greater level of uncertainty in the estimated NPV of scenario costs than are the BEV scenarios. This is principally due to the significant uncertainty in fuel cell system costs for FCVs. The high cost estimates for FCVs reflect a relatively pessimistic cost reduction rate for automotive fuel cell systems (characterized by an 85% MPF slope). While this potential for slow cost reduction cannot, in my opinion, be ruled out at this early stage of fuel cell system commercialization, it is also probably unlikely due to the fact that fuel cell systems appear to be amenable to automated production, and because the automobile industry is extremely adept at driving down costs through volume manufacturing techniques. As FCV commercialization proceeds, it will at least in principle be possible to narrow the uncertainties in fuel cell system costs. In all likelihood, this would improve the relative attractiveness of FCVs relative to BEVs, because the reduction in uncertainty would likely result in a lowering of the high case FCV cost estimates.

Hypothesis Tests

In Chapter 1, four hypotheses were proposed with regard to the potential relative costs of the three ZEV types. These hypotheses are assessed below, given the scenario cost results shown above in Figures 7-11 through 7-18, and the ZEV retail price and lifecycle cost results presented in Figures 7-19 through 7-22 (at end of chapter).

Hypothesis 1:

H_1: Lifecycle costs for BEVs are always lower than lifecycle costs for DHFCVs and DMFCVs, under comparable production volume assumptions.

H_{1a}: Lifecycle costs for DHFCVs and/or DMFCVs in some cases drop below those of BEVs, under comparable production volume assumptions.

DHFCV and DMFCV lifecycle costs ultimately reach lower levels than BEV lifecycle costs in both the low cost and central cost cases. Hence, Hypothesis 1 is rejected and the alternative hypothesis is accepted.

Hypothesis 2:

H_2: Under the high production volume scenarios, the purchase prices of BEVs, DHFCVs, and DMFCVs exceed those of comparable conventional vehicles in all cases.

H_{2a}: Under the high production volume scenarios, the purchase prices of BEVs, DHFCVs, and/or DMFCVs drop below those of comparable conventional vehicles in at least the low cost case.

At no time does the estimated purchase price for any of the ZEVs reach the $20,155 purchase price of the mid-sized (Taurus) conventional vehicle. Hence, Hypothesis 2 is not rejected.

Hypothesis 3:

H_3: In 2026, DMFCVs have higher initial prices and/or lifecycle costs than DHFCVs or BEVs.

H_{3a}: In 2026, DMFCVs have lower initial prices and lifecycle costs than DHFCVs and BEVs.

Only in the high cost case do the estimated purchase prices for DMFCVs exceed those for BEVs in 2026. In all other cases, the estimated purchase prices for DMFCVs are lower than for DHFCVs and for BEVs. However, the lifecycle costs for DMFCVs are higher than for DHFCVs in all cases, and only in the low cost cases and high production volume central cost case are lifecycle costs for DMFCVs lower than for BEVs. Hence, Hypothesis 3 is not rejected.

Hypothesis 4:

H_4: The net present value of vehicle, emissions, and infrastructure costs, over the time period 2003-2043, is lower for BEVs than for DHFCVs and DMFCVs.

H_{4a}: The net present value of vehicle, emissions, and infrastructure costs, over the time period 2003-2043, is lower for DHFCVs and/or DMFCVs than for BEVs.

For all five defuzzification measures in the low production volume case, and for four out of five measures in the high production volume case, the net present value of vehicle, emissions, and infrastructure costs for BEVs is lower than for the other ZEV types. However, in the high production volume central cost case, and in both the low and high production volume low cost cases, the net present value of costs for DHFCVs is lower than for BEVs. Hence, in certain cases, total vehicle, infrastructure, and emissions costs for BEVs exceed those for DHFCVs. But, in an overall sense, and within the context of the range of uncertainty in these costs estimated here, costs for BEVs are generally lower. Thus, Hypothesis 4 is not rejected.

Comparisons with Conventional Vehicles

The primary focus of this analysis has been to compare the relative vehicle, infrastructure, and emissions-related costs associated with three types of ZEVs that are owned and operated in the SCAB. However, it is also interesting to compare the ZEV types against a conventional vehicle baseline. Clearly, early generation ZEVs will be much more expensive to manufacture than conventional vehicles, and these high costs would translate into high purchase prices unless the vehicles are sold with a heavy subsidy. However, as the analyses in Chapters 2 through 4 illustrate, ZEVs in higher volume production may only carry a price premium of a few thousand dollars. Furthermore, their greater efficiency and potential for reduced maintenance costs may make them nearly competitive with conventional vehicles on a lifecycle cost basis. This brings up another interesting question, which is that if emission-related costs are also considered, how do the relative costs of owning and operating ZEVs and conventional vehicles compare?

Table 7-1 and Figures 7-21 and 7-22 compare the relative lifecycle costs for the three ZEV types and for the conventional ICE Taurus, with Table 7-1 showing the detailed breakdown of lifecycle costs by cost category. The cost estimates for the ZEVs in Table 7-1 are for the later generation vehicles in the highest production volume (i.e., year 2026, high production volume case), and with the central component and fuel cost assumptions. As shown in the table, the BEVs, DHFCVs, and DMFCVs carry a lifecycle cost premium of $0.0510 per mile, $0.0087 per mile, and $0.0384 per mile, respectively. All of the ZEVs have higher vehicle costs than the conventional vehicle, but they have lower fuel and maintenance costs. For DHFCVs, this means that lifecycle costs almost reach parity with those of the conventional vehicle. For BEVs, lifecycle costs remain higher largely due to the cost of the battery pack (including battery replacement costs). For DMFCVs, costs are higher than for conventional vehicles mainly due to higher vehicle costs.

One interesting feature apparent in the table is that the baseline lifecycle cost calculation assume that fuel taxes amount to the same cost per mile ($0.0175/mi) for all vehicle types. Since the ZEVs are more efficient than conventional vehicles, a fuel tax that was the same for electricity, methanol, and hydrogen on an energy content basis would result in a lower per-mile fuel tax for the ZEVs. Furthermore, government policies could in theory be enacted to eliminate fuel taxes for fuels that were considered to be socially beneficial, further increasing the relative attractiveness of ZEV lifecycle costs in comparison

with costs for conventional vehicles. This point will be addressed further in a later section in this chapter.

Vehicle Lifecycle Costs Plus Emission-Related Costs

In order to compare vehicle lifecycle costs for ZEVs and conventional vehicles that include fuelcycle emission-related costs, it is necessary to characterize the fuelcycle emissions of criteria pollutants and GHGs for conventional vehicles. This is somewhat complex, as conventional vehicle emissions vary with vehicle vintage, age, and emission control equipment, as well as with the fuel used. Furthermore, while vehicles are designed to meet emission standards when tested over certain driving cycles, emissions can be much higher in the "real world" due to off-cycle emissions from harder accelerations and higher speeds than in the test cycles, and emission control systems can also malfunction in older vehicles.

Table 7-2 presents emission estimates for various stages of the conventional gasoline vehicle fuel cycle, including emissions from petroleum extraction, gasoline production, gasoline distribution and marketing, vehicle exhaust (from properly functioning vehicles operated under "on-cycle" conditions), vehicle evaporative losses, and vehicle malfunctioning and fuel enrichment. These estimates rely on only a few of many possible sources, and the vehicle exhaust emission estimates are average emissions for light-duty vehicles of different approximate vintages (including future projections). However, the estimates do include recent analysis of emissions from actual vehicle operation under real driving conditions (An, et al., 1995; Ross, et al., 1995).

Two sets of complete fuelcycle emission estimates for gasoline vehicles have been calculated, to serve as a baseline for comparison. First, a set of near-term fuelcycle emission estimates have been calculated based on the following estimates for various stages in the conventional vehicle fuelcycle:

- upstream emissions of NMOG, CO, and NO_x for 1992 (Acurex, 1996b);
- upstream emissions of PM, SO_x, and GHGs for 2000 (Delucchi, 1997);
- vehicle exhaust GHG emissions (total CO_2-equivalents) for 2000 (Delucchi, 1997);
- measured PM exhaust emissions (CARB, 1997);
- evaporative emissions of NMOG (Ross, et al., 1995); and
- vehicle exhaust, malfunctioning, and off-cycle NMOG, CO, and NO_x emissions for early 1990s vintage, California vehicles (An et al., 1995).

Second, a lower set of future fuelcycle emissions have been estimated based on vehicles that achieve CARB's low-emission vehicle (LEV) standard, and on projected future upstream, malfunctioning, and off-cycle emissions. The

separate emission estimates that compose this set of overall fuelcycle emission estimates are:

- upstream emissions of NMOG, CO, and NO_x for 2010 (Acurex, 1996b);
- upstream emissions of PM, SO_x, and GHGs for 2015 (Delucchi, 1997);
- vehicle exhaust GHG emissions (total CO_2-equivalents) for 2015 (Delucchi, 1997);
- vehicle exhaust NMOG, CO, and NO_x emission estimates that meet the CARB LEV 50,000 mile standard (CARB, 1997);
- measured PM exhaust emissions (CARB, 1997);
- evaporative emissions of NMOG estimated by the EMFAC7G model for vehicles with "enhanced evaporative emissions control" systems (CARB, 1997);
- malfunctioning, and off-cycle NMOG, CO, and NO_x emissions projected for 2010 vintage vehicles (Ross et al., 1995).

The in-basin and out-of-basin fuelcycle emission estimates that result from summing these estimates from the various stages in the gasoline vehicle fuelcycle are shown in Table 7-2. For upstream emissions, estimates for NMOG, CO, and NO_x are based on the Acurex study (1996b) because these estimates are specific to fuel use in the SCAB, and because they are separated into in-basin and out-of-basin components. Also, for near-term NMOG, CO, and NO_x exhaust emissions, the An et al. (1995) estimates are used because they are for California vehicles running on reformulated gasoline. As in the emission estimates associated with the BEV, DHFCV, and DMFCV fuelcycles, emissions of particulates from tire and brake wear and from road dust have not been included. See the notes to the table for additional details of the various emissions estimates.

Figures 7-23 through 7-25 compare the total vehicle lifecycle plus emission-related costs for year 2026, high production volume ZEVs, the near-term ICEV, and the future low-emission ICEV. Figure 7-23 shows that with central case cost assumptions, the DHFCV is the lowest total lifecycle cost vehicle, followed by the ICE LEV, the DMFCV, the BEV, and the near-term ICEV. This finding is significant, because it shows that the inclusion of emission-related externality values (for vehicle operation in the SCAB) allows at least one ZEV type to overcome the lifecycle cost disadvantage that it faces relative to even a future, low-emission ICEV. With regard to near-term ICEV technology, the inclusion of emission-related externalities allows all three of the ZEV types to compare favorably.

Figure 7-23:

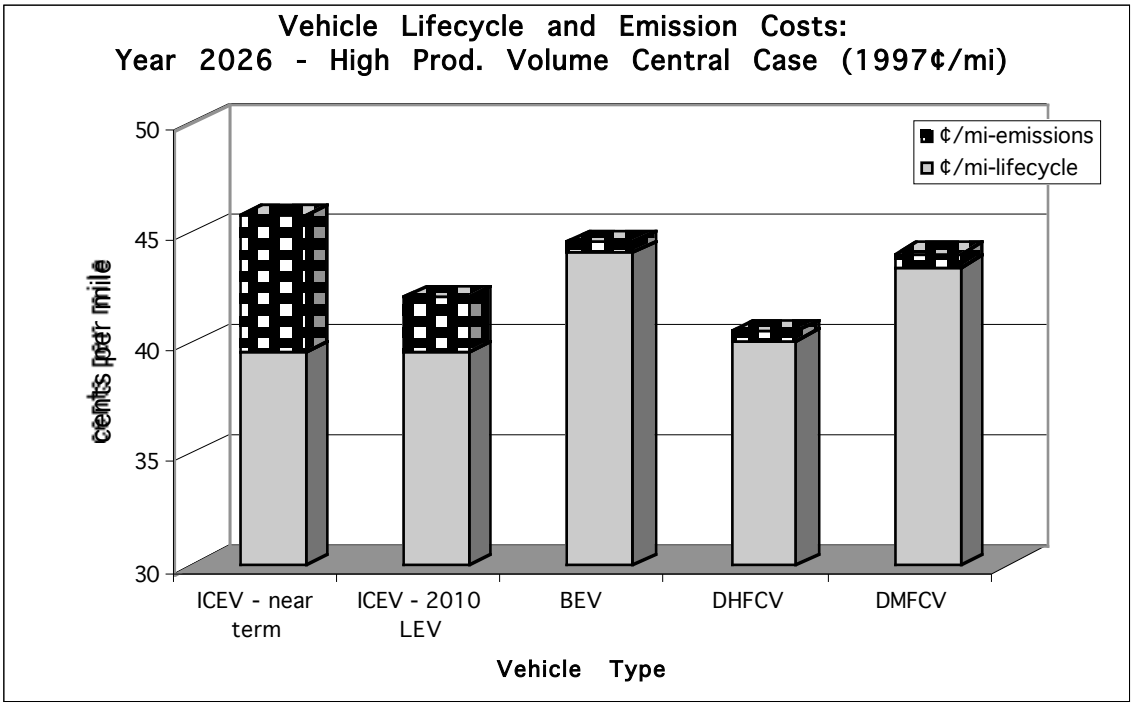

Figure 7-24:

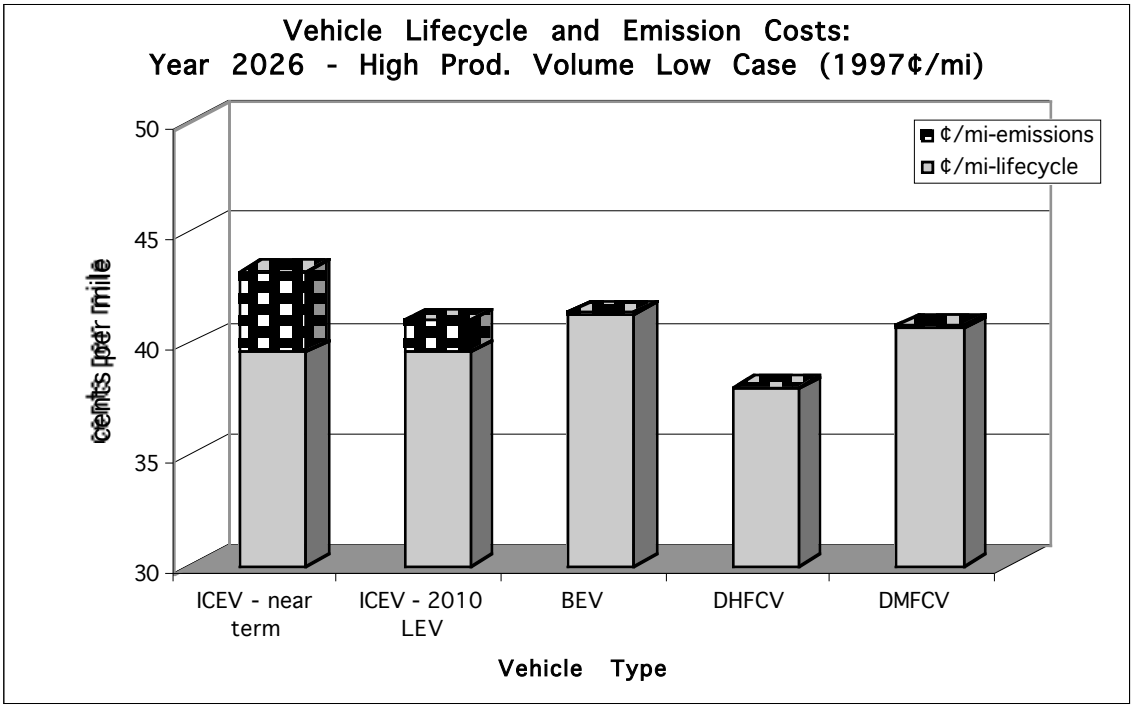

Figure 7-25:

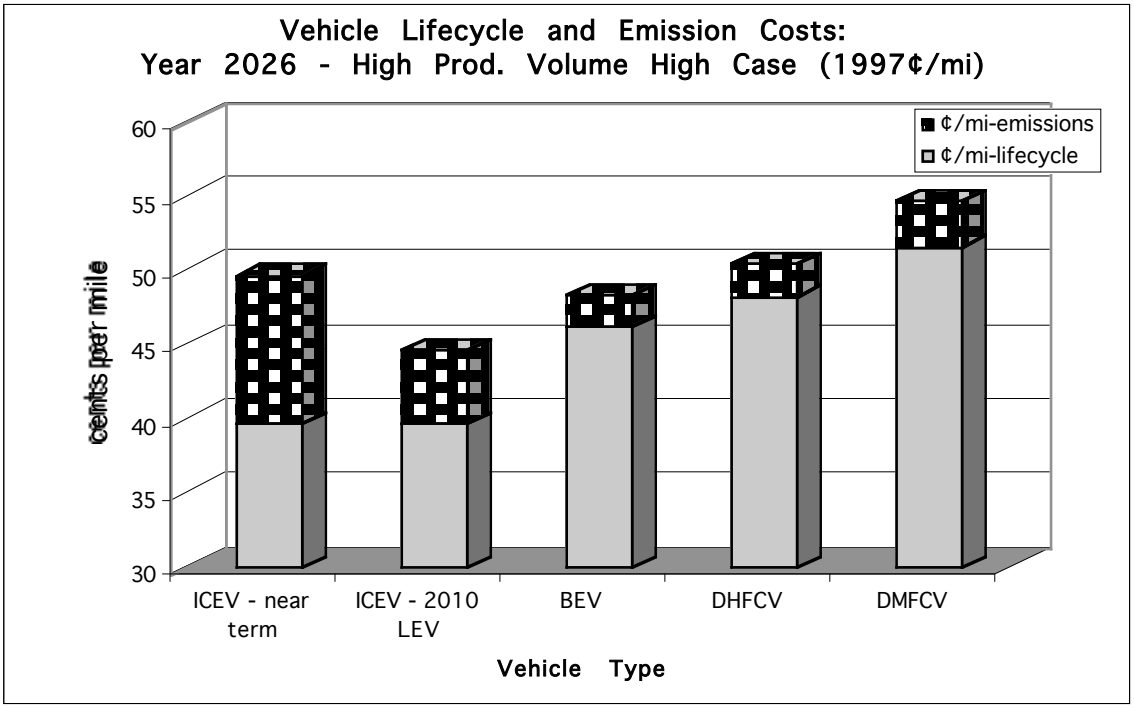

Vehicle Lifecycle Costs, Emission-Related Costs, and Infrastructure Costs

The above comparisons show that high-volume production ZEVs, and DHFCVs in particular, look attractive compared with ICEVs when total vehicle lifecycle and emissions costs are considered for vehicle operation in the SCAB. However, introduction of the ZEVs also entails significant infrastructure support costs, as discussed in Chapter 5. Including these infrastructure support costs may have an impact on the total lifecycle cost estimates for ZEVs, and this could alter the above findings.

Figures 7-26 through 7-29 show comparisons of the different vehicle types when infrastructure support costs for ZEVs are included along with vehicle lifecycle and emission-related costs. The infrastructure cost components were calculated by spreading the total infrastructure support costs estimated in Chapter 5 (for vehicle introduction in the SCAB) over the total VMT for the ZEVs. For BEVs and DHFCVs, the infrastructure support costs are spread over the total VMT of vehicles introduced from 2003 to 2026 (about 324,000 total vehicles traveling 165,000 miles each). For DMFCVs, the infrastructure support costs are spread over the total VMT of the DMFCVs introduced from 2011 to 2026 (about 276,000 total vehicles traveling 165,000 miles each).

Figure 7-26 shows that there is a significant level of uncertainty in Year 2026 total lifecycle costs for ZEVs, particularly for the two types of FCVs. The uncertainty is asymetrical for DHFCVs and DMFCVs, with the high cost case reflecting the relatively pessimistic 85% slope for the fuel cell system manufacturing progress function. The two lowest cost cases appear to be the internal combusion engine LEV and the DHFCVs, but as the figure clearly shows the uncertainties are significant enough, and the results close enough for all

vehicle types, that it is not possible to unequivocally determine the "best" Year 2026 vehicle type for the SCAB.

Figure 7-26:

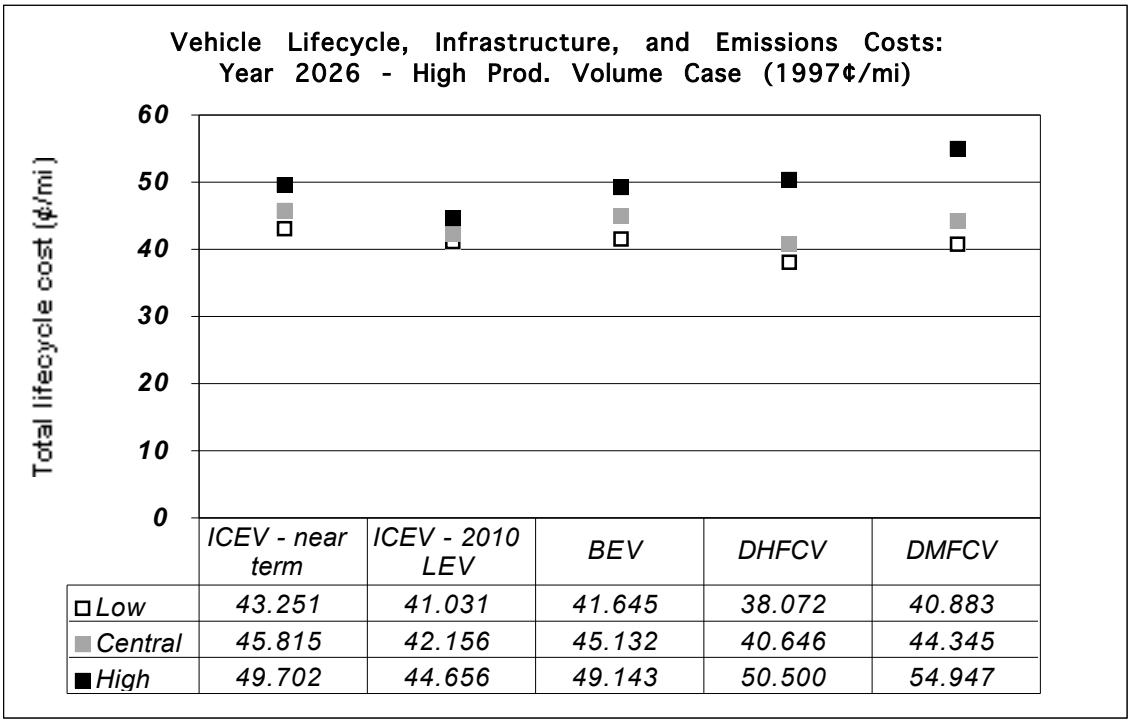

	ICEV - near term	ICEV - 2010 LEV	BEV	DHFCV	DMFCV
Low	43.251	41.031	41.645	38.072	40.883
Central	45.815	42.156	45.132	40.646	44.345
High	49.702	44.656	49.143	50.500	54.947

Figure 7-27 shows that in the central case, the inclusion of infrastructure costs has a relatively small impact on the total lifecycle costs of the ZEVs. The impact is greatest for BEVs, with a cost of about 0.53¢ per mile, followed by DMFCVs with about 0.25¢ per mile, and DHFCVs with about 0.049 ¢ per mile.[50] The inclusion of these costs does not change the finding that, with central case assumptions, the DHFCV has the lowest lifecycle cost, followed by the ICE LEV, the DMFCV, the BEV, and finally the near-term ICEV.

[50] Recall that much of the infrastructure support costs for DHFCVs is included in the hydrogen fuel cost estimates used in Chapter 3.

Figure 7-27:

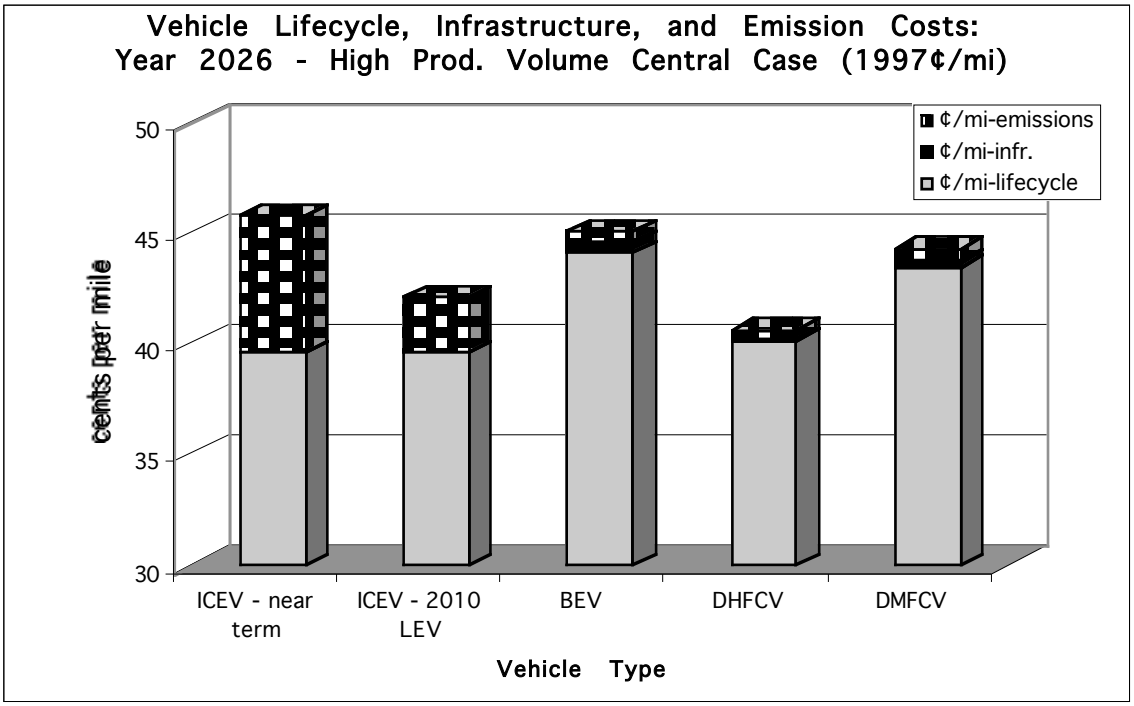

Figure 7-28 shows similarly that the inclusion of infrastructure costs with low cost assumptions does not significantly change the results. The infrastructure cost component for BEVs, DHFCVs, and DMFCVs is now about 0.21¢ per mile, about 0.013¢ per mile, and about 0.064 ¢ per mile, respectively.

Figure 7-28:

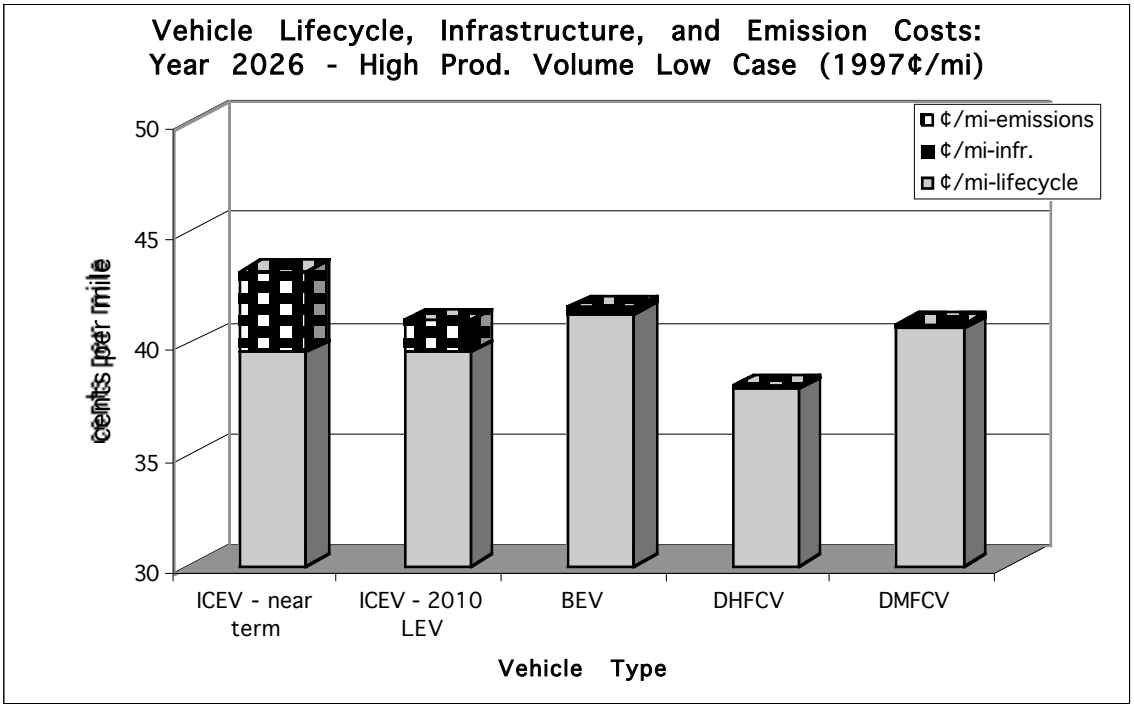

Finally, Figure 7-29 shows that for the high cost assumption case, the inclusion of infrastructure costs once again has relatively little effect on the final cost estimates. The infrastructure cost component for BEVs, DHFCVs, and DMFCVs in the high cost case is 0.841¢ per mile, 0.084¢ per mile, and about 0.281¢ per mile, respectively.

Figure 7-29:

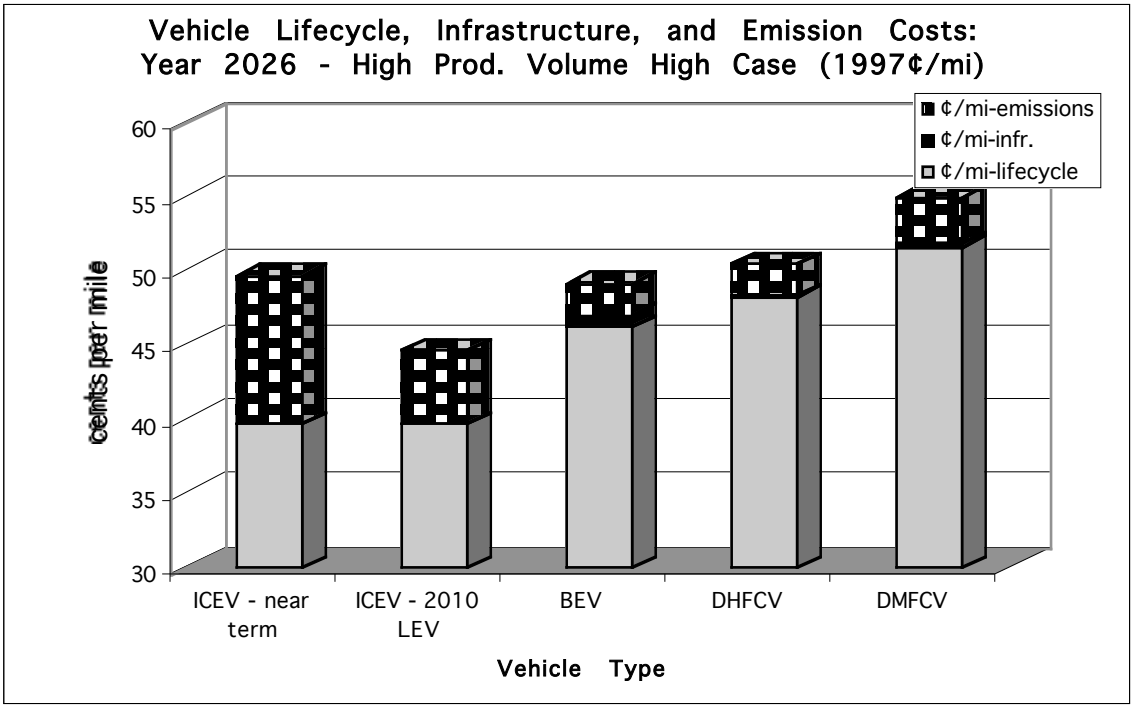

The Value of Including Uncertainty in Key Input Variables

A critical aspect of the analysis conducted here is the explicit inclusion of uncertainties in estimates of key ZEV component costs, fuel costs, fuelcycle emissions, and emission damage or control values. Rather than using point estimates for all variables and then conducting *post hoc* sensitivity analysis, uncertainty in key variables has been included from the very beginning of the analysis, and then propagated through the modeling effort using the mathematics of fuzzy sets. This method has the advantages of reducing the need for later sensitivity analysis, as well as allowing results to be presented in a form that conveys the overall level of uncertainty that arises from the inclusion of uncertainty in key input variables. However, since the results are themselves uncertain, making definitive statements with regard to the relative costs of different ZEV types, and of ZEVs relative to ICEVs, becomes more difficult than if point estimates are used and the magnitude of results is clearly differentiated.

One interesting question is the degree to which, if any, including uncertainty in key variables leads to any different conclusions than if point estimates were used. In order to explore this issue, I have made several comparisons of the results of the high production volume scenario, total vehicle plus infrastructure plus emissions NPV estimates. The comparisons include the following: 1) all of the low case values; 2) all of the central case values (i.e., the same as the "TFN Modes" defuzzification technique); 3) all of the high case values; 4) the results of Chang's defuzzification technique; 5) the results of Kaufman and Gupta's defuzzification technique; 6) the results of the MATLAB centroid defuzzification techniqe, and 7) the results of the MATLAB bisector defuzzification technique. The results of these comparisons, in terms of the ranking of the three different ZEV production and use scenarios, are as follows:

Low Case Values:	DHFCV<BEV<DMFCV
Central Case Values:	DHFCV<BEV<DMFCV
High Case Values:	BEV<DHFCV<DMFCV
Chang's Method:	BEV<DHFCV<DMFCV
Kaufman and Gupta's Method:	BEV<DHFCV<DMFCV
MATLAB Centroid Method:	BEV<DHFCV<DMFCV
MATLAB Bisector Method:	BEV<DHFCV<DMFCV

What these comparisons show is that the ranking order of the different scenarios does vary in some cases, depending on the type of comparison that is done. In other words, had I used point estimates instead of fuzzy-set distributions to characterize key input values, I would have obtained different conclusions regarding the relative attractiveness of the BEV and DHFCV scenarios depending on whether the assumed point values were relatively optimistic (i.e., similar to the low case values), or pessimistic (similar to the high case values).

Furthermore, when only point values are used, there is a significant possibility of either intentionally (e.g., for advocacy purposes) or unintentionally making relatively optimistic assumptions about one set of technologies and relatively pessimistic assumptions about another. This would be analogous to, for example, comparing the low case DHFCV and DMFCV estimates with the high case BEV estimates. This clearly could lead to a different conclusion than if uncertainty in key variables were included, and any results and comparisons were put in the context of the overall level of uncertainty in the analysis. In the latter case, where uncertainty is included, completely unequivocal conclusions about the relative ranking of the various cases can be made only where there is no "overlap" between the results, or where all possible comparisons yield consistent conclusions. In all other cases, the results may indicate that one ranking order is most likely, but that there is at least the possibility of an alternate result.

For example, with regard to the comparisons shown above, the fact that four out of five defuzzification techniques yields the ranking order "BEV<DHFCV<DMFCV" suggests that it is likely that the NPV of the total costs associated with the high production volume BEV scenario would in fact be the lowest, followed by the DHFCV and DMFCV scenarios. However, the fact that some possible comparisons yield different results (as is obvious by the overlap in the triangles shown in Figure 7-16) makes it impossible to make this a completely unequivocal conclusion. In contrast, where point estimates are used exclusively, all results appear unequivocal because the only possibility is to achieve a distinct, "crisp" set of results, with a clearly implicit ranking order. Only through the somewhat burdensome process of sensitivity analysis can possible variations in the results be explored, and often these alternate "sensitivity analysis" cases are de-emphasized by appearing as an "add-on" to the primary analysis, and buried in an appendix.

Uncertainty Bands and the Degree of Uncertainty

In Chapter 1, the notion was introduced of an uncertainty band for fuzzy set distributions that is analogous to the concept of the confidence interval for probability distributions. For purposes of this analysis, the uncertainty band is set at the level of $\mu(x)$ equal to 0, where the "low" and "high" cases are

established. This uncertainty band provides a measure of the relative level of uncertainty in each alternative. Again using the results of the high production volume scenario for the NPV of total vehicle plus infrastructure plus emission costs, the following uncertainty bands can be calculated:

	Net Present Values (Billions of Year 2000 $s)			
	Low	Central	High	Uncertainty Band
BEV Scenario:	107.0	113.9	124.1	17.1
DHFCV Scenario	99.4	110.6	143.0	43.6
DMFCV Scenario	108.4	120.4	150.1	41.7

As a further measure, these absolute magnitudes of variation in the estimates can be normalized to the maximum value (i.e. where the right extent of the distribution reaches $\mu(x) = 0$), in order to provide a relative measure of the proportion of the total result that is uncertain. These relative uncertainties would be the following, for the above example:

	Values (Billions of Year 2000 $s)			**Relative (normalized)**
	Low	Central	High	Uncertainty Band
BEV Scenario:	107.0	113.9	124.1	13.8%
DHFCV Scenario	99.4	110.6	143.0	30.5%
DMFCV Scenario	108.4	120.4	150.1	27.8%

With these relative measures, a measure of a 100% uncertainty band would show that degree of uncertainty would extend over the entire range of the variable, whereas a 0% uncertainty band would respresent the special case of a "crisp" or "point" estimate. Note that in the above "high production volume" example, the DHFCV scenario has both the highest magnitude uncertainty band and the highest relative uncertainty band, followed by the DMFCV scenario and the BEV scenario.

Additional Sensitivity Analysis

In the MATLAB/Simulink fleet-level vehicle, infrastructure, and emissions cost analysis model, several key input variables have been expressed as TFNs in order to propagate important uncertainties through the model. In this way, the final result reflects underlying uncertainties in vehicle costs, infrastructure costs, emission levels, and emission-related damage and control costs. However, there are additional sources of potential variability in the results that were not included as fuzzy set distributions. This was done because it is necessary to focus the analysis to some degree and to take at least a few aspects of the scenario analyses as given. These aspects include the assumed driving ranges of the vehicles, the hybridization of the FCVs by including a battery pack as well as a fuel cell system, and the choice of a discount rate for calculating the net present values of total scenario costs. The effect of varying these assumptions can be explored through more traditional sensitivity analysis, and this is done in the sections that follow.

Sensitivity of Vehicle Costs to Assumed Vehicle Driving Range

In Chapters 2 through 4, specific vehicle driving ranges were assumed for BEVs and FCVs. Driving ranges for BEVs were determined by the range possible for

vehicles using battery modules composed of 100 Ah cells. These ranges vary somewhat depending on the generation of the battery technology, because later generation battery technologies achieve the same battery pack energy in a lighter weight battery pack, thus leading to a lighter and more efficient vehicle. For FCVs, the vehicle range was assumed to be 300 miles. This range was assumed so that FCVs would not face a significant disadvantage in the market, due to driving range, in comparison with conventional vehicles.

In principle, BEV driving ranges could be significantly higher or lower than assumed in Chapter 2, and this would have an effect on both vehicle purchase price and lifecycle cost. In order to investigate the effect of variations in BEV driving range on initial and lifecycle costs, I have performed additional runs of the Lotus 1-2-3 model with different assumed driving ranges. These runs are based on the Generation 4 vehicle design, for year 2026 production in the high production volume case, using central case component cost assumptions. However, due to changes in the masses of vehicles with different-size battery packs, motor and controller costs vary with driving range. Also, the $ per kg cost of the battery pack changes with vehicle driving range because the Ah capacity of the battery pack cells is different, and lower capacity cells tend to have higher costs per unit mass (and per kWh).[51] Figure 7-30 shows the variation in vehicle purchase prices by BEV driving range, for driving ranges of 100 miles, 126 miles (the reference case), 150 miles, and 200 miles. Table 7-3 presents some of the important differences between these vehicles, including drivetrain power levels, vehicle masses, and key component costs.

Figure 7-30:

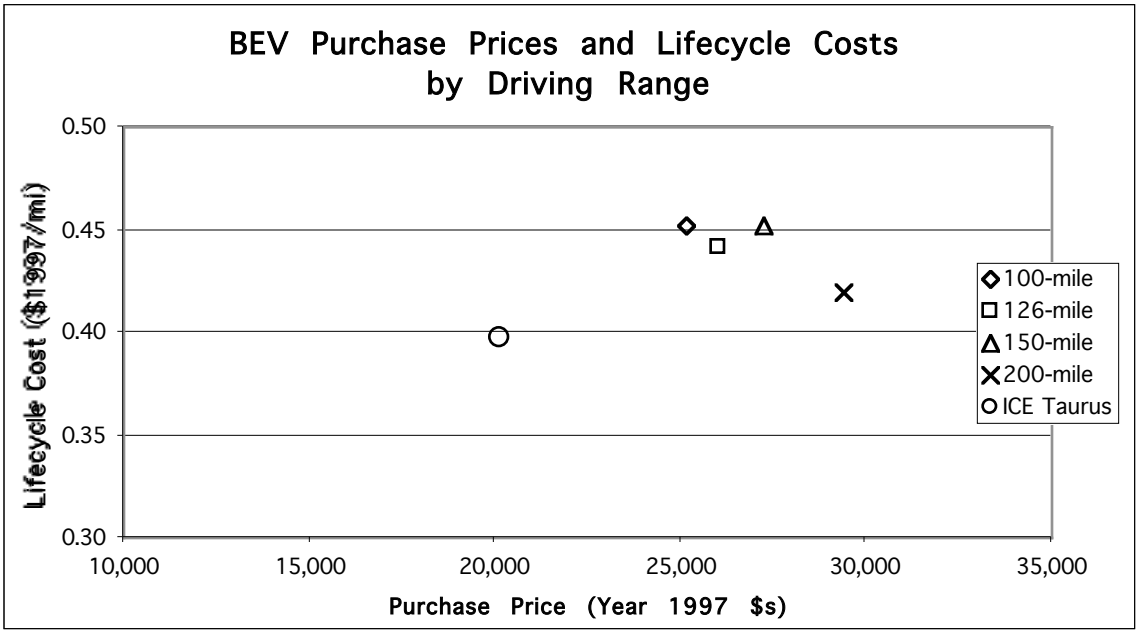

Figure 7-30 shows that while BEV purchase prices increase with driving range, lifecycle costs do not necessarily increase. In fact, the BEV with the lowest

[51] The relationship between NiMH cell capacity and battery cost is discussed in Chapter 3.

lifecycle cost is the one with the highest driving range. This is because of the cost of battery replacement. Even though the 200-mile range BEV has the largest and most expensive battery pack, with a lifetime of 14.3 years it lasts almost the lifetime of the vehicle. The Lotus 1-2-3 model calculates battery replacement costs with the assumption that if a battery needs to be replaced near the end of the vehicle life, the driver chooses to accept a degraded level of performance for the remainder of the vehicle life, rather than replace the battery. Thus, instead of paying a high cost for a new battery for a vehicle that itself has only a fraction of its worth than when new, the driver instead does not replace the battery and lives with a shorter vehicle range until the vehicle itself is retired. As shown in Table 7-3, the lifecycle cost of the battery is much lower for the 200-mile range BEV than for the shorter range BEVs. This is because the battery is not replaced during the life of the vehicle. Even though the initial cost of the battery is higher, and the vehicle is heavier and has a more powerful and expensive drivetrain, the elimination of the battery replacement cost more than offsets the contribution of the higher initial purchase price to the overall vehicle lifecycle cost.

Also, the battery and vehicle lifecycle costs for the 126-mile (base case) vehicle are lower than for the 100-mile and 150-mile vehicles. This is because the battery life is almost exactly one-half the life of the vehicle. Since the battery is replaced half-way through the life of the vehicle, the two battery packs are used nearly optimally such that little battery life is left when the vehicle is scrapped. Vehicles that are retired when some battery life is left are awarded a salvage-value credit in the Lotus 1-2-3 model, but at a loss of 30% of the initial cost of the remaining battery life. Thus, the 126-mile range BEV assumed here as a base case is a relatively low-lifecycle cost BEV. Only by going to a vehicle with a longer range and a battery pack that lasts the life of the vehicle, can a lower lifecycle cost be achieved. However, the 200-mile range, "single battery pack" vehicle has an initial purchase price that is about $3,500 higher than the 126-mile range, base case BEV.

In reality, of course, battery cycle life is an uncertain parameter because of the lack of experience with advanced batteries over many years of use. The NiMH battery cycle lives estimated in the Lotus 1-2-3 model are based on cycle life versus depth-of-discharge data supplied by Ovonic Battery Company for batteries that have been cycled under laboratory conditions. In real world conditions, it is unclear how consumers would choose to recharge their vehicles (i.e., "top-off" the batteries each evening, always wait until they reach a relatively deep discharge depth, or some mix of these two). This consumer behavior has implications for the durability of the battery pack (as well as vehicle efficiency because of the low efficiency of "top-off" recharging). It is unlikely that batteries used in the real world will achieve the same cycle lives as batteries that are cycled optimally under laboratory conditions, and as a result the estimates presented here may overestimate battery cycle lives and underestimate battery replacement costs. The relatively low lifecycle cost for the 200-mile range BEV would not be realized if the battery pack had to be replaced; the resulting lifecycle cost would likely be close to that of the other cases.

Similarly, FCV purchase prices and lifecycle costs will vary with different assumed driving ranges. Higher driving ranges will necessitate a greater quantity of hydrogen or methanol stored, and this will increase the weight of the vehicle, the required drivetrain power to achieve a given level of performance,

and the cost of the vehicle. Figure 7-31, below, shows the purchase prices and lifecycle costs of DHFCVs with 200-mile, 250-mile, 300-mile, and 400-mile driving ranges. Figure 7-32 shows the purchase prices and lifecycle costs of DMFCVs with the same set of driving ranges. Tables 7-4 and 7-5 also present these costs, along with important characteristics for each vehicle. Figures 7-31 and 7-32 show that, in comparison with BEVs, the variations in FCV purchase prices and lifecycle costs are relatively modest with different assumed driving ranges, particularly for DMFCVs.

Figure 7-31:

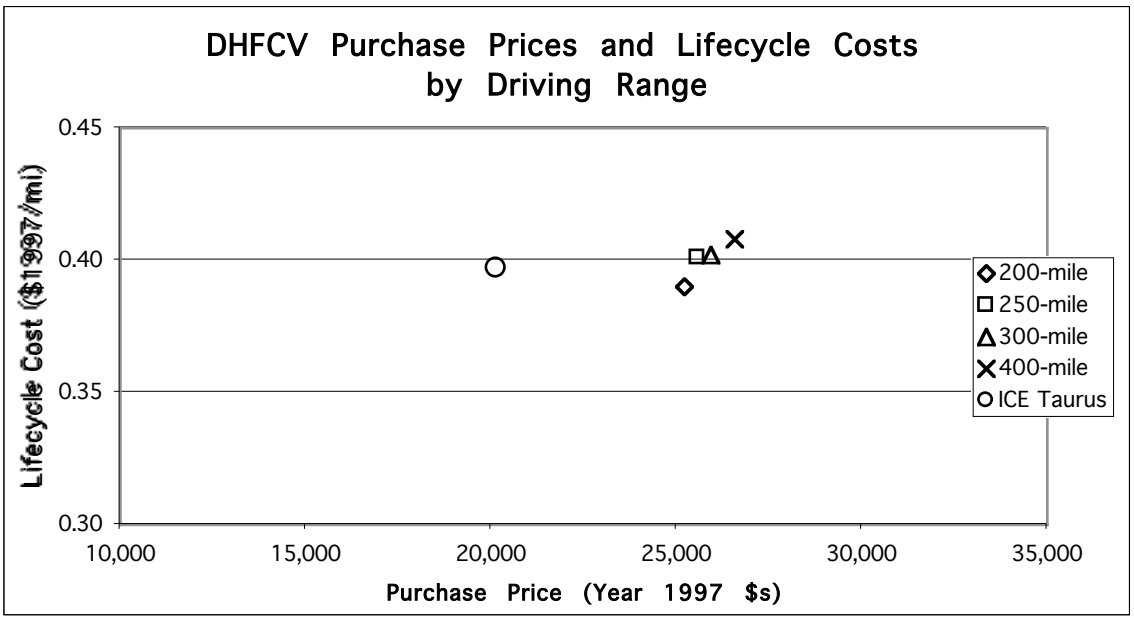

Figure 7-32:

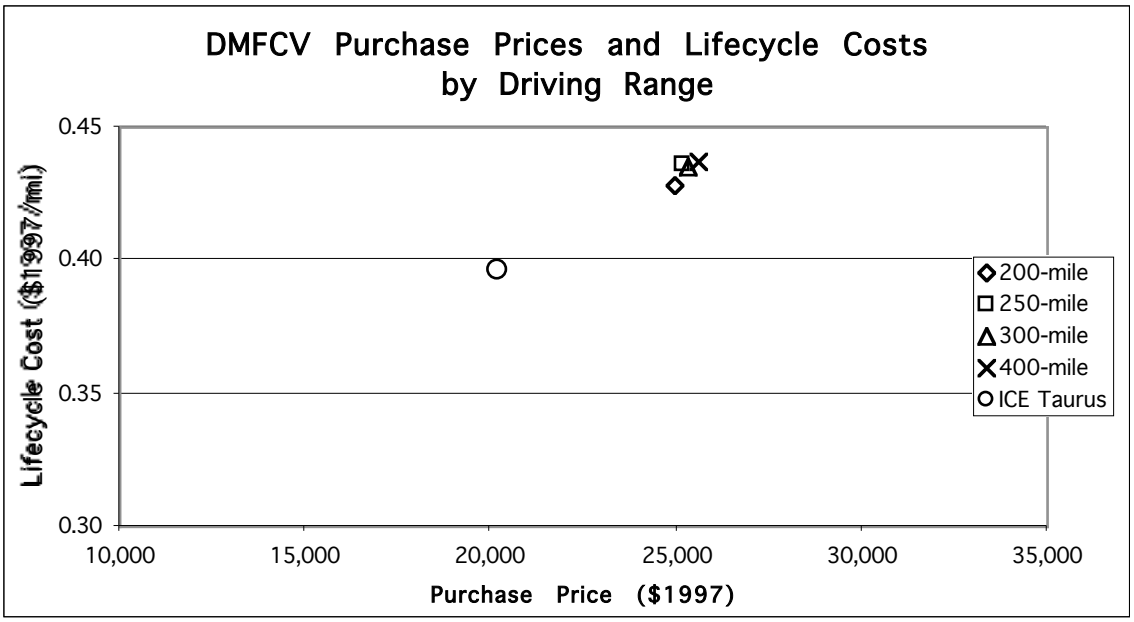

Sensitivity of Vehicle Costs to Hybrid Vehicle Configuration

As discussed in Chapters 3 and 4, FCVs can be hybrid power system vehicles, with a peak power battery or ultracapacitor used in conjunction with the fuel cell system, or pure fuel cell power system vehicles. The advantages of hybridization include the ability to recapture regenerative braking energy and the possibility of using battery power to propel the vehicle in a "limp back" mode in the event of a fuel cell system failure or empty fuel tank. Despite the efficiency gain from regenerative braking in hybrid FCVs, it is unclear if hybrids would necessarily be more efficient, since the larger fuel cell system in a pure FCV would tend to operate at a lower percentage of its peak power. This means that the fuel cell system would tend to be more efficient than the smaller fuel cell system in a hybrid FCV. Some model results have shown that the relative efficiency advantage of hybrid and pure FCVs depends on the driving cycle over which the simulations are conducted (Friedman, 1999; Thomas, et al., 1998a).

The DHFCV and DMFCV cost analyses conducted in Chapters 3 and 4 assumed a hybrid vehicle design, because particularly in the early years of FCV introduction the high costs of fuel cell systems suggest that this strategy will be most cost-effective. However, it is worth investigating the potential costs of both hybrid and non-hybrid FCVs because of the non-linear nature of fuel cell system costs. Even though pure FCVs need much larger fuel cell systems than hybrid FCVs, the $ per net-kW costs of the larger systems are lower because some of the components in the fuel cell system do not scale directly with system power. In one of the cases presented below, for example, the Generation 4 non-hybrid DHFCV has a 72.9 kW-net fuel cell system with a cost of $39.17 per kW-net, while the Generation 4 hybrid DHFCV has a 20.9 kW-net fuel cell system with a cost of $76.69 per kW-net. The per-kW cost of the small, hybridized fuel cell system is nearly double that of the much larger, non-hybridized system. This effect, coupled with the cost savings from eliminating the battery pack and the additional control electronics needed to manage the more complex hybrid power system, could make the costs of pure FCVs competitive with those of hybrid FCVs.

In order to investigate this issue, I have performed additional runs of the Lotus 1-2-3 spreadsheet model with non-hybrid FCV configurations. Figure 7-33 shows the results for hybrid and non-hybrid DHFCVs with high production volume, central case cost assumptions. The cases reflect vehicle costs at the end of each vehicle technology generation. In order to estimate the costs of fuel cell systems for the non-hybrid DHFCVs in the year 2006, 2010, and 2014 cases, the same proportional costs were assumed as predicted by Equation 3-3 for fuel cell systems in high volume production. In other words, if the $ per kW cost of a 70-kW fuel cell system for a non-hybrid DHFCV in high volume production is $40.78 per net kW, and the cost of a 20-kW fuel cell system for a hybrid DHFCV is $79.10 per net kW, then the same 1:1.94 ratio was used to estimate the proportional costs of the fuel cells in lower volume production (using the hybrid fuel cell system cost predicted by the MPF framework.

Figure 7-33 shows that, as expected, in the early years of production the purchase prices and lifecycle costs estimated for 300-mile range hybrid DHFCVs are lower than for comparable non-hybrid DHFCVs. As time progresses, however, and fuel cell system technology cost and power density become "learned out," the gap between the two vehicle types closes. By 2026, the non-

hybrid DHFCVs actually have slightly lower purchase prices and lifecycle costs than the hybrid DHFCVs. This advantage comes despite the fact that the non-hybrid DHFCVs are slightly heavier and require a more powerful and expensive drivetrain (68 kW for the non-hybrid versus 65 kW for the hybrid).

Figure 7-33:

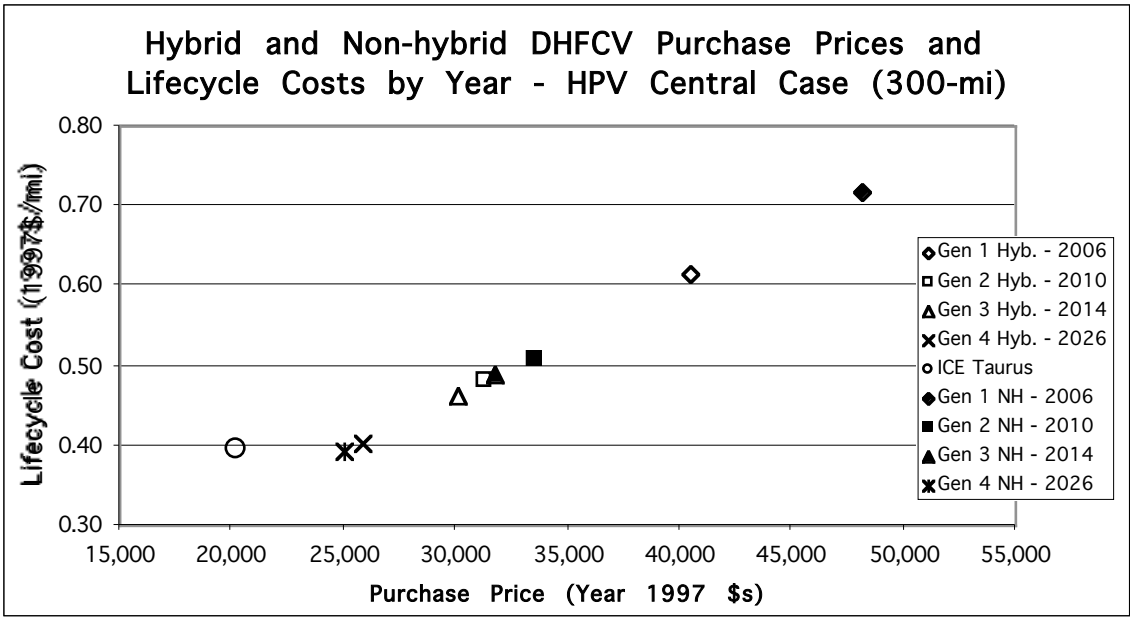

Note: HPV = high production volume case.

In order to investigate whether or not this year 2026 non-hybrid DHFCV advantage extends across variations in vehicle driving range, Figure 7-34 presents cost estimates for both vehicle types with driving ranges of 200 miles, 250 miles, 300 miles, and 400 miles. The purchase price advantage for the non-hybrid DHFCVs extends across all driving ranges, and the lifecycle cost advantage extends across all driving ranges except 200 miles, where the hybrid DHFCV has a slight advantage. In general, hybrid DHFCVs have lifecycle costs that are more sensitive to variations in driving range than non-hybrid DHFCVs.

Figure 7-34:

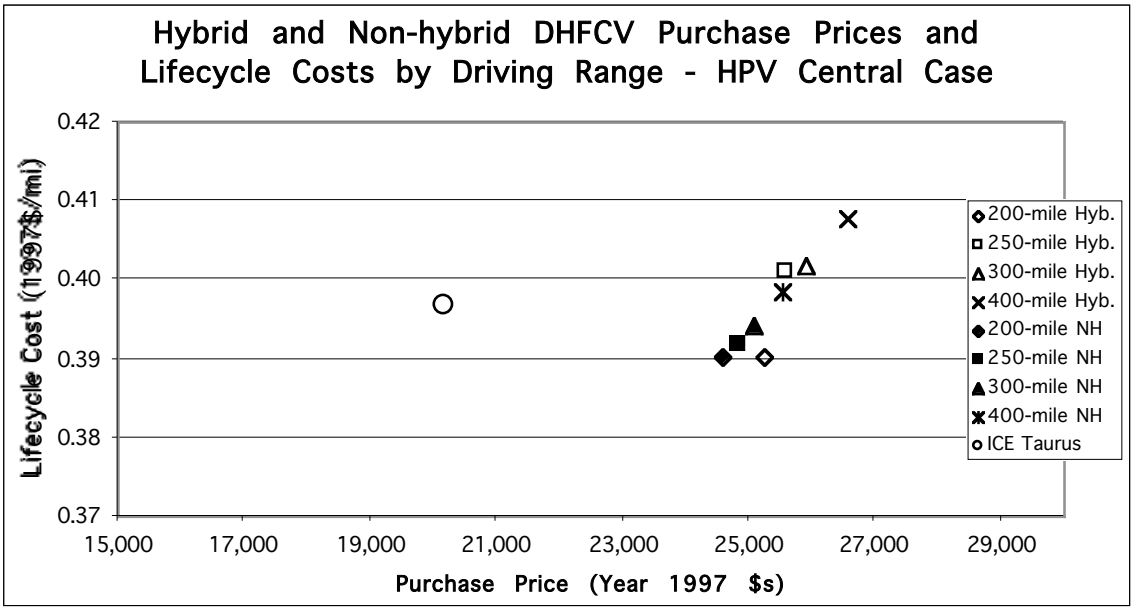

Note: HPV = high production volume case; NH = non-hybrid vehicle.

For DMFCVs, Figure 7-35 shows that, in contrast with DHFCVs, the hybrid DHFCVs have lower purchase prices and lifecycle costs in both 2014 and 2026. However, the gap between the hybrid and non-hybrid vehicles is closed considerably by 2026.

Figure 7-35:

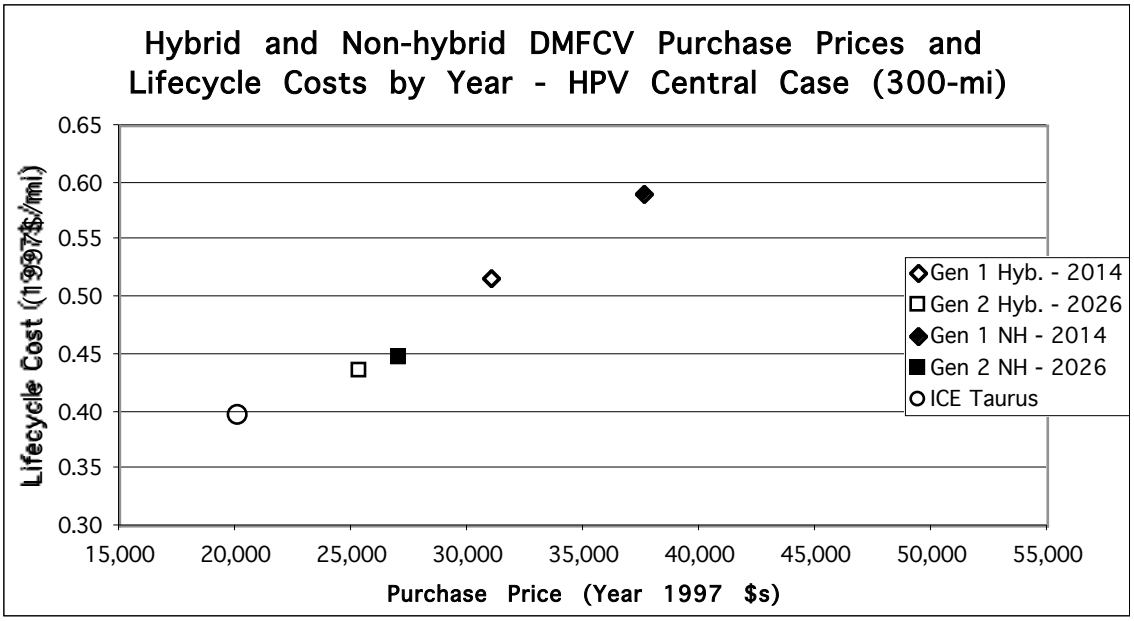

Note: HPV = high production volume case; NH = non-hybrid vehicle.

Figure 7-36 shows that for year 2026 vehicles with different driving ranges, the purchase price and lifecycle cost advantage of the hybrid DMFCVs extends across all driving ranges. As in the DHFCV case, the non-hybrid DMFCVs have purchase prices and lifecycle costs that are less sensitive to variations in driving range than the hybrid DMFCVs.

Figure 7-36:

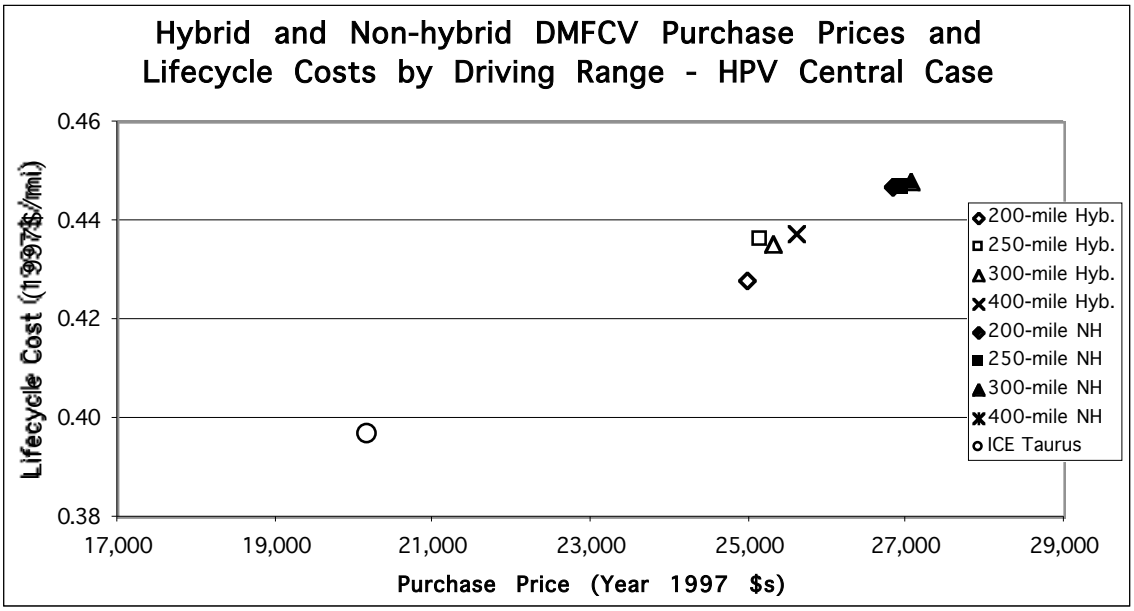

Note: HPV = high production volume case; NH = non-hybrid vehicle.

Sensitivity of Scenario Net Present Values to Assumed Discount Rate

The discount rate used to calculate the net present values of total scenario costs was assumed to be 3.65% in the reference case. This rate was selected because it is the rate needed to reproduce the total costs of vehicle ownership calculated with the Lotus 1-2-3 model, from the calculated "cents per mile" levelized costs. Since the annual VMT schedule used in the MATLAB/Simulink model varies over time with vehicle age, the 3.65% rate was required rather than the 3.1% rate used in the Lotus 1-2-3 model, which assumes the same average VMT for each year.

In principle, any choice of a discount rate is subjective. While most analysts agree that the use of some positive discount rate is justifiable because of the social time preference for money (and also because consumption tends to grow over time), there is much less agreement about what exact discount rate should be used for calculations of cost and benefit streams over any particular time horizon. For issues that involve potential impacts that extend across generations, such as future climate change damages from present GHG emissions, the discounting issue becomes even more complicated because questions of inter-generational equity are raised (Lind, 1995; Manne, 1995; Mohr, 1995). The use of a discount rate typical for shorter-term decisions, such as 5%, leads to calculations of negligible damage net present values when the damages occur many years in the future. This makes any sort of decision to mitigate

potential future damages, in this example by reducing GHG emissions, impossible to justify (unless a potential policy is a "no regrets" one).

Furthermore, the sensitivity of the final result to the choice of a discount rate increases with longer time horizons. For example, the difference between the net present value of a dollar discounted for 20 years at 3% is approximately double the value of the same dollar discounted at 7%. But, the net present value of a dollar discounted at 3% for 200 years is about three orders of magnitude greater than the value of a dollar discounted at 7%. The wide range in GHG damage values shown in Table 6-9 is partly due to the sensitivity of future damage net present values to the assumed discount rate.

One basic and reasonable approach to dealing with discount rate sensitivity is to simply calculate net present values of economic cost (and/or benefit) streams with a range of different discount rates, and determine how the choice of a discount rate affects the results. Norgaard (1986) advocates this approach. In order to investigate the discount rate sensitivity of the total scenario cost results presented in Figures 7-15 and 7-16, which were computed with a discount rate of 3.65%, the total scenario cost net present values have also been computed using discount rates of 3%, 5%, and 7%. Table 7-6 presents the high and low production volume scenario rankings for each discount rate, based on the various TFN defuzzification methods discussed above.

In general, the choice of a discount rate changes the calculated net present value of each total scenario cost (of course), but only in a few cases does it have an effect on the scenario ranking. The 3% and 3.65% discount rates produce identical rankings with all defuzzification methods. With the 5% discount rate, the rankings are again unchanged except that in the high production volume case, Chang's method ranks the DMFCV scenario second and the DHFCV scenario third, while with the 3% and 3.65% discount rates the defuzzified net present value of the DHFCV scenario is lower. With the 7% discount rate, however, the DMFCV case and the DHFCV case change positions in the low production volume scenario with Kaufman and Gupta's method and with the two MATLAB "defuzz" methods, and in the high production volume scenario with Chang's Method.

This switching occurs because the DMFCV scenarios have relatively low vehicle costs in early years, relative to the DHFCV scenarios, as a result of the assumption that the vehicles introduced from 2003 to 2010 are moderately costly BEVs rather than more expensive FCVs. The 7% discount rate diminishes costs that occur later in the scenarios, and therefore in effect emphasizes earlier costs. Since early generation BEVs have lower costs than early generation DHFCVs, the BEV and DMFCV scenarios benefit from the higher discount rate. In the low production volume cases, the total costs for the DMFCV and DHFCV scenarios are quite similar. As a result, some switching in rank occurs with different defuzzification methods, and with different discount rates. In the high production volume cases, it is the total BEV and DHFCV scenario costs that are closest in magnitude, and among which some switching in rank occurs with different defuzzification methods.[52]

---

[52] Except that Chang's method often seems to favor the DMFCV case over the DHFCV case. This may be because its "(c-a)" parameter in effect penalizes the range of variation in TFNs, which are highest in the DHFCV scenario net present values.

Sensitivity of Vehicle Retail Prices to ZEV Pricing Strategies

The ZEV purchase prices shown in Tables 2-24 and 2-25, 3-7 and 3-8, and 4-3 and 4-4 are based on retail-level vehicle prices as calculated in the Lotus 1-2-3 spreadsheet model. The purchase prices assume traditional automobile industry accounting practices. In general, the automobile industry practices "cost-plus" pricing, where the purchase price of the vehicle covers the manufacturing cost, plus division and corporate level costs, warranty costs, dealer costs, and manufacturer and dealer profit. Once these additional costs are included, the markups from the manufacturing to the retail level are on the order of 80-100%. In other words, the final purchase price of a vehicle is perhaps double its manufacturing cost.

The exact level of markup differs from component to component in the Lotus 1-2-3 model because the various markups are calculated through somewhat complex formulas that include the cost of "holding money," costs for testing and validating different components, and the various other division, corporate, dealer, and warranty costs. For example, the total vehicle manufacturing cost for one BEV case is estimated to be $14,108, and the retail price is estimated to be $26,813, for a total markup of about 90%. The battery pack in this vehicle has an OEM cost of $6,863, but at the retail level the battery cost is $12,590, resulting in a markup of about 83%.

A shortcoming of some previous EV cost studies is that some of these additional markups have not been included. In some studies, the total vehicle price was estimated by simply adding the costs of a vehicle "glider," the OEM costs of any additional EV components, and manufacturer and dealer profit, but excluding division and corporate level costs (e.g. Moomaw, et al., 1994). Some other cost studies include all of the markups, but make relatively charitable assumptions for some types of EVs by arguing, for example, that the markup on a BEV battery pack could be proportionally lower than the markup on other vehicle components. For example, ANL's BEV cost studies assume considerably lower markup on BEV battery packs than for other vehicle components (Cuenca, 1996). Thus, the vehicle purchase prices shown in this analysis are relatively conservative (on the high side), in that arguments can be made for lower markups on certain costly and novel EV components. However, the estimates shown here are probably more consistent with conventional industry accounting practices.

A more fundamental vehicle price issue is that regardless of the estimated vehicle retail price that manufacturers would charge in order to recoup all costs plus profit, it is likely that manufacturers would have to price EVs differently in early years of production than they price conventional vehicles. With the present generation of BEVs and hybrid EVs, manufacturers have either leased vehicles, rather than allowing outright purchases (as with the Honda EV-Plus and GM EV-1), or they have sold the vehicles at prices that are significantly below the full "cost-plus" price (as is the case with the Toyota Prius in Japan).

In a study of potential automobile industry BEV pricing strategies, Green Car Media has shown that several different pricing models are possible. In comparison with the traditional "cost-plus" model, one of the pricing models provided a similar level of overall manufacturer profit after five years, even though the BEVs were sold at a significant loss in the first two years (EPRI, 1996). This "customer oriented" pricing scheme uses lower initial vehicle prices to help

build volume in early years, at the expense of profit, but then profits are recouped in later years when vehicle manufacturing costs are lower. If early generation FCV manufacturing costs turn out to be near the levels estimated here, manufacturers will clearly have to sell (or lease) the vehicles at an initial loss in order to build volume. With lower manufacturing costs in later years, these lost profits may be at least partially recouped, but it is likely that some cross-subsidization with other vehicle lines will also be needed. Thus, the BEV and FCV retail purchase prices estimated here are shown for illustrative purposes, but the actual prices at which vehicles are sold in the market are likely to be quite different, particularly in the early years of vehicle introduction.

Policies and Incentives

EVs are a unique technology from an environmental policy perspective. They are consumer products, meaning that they will only come to be used if consumers choose to buy them, but they also have the potential to provide significant public benefits in the form of reduced air pollution. Unlike other technologies to reduce air pollution, such as pollution control devices for powerplants, the government cannot simply mandate their use in all settings (although California and other states have mandated a small percentage of EV sales with the ZEV mandate).

With regard to mobile-source pollution control measures, there are several important differences between requiring EVs and, for example, requiring pollution control equipment for conventional vehicles. First, while installing catalytic converters for conventional vehicles adds cost that ultimately is passed on to consumers, the additional cost is relatively low. At least in the near term, the incremental costs for EVs will be much higher than the incremental costs of catalyst-equipped versus non-catalyst-equipped conventional vehicles. Second, conventional vehicle performance is only slightly affected by the inclusion of a catalytic converter, and the change is thus relatively transparent to consumers. In contrast, BEVs are likely to have limited driving ranges and long refueling times for many years to come, although FCVs in principle could be similar in virtually all respects to conventional vehicles. Third, BEVs and hydrogen and methanol powered FCVs require access to non-conventional refueling sources. Not everyone will have easy access to these sources (at least in the near term), and this could make EV use impractical for many.

Thus, on one hand, the potential air quality (and other) benefits of EV use suggest a government role in encouraging their proliferation. However, their unique attributes impose barriers against a widespread mandate for their use. The combination of these factors suggests that other policy measures may be appropriate. These policies may include incentives to consumers for EV purchase, incentives to fuel providers for provision of the necessary fuels, and additional policies that could enhance the attractiveness of EV use. Existing and proposed federal policies that fall into these categories are discussed below. There also are a variety of existing state-level and air quality management district (AQMD) policies, although these vary widely from state to state and district to district. The state-level and AQMD policies to encourage EV use in California, that were in effect as of 1994, are discussed in Lipman et al. (1994)

The existing federal tax credit for EVs, of 10% of the price of the vehicle with a maximum credit of $4,000, is scheduled to expire in 2004, just a year after

the full sales requirements of the ZEV mandate take effect (Energy Policy Act of 1992, Title XIX, Section 1913).[53] Two new, companion bills have recently been introduced, one in the House and one in the Senate, that would extend the existing federal tax credit to 2010. These new bills are each called the "Alternative Fuels Promotion Act" (S. 1003 and H.R. 2252). The House bill was sponsored by U.S. Representatives Dave Camp (R-MI) and Sander Levin (R-MI) and introduced on June 17, 1999. The Senate bill was introduced on May 11, 1999 by John Rockefeller (D-WV), Michael Crapo (R-ID), Richard Bryan (D-NV), and Orrin Hatch (R-UT). Both bills would also add an additional $5,000 tax credit for any EV with a 100 or greater mile driving range, provide up to a $30,000 tax credit for constructing alternative fuel refueling stations, and provide a $0.50 per gallon-equivalent of gasoline (on an energy basis) tax credit to sellers of alternative fuels through 2007. The Senate bill would also extend a high-occupancy vehicle lane exemption to AFVs (H.R. 2252 and S. 1003).

If enacted into law, these bills would have a significant impact on the costs of EVs to consumers, and the costs to fuel providers of constructing electricity, methanol, and hydrogen refueling stations and providing hydrogen or methanol fuel. Since no phase-out schedule is indicated for the $5,000 additional tax credit per EV, if it assumed to apply to all BEVs and FCVs sold from 2003 to 2026, and if the existing 10% tax credit follows the proposed new phase-out schedule (7.5% in 2008, 5% in 2009, and 2.5% in 2010), then the total value of the tax subsidy can be calculated for each scenario examined here. For BEVs, the total value of the subsidy would range from 18.0% to 20.8% of the total (undiscounted) cost of the vehicles from 2003 to 2026, depending on the specific low or high production volume and SCAB sales scenario and low, central, or high cost case. For DHFCVs, the total value of the subsidy would range from 12.3% to 19.5% of the total vehicle cost, again depending on the specific case. Finally, for the DMFCV scenarios, with BEVs sold in the years from 2003 to 2010, the total value of the subsidy would range from 13.0% to 20.2% of the total cost of the vehicles.

Since the existing federal tax credit for EVs is scheduled to phase out in 2004, the impact on post-2004 EV purchasers of the enactment into law of either H.R. 2252 or S. 1003 would clearly be quite significant. In fact, there would be a significant impact on EV purchasers from 2002 to 2004 as well, due to the change in the tax credit phase-out schedule. Note that in the later years of the various EV scenarios, the gap in estimated purchase prices between the BEVs/FCVs and the conventional Taurus is about $5,000 to $8,000 (in the central cases). The proposed $5,000 tax credit would thus likely go far to compensate consumers for the incremental cost of BEV or FCV purchases in those years, if the credit were to remain in effect for that long.

In addition to these tax credits for private consumers, the 1992 Energy Policy Act contains provisions for government and private fleet purchases of AFVs. These AFVs may include BEVs and FCVs, but there are no specific

---

[53] The federal tax credit is phased out according to the following schedule: in 2002 the credit is reduced to 7.5 percent of the cost of any qualified EV, in 2003 the credit is reduced to 5 percent, and in 2004 the credit is reduced to 2.5 percent. A "qualified EV" is any motor vehicle that is powered by an electric motor drawing current from rechargeable batteries, fuel cells, or other portable sources of electrical current, so the credit applies to FCVs as well as BEVs (Energy Policy Act of 1992, Title XIX, Section 1913).

requirements for the purchase of any specific type of AFV. So, any decision to purchase BEVs or FCVs would be up to each government agency or other fleet owner. There are differing requirements for federal, state, and other fleets to purchase AFVs. After a phase-in period from 1993 to 1999, the percentages of AFVs that must be purchased are now as follows: 75% of all vehicles for federal fleets (42 USC §13212); 50% of all vehicles for state fleets, rising to 75% in 2000 (42 USC §13257); and 20% for other fleets, rising to 30% in 2002, 40% in 2003, 50% in 2004, 60% in 2005, and 70% in 2006 and thereafter (42 USC §13257).

For purposes of the federal fleet requirements, the term "federal fleet" means a group of 20 or more light duty motor vehicles that are:

- used primarily in a metropolitan area with a 1980 population of more than 250,000;
- centrally fueled or capable of being centrally fueled; and
- owned or controlled by a Federal executive department, military department, Government corporation, independent establishment, or executive agency; the United States Postal Service, the Congress, the courts of the U.S., or the executive office of the President.

Some vehicles, including law enforcement vehicles, emergency vehicles, or those used for purposes of national security, are excluded from the AFV federal fleet requirements (42 USC §13212). The definition of a "fleet" used under the requirements for state and other fleets is similar to that of a "federal fleet" given above, with the additional provision that the fleet must be owned or operated by a governmental entity or other person that owns or controls at least 50 light duty vehicles (Energy Policy Act of 1992, Title III, Section 301).

These fleet AFV purchase requirements provide a potentially attractive niche for BEVs and FCVs. Particularly where fleet vehicles are used heavily, the higher efficiency and lower maintenance requirements of BEVs and FCVs could make them economically attractive, even if capital costs are higher than for some other AFV types. Furthermore, the capacity for these vehicles to be centrally refueled eases the infrastructure issues that BEVs and FCVs face, because dedicated recharging or hydrogen or methanol refueling stations could be built to support the fleet. Since the number of BEVs or FCVs in the fleet would be known, the optimal size of recharging or refueling station could be built, and it could be operated in an efficient manner.

Potential Policies to Encourage ZEV Purchase and Use

In addition to these existing and proposed mandated ZEV sales requirements, ZEV tax credits, AFV fleet purchase requirements, and ZEV HOV lane exemptions, there are a variety of additional policy measures that could be enacted. First, another type of vehicle purchase or registration incentive, that would have a lesser impact on government budgets, would be a revenue-neutral "feebate" scheme. This type of incentive would reward efficient and/or clean vehicles, while penalizing less efficient and/or less clean vehicles. One version of

this type of incentive, the "Drive-Plus" program, was proposed in California but was not enacted into law.

The feebate scheme could either be in the form of a one-time tax credit or penalty for vehicle purchase, or applied to the annual vehicle registration fee. If applied at the federal level as a tax credit or penalty for vehicle purchase, the feebate policy could replace the existing "gas guzzler" tax on inefficient vehicles and the federal tax credit for EVs. The new feebate scheme could provide a more coherent framework for rewarding or penalizing the broad variety of EVs and other AFVs that are now and soon will be offered in the market. One potential drawback with this type of incentive program is that if it were applied to vehicle registration fees it would be regressive, since less efficient and higher emitting vehicles tend to be held by lower income people. In order to offset this, progressive measures could be included, perhaps in the form of a penalty waiver for lower income drivers.

Other types of potential incentives include a simple registration fee waiver for certain types of clean and/or efficient vehicles, incentives to manufacturers for producing EVs (perhaps in the form of accelerated depreciation of EV production capital expenditures), and designated parking spaces for certain types of vehicles. Various packages of these incentives could be offered through different levels of government, in order to incentivize simultaneously the production, sale, and use of EVs.

Past experience has shown that it would probably be much more politically feasible to enact policies to incentivize the purchase and use of clean and/or efficient vehicles, rather than penalizing conventional vehicles through measures such as increased taxes on gasoline (although as discussed above the existing gas-guzzler tax could probably be revised into part of a larger incentive scheme). The budgetary impact of such measures would of course have to be considered, but the social benefits of EV use, especially in heavily polluted urban areas, provide a potentially powerful justification for a reasonable level of government expenditure or revenue loss.

Additional Issues and Questions

The present analysis has sought to investigate many of the important vehicle cost, emissions, and infrastructure issues that will confront BEVs and certain types of FCVs as they enter the marketplace. However, this analysis has necessarily been limited in scope in several important dimensions. These limitations have been discussed at various places in the preceding chapters. The following sections review these limitations, and discuss how future analyses might be expanded to include a broader array of vehicle types and issues.

First, the analysis of FCVs in Chapters 3 and 4 focused only on direct-hydrogen and direct-methanol FCVs. Much manufacturer effort and government funding are at present directed at developing indirect-methanol FCVs, as well as potential other indirectly-fueled FCVs that would run on a low-sulfur type of reformulated or synthetic gasoline. These vehicles would require an onboard fuel reformer, which entails additional system complexity and cost, but which would alleviate the refueling infrastructure and onboard fuel storage issues for direct-hydrogen FCVs. Since these reformer systems are presently at a relatively early stage of development, with unknown manufacturing costs and also uncertain emissions characteristics, indirectly fueled FCVs have not been

included in this analysis. However, developments are occurring rapidly, and within a few years much more will be known about the potential attributes of these vehicle types. At that time, this effort will be revisited and, if funding can be obtained, analysis of indirectly-fueled FCV types will be added. Their potential purchase prices, lifecycle costs, and emission-related costs will be analyzed in comparison with the other vehicle types assessed here. It is worth noting again that, at present, these indirectly-fueled FCVs would not meet the full ZEV mandate requirements for major manufacturers, but this may change with future revisions of the ZEV mandate.

Second, the analysis of the infrastructure and emission-related costs for direct-hydrogen FCVs included only the scenario in which hydrogen would be produced in a decentralized fashion, with small-scale steam reformation at service stations, and stored onboard the vehicles as a compressed gas. There are many other ways in which hydrogen could in principle be provided and stored. These include: production of hydrogen via large-scale steam reformation, coupled with truck delivery of liquid hydrogen or pipeline delivery of gaseous hydrogen; hydrogen production via electrolysis (either with solar, wind, or grid power); hydrogen production from biomass feedstocks; and storage of hydrogen with any of the myriad hydrogen storage technologies discussed in Chapter 3. Future revisions to this analysis may consider an expanded array of hydrogen production and storage strategies.

Third, this analysis did not consider all categories of social costs, but rather focused on the types of costs that are likely to produce significant differences among the three ZEV types assessed. A full social cost analysis would consider many additional potential costs to society of changes in vehicle technology. These additional social costs might include:

- damage or control costs from an expanded array of pollutants from fuel production and vehicle operation (including, for example, toxic pollutants such as benzene and butadiene);
- damage or control costs from emissions from vehicle manufacture;
- damage costs from emissions of PM from road dust and tire and brake wear;
- costs associated with changes in energy use patterns (such as, for example, the reduced risk of marine oil spills and the potential effects on the U.S. economy of oil import reductions);
- potential health and mortality costs associated with safety differences among vehicles and fuels;
- the external costs of vehicle noise; and
- possible "hedonic" costs and benefits from differences in the satisfaction that vehicle users derive from various attributes of different types of vehicles (such as, for example, differences in interior vehicle noise, driving enjoyment, satisfaction over driving a less polluting vehicle, etc.).

The inclusion of all of these types of costs might significantly affect the relative social costs of the different ZEV types assessed here, and the relative social costs of ZEVs and conventional vehicles.

Finally, one issue that has been addressed only incompletely here is that there may be electronic control issues for hybrid FCVs beyond those discussed in Chapters 3 and 4. For the present analysis, the electronic controls needed for all FCVs are assumed to be slightly higher ($3 per kW) than those for BEVs due to the additional complexity of controlling the fuel cell stack auxiliary systems (e.g., the air compressor, the fuel flow controls, and the thermal management system). However, it is possible that hybrid FCVs would require an additional high-power DC/DC converter to regulate the voltage of their dual DC power sources. If required, this additional DC/DC converter would be more costly than the (~$70) low-power DC/DC converter that is integrated into the main motor inverter/controller to provide 12V power to auxiliary systems, because it would operate with higher current levels. The manufacturing cost of this additional converter might be on the order of $250 to $350 in high volume production (based on cost estimates for simple brush DC motor controllers). The costs of this additional DC/DC converter have not been included for the hybrid FCVs here because it is not entirely clear that the main inverter/controller could not be modified (at low cost) to manage the dual power system, and because cost estimates for this novel component are not yet available. In future revisions, if it appears that this component will in fact be required for hybrid FCVs, then its cost will be included. It is worth noting that the other publicly available hybrid FCV cost analyses conducted to date also do not include the costs of an additional high-power DC/DC converter (DeLuchi, 1992; Ogden, et al., 1999; Thomas, et al., 1998a).

Conclusions

The automobile industry is entering a period of rapid technological innovation. New vehicle types, many of which are based in part or in full on electric drive systems, are beginning to compete with conventional, gasoline ICE vehicles. Just as gasoline, electric, and steam powered vehicles competed in the market in the early 1900s, with the ultimate outcome of the competition impossible to predict, it also is impossible at this point to know how the emerging competition among conventional vehicles, hybrid gasoline/electric and diesel/electric vehicles, BEVs, FCVs, and other AFVs will ultimately play out. The dynamics of technological innovation and diffusion are extremely complex, and social, economic, regulatory, and political factors all will have an influence on technological evolution in the automotive industry. Ultimately, however, technological change is inevitable. In the words of Joseph Schumpeter (1939) the "winds of creative destruction" will blow, resulting in new waves of technologies that will supplant the old.

James Utterback, building on the work of William Abernathy, has postulated that new technologies move from a "fluid phase," in which designs are experimental and no clear favorite has emerged, to a "specific phase." When the specific phase is achieved, a dominant product design is established, competition drives many firms from the industry, and technology production cost, rather than design, begins to dominate as the crucial factor in the competition of the industry (Utterback, 1994; Utterback and Suarez, 1991). At present, the

automobile industry is in the fluid phase. Many industry experts believe that new vehicle designs based on fuel cells, electric drive systems, and lightweight materials are likely to compose the next “dominant design.”

For other individuals, however, it is difficult to envision radical change in motor vehicle technology. The motor vehicle system has for many years been almost entirely dominated by a mature, "locked-in" technology: the steel-bodied, gasoline-fueled, ICE vehicle. This lock-in situation has several important implications. First, the entire motor vehicle system, including vehicle refueling infrastructure, has been built over decades to support gasoline vehicles exclusively. Any major changes to this infrastructure will be expensive. Second, the characteristics of gasoline automobiles have come to define how we believe a vehicle should perform, and vehicles that offer performance differences compared to conventional vehicles will face an uncertain consumer response, particularly since the characteristics of new vehicle technologies are themselves changing rapidly. Third, to the extent that new technologies are to be adopted, early adoptions will lead to improvements in the technology that will benefit later users, but there is no market mechanism for early adopters to be compensated for their experimentation that later provides benefits to others. Since there is no compensatory mechanism, few are likely to be willing to gamble on producing and purchasing new technologies, and the market is likely to undersupply experimentation as a result (Cowan and Kline, 1996). Hence, in the absence of policy intervention, we may remain locked-in to the existing technology, even if the benefits of technology switching overwhelm the costs.

There are numerous examples, however, of an entrenched or locked-in technology being first challenged and ultimately replaced by a competing technology. This process is generally enabled by a new wave of technology, and it is sometimes achieved through a process of hybridization of the old and the new. Technological "leapfrogging" is another possibility, but this seems to occur relatively rarely. A prime example of the hybridization concept is in the case of utility-scale power generating systems, where the competition between gas and steam powered generators dates back to the beginning of the century. From about 1910 to 1980, the success of steam turbines led to a case of technological lock-in, and to the virtual abandonment of gas turbine research and development. However, partly with the aid of "spillover" effects from the use of gas turbines in aviation, the gas turbine was able to escape the lock-in to steam turbine technology. First, gas turbines were used as auxiliary devices to improve steam turbine performance, and then they slowly became the main component of a hybridized, "combined-cycle" system. In recent years, orders for thermal power stations based primarily on gas turbines have increased to more than 50% of the world market, up from just 15-18% in 1985 (Islas, 1997).

Brian Arthur (1989) has shown that increasing returns to adoption, or "positive feedbacks," can be critical to determining the outcomes of technological competitions in situations where increasing returns occur. These increasing returns can take various forms, including the following: industrial learning (e.g., learning-by-doing in manufacturing, along with economies of scale, leads to production cost declines); network related externalities (e.g., networks of complementary products, once developed, encourage future users); returns on information (e.g. information about product quality and reliability decreases uncertainty and reduces risk to future adopters); and/or better compatibility

with other technologically interdependent systems. Where increasing returns are important, as in most technology markets, the success with which a challenger technology can capture these effects and enter the virtuous cycle of positive feedbacks may, in conjunction with chance historical events,[54] determine whether or not the technology is ultimately successful.

Thus, due to the present lock-in to ICE vehicle technology, the complicated nature of technological evolution, and the present rapid pace of new motor vehicle technology development, it is not at this point clear what set of motor vehicle technologies will supplant the internal combustion engine, or when this will occur. For a variety of reasons, however, automotive fuel cell technology looks very promising, particularly for use along the California South Coast. First, the air pollution problem is serious enough in the region that regulators are insisting that zero tailpipe-emission vehicles be included in the regulated mix of motor vehicles. Second, BEVs are likely to suffer from limited driving ranges and long recharge times for quite some time. Third, fuel cell vehicles can be powered by a range of different fuels, and this flexibility offers choices in the manner in which they are brought to market. Fourth, fuel cells are an inherently efficient and "clean" technology, in principle free from any emissions other than water vapor, and also free from the efficiency limitations of heat engines.

This analysis has shown that the discounted net present value of the total vehicle, infrastructure, and emission-related costs associated with various multi-year scenarios of ZEV introduction is likely to be lower for BEVs than for DHFCVs or DMFCVs. This is largely because the manufacturing costs of BEVs in the early years of the scenarios are likely to be lower than the costs of FCVs, and net present values calculated with a positive discount rate emphasize near-term costs relative to long-term costs. However, after several years of technology evolution and cost reduction, the manufacturing costs and retail prices for all three ZEV types become quite comparable. Only if fuel cell technology cost reductions are very slow are the costs of hybrid or "pure" FCVs likely to significantly exceed the costs of comparable BEVs, after ten or fifteen years of technology development. It is important to note, though, that based on how close the final scenario net present value, vehicle retail price, and vehicle lifecycle cost results are for all three ZEV scenarios, and the degree of overlap in the uncertainty bands around the results, it is not possible at this time to unequivocally say which ZEV type would be a superior choice for the Los Angeles area. Doing so will require uncertainties in key input variables to be narrowed, and this will only be possible in time with improved data.

However, this analysis has shown that likely FCV technology cost reductions, coupled with improved system power densities, could result in FCVs with lifecycle costs that are very comparable with those of conventional vehicles. When emission-related and infrastructure costs are included along with vehicle

---

[54]Consider, for example, the case of the "Dymaxion Car;" the 1933 vehicle designed by Buckminster Fuller. With one wheel in the rear and two in front, the 20-foot, 11-seat car could perform a U-turn in less than its own length, achieve about 30 miles per gallon due to its raindrop shape, and reportedly reach a top speed of 120 mph. Due to a crash while racing in 1935 (that may have been the fault of another vehicle) and the subsequent bad publicity, investors were scared away and the project to produce the vehicle was halted (Rennie, 1997).

lifecycle costs, the central case results show that DHFCVs used in the SCAB could have lower total costs than even gasoline LEVs. The total costs associated with BEVs and DMFCVs are likely to fall in between the total costs of present-day ICE vehicles, and the costs of future ICE LEVs.

This finding, that certain ZEV types can over a reasonably short timeframe compete favorably with conventional vehicles on a lifecycle cost basis, is significant. It suggests that if consumers can be educated to consider vehicle lifecycle costs as well as initial purchase prices, then vehicle purchase price incentives may not be needed in the future in order for consumers to find ZEV purchases attractive. Furthermore, the lower external costs of ZEVs, relative to even ICE LEVs, has potentially profound implications for urban air quality as well as climate change. Particularly given the explosion of automobile use that is occurring in the developing world, the timely production and adoption of ZEV and/or near-ZEV technologies could affect the future health of millions, if not billions, of individuals. Perhaps even more significantly, BEV and FCV technologies offer a flexibility of energy supply that includes the potential use of renewable solar, wind, and biomass fuel sources. Pathways of vehicle development and fuel production that result in greater reliance on these renewable energy sources are almost certainly the best hope for alleviating the climate change impacts of motor vehicle use. Historical perspective may show that reducing the rate and extent of climate change is among the most important challenges that the present generation will face, in the struggle to balance the needs and wants of human civilization with the limits of a small and fragile planet.

Tables and Large Figures for Chapter 7

Table 7-1: Lifecycle Cost Breakdowns for Year 2026, High Production Volume, Central Case, Mid-Sized Vehicles (1997¢/mi)

Lifecycle cost category	Gasoline ICEV	BEV	DHFCV	DMFCV
Purchased electricity ($0.065/kWh)	0.00	2.73	0.00	0.00
Vehicle (excluding battery, fuel cell, and hydrogen storage)	17.61	14.65	14.26	14.48
Battery, tray, and aux. (+ recharger for BEV)	0.00	10.93	2.68	2.71
Fuel, excluding excise taxes[a]	5.56	inc. in elect.	3.02	6.66
Fuel storage system	inc. in vehicle	0.00	1.28	0.08
Fuel cell system	0.00	0.00	2.84	3.47
Insurance[b]	6.77	7.88	7.86	7.72
Maintenance and repairs (excluding oil and inspection)	4.88	3.72	4.17	4.32
Oil	0.17	0.00	0.00	0.00
Replacement tires[c]	0.50	0.45	0.32	0.32
Parking, tolls, and fines	1.05	1.05	1.05	1.05
Registration fees[d]	0.50	0.48	0.45	0.46
Vehicle safety and emissions inspection fees	0.60	0.21	0.21	0.21
Federal, state, and local fuel excise taxes[e]	1.75	1.75	1.75	1.75
Accessories	0.30	0.30	0.30	0.30
Total lifecycle cost	**39.68 ¢/mi**	**44.15 ¢/mi**	**40.19 ¢/mi**	**43.52 ¢/mi**

Notes:

[a]Based on fuel costs of $1.20/gallon for gasoline, $9.47/MMBTU for hydrogen, and $0.91/gallon ($14.01/MMBTU) for methanol.

[b]Calculated with a complex formula that estimates physical damage and liability insurance premiums as a function of VMT and vehicle value. Insurance premiums related to theft and damage costs are estimated to be proportional to vehicle value, while premiums for personal injury related costs are assumed to be independent of vehicle value. See Delucchi (1999) for details.

[c]Calculated as a function of VMT and vehicle mass. Tire wear is estimated to be proportional to vehicle mass, and a linear function of VMT. If a scheduled tire replacement falls near the

vehicle scrappage date (i.e., if the owner would get 20% or less of the full life of the last set of tires) then no final tire replacement occurs and the last set of tires is worn past the usual point of replacement (presumably the DHFCVs and DMFCVs shown in the table have one less tire replacement then the ICEV and BEV due to this assumption, and this along with their somewhat lower mass accounts for their significantly lower cost of tire replacement).

[d]Calculated as a linear function of vehicle mass, with a fee of $50 per year for the baseline ICEV (based on the fact that most states charge vehicle mass-based registration fees with a range of fees of $20 to $100 per year).

[e]Fuel taxes are assumed to be proportional to VMT, such that all vehicles have the same per-mile fuel tax.

Table 7-2: Fuelcycle Emissions for Light-Duty Gasoline ICE Vehicles (g/mi)

	GHGs (gCO_2-eq)	NMOG	CO	NOx	PM_{10}	SOx
Petroleum Extraction and Gasoline Production:						
Acurex (1996b) – 1992	[58.73][a]	(.05024) .1294	(.01070) .00655	(.01968) .07587	N.E.	N.E.
Acurex (1996b) – 2010	[44.03][a]	(.02125) .09161	(.00278) .00555	(.00973) .09543	N.E.	N.E.
Delucchi (1997) - 2000	[109.73]	[0.054]	[0.231]	[0.305]	[0.034]	[0.373]
Delucchi (1997) - 2015	[87.73]	[0.045]	[0.193]	[0.255]	[0.029]	[0.312]
Gasoline Distribution and Dispensing:						
Acurex (1996b) – 1992	(0.68)[a]	(.05044)	(.00287)	(.00614)	N.E.	N.E.
Acurex (1996b) – 2010	(0.46)[a]	(.00680)	(.00205)	(.00240)	N.E.	N.E.
Delucchi (1997) - 2000	(6.21)	(0.103)	(0.0098)	(0.025)	(0.0049)	(0.015)
Delucchi (1997) - 2015	(4.95)	(0.086)	(0.0082)	(0.021)	(0.0041)	(0.012)
Exhaust Emissions:						
An et al. (1995) - ~1990	N.E.	(0.34)	(4.0)	(0.37)	N.E.	N.E.
Ross et al. (1995) – 2000	N.E.	(0.22)	(2.9)	(0.26)	N.E.	N.E.
Ross et al. (1995) – 2010	N.E.	(0.11)	(1.4)	(0.13)	N.E.	N.E.
Delucchi (1997) – 2000[b]	(454.4)	N.R.	N.R.	N.R.	N.R.	N.R.
Delucchi (1997) – 2015[b]	(370.7)	N.R.	N.R.	N.R.	N.R.	N.R.
CARB (1997) – LEV Std.	--	(0.075)	(3.4)	(0.20)	(0.0006-0.0008)[c]	--
Evaporative Emissions:						
Ross et al. (1995)	--	(0.37)	--	--	--	--
CARB (1997) – EMFAC7G	--	(0.07)	--	--	--	--
Off-Cycle and Malfunction:						
An et al. (1995) - ~1990	N.E.	(0.60)	(12.0)	(1.07)	N.E.	N.E.
Ross et al. - 2000	N.E.	(0.54)	(8.0)	(0.69)	N.E.	N.E.
Ross et al. - 2010	N.E.	(0.24)	(5.0)	(0.32)	N.E.	N.E.
Total Modeled Emissions:						
In-basin – near term	[570]	(1.411)	(16.014)	(1.466)	(0.006)	(0.015)
Out-of-basin – near term		0.129	0.007	0.076	0.034	0.373
In-basin – future LEV	[463]	(0.413)	(8.405)	(0.532)	(0.005)	(0.012)
Out-of-basin – future LEV		0.092	0.006	0.095	0.029	0.312

Notes: CO = carbon monoxide; GHGs = greenhouse gases; LEV = low-emission vehicle; N.E. = not estimated; NMOG = non-methane organic gases; NOx = oxides of nitrogen; N.R. = not explicitly reported; PM_{10} = particulate matter less than 10 microns in diameter; SOx = oxides of sulfur. Values in parentheses are in-basin emissions. Values in brackets are mostly out-of-basin but may contain an in-basin component. All others are out-of-basin. All GHG estimates reflect

Acurex's assumptions of 23.0 mpg for year 1992-2000 vehicles, and 27.5 mpg for 2010-2015 vehicles.

[a] These estimates include emissions of CO_2 and CH_4 only.

[b] These figures were calculated from Delucchi's estimates of 354.3 gCO_2-eq. in 2000 and 345.6 gCO_2-eq. to reflect the mpg estimates used here (Delucchi's estimates are based on 29.5 mpg in 2000 and 2015).

[c] There is currently no PM standard for light-duty gasoline vehicles in California. Recent tests by the Environmental Research Consortium (the Big 3), reported in CARB (1997) have measured PM levels shown in the table for light-duty vehicles running on California Phase 2 gasoline. The 0.0006 g/mi estimate was the average of tests of six low-mileage vehicles, and the 0.0008 g/mi estimate was the average of tests of three high-mileage vehicles.

Table 7-3: BEV Purchase Prices, Lifecycle Costs and Characteristics by Driving Range (Generation 4, Central Case, year 2026, High Production Volume)

Category	**100-mile Range**	**126-mile Range (base case)**	**150-mile Range**	**200-mile Range**
Vehicle mass	1,232 kg	1,306 kg	1,381 kg	1,557 kg
Drivetrain power	65 kW	69 kW	73 kW	81 kW
Motor/controller OEM cost	$702/$806	$745/$829	$788/$867	$875/$928
Battery pack energy	22.2 kWh	28.8 kWh	36.3 kWh	53.3 kWh
Battery cell capacity	77 Ah	100 Ah	126 Ah	185 Ah
Battery OEM cost	$3,969	$4,421	$5,123	$6,354
Battery OEM cost per kg	$20.26/kg	$17.68/kg	$16.98/kg	$14.87/kg
Battery cycle life	1,801 cycles (6.1 years)	1,708 cycles (8.0 years)	1,635 cycles (9.8 years)	1,507 cycles (14.3 years)
Battery lifecycle cost	12.39 ¢/mi	10.74 ¢/mi	11.28 ¢/mi	6.89 ¢/mi
Vehicle purchase price	**$25,189**	**$25,990**	**$27,221**	**$29,400**
Vehicle lifecycle cost	**45.23 ¢/mi**	**44.15 ¢/mi**	**45.21 ¢/mi**	**41.95 ¢/mi**

Table 7-4: DHFCV Purchase Prices, Lifecycle Costs and Characteristics by Driving Range (Generation 4, Central Case, year 2026, High Prod. Volume)

Category	**200-mile Range**	**250-mile Range**	**300-mile Range (base case)**	**400-mile Range**
Vehicle mass	1,196 kg	1,211 kg	1,227 kg	1,256 kg
Drivetrain power	63 kW	64 kW	65 kW	66 kW
Motor/controller OEM cost	$680/$791	$691/$798	$702/$806	$713/$814
Battery pack energy	5.18 kWh	5.18 kWh	5.18 kWh	5.18 kWh
Battery module peak power	650 W/kg	650 W/kg	650 W/kg	650 W/kg
Battery cell capacity	18 Ah	18 Ah	18 Ah	18 Ah
Fuel cell system power (gross/net)	24.0/19.3 kW	25.0/20.1 kW	26.0/20.9 kW	28.0/22.5 kW
Fuel cell system OEM cost	$1,592	$1,658	$1,724	$1,857
Hydrogen stored	4.63 kg	5.70 kg	6.79 kg	9.02 kg
Vehicle purchase price	**$25,238**	**$25,572**	**$25,910**	**$26,569**
Vehicle lifecycle cost	**39.01 ¢/mi**	**40.10 ¢/mi**	**40.19 ¢/mi**	**40.79 ¢/mi**

Table 7-5: DMFCV Purchase Prices, Lifecycle Costs and Characteristics by Driving Range (Generation 4, Central Case, year 2026, High Prod. Volume)

Category	**200-mile Range**	**250-mile Range**	**300-mile Range (base case)**	**400-mile Range**
Vehicle mass	1,211 kg	1,226 kg	1,241 kg	1,269 kg
Drivetrain power	64 kW	65 kW	65 kW	67 kW
Motor/controller OEM cost	$691/$798	$702/$806	$702/$806	$724/$821
Battery pack energy	5.18 kWh	5.18 kWh	5.18 kWh	5.18 kWh
Battery module peak power	650 W/kg	650 W/kg	650 W/kg	650 W/kg
Battery cell capacity	18 Ah	18 Ah	18 Ah	18 Ah
Fuel cell system power (gross/net)	25.5/20.3 kW	26.5/21.1 kW	27.5/21.9 kW	29.0/23.0 kW
Fuel cell system OEM cost	$1,938	$2,014	$2,090	$2,204
Methanol stored	44.5 kg	54.6 kg	64.8 kg	85.7 kg
Vehicle purchase price	**$24,965**	**$25,146**	**$25,302**	**$25,613**
Vehicle lifecycle cost	**42.77 ¢/mi**	**43.65 ¢/mi**	**43.52 ¢/mi**	**43.73 ¢/mi**

Table 7-6: Sensitivity of Scenario Cost Net Present Values to Discount Rate

Discount Rate and Case	Defuzzification Method	Result
3.00% Discount Rate:		
Low Production Volume	Chang's Method	BEV<DMFCV<DHFCV
	Kaufman and Gupta's Method	BEV<DHFCV<DMFCV
	TFN Modes	BEV<DHFCV<DMFCV
	MATLAB Centroid	BEV<DHFCV<DMFCV
	MATLAB Bisector	BEV<DHFCV<DMFCV
High Production Volume	Chang's Method	BEV<DHFCV<DMFCV
	Kaufman and Gupta's Method	BEV<DHFCV<DMFCV
	TFN Modes	DHFCV<BEV<DMFCV
	MATLAB Centroid	BEV<DHFCV<DMFCV
	MATLAB Bisector	BEV<DHFCV<DMFCV
3.65% Discount Rate:		
Low Production Volume	Chang's Method	BEV<DMFCV<DHFCV
	Kaufman and Gupta's Method	BEV<DHFCV<DMFCV
	TFN Modes	BEV<DHFCV<DMFCV
	MATLAB Centroid	BEV<DHFCV<DMFCV
	MATLAB Bisector	BEV<DHFCV<DMFCV
High Production Volume	Chang's Method	BEV<DHFCV<DMFCV
	Kaufman and Gupta's Method	BEV<DHFCV<DMFCV
	TFN Modes	DHFCV<BEV<DMFCV
	MATLAB Centroid	BEV<DHFCV<DMFCV
	MATLAB Bisector	BEV<DHFCV<DMFCV
5.00% Discount Rate:		
Low Production Volume	Chang's Method	BEV<DMFCV<DHFCV
	Kaufman and Gupta's Method	BEV<DHFCV<DMFCV
	TFN Modes	BEV<DHFCV<DMFCV
	MATLAB Centroid	BEV<DHFCV<DMFCV
	MATLAB Bisector	BEV<DHFCV<DMFCV
High Production Volume	Chang's Method	BEV<DMFCV<DHFCV
	Kaufman and Gupta's Method	BEV<DHFCV<DMFCV
	TFN Modes	DHFCV<BEV<DMFCV
	MATLAB Centroid	BEV<DHFCV<DMFCV
	MATLAB Bisector	BEV<DHFCV<DMFCV
7.00% Discount Rate:		
Low Production Volume	Chang's Method	BEV<DMFCV<DHFCV
	Kaufman and Gupta's Method	BEV<DMFCV<DHFCV
	TFN Modes	BEV<DHFCV<DMFCV
	MATLAB Centroid	BEV<DMFCV<DHFCV
	MATLAB Bisector	BEV<DMFCV<DHFCV
High Production Volume	Chang's Method	BEV<DMFCV<DHFCV
	Kaufman and Gupta's Method	BEV<DHFCV<DMFCV
	TFN Modes	DHFCV<BEV<DMFCV
	MATLAB Centroid	BEV<DHFCV<DMFCV
	MATLAB Bisector	BEV<DHFCV<DMFCV

Figure 7-33:

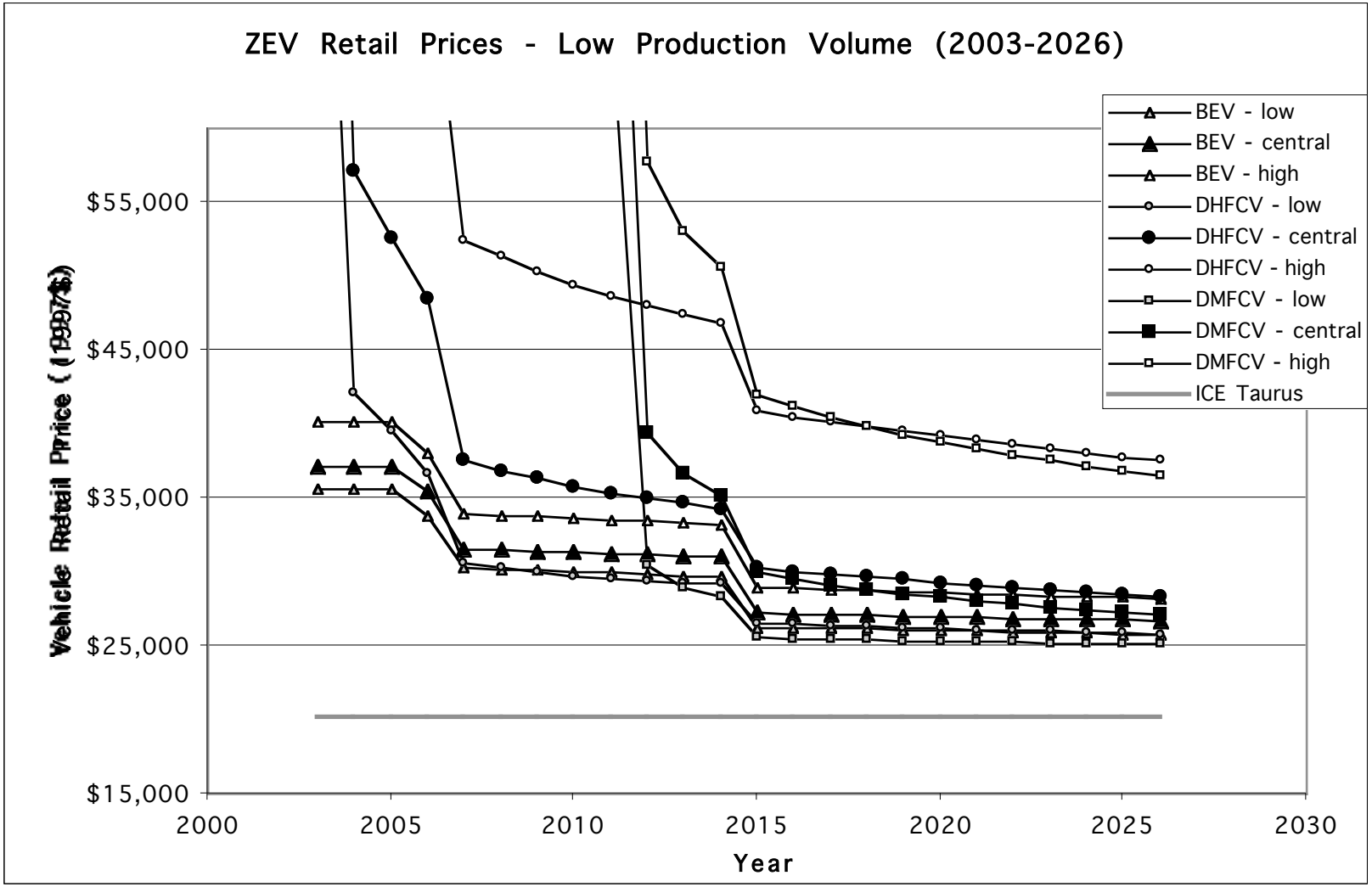
ZEV Retail Prices - Low Production Volume (2003-2026)
BEV - low
BEV - central
BEV - high
DHFCV - low
DHFCV - central
DHFCV - high
DMFCV - low
DMFCV - central
DMFCV - high
ICE Taurus
$55,000
$45,000
$35,000
$25,000
$15,000
2000
2005
2010
2015
2020
2025
2030
Year

Figure 7-34:

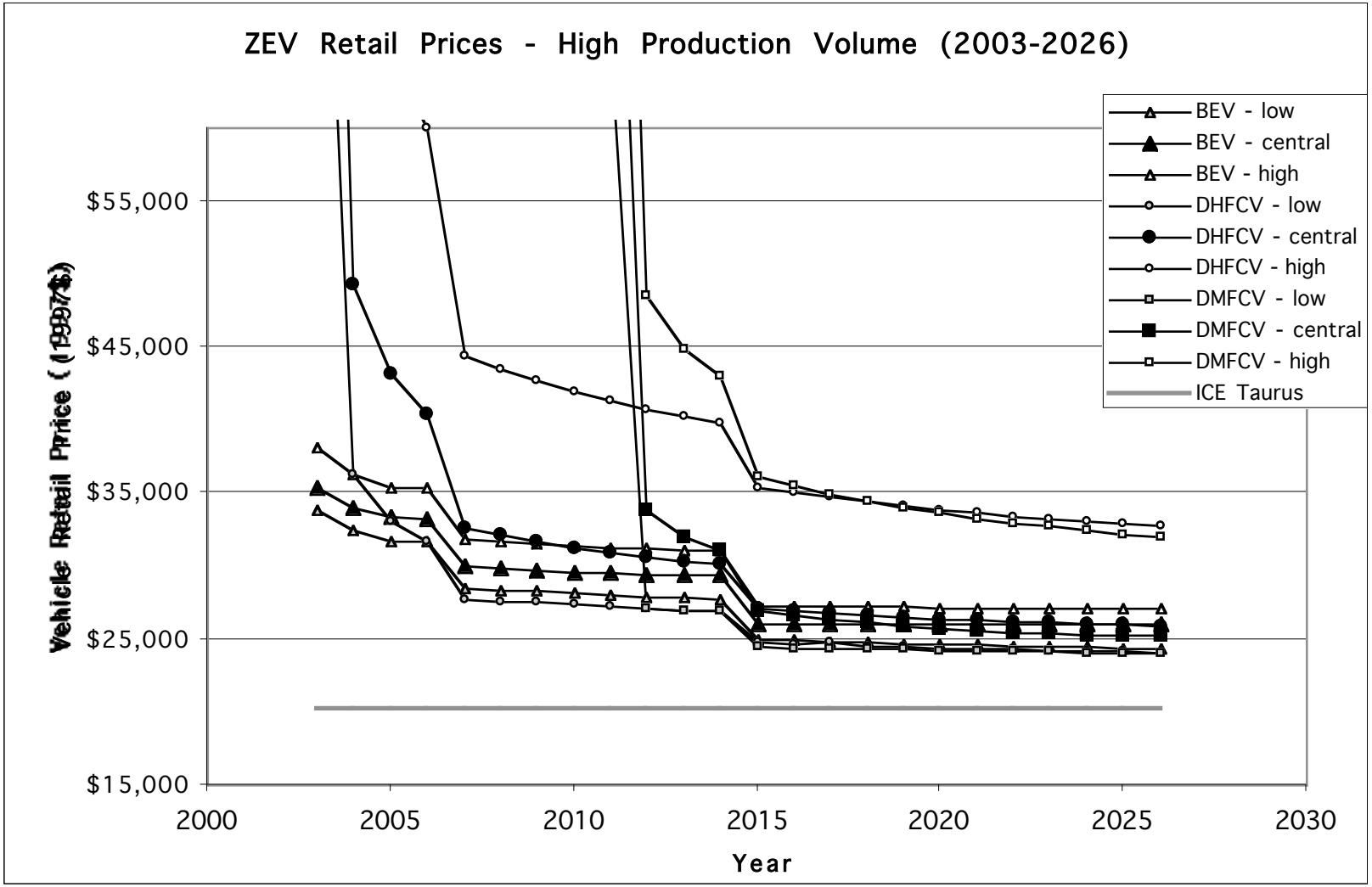
ZEV Retail Prices - High Production Volume (2003-2026)
BEV - low
BEV - central
BEV - high
DHFCV - low
DHFCV - central
DHFCV - high
DMFCV - low
DMFCV - central
DMFCV - high
ICE Taurus
$55,000
$45,000
$35,000
$25,000
$15,000
2000
2005
2010
2015
2020
2025
2030
Year

Figure 7-35:

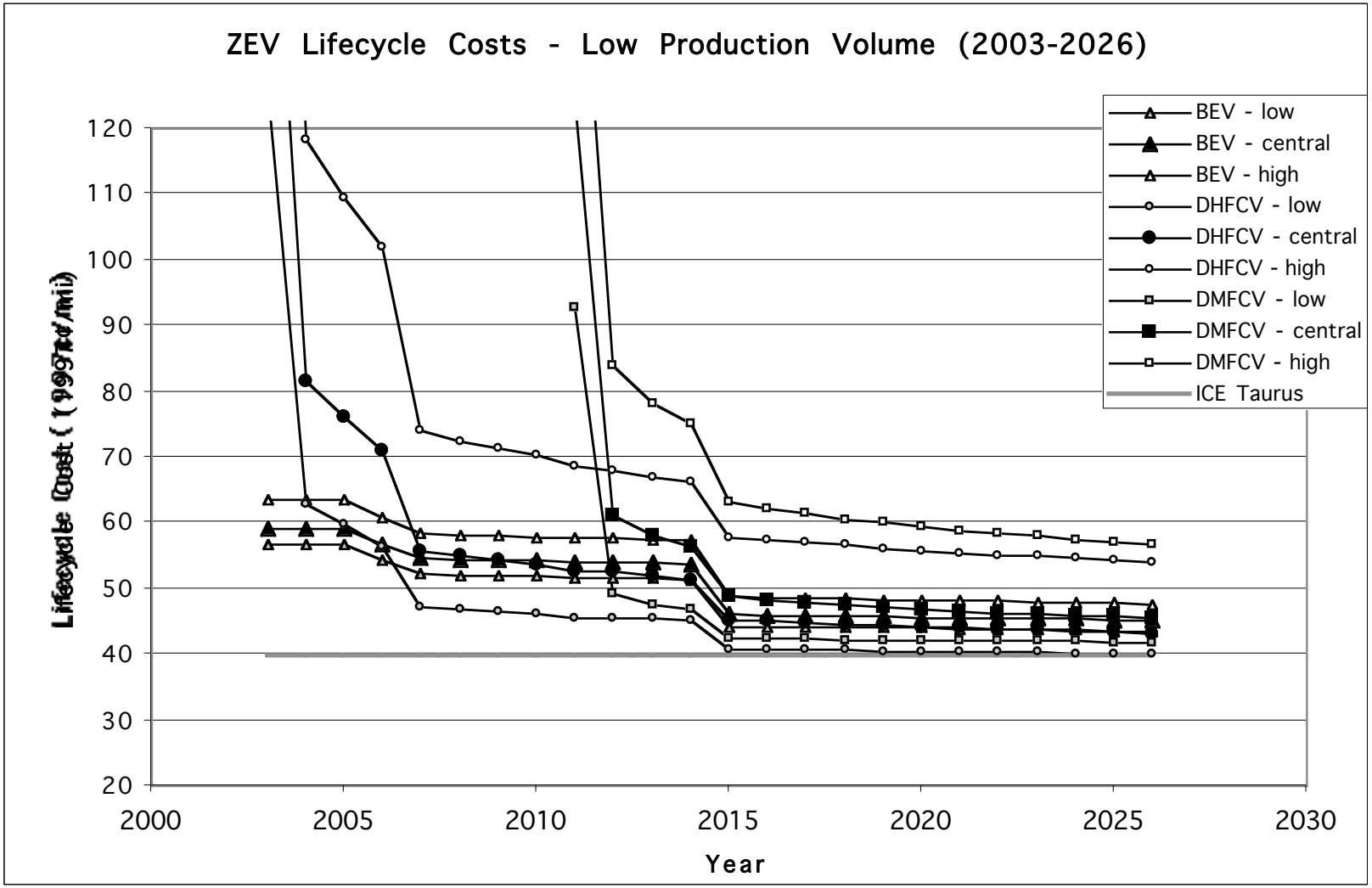
ZEV Lifecycle Costs - Low Production Volume (2003-2026)
BEV - low
BEV - central
BEV - high
DHFCV - low
DHFCV - central
DHFCV - high
DMFCV - low
DMFCV - central
DMFCV - high
ICE Taurus
120
110
100
90
80
70
60
50
40
30
20
2000
2005
2010
2015
2020
2025
2030
Year

Figure 7-36:

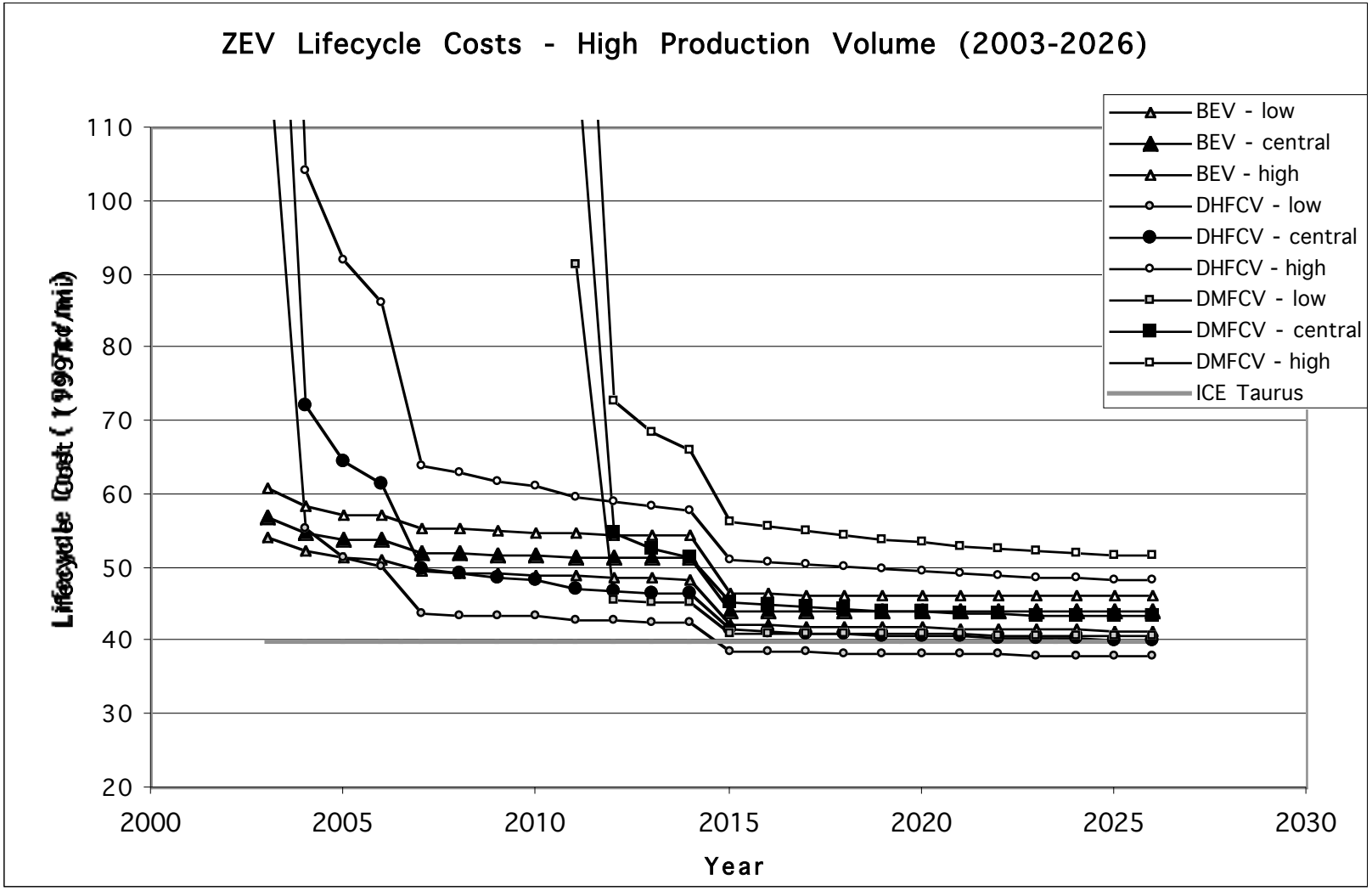
ZEV Lifecycle Costs - High Production Volume (2003-2026)
BEV - low
BEV - central
BEV - high
DHFCV - low
DHFCV - central
DHFCV - high
DMFCV - low
DMFCV - central
DMFCV - high
ICE Taurus
110
100
90
80
70
60
50
40
30
20
2000
2005
2010
2015
2020
2025
2030
Year

References

M.G. Abdel-Kader et al., *Investment Decisions in Advanced Manufacturing Technology: A Fuzzy Set Theory Approach*, Ashgate Publishing Ltd., Aldershot (1998).

W.J. Abernathy and K. Wayne, "Limits of the Learning Curve," *Harvard Business Review* **52**(5): 109-119 (1974).

American Council for an Energy Efficient Economy, *Development of Cost Estimates for Fuel Economy Technologies*, Manufacturing cost estimates prepared by L.H. Lindgren for M. Ledbetter, Washington, D.C., (1990).

S.M. Aceves et al., "Insulated Pressure Vessels for Hydrogen Storage on Vehicles," *International Journal of Hydrogen Energy* **23**(7): 583-591 (1998).

Acurex Environmental Corporation, *Evaluation of Fuel-Cycle Emissions on a Reactivity Basis: Volume 1 - Main Report*, FR-96-114, Prepared for California Air Resources Board, Mountain View, September 19 (1996a).

Acurex Environmental Corporation, *Evaluation of Fuel-Cycle Emissions on a Reactivity Basis: Volume 2 - Appendices*, FR-96-114, Prepared for California Air Resources Board, Mountain View, September 19 (1996b).

J. Adams, *Presentation to CARB Zero Emission Technology Review Workshop*, GM Ovonics, El Monte, California (1995).

W. Almeida, Personal Communication, Vista Metals, Inc., April 20 (1998).

C.v. Altrock and B. Krause, "Multi-criteria decision making in German automotive industry using fuzzy logic," *Fuzzy Sets and Systems* **63**: 375-380 (1994).

K.A.G. Amankawah et al., "Hydrogen storage on superactivated carbon at refrigeration temperatures," *International Journal of Hydrogen Energy* **14**: 437-447 (1990).

American Methanol Institute, "http://www.methanol.org/methanol/fact/Wldexp.pdf," June 24 (1999a).

American Methanol Institute, "http://www.methanol.org/methanol/fact/Wldmeohs.pdf," June 24 (1999b).

American Methanol Institute, "http://www.methanol.org/methanol/fact/Meoh89.pdf," June 24 (1999c).

AMM Online, "http://www.amm.com/ref/platgrp.htm," August 3 (1999).

F. An et al., "Vehicle Total Life-Cycle Exhaust Emissions," *Society of Automotive Engineers* **951856**: 147-157 (1995).

B.A. Andersson and I. Rade, *Large-Scale Electric-Vehicle Battery Systems: Long-Term Material Constraints*, Hamburg, Germany (1998).

L. Argote and D. Epple, "Learning Curves in Manufacturing," *Science* **247**(February 23): 920-924 (1990).

W.B. Arthur, "Competing Technologies, Increasing Returns, and Lock-In By Historical Events," *The Economic Journal* **99**(March): 116-131 (1989).

T.C. Austin and L.C. Caretto, *Powerplant Emissions and Energy Consumption Associated with Electric Vehicle Recharging* (1995).

Automotive News, "Car and Truck Production Figures," *Automotive News*, December 28, p. 46 (1998).

B. Bahar, *Membrane Electrode Assemblies Economic Considerations*, Intertech Conferences, Chicago (1996).

Ballard, "http://www.ballard.com/viewpressrelease.asp?sPrID=90," August 5 (1999).

Ballard Power Systems Inc., *1998 Annual Report: Building Customer Relationships*, Vancouver, (1998).

H. Bandemer and S. Gottwald, *Fuzzy Sets, Fuzzy Logic, Fuzzy Methods*, John Wiley and Sons, New York (1995).

A. Banerjee and A. T-Raissi, *Systems Study of Metal Hydride Storage Requirements (Draft)*, Report for NREL, FSEC-CR-760-94, Florida Solar Energy Center, Cape Canaveral, (1994).

T. Banisch, Personal Communication, Kensington, Inc., May 5 (1998).

K. Barnes, Personal Communication, Unique Mobility, Inc., September 23, 1998 (1998).

J. Bennett, Personal Communication, Hollingsworth-Vose Co., October 30 (1997).

J.M. Bentley, P. Teagan, D. Walls, E. Balles, and T. Parish, *The Impact of Electric Vehicles on CO2 Emissions*, EGG-EP-10296, EG&G Idaho, Inc., Cambridge, May (1992).

G.D. Berry, *Hydrogen as a Transportation Fuel: Costs and Benefits*, UCRL-ID-123465, Lawrence Livermore National Laboratory, Livermore, March (1996).

G.D. Berry and S.M. Aceves, "Onboard Storage Alternatives for Hydrogen Vehicles," *Energy and Fuels* **12**(1): 49-55 (1998).

B. Bonnice, Personal Communication, SatCon Technology Corp., March 24 (1999).

Booz-Allen & Hamilton Inc., *Zero-Emission Vehicle Technology Assessment*, 95-11, New York State Energy Research and Development Authority, McLean, August (1995).

R.H. Borgwardt, "Methanol Production from Biomass and Natural Gas as Transportation Fuel," *Industrial Engineering Chemical Research* **37**(9): 3760-3767 (1998).

Boston Consulting Group, *Perspectives on Experience*, Boston (1972).

K. Bradsher, "Can Motor City Come Up With A Clean Machine?," *The New York Times*, May 19, pp. D1,21 (1999).

D. Brandmeyer, Personal Communication, Battelle, November 11 (1997).

S.F. Brown, "The Automakers' Big-Time Bet on Fuel Cells," *Fortune*, March 30, pp. 122 B-D (1998).

C. Bruhl, "The Impact of the Future Scenarios for Methane and Other Chemically Active Gases on the GWP of Methane," *Chemosphere* **26**(1-4): 731-738 (1993).

A.F. Burke, *A Method for the Analysis of High Power Battery Designs*, Report for the California Air Resources Board, UCD-ITS-RR-99-6, Institute of Transportation Studies, Davis, February (1999).

A.F. Burke and M. Miller, *Assessment of the Greenhouse Gas Emission Reduction Potential of Ultra-Clean Hybrid-Electric Vehicles*, Institute of Transportation Studies - Davis, Davis, December (1997).

M. Cahill, Personal Communication, Eltech Corp., September 11 (1997).

CALSTART, "Japan Firms Improve Nickel-Battery Process," *CALSTART NewsNotes*, No. 4/7/98 (1998).

California Air Resources Board, *Proposed Amendments to the Low-Emission Vehicle Regulations to Add an Equivalent Zero-Emission Vehicle Standard*, Preliminary Draft Staff Report, Mobile Source Division, June 11 (1996).

California Air Resources Board, *Proposed Amendments to California's Low-Emission Vehicle Regulations "LEV II"*, Draft Staff Report, California Environmental Protection Agency, Sacramento, November 7 (1997).

California Air Resources Board, *1998 Zero-Emission Vehicle Biennial Program Review*, California Environmental Protection Agency, Sacramento, July 6 (1998a).

California Air Resources Board, *Proposed California Zero-Emission and Hybrid Electric Vehicle Exhaust Emission Standards and Test Procedures for 2003 and Subsequent Model Passenger Cars, Light-Duty Trucks and Medium-Duty Vehicles*, California Environmental Protection Agency, Sacramento, September 18 (1998b).

California Air Resources Board, *Fact Sheet: Zero Emission Vehicles*, California Environmental Protection Agency, Sacramento, June (1998c).

California Energy Commission, *Emission Offsets - Constraints and Opportunities for Powerplant Development Projects*, P700-97-002, Environmental Protection Office, Sacramento, August (1997).

California Energy Commission, *Results of the Delphi IX Survey of Oil Price Forecasts*, Sacramento, (1998).

California Energy Commission, *Fuels Report - Draft*, Committee Report, P300-99-001CD, Sacramento, April (1999a).

California Energy Commission, "http://www.energy.ca.gov/afvs/m85/m85stations.html," May 21 (1999b).

California Energy Commission, "http://www.energy.ca.gov/electricity/system_power.html," June 16 (1999c).

A. Chambers et al., "Hydrogen Storage in Graphite Nanofibers," *Physical Chemistry B* **102**(22): 4253-4256 (1998).

F. Chapman, C. Calwell, and D. Fisher, *What's the Charge?: Estimating the Emissions Benefits of Electric Vehicles in Southern California*, Environmental Defense Fund and Natural Resources Defense Council, (1994).

P. Chen et al., "High H2 Uptake by Alkali-Doped Carbon Nanotubes Under Ambient and Moderate Temperatures," *Science* **285**: 91-93 (1999).

C.-Y. Chiu and C.S. Park, "Fuzzy Cash Flow Analysis Using Present Worth Criterion," *The Engineering Economist* **39**(2): 113-137 (1994).

W.R. Cline, *Global Warming: The Economic Stakes*, Institute for International Economics, Washington, D.C. (1992).

P. Conley, "Experience curves as a planning tool," *IEEE Spectrum* **June 1970**: 63-68 (1970).

D. Corrigan, Personal Communication, Ovonic Battery Company, October 18 (1998).

D.A. Corrigan et al., *Ovonic Nickel-Metal Hydride Batteries for Electric Vehicles*, Florence, Italy (1997).

R. Cowan and D. Kline, *The Implications of Potential "Lock-In" in Markets for Renewable Energy*, Newport Beach, California (1996).

R. Cuenca, Personal Communication, Argonne National Laboratory, June (1996).

R.M. Cuenca,*Simple Cost Model For EV Traction Motors*, Riverside, California (1995).

N. Cui and J.L. Luo, "Electrochemical study of hydrogen diffusion behavior in Mg2Ni-Type hydrogen storage alloy electrodes," *International Journal of Hydrogen Energy* **24**: 37-42 (1999).

Daimler-Benz, *Technology '96*, Daimler-Benz AG, Stuttgart, March 31 (1996).

DaimlerChrysler, "DaimlerChrysler NECAR 4 Press Conference," (1999a).

DaimlerChrysler, *NECAR 4: The Alternative*, Corporate Communications, Stuttgart, March (1999b).

K.G. Darrow, *Light Duty Full Fuelcycle Emissions Analysis, Topical Report*, GRI-93/0472, Gas Research Institute, Chicago, April (1994).

S.C. Davis, *Transportation Energy Data Book: Edition 17*, ORNL-6919, Office of Transportation Technologies, U.S. Department of Transportation, Washington, D.C., August (1997).

S.C. Davis, *Transportation Energy Data Book: Edition 18*, ORNL-6919, Office of Transportation Technologies, U.S. Department of Transportation, Washington, D.C., August (1998).

M.A. Delucchi, *The Annualized Social Cost of Motor-Vehicle Use, Based on 1990-1991 Data: Summary of Theory, Data, Methods, and Results*, UCD-ITS-RR-96-3 (1), Institute of Transportation Studies - Davis, Davis, April (1996a).

M.A. Delucchi, *A Revised Model of Emissions of Greenhouse Gases from the Use of Transportation Fuels and Electricity*, UCD-ITS-RR-97-8, Institute of Transportation Studies - Davis, Davis, February (1997).

M.A. Delucchi, *Motor Vehicle Lifecycle Cost and Performance Model - Draft*, Institute of Transportation Studies, Davis, (1999).

M.A Delucchi and S. Hsu, *The External Cost of Noise from Motor Vehicles*, UCD-ITS-RR-96-3 (14), Institute of Transportation Studies - Davis, Davis, April (1996).

M.A. Delucchi and T.E. Lipman, *Emissions of Non-CO2 Greenhouse Gases from the Production and Use of Transportation Fuels and Electricity*, UCD-ITS-RR-97-5, Institute of Transportation Studies - Davis, Davis, February (1997).

M.A Delucchi and J. Murphy, *U.S. Military Expenditures to Protect the Use of Persion-Gulf Oil for Motor Vehicles*, UCD-ITS-RR-96-3 (15), Institute of Transportation Studies - Davis, Davis, April (1996).

M.A. DeLuchi, "Hydrogen vehicles: an evaluation of fuel storage, performance, safety, and cost," *International Journal of Hydrogen Energy* **14**: 81-130 (1989).

M.A. Deluchi, *Emissions of Greenhouse Gases from the Use of Transportation Fuels and Electricity*, ANL/ESD/TM-22, Center for Transportation Research, Argonne National Laboratory, Argonne, November (1991).

M.A. DeLuchi, *Hydrogen Fuel-Cell Vehicles*, UCD-ITS-RR-92-14, Insitute of Transportation Studies, September 1 (1992).

A.C. Dillon et al., "Storage of hydrogen single-walled carbon nanotubes," *Nature* **386**(March 27): 377-379 (1997).

R.N. Dino, "Forecasting the Price Evolution of New Electronic Products," *Journal of Forecasting* **4**(1): 39-60 (1985).

K. Dircks,*Recent Advances in Fuel Cells for Transportation Applications*, Brussels (1998).

L.S. Dixon and S. Garber, *California's Ozone-Reduction Strategy for Light-Duty Vehicles*, ISBN: 0-8330-2392-6, Rand Institute for Civil Justice, Santa Monica, (1996).

K.K. Dompere, "The theory of social costs and costing for cost-benefit analysis in a fuzzy decision space," *Fuzzy Sets and Systems* **76**: 1-24 (1995).

W. Donitz, "Fuel Cells for Mobile Applications, Status, Requirements and Future Applications Potential," *International Journal of Hydrogen Energy* **23**(7): 611-615 (1998).

H. Dowlatabadi, A.J. Krupnick, and A. Russell, *Electric Vehicles and the Environment: Consequences for Emissions and Air Quality in Los Angeles and U. S. Regions*, Discussion Paper, QE91-01, Resources for the Future, Washington, D. C., October (1990).

B. Duret and A. Saudin, "Microspheres for On-Board Hydrogen Storage," *International Journal of Hydrogen Energy* **19**(9): 757-764 (1994).

J.M. Dutton and A. Thomas, "Treating Progress Functions as a Managerial Opportunity," *Academy of Management Review* **9**(2): 235-247 (1984).

EA Engineering, Science, and Technology, Inc., *Methanol Refueling Station Costs*, For the American Methanol Foundation, Silver Spring, February 1 (1999).

Edison EV, "http://www.edisonev.com/azpubl1.htm," May 16 (1999a).

Edison EV, "http://www.edisonev.com/efaq2.htm," May 16 (1999b).

Energy and Environmental Analysis, Inc., *Assessment of Costs of Body-in-White and Interior Components for an Electric Vehicle*, Prepared for California Air Resources Board, Arlington, March (1998a).

Energy and Environmental Analysis, Inc., *Briefing on Technology and Cost of Toyota Prius*, U.S. DOE, Office of Transportation Technologies, Arlington, April 23 (1998b).

Energy Information Administration, *Emissions of Greenhouse Gases in the United States 1985-1991*, DOE/EIA-0573, U. S. Department of Energy, Washington, D. C., September, 1993 (1993b).

Energy Information Administation, *Electricity Generation and Environmental Externalities: Case Studies*, DOE/EIA - 0598, Energy Information Administration Office of Coal, Nuclear, Electric, and Alternate Fuels, U.S. Department of Energy, Washington, D. C., September (1995a).

Energy Information Administation, *The Effects of Title IV of the Clean Air Act of 1990 on Electric Utilities: An Update*, DOE/EIA-0582(97), U.S. Department of Energy, Energy Information Administration, Office of Coal, Nuclear, Electric, and Alternate Fuels, Washington, D. C., March (1997).

Energy Information Administation, *Annual Energy Outlook 1999*, DOE/EIA-0383(99), U.S. Department of Energy, Washington, D. C., December (1998).

P. Ekdunge and M. Raberg, "The Fuel Cell Vehicle Analysis of Energy Use, Emissions, and Cost," *International Journal of Hydrogen Energy* **23**(5): 381-385 (1998).

Electric Power Research Institute, *Pricing for Success: Using Auto Industry Models to Review Electric Vehicle Costing and Pricing*, TR-107094, Prepared by Green Car Media, Palo Alto, October (1996).

Engineering Systems Management, Inc., *Life-Cycle Cost Analysis of Conventional and Fuel Cell/Battery Powered Urban Passenger Vehicles*, DE-AC02-91CH10491, For U.S. DOE, Gaithersburg, November 30 (1992).

T. Evashenk, Personal Communication, California Air Resource Board, April 7 (1999).

R. Ewald, "Requirements for Advanced Mobile Storage Systems," *International Journal of Hydrogen Energy* **23**(9): 803-814 (1998).

S. Fankhauser, "The Social Costs of Greenhouse Gas Emissions: An Expected Value Approach," *The Energy Journal* **15**: 157-184 (1994).

Federal Register, "National Ambient Air Quality Standards for Particulate Matter: Proposed Decision," **61**: 65638-65713 (1996).

M.A. Fetcenko et al., *Selection of Metal Hydride Alloys for Electrochemical Applications,* Vol. 92-5, ed. by D. A. Corrigan and S. Srinivasan, The Electrochemical Society, Phoenix, Arizona (1992).

E. Figenbaum, "Th!NK - a unique city car," *Eletric and Hybrid Vehicle Technology '98* : 47-51 (1998).

D.J. Friedman, *Analysis of an Advanced Mid-Sized Direct-Hydrogen Fuel Cell Vehicle*, UC Davis (1999).

D.J. Friedman and R.M. Moore, *Maximizing the efficiency of a direct-hydrogen PEM fuel cell system*, Electrochemical Society, Boston (1998).

Fuel Cells 2000, "http://www.fuelcells.org/fuel/fcnews.shtml," July 26 (1999).

M. Fulmer and S. Bernow, "A Social Cost Analysis of Alternative Fuels for Light Vehicles," in *Transportation and Energy: Strategies for a Sustainable Transportation System*, ed. by D. S. a. S. A. Shaheen, American Council for an Energy Efficient Economy, Washington, D.C., pp. 139-159 (1995).

General Motors, "GM EV1 Engineering Overview," *Press Release from General Motors Advanced Technology Vehicles* (1996a).

General Motors, "GM EV1 Manufacturing Overview," *Press Release from General Motors Advanced Technology Vehicles* (1996b).

General Motors, "GM EV1 Structure," *Press Release from General Motors Advanced Technology Vehicles* (1996c).

General Motors, "GM EV1 Exterior Panels," *Press Release from General Motors Advanced Technology Vehicles* (1996d).

General Motors, "GM EV1 Aerodynamics," *Press Release from General Motors Advanced Technology Vehicles* (1996e).

P. Ghemawat, "Building strategy on the experience curve," *Harvard Business Review* **March-April, 1985**: 143-149 (1985).

P. Gifford, Personal Communication, GM Ovonic Company, September 17 (1998).

T. Glennon, Personal Communication, Glenntech Enterprises, September 2 (1998).

GM Ovonic, "Product Literature," (n.d.).

K. Goeke, T. Kelly, and H.D. Nix, *1998 Baseline Energy Outlook*, P300-98-012, California Energy Commission, Sacramento, August (1998).

T.F. Golob, D. Brownstone, D.S. Bunch, and R. Kitamura, *Forecasting Electric Vehicle Ownership and Use in the California South Coast Air Basin*, UCI-ITS-RR-96-3, Institute of Transportation Studies - Irvine, Irvine, August (1996).

R. Goodland and S.E. Serafy, "The urgent need to internalize CO2 emission costs," *Ecological Economics* **27**: 79-90 (1998).

G. Hall and S. Howell, "The Experience Curve from the Economist's Perspective," *Strategic Management Journal* **6**: 197-212 (1985).

J.K. Hammitt et al., "A welfare-base index for assessing environmental effects of greenhouse-gas emissions," *Nature* **381**(May 23): 301-3023 (1996).

J.G. Hansel et al., "Safety considerations in the design of hydrogen powered vehicles," *International Journal of Hydrogen Energy* **18**: 783-790 (1993).

K.S. Hardy, *Advanced Vehicle Systems Development*, DOE/CS-54209-22, Jet Propulsion Laboratory, 1985 (1985).

D. Harvey, Personal Communication, Eupec Corp., Septermber 9 (1998).

H. Hasuike, *Economic Study of Advanced Batteries for Electric Vehicles* (1991).

H.H. Hinterhuber, "Strategic cost management: preliminary lessons from European companies," *International Journal of Technology Management* **13**(1): 1-14 (1997).

R.L. Hodkinson, *Toward 4 Dollars per Kilowatt*, Orlando, FL (1997).

J.P. Holdren, "Energy Hazards: What to Measure, What to Compare," *Technology Review* **85**(3): 32-39,74-35 (1982).

R. Hwang, M. Miller, A.B. Thorpe, and D. Lew, *Driving Out Pollution: The Benefits of Electric Vehicles*, Union of Concerned Scientists, Berkeley, November, 1994 (1994).

R. Hwang and D. Taylor, *Electric Vehicle Air Quality Impacts: Evaluation of Methods Used in South Coast Air Basin*, Orlando, Florida (1997).

Hydrogen and Fuel Cell Letter, "Carbon Nanotubes Look Promising for H2 Storage, Fuel Cell Components, and Other Uses," *Hydrogen and Fuel Cell Letter* **XII**(8) (1997).

Hydrogen and Fuel Cell Letter, "Energy Partners Develops Low-Cost Collector Plate Manufacturing Process," *Hydrogen and Fuel Cell Letter* **14**(5) (1999a).

Hydrogen and Fuel Cell Letter, "Five Years in the Making, US$18 Million Hydrogen Production/Fueling Station Opens in Munich," *Hydrogen and Fuel Cell Letter* **14**(6): 1-2 (1999b).

J. Hynes, Personal Communication, Hudson Tool and Die, April 9 (1998).

Intergovernmental Panel on Climate Change, *Climate Change 1995: The Science of Climate Change*, Cambridge University Press, Cambridge (1996a).

J. Islas, "Getting round the lock-in in electricity generating systems: the example of the gas turbine," *Research Policy* **26**: 49-66 (1997).

B.D. James et al., *Onboard Hydrogen Storage in Fuel Cell Vehicles,* Vol. CD-ROM, EVS-14, Orlando, Florida (1997).

V. Jansen, Personal Communication, Oremet Wah-Chang, May 1 (1998).

C. Johnson et al., "Impact of Aircraft and Surface Emissions of Nitrogen Oxides on Tropospheric Ozone and Global Warming," *Nature* **355**: 69-71 (1992).

F.R. Kalhammer, A. Kozawa, C.B. Moyer, and B.B. Owens, *Performance and Availability of Batteries for Electric Vehicles: A Report of the Battery Technical Advisory Panel*, California Air Resources Board, El Monte, December 11, 1995 (1995).

F.R. Kalhammer, P.R. Prokopius, V.P. Roan, and G.E. Voecks, *Status and Prospects of Fuel Cells as Automobile Engines: A Report of the Fuel Cell Technical Advisory Panel*, California Air Resources Board, Sacramento, July (1998).

D. Kasler, "Honda unplugs electric cars," *Sacramento Bee*, April 30, pp. A1,18 (1999).

C. Kazimi, "Evaluating the Environmental Impacts of Alternative-Fuel Vehicles," *Journal of Environmental Economics and Management* **33**: 163-185 (1997).

Kitco Inc., "http://www.kitco.com/gold.live.html," May 25 (1999).

B. Knosp et al., "Evaluation of Zr(Ni, Mn)2 Laves Phase Alloys as Negative Active Material for Ni-MH Electric Vehicle Batteries," *Journal of the Electrochemical Society* **145**(5): 1478-1482 (1998).

G. Kochek, Personal Communication, Advanced D.C. Motors, Inc., September (1995).

V.C.Y. Kong et al., "Development of hydrogen storage for fuel cell generators I: Hydrogen generation using hydrolysis hydrides," *International Journal of Hydrogen Energy* **24**: 665-675 (1999).

B. Kosko, *Fuzzy Thinking: The New Science of Fuzzy Logic*, Hyperion Books, New York (1993).

M. Krebs, "From One Platform Many Models Grow," *The New York Times*, May 19, p. 7 (1999).

Los Angeles Department of Water and Power, "http://www.ladwp.com/services/electran/rates.htm," May 20 (1999).

M. Ledbetter and M. Ross, *A Supply Curve of Conserved Energy for Automobiles,* Vol. 4, ed. by W. W. S. P.A. Nelson, and R.H. Till, American Institute of Chemical Engineers, New York (1990).

P. Leiby,*The Costs of Oil Imports*, UC Davis (1997).

R.C. Lind, "Intergenerational equity, discounting, and the role of cost-benefit analysis in evaluating global climate policy," *Energy Policy* **23**(4/5): 379-389 (1995).

T.E. Lipman, *The Cost of Manufacturing Electric Vehicle Batteries*, Report for California Air Resources Board, UCD-ITS-RR-99-5, Institute of Transportation Studies, Davis, May (1999a).

T.E. Lipman, *The Cost of Manufacturing Electric Vehicle Drivetrains*, Report for California Air Resources Board, UCD-ITS-RR-99-7, Institute of Transportation Studies, Davis, May (1999b).

T.E. Lipman, *A Review of Electric Vehicle Cost Studies: Assumptions, Methodologies, and Results*, Report for California Air Resources Board, UCD-ITS-RR-99-8, Institute of Transportation Studies, Davis, May (1999c).

T.E. Lipman and M.A. Delucchi, "Hydrogen-fuelled vehicles," *International Journal of Vehicle Design* **17**(5/6 (Special Issue)): 562-589 (1996).

T.E. Lipman, K.S. Kurani, and D. Sperling, *Incentive Policies for Neighborhood Electric Vehicles*, UCD-ITS-RR-94-20, Institute of Transportation Studies - Davis, August (1994).

T.E. Lipman and D. Sperling, "Forecasting Cost Path of Electric Vehicle Drive System: Monte Carlo Experience Curve Simulation," *Transportation Research Record* **1587**: 19-26 (1997).

T. Litman, *Transportation Cost Analysis: Techniques, Estimates, and Implications*, Victoria Transport Policy Institute, Victoria, July 16 (1996).

F.J. Liu et al., "Effects of Ni-substitution and F-treatment on the hydriding behaviors and microstructures of AB2-compound (Ti,Zr)(Mn,Cr)2," *Journal of Alloys and Compounds* **232**: 232-237 (1996).

F.D. Lomax, B.D. James, G.N. Baum, C.E. Thomas, *Detailed Manufacturing Cost Estimates for Polymer Electrolyte Membrane (PEM) Fuel Cells for Light Duty Vehicles*, Directed Technologies, Inc., Arlington, October (1997).

A.B. Lovins,*Hypercars: The Next Industrial Revolution,* Vol. 1, Osaka (1996).

A.B. Lovins and B.D. Williams,*A Strategy for the Hydrogen Transition*, Vienna, Virginia (1999).

R.D. MacDowall, "Comparative Evaluation of Acoustical Noise Levels of Soleq Evcort EV and ICE Counterpart," *SAE Technical Paper Series* **SP-817**(900138): 23-25 (1990).

J. Maceda, Personal Communication, H-Power Corp., October 18 (1991).

J.J. MacKenzie, R.C. Dower, D.D.T. Chen, *The Going Rate: What it Really Costs to Drive*, World Resources Institute, Washington, D.C., June (1992).

C. Madery and J.-L. Liska,*SAFT Nickel-Metal Hydride Modules for Electric Vehicle Application*, ed. by A. F. Burke, Institute of Transportation Studies - Davis, UC Davis (1999).

D.C. Magnuson and H.F. Gibbard, "Status and prospects of metal hydrides for nickel-metal hydride secondary batteries," *Materials Letters* **21**: 1-2 (1994).

Malcolm Pirnie, Inc., *Evaluation of the Fate and Transport of Methanol in the Environment*, Prepared for the American Methanol Institute, 3522-002, Oakland, January (1999).

A. Manne, "The rate of time preference: Implications for the greenhouse debate," *Energy Policy* **23**(4/5): 391-394 (1995).

J. Mark, J.M. Ohi, and D.V. Hudson, Jr., *Fuel Savings and Emissions Reductions from Light Duty Fuel Cell Vehicles*, NREL/TP-463-6157, National Renewable Energy Laboratory, Golden, April (1994).

D. Martin and L. Michaelis, *Global Warming Due to Transport*, Florence (1992).

A.E. Mascarin et al., *Costing the Ultralight in Volume Production: Can Advanced Composite Bodies-in-White Be Affordable?*, Detroit (1995).

N. Mattson and C. Wene, "Assessing New Energy Technologies Using an Energy System Model with Endogenized Experience Curves," *International Journal of Energy Research* **21**: 385-393 (1997).

D.R. McCubbin and M.A. Delucchi, *The Social Cost of The Health Effects of Motor Vehicle Air Pollution*, UCD-ITS-RR-96-3 (11), Institute of Transportation Studies - Davis, Davis, August (1996).

P. Miller and J. Moffett, *The Price of Mobility: Uncovering the Hidden Costs of Transportation*, Natural Resources Defense Council, New York, October (1993).

E. Mohr, "Greenhouse policy persuasion: towards a positive theory of discounting the climate future," *Ecological Economics* **15**: 235-245 (1995).

S. Montgomery, Personal Communication, OMG, Inc., November 17 (1997).

W.R. Moomaw, C.L. Shaw, W.C. White, and J.L. Sawin, *Near-Term Electric Vehicle Costs*, Northeast Alternative Vehicle Consortium, Boston, October (1994).

R.B. Moore and V. Raman, "Hydrogen Infrastructure for Fuel Cell Transportation," *International Journal of Hydrogen Energy* **23**(7): 617-620 (1998).

R.M. Moore, Personal Communication, Fuel Cell Vehicle Modeling Center, UC Davis, July 29 (1999).

R.M. Moore et al., *A Fuel Control Strategy that Optimizes the Efficiency of a Direct-Methanol Fuel Cell in an Automotive Application,* Vol. SAE Paper Number: 99FTT-44, Costa Mesa, CA (1999a).

R.M. Moore et al.,*A Comparison Between Direct-Methanol and Direct-Hydrogen Fuel Cell Vehicles,* Vol. SAE Paper Number: 99FTT-48, Costa Mesa, CA (1999b).

M.G. Morgan and M. Henrion, *Uncertainty: A Guide to Dealing with Uncertainty in Quantitative Risk and Policy Analysis*, Cambridge University Press, Cambridge (1990).

M. Mumma, Personal Communication, Cell-Con Inc., July 6 (1998).

O.J. Murphy et al., "Low-cost light weight high power density PEM fuel cell stack," *Electrochimica Acta* **43**(24): 3829-3840 (1998).

NASA, "http://www.jpl.nasa.gov/releases/97/fuelcel3.html," August 3 (1997).

National Science Foundation, "http://www.nsf.gov/sbe/srs/s2194/s2194001.xls," June 16 (1999).

National Highway Traffic Safety Administration, *Automotive Fuel Economy Program: Twenty-Third Annual Report to Congress*, U.S. Department of Transportation, Washington, D.C., (1998).

Nordhaus, *Managing the Global Commons: The Economics of Climate Change*, The MIT Press, Cambridge (1994).

R.B. Norgaard, "Environmental Evaluation Techniques and Optimization in an Uncertain World," *Land Economics* **62**(2): 210-213 (1986).

G.P. Nowell, *The Promise of Methanol Fuel Cell Vehicles*, For the American Methanol Institute, Washington, D.C., (1998).

K. Numajiri, Personal Communication, Sumitomo Corp., September 11 (1997).

NYSERDA, *Zero-Emission Vehicle Technology Assessment*, 95-11, New York State Energy Research and Development Authority, August (1995).

D. Oei, J.A. Adams, A.A. Kinnelly, G.H. Purnell, R.I. Sims, M.S. Sulek, D.A. Wenette, B. James, F. Lomax, G. Baum, S. Thomas, and I. Kuhn, *Direct-Hydrogen-Fueled Proton-Exchange-Membrane Fuel Cell System for Transportation Applications: Conceptual Vehicle Design Report for Battery Augmented Fuel Cell Powertrain Vehicle*, DOE/CE/50389-503, U.S. Department of Energy, Dearborn, July (1997b).

D. Oei, A. Kinnelly, R. Sims, M. Sulek, D. Wenette, B. James, F. Lomax, G. Baum, S. Thomas, and I. Kuhn, *Direct-Hydrogen-Fueled Proton-Exchange-Membrane Fuel Cell System for Transportation Applications: Conceptual Vehicle Design Report for Pure Fuel Cell Powertrain Vehicle*, DOE/CE/50389-501, U.S. Department of Energy, Dearborn, February (1997a).

J. Ogden, E.D. Larson, and M.A. Delucchi, *A Technical and Economic Assessment of Renewable Transportation Fuels and Technologies*, Office of Technology Assessment, U.S. Congress, Washington, D.C., May 27 (1994).

J.M. Ogden et al., "Fuels for Fuel Cell Vehicles: Vehicle Design and Infrastructure Issues," *SAE Technical Paper Series* **982500**: 1-25 (1998).

J.M. Ogden et al., "A Comparison of Hydrogen, Methanol, and Gasoline as Fuels for Fuel Cell Vehicles: Implications for Vehicle Design and Infrastructure Development," *Journal of Power Sources* **79**: 143-168 (1999).

J.M. Ogden and R.H. Williams, *Solar Hydrogen: Moving Beyond Fossil Fuels*, World Resources Institute, Washington, D.C. (1989).

S. Osawa and H. Kosaka,*Honda EV-Plus - Technical Feedback from First-Year Marketing Experience*, Brussels (1998).

Office of Technology Assessment, *Advanced Vehicle Technology: Visions of a Super-Efficient Family Car*, OTA-ETI-638, Office of Technology Assessment, U.S. Congress, Washington, D.C., September (1995).

N. Otto, Personal Communication, Ballard Power Systems Inc., April 20 (1999).

S.R. Ovshinsky et al.,*Advanced Materials for Next Generation NiMH Portable, HEV, and EV Batteries*, Ft. Lauderdale, Florida (1998).

Panasonic EV Energy Co., "Product Literature," (n.d.).

P.G. Patil and J. Ohi,*The Federal Government's Role in Fuel Cell Research and Development*, University of California - Irvine (1998).

D.W. Pearce et al., "The Social Costs of Climate Change: Greenhouse Damage and the Benefits of Control," in *Climate Change 1995: Economic and Social Dimensions of Climate Change*, ed. by J. P. Bruce, H. Lee and E. F. Haites, Cambridge University Press, Cambridge, pp. 179-224 (1996).

J. Perry, "Ford's Mountain, and Its Mouse," *The New York Times*, May 19, p. 21 (1999).

W. Peschka and W.J.D. Escher, "Germany's contribution to the demonstrated technical fesibility of the liquid-hydrogen fueled passenger automobile," in *Alternative Fuels: Alcohols, Hydrogen, Natural Gas and Propane*, Vol. SP-982, Society of Automotive Engineers, Inc., Warrendale (1993).

T.W. Petersik, "The Impact of International Learning on Technology Cost," in *Issues in Midterm Analysis and Forecasting*, Energy Information Administration, Washington, D.C. (1997).

B. Pladson, Personal Communication, Bison ProFab, May 4 (1998).

Powerball Technologies, "http://www.powerball.net/inside/products/index.html," May 28 (1999).

Praxair Corp., "http://www.praxair.com/Praxair.nsf," June 15 (1999).

B. Purcell, "Stepping Ahead," *Eletric and Hybrid Vehicle Technology '98* : 42-45 (1998b).

R. Purcell, *A Discussion of General Motors' EV-1 Program,* Vol. UCD-ITS-RR-98-8, ed. by T. E. Lipman, D. Santini and D. Sperling, ITS-Davis, Asilomar Conference Center, Pacific Grove, California (1998a).

J.E. Quinn et al., *Projected Costs for Sodium-Sulfur Electric Vehicle Batteries*, ed. by W. D. Jackson, IEEE, Washington, D.C. (1989).

D.V. Ragone et al.,*Power-Energy Curves Revisited*, Deerfield Beach, Florida (1995).

K. Rajashekara and R. Martin, "Electric Vehicle Propulsion Systems Present and Future Trends," *Journal of Circuits, Systems, and Computers* **5**(1): 109-129 (1995).

T.R. Ralph et al., "Low Cost Electrodes for Proton Exchange Membrane Fuel Cells," *Journal of the Electrochemical Society* **144**(11): 3845-3857 (1997).

W.G. Rankin, Personal Communication, Unique Mobility, Inc., September 25, 1998 (1998).

N.S. Rau, S.T. Adelman, and D.M. Kline, *EVTECA - Utility Analysis Volume 1: Utility Dispatch and Emissions Simulations*, TP-462-7899, National Renewable Energy Laboratory, Golden, (1996).

G.F. Ray, "Full Circle: The diffusion of technology," *Research Policy* **18**: 1-18 (1989).

J.M. Reilly, "Climate-Change Damage and the Trace-Gas-Index Issue," in *Economic Issues in Global Climate Change: Agriculture, Forestry, and Natural Resources*, ed. by J. M. Reilly and M. Anderson, Westview Press, Boulder, pp. 72-88 (1992).

D.E. Reisner et al.,*Bipolar Nickel-Metal Hydride EV Battery*, Vol. II, Osaka, Japan (1996).

J. Rennie, "13 Vehicles That Went Nowhere," *Scientific American*, Vol. 277, No. 4, October, pp. 64-67 (1997).

H.-H. Rogner, "Hydrogen Technologies and the Technology Learning Curve," *International Journal of Hydrogen Energy* **23**(9): 833-840 (1998).

M. Ross et al., "Real-World Emissions from Model Year 1993, 2000, and 2010 Passenger Cars," *Society of Automotive Engineers* (1995).

Sacramento Bee, "Toyota to Introduce Fuel Cell Vehicle in 2003," , July 2, p. C10 (1999).

T. Sakai et al., *Nickel-Metal Hydride Batteries Using Rare-Earth Based Hydrogen Storage Alloys,* Vol. 92-5, ed. by D. A. Corrigan and S. Srinivasan, The Electrochemical Society, Phoenix, Arizona (1992).

G.D. Sandrock, Material from DOE Contractor's Meeting (1997).

R. Savoie, Personal Communication, Ballard Power Systems, April 29 (1998).

South Coast Air Quality Management District, *Air Quality Management Plan*, South Coast Air Quality Management District, (1997).

R. Schmalensee, "Comparing Greenhouse Gases for Policy Purposes," *The Energy Journal* **14**: 245-255 (1993).

J. Schumpeter, *Business Cycles: A Theoretical, Historical, and Statistical Analysis of the Capitalist Process*, McGraw Hill, New York (1939).

K. Scott et al., "Material aspects of the liquid feed direct methanol fuel cell," *Journal of Applied Electrochemistry* **28**: 1389-1397 (1998).

W.R. Scott and D. Rusta, *Sealed-Cell Nickel-Cadmium Battery Applications Manual*, Prepared for NASA, NAS5-23514, TRW, Redondo Beach, May 5 (1978).

Shell International Petroleum,*The evolution of the world's energy system 1860-2060*, Paris, France (1994).

K.P. Shine et al., "Radiative Forcing of Climate," in *Climate Change, the IPCC Scientific Assessment*, ed. by J. T. Houghton, G. J. Jenkins and J. J. Ephraums, Cambridge University Press, Cambridge, pp. 42-68 (1990).

W. Short, D.J. Packey, and T. Holt, *A Manual for the Economic Evaluation of Energy Efficiency and Renewable Energy Technologies*, NREL/TP-462-5173, National Renewable Energy Laboratory, Golden, March (1995).

Sierra Research, Inc. and Charles River Associates, *The Cost-Effectiveness of Further Regulating Mobile Source Emissions*, SR94-02-04, Sacramento, February 28 (1994).

W. Silvert, "Ecological impact classification with fuzzy sets," *Ecological Modelling* **96**: 1-10 (1997).

S. Slagle, Personal Communication, JMC-USA, Inc., May 11 (1998).

K. Small and C. Kazimi, "On the costs of air pollution from motor vehicles," *Journal of Transportation Economic Policy* **29**: 7-32 (1995).

P.N. Smith, "Application of Fuzzy Sets in the Environmental Evaluation of Projects," *Journal of Environmental Management* **42**: 365-388 (1994).

R.H. Socolow, "Failures in Discourse," in *Boundaries of Analysis: An Inquiry into the Tocks Island Dam Controversy*, ed. by H. A. Feiveson, F. W. Sinden and R. H. Socolow, Ballinger Publishers, Cambridge (1976).

Southern California Edison, "Schedule TOU-EV-1: Domestic Time-of-Use EV Recharging," (1998a).

Southern California Edison, "Schedule TOU-EV-2: Domestic Time-of-Use EV Recharging," (1998b).

D. Sperling, *Future Drive*, Island Press, Washington, D.C. (1995).

D. Sperling and M.A. DeLuchi, "Transportation Energy Futures," *Annual Review of Energy* **14**: 375-424 (1989).

A.E. Steck, *Membrane Materials in Fuel Cells*, ed. by O. Savandogo, P. R. Roberge and T. N. Veziroglu, Les Editions de l'Ecole Polytechnique de Montreal, Montreal (1995).

M.R. Swain et al., "Comparison of Hydrogen, Natural Gas, Liquified Petroleum Gas, and Gasoline Leakage in a Residential Garage," *Energy and Fuels* **12**: 83-89 (1998).

J. Tachtler and A. Szyszka, "Car fueling with liquid hydrogen," *International Journal of Hydrogen Energy* **19**: 377-385 (1994).

A. Tanghetti, Personal Communication, California Energy Commission, April 15 (1999).

Y. Tao and Y. Xinmiao, "Fuzzy Comprehensive Assessment, Fuzzy Clustering Analysis and its Application to Urban Traffic Environment Quality Evaluation," *Transportation Research - D* **3**(1): 51-57 (1998).

Transportation Design and Manufacturing, Inc.,, *UEV/WEV Manufacturing Plan*, Livonia, June 4 (1997).

W.P. Teagan et al., "Cost reductions of fuel cells for transportation applications: fuel processing options," *Journal of Power Sources* **71**: 80-85 (1998).

C.E. Thomas, B.D. James, F.D. Lomax, and I.F. Kuhn, *Integrated Analysis of Hydrogen Passenger Vehicle Transportation Pathways*, Directed Technologies, Inc., Arlington, March (1998a).

C.E. Thomas, B.D. James, F.D. Lomax, "Market Penetration Scenarios for Fuel Cell Vehicles," *International Journal of Hydrogen Energy* **23**(10): 949-966 (1998b).

C.E. Thomas et al., "Affordable Hydrogen Supply Pathways for Fuel Cell Vehicles," *International Journal of Hydrogen Energy* **23**(6): 507-516 (1998c).

R.S.J. Tol, "The Damage Costs of Climate Change: Toward More Comprehensive Calculations," *Environmental and Resource Economics* **6**: 353-374 (1995).

R.S.J. Tol, "The Marginal Costs of Greenhouse Gas Emissions," *The Energy Journal* **20**(1): 61-81 (1999).

U.S. Department of Commerce, *A Competitive Assessment of the U.S. Electric Motor Industry*, International Trade Administration, Washington, D.C., August (1988).

U.S. Department of Energy, *Encouraging the Purchase and Use of Electric Motor Vehicles*, Office of Transportation Technologies, U.S. Department of Energy, Washington, D.C., May (1995).

U.S. Department of Energy, *Scenarios of U.S. Carbon Reductions: Potential Impacts of Energy Technologies by 2010 and Beyond*, Office of Energy Efficiency and Renewable Energy, Washington, D.C., (1998a).

U.S. Department of Energy, *Total Energy Cycle Assessment of Electric and Conventional Vehicles: An Energy and Environmental Analysis, Volume I: Technical Report*, Office of Energy Efficiency and Renewable Energy, Washington, D.C., January (1998b).

U.S. Department of Energy, *Fuel Cells for Transportation 98: Annual Contractor's Report*, Office of Advanced Automotive Technologies, Washington, D.C., November (1998c).

U.S. Department of Energy, *Fuel Cells for Transportation 98: Annual National Laboratory Report*, Office of Advanced Automotive Technologies, Washington, D.C., November (1998d).

U.S. Environmental Protection Agency, *Chemical Summary for Methanol*, Fact Sheet, EPA 749-F-94-013a, Office of Pollution Prevention and Toxics, Washington, D.C., August (1994).

U.S. Environmental Protection Agency, *The Benefits and Costs of the Clean Air Act, 1970 to 1990*, Office of Air and Radiation, Washington, D.C., October (1997).

U.S. Environmental Protection Agency, *National Air Quality and Emission Trends Report, 1997: Fact Sheet*, 454/R-98-016, Office of Air Quality Planning and Standards, Washington, D.C., December 10 (1998).

U.S.Geological Survey, "http://greenwood.cr.usgs.gov/pub/fact-sheets/fs-0145-97/fs-0145-97.html," (1998).

U.S. Government Accounting Office, *Electric Vehicles: Likely Consequences of U.S. and Other Nations' Programs and Policies*, GAO/PEMD-95-7, Washington, D.C., December (1994).

J.M. Utterback, *Mastering the Dynamics of Innovation*, Harvard Business School Press, Boston (1994).

J.M. Utterback and F.F. Suarez, *Innovation, Competition, and Industry Structure*, Working Paper, WP # 29-90, Sloan School of Management, MIT, Cambridge, (1991).

R.F. Veit, "Fuel of the Future?," *Electric and Hybrid Vehicle Technology '98* : 124-127 (1998).

S. Venkatesan et al., *Rechargeable Ovonic Ni/MH Batteries for Consumer, Electric Vehicle, and Military Applications*, Cherry Hill, NJ (1994).

A. Vyas and R. Cuenca, *EV Cost Model*, Washington, D.C. (1999).

A. Vyas et al., "An Assessment of Electric Vehicle Life Cycle Costs to Consumers," *SAE Technical Paper Series* **982182** (1998).

A.D. Vyas, H.K. Ng, D.J. Santini, and J.L. Anderson, *Electric and Hybrid Electric Vehicles: A Technology Assessment Based on a Two-Stage Delphi Study*, ANL/ESD-36, Argonne National Laboratory, U.S. Department of Energy, Argonne, December (1997).

J. Wallace, "Electric Dreams," *Eletric and Hybrid Vehicle Technology '98* : 10-16 (1998).

M.-J. Wang and G.-S. Liang, "Benefit/Cost Analysis Using Fuzzy Concept," *The Engineering Economist* **40**(4): 359-376 (1995).

M.Q. Wang and D.J. Santini, "Monetary Values of Air Pollutant Emissions in Various U.S. Regions," *Transportation Research Record* **1475**: 33-41 (1994).

Q. Wang, *Development and Use of the Greet Model to Estimate Fuel-Cycle Energy Use and Emissions of Various Transportation Technologies and Fuels*, ANL/ESD-31, Argonne National Laboratory Center for Transportation Research, Argonne, March (1996).

Q. Wang et al., "Emissions Impacts of Electric Vehicles," *Journal of the Air and Waste Management Association* **40**: 1275-1284 (1990).

J. Werth, "Patent Application of John Werth for Hydrogen Generating System," Docket HPOW-102: (1992).

R. Whitaker, "Investment in volume building: the 'virtuous cycle' in PAFC," *Journal of Power Sources* **71**: 71-74 (1998).

J. Willand, *State-of-the Art and Development Trends for Fuel Cell Vehicles*, European Fuel Cell Group, Jalich, Germany (1996).

S. Wood, Personal Communication, September 2 (1998).

S.C. Wood and G.S. Brown, "Commercializing Nascent Technology: The Case of Laser Diodes at Sony," *Journal of Product Innovation and Management* **15**: 167-183 (1998).

T.P. Wright, "Factors Affecting the Cost of Airplanes," *Journal of Aeronautical Science* **3** (122) (1936).

T.S. Yau, H.W. Zaininger, M.J. Bernard, M.K. Singh, and C.L. Saricks, *Utility Emissions Associated with Electric and Hybrid Vehicle Charging*, DOE/CE-0395, Office of Transportation Technologies, U.S. Department of Energy, Washington, D.C., April (1993).

L.E. Yelle, "Adding Life Cycles to Learning Curves," *Long Range Planning* **16**: 82-87 (1983).

D. Yergin, *The Prize: The Epic Quest for Oil, Money, and Power*, Simon and Shuster, New York (1991).

K.S. Young, "Advanced composites storage containment for hydrogen," *International Journal of Hydrogen Energy* **17**: 505-507 (1992).

P. Young, "Technological Growth Curves: A Competition of Forecasting Models," *Technological Forecasting and Social Change* **44**: 375-389 (1993).

L. Zadeh, "The concept of a linguistic variable and its applications to approximate reasoning," *Information Science* **8**: 199-239 (1975).

P. Zhang et al., "Recovery of metal values from spent nickel-metal hydride rechargeable batteries," *Journal of Power Sources* **77**: 116-122 (1999).

H.-J. Zimmermann, *Fuzzy Set Theory and its Applications, 2nd Ed.*, Kluwer Academic Publishers, Boston (1991).

Appendix A: Fuzzy Sets and Fuzzy Set Mathematics

Fuzzy Sets and Probability Distributions

Fuzzy set theory and probability theory arise from different mathematical fields, but in practice they can be used in a similar fashion to characterize uncertain variables. Both are capable of characterizing variation/uncertainty using classic distributional forms, such as normal (i.e., Gaussian), Poisson, and so on, as well as irregular forms. A key difference between the two is that while probability distributions are normalized such that the entire area within the distribution is equal to 1 (i.e., 100%), fuzzy set distributions are typically normalized such that the maximum membership function value, $\mu(x)$, is equal to 1. Such fuzzy sets are called "normal" fuzzy sets. Figure A-1, below, shows corresponding fuzzy set and probability distributions.

Figure A-1: Probabilistic and Fuzzy Set-Based Depictions of Variation

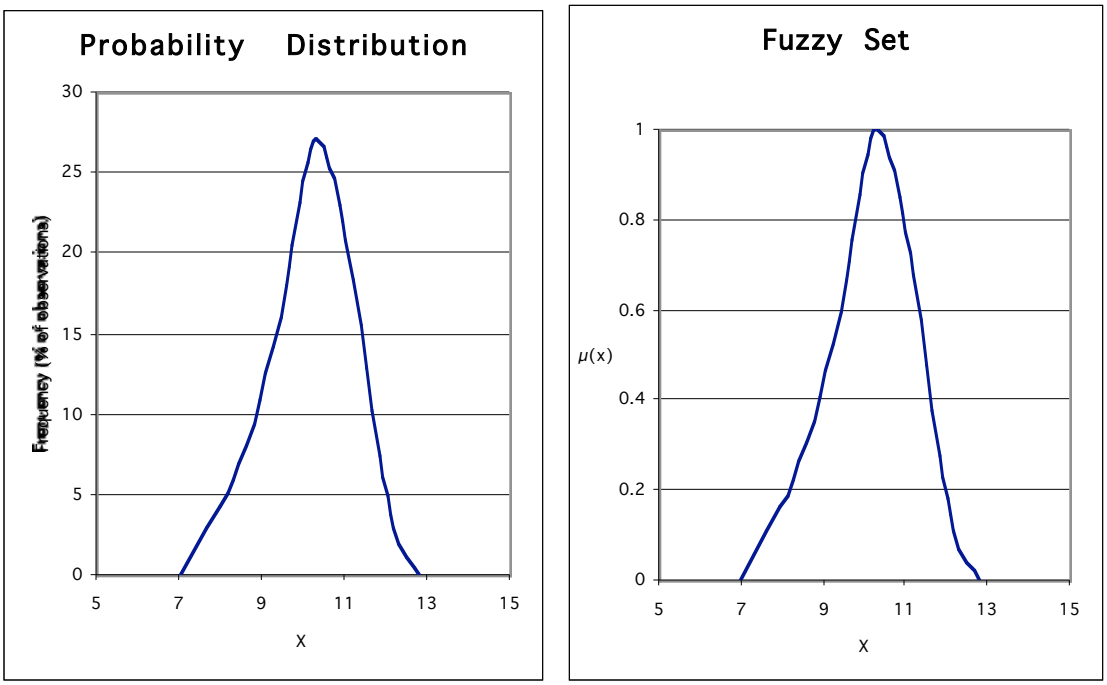

Fuzzy Sets Defined

A fuzzy set is defined as a set of "membership function" values across a certain range of interest. This range of interest is known as the "universe of discourse" in the lexicon of fuzzy set theory. For each value in the range (the values can be represented as "x", which are elements in the universe **R**), there is a corresponding membership function value, $\mu(x)$. For "normal" fuzzy sets, these membership function values will be in the range of 0 to 1, with 0 denoting a zero degree of membership in the set, and 1 denoting a complete degree of membership, at the corresponding x value. Fuzzy sets differ from conventional

sets in that in fuzzy set theory partial membership in a set is allowed, whereas in conventional set theory elements are either entirely in or out of a given set.

Fuzzy sets A and B can thus be defined as a series of values of x and $\mu(x)$. Fuzzy set A is defined as a set of membership function values $\mu a(x)$, across values of x in the universe of discourse **R**, and fuzzy set B is defined as a set of membership function values $\mu b(x)$ across the values of x.

For example, the following values for x and $\mu a(x)$ define the fuzzy set A. Since fuzzy set A is triangular in shape, it is known as a triangular fuzzy set.

x	0	1	2	3	4	5	6
$\mu a(x)$	0	0	0.5	1.0	0.67	0.33	0

Figure A-2:

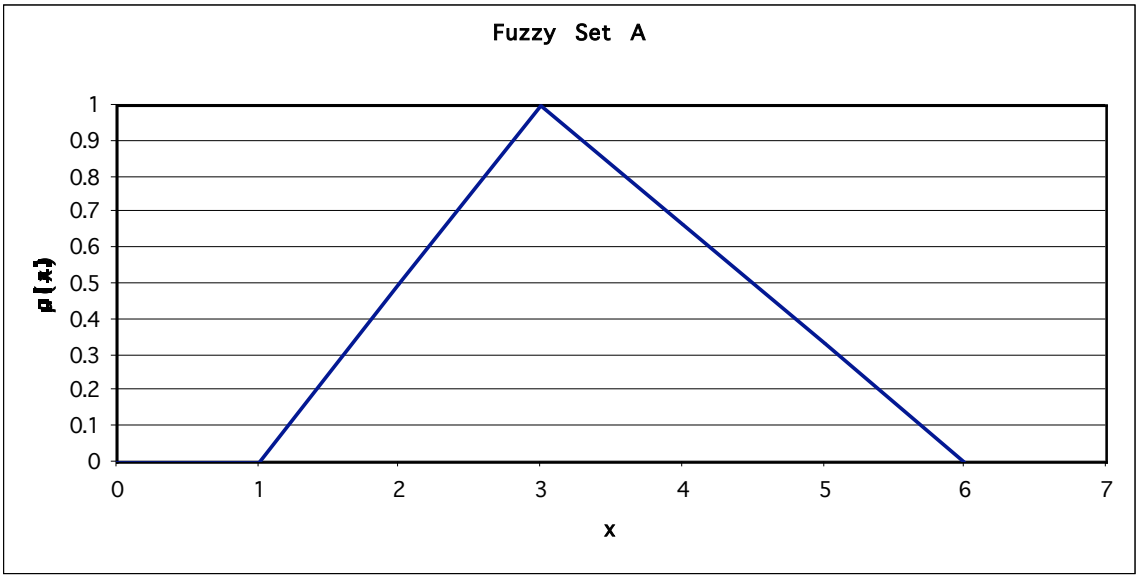

Of course, there are in fact an infinite number of points along x, and an infinite number of values of $\mu(x)$. Simple triangular fuzzy sets can be depicted with just three sets of x and $\mu(x)$ values, while more complex set forms may require many more sets of values to be adequately defined and graphically depicted.

General Procedure for Performing Fuzzy Set Addition

Two fuzzy sets, A and B, can be added to form fuzzy set S, by the following rule:

Sum $S := A \oplus B$ determined as:

$$\mu_S(a) = \sup_{x \in \mathbf{R}} \min\{\mu_A(x), \mu_B(a - x)\} \text{ for all } a \in \mathbf{R}$$

Where:

μa(x) is the membership function of fuzzy set A across the values of x, which are included in the "universe of discourse" **R**

μb(x) is the membership function of fuzzy set B across the values of x

μs(a) is the membership function of fuzzy set S across the values of a, which are also included in the "universe of discourse" **R**

μb(a-x) is the membership function of fuzzy set B across the values of "a-x"

min{c,d} takes the minimum of the two values, c and d

sup is the supremum, or height, of all of the values in a given set of membership function values (i.e., the maximum membership function value).

Step 1: Define fuzzy sets A and B

See above for definition of fuzzy set A.

Next, fuzzy set B can be defined in a similar manner as fuzzy set A.

Step 2: Introduce the Values for the Range "a" in the Universe of Discourse **R**

Having defined two fuzzy sets, A and B, we now need to introduce a new range of values, "a". Like "x," "a" is also a range of values across which membership function values for a fuzzy set can be defined. In order to perform fuzzy addition of two sets that are defined across a universe of discourse "x," "a" will need to be a somewhat larger range of values, also within the universe of discourse **R**.

Step 3: Evaluate μa(x) and μb(a-x) for Each Value of "x" and "a"

First, for each value of x, μa(x) needs to be defined. A few such values are shown in the above table. As noted above, however, there are in principle an infinite number of values of x and μa(x) (and a and μb(a-x)) and it would be impossible to define all of them. In practice, the resolution with which μa(x) and μb(a-x) will

need to be defined will differ according to the complexity of fuzzy sets A and B. For simple fuzzy set forms, ten or so values will probably be adequate, but for more complex forms more values may be needed in order to assure that important values are not excluded. Next, for each value of a and x, μb(a-x) needs to be defined. This is done by calculating the value of "a-x" and then determining the value of μb for that a-x value. In a spreadsheet, this can be done by defining fuzzy sets A and B with functions, and then evaluating the functions for each value of "x" and μa(x) and "a-x" and μb(a-x).

Step 4: Select the minimum value of μa(x) and μb(a-x) for each value of x and a

For each x and a value, the lower of the two values of μa(x) and μb(a-x) must be selected. In a spreadsheet, this can easily be done with an "IF" logic function. If μa(x) is lower than μb(a-x) at a certain value of x and a, then it is chosen, and vice versa if μb(a-x) is lower.

Step 5: Calculate the supremum of values for each value of "a"

From step 4, a matrix of values has been obtained as the lesser of μa(x) and μb(a-x) for each "x" and "a" value. Now, μs(a) can be calculated as the supremum or highest μ value across all values of "x," for each value of "a." This can be done in a spreadsheet with a "MAX" function. The resulting set of μs(a) and "a" values define the fuzzy set S. This fuzzy set S is the sum of the fuzzy sets A and B.

General Procedure for Performing Fuzzy Set Subtraction

Two fuzzy sets, A and B, can be subtracted to form fuzzy set S, by the following rule:

Difference $S := A \ominus B$ determined as

$$\mu_S(a) = \sup_{x \in \mathbf{R}} \min\{\mu_A(x), \mu_B(x - a)\} \text{ for all } a \in \mathbf{R}$$

Where:

μa(x) is the membership function of fuzzy set A across the values of x, which are included in the "universe of discourse" **R**

μb(x) is the membership function of fuzzy set B across the values of x

μs(a) is the membership function of fuzzy set S across the values of a, which are also included in the "universe of discourse" **R**

μb(x-a) is the membership function of fuzzy set B across the values of "x-a"

min{c,d} takes the minimum of the two values, c and d

sup is the supremum, or height, of all of the values in a given set of membership function values (i.e., the maximum membership function value).

Step 1: Same as above for fuzzy set addition

Step 2: Same as above for fuzzy set addition

Step 3: Evaluate μa(x) and μb(x-a) for Each Value of "x" and "a"

As above for fuzzy set addition, but instead of μb(a-x), μb(x-a) is determined for each "a" and "x" value.

Step 4: Same as above, except with the minimum of μa(x) and μb(x-a) for each "a" and "x" value

Step 5: Same as above for fuzzy set addition. The resulting fuzzy set S is the difference between fuzzy sets A and B.

General Procedure for Performing Fuzzy Set Multiplication

Two fuzzy sets, A and B, can be multiplied to form fuzzy set S, by the following rule:

Product $S := A \quad B$ determined as

$$\mu_S(a) = \sup_{\substack{x,y \in \mathbf{R} \\ a = xy}} \min\{\mu_A(x), \mu_B(y)\} \text{ for all } a \in \mathbf{R}$$

Where:

μa(x) is the membership function of fuzzy set A across the values of x, which are included in the "universe of discourse" **R**

μb(y) is the membership function of fuzzy set B across the values of y, which are also included in the "universe of discourse" **R**

μs(a) is the membership function of fuzzy set S across the values of a, which are also included in the "universe of discourse" **R**

min{c,d} takes the minimum of the two values, c and d

sup is the supremum, or height, of all of the values in a given set of membership function values (i.e., the maximum membership function value).

Step 1: Same as above for fuzzy set addition and subtraction, except that fuzzy set A is defined over the range "x" and fuzzy set B is defined over the range "y". Two different ranges are needed because the values of range "a" (see below) are the product of elements of "x" and "y".

Step 2: Choose the Minimum Value of μa(x) and μb(y) for Each Value of "a" In this case, it is necessary to determine all of the possible values of "a" as the product of values of "x" and "y". Then, for each value of "a", choose the minimum of μa(x) and μb(y) values that produce that value of "a" in each instance. In other words, a value of "a" of 0.04 can be obtained for values of x and y of 0.2 and 0.2. The minimum of μa(0.2) and μb(0.2) would then be chosen. However, a value of "a" of 0.04 can also be obtained from a value of x of 4 and of y of 0.01. The minimum of μa(4) and μb(0.01) would also be chosen among the set of minimized a=0.04 values.

Step 3: Calculate the supremum of the minimum μa(x) and μb(y) values for each value of a. The resulting set of μs(a) and "a" values define the fuzzy set S. This fuzzy set S is the product of the fuzzy sets A and B.

Appendix B:

Key Component Costs for BEVs, DHFCVs, and DMFCVs

Table B-1: Key BEV Component Costs (Low Production Volume Scenario)

	Electric Motor (1997$)			Motor Controller (1997$)			NiMH Battery (1997$/lb)		
	Low	Central	High	Low	Central	High	Low	Central	High
Generation 1									
2003	645	886	1901	1912	2052	2576	10.26	11.13	12.00
2004	645	886	1901	1912	2052	2576	10.26	11.13	12.00
2005	645	886	1901	1912	2052	2576	10.26	11.13	12.00
2006	607	886	1601	1529	1663	2172	9.23	10.10	10.97
Generation 2									
2007	561	821	1485	1458	1606	2115	8.83	9.56	10.30
2008	559	821	1467	1434	1581	2089	8.78	9.52	10.26
2009	556	821	1449	1411	1557	2064	8.73	9.48	10.23
2010	554	821	1431	1389	1533	2039	8.69	9.44	10.19
Generation 3									
2011	552	821	1413	1366	1509	2015	8.64	9.40	10.16
2012	549	821	1396	1344	1486	1990	8.60	9.36	10.12
2013	547	821	1379	1323	1463	1966	8.55	9.32	10.08
2014	544	821	1362	1301	1440	1943	8.51	9.28	10.05
Generation 4									
2015	497	745	1023	980	1093	1722	8.50	9.18	9.77
2016	495	745	1018	973	1085	1707	8.50	9.13	9.71
2017	493	745	1014	966	1078	1693	8.50	9.08	9.66
2018	490	745	1009	959	1070	1678	8.45	9.03	9.61
2019	488	745	1005	952	1063	1664	8.40	8.98	9.56
2020	486	745	1000	945	1056	1650	8.36	8.93	9.51
2021	483	745	996	938	1048	1636	8.31	8.88	9.45
2022	481	745	992	931	1041	1622	8.26	8.83	9.40
2023	479	745	987	925	1034	1608	8.22	8.79	9.35
2024	476	745	983	918	1027	1595	8.17	8.74	9.30
2025	474	745	979	911	1020	1581	8.13	8.69	9.25
2026	472	745	974	905	1012	1568	8.08	8.64	9.20

Table B-2: Key BEV Component Costs (High Production Volume Scenario)

	Electric Motor (1997$)			Motor Controller (1997$)			NiMH Battery (1997$/lb)		
	Low	Central	High	Low	Central	High	Low	Central	High
Generation 1									
2003	607	886	1601	1529	1663	2172	9.23	10.10	10.97
2004	571	886	1348	1222	1347	1831	8.30	9.17	10.04
2005	556	886	1248	1105	1226	1696	7.92	8.78	9.64
2006	551	886	1219	1073	1192	1658	7.81	8.67	9.53
Generation 2									
2007	507	821	1109	993	1110	1587	7.79	8.63	9.47
2008	503	821	1085	964	1079	1553	7.71	8.57	9.41
2009	499	821	1061	936	1049	1519	7.64	8.50	9.35
2010	495	821	1038	910	1021	1487	7.57	8.43	9.29
Generation 3									
2011	492	821	1016	884	993	1456		8.37	9.24
2012	488	821	995	860	967	1426	7.43	8.31	9.18
2013	484	821	974	837	942	1397	7.37	8.31	9.18
2014	481	821	954	814	918	1369	7.30	8.31	9.18
Generation 4									
2015	432	745	898	791	890	1339	7.28	8.02	8.55
2016	429	745	892	782	881	1321	7.21	8.02	8.55
2017	426	745	886	773	871	1303	7.15	8.02	8.55
2018	423	745	880	765	862	1286	7.09	8.02	8.55
2019	420	745	874	757	853	1270	7.03	8.02	8.55
2020	417	745	869	749	845	1255	6.97	8.02	8.55
2021	414	745	863	741	837	1240	6.92	8.02	8.55
2022	411	745	858	734	829	1226	6.87	8.02	8.55
2023	409	745	858	727	829	1226	6.82	8.02	8.55
2024	407	745	858	721	829	1226	6.77	8.02	8.55
2025	404	745	858	715	829	1226	6.72	8.02	8.55
2026	402	745	858	709	829	1226	6.68	8.02	8.55

Table B-3: Key DHFCV Component Costs (Low Production Volume Scenario)

	Electric Motor (1997$)			Motor Controller (1997$)			NiMH Battery (1997$/lb)			Fuel Cell System (1997$/kW-pk)			Hydrogen Tank (1997$/Ft^3/1000 psi)		
	Low	Mid	High	Low	Mid	High	Low	Mid	High	Low	Mid	High	Low	Mid	High
Generation 1															
2003	645	886	1901	1912	2052	2576	18.57	20.17	21.79	1125.21	1760.16	2550.29	33.45	40.66	47.38
2004	645	886	1901	1912	2052	2576	18.57	20.17	21.79	183.12	430.47	914.43	33.45	40.66	47.38
2005	645	886	1901	1912	2052	2576	18.57	20.17	21.79	137.70	345.08	778.41	33.45	40.66	47.38
2006	607	886	1601	1529	1663	2172	16.69	18.31	19.94	116.48	303.06	708.17	25.59	32.48	38.94
Generation 2															
2007	517	756	1380	1403	1527	2073	16.62	18.24	19.87	94.29	257.24	628.49	25.30	32.17	38.62
2008	514	756	1363	1380	1503	2048	16.49	18.12	19.74	85.96	239.44	596.50	24.82	31.67	38.09
2009	512	756	1346	1357	1480	2023	16.37	17.99	19.62	79.43	225.21	570.47	24.36	31.17	37.56
2010	510	756	1329	1335	1457	1999	16.25	17.87	19.50	74.11	213.41	548.54	23.90	30.68	37.05
Generation 3															
2011	508	756	1313	1312	1434	1974	16.13	17.75	19.38	70.53	203.36	529.60	23.46	30.20	36.54
2012	506	756	1296	1291	1412	1950	16.01	17.63	19.25	70.53	194.62	512.93	23.02	29.73	36.04
2013	504	756	1280	1269	1390	1927	15.89	17.51	19.13	70.53	186.91	498.04	22.59	29.26	35.55
2014	501	756	1264	1248	1368	1903	15.77	17.39	19.02	70.53	180.01	484.58	22.17	28.80	35.06
Generation 4															
2015	464	702	968	1183	1053	1696	10.91	11.69	12.46	76.55	173.77	472.29	21.75	28.35	34.58
2016	462	702	963	1163	1045	1681	10.85	11.62	12.39	76.55	168.73	462.27	21.35	27.90	34.10
2017	460	702	959	1143	1038	1667	10.80	11.56	12.32	76.55	164.03	452.86	20.95	27.47	33.64
2018	458	702	955	1123	1031	1653	10.74	11.50	12.25	76.55	159.62	443.97	20.56	27.04	33.18
2019	456	702	950	1104	1024	1639	10.68	11.43	12.18	76.55	155.48	435.55	20.17	26.61	32.72
2020	454	702	946	1086	1017	1625	10.63	11.37	12.12	76.55	151.57	427.54	19.79	26.19	32.27
2021	452	702	942	1067	1010	1611	10.57	11.31	12.05	76.55	147.87	419.91	19.42	25.78	31.83
2022	450	702	938	1049	1003	1597	10.51	11.25	11.99	76.55	144.35	412.61	19.06	25.38	31.39
2023	448	702	933	1031	996	1584	10.46	11.19	11.92	76.55	141.00	405.61	18.71	24.98	30.96
2024	446	702	929	1014	989	1570	10.40	11.13	11.85	76.55	137.80	398.89	18.36	24.59	30.54
2025	444	702	925	997	982	1557	10.35	11.07	11.79	76.55	134.74	392.42	18.01	24.20	30.12
2026	442	702	921	980	975	1544	10.29	11.01	11.73	76.55	131.81	386.18	17.68	23.82	29.71

Table B-4: Key DHFCV Component Costs (High Production Volume Scenario)

	Electric Motor (1997$)			Motor Controller (1997$)			NiMH Battery (1997$/lb)			Fuel Cell System (1997$/kW-pk)			Hydrogen Tank (1997$/Ft^3/1000 psi)		
	Low	Mid	High	Low	Mid	High	Low	Mid	High	Low	Mid	High	Low	Mid	High
Generation 1															
2003	607	886	1601	1529	1663	2172	16.69	18.31	19.94	1125.21	1760.16	2550.29	25.59	32.48	38.94
2004	571	886	1348	1222	1347	1831	15.01	16.63	18.25	137.70	345.08	778.41	19.57	25.95	32.01
2005	556	886	1248	1105	1226	1696	14.31	15.92	17.54	87.43	242.61	602.25	17.36	23.46	29.31
2006	551	886	1219	1073	1192	1658	14.11	15.72	17.33	66.88	197.07	517.62	16.75	22.77	28.56
Generation 2															
2007	467	756	1025	945	1053	1552	13.92	15.52	17.13	70.53	172.15	469.09	16.18	22.12	27.84
2008	463	756	1002	917	1024	1518	13.73	15.33	16.94	70.53	161.15	447.06	15.63	21.49	27.15
2009	460	756	980	890	995	1485	13.55	15.15	16.75	70.53	151.86	428.13	15.11	20.89	26.49
2010	456	756	959	864	968	1454	13.37	14.97	16.62	70.53	143.82	411.51	14.62	20.31	25.85
Generation 3															
2011	453	756	938	839	942	1423	13.19	14.96	16.62	70.53	136.76	396.69	14.14	19.76	25.23
2012	449	756	918	815	917	1394	13.03	14.96	16.62	70.53	130.46	383.30	13.69	19.23	24.64
2013	446	756	899	792	893	1365	12.86	14.96	16.62	70.53	124.79	371.08	13.26	18.72	24.07
2014	443	756	880	771	870	1338	12.70	14.96	16.62	70.53	119.63	359.85	12.85	18.24	23.53
Generation 4															
2015	409	702	847	713	858	1318	9.33	10.24	10.89	76.55	114.90	349.45	12.46	17.77	23.01
2016	406	702	841	694	849	1300	9.25	10.24	10.89	76.55	111.05	340.87	12.10	17.33	22.51
2017	403	702	835	676	840	1283	9.17	10.24	10.89	76.55	107.42	332.72	11.75	16.91	22.03
2018	400	702	829	659	831	1267	9.10	10.24	10.89	76.55	104.00	324.97	11.41	16.51	21.57
2019	398	702	824	642	823	1251	9.03	10.24	10.89	76.55	100.77	317.59	11.10	16.13	21.13
2020	395	702	818	627	814	1236	8.96	10.24	10.89	76.55	97.71	310.54	10.80	15.77	20.72
2021	393	702	813	612	807	1221	8.89	10.24	10.89	76.55	94.82	303.82	10.52	15.42	20.33
2022	391	702	813	598	806	1220	8.83	10.24	10.89	76.55	92.08	297.40	10.26	15.40	20.30
2023	389	702	813	585	806	1220	8.77	10.24	10.89	76.55	89.48	291.26	10.01	15.40	20.30
2024	387	702	813	572	806	1220	8.71	10.24	10.89	76.55	87.02	285.40	9.78	15.40	20.30
2025	385	702	813	561	806	1220	8.65	10.24	10.89	76.55	84.68	279.79	9.56	15.40	20.30
2026	383	702	813	550	806	1220	8.60	10.24	10.89	76.55	82.46	274.42	9.35	15.40	20.30

Table B-5: Key DMFCV Component Costs (Low Production Volume Scenario)

	Electric Motor (1997$)			Motor Controller (1997$)			NiMH Battery (1997$/lb)			Fuel Cell System (1997$/kW-pk)		
	Low	Mid	High	Low	Mid	High	Low	Mid	High	Low	Mid	High
Generation 1												
2003												
2004												
2005												
2006												
Generation 2												
2007												
2008												
2009												
2010												
Generation 3												
2011	528	778	1082	1037	1155	1802	16.13	17.75	19.38	1125.21	1760.16	2550.29
2012	526	778	1078	1029	1147	1786	16.01	17.63	19.25	147.05	363.11	807.83
2013	523	778	1073	1022	1139	1771	15.89	17.51	19.13	109.33	288.54	683.30
2014	521	778	1068	1015	1131	1756	15.77	17.39	19.02	91.50	251.31	617.90
Generation 4												
2015	464	702	968	1183	1053	1696	10.91	11.69	12.46	92.41	227.29	574.30
2016	462	702	963	1163	1045	1681	10.85	11.62	12.39	92.41	212.58	546.99
2017	460	702	959	1143	1038	1667	10.80	11.56	12.32	92.41	200.63	524.41
2018	458	702	955	1123	1031	1653	10.74	11.50	12.25	92.41	190.59	505.18
2019	456	702	950	1104	1024	1639	10.68	11.43	12.18	92.41	181.97	488.42
2020	454	702	946	1086	1017	1625	10.63	11.37	12.12	92.41	174.42	473.58
2021	452	702	942	1067	1010	1611	10.57	11.31	12.05	92.41	167.72	460.25
2022	450	702	938	1049	1003	1597	10.51	11.25	11.99	92.41	161.69	448.15
2023	448	702	933	1031	996	1584	10.46	11.19	11.92	92.41	156.22	437.06
2024	446	702	929	1014	989	1570	10.40	11.13	11.85	92.41	151.21	426.81
2025	444	702	925	997	982	1557	10.35	11.07	11.79	92.41	146.60	417.29
2026	442	702	921	980	975	1544	10.29	11.01	11.73	92.41	142.32	408.39

Table B-6: Key DMFCV Component Costs (High Production Volume Scenario)

	Electric Motor (1997$)			Motor Controller (1997$)			NiMH Battery (1997$/lb)			Fuel Cell System (1997$/kW-pk)		
	Low	Mid	High	Low	Mid	High	Low	Mid	High	Low	Mid	High
Generation 1												
2003												
2004												
2005												
2006												
Generation 2												
2007												
2008												
2009												
2010												
Generation 3												
2011	465	778	964	854	959	1433	13.19	14.96	16.62	1125.21	1760.16	2550.29
2012	462	778	956	843	947	1412	13.03	14.96	16.62	85.61	238.68	595.13
2013	458	778	949	833	936	1392	12.86	14.96	16.62	83.60	188.40	500.93
2014	454	778	943	823	925	1373	12.70	14.96	16.62	83.60	163.09	450.98
Generation 4												
2015	409	702	847	713	858	1318	9.33	10.24	10.89	92.41	146.63	417.36
2016	406	702	841	694	849	1300	9.25	10.24	10.89	92.41	136.48	396.09
2017	403	702	835	676	840	1283	9.17	10.24	10.89	92.41	128.14	378.33
2018	400	702	829	659	831	1267	9.10	10.24	10.89	92.41	121.11	363.09
2019	398	702	824	642	823	1251	9.03	10.24	10.89	92.41	115.04	349.74
2020	395	702	818	627	814	1236	8.96	10.24	10.89	92.41	109.71	337.87
2021	393	702	813	612	807	1221	8.89	10.24	10.89	92.41	104.98	327.19
2022	391	702	813	598	806	1220	8.83	10.24	10.89	92.41	100.72	317.48
2023	389	702	813	585	806	1220	8.77	10.24	10.89	92.41	96.87	308.59
2024	387	702	813	572	806	1220	8.71	10.24	10.89	92.41	95.64	300.40
2025	385	702	813	561	806	1220	8.65	10.24	10.89	92.41	95.64	292.82
2026	383	702	813	550	806	1220	8.60	10.24	10.89	92.41	95.64	285.77

This page left intentionally blank